**Joint Pathology Center**
**Veterinary Pathology Services**

*Conference Coordinator*
**Matthew C. Reed, DVM**
**Captain, Veterinary Corps, U.S. Army**
**Veterinary Pathology Services**
**Joint Pathology Center**

## WEDNESDAY SLIDE CONFERENCE 2014-2015

# Conference 1

**3 September 2014**

**Conference Moderator:**
Sarah Hale, DVM, Diplomate ACVP
Chief, Extramural Programs
Joint Pathology Center
Forest Glen Annex, Bldg. 161
2460 Linden Lane
Silver Spring, MD 20910

**CASE I:** Ex58B/Ex58G (JPC 3134882).

**Signalment:** A 7-year-old intact male German shepherd dog.

**History:** A 7-year-old intact male German shepherd dog was presented with hind limb paresis of 3 days duration and back pain. The referring veterinarian had treated the dog with prednisone and cephalexin for 3 days but the dog had deteriorated neurologically despite treatment. Neurological examination at presentation revealed paralysis of the right hind limb and paresis with minimal voluntary movement of the left hind limb. The dog appeared to be mainly in pain during postural shifts. All spinal reflexes were absent in the right hind limb. A weak withdrawal reflex was detected in the left hind limb. The neuroanatomic diagnosis was a lesion located in L4-S1 spinal cord segments and more severe on the right side. MRI examination was done 4 days post-admission and demonstrated an intramedullary increased signal intensity from the conus medularis to the level of L1. A surgical intervention was attempted but the dog's condition continued to deteriorate and it was

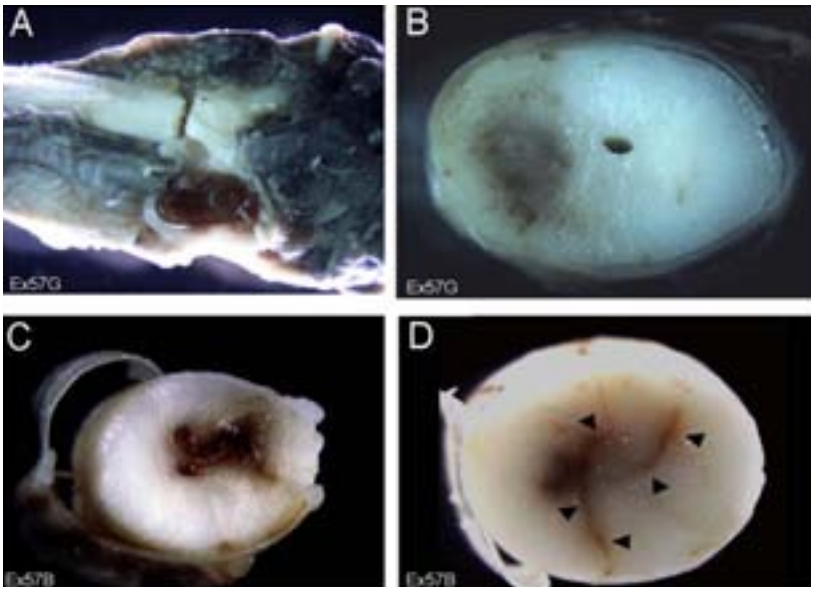


*1-1. Lumbar spinal cord, dog: At necropsy, following incision of the dura, a single nematode was found embedded in the spinal parenchyma at $L_1$ –$L_2$ spinal segments on the left (Fig 1A). There were multiple, randomly distributed foci of hemorrhage and necrosis with or without cavitation involving the gray and white matter (Fig 1B). The lumbar segment was the most severely affected. Many necrohemorrhagic foci were continuous through multiple transverse sections and formed one or more tracts. The lesion was mostly located on the right side of the cord but moved to the left at $L_1$-$L_2$. Similar lesions were seen in the second case (Fig. 1C and D). (Photo courtesy of: Department of Veterinary Resources, Weizmann Institute, Israel. http://www.weizmann.ac.il/vet/*

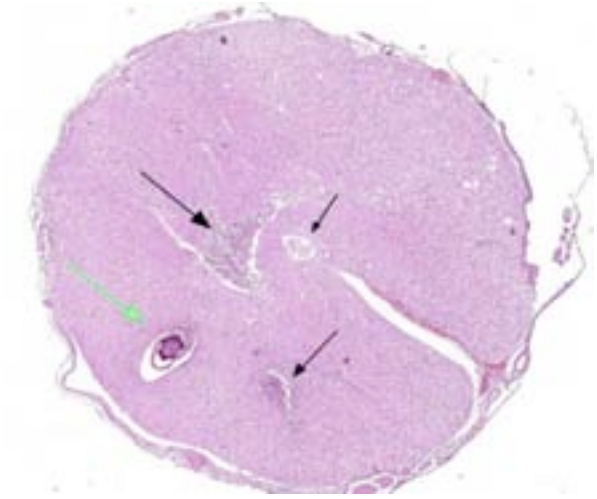

*1-2. Lumbar spinal cord, dog: There are multiple areas of cavitation and necrosis (black arrows) within both the grey and white matter (black arrows). A transverse section of an adult spirurid nematode is present within one area of necrosis (green arrow). (HE 9X)*

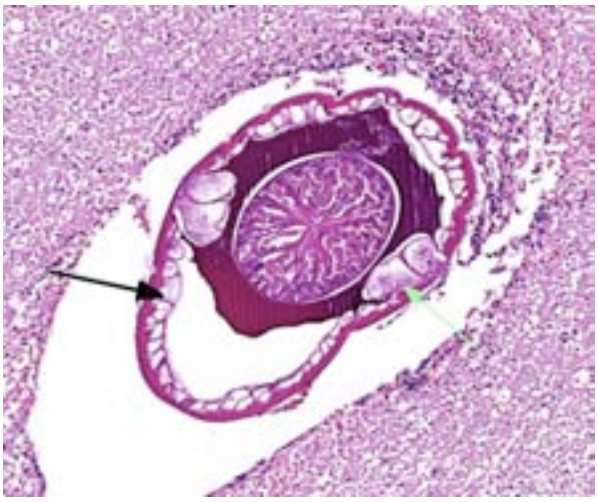

*1-3. Lumbar spinal cord, dog: The adult S. lupi exhibits a thick smooth eosinophilic cuticle, polymyarian-coelomyarian musculature (black arrow), a pseudocoelom which contains abundant dark red material, large lateral chords (green arrow), and a large centrally located gastrointestinal tract. (HE 120X)*

euthanized. Most of the slides submitted are from this case (Ex57G). Additional slides are from another dog with a history of acute progressive paraparesis and severe back pain beginning 3 days before presentation (Ex57B).

**Gross Pathologic Findings:** At necropsy, following incision of the dura, a single nematode was found embedded in the spinal parenchyma at $L_1$ –$L_2$ spinal segments on the left. Transverse sections of the spinal cord showed macroscopic changes from the caudal thoracic to the lumbar area. There were multiple, randomly distributed foci of hemorrhage and necrosis with or without cavitation involving the gray and white matter. The lumbar segment was the most severely affected. Many necrohemorrhagic foci were continuous through multiple transverse sections and formed one or more tracts. The lesion was mostly located on the right side of the cord but moved to the left at $L_1$-$L_2$. Similar lesions were seen in the second case.

**Laboratory Results:** CBC and serum biochemistry were unremarkable. Serological tests for *Toxoplasma gondii* and *Neospora caninum* were negative. Fecal flotation yielded *S. lupi* eggs. CSF analysis revealed mild mixed pleocytosis (40 cells/µl, reference interval: 0-8 cells/µl) with neutrophils (65%) and eosinophils (35%), and protein concentration of 22 mg/dl (RI: <25 mg/dl). Endoscopy demonstrated 3 typical *S. lupi* nodules in the caudal esophagus.

**Histopathologic Description:** In a random distribution within the white matter, there are several foci of necrosis and acute hemorrhage with mild gitter cell and variable neutrophilic infiltration. In the tissue around the tract, astrocytes show mild hypertrophy. Scattered vacuoles, some containing swollen axons (spheroids) and other cellular debris, are present in the white matter near the necrotic foci as well as further away. There is slight hemorrhage and mild gitter cell infiltration in the meninges within the ventral median fissure of one sample (lumbar intumescence). In another sample, there is widespread hemorrhage in the connective tissue external to the dura mater. There are several sections of a nematode with a smooth cuticle, coelomyarian-polymyarian muscles, large lateral hypodermal chords, abundant amphophilic to basophilic fluid in the pseudocoelom and an intestine composed of individual cuboidal cells, each with a prominent brush border. These features are typical of an adult spirurid, including *Spirocerca lupi.* Unfortunately, the parasite was dislodged during tissue processing. Sections from the second block (Ex57B) show a similar lesion but in this sample the tracts are present in the gray and white matter and there is mild to moderate inflammatory infiltration. Within one of the tracts there is a single transverse section at the level of the esophagus of a nematode with morphologic features as described above.

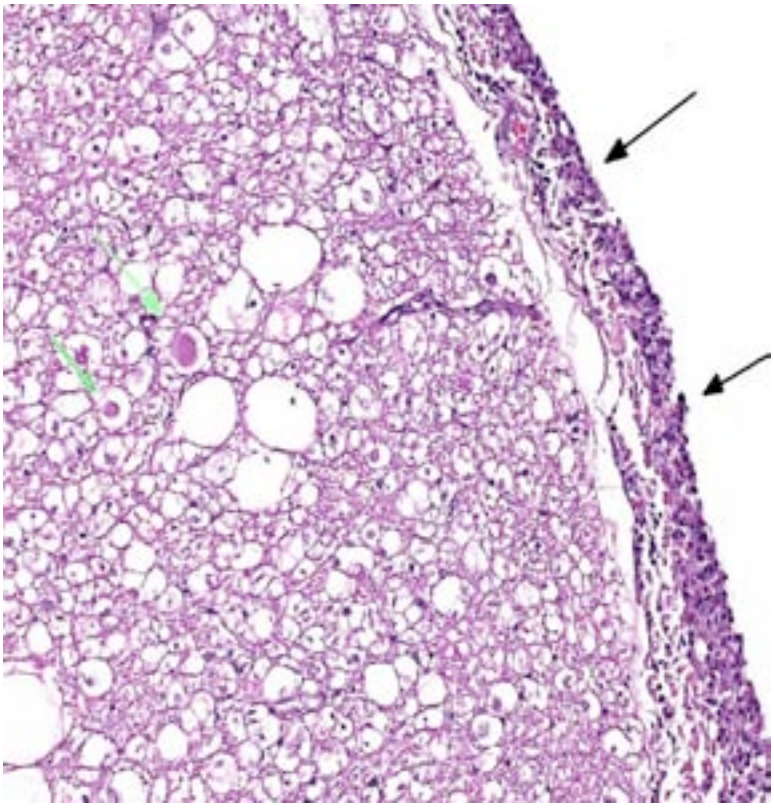

*1-4. Lumbar spinal cord, dog: Within the lateral funiculi, there are moderate numbers of dilated axon sheaths which contain mildly to moderately swollen axons (spheroids) (green arrows), and the overlying meninges are expanded by moderate numbers of neutrophils, eosinophils, histiocytes and lymphocytes. (HE 144X)*

**Contributor's Morphologic Diagnosis:** Spinal cord: Multifocal necrosis and hemorrhage with mild acute histiocytic and neutrophilic meningomyelitis and intralesional spirurid nematode.

**Contributor's Comment:** *Spirocerca lupi* is primarily a parasite of dogs. Its distribution is worldwide but it is most prevalent in warm climates. Adult parasites live in a nodular mass in the esophageal wall of the host. The female lays embryonated eggs which are transferred through a tract in the nodules and excreted with feces. The eggs are ingested by an intermediate host, corprophagus beetles, and develop to infective L3 within 2 months.

Carnivores are infected by ingestion of the beetles or a variety of paratenic hosts (birds, lizards, mice, rabbits etc.). In the carnivore host, the infective larvae penetrate the gastric mucosa and migrate within the walls of the gastric arteries to the thoracic aorta. About 3 months post-infection the larvae leave the aorta and migrate to the esophagus where they incite the development of fibro-inflammatory tissue (granulomas) as they mature to adults over the next 3 months. Lesions associated with *S. lupi* infestation are mainly due to migration and persistence of the parasite in tissues. Esophageal nodular masses (granulomas) and aortic scars and aneurysms are the most common lesions. Other lesions include spondylitis and spondylosis of the caudal thoracic vertebrae, neoplastic transformation of the esophageal granulomas, hypertrophic osteopathy, and aberrant migration into a wide variety of tissues including thoracic viscera, GIT, urinary system and subcutaneous tissue.[5]

More recently, several reports from Israel and South Africa describe aberrant migration into the spinal cord.[1,2,3] In one report (n=4) *S. lupi* was located in the extradural space and elicited signs typical of thoracolumbar IVD prolapse or spinal trauma.[2] In the remaining cases (n=5), tracts were present within the spinal cord as in the two cases used here.[2,3] Although confirmation of the diagnosis is difficult in cases which recover, the neurologists at the Veterinary School of the Hebrew University estimate that in the past 2-3 years, approximately 10-15 cases are seen annually (Dr. Orit Chai, personal communication). The reason for the increase in the occurrence of this form of canine spirocercosis is unknown but it may in part be attributable to failure in making the correct diagnosis in the past. Currently, a tentative diagnosis is based on the neurological signs, eosinophilic CSF pleocytosis and evidence of *S. lupi* infection in other tissues (by thoracic radiography, esophagoscopy and fecal floatation). The presenting signs of an acute nonsymmetrical paraparesis / plegia and high CSF eosinophil counts, observed in the present case, are similar to previously reported spinal intramedullary spirocercosis cases.[1]

The cause of aberrant migration of *S. lupi* is unknown. It has been suggested that aberrant migration occurs when a worm in the thoracic arterial wall enters the intercostal arteries and through their spinal branches arrives at the

extradural space. To enter the spinal cord it must then further penetrate the dura mater and the leptomeninges. The location reported in most intradural and extradural cases is T4-L1. In this region the aorta lies closely parallel to the vertebral column and the intercostal arteries supply the spinal branches that enter the spinal canal via the intervertebral foramina.[3]

Verminous encephalomyelitis may arise from aberrant wanderings of a parasite within its normal host (e.g., *Dirofilaria immitis* in the CNS of dogs and cats and *Strongylus vulgaris* in the brain of horses); or more commonly, infection of an aberrant host (e.g., *Paralephastrongylus tenuis*, the meningeal worm of white-tailed deer infesting sheep, goats and other herbivores). Other than regions where *S. lupi* is prevalent, cerebrospinal helminthosis is uncommon in dogs and cats. Nematodes, which may cause aberrant migration into the CNS of dogs include *Angiostrongylus cantonensis* in Australia, *Angiostrongylus vasorum* and *Dirofilaria immitis*.[6] There is a report of neurologic dysfunction in 3 dogs due to intracranial hemorrhage from consumptive coagulopathy associated with *Angiostrongylus vasorum* infection of the lung.[3]

**JPC Diagnosis:** Spinal cord: Meningomyelitis, necrotizing, eosinophilic, multifocal, marked, with adult spirurid nematode.

**Conference Comment:** This is an excellent example of aberrant migration in a normal host of a common and readily identifiable nematode. Conference participants reviewed the features of nematodes on histologic section of which they used the coelomyarian-polymyarian musculature that projects into the pseudocoelom, prominent lateral chords and eosinophilic material within the pseudocoelom in the present case to facilitate identification of a spirurid nematode, specifically *Spirocerca lupi.* Other spirurids of veterinary importance include: *Trichospirura leptostoma* inhabiting pancreatic ducts of the common marmoset, *Physaloptera* spp. residing in the stomach of many mammals, *Draschia megastoma* in the stomach of horses, and *Gongylonema* spp. found in the many different tissues and species.

The contributor provides an excellent overview of the complex pathogenesis of *Spirocerca* and appropriately conveys the tremendous variety of lesions associated with infection. Of significance is the pathognomonic lesion of thoracic spondylitis and its ability to induce malignant transformation, with esophageal fibrosarcoma or osteosarcoma being most characteristic.[7] This ability is not exclusive to *Spirocerca,* however. The acronym SOCCS-T is often used at JPC to facilitate remembering the following neoplasm-inducing parasites: *Spirocerca lupi, Opisthorchis felineus* (cholangiocarcinoma in cats and people), *Cysticercus fasciolaris* (hepatic sarcoma in rats), *Clonorchis sinensis* (cholangiocarcinoma in cats and people), *Schistosoma hematobium* (transitional cell carcinoma of urinary bladder in people) and *Trichosomoides crassicauda* (papillomas of rat urothelium).

Just as the contributor noted, it is the extensive migration of *Spirocerca* which most commonly causes lesions, as was the case in this dramatic example. Up to 80% of the section of spinal cord was affected in some slides, leading participants to speculate on how rapid the migration must have occurred to cause such extensive lesions in a relatively short period of time. Conference participants also discussed the clinicopathologic findings of pleocytosis, along with elevated neutrophils, eosinophils and protein, as expected findings of a cerebrospinal fluid analysis in this case. This is to contrast with an albuminocytologic dissociation, in which elevated protein levels does not accompany pleocytosis (seen with neoplastic or degenerative diseases such as Guillain-Barre syndrome in people).

**Contributing Institution:** Department of Veterinary Resources
Weizmann Institute, Israel
http://www.weizmann.ac.il/vet/

**References:**

1. Chai O, Shelef I, Brenner O, Dogadkin O, Aroch I, Shamir MH. Magnetic resonance imaging findings of spinal intramedullary sprocercosis. *Vet Radiol Ultrasound*. 2008;49:456-9.
2. Du Plessis CJ, Keller N, Millward IR. Aberrant extradural spinal migration of *Spirocerca lupi*: four dogs. *J Small Anim Pract.* 2007;48:275-278.
3. Dvir E, Perl S, Loeb E, et al. Spinal intramedullary aberrant Spirocerca lupi migration in three dogs. *J Vet Intern Med.* 2007;21:860-864.
4. Garosi LS, Platt SR, McConnell JF, Wray JD, Smith KC. Intracranial hemorrhage associated

with *Angiostrongylus vasorum* infection in three dogs. *J Small Anim Pract.* 2005;46:93-99.
5. Mazaki-Tovi M, Baneth G, Aroch I, et al. Canine spirocercosis: Clinical, diagnostic, pathologic and epidemiologic characteristics. *Vet Parasitol.* 2002;107:235-250.
6. Summers BA. Inflammatory diseases of the central nervous system. In: Summers BA, Cummings JF, de LaHunta A, eds. *Veterinary Neuropathology*. St. Louis, MO: Mosby-Year Book; 1995:159-162.
7. Van der Merwe LL, Kirberger RM, Clift S, Williams M, Keller N, Naidoo V. Spirocerca lupi infection in the dog: a review. *Vet J.* 2008;176(3): 294-309.

**CASE II:** L10-13908 (JPC 3167326).

**Signalment:** 11-year-old male rhesus macaque (*Macaca mulatta*).

**History:** This macaque was used for long-term visual and behavioral studies. A cranial head-stage implant was maintained on this animal for 4 years, which was associated with chronic purulent discharge. This purulent discharge was treated regularly with mechanical flushing and debridement, as well as anti-microbial therapy (based on routine culture and sensitivity results). No clinical signs were noted at the end of study period, although a physical examination just prior to barbiturate euthanasia revealed an enlarged liver upon abdominal palpation.

**Gross Pathologic Findings:** This macaque was presented dead in good body condition. Diffusely, the liver was enlarged (liver weight = 0.85 g; body weight = 6.8 kg), with rounded margins, and was pale red/tan and firm. A thick, viscous, pale green to pale yellow, opaque, odoriferous film of purulent material (biofilm) was noted in the subcutaneous tissues underneath the cranial head-stage implant. All other organs and tissues were within normal gross limits.

**Laboratory Results:** Mixed bacteria were isolated from the biofilm under the cranial head-stage implant, including *Staphylococcus* spp., *Streptococcus* spp., and *Enterococcus* spp. These were all resistant to most antimicrobials except enrofloxacin and ciprofloxacin.

**Histopathologic Description:** Sections of liver are examined. There is extensive effacement of normal hepatic lobular architecture due to the presence of massive amounts of amorphous, homogenous sheets of eosinophilic hyaline acellular material that appears to originate in and expand the space of Disse. This material is congophilic and displays bright-green birefringence when viewed under polarized light. Multifocally and extensively, the amyloid deposits in the space of Disse often expand outward to involve adjacent sinusoidal spaces (resulting loss of the sinusoidal lumen), and the amount of amyloid present results in massive to total loss of normal hepatocytes and hepatic lobular architecture, with remaining hepatocytes appearing sparse, compacted/atrophied, and displaced into thin, often tortuous hepatic cords. Occasional portal triads and central veins are still recognizable.

**Contributor's Morphologic Diagnosis:** Liver, hepatic amyloidosis, severe, diffuse, chronic.

**Contributor's Comment:** **Amyloid** refers to a heterogenous group of protein fibrils that share a common ultrastructural feature, namely that extracellular cross polymerization of the fibrils results in the formation of insoluble β-pleated sheets.[1] Biochemically, at least 20 different types of amyloid protein have been discovered in humans and animals. **Amyloidosis** refers to human and animal diseases that are characterized by the extracellular deposition of amyloid in various tissues, often resulting in dysfunction of compromised organs.[1]

Amyloidosis can be classified by the biochemical composition of the amyloid protein involved.[9] Amyloidosis can also be classified on the basis of whether it results from a primary or secondary disease process, and whether amyloid deposition is localized to one tissue or multiple tissues (systemic).[10] More typically, classification of amyloidosis often reflects a combination of all these systems.[10]

The two most traditionally recognized forms of systemic amyloidosis in humans and animals are:

1. **Primary amyloidosis (AL),** characterized by the deposition of immunoglobulin light chain that is overproduced by plasma cell/B-cell dyscrasias (e.g., multiple myeloma, B-cell proliferations).[1,10]

2. **Secondary/reactive systemic amyloidosis (AA),** characterized by the deposition of serum amyloid A (SAA), is produced as a liver-derived acute phase protein as part of inflammatory processes. In this form, a chronic-active inflammatory process usually occurs that results in sustained production of SAA, but a defect in the degradation of SAA (perhaps due to excessive levels of SAA that overwhelm the enzymatic degradation pathway; a defect in the enzymatic degradation pathway; or a structural difference of the SAA fibril that

*2-1. Liver, rhesus macaque: The liver was diffusely enlarged (liver weight = 0.85 g; body weight = 6.8 kg) with rounded margins. (Photo courtesy of: Veterinary Services Center, Department of Comparative Medicine, Stanford School of Medicine (http://med.stanford.edu/compmed/). (HE 0.63X)*

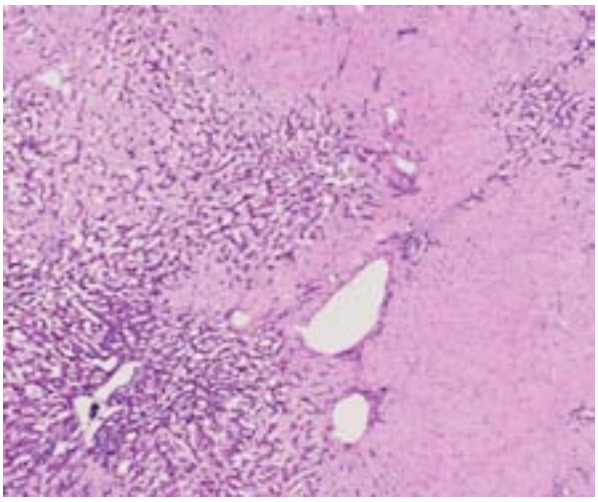

*2-2. Liver, rhesus macaque: Large areas of amyloid surround and replace hepatic parenchyma. (HE 34X)*

makes it resistant to degradation), leading to the development of AA amyloidosis.[1,10]

There are several types of amyloidosis that occur in macaques, the major type being **secondary/ reactive amyloidosis (AA)**. This has been reported in rhesus macaques, in association with enterocolitis (usually associated with *Shigella* spp. infection),[2,4] osteoarthritis,[2,3,4] and chronic indwelling venous catheters.[6] In pig-tailed macaques, secondary/reactive amyloidosis is associated with enterocolitis, retroperitoneal fibromatosis, and glomerulonephritis.[10] In most reported cases, advancing age is a predisposing factor for the deposition of AA amyloid.[2,3,4,6,12,15] The deposition can be systemic or (more rarely) localized, with typical tissues that are affected being small intestines, liver, spleen, and kidney.[8] A notable localized form of secondary/reactive amyloidosis appears to be **intestinal amyloidosis (AA),** which has been reported in cynomolgus macaques[14] and pig-tailed macaques.[7] In this form, there is localized deposition of AA amyloid in the lamina propria of the small intestines (and less often, the large intestines), and may occur as an incidental lesion in aged macaques.[7,14] However, it is more commonly linked to a clinical syndrome of weight loss and diarrhea resulting from protein-losing enteropathy.[7]

Other distinct forms of amyloidosis in macaques include:

- **Cerebral amyloidosis (Aβ),** which involves the deposition of amyloid β protein precursor as either plaques (senile amyloid plaques) within the neuropil and/ or as deposits within vessels walls (cerebral amyloid angiopathy) of the brain. This has been reported in rhesus macaques[14] and cynomolgus macaques[11] which are used animal models for Alzheimer's disease research.

- **Pancreatic islet amyloidosis (AIAAP),** where amylin (islet-associated polypeptide) accumulation is localized to endocrine pancreatic islets, is often associated with diabetes mellitus. This has been documented in cynomolgus macaques[5,16] and Celebes-crested macaques,[5] and provide a nonhuman primate model for diabetes mellitus research.

In general, clinical presentation of macaques affected with secondary/reactive amyloidosis reflects the type of tissues that are involved, the amount of amyloid involved, and the primary inciting causes (if any can be identified) that may be involved. For example, amyloidosis involving the gastrointestinal tract or liver can present similarly with weight loss due to hypoproteinemia (via protein-losing enteropathy and decreased hepatic function respectively). Intestinal amyloidosis may also present with diarrhea, due

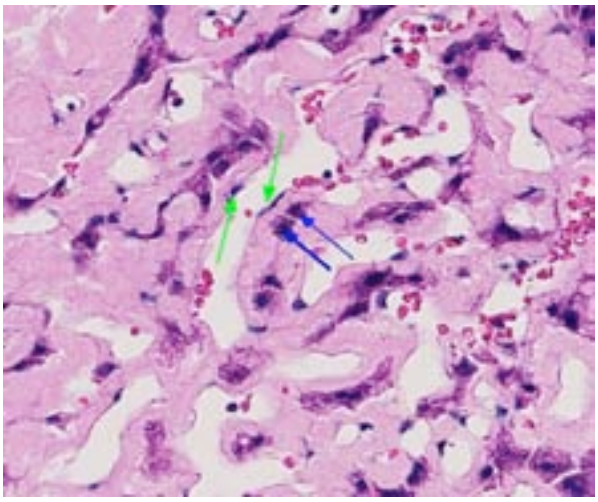

*2-3. Liver, rhesus macaque: Amyloid fills the space of Disse between hepatocytes (blue arrows) and endothelial cells (green arrows). (HE 284X)*

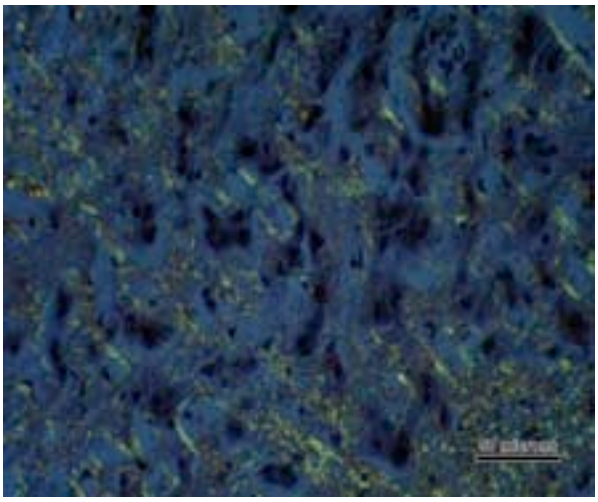

*2-4. Liver, rhesus macaque: Material within the space of Disse is congophilic and displays bright-green birefringence when viewed under polarized light. (HE 400X)*

to both the presence of amyloid with the mucosa and the primary instigating pathogen (e.g., shigellosis).

Noninvasive, antemortem diagnosis of secondary/ reactive amyloidosis in macaques is difficult. Clinical biochemistry studies of macaques with amyloidosis have consistently revealed significant elevations in γ-glutamyl transferase, aspartate aminotransferase, and alkaline phosphatase, and significant decreases in total protein and albumin.[6,8,9] Serum electrophoresis may reveal hypergammaglobulinemia (polyclonal gammopathy) as well.[6] Immunoassays have also revealed elevations in SAA early in the disease course and elevations in macrophage colony-stimulating factor later in the disease course.[9] Diagnostic imaging (e.g., radiography, magnetic resonance imaging) can be used to evaluate hepatomegaly if the liver contains significant amounts of amyloid, but are very insensitive for mild and subclinical cases.[8]

The diagnosis and differentiation of secondary/ reactive amyloidosis can be achieved using several methods:

1. **Gross pathology** is often unrewarding in mild to moderate or subclinical cases. In severely affected animals however, gross examination may reveal enlarged livers that are often described as pale, friable to firm, and waxy; prominent white pulp areas on the cut surfaces of spleens; or thickened gastrointestinal mucosa. Chronically-affected animals may also display emaciation associated with weight loss.[2,3,4,8,12]

2. **Histopathology** of tissues obtained as biopsy specimens or from necropsy is the traditional gold standard for diagnosis of secondary/reactive amyloidosis. Amyloid appears as amorphous, acellular, homogenous eosinophilic extracellular material on H&E sections, and occurs most prominently in the space of Disse in the liver, the follicular white pulp areas in the spleen, the lamina propria of the gastrointestinal tract, the medullary interstitium of the kidneys, and the corticomedullary junction of the adrenal glands.[2,3,4,8,12]

   Other histochemical and immunohistochemical stains can be performed to definitively confirm the presence of AA amyloid in tissues. The most commonly used histochemical stain is Congo red. Like all amyloid, AA amyloid appears orange to rosy-pink with Congo red staining, and will display bright green birefringence when examined with polarized light. However, AA amyloid (in contrast to other types of amyloid) loses its congophilic and birefringence properties if treated with potassium permanganate prior to Congo Red staining.[2,3,12] Antibodies for most

types of amyloid proteins (including AA amyloid) are commercially available.

We believe that the case of hepatic amyloidosis presented here represents severe localized secondary/reactive amyloidosis in the liver. Observable amyloid deposition was not noted in all other tissues examined histologically. The cause of the amyloidosis was most likely the chronic infection of the subcutaneous tissues under the cranial head-stage implant ("peri-implantitis") in this macaque, which is a common cause of secondary/reactive amyloidosis in macaques observed in our institution.

**JPC Diagnosis:** Liver, space of Disse: Amyloidosis, diffuse, severe, with marked hepatocellular atrophy and loss.

**Conference Comment:** The contributor provides an excellent overview of amyloidosis with emphasis on the variety of manifestations in nonhuman primates. This case is an exceptional example of hepatic amyloidosis, as it nicely illustrates the expansion of the perisinusoidal space with amyloid. This area, known as the space of Disse, is the narrow space between the plates of hepatocytes and sinusoidal lining cells where amyloid is known to accumulate within the liver. For reviewing the important ultrastructural appearance of amyloid with its randomly oriented fibrils in this characteristic location, we refer the reader to the EM case from the 2013 WSC (conference 6, case 4).

Conference participants noted the severity of the lesion in this case and were amazed as to the lack of clinical signs in this animal. Participants agreed the source of amyloid is most likely due to the chronic inflammation in response to the implant, resulting in reactive amyloid A (AA). Not likely applicable in this instance, but of academic interest, is the recent evidence suggesting AA amyloidosis is transmissible, both within and between species.[13] While currently only demonstrable experimentally, the possibility of amyloid transmission between species and the presence of amyloid in skeletal muscle of food animals such as poultry and cattle suggests a potential public health concern worthy of further investigation.

**Contributing Institution:** Veterinary Services Center
Department of Comparative Medicine
Stanford School of Medicine
(http://med.stanford.edu/compmed/)

**References:**

1. Addie DD, Jarrett O. Feline coronavirus infections. In: Greene CE, ed. *Infectious Diseases of the Dog and Cat*. 3rd ed. St. Louis, MO: Saunders; 2006:91-100.
2. Bradshaw JM, Pearson GR, Gruffydd-Jones TJ. A retrospective study of 286 cases of neurological disorders of the cat. *J Comp Path.* 2004;131:112–120.
3. Brown CC, Baker DC, Barker IK. Alimentary system. In: Maxie MG, ed. *Jubb, Kennedy, and Palmer's Pathology of Domestic Animals*. Vol. 2. 5th ed. London, UK: Saunders Elsevier; 2007:290-293.
4. Diaz JV, Poma R. Diagnosis and clinical signs of feline infectious peritonitis in the central nervous system. *Can Vet J.* 2009;50(10):1091–1093.
5. Foley JE, Leutenegger C. A review of coronavirus infection in the central nervous system of cats and mice. *J Vet Intern Med.* 2001;15(5):438–444.
6. Foley JE, Lapointe JM, Koblik P, Poland A, Pedersen NC. Diagnostic features of clinical neurologic feline infectious peritonitis. *J Vet Intern Med.* 1998;12(6):415–423.
7. Giori L, Giordano A, Giudice C, Grieco V, Paltrinieri S. Performances of different diagnostic tests for feline infectious peritonitis in challenging clinical cases. *J Small Anim Pract*. 2011;52:152-157.
8. Gunn-Moore DA, Reed N. CNS disease in the cat: current knowledge of infectious causes. *J Fel Med Surg*. 2011;13(11):824–836.
9. Keel SB, Abkowitz JL. The microcytic red cell and the anemia of inflammation. *N Engl J Med*; 2009;361(19):1904-1906.
10. Kent M. The cat with neurological manifestations of systemic disease. Key conditions impacting on the CNS. *J Fel Med Surg*. 2009;11(5):395–407.
11. Kipar A, Meli ML. Review of feline infectious peritonitis: Still an enigma? *Vet Pathol*. 2014:51(2):505-526.
12. MacLachlan NJ, Dubovi EJ. *Fenner's Veterinary Virology*. 4th ed. London, UK: Academic Press; 2011:393-412.

13. Murakami T, Ishiguro N, Higuchi K. Transmission of systemic AA amyloidosis in animals. *Vet Pathol.* 2014;51(2):363-371.
14. Myrrha LW, Miquelitto Figueira Silva F, Fernandes de Oliveira Peternelli E, Silva Junior A, Resende M, Rogéria de Almeida M. The paradox of feline coronavirus pathogenesis: a review. *Adv Virol*. 2011;2011:1-8.
15. Rand JS, Parent J, Percy D, Jacobs R. Clinical, cerebrospinal fluid, and histological data from twenty-seven cats with primary inflammatory disease of the central nervous system. *Can Vet J.* 1994;35(2):103–110.
16. Sharif S, Suri Arshad S, Hair-Bejo M, Rahman Omar A, Allaudin Zeenathul N, Alazawy A. Diagnostic methods for feline coronavirus: a review. *Vet Med Int*. 2010;2010:1-7.
17. Singh M, Foster DJ, Child G, Lamb WA. Inflammatory cerebrospinal fluid analysis in cats: Clinical diagnosis and outcome. *J Fel Med Surg.* 2005;7(2):77–93.
18. Tsai HY, Ling-Ling C, Chao-Nan L, Bi-Ling S. Clinicopathological findings and disease staging of feline infectious peritonitis: 51 cases from 2003 to 2009 in Taiwan. *J Feline Med Surg.* 2010;13:74-80.
19. Wise AG, Kiupel M, Maes RK. Molecular characterization of a novel coronavirus associated with epizootic catarrhal enteritis (ECE) in ferrets. *Virology.* 2006;349:164–174.

**CASE III:** 2013910414 (JPC 4048844).

**Signalment:** 11-year, 8-month-old male Papillon, dog (*Canis familiaris*).

**History:** The dog had been bitten on the left femoral skin, and a 12 x 16 mm dermal mass formed at first in the region. The mass was covered with crust. On fine needle aspiration, only lipocytes were found. He was fitted with an Elizabethan collar to prevent self-trauma and was topically treated with antibiotics and steroids with no clinical improvement. The mass increased in size for two years.

**Gross Pathology:** The masses were arranged in a pattern resembling a horse's hoof, and some masses were ulcerated.

**Laboratory Results:** None

**Histopathologic Description:** The multiple variably sized masses are present in the dermis and subcutis, with multiple small masses around large masses. Various-sized swollen peripheral nerve fascicles are observed in each mass, with perineurial hyperplasia. In the large mass, perineurial hyperplasia and fibrosis is more remarkable. Swollen nerve fascicles in each mass consist of thin, unmyelinated nerves with hypertrophic Schwann cells and a thickened perineurium.
Immunohistochemically, nerve fascicles include neurofilament-positive axons with GFAP-positive Schwann cells. Hyperplastic perineurium is positive for type 4 collagen and nerve growth factor receptor (NGFR). Small nerve fibers, which are positive for GFAP and PGP9.5, are included in hyperplastic perineurium. These lesions show no significant proliferative activity based on Ki-67 staining.

**Contributor's Morphologic Diagnosis:** Skin: Multiple traumatic neuroma with swollen nerve fascicles and perineurial hyperplasia.

**Contributor's Comment:** The present case was characterized by swollen peripheral nerve fascicles with perineurial hyperplasia and fibrosis. Each nerve fascicle consisted of thin to unmyelinated nerve fibers, including axons and Schwann cells. Axons in swollen nerve fascicles and hyperplastic perineurium had Schwann cells as well as normal nerve fibers, suggesting a non-neoplastic lesion. The lack of proliferative activity also indicated that our case was non-neoplastic. The histological features resembled traumatic neuroma except swollen large-sized nerve fascicles and perineurial hyperplasia. Perineurial hyperplasia and fibrosis were observed in Morton's neuroma, which is one subtype of traumatic neuroma in humans. With clinical findings and histological features, it was suggested that peripheral nerves of affected area were the result of self-inflicted injury. Thus, the present case was diagnosed as unique subtype of traumatic neuroma.

Traumatic neuroma is a reactive and non-neoplastic proliferative nerve disease to injury or surgery at the proximal end of an injured peripheral nerve.[6,16] In the dog, it has been reported following tail docking.[7] Microscopically, small nerve fascicles including axons with their investiture of myelin, Schwann cells, and fibroblasts proliferate with abundant fibrous stroma.[16] Many axons were seen in a parallel distribution within fascicles.[4] Ascertaining the presence of axons by immunohistochemical examination is useful in distinguishing "non-neoplastic" neuroma from neoplasms such as Schwanoma and neurofibroma.[2]

Morton's neuroma (localized interdigital neuritis) is not a true tumor and one subtype of traumatic neuroma caused by chronic or repeated mild trauma to the region. The lesion is commonly seen in the interdigital plantar nerve of third and fourth toes in women.[13,16] Histologically, proliferative changes characterize traumatic neuromas, whereas degenerative changes are the hallmark of Morton's neuroma. As the lesion progresses, the fibrosis becomes marked and envelops the epineurium and perineurium in a concentric fashion and even extends into the surrounding tissue.[8,16] Similarly, when hands are injured due to vibration from hand held power tools, demyelination and perineurial and endoneural fibrosis can develop in the nerves in fingers and wrists.[14]

The present case needs to be differentiated from a neoplasm because the histological features of hyperplastic perineurium with fibrosis are similar to Schwannoma, neurofibroma and perineurioma. Schwannoma or neurofibroma with plexiform pattern most closely resembled the present case.[13,16] With continued growth in these tumors, the

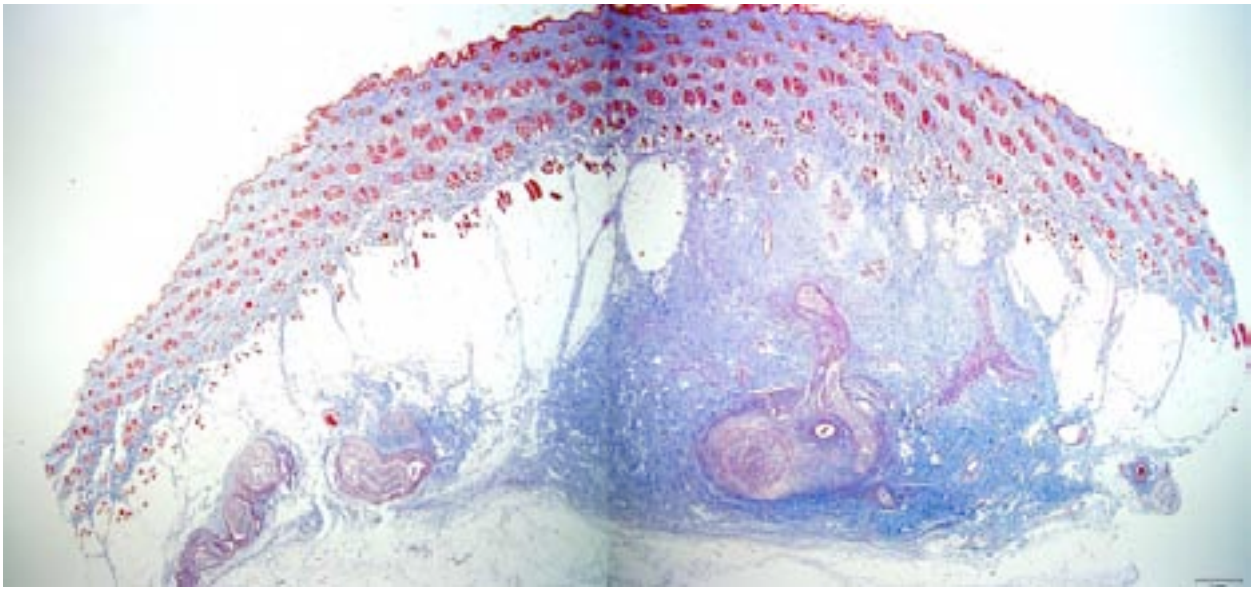

*3-1. Haired skin, dog: This tiled image shows the extent of a neuroma that arose over two years following a dog bite at the site. The mass is composed of clusters of large caliber nerve fibers surrounded by fibrous connective tissue. (Masson's Trichrome, 0.3X) (Photo courtesy of: Department of Pathology, Faculty of Pharmaceutical Sciences, Setsunan University, 45-1 Nagaotohge-cho, Hirakata, Osaka 573-0101, Japan. http://www.setsunan.ac.jp/~p-byori/)*

fascicular components infiltrate surrounding soft tissue. The pathological features are similar to the present case at first. Schwannoma is composed of mainly Schwann cells with characteristic patterns and containing few axons. Neurofibroma consists of a mixture of Schwann cells, axons and fibroblasts, and the number of axons is very low.[13,15] Perineuroma has multiple forms: intraneural, extraneural, sclerosing, reticular, and hybrid features with neurofibroma or schwannoma.[16] Intraneural perineurioma is composed of concentric layers of perineurial cells ensheathing an axon and Schwann cell. Extraneural perineurioma is an extremely elongated spindle cell lesion arranged in parallel bundles. In the present case, perineurial cells do not proliferate inside nerve fascicles, but increase in the margin of nerve fascicles, which is a normal site. Additionally, many nerve fibers randomly proliferate in hyperplastic perineurium.

Human perineurial cells are immunoreactive for epithelial membrane antigen (EMA), but negative for S-100.[4,11,13,16,17] GFAP and S100 commonly stain Schwann cells. Thus, immunostaining for these proteins is always used to distinguish between perineurial cell and Schwann cells. However, in canine perineurioma, the tumor cells are negative for EMA.[10] The basement membrane between perineurial cells are positive for type 4 collagen and laminin.[16] Additionally, positive staining for type 4 collagen and NGFR can help identify nerve origin.[3,4] Thus, our results indicate that immunohistochemistry for type 4 collagen and NGFR might be useful for identifying perineurial cells of the dog.

**JPC Diagnosis:** Haired skin: Neuroma.

**Conference Comment:** This case provides an interesting diagnostic exercise in distinguishing neoplastic from non-neoplastic proliferative peripheral nerve lesions. Neuroma is a well-known entity, which has been described in the literature for over 50 years.[15] Its name perhaps inappropriately implies neoplasia, as the contributor previously discusses.

Neuroma development following trauma, most commonly observed subsequently to tail-docking or digital neurectomy in horses, is presumed to arise when the normal regenerative growth of a disrupted nerve fiber encounters a physical obstruction such as scar tissue.[7] This results in a haphazard arrangement of axons and disorganized microfascicular architecture, observed in this case as numerous Schwann cells and few axons haphazardly arranged and surrounded by a variably thick fibrotic perineurium.

The classification of a non-neoplastic lesion implies the proliferating cell population still

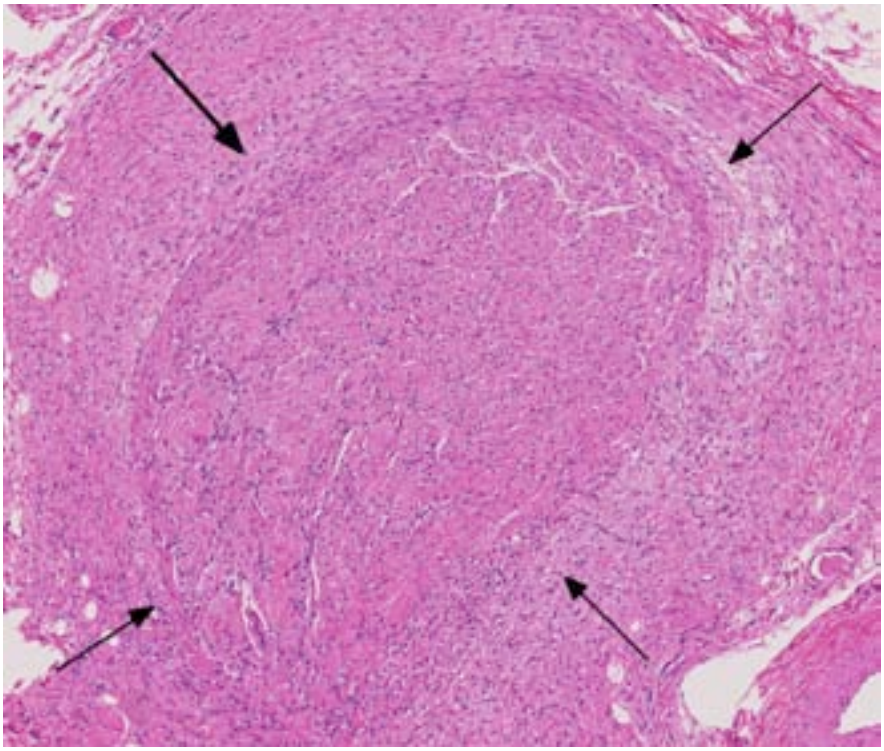

*3-2. Haired skin, dog: Proliferating nerve bundles are surrounded by a markedly thickened perineurium. (HE 61X)*

possesses control over its growth cycle and/or stability of its genome. This is an opportunity for the reader to review the hallmarks of neoplasia and independently consider whether any of these may apply in this case. The following six hallmarks are acquired in succession and lead to cells becoming neoplastic and eventually malignant: sustained proliferative signaling, evasion of growth suppressors, resisting cell death, enabling replicative immortality, induction of angiogenesis and the activation of invasion and/or metastasis. Recently, two further hallmarks have been added: the reprogramming of energy metabolism and evasion of the immune response. Two characteristics described as crucial to the acquisition of these hallmarks are genomic instability and tumor-promoting inflammation. When mutations are permanently acquired in the genome, the cell may develop a selective advantage that enables its outgrowth and eventual dominance in the local environment that may be fueled by growth and survival factors supplied by secondary inflammatory cells.[9]

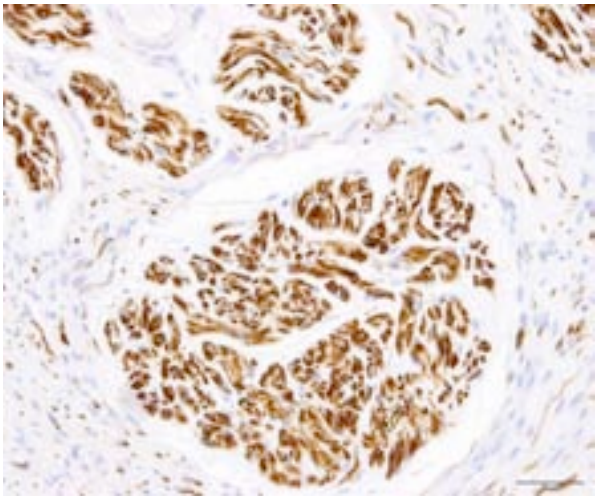

*3-3. Haired skin, dog: Nerve fibers demonstrate strong intracytoplasmic immunostaining for anti-glial fibrillary acidic protein. (GFAP 100X)*

Conference participants reviewed the most common neural tumors of domestic animals. Schwannomas, which originate from a single nerve and extend in conjunction with but external to it, facilitates its involvement with plexus arrangements such as the brachial plexus and other common sites including the heart base, spinal nerve roots and the tongue.[12] Neurofibromatosis is a well-recognized variant of Schwannomas observed in cattle in which multiple sites are involved. Peripheral nerve sheath tumors are of controversial origin, but often found on the distal limbs of dogs and graded according to soft tissue sarcoma criteria.[5] Ganglioneuromas are rare tumors reported in many species and are composed of ganglion and glial cells. Ganglioneuroblastomas are similar but are composed of poorly differentiated ganglion cells with more atypia.[12]

**Contributing Institution:** Department of Pathology, Faculty of Pharmaceutical Sciences, Setsunan University, 45-1 Nagaotohge-cho, Hirakata, Osaka 573-0101, Japan
http://www.setsunan.ac.jp/~p-byori/

**References:**

1. Antunes SL, Chimelli L, Jardim MR, et al. Histopathological examination of nerve samples from pure neural leprosy patients: Obtaining maximum information to improve diagnostic efficiency. *Mem Inst Oswaldo Cruz*. 2012;107(2): 246-253.

2. Arishima H, Takeuchi H, Tsunetoshi K, Kodera T, Kitai R, Kikuta K. Intraoperative and pathological findings of intramedullary amputation neuroma associated with spinal ependymoma. *Brain Tumor Pathol*. 2013;30:196-200.

3. Chijiwa K, Uchida K, Tateyama S. Immunohistochemical evaluation of canine peripheral nerve sheath tumors and other soft tissue sarcomas. *Vet Pathol.* 2004;41:307-318.

4. Chrysomali E, Papanicolaou SI, Dekker NP, Regezi JA. Benign neural tumors of the oral cavity: a comparative immunohistochemical study. *Oral Surg Oral Med Oral Pathol Oral Radiol Endod*. 1997;84:381-390.

5. Dennis MM, McSporran KD, Bacon NJ, Schulman FY, Foster RA, Powers BE. Prognostic factors for cutaneous and subcutaneous soft tissue sarcomas in dogs. *Vet Pathol.* 2011;48(1):73-84.

6. Ginn PE, Mansell JL, Rakich PM. Neoplastic and reactive disease of the skin and mammary glands. In: *Jubb & Kennedy Pathology of Domestic Animals*. Vol. 1. St Louis, MO: Sanders Elserver; 2006:761-767.

7. Gross TL, Carr SH. Amputation neuroma of docked tails in dogs. *Vet Pathol*. 1990;27:61-62.

8. Guiloff RJ, Scadding JW, Klenerman L. Morton's metatarsalgia. Clinical, electrophysiological and histological observations. *J Bone Joint Surg Br.* 1984;66:586-591.

9. Hanahan D, Weinberg RA. Hallmarks of cancer: the next generation. *Cell*. 2011;144:646-674.

10. Higgins RJ, Dickinson PJ, Jimenez DF, Bollen AW, Lecouteur RA. Canine intraneural perineurioma. *Vet Pathol*. 2006;43:50-54.

11. Hirose T, Tani T, Shimada T, Ishizawa K, Shimada S, Sano T. Immunohistochemical demonstration of EMA/Glut1-positive perineurial cells and CD34-positive fibroblastic cells in peripheral nerve sheath tumors. *Mod Pathol.* 2003;16:293-298.

12. Maxie MG, Youssef S. Nervous system. In: *Jubb & Kennedy Pathology of Domestic Animals*. Vol. 1. St Louis, MO: Sanders Elsevier; 2006:455.

13. Rosai J. Tumors and tumor-like conditions of peripheral nerves. In: *Rosai and Ackerman's Surgical Pathology*. St. Louis, MO: Elsevier Mosby; 2004:2263-2271.

14. Stromberg T, Dahlin LB, Brun A, Lundborg G. Structural nerve changes at wrist level in workers exposed to vibration. *Occup Environ Med*. 1997;54:307-311.

15. Swanson HH. Traumatic neuromas: a review of the literature. *Oral Surg Oral Med Oral Pathol.* 1961;14:317-326.

16. Weiss SW, Goldblum GJ. Benign tumors of peripheral nerves. In: *Enzinger and Weiss's Soft Tissue Tumors*. St. Louis, MO: Mosby; 2013:784-854.

17. Yamaguchi U, Hasegawa T, Hirose T, et al. Sclerosing perineurioma: a clinicopathological study of five cases and diagnostic utility of immunohistochemical staining for GLUT1. *Virchows Arch*. 2003;443:159-163.

**CASE IV:** 07N1149 (JPC 3100109).

**Signalment:** Neonate female American Quarter horse, *Equus caballus.*

**History:** The foal gasped at birth then stopped breathing. The foal was dead on arrival to the University of California, Davis Veterinary Medical Teaching Hospital. Intubation was unsuccessful.

**Gross Pathological Findings:** The mucous membranes of the oral cavity were diffusely tinged blue (cyanosis). Approximately 20% of the pulmonary parenchyma was aerated and the remaining lung tissue was atelectic (fetal atelectasis). Foci of epicardial hemorrhages were present on the right ventricle, adjacent to the atrio-ventricular junction. Pinpoint hemorrhages were scattered throughout the thymus and on the mucosal surface of the esophagus.

**Histopathologic Description:** Skeletal muscle (diaphragm, semitendinosis): Within numerous swollen myofibers are discrete glassy to compact granular, lightly basophilic, oval to variably shaped and sized inclusion bodies that are up to approximately 50 µm in length. The inclusions disrupt and/or replace the normal cytoplasmic myofibril architecture.

Heart: Intracytoplasmic inclusions, similar to those previously described, are within numerous variably swollen and disrupted myocytes.

Brainstem: A few to moderate numbers of large neuronal cell bodies contain intracytoplasmic inclusion bodies, similar to those previously described.

**Contributor's Morphologic Diagnoses:** 1. Heart, Skeletal muscle (diaphragm, intercostal, thigh): Severe multifocal myofiber degeneration with intracytoplasmic inclusions.
2. Brainstem: Moderate neuronal degeneration with intracytoplasmic inclusions.

**Laboratory Results:** Period acid-Schiff staining of formalin-fixed, paraffin-embedded tissues collected at the time of necropsy, sectioned at 5 µm, show intensely PAS-positive, large intracytoplasmic inclusions within swollen skeletal muscle fibers (tongue, diaphragm, intercostal, semitendinosis, quadricep), in cardiac myocytes, and within large neuronal cell bodies in the brainstem.

Genotyping was performed at the Veterinary Genetics Laboratory at the University of California, Davis. DNA used for analysis was isolated from formalin fixed paraffin embedded skeletal muscle tissue. Analysis showed the foal to be homozygous for the single nucleotide polymorphism responsible for glycogen branching enzyme deficiency.

Transmission electron microscopy was performed on formalin fixed skeletal muscle and brainstem at the California Animal Health and Food Safety Laboratory, Davis Branch. Transmission electron

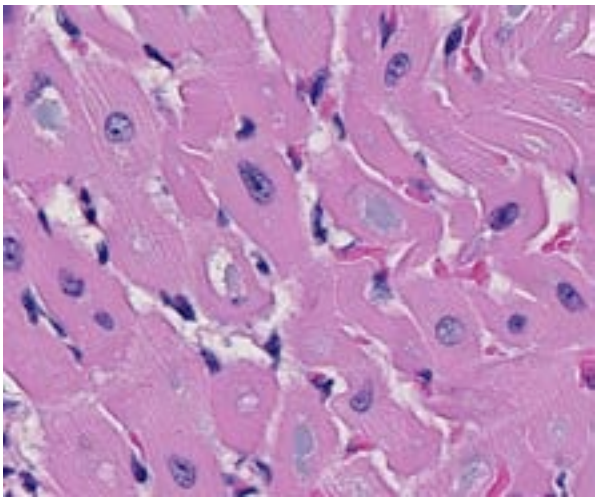

*4-1. Heart, foal: Cardiomyocytes contain one or multiple amphophilic cytoplasmic inclusions. (HE 400X)*

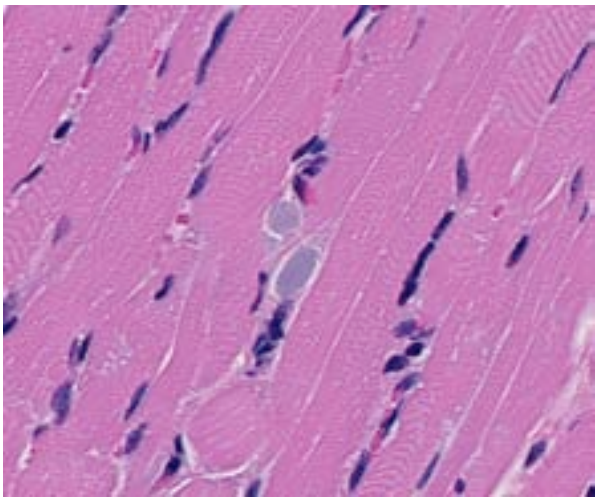

*4-2. Skeletal muscle, foal: Rhabdomyocytes contain one or multiple amphophilic cytoplasmic inclusions. (HE 400X)*

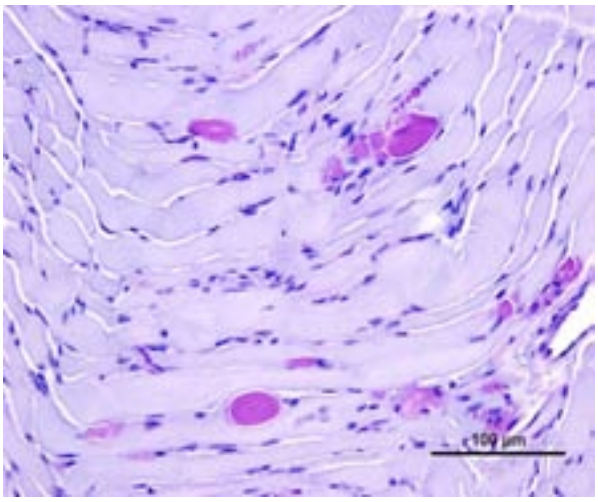

*4-3. Skeletal muscle, foal: PAS-positive inclusions displace myofibrils within swollen muscle fibers. (PAS 200X) (Photo courtesy of: University of California, Davis, Veterinary Medical Teaching Hospital, VM3A, Anatomic Pathology, One Shields Avenue, Davis, CA 95616 http://www.vetmed.ucdavis.edu/pmi/)*

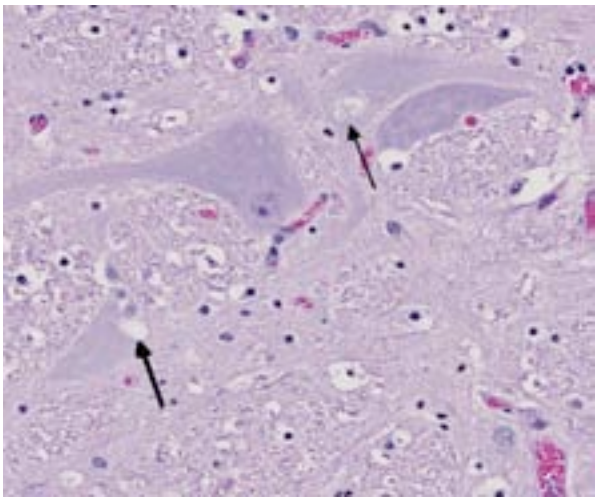

*4-4. Brainstem, foal: Brainstem neurons contain multifocal intracytoplasmic inclusions. (HE 400X)*

microscopy revealed large electron dense filamentous to granular inclusions in degenerate skeletal muscle fibers. Similar inclusions are seen within degenerate neuronal cell bodies within the brainstem.

**Contributor's Comment:** Glycogen branching enzyme deficiency, or glycogen storage disease IV, is a fatal hereditary condition that occurs in American Quarter horse and American Paint horse lineages. The inheritance pattern is autosomal recessive. The genetic mutation responsible for this disease has been identified in the glycogen branching enzyme 1 gene (*GBE*1) as a cytosine to adenosine substitution at base 102 that results in a tyrosine to stop mutation in codon 34 of exon 1.[7] Homozygous foals are either stillborn, die shortly after birth, or are euthanized within the first few months of life due to worsening clinical signs. Clinical signs vary and may include progressive muscle weakness, hypoglycemic seizures, respiratory failure, or sudden death. A study performed to assess the carrier frequency of this allelic mutation in populations of Quarter horses and Paint horses estimated that 8.3% of Quarter horses and 7.1 % of Paint horses are heterozygous for the mutated form of *GBE*1.[4]

Normal glycogen is present in the cytosol in the form of small electron dense granules that range in diameter from 10 to 40 nm and are comprised of glucose molecules that have α 1, 4 linkages between glucose residues and α 1, 6 glycosidic bonds at every 10$^{th}$ residue that create a branched polymer.[3] Branching of the polymer increases water solubility and provides a larger number of terminal residues which are the sites for enzymatic action of glycogen phosphorylase and glycogen synthase; enzymes that are responsible for glycogen degradation and synthesis, respectively. While glycogen synthase catalyzes the synthesis of α-1, 4 linkages between glucose residues, glycogen branching enzyme is responsible for the formation of the α 1, 6 glycosidic bonds that create the branched form of the glucose polymer, glycogen. Animals born deficient of this enzyme form non-branching, PAS-positive, diastase-resistant glucose polymers that form large aggregates within the cytoplasm of various tissues including skeletal muscle, brain, spinal cord, heart, liver. Glucose polymers that have only α -1, 4 linkages between glucose residues or those having few α-1, 6 glycosidic bonds (1 per 30 glucose residues) are amylose and amylopectin, respectively.[3] Amylose and amylopectin are starches that serve as nutritional reservoirs for plants and are not normal storage forms of glucose in mammalian species. Glycogen branching enzyme deficiency (equine glycogen storage disease IV) has previously been termed "amylopectinosis" prior to identification of the genetic mutation responsible for this disease.[2] Also, prior to discovering the genetic mutation and inheritance pattern, Valberg, et al. reported that glycogen branching enzymatic activity was virtually absent in affected foals and that some of the half-siblings of the affected foals

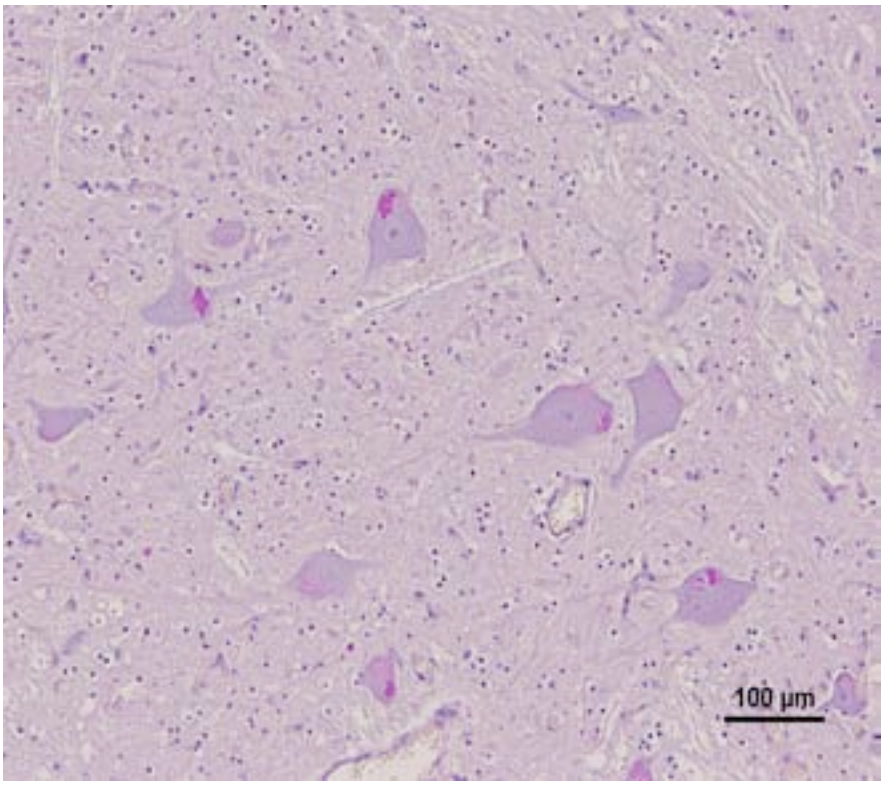


*4-5. Brainstem foal: Brainstem inclusions are also PAS-positive. (PAS 200X) (Photo courtesy of: University of California, Davis, Veterinary Medical Teaching Hospital, VM3A, Anatomic Pathology, One Shields Avenue, Davis, CA 95616 http://www.vetmed.ucdavis.edu/pmi/)*

had an approximately 50% decrease in GBE activity.[6]

The breed of the foal (Quarter horse) and the character and staining properties of the numerous intracytoplasmic inclusions seen within all examined skeletal muscles, heart, and brainstem were consistent with glycogen branching enzyme deficiency, also referred to as glycogen storage disease IV. This diagnosis was confirmed by genotype analysis. The hemorrhages seen in multiple organs are considered agonal. The partial aeration of the lung parenchyma may have occurred during attempts at resuscitation or at the time of parturition when the foal was reported to have gasped for air prior to ceasing to breathe.

**JPC Diagnosis:** 1. Skeletal muscle: Glycogen-like inclusions, intrasarcoplasmic, many, with multifocal mild rhabdomyocyte degeneration.
2. Cardiac muscle: Glycogen-like inclusions, intrasarcoplasmic, many.
3. Brainstem, gray matter, neurons: Glycogen-like inclusions, intracytoplasmic, rare.

**Conference Comment:** The contributor adeptly describes the pathogenesis behind the defect in glycogen metabolism and formation of inclusions in this important entity of American quarter and paint horses as well as Norwegian forest cats. Glycogen is a crucial source of energy stored in myocytes and in variable amounts within hepatocytes. When glucose is found in excess, it is converted into glycogen and stored in hepatocytes, thus glycogen concentration within the liver is highest shortly after eating, or in animals with abnormal glucose metabolism such as those with diabetes. Renal tubular epithelial cells and B-cells of the islets of Langerhans also can convert glucose to glycogen, resulting in intracellular accumulation in diabetics.[1]

Glycogen is demonstrated histologically using the PAS reaction on two serial sections. Pretreatment of one section with diastase enables its comparison between the intensity of magenta staining of the two sections to determine whether glycogen is present. If glycogen is present, diastase will digest it and remove it from the tissue (diastase-sensitive), thus removing the magenta color. The inclusions in this case are diastase-resistant because, as the contributor describes, the deficient glycogen branching enzyme (GBE) is necessary to form the glycosidic bonds between glucose molecules, creating the branching polymer glycogen. This is in contrast to other glycogen storage diseases such as type I and III which involve deficiencies in the conversion of glycogen to glucose, thus resulting in excess accumulation of glycogen.[1] All types of glycogen storage diseases are characterized by defects in the glycogen metabolic pathway and ultimately result in the failure of adequate utilization of energy resources leading to generalized muscle weakness or death.

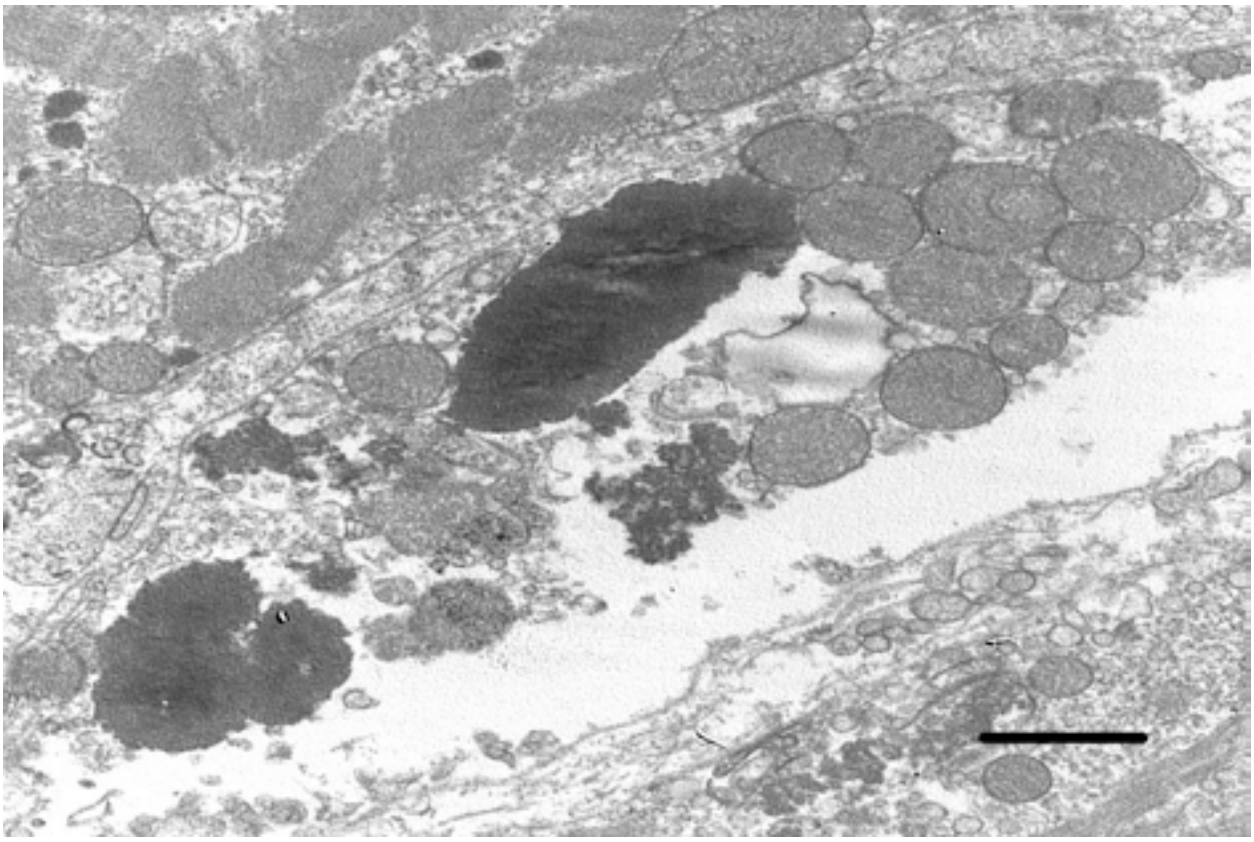

*4-6. Skeletal muscle, foal: Transmission electron micrograph of formalin fixed skeletal muscle showing large electron dense intracytoplasmic inclusions within a degenerate skeletal muscle fiber. Bar = 1 µm (Photo courtesy of: University of California, Davis, Veterinary Medical Teaching Hospital, VM3A, Anatomic Pathology, One Shields Avenue, Davis, CA 95616 http://www.vetmed.ucdavis.edu/pmi/).*

Another storage myopathy commonly recognized in the American Quarter horse, though reported in many other breeds, is equine polysaccharide storage myopathy. A definitive abnormality of the glycolytic or glycogenolytic pathway has not yet been identified for this entity, although a point mutation in skeletal muscle glycogen synthase I (GYS1) gene has been associated with some cases. This disease results in the accumulation of intracytoplasmic glycogen within type 2 fibers, which can become amylase-resistant inclusions as the glycogen becomes ubiquitinated in chronic cases. Episodes of exertional rhabdomyolysis is often associated with this condition.[5]

A second major group of storage diseases worthy of mention in domestic animals are those of lysosomes, characterized by a deficiency of lysosomal acid hydrolases leading to the excess accumulation of insoluble metabolites within lysosomes. For a case example and in-depth discussion of the numerous types of lysosomal storage diseases, we refer the reader to WSC 2013 (conference 5, case 2).

**Contributing Institution:** University of California, Davis
Veterinary Medical Teaching Hospital, VM3A, Anatomic Pathology
One Shields Avenue
Davis, CA 95616
http://www.vetmed.ucdavis.edu/pmi/

**References:**

1. Myers RK, McGavin MD, Zachary JF. Cellular adaptations, injury and death: Morphologic, biochemical, and genetic bases. In: Zachary JF, McGavin MD, eds. *Pathologic Basis of Veterinary Disease*. 5th edition. St. Louis, MO: Elsevier Mosby; 2012:35,54-55.
2. Render JA, et al. Amylopectinosis in a fetal and neonatal Quarter horse. *Vet Pathol*. 1999;36:157-160.
3. Stryer L. *Biochemistry*. 4th edition. New York: WH Freeman and Company; 1995:472-473, 581-588.
4. Valberg SJ, et al. Glycogen branching enzyme deficiency in Quarter horse foals. *J Vet Intern Med.* 2001;15:572- 580.

5. Valentine BA, McGavin MD. Skeletal muscle. In: Zachary JF, McGavin MD, eds. *Pathologic Basis of Veterinary Disease*. 5th edition. St. Louis, MO: Elsevier Mosby; 2012:902-904.
6. Wagner ML, et al. Allele frequency and likely impact of the glycogen branching enzyme deficiency gene in Quarter horse and Paint horse populations. *J Vet Intern Med* 2006;20:1207-1211.
7. Ward TL, et al. Glycogen branching enzyme (*GBE1*) mutation causing equine glycogen storage disease IV. *Mamm Genome* 2004;15:570-577.

**Joint Pathology Center**
**Veterinary Pathology Services**

*Conference Coordinator*
**Matthew C. Reed, DVM**
**Captain, Veterinary Corps, U.S. Army**
**Veterinary Pathology Services**
**Joint Pathology Center**

## WEDNESDAY SLIDE CONFERENCE 2014-2015

# Conference 2

**10 September 2014**

**Conference Moderator:**
Cary Honnold, DVM, Diplomate ACVP, ACVPM
Deputy Director, WRAIR Veterinary Service Program
Walter Reed Army Institute of Research
Forest Glen Annex
2460 Linden Lane
Silver Spring, MD 20910

**CASE I:** 11857 (JPC 4033346).

**Signalment:** 5-month-old male crossbreed calf (*Bos taurus*).

**History:** This was one of 38 calves with ages varying from 1-6 months out of a herd of 78. The affected animal was acutely dyspneic and febrile. Additionally, it showed lethargy, tremors, bruxism, open mouth breathing, dehydration, rapid and noisy breathing, coughing, serous or mucopurulent nasal discharge, recumbency and finally, death.

**Gross Pathology:** There were areas of consolidation, edema and emphysema in cranioventral regions of the apical and cardiac

*1-1. Presentation, calf: This calf was acutely dyspneic and febrile and demonstrated open mouth breathing with a serous nasal discharge. (Photo courtesy of: Animal Pathology Department / Veterinary Diagnostic Laboratory, Veterinary Faculty; Federal University of Pelotas. 96010-900 Pelotas, RS, Brazil. http://www.ufpel.edu.br/fvet/oncovet/; http://www.ufpel.edu.br/fvet/lrd/)*

*1-2. Lung, calf: The cranioventral lungs have multifocal to coalescing depressed areas of red-brown consolidation with edema, which were rubbery and firm. (Photo courtesy of: Animal Pathology Department / Veterinary Diagnostic Laboratory, Veterinary Faculty; Federal University of Pelotas. 96010-900 Pelotas, RS, Brazil. http://www.ufpel.edu.br/fvet/oncovet/; http://www.ufpel.edu.br/fvet/lrd/)*

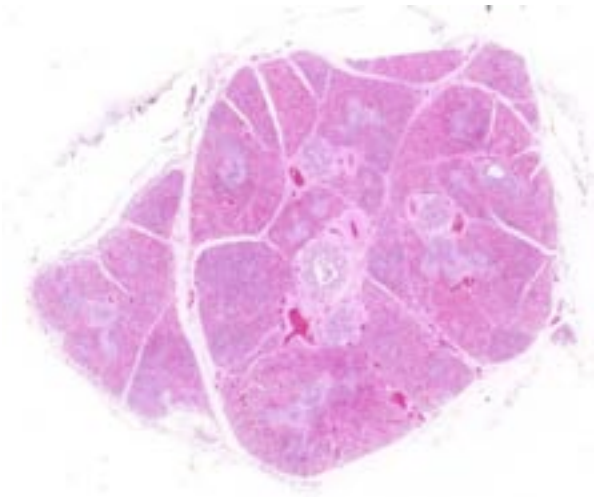

*1-3. Lung, calf: At subgross examination airways are pale and architecture is distorted (necrosis). The parenchyma is markedly congested and interlobular septa and pleural connective tissue is expanded by edema and emphysema. (0.63X)*

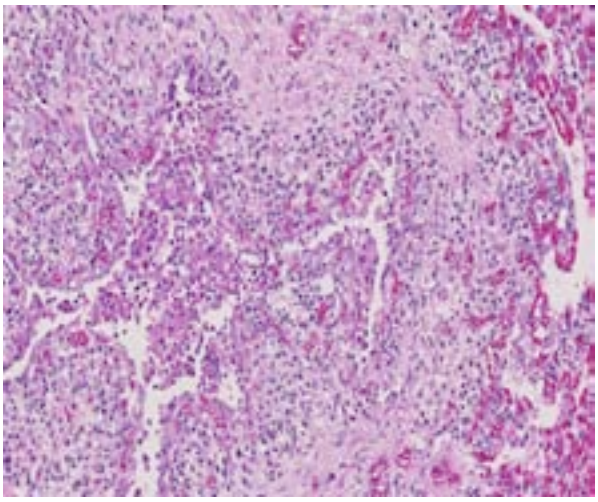

*1-4. Lung, calf: Bronchiolar epithelium is necrotic or attenuated, and the lumen contains numerous neutrophils and macrophages admixed with cellular debris. Numerous histiocytes and fewer neutrophils, lymphocytes, and plasma cells expand the submucosa. (HE 144X)*

lung lobes, which were red-brown and rubbery to firm.

**Laboratory Results:** Immunohistochemistry was positive for BRSV (polyclonal anti−BRSV, VMRD Inc., Pullman, WA) and negative for parainfluenza type−3 virus (VMRD Inc., Pullman, WA). No bacterial growth on microbiological cultures.

**Histopathologic Description:** Bronchiolar lumens contain a copious quantity of necrotic epithelial cells and neutrophils. Some lymphocytes and plasma cells encircle bronchioles and blood vessels. Mononuclear cells also thicken alveolar septa. Alveoli contain numerous neutrophils and macrophages and eventually some fibrin. Syncytial cells are prominent and appear as multinucleate cells closely associated with the bronchiolar epithelium, and in the alveoli. Some proliferation of type II pneumocytes appears as scattered tombstone-like cells or complete cuboidal epithelialization of the alveoli.

**Contributor's Morphologic Diagnosis:** Lung: Bronchiolitis, necrotizing and pneumonia bronchointerstitial, suppurative, subacute, multifocal, moderate, with marked hyperplasia of type II pneumocytes and epithelial syncytia, crossbreed, bovine.

**Contributor's Comment:** The bovine respiratory disease (BRD) pneumonias constitute a significant proportion of feedlot diseases. Bovine herpesvirus-1 (BHV-1) (infectious bovine rhinotracheitis virus); parainfluenza virus-3 (PI-3); and bovine respiratory syncytial virus (BRSV) are recognized as primary respiratory pathogens.[7] Bovine viral diarrhea virus 1 and 2 [BVDV-1–2], bovine adenovirus A–D [BAdV-A–D], and bovine coronavirus [BCoV]), bacteria (*Mannheimia haemolytica, Pasteurella multocida*, and *Histophilus somni*), and *Mycoplasma* spp. have also been recognized as additional agents associated with severe BRD.[5,7]

Among those etiologic agents, bovine respiratory syncytial virus (BRSV) seems to be a major contributor to the bovine respiratory disease of BRD complex.[2] This virus belongs to the *Pneumovirus* genus within the subfamily *Pneumovirinae*, family *Paramyxoviridae*, and is an enveloped, non-segmented, negative-stranded RNA.[8] By electron microscopy, the morphology of the RSV virions appears to be either very pleomorphic, with a shape roughly rounded and a diameter between 150 and 35 nm, or filamentous with a length that can reach 5µm and a diameter between 60 and 100 nm.[10]

The bovine respiratory syncytial virus (BRSV) has been recognized as a pathogen in cattle responsible of an acute respiratory disease syndrome in beef and dairy calves since the early 1970s. The impact of BRSV infection on the cattle industry results in economic losses due to the morbidity, mortality, treatment and prevention

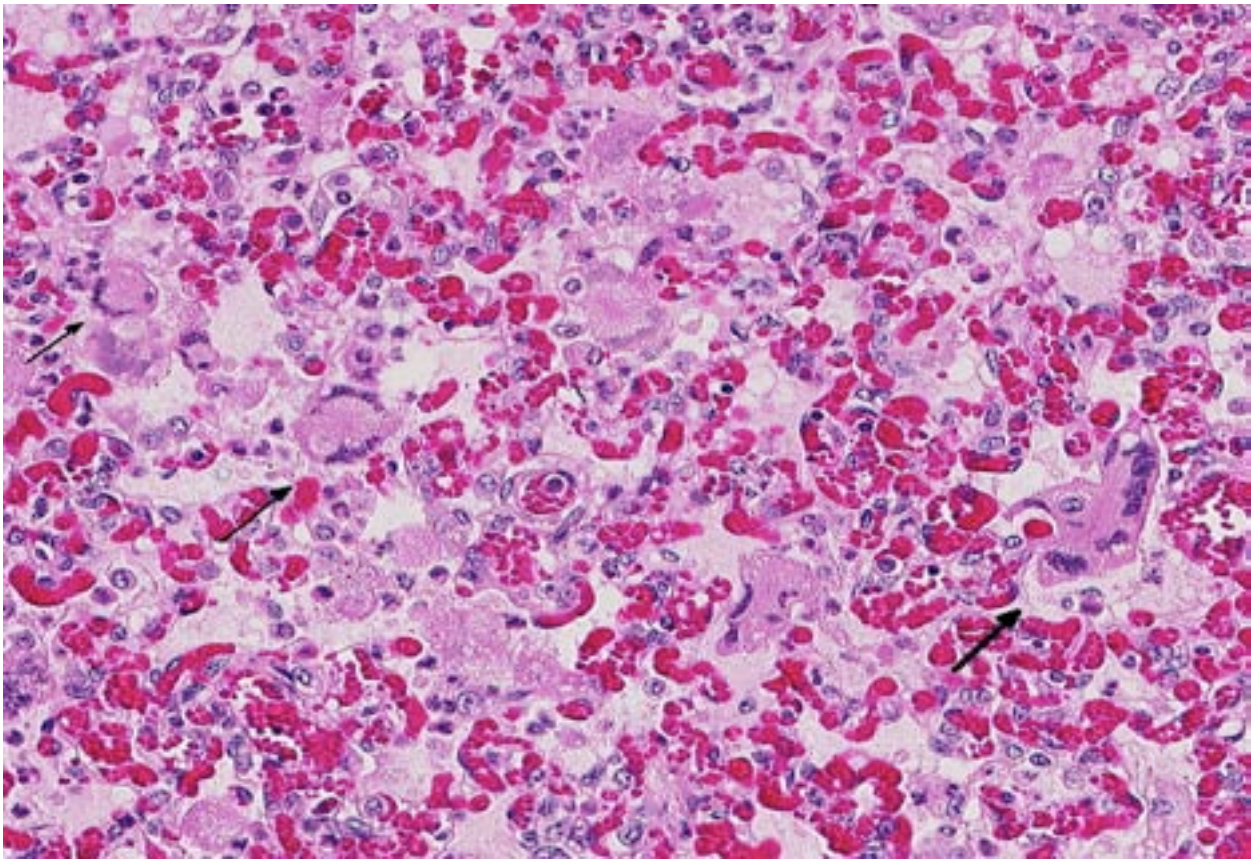

*1-5. Lung, calf: Multifocally, alveolar spaces contain large multinucleated viral syncytia characteristic of bovine respiratory syncytial virus (BRSV). (HE 224X)*

costs that eventually lead to loss of production and reduced carcass value.[8] BRSV causes acute outbreaks of respiratory disease in 2-week to 5-month-old dairy and beef calves. This virus could also predispose to bacterial pneumonia in feedlot beef cattle and occasionally cause respiratory disease in naive adult dairy cows.[3]

The virus replicates predominantly in ciliated respiratory epithelial cells but also in type II pneumocytes. It appears to cause little or no cytopathology in ciliated epithelial cell cultures in vitro, suggesting that much of the pathology is due to the host's response to virus infection. RSV infection induces an array of pro-inflammatory chemokines and cytokines that recruit neutrophils, macrophages and lymphocytes to the respiratory tract resulting in respiratory disease.[10]

Microscopic lesions in BRSV infections consist of bronchointerstitial pneumonia, characterized by necrotizing bronchiolitis, formation of bronchiolar epithelial syncytia, and exudative or proliferative alveolitis. The subacute lesions of BRSV represent early repair of the previous lesions and additional lymphocyte-mediated lysis of virus infected cells. Bronchiolitis obliterans may occur as early as 10 days after infection.[2,4]

**JPC Diagnosis:** Lung: Bronchointerstitial pneumonia, necrotizing and suppurative, diffuse, with rare multinucleated viral syncytia.

**Conference Comment:** This is an excellent example of bovine respiratory syncytial virus (BRSV) infection, containing all the pertinent histologic features as dutifully described above by the contributor. There is some slide variation in terms of the numbers of viral syncytia contained within several sections. Additionally, the presence of suppurative inflammation led many to speculate on the additional presence of one of the many secondary bacterial pathogens associated with this entity.

BRSV is one of many components of the commonly described bovine respiratory disease complex (BRDC), a pathologically complex and economically important disease which costs the

U.S. cattle industry up to $1 billion per year.[8] While complex in its pathogenesis, the disease is ultimately a manifestation of the stress which cattle experience during weaning, processing, shipping and commingling. For this reason, it is logical that clinical signs of BRDC generally occur 7-10 days following this series of events resulting in the leading cause of morbidity and mortality in U.S. feedlots.[8]

BRSV is the largest player in the BRDC, with seroconversion estimates in some geographic areas of over 70% in calves under 12 months old.[8] With the addition of the aforementioned primary viral pathogens and the bacterial pathogens *Mannheimia haemolytica, Bibersteinia trehalosi, Histophilus somni, Pasteurella multocida, Mycoplasma bovis* and *Trueperella pyogenes*, assigning a specific etiologic diagnosis to gross or histopathologic lesions can prove to be an arduous task for the aspiring pathologist. Conference participants compared and contrasted the gross pathology of two other readily identifiable bacterial pathogens - *M. haemolytica* was described as resembling a "brush fire" histologically due to the "advancing front of coagulative necrosis" caused by bacterial toxins, while lesions of *M. bovis* often appear as "golf balls" due to its predilection for causing suppurative bronchiolitis with bronchiectasis.

A recent study compared the susceptibility of bovine airway epithelial cells to three different respiratory pathogens associated with the BRDC, with the differences between them perhaps due to direct correlation to the variation in disease manifestation. PI-3 readily entered the apical membrane of ciliated epithelial cells. These cells were largely resistant to BHV-1; however, when tight junctions were opened or the epithelial monolayer was damaged, BHV-1 infected basal cells. BRSV, in contrast, was unable to infect either epithelial or basal cells; however, the submucosal cells were susceptible though not specifically identified. The results led the authors to speculate on how BHV-1 and BRSV are able to cross the epithelial barrier as is apparently necessary to incite infection, even suggesting such bacterial pathogens as *M. haemolytica* are actually primary initiators.[6] This is in contrast with well-established data elsewhere of reduced ciliary clearance by epithelial degeneration and necrosis as a result of BRSV infections leading to secondary bacterial invasion.[3]

In large part thanks to its human relative, RSV, much has been described in regard to the immunopathogenic mechanisms of BRSV. The nonstructural proteins of RSV, NS1 and NS2, are instrumental in mediating resistance to IFN-stimulated responses, specifically by blocking phosphorylation and activation of IRF-3.[8] This interruption of the MyD88-independent pathway, which occurs exclusively through TLR 3 or TLR 4 signaling, reduces activated interferon thus limiting the innate immune response. While TLR 3 recognition of double-stranded, viral RNA utilizes only MyD88-independent signaling,[1] TLR 4 has the additional option of mediating NF-κB activation in concert with MD2 and CD14 when it recognizes the F protein of BRSV.[8] It is this fusion protein that is also responsible for mediating fusion of the viral envelope and the formation of viral syncytia seen histologically in both BRSV and PI-3 cases. The persistence of the virus in the face of widespread vaccination and in spite of the advances in the understanding of its pathogenic mechanisms has led to researchers developing improved technologies. Some promising examples include live attenuated vaccines which are devoid of either NS1 or NS2 and are capable of inducing robust antibody responses.[8]

Given the endemicity of these prominent respiratory pathogens and their considerable economic impact, significant opportunity for discovery remains in the complex pathogenesis of BRDC; though we leave the reader to speculate where in the process of beef production the most impactful of those opportunities lie, whether it is management considerations, preventive therapy, or treatment.

**Contributing Institution:** Animal Pathology Department
Veterinary Diagnostic Laboratory
Veterinary Faculty
Federal University of Pelotas
96010-900 Pelotas
RS, Brazil
http://www.ufpel.edu.br/fvet/oncovet/
http://www.ufpel.edu.br/fvet/lrd/

**References:**

1. Ackermann MR. Inflammation and healing. In: Zachary JF, McGavin MD, eds. *Pathologic Basis of Veterinary Disease.* 5th ed. St. Louis, MO: Elsevier Mosby; 2012:111-112.

2. Brodersen BW. Bovine respiratory syncytial virus. *Vet Clin North Am Food Anim Pract* 2010;26(2):323–333.
3. Caswell JL. Failure of respiratory defenses in the pathogenesis of bacterial pneumonia of cattle. *Vet Pathol.* 2014;51(2):393-409.
4. Caswell JL, Williams KJ. Respiratory system. In: Maxie MG, ed. *Jubb, Kennedy and Palmer's Pathology of Domestic Animals*. 5th ed. Vol. 2. Philadelphia, PA: Saunders Elsevier; 2007:596-598.
5. Fulton RW, Blood KS, Panciera RJ, et al. Lung pathology and infectious agents in fatal feedlot pneumonias and relationship with mortality, disease onset, and treatments. *J Vet Diagn Invest*. 2009;21:464-477.
6. Kirchhoff J, Uhlenbruck S, Goris K, Keil GM, Herrler G. Three viruses of the bovine respiratory disease complex apply different strategies to initiate infection. *Vet Res.* 2014;45:20.
7. Panciera RJ, Confer AW. Pathogenesis and pathology of bovine pneumonia. *Vet Clin North Am Food Anim Pract.* 2010; 26(2):191–214.
8. Sacco RE, McGill JL, Pillatzki AE, Palmer MV, Ackermann MR. Respiratory syncytial virus infection in cattle. *Vet Pathol.* 2014;51(2): 427-436.
9. Sarmiento-Silva RE, Nakamura-Lopez Y, Vaughan G. Epidemiology, molecular epidemiology and evolution of bovine respiratory syncytial virus. *Viruses*. 2012;4:3452-3467.
10. Valarcher J-F, Taylor G. Bovine respiratory syncytial virus infection. *Vet Res.* 2007;38:153–180.

**CASE II**: 2014A (JPC 4048859).

**Signalment:** Four-week-old male crossbred pig *(Sus scrofa)*.

**History:** A respiratory disease in a pig herd quickly spread from the finishing unit to the growing and breeding units. The affected animals showed prostration with respiratory signs including sneezing. The disease disappeared two weeks after onset, except in the breeding unit. The presently examined pig was one of two in the breeding unit submitted for necropsy.

**Gross Pathology:** Patchy, mottled, dark-red, and consolidated foci were found in the cranial, middle, and caudal lobes of the lung. Affected pulmonary lobules were well demarcated from normal areas. No gross lesions were detected in other organs.

**Laboratory Results:** Virology: Influenza A virus (subtype; H1N2) was isolated from the samples of nasal discharge and lung tissue. No pathologic bacteria were isolated from the lungs. Immunohistochemistry: Type A influenza virus matrix antigen was detected in the lung. Antigens of porcine reproductive and respiratory syndrome virus (PRRSV), porcine circovirus type 2 (PCV2), *Mycoplasma hyopneumoniae* and *Mycoplasma hyorhinis* were negative in the lung.

**Histopathologic Description:** Necrosis and desquamation of the bronchial epithelial cell layer was multifocally found in the affected lobes of the lung. The lumen of the involved bronchioles was extended, and some bronchioles were obstructed by necrotic cell debris, macrophages, and neutrophils. Necrotic cell debris and the inflammatory cells were also found in bronchia, alveolar ducts, and adjacent alveolar lumina. Hyaline membranes, formed by cellular debris accumulation and exudative proteins, were occasionally observed in some sections of alveolar wall. Slight lymphocyte accumulation was noted around bronchioles and adjacent vessels. Some bronchioles were found to have a hyperplastic epithelial cell layer. Alveolar septa were slightly thickened with lymphohistocytic infiltration and hyperplasia of type II pneumocytes.

Immunohistochemical analysis to detect type A influenza virus revealed presence of influenza virus matrix antigens in the epithelial cells, with necrotic changes in some bronchioles and adjacent alveolar walls. Other major pathological findings in this case were basophilic intranuclear inclusion bodies (cytomegalic inclusion bodies) in

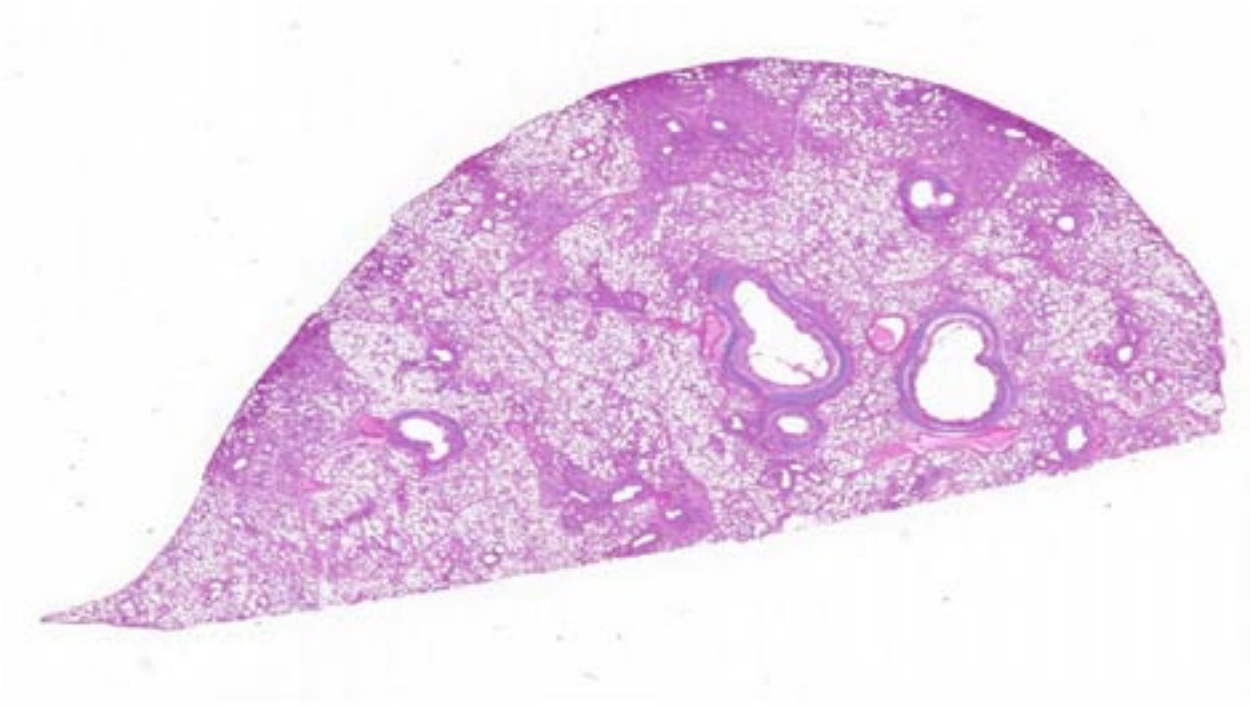

*2-1. Lung, pig: There are patchy areas of atelectasis scattered throughout the section centered on small airways. (HE 0.63x)*

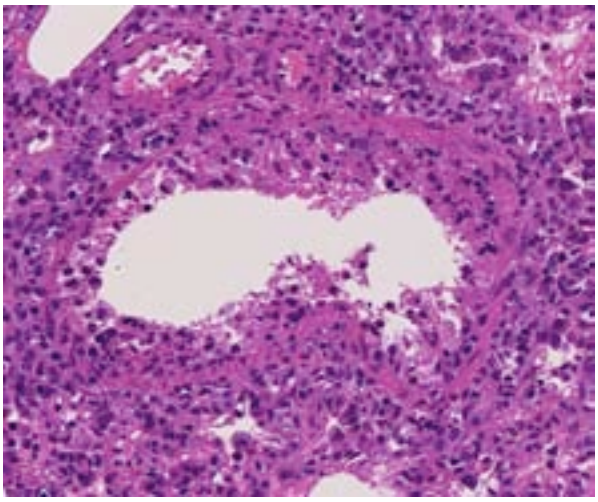

*2-2. Lung, pig: There is diffuse necrosis of the epithelium of small bronchioles within areas of atelectasis. (HE 248X)*

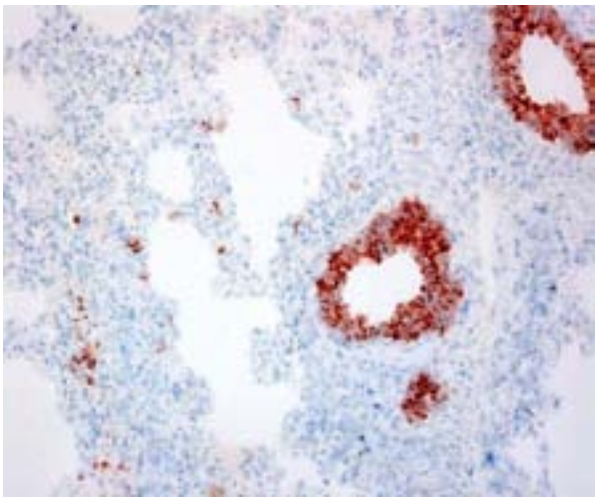

*2-3. Lung, pig: Immunohistochemical analysis to detect type A influenza virus revealed presence of influenza virus matrix antigens in the epithelial cells, with necrotic changes in some bronchioles and adjacent alveolar walls. (Photo courtesy of: National Institute of Animal Health, Japan. http://www.naro.affrc.go.jp/org/niah/)*

epithelial cells of nasal mucous glands with slight lymphocytic infiltration in the lamina propria and slight inflammatory exudates in the nasal cavity.

**Contributor's Morphologic Diagnosis:** Lung: Pneumonia, bronchointerstitial, necrotizing, multifocal, moderate, subacute.

**Contributor's Comment:** Influenza virus infections are a common cause of swine pneumonia worldwide. Swine influenza viruses are type A viruses, and major epidemic subtypes —defined by the nature of the hemagglutinin (H) and neuraminidase (N)—are H1N1, H1N2, or H3N2.[6] Influenza virus infections in swine cause acute respiratory disease with high morbidity and function as a major etiology of porcine respiratory disease complex (PRDC), as the virus infections act synergistically with other viral and bacterial infections in the respiratory tract. Further, swine influenza virus infections are not limited in significance to merely swine production but represent major public health concerns, as pigs are susceptible to infection of avian and human influenza viruses and often result in appearance of reassortment viruses in pigs.

The common microscopic findings in swine influenza infections are necrotizing bronchitis and bronchiolitis.[3] The influenza virus primarily infects the epithelial cells lining the surface of the respiratory tract, and infection induces cytolysis of infected cells.[9] Cell death induced by the viral infection also occurs through apoptosis induced by the viral components.[7] The term 'bronchointerstitial pneumonia' is used in veterinary pathology to describe cases with pulmonary lesions showing histologic features of both bronchopneumonia and interstitial pneumonia.[11] This combined type of pneumonia is frequently seen in many viral infections in which viruses replicate within and cause necrosis of bronchial, bronchiolar, and alveolar cells. The term has also frequently been used in microscopic examination of influenza virus infections in animals.[8] Although histopathologic features of swine influenza are considerably characteristic, immunohistochemical evaluation with sections of formalin-fixed tissue can prove nevertheless useful in differential diagnosis.[10] Similar histological lesions are necrotizing bronchopneumononia induced by PCV2, interstitial pneumonia induced by PRRSV, or mycoplasmal pneumonia.[2,4] Of note, findings on immunohistochemistry were negative for all three diseases in the present case.

**JPC Diagnosis:** Lung: Pneumonia, bronchointerstitial, necrotizing, multifocal, moderate, with type II pneumocyte hyperplasia.

**Conference Comment:** In swine, influenza viruses specifically target airway epithelial cells, leading to its hallmark histopathologic lesion of necrotizing bronchitis and bronchiolitis.[6] We typically reserve the diagnosis of bronchointerstitial pneumonia for those cases in which pathogens target both airway epithelium as

well as either pneumocytes or vascular endothelium within alveolar septa. This seems to occur exclusively with viral infections, and this case represents an excellent example. Of note is the affinity for the terminal airways in this case, as many bronchioles are barely evident among the extensive inflammation and necrosis in the periphery of the section with relative sparing of the larger airways.

All influenza viruses of significance in swine are type A viruses, with the subtypes H1N1, H1N2 or H3N2 being most common.[6] Influenza is an orthomyxovirus, a single-stranded RNA virus which is well known for its ability to constantly adapt through spontaneous mutations of its hemaglutinin and neuraminidase proteins (antigenic drift) or via recombination of genes with those in strains infecting other species (antigenic shift).[5] It is this talent of recombination which enables cross-species transmission and earns it the distinction of being the deadliest virus known to man, with the 1918 pandemic of H1N1 killing up to 40 million people worldwide.[5]

Early studies demonstrated influenza receptors of both avian and human viruses within the trachea of swine, leading to the labeling of swine as a "mixing vessel" from which pandemic influenza may arise. It has since been determined that avian influenza can infect humans just as readily as swine, negating the need for the pig as an intermediate host.[6] Thus it is the avian viruses which have been given the most attention as of late, the most noteworthy being the H5N1 strain known as highly pathogenic avian influenza. (see WSC 2012 conf 14, case 4 or WSC 2013 conf 7, case 4 for two examples).

Influenza is capable of cross-infection between swine and people, with the 2009 H1N1 pandemic being the most well-known example. Triple reassortments, which are influenza viruses circulating in swine that possess both avian- and human-origin genes, have been identified which add to the circulating pool likely resulting in the increased incidence of newly reassorted viruses.[6] Newly reassorted viruses pose a significant biosecurity and management problem for the swine industry, with the need for protection against the increasingly antigenically diverse viruses being of significant concern.

In addition to hemagglutinin (used for attachment to and internalization of host cells) and neuraminidase (which prevents viral progeny aggregration), the proteins that influenza is classified by, there are several others important for disease pathogenesis and diagnostics. The polymerase PB2 directs cell processes toward virus replication and is considered most significant of the polymerases with regard to pathogenicity. The nonstructural protein PB1-F2 also contributes to virulence through four mechanisms: inducing apoptosis, IFN suppression, increasing viral replication rates or delaying viral clearance, and increasing inflammation. NS1, another nonstructural protein, interferes with antiviral response and exhibits both proapoptotic and antiapoptotic activities. It also is only expressed in infected cells, making its antibodies a useful naturally occurring DIVA (Differentiating Infected from Vaccinated Animals) tool. The nucleoprotein (NP) is a highly-conserved, internal protein in all type A influenza viruses and thus an appropriate target for ELISA.[6] This could potentially alleviate the demonstrated problems associated with antigenic variation when detecting hemagglutinin antibody.

Early detection of different subtypes of influenza virus, most notably H5N1 which experimentally only induces subclinical disease in swine[1], is a significant public health concern. New techniques utilizing oral secretions collected by the suspension of absorbent ropes within the pens of swine may be the way forward for rapid screening in large facilities, though antibody-based diagnostics from oral fluids are not yet a proven technology.[6]

**Contributing Institution:** Department of Embryology, Histology and Pathology
Ecole Nationale Vétérinaire d'Alfort
7, avenue du Général de Gaulle
94704 MAISONS-ALFORT CEDEX
http://www.vet-alfort.fr/

**References:**

1. Buehler J, Lager K, Vincent A, Miller C, Thacker E, Janke B. Issues encountered in development of enzyme-linked immunosorbent assay for use in detecting *Influenza A* virus subtype H5N1 exposure in swine. *J Vet Diagn Invest.* 2014;26(2):277-281.
2. Grau-Roma L, Segales J. Detection of porcine reproductive and respiratory syndrome virus,

porcine circovirus type 2, swine influenza virus and Aujeszky's disease virus in cases of porcine proliferative and necrotizing pneumonia (PNP) in Spain. *Vet Microbiol.* 2007;119(2-4):144-151.
3. Haesebrouck F, Pensaert MB. Effect of intratracheal challenge of fattening pigs previously immunised with an inactivated influenza H1N1 vaccine. *Vet Microbiol.* 1986;11(3):239-249.
4. Hansen MS, Pors SE, Jensen HE, Bille-Hansen V, Bisgaard M, Flachs EM, et al. An investigation of the pathology and pathogens associated with porcine respiratory disease complex in Denmark. *J Comp Pathol.* 2010;143(2-3):120-131.
5. Husain AN. The lung. In: Kumar V, Abbas AK, Aster JC, eds. *Robbins and Cotran Pathologic Basis of Disease*. 9th ed. Philadelphia, PA:Elsevier Saunders; 2015:76.
6. Janke BH. Influenza A virus infections in swine: pathogenesis and diagnosis. *Vet Pathol.* 2014;51(2):410-426.
7. Mori I, Komatsu T, Takeuchi K, Nakakuki K, Sudo M, Kimura Y. In vivo induction of apoptosis by influenza virus. *J Gen Virol.* 1995;76(Pt 11): 2869-2873.
8. Prescott JF, Wilcock BP, Carman PS, Hoffman AM. Sporadic, severe bronchointerstitial pneumonia of foals. *Can Vet J.* 1991:32(7): 421-425.
9. Seo SH, Webby R, Webster RG. No apoptotic deaths and different levels of inductions of inflammatory cytokines in alveolar macrophages infected with influenza viruses. *Virology.* 2004;329(2):270-279.
10. Vincent LL, Janke BH, Paul PS, Halbur PG. A monoclonal-antibody-based immunohistochemical method for the detection of swine influenza virus in formalin-fixed, paraffin-embedded tissues. *J Vet Diagn Invest.* 1997;9(2): 191-195.
11. Lopez A. Respiratory system, mediastinum, and pleurae. In: Zachary JF, McGavin MD, eds. *Pathologic Basis of Veterinary Disease*. 5th ed. St. Louis, MO: Elsevier Mosby;2012:458-538.

**CASE III**: 09N2904 (JPC 4019370).

**Signalment:** 11-year-old, castrated male domesticated alpaca (*Vicugna pacos*).

**History:** This adult male alpaca was presented to the VMTH for partial anorexia and lethargy with drooling. He was recently switched to new grass hay in which alfalfa and weeds were present. He was allowed access to fresh grass in a pasture for a few hours but developed diarrhea that resolved. He shared his enclosures with goats (all healthy).

Over the course of a 3-day hospitalization, the alpaca was noted to be anxious, depressed, and colicky with decreased gastrointestinal motility and intermittent recumbency (both sternal and lateral). He was treated intensively with fluids, antibiotics and supportive care. Facial and pulmonary edema, oliguria and azotemia developed over the 3 days with initial partial response to diuretics followed by apparent anuria. Sinus tachycardia was present initially, but by early on day 3 arrhythmias were noted. Ventricular tachycardia (up to 190 bpm) with runs of premature ventricular contractions developed and worsened in spite of I.V. lidocaine. The alpaca went into cardiac arrest and could not be resuscitated.

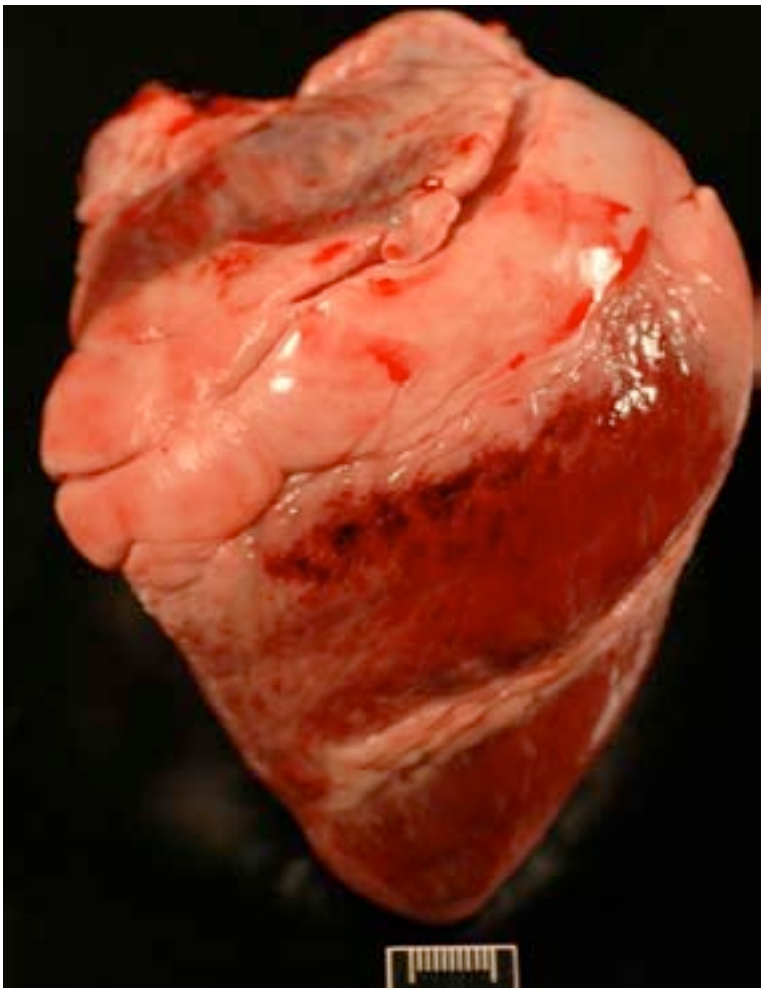

*3-1. Heart, alpaca: There are coalescing petechiae on the epicardial surface. (Photo courtesy of: University of California, Davis, Veterinary Medical Teaching Hospital, Anatomic Pathology Service)*

**Gross Pathology:** There was diffuse subcutaneous edema, mild abdominal effusion, and pulmonary congestion and edema. On the epicardial surface of the right ventricle there was a focally extensive area of petechiation. The heart silhouette, weight, and measurements were considered normal. The mucosal surface of the pylorus and entire duodenum was diffusely discolored dark red to purple and thickened, and serosal surfaces of the entire bowel were reddened. The cortical surfaces of the kidneys were mottled dark red to purple, and in the right kidney there were wedge shaped areas of red-purple discoloration which tapered into the medulla. The bladder contained urine.

**Laboratory Results:** Abnormal lab work included: elevated BUN (62 increasing to 116); elevated creatinine (4.8 increasing to 8.4); hyperglycemia (410 to 690); leukocytosis with neutrophilia, lymphocytopenia and monocytosis (11,620 with 73% neutrophils, 10% bands, 4% lymphocytes and 13% monocytes). Serum collected on day 2 and analyzed at the California Animal Health and Food Safety Lab was positive for oleandrin.

**Histopathologic Description:** Heart (left ventricular myocardium): Multiple foci of hemorrhage are present in the subendocardial and subepicardial myocardium. Myofibers in these foci and in scattered foci throughout the sections are pale, granular to fibrillar or fragmented and the endomysium and perimysium are expanded by a combination of edema and cells with variably pyknotic to plump nuclei. Adjacent myofibers

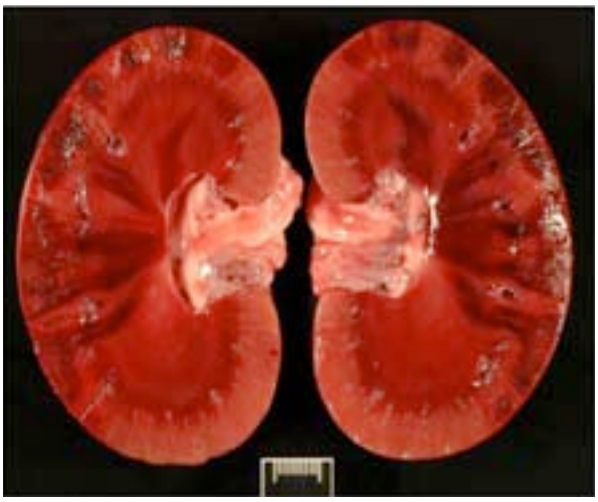

*3-2. Kidney, alpaca: There are multiple wedge-shaped areas of necrosis which encompass both the cortex and medulla. (Photo courtesy of: University of California, Davis, Veterinary Medical Teaching Hospital, Anatomic Pathology Service)*

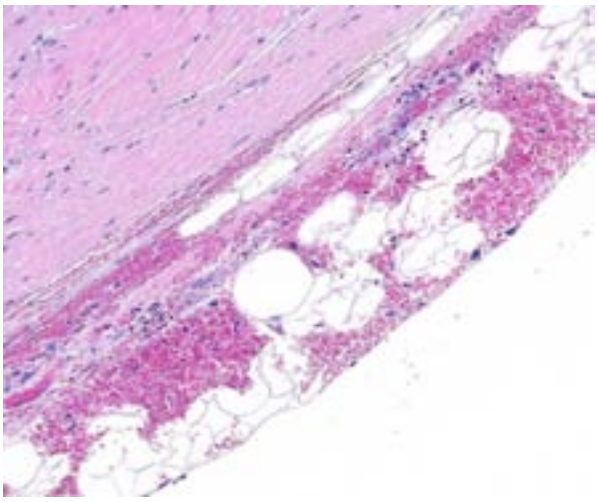

*3-3. Heart, alpaca: There is multifocal hemorrhage within the endocardium. (HE 50X)*

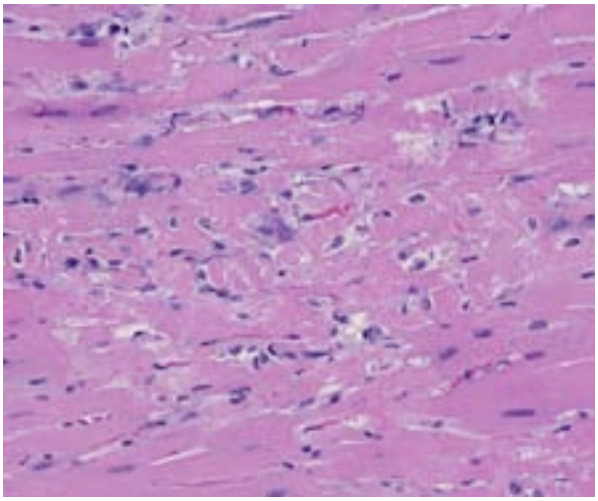

*3-4. Heart, alpaca: There are widely scattered areas of myocardial degeneration and necrosis. (HE 280X)*

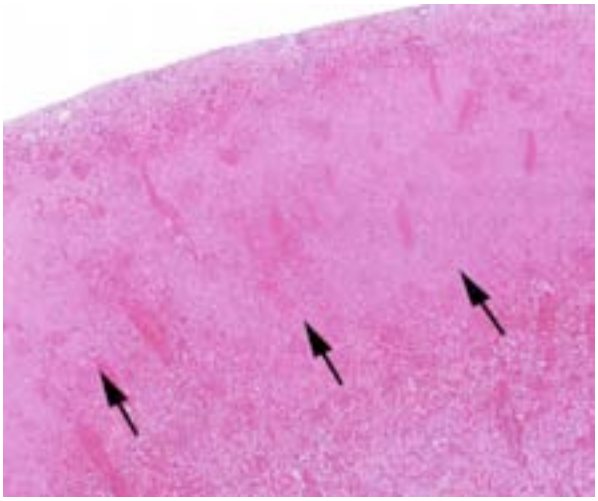

*3-5. Kidney, alpaca: There are coalescing areas of architectural loss within the renal cortex, corresponding to areas of coagulative necrosis. (HE 14X)*

occasionally have centrally located hypertrophied nuclei. The endocardial hemorrhage in two sections surrounds Purkinje fibers which are vacuolated and fragmented. Scattered individual myofibers are hyalinized and are brightly eosinophilic (Zenker's necrosis) or lightly basophilic (early mineralization). Rarely, necrotic fibers are surrounded by neutrophils or mononuclear cells (myophagia).

Kidney: There are large wedge shaped areas of acute infarction characterized by hemorrhage and coagulative necrosis of the cortex and medulla. Cells of the infracted glomeruli and tubules have loss of cellular detail and karyolytic nuclei. Glomeruli multifocally contain abundant fibrin within capillaries. Small numbers of renal tubules exhibit acute tubular necrosis in which epithelial cells are hypereosinophilic, have pyknotic nuclei, and slough into the lumen (cellular casts). Surrounding tubular epithelium is multifocally attenuated. There is multifocal mineralization of necrotic tubules.

**Contributor's Morphologic Diagnosis:** 1. Heart (left ventricle): Moderate multifocal subacute myocardial degeneration and necrosis with associated hemorrhage compatible with oleandrin intoxication.
2. Kidneys: Severe multifocal acute infarction and multifocal acute tubular necrosis.

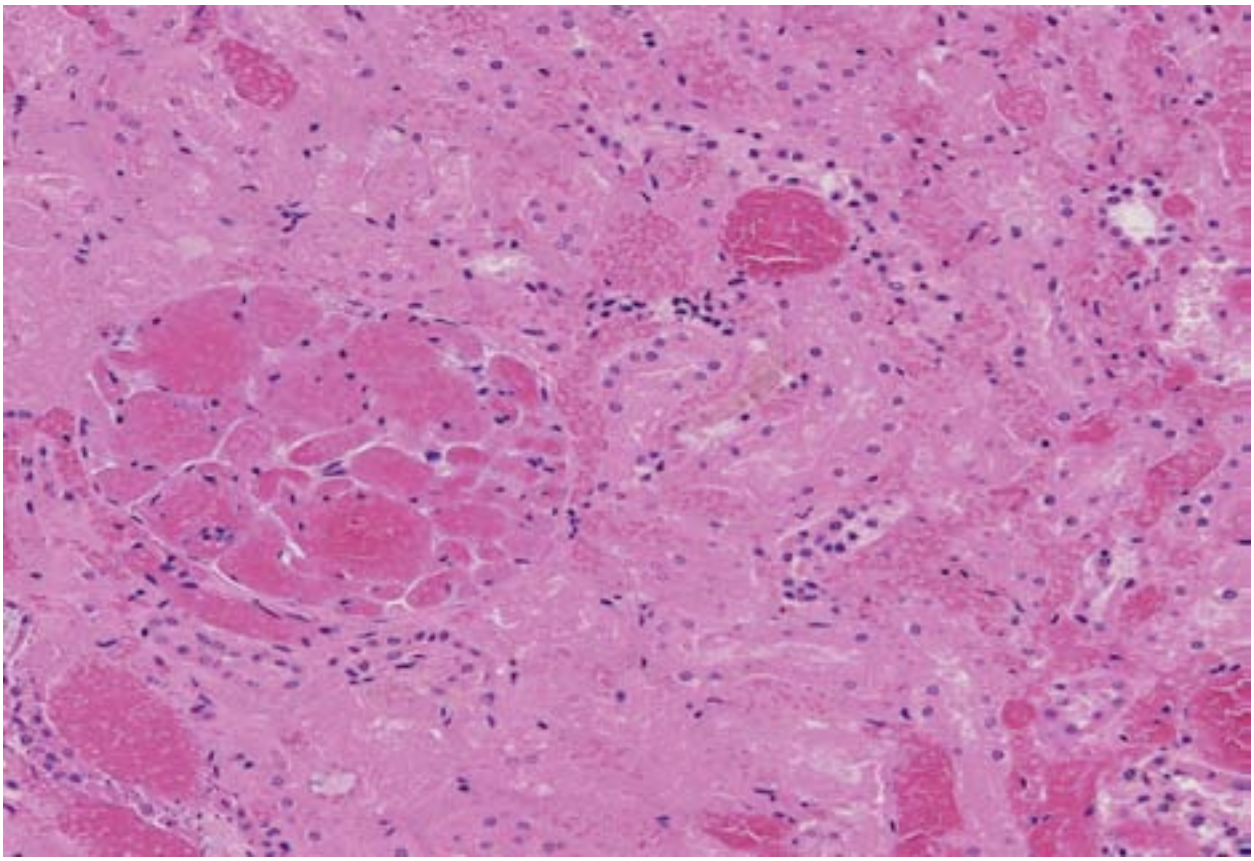

*3-6. Kidney, alpaca: Higher magnification of areas of renal infarction. (HE 320X)*

ADDITIONAL DIAGNOSES (TISSUES NOT ON SLIDE):

1. Stomach (C3), small intestine and colon: Moderate diffuse congestion and multifocal transmural hemorrhage with multifocal superficial necrosis.

2. Adrenals: Severe multifocal subacute medullary hemorrhage and necrosis.

3. Pelvic limbs: Mild multifocal myonecrosis with hemorrhage and multifocal myofiber regeneration.

**Contributor's Comment:** Oleander intoxication in this alpaca was confirmed by finding oleandrin in the serum antemortem and the fact that oleander was present on the property. Pink oleander (*Nerium oleander*) is a popular showy flowering ornamental shrub that was widely planted in California in median strips of freeways, verges of country roads, parks, farmsteads and urban homes. Unfortunately, all parts of the plant are highly toxic with over 35 bio-active compounds having been isolated from this plant.[14]

The most studied of the toxic principals are cardioactive glycosides including oleandrin. The heart and GI tract are the primary targets of intoxication, though neurological signs have been reported and renal tubular degeneration has been seen in some cases. South American camelids (llamas and alpacas)[6] and horses account for the majority of cases in our VMTH pathology archives, although much of the literature is concerned with intoxications in humans, cattle, and other commercial livestock.[1-4,8,15] Birds and rodents are fairly resistant experimentally, as are primates, though experimental or natural intoxication has been reported.[10,13]

The cardioactive glycosides of oleander exert a positive inotropic effect, caused by interference with normal calcium channel mechanisms and eventual intracellular accumulation of calcium.[10] The underlying mechanism for renal failure is undetermined at this time, but is a common finding with oleander toxicity in New World camelids.[6] Two possible mechanisms include inhibition of the $Na^{+}$-$K^{+}$ ATPase pump in the renal tubules causing direct tubular injury, or infarction

due to hypoperfusion secondary to cardiac damage. It is also possible that it is a combination of both mechanisms, as in this case both infarction and acute tubular necrosis were observed.

Other cardiotoxic plants, zoo or wild animals that might be exposed include: foxglove (*Digitalis lannata or D. purpurea),* yellow oleander (*Thevetia peruviana*), rhododendrons and azaleas (*Rhododendron* spp.), mountain laurel (*Kalmia latifolia*), kalanchoe (*Kalanchoe blossfeldiana* and its hybrids), milkweeds (*Asclepias* species), lily of the valley (*Convallaria majalis*), Dogbane (*Apocynum cannabinum*), avocado (*Persea Americana* Guatamalan variety). Other cardiotoxins include ionophores such as monensin and salinomyocin, which was responsible for a large alpaca mortality event through contamination of a commercial feed.[5]

**JPC Diagnosis:** 1. Heart, myocardium: Necrosis and degeneration, multifocal, moderate.
2. Heart, epicardium: Hemorrhage, acute, multifocal.
3. Kidney, cortex: Infarcts, acute, multifocal and coalescing.

**Conference Comment:** Arriving at a precise etiologic diagnosis proved challenging for conference participants in this case, whom at best could consider oleander on a differential list which included other cardiac toxins such as monensin (ionophore used as coccidiostat that also acts on Na+/K+ pumps), coffee senna or western water hemlock (plants known to cause muscular & myocardial necrosis in livestock), yew (*Taxus sp.),* gossypol (toxic alcohol from cottonseed meal), locoweed (plants better known for "star gazing" in cattle but which cause myocardial degeneration), or cantharidin (toxic principle from blister beetles that causes gastric, cystic and myocardial necrosis) in addition to the aforementioned cardiotoxic plants listed by the contributor.[9]

To further complicate the picture, ischemic myocardial necrosis also occurs in disseminated intravascular coagulopathy, vitamin E/selenium deficiency, and inflammatory diseases such as periarteritis nodosa. Subendocardial necrosis is observed following acute brain injury ("brain-heart syndrome") or in catecholamine excess from a functional pheochromocytoma.[9] The presence of renal necrosis does not assist in narrowing down the list, as the potential candidates for inducing renal infarcts or toxic tubular necrosis is equally extensive with significant overlap from the cardiotoxic differentials. As the contributor points out, identifying the geographic location as California in the present case significantly elevates oleander from others on the list. The gross and microscopic findings of endocardial hemorrhage, while considered non-specific at best, have been reported as commonly occurring in oleandrin toxicity[4], is prominent in the distributed sections, and may have yielded some assistance in narrowing this relatively long list of ruleouts.

Some discussion among participants revolved around the presence of apparent vascular necrosis of some larger arteries and whether to attribute those to vasculitis, injury due to hypertension or the renal infarct, with the most favorable opinion being secondary injury from a period of hypertension.

Oleandrin toxicity is most often associated with horses, though it is known to be toxic to many species. Participants briefly contrasted the manifestations of toxin ingestion as reported in horses with the current case. In the horse, mortality appears to be more common, with a rate of 50% (30 cases) versus 25% in camelids (12 cases). The clinical signs between species are similar, with the triad of gastrointestinal, cardiac and renal disease consistently present in each species.[7,12]

**Contributing Institution:** University of California, Davis
Veterinary Medical Teaching Hospital
Anatomic Pathology Service

**References:**
1. Ada SE, Al-Yahya MA, Farhan AH. Acute toxicity of various oral doses of dried *Nerium oleander* leaves in sheep. *Am J Chin Med.* 2001;29:525–532.
2. Aslani MR, Movassaghi AR, Mohri M, Abbasian A, Zarehpour M. Clinical and pathological aspects of experimental oleander (Nerium oleander) toxicosis in sheep. *Vet Res Commun*. 2004;28(7):609-16.
3. Barbosa RR, Fontenele-Neto JD, Soto-Blanco B. Toxicity in goats caused by oleander (Nerium oleander). *Res Vet Sci*. 2008;85(2):279-81, 26.

4. Galey FD, Holstege DM, Plumlee KH, Tor E, Johnson B, Anderson ML, Blanchard PC, Brown F. Diagnosis of oleander poisoning in livestock. *J Vet Diagn Invest.* 1996;8:358-364.
5. Hughes KJ, Dart AJ, Hodgson DR. Suspected *Nerium oleander* (oleander) poisoning in a horse. *Aust Vet J.* 2002;80:412–415.
6. Kosal DE, Anderson ME. An unaddressed issue of agricultural bioterrorism: A case study on feed security. *J Anim Sci*. 2004;82:3394–3400.
7. Kozikowski TA, Madgesian KG, Puschner B. Oleander intoxication in New World camelids: 12 cases (1995-2006). *JAVMA.* 2009;235:305-309.
8. Langford SD, Boor PJ. Oleander toxicity: An examination of human and animal toxic exposures. *Toxicology*. 1996;109(1):1-13.
9. Maxie MF, Robinson WF. Cardiovascular system. In: Maxie MG, ed. *Jubb, Kennedy, and Palmer's Pathology of Domestic Animals*. Philadelphia, PA: Elsevier Saunders; 2007:33.
10. Omidi A, Razavizadeh AT, Movassaghi AR, Aslani MR. Experimental oleander (Nerium oleander) intoxication in broiler chickens (Gallus gallus). *Hum Exp Toxicol*. 2011 May 16. [Epub ahead of print]
11. Poindexter BJ, Feng W, Dasgupta A, Bick RJ. Oleandrin produces changes in intracellular calcium levels in isolated cardiomyocytes: A real-time fluorescence imaging study comparing adult to neonatal cardiomyocytes. *J Toxicol Environ Health A*. 2007;70(6):568-74.
12. Renier AC, Kass PH, Magdesian KG, Madigan JE, Aleman M, Pusterla N. Oleander toxicosis in equids: 30 cases (1995-2010). *JAVMA*. 2013;242(4):540-549.
13. Schwartz WL, Bay WW, Dollahite JW, Storts RW, Russell LH. Toxicity of Nerium oleander in the monkey (Cebus apella). *Vet Pathol*. 1974;11(3):259-77.
14. Sharma P, Choudhary AS, Parashar P, Sharma MC, Dobhal MP. Chemical constituents of plants from the genus Nerium. *Chem Biodivers*. 2010;7(5):1198-207.
15. Soto-Blanco B, Fontenele-Neto JD, Silva DM, Reis PF, Nóbrega JE. Acute cattle intoxication from Nerium oleander pods. *Trop Anim Health Prod*. 2006;38(6):451-454.

**CASE IV:** 12-12710 (JPC 4048081).

**Signalment:** 8-month-old Angus heifer.

**History:** This was the sixth calf to die from a group of approximately 225. The first calf died in September, just before weaning and had shown bloody diarrhea that did not respond to treatment with oxytetracycline. The group was treated with a coccidiostat in the water. Calves had been vaccinated for clostridial agents plus IBR, BVD and PI3. Several other calves died in the course of a few days in late October.

This heifer was found sick and treated with penicillin and banamine, but died. It was submitted for necropsy to the Washington Animal Disease Diagnostic Laboratory at Washington State University.

**Gross Pathology:** Multifocally, throughout the jejunum, ileum, cecum, and colon, were widely scattered, linear to elliptical areas of mucosal ulceration that ranged from 0.5 to 8.0 cm in length, with the ileum being most severely affected. The edges of the ulcers were raised and there were multifocal areas of hemorrhage within the surrounding mucosa. Throughout the small intestines were segmental regions of hyperemia. Within the colon there was a single dark red, blood-stained fecal ball. Other minor lesions included mesenteric lymphadenopathy and mild, mucopurulent tracheitis.

**Laboratory Results:** Feces from this heifer were cultured for *Salmonella* spp. and were negative. Anaerobic cultures of feces isolated *Clostridium perfringens* type A.

The sera from two herdmates of this heifer were tested by antigen ELISA for persistent infection with BVDV. Both were positive.

**Histopathologic Description:** In a section of ileum, Peyer's patches were moderately to markedly hypocellular and were partially to completely replaced by ectatic intestinal crypts (crypt herniation) that were often filled with karyorrhectic cellular debris admixed with many degenerate neutrophils. The overlying mucosa was extensively ulcerated. The ulcers were covered by large coagula composed of numerous degenerate neutrophils admixed with abundant necrotic cellular debris and mixed bacterial colonies. Numerous neutrophils infiltrated the adjacent lamina propria and submucosa. Remaining crypts in the adjacent, less severely affected mucosa, were mildly to markedly ectatic and filled with abundant mucus admixed with necrotic cellular debris and many degenerate

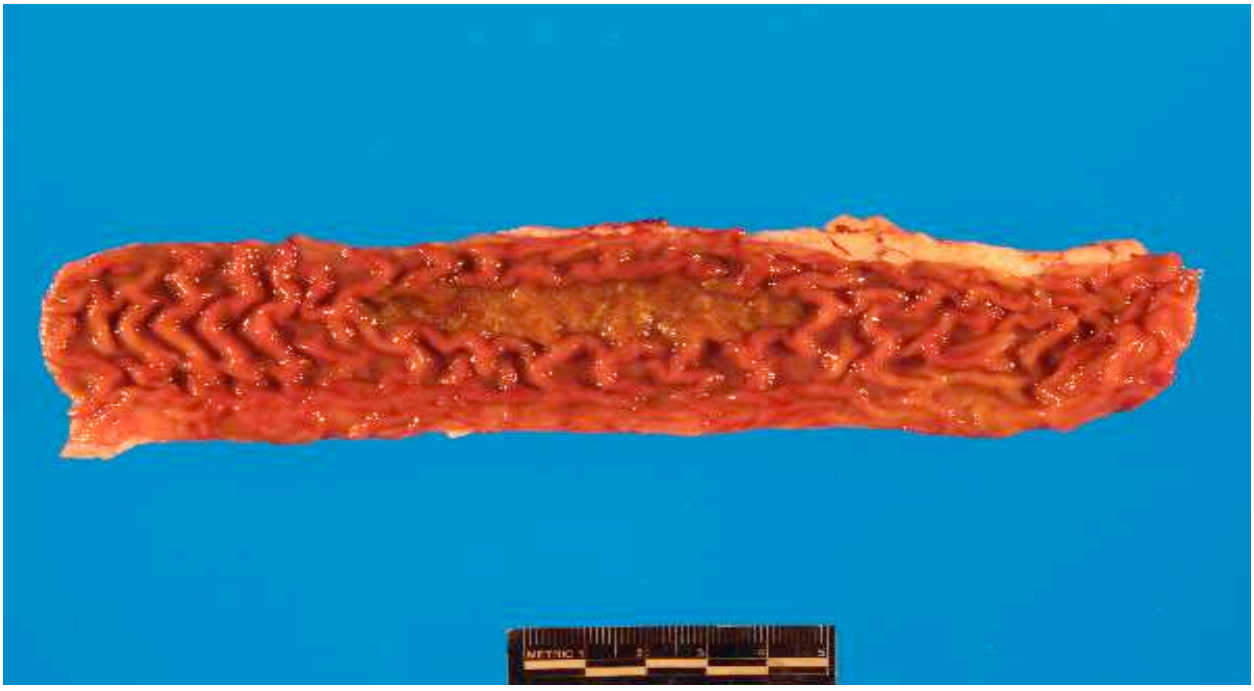

*4-1. Ileum, calf: There are multifocal elliptical areas of necrosis, most prominently in the ileum. (Photo courtesy of: Department of Veterinary Microbiology and Pathology, College of Veterinary Medicine, Pullman, WA 99164-7040 http://www.vetmed.wsu.edu/depts-vmp/index.aspx)*

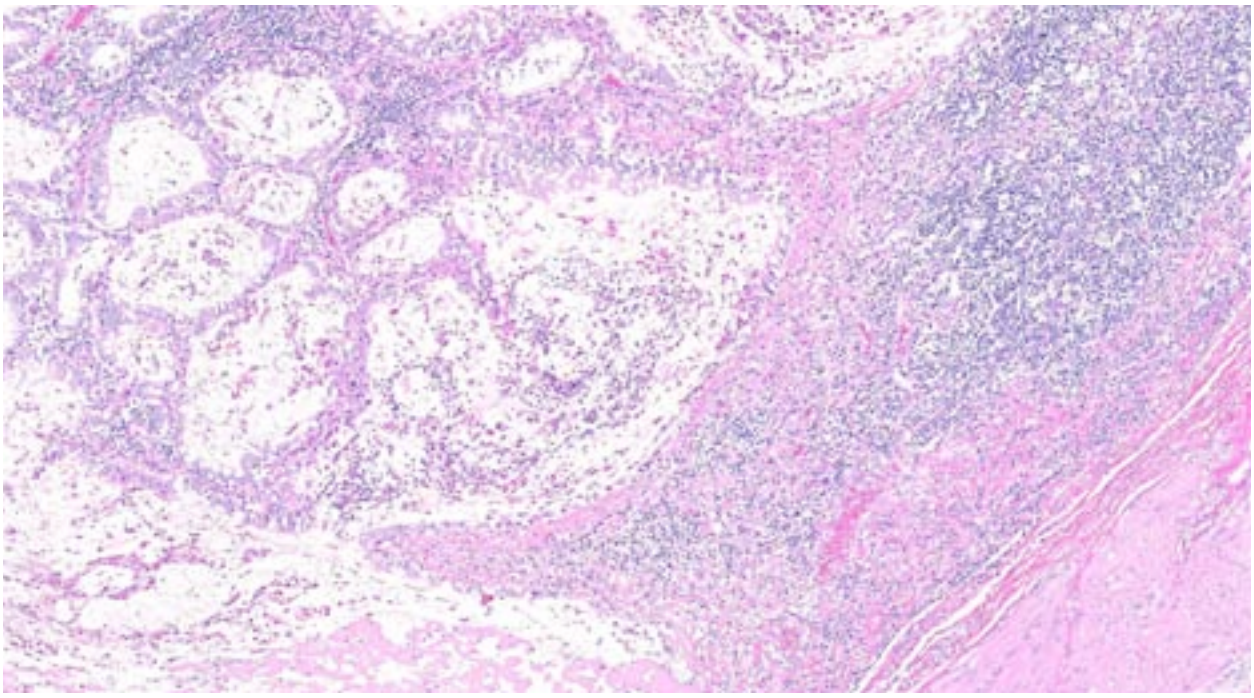

*4-2. Ileum, calf: Crypts overlying Peyer's patches are widely dilated and contain abundant necrotic debris. (HE 37X)*

neutrophils. The lamina propria in these regions was moderately expanded, and crypts elevated by increased numbers of lymphocytes, plasma cells, neutrophils, and varying amounts of edema.

A replicate section immunostained for the presence of bovine viral diarrhea virus (BVDV) revealed positive immunoreactivity in the crypt epithelial cells and macrophages. Positive controls had appropriate immunoreactivity and a replicate slide stained with a non-specific antibody (isotype control) had no immunoreactivity in those areas.

**Contributor's Morphologic Diagnosis:** Enterocolitis, necrotizing and ulcerative, multifocal, severe with Peyer's patch necrosis and crypt herniation associated with BVDV infection.

**Contributor's Comment:** Lesions present were compatible with mucosal disease caused by persistent infection with bovine viral diarrhea virus.

Bovine viral diarrhea virus (BVDV) is an RNA virus of the genus *Pestivirus* that causes a wide variety of clinical disease primarily in cattle which is its natural host.[3] A highly mutable virus, BVDV has developed two primary genotypes, 1 and 2, with both cytopathic (cp) and noncytopathic (ncp) forms within each genotype. Type 1 genotypes are considered to be more prevalent but less virulent than type 2 genotypes, although exceptions occur. Cytopathogenicity in vitro does not correlate with virulence.

In naïve, immunocompetent non-pregnant cattle, infection with BVDV can cause mild clinical disease characterized by fever and leukopenia, or they may develop classic bovine virus diarrhea, including oculonasal discharge, oral erosions and enteritis. Highly virulent strains (usually type 2 genotypes) may cause acute, severe disease with high morbidity and mortality with lesions indistinguishable from mucosal disease (described later). Transiently infected or vaccinated cattle develop neutralizing antibodies that are protective against reinfection.

Infection of naïve pregnant animals can result in fetal loss, congenital defects or birth of live, persistently infected (PI), immunotolerant calves. Infected fetuses may be aborted or may develop hydrancephaly, cerebellar hypoplasia, thymic atrophy, osteosclerosis or cataracts and other ocular lesions. PI status requires infection of the fetus early in gestation (40 -125 days).[4] PI cattle are immunotolerant and do not develop antibodies to BVDV. They shed large amounts of virus and are an important source of infection for the herd. Detection and removal of PI animals is an

important management strategy on cattle ranches. PI status can be detected by PCR for BVDV on buffy coats, but this does not distinguish from transiently infected cattle. Antigen ELISA on serum or ear notch supernatants, however, detects animals with high viral shedding and is the preferred method for screening for BVDV PI animals.[5] PCR on pooled samples from ear notch supernatants, with subsequent individual testing on positive pools is an efficient way to screen large herds.[8]

PI calves are often unthrifty and most succumb to mucosal disease before 2 years of age. Mucosal disease occurs when a calf persistently infected with an ncp strain of BVD becomes infected with a similar cp strain, or when the ncp resident strain mutates to become cp. The classic clinical presentation of mucosal disease is a small calf with oculonasal discharge and severe diarrhea. Gross lesions include coronitis, nasal and oral erosions, and ulcerative lesions throughout the gastrointestinal tract, including esophageal ulcers and characteristic, severe enteric ulcerations overlying Peyer's patches.[3,4] The epithelial necrosis and herniation of crypts into severely depleted Peyer's patch lymphoid follicles is characteristic of BVD; rinderpest causes similar lesions but is distinguished by characteristic multinucleate syncytial cells with morbillivirus cytoplasmic inclusions.[3] Diagnosis of BVD can be confirmed by immunohistochemical demonstration of viral antigens within ulcerative lesions in the skin and throughout the gastrointestinal tract.

**JPC Diagnosis:** Small intestine: Enteritis, necrotizing, diffuse, severe, with focally extensive Peyer's patch necrosis and crypt abscessation.

**Conference Comment:** In an era in which ivermectin has virtually eliminated a multitude of picturesque lesions in domestic animals, veterinary pathologists can find consolation in the persistence of bovine pestivirus, or BVDV, and its ability to induce a tremendous variety of pathology. This case is an exceptional example of the classic presentation of ulceration and Peyer's patch necrosis within the gastrointestinal tract associated with the form of infection known as mucosal disease (MD), or which can be seen in acute infections of highly virulent strains.[4] Linear ulcerations within the alimentary tract are classic, but one must also consider lesions from the brain to the reproductive tract, to include cerebellar hypoplasia, leukomalacia, retinitis, retinal atrophy, cataracts, myocardial necrosis, metaphyseal osteosclerosis, orchitis, oophoritis and thymic atrophy as possibly being associated with BVDV infection. Additionally, there are reports of disease in other species to include white-tail deer, sheep, goats, mouse deer, mountain goats and alpacas.[4,7]

The economic impact of the BVDV is significant, with the bulk of the expenses due to the acute transient infections which can compromise the immune system and exacerbate other bacterial or viral infections. Eradication efforts have been underway throughout Europe and in areas within the U.S. with restricted animal movement such as in the Upper Peninsula of Michigan.[6] These efforts focus on identifying the beating heart of the disease, the reservoir and source of infection known as the persistently infected (PI) calf.

As the contributor describes in detail, the PI calf develops in-utero following exposure to the virus, specifically a non-cytopathic (ncp) strain. For the calf to become immunotolerant to BVDV, the virus must avert the immune system by infecting the fetus before the humoral immune system is fully developed (~125 days gestation). Also, the virus must suppress the innate immune response through inhibition of type I IFN signaling. Type I IFN signaling is normally stimulated through the recognition of viral double-stranded (ds) RNA via TLR 3 (as discussed in case I) or RIG-1. Non-cytopathic strains, which already have less dsRNA to begin with compared with cytopathic strains, achieve this suppression through the expression of $E^{rns}$ glycoprotein. $E^{rns}$ exhibits RNAse activity and degrades extracellular RNA, thus decreasing stimulation of TLR 3 and RIG-1. Similarly, the glycoprotein $N^{pro}$ degrades IRF-3 which is also involved in IFN signaling, though in conjunction with IRF-7 through TLR 7, 8, and 9.[1] Expression of both $E^{rns}$ and $N^{pro}$ is necessary to induce persistent infection.[4] These underpinned mechanisms of disease pathogenesis elaborately correlate with the ncp strain's ability and cp strain's inability to produce a PI animal.

The difference between cp and ncp strains was demonstrated in vitro as the ability to induce apoptosis in bovine turbinate cells. This corresponds with the continual expression of NS3 protease in cp strains versus little to no expression

in ncp strains. NS3 induces apoptosis through both intrinsic (caspase 9) and extrinsic (caspase 8) pathways. Activated caspase 8 incites apoptosis of B- and T-lymphocytes in ileal Peyer's patches, which may correlate activation of the extrinsic pathway with the Peyer's patch necrosis observed in this case. Additionally, the antiapoptotic BCL-2 protein is upregulated by ncp BVDV, which may also relate to the difference in disease manifestation between the two strains.[4]

Bovine pestivirus shares its genus with other prominent diseases of domestic animals such as Classical swine fever virus and Border disease virus of sheep. Additionally, a closely related virus that causes similar clinical presentations as BVDV has been circulating in Brazilian cattle with reports of cases in Europe and Asia as well indicating possible widespread dissemination. To date, this virus has been called "Hobi-like", "BVDV-3" or "atypical pestivirus" [2], and in time may add itself to the list of economically important Pestiviruses.

**Contributing Institution**: Department of Veterinary Microbiology and PathologyCollege of Veterinary Medicine,
Pullman, WA 99164-7040

**References:**

1. Ackermann MR. Inflammation and healing. In: Zachary JF, McGavin MD, eds. *Pathologic Basis of Veterinary Disease.* St. Louis, MO: Elsevier Mosby; 2012:111-112.
2. Bauermann FV, Ridpath JE, Weiblen R, Flores EF. Hobi-like viruses: An emerging group of pestiviruses. *J Vet Diagn Invest.* 2013;25(1):6-15.
3. Brown CC, Baker DC and Barker IK. The Alimentary system. In: Maxie MG, ed. *Pathology of Domestic Animals.* 5th edition. Vol. 2. St. Louis, MO: Saunders Elsevier; 2007:140-147; 149-151.
4. Brodersen BW. Bovine viral diarrhea virus infections: Manifestation of infection and recent advances in understanding pathogenesis and control. *Vet Pathol*. 2014;51:453-464.
5. Cornish TE, van Olphen AL, Cavender JL, et al. Comparison of ear notch immunohistochemistry, ear notch antigen capture ELISA and buffy coat virus isolation for detection of calves persistently infected with bovine viral diarrhea virus. *J Vet Diagn Invest*. 2005;17:110-117.
6. Grooms DL, Bartlett BB, Bolin SR, Corbett EM, Grotelueschen DM, Cortese VS. Review of the Michigan Upper Peninsula bovine viral diarrhea virus eradication project. *J Am Vet Med Assoc*. 2013;15;243(4):548-54.
7. Jarvinen JA, O'Connor AM. Seroprevalence of bovine viral diarrhea virus in alpacas in the United States and assessment of risk factors for exposure, 2006-2007. *J Am Vet Med Assoc.* 2014;15;245(6):696-703.
8. Kennedy JA, Mortimer RG, Powers B. Reverse transcription-polymerase chain reaction on pooled samples to detect bovine viral diarrhea virus by using fresh ear-notch supernatants. *J Vet Diagn Invest*. 2006;18:89-93.

**Joint Pathology Center**
**Veterinary Pathology Services**

*Conference Coordinator*
**Matthew C. Reed, DVM**
**Captain, Veterinary Corps, U.S. Army**
**Veterinary Pathology Services**
**Joint Pathology Center**

## WEDNESDAY SLIDE CONFERENCE 2014-2015

# Conference 3

**17 September 2014**

**Conference Moderator:**
Paul Facemire, DVM, Diplomate ACVP
Deputy Chief, Global Health Engagements
Office of the Surgeon General
7700 Arlington Blvd
Falls Church, VA 22042

---

**CASE I:** 12-3003 (JPC 4019855)

**Signalment:** 8-week-old female domestic shorthair feline (*Felis catus).*

**History:** The kitten reportedly developed pale, unformed stools, anorexia, rapid weight loss and death within 2 weeks of purchase from a pet store. The owner of the pet store reported that multiple kittens both living at the store and recently purchased from the store had developed similar clinical signs, with most of the affected kittens recovering after supportive treatment. In addition, two apparently well-grown kittens had died suddenly within the previous 2 months.

**Gross Pathology:** The kitten presented within 12 hours of death and was judged to be in an adequate state of post-mortem preservation, in very poor body condition (315g) and moderately dehydrated. Pasty, yellow-grey feces stained the tail and perineum. A small amount of kibble was

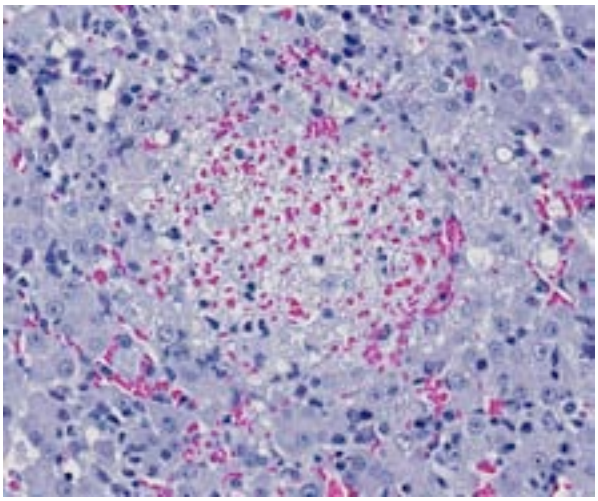

*1-1. Liver, kitten: Multiple foci of necrosis are infiltrated by low numbers of neutrophils. (HE 164X)*

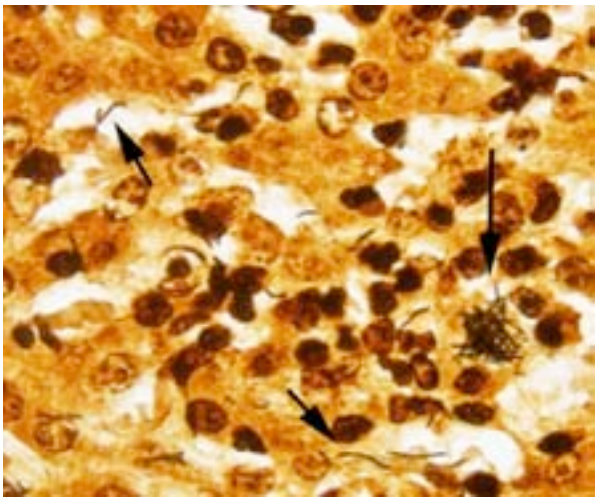

*1-2. Liver, kitten: Filamentous bacilli consistent with Clostridium piliforme are present within hepatocytes and extracellularly within necrotic foci. (Warthin-Starry 4.0, 60X)*

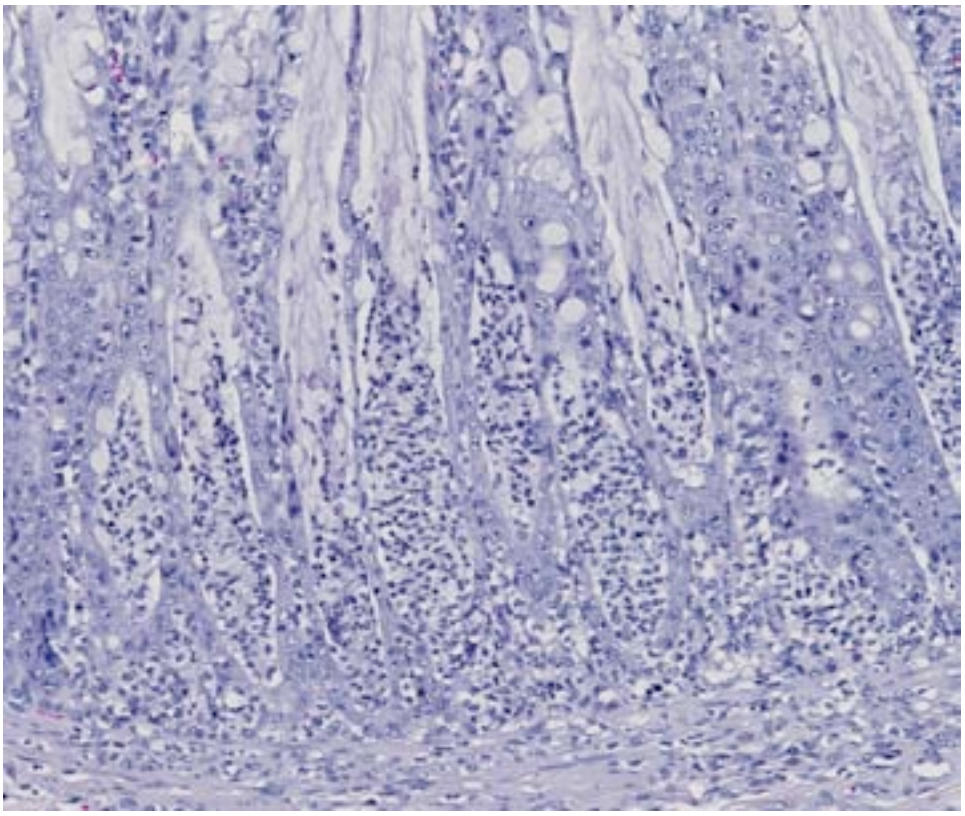

*1-3. Colon, cat: Colonic glands are diffusely expanded and contain numerous necrotic epithelial cells, degenerate neutrophils, and moderate amounts of mucus (crypt abscesses). (HE 120X)*

present in the stomach. The intestine and colon contained scant yellow mucoid content. There was patchy reddening of the serosal surface of the small intestine and proximal colon. Moderate numbers of pale, randomly scattered 1-2mm diameter foci were scattered throughout the hepatic parenchyma. The lungs were diffusely mottled red and tan and were slightly wet (congestion and oedema). No other abnormalities were detected on gross examination.

**Laboratory Results:** Culture of colonic contents produced a scant growth of *E. coli* and an *Enterococcus* species. There was no growth of *Campylobacter* or *Salmonella* spp. Low numbers of coccidial (1+) oocysts were seen on fecal flotation examination. ELISA for *Giardia* and cryptosporidia were negative, as was PCR for *Tritrichomonas fetus.*

**Histopathologic Description:** Liver: Multifocally disrupting the hepatic parenchyma are low numbers of randomly scattered, variably sized foci of lytic necrosis characterized by loss of normal hepatic architecture and replacement by karyorrhectic debris, eosinophilic fibrillar material (fibrin), scattered erythrocytes and occasional degenerate neutrophils. Hepatocytes around the margins of necrotic foci are often swollen with vesicular nuclei and vacuolated cytoplasm (degenerate). Moderate numbers of neutrophils, macrophages and fewer lymphocytes separate foci of necrosis from the surrounding normal hepatic parenchyma. Smaller foci of similar inflammatory cells without significant central necrosis are also scattered throughout. Faintly visible, slender, 4-20 μm long bacilli are rarely visible arranged in sheaves and stacks within degenerate and intact hepatocytes surrounding foci of inflammation and necrosis.

PROXIMAL COLON: The mucosa is multifocally eroded, with affected areas overlain by mats of bacteria admixed with karyorrhectic debris, mucin and degenerate neutrophils. Enterocytes are multifocally hypereosinophilic, rounded up and dissociated with pyknotic nuclei (necrosis). There is diffuse goblet cell hyperplasia. Colonic crypts contain excess mucin within which large numbers of faintly basophilic bacilli are often visible. In addition crypts multifocally contain karyorrhectic debris and degenerate neutrophils (crypt abscesses). Crypt enterocytes are multifocally crowded, with slightly basophilic cytoplasm, vesicular nuclei and increased mitotic figures (regeneration). Moderate numbers of neutrophils and macrophages and fewer lymphocytes and plasma cells diffusely expand the lamina propria, multifocally extend into the submucosa, and rarely infiltrate the tunica muscularis.

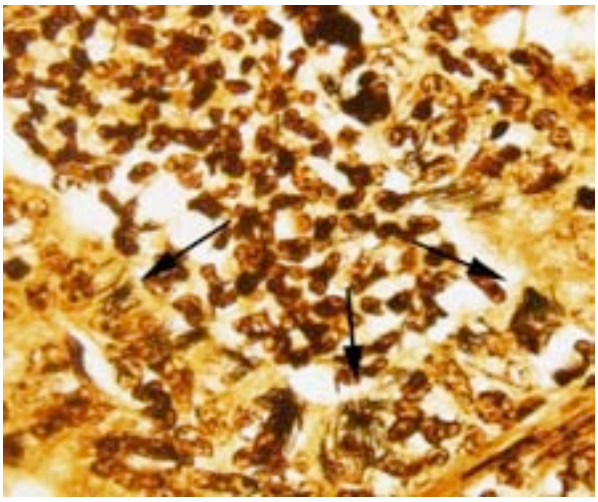

*1-4. Colon, kitten: Clusters of C. piliforme are present within glandular epithelium lining crypt abscesses. (Warthin-Starry 4.0, 600X)*

OTHER TISSUES (not present on submitted slides): Similar, but less severe lesions to those in the colon are present in sections of ileum. A small focus of myocardial necrosis and neutrophil infiltration disrupts the left ventricular myocardium. Alveoli within the lungs diffusely contain lightly eosinophilic homogeneous material (oedema).

SPECIAL STAINS: Low to moderate numbers of slender, silver positive, 4-20 μm long bacilli arranged in criss-crossed stacks are visible within hepatocytes surrounding foci of necrosis in the liver on Warthin-Starry stained sections. The bacteria are difficult to discern with Gram stain. Myriad silver positive, 4-20μm long bacilli arranged in sheaves and crisscrossed stacks are visible within colonic crypts and within crypt enterocytes, and occasionally within the lamina propria on Warthin-Starry stained sections.

**Contributor's Morphologic Diagnosis:**

LIVER: Moderate, subacute, multifocal, necrotizing and suppurative hepatitis with intracellular argyrophilic bacilli.

COLON: Severe, subacute, multifocal, necrotizing and suppurative colitis with crypt abscesses, goblet cell hyperplasia and myriad intralesional argyrophilic bacilli.

**Contributor's Comment:** Based on the characteristic lesions in the liver, intestinal tract and heart and intralesional argyrophilic bacteria, Tyzzer's disease was diagnosed as the cause of death in this kitten.

Tyzzer's disease is a commonly fatal disease of primarily young animals caused by the gram-negative anaerobe *Clostridium piliforme*. Spontaneous disease is reported in a range of wild[9,10] and domestic[4,5,6] species, but is particularly well-recognized in laboratory animals (mice, rats, rabbits, gerbils, hamsters and guinea pigs)[8] and foals.[1] Rare cases are reported in cats.[4,7] Disease usually occurs as isolated cases or epizootics with low morbidity and high mortality. Antemortem clinicopathologic findings vary between species. Reports in kittens describe diarrhea, emaciation and depression,[4] while foals developed lethargy, recumbency, fever and seizures, metabolic acidosis, hypoglycemia and increased liver enzymes.[1] Definitive diagnosis is often possible based on characteristic gross and histologic lesions, with silver-positive bacterial rods visible in histological sections of affected liver. Serological tests, PCR and EM have also been utilized in the diagnosis.[1,4,5,9] The organism is extremely fastidious and culture is unrewarding.[7]

Among rodents, B6 mice are resistant to infection compared to CBA/N and DBA/2 mice, and B-lymphocyte function appears to be particularly important in disease resistance.[8] Infected rats may develop a characteristic megaloileitis.[8] Gerbils are recognized to be highly susceptible to Tyzzer's disease and are a useful sentinel animal to detect its presence in research facilities.[8] In rabbits, outbreaks are characterized by profuse diarrhea and high mortality among weanlings. Surviving animals may develop stenosis of the intestinal tract.[8]

The pathogenesis of Tyzzer's disease is only partially elucidated. It is thought that rodents and rabbits may be an important source of infection through shedding of spores in feces.[8,12] The spores may remain infective in contaminated environments for up to a year.[8] Ingested spores are carried through the digestive tract into the small intestine and are able to penetrate mucosal epithelial cells and replicate within them.[12] Bacteria may reach the liver by penetrating capillaries within the lamina propria that drain into the portal venous system, or within macrophages (leukocyte trafficking).[12] Once in the liver, the bacteria penetrate sinusoidal

endothelial cells and adjacent hepatocytes and replicate within them.[12] Lysis of infected cells results in the characteristic areas of lytic necrosis, which may be seen grossly as multiple 2-3mm yellow-grey foci scattered throughout the hepatic parenchyma.[8,12]

Predisposing factors are an important consideration and are frequently reported in cases of Tyzzer's disease.[3,4,6,8] Stress associated with weaning, overpopulation, poor hygiene, immunosuppression due to disease or corticosteroid treatment, and concurrent infections are possible contributing factors.[8] Kittens with Tyzzer's disease in one report were co-infected with feline panleukopenia virus.[4] In reports of Tyzzer's disease in dogs, previous or concurrent infection with distemper, parvovirus and coccidia were described and likely contributed to susceptibility to Tyzzer's.[3,6]

No significant concurrent disease processes were noted in the present case, but the history of diarrhea and recovery in other kittens from the pet store suggest the possibility of an underlying infectious enteritis that was not detected by routine diagnostic screening. The stress of transport and re-homing, housing conditions and access to rodent feces may also have been factors in disease susceptibility, as kittens came from various sources and were housed in cages adjacent to rodents and rabbits. The two other kittens from the pet store that died "suddenly" may also have had Tyzzer's disease; however, no diagnostics were undertaken on those kittens, so other causes of death cannot be ruled out.

Prevention of death from Tyzzer's disease involves maximizing nutritional status, maintaining adequate hygiene of rearing areas, vaccination to prevent predisposing disease conditions, controlling wild rodents, management of parasite burdens, and prompt intensive care of affected individuals.[1,8]

**JPC Morphologic Diagnosis:** 1. Liver: Hepatitis, necrotizing, multifocal, random, with numerous intracytoplasmic filamentous bacilli. 2. Colon: Colitis, necrotizing, diffuse, moderate, with mild mucosal hyperplasia and numerous intracytoplasmic filamentous bacilli.

**Conference Comment:** The contributor does an excellent job of highlighting important characteristics of Tyzzer's disease, a diagnosis more commonly assigned to rodents or foals. The liver is the principle target of the bacteria with hepatic necrosis evident regardless of species. Intestinal involvement is variable, but colitis with crypt abscesses is a common component with this disease in cats.[2] Conference participants briefly discussed the merits of using the term "crypt abscess" in the colon, with most favoring it as an accurate term throughout the intestinal tract albeit with the reminder that it actually refers to exfoliated epithelial cells admixed with fewer inflammatory cells.[2]

Necrotizing colitis in kittens is much more common than the occurrence of Tyzzer's disease in this species, thus participants also reviewed the more typical etiologies often associated with this lesion. *Tritrichomonas foetus* causes persistent large-bowel diarrhea in cats less than 1 year of age, with chronic colitis and variably apparent crescent-shaped organisms being the corresponding histologic findings.[2] Although feline panleukopenia virus (FPV, feline parvovirus) more commonly causes small intestinal disease, colonic lesions may also be involved. Feline leukemia virus can cause cryptal necrosis similar to FPV. The small gram-negative bacteria, *Anaerobiospirillum* is associated with ileocolitis in cats in which it causes crypt abscesses and may lead to septicemia or renal failure.[2]

**Contributing Institution:** Massey University, New Zealand

**References:**

1. Borchers A, Magdesian KG, Halland S, Pusterla N, Wilson WD. Successful treatment and polymerase chain reaction (PCR) confirmation of Tyzzer's disease in a foal and clinical and pathologic characteristics of 6 additional foals (1986-2005). *J Vet Intern Med.* 2006;20:1212-8.
2. Brown CC, Baker DC, Barker IK. Alimentary system. In: Maxie MG, ed. *Jubb, Kennedy, and Palmer's Pathology of Domestic Animals.* 5th ed. Vol. 2. Philadelphia, PA: Elsevier Saunders; 2007;114, 227, 278-279.
3. Headley SA, Shirota K, Baba T, Ikeda T, Sukura A. Diagnostic exercise: Tyzzer's disease, distemper, and coccidiosis in a pup. *Vet Pathol.* 2009;46:151-4.
4. Ikegami T, Shirota K, Goto K, Takakura A, Itoh T, Kawamura S, et al. Enterocolitis associated

with dual infection by Clostridium piliforme and feline panleukopenia virus in three kittens. *Vet Pathol*. 1999;36:613-5.
5. Ikegami T, Shirota K, Une Y, Nomura Y, Wada Y, Goto K, et al. Naturally occurring Tyzzer's disease in a calf. *Vet Pathol.* 1999;36:253-5.
6. Iwanaka M, Orita S, Mokuno Y, Akiyama K, Nii A, Yanai T, et al. Tyzzer's disease complicated with distemper in a puppy. *J Vet Med Sci.* 1993;55:337-9.
7. Kovatch RM, Zebarth G. Naturally occurring Tyzzer's disease in a cat. *J Am Vet Med Assoc.* 1973;163:136-8.
8. Percy DH, Barthold SW. Pathology of Laboratory Rodents and Rabbits. 3rd edition, Blackwell Publishing, Ames, Iowa: 2007;57-8, 138-40, 187-8, 208, 225-6, 271-3.
9. Raymond JT, Topham K, Shirota K, Ikeda T, Garner MM. Tyzzer's disease in a neonatal rainbow lorikeet (*Trichoglossus haematodus)*. *Vet Pathol.* 2001;38:326-7.
10. Simpson VR, Hargreaves J, Birtles RJ, Marsden H, Williams DL. Tyzzer's disease in a Eurasian otter (*Lutra lutra)* in Scotland. *Vet Rec.* 2008;163:539-43.
11. Young JK, Baker DC, Burney DP. Naturally occurring Tyzzer's disease in a puppy. *Vet Pathol.* 1995;32:63-5.
12. Zachary JF. Mechanisms of microbial infections. In: Zachary JF, McGavin DM, eds. Pathologic Basis of Veterinary Disease. 5th ed. St. Louis, MO: Elsevier Mosby; 2012:174.

**CASE II:** B2944 (JPC 4041409)

**Signalment:** 9-year-old neutered male domestic short hair feline (*Felis cattus*).

**History:** This cat presented with a chronic history of inappetence, lethargy, weight loss and inappropriate defecation. Physical examination revealed a thin cat and abdominal palpation identified a firm, irregular mass present in the caudal abdomen. Biochemistry and hematology samples were obtained and analyzed but were largely unremarkable. Abdominal ultrasonographic evaluation was performed which revealed a large mass in the descending colon. The colonic mass was identified and resected during exploratory laparotomy. Fine needle aspirates of the enlarged mesenteric lymph nodes adjacent to the mass revealed a mixed cellular population consistent with a reactive lymph node. The surgery and recovery period went well without any complications.

**Gross Pathology:** A solid mass measuring 2.5 x 3.5 x 1.5cm focally expanded the colonic wall. The cut surface was characterised by firm, white tissue which extended into and partially occluded the colonic lumen.

**Laboratory Results:** Cobalamin levels were within normal limits, but the folate levels were slightly decreased, at 8.1 µg/L (reference 13.4-38 µg/L).

**Histopathologic Description:** Colon: An unencapsulated, moderately cellular, infiltrative, exophytic mesenchymal mass markedly expands and effaces the mucosa and submucosa, compressing adjacent mucosa and extending into and largely occluding the colonic lumen. Multifocally, the neoplasm infiltrates and destroys the underlying tunica muscularis and extends to the serosa. The neoplastic fusiform or polygonal cells are arranged in sheets and interlacing streams and bundles supported by a fibrovascular stroma. The cells have indistinct borders and contain moderate amounts of eosinophilic fibrillar cytoplasm. They contain a single oval to elongate nucleus, finely stippled chromatin and 1-2 distinct nucleoli. Six mitotic figures are observed in 10 HPFs. There is moderate anisocytosis, moderate to marked anisokaryosis and moderate cellular pleomorphism. Occasional karyomegalic cells are observed. The surface of the exophytic mass is widely ulcerated and replaced by abundant fibrin embedded with necrotic debris, degenerating neutrophils and myriad bacterial colonies.

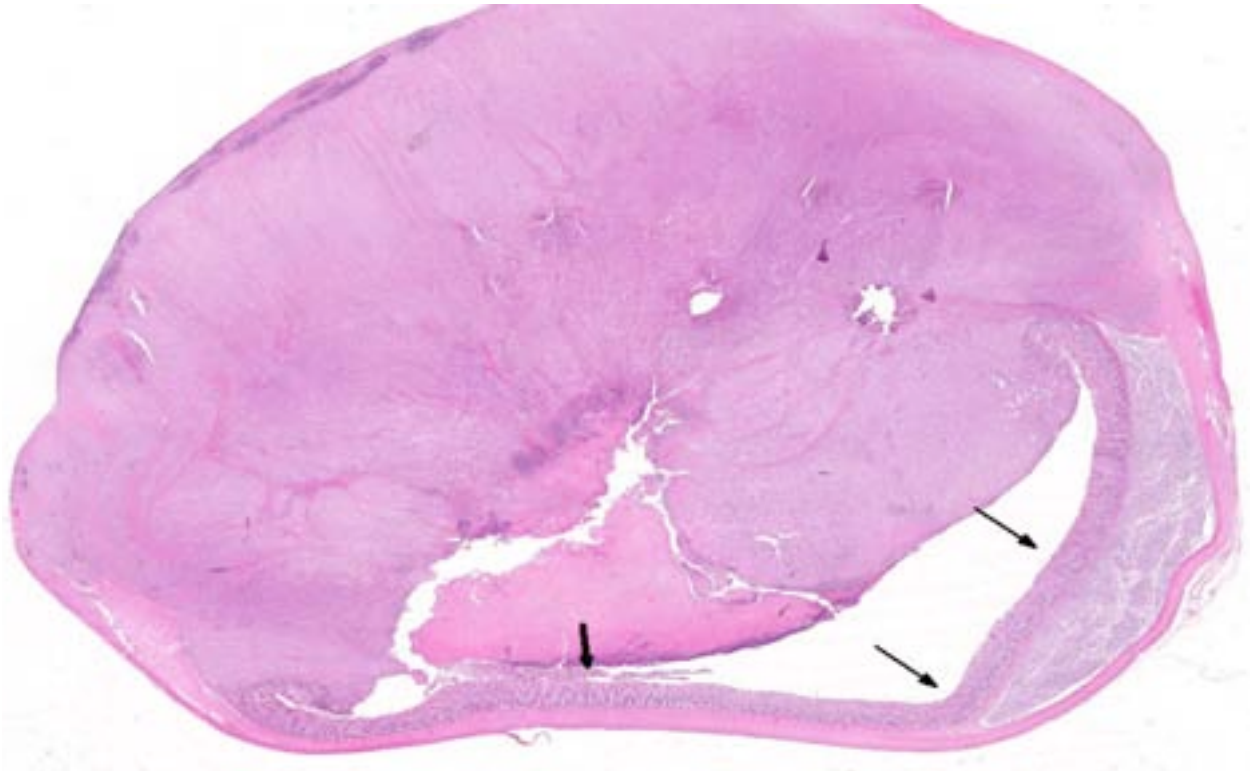

*2-1. Colon, cat: The colon is asymmetrically and transmurally expanded and effaced by a large infiltrative mesenchymal neoplasm. (HE 3X)*

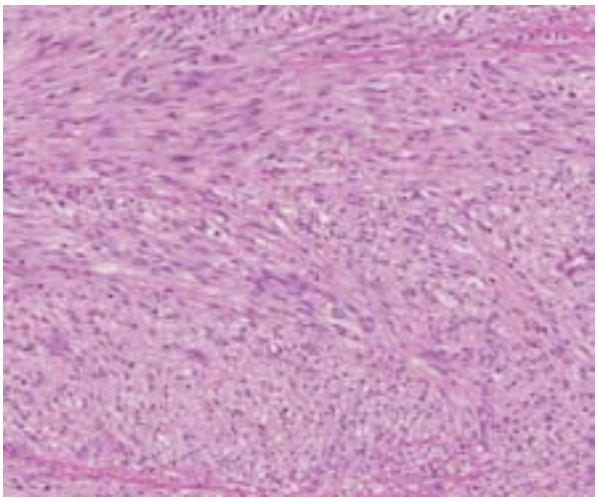

*2-2. Colon, cat: Neoplastic cells are spindled and elongate, and arranged in broad streams and bundles on a fine fibrous matrix. (HE 116X)*

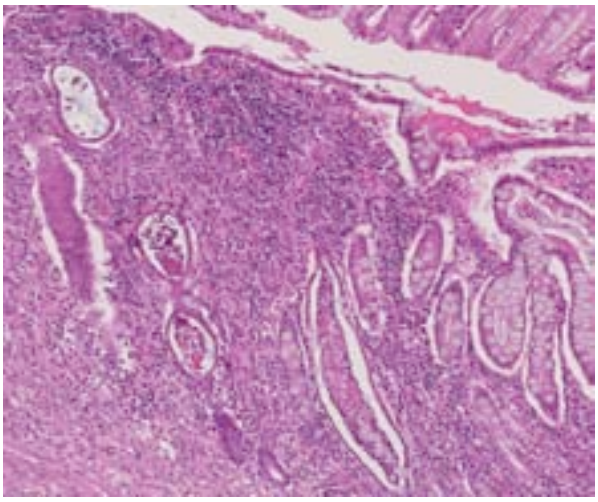

*2-3. Colon, cat: The neoplasm infiltrates and replaces the mucosa, and remaining glands are dilated and filled with necrotic debris (crypt abscesses). (HE 77X)*

Multifocally, small to moderate nodular aggregates of lymphocytes border the neoplastic mass.

The neoplastic cells did not express alpha smooth muscle actin. Additional tissue sections were immunohistochemically stained for CD117 (c-KIT) and revealed scattered neoplastic cells exhibiting weak to moderate CD117 (c-KIT) positivity.

**Contributor's Morphologic Diagnosis:** Colon: Gastrointestinal stromal tumor, intermediate to high grade.

**Contributor's Comment:** Lymphoma and mast cell tumors are the most frequently encountered types of haematopoietic neoplasia in the feline intestine and adenocarcinomas are the most commonly described non-hematopoietic neoplasm.[9,13] Gastrointestinal stromal tumors (GISTs) account for the majority of mesenchymal tumors in the human gastrointestinal tract.[6,13] They have been previously reported in the dog, ferret, horse and nonhuman primate, however, GISTs are rarely described in cats.[13,6,7]

GISTs are described as a distinctive group of primary mesenchymal gastrointestinal tumors assumed to be derived from the interstitial cells of Cajal (ICC) or their progenitor stem cells.[12] Immunohistochemistry has enabled their recognition as a unique group of gastrointestinal mesenchymal tumours by their cytoplasmic immunoreactivity for c-KIT protein (CD117).[12]

CD117 (KIT) protein is a transmembrane growth factor receptor belonging to the tyrosine kinase family whose ligand is the stem cell factor.[6,13] In the gastrointestinal tract immunohistochemical identification of the CD117 antigen is consistently demonstrable in the ICC (myofibroblasts). These cells are the autonomic nerve-related GI pacemaker cells dispersed between the intestinal smooth muscle cells that co-ordinate intestinal motility and peristalsis.[4,12,13]

Prior to their immunohistochemical characterization, GISTs were classified as leiomyomas, leiomyosarcomas, leioblastomas or schwannomas based on their histological appearance and apparent origin from the tunica muscularis.[13] It is now suggested that these ICC are the histogenic origin of the neoplastic mesenchymal cells in GISTs due to their immunohistochemical similarity producing diffuse strong cytoplasmic expression of CD117.[13,6] The variability in histologic appearance is likely due to different pathways of differentiation within these tumours.

GISTs are more frequently observed in the intestinal tract of the veterinary companion animals, in particular the cecum in horses in comparison to humans where the stomach is the most common site of origin.[4,6,7,13] In a prior study in dogs, GISTs occurred in older animals with no overt sex predisposition and a relatively low incidence of metastasis.[5]

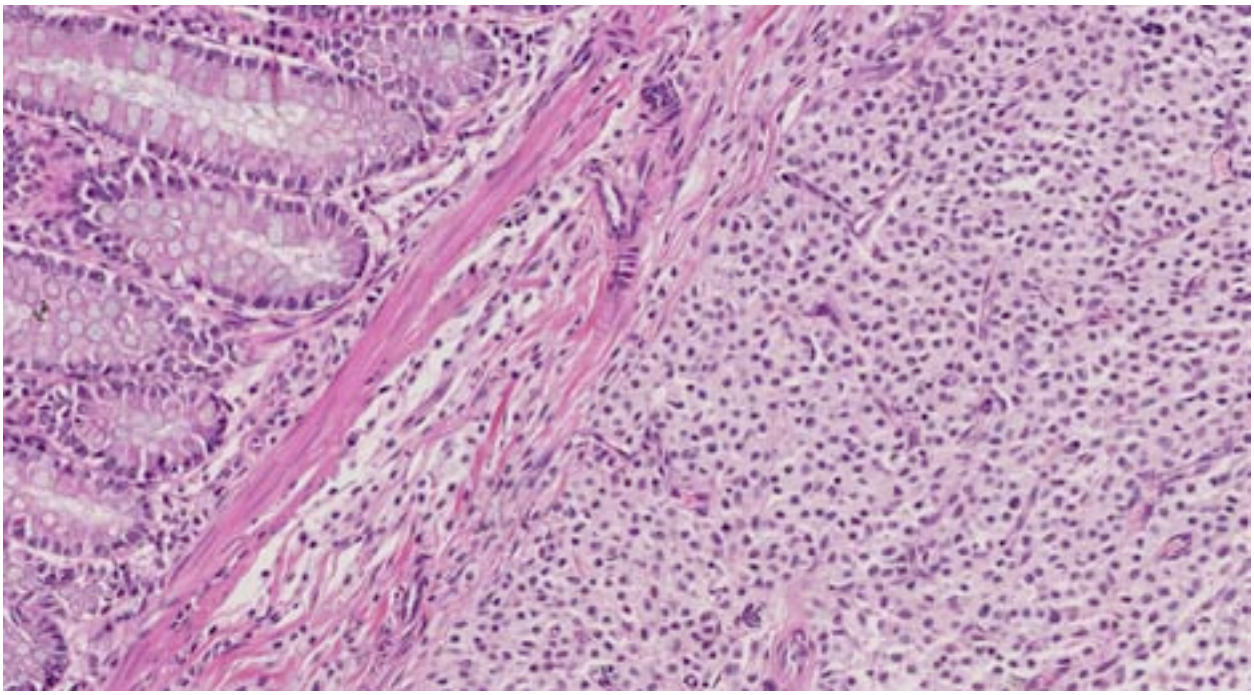

*2-4. Colon, cat: A second neoplasm composed of well-differentiated mast cells expands the submucosa. (HE 164X)*

In humans, GISTs tend to be more densely cellular than smooth muscle tumors and several histological patterns have been identified of which the most commonly described is the spindloid pattern composed of fusiform cells arranged in whorls or interlacing fascicles or whorls with elongated or cigar-shaped nuclei with perinuclear vacuoles.[14] Less commonly observed is the polygonal or epithelioid variant.[14]

These tumors can express CD34 and SMA in addition to the more consistent expression of CD117 and vimentin.[7] Desmin and S-100 are usually not expressed.[13] In contrast leiomyomas are typically positive for SMA and desmin which are markers of smooth muscle differentiation. These tumors do not express CD117 and usually have an indolent course.[6] Tumors that do not express SMA or CD117 have been described as GIST-like tumors.[11,12]

Prior reports of canine, equine and feline GISTs are histologically and immunohistochemically comparable with the human spindloid variant.[4,13] Smooth muscle differentiation resulting in the co-expression of SMA in some tumours supports the hypothesis that GISTs develop from a pluripotential ICC or its progenitor cell type which can differentiate into smooth muscle cells.[4,13]

Alteration of the gene encoding the tyrosine kinase receptor KIT is considered an early molecular event in the development of GISTs.[13] This enables ligand-independent receptor activation and subsequent signal transduction leading to cellular proliferation.[6] In human, canine and feline GISTs the majority of mutations have been identified in the juxtamembrane domain (exon 11) of the gene.[6,13] These KIT mutations are potential targets for therapeutic invention with tyrosine kinase inhibitors.[13]

It is difficult to determine the degree of malignancy of GISTs as their biological behaviour is not well characterised in animals.[13] In this case, following diagnosis, the cat was treated with toceranib phosphate (Palladia) for 10 months with no recurrence or metastatic spread of the tumor 2 years after surgical resection.

**JPC Morphologic Diagnosis:** 1. Colon: Gastrointestinal stromal tumor. 2. Colon: Mast cell tumor, well-differentiated.

**Conference Comment:** As occasionally occurs with WSC submissions, the serial sectioning of 180+ slides may uncover distinctive pathologic processes which were not originally identified by the contributor. In this example, some conference participants had, in addition to the described

GIST, a well-circumscribed, densely cellular neoplasm composed of round cells which separates the muscular layers of the colon from the submucosa. The neoplastic cells have faintly granular cytoplasm, a centrally-placed nucleus, and stain multifocally for CD117 which is most indicative of a mast cell tumor. As the contributor outlines, mast cell tumors are quite common within the intestine of cats, accounting for the third most frequently encountered neoplasm within this location.[10]

The contributor thoroughly discusses the immunohistochemical characteristics of GISTs, which became important in their differentiation from tumors of muscle origin. Although these are typically discovered as incidental findings at necropsy[4], this case portrays the magnitude to which these tumors can grow and cause functional obstructions as observed clinically in this cat. They have also been reported to induce paraneoplastic hypoglycemia by their production of insulin-like growth factors and erythrocytosis from their production of erythropoietin.[3]

An abdominal mass in the cat must also include the non-neoplastic lesion, eosinophilic sclerosing fibroplasia, as a possible differential which may also lead to obstructive clinical signs. This mass of eosinophils, fibroblasts and collagen may be found throughout the gastrointestinal tract in cats of all ages. It is hypothesized this is an inflammatory response to a bacteria and may be related to the cat's affection for recruiting eosinophils in other dermatologic and oral conditions known collectively as the eosinophilic granuloma complex.[5]

**Contributing Institution:** Royal Veterinary College
Dept Pathology and Pathogen Biology
Hawkshead Lane, North Mymms, Herts
UK AL9 7TA
www.rvc.ac.uk

**References:**

1. Atzwanger BL, Fletcher JA, Fletcher CD. Gastrointestinal stromal tumors. Virchows Arch 456:111-127, 2010.
2. Bettini G, Morini M. Marcato P. Gastrointestinal spindle cell tumors of the dog: Histological and immunohistochemical study. *J Comp Path*. 2003;129:283-293.
3. Brown C, Baker D, Barker I. Alimentary system. In: Maxie MG, ed. *Jubb, Kennedy, and Palmer's Pathology of Domestic Animals*. 5th edition. Vol. 2. 2007;127-128.
4. Cooper BJ, Valentine BA. Tumors of muscle. In: Meuten DJ, ed. *Tumors in Domestic Animals*. 4th ed. 2002;328-333.
5. Craig LE, Hardam EE, Hertzke DM, Flatland B, Rohrbach BW, Moore RR. Feline gastrointestinal eosinophilic sclerosing fibroplasias. *Vet Pathol.* 2009;46:63-70.
6. Frost D, Lasota J, Miettinen M. Gastrointestinal stromal tumors and leiomyomas in the dog: A histopathologic, immunohistochemical and molecular genetic study of 50 cases. *Vet Pathol.* 2003;40:42-54.
7. Gillespie V, Farrelly K, Craft D, Luong R. Canine gastrointestinal stromal tumors: Immunohistochemical expression of CD34 and examination of prognostic indicators including proliferation markers Ki67 and AgNOR. *Vet Pathol*. 2011;48:283-291.
8. Hanazono, K, Fukumoto S and Hirayama K. Predicting metastatic potential of gastrointestinal stromal tumors in dog by ultrasonography. *J Vet Med Sci*. 2012;74:1477-1482.
9. Head KW, Else RW, Dubielzig RR. Tumors of the alimentary tract. In: Meuten DJ, ed. *Tumors in Domestic Animals*. 4th edition. 2002;461-476.
10. Henry C, Herrera C. Mast cell tumors in cats. *J Fel Med Surg.* 2013;15:41-47.
11. Luc A, Prata D, Huet H, Lagadic M, Bernex F. A KIT positive gastrointestinal stromal tumor in a ferret (Mustela putorius furo). *J Vet Diagn Invest*. 2009;21:915-917.
12. Maas C, Haar G, Gaag I. Reclassification of small intestinal and caecal smooth muscle tumors in 72 Dogs: Clinical, histologic, and immunohistochemical evaluation. *Veterinary Surgery*. 2007;36:302-313.
13. Morini M, Gentilini F, Spadari A. Cytological, immunohistochemical and mutational analysis of a gastric gastrointestinal stromal tumor in a cat. *J Comp Path*. 2011;145:152-157.
14. Morini M, Bettini G, Preziosi R, Mandrioli L. C-kit gene product (CD117) immunoreactivity in canine and feline paraffin sections. *Journal of Histochemistry & Cytochemistry*. 2004;52:705–708.

**CASE III:** 12-8651 (JPC 4032480)

**Signalment:** 4-year-old intact male miniature Schnauzer dog *(Canis familiaris)*.

**History:** The dog had experienced some weight loss in the past several months. Firm nodules were palpated on the testicles. The referring veterinarian submitted the testicles to rule out infection and neoplasia.

**Gross Pathology:** At castration surgery the testes and epididymis were thickened by white material. Both testicles were submitted for histopathology. At sectioning, multiple cystic nodules were present within the tunics.

**Laboratory Results:** None.

**Histopathologic Description:** Both testicles were equally affected. The testicular cords (between the pampiniform plexus and spermatic duct), tunica albuginea and the stroma of the epididymis were multifocally expanded by many cross sections of variably sized and variably degenerate acoelomate larvae within cystic spaces lined by either streams of fibrous connective tissue or a thick bands of inflammatory cells. Cestode larvae ranged from 1,000 x 600 µm to 1,600 to 900 µm and had thick (45 µm), convoluted hyaline cuticles overlying single layers of palisading epithelial cells. Within the loose mesenchymal parenchyma digestive tracts were not observed, and there were numerous, 50 x 40 µm, oval to pleomorphic, clear vesicles with widely scattered, small, weakly basophilic concretions (calcareous corpuscles). No scolices were observed. Inflammatory infiltrates flanking parasites were composed of moderate numbers of lymphocytes, plasma cells, epithelioid macrophages, neutrophils and eosinophils; granulocytes were predominantly within areas of degenerating larvae. Within the testicular parenchyma spermatogenesis was present; epididymal ducts were histologically within normal limits and contained some sperm.

**Contributor's Morphologic Diagnosis:** Periorchitis, epididymitis and funiculitis, lymphohistiocytic and pyogranulomatous, severe, bilateral and multifocal, chronic with intralesional cestode larvae (most likely *Mesocestoides* sp.).

**Contributor's Comment:** Mesocestoides spp. are tapeworm parasites with unusual 3 host life cycles.[7] The first intermediate hosts are purported to be coprophagous insects, which are ingested by a variety of small reptiles and rodents. Within the second intermediate host, the metacestode, called a tetrathyridium, penetrates the intestinal wall and undergoes asexual replication within the peritoneal cavity. Ingestion of the second host by the definitive host completes the life cycle; infection with adult *Mesocestoides* are largely asymptomatic. Proglottids from adult parasites are not directly infectious to definitive or secondary intermediate host species.[7] Definitive hosts are mainly wild and domestic canids, although

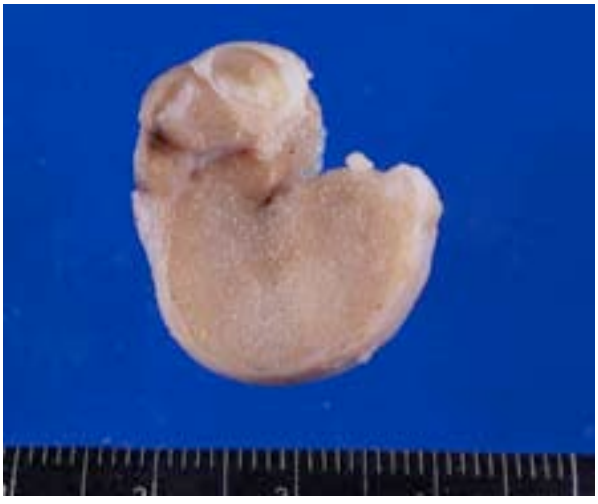

*3-1. Testis, dog: At sectioning, multiple cystic nodules were present within the vaginal tunics. (Photo courtesy of: Department of Veterinary Microbiology and Pathology, College of Veterinary Medicine, Washington State University, Pullman, WA 99164-7040, www.vetmed.wsu.edu)*

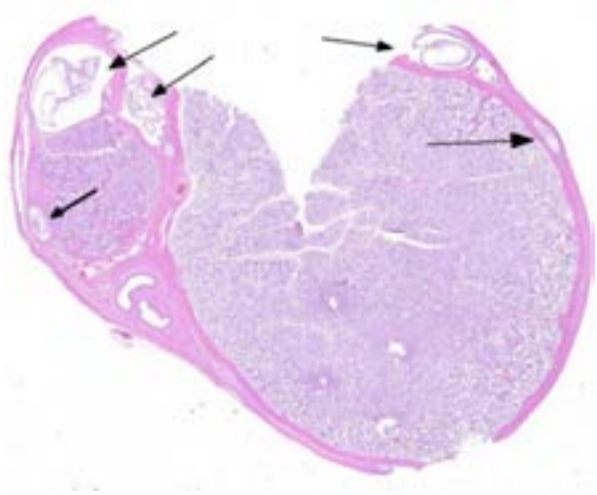

*3-2. Testis, dog: Within the vaginal tunics, there are numerous cross sections of degenerating cestode parasites. (HE 0.63X)*

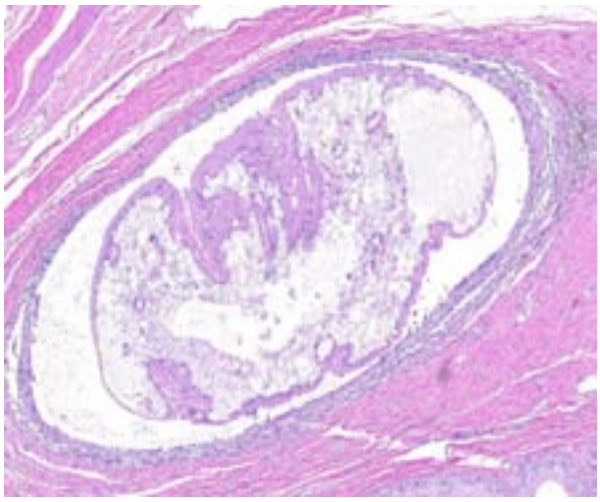

*3-3. Testis, dog: Degenerating cestode paraasites are surrounded by a dense fibrous capsule which is lined by epithelioid macrophages, lymphocytes, and plasma cells. (HE 120X)*

multiple species, including humans[5], can become infected. Distribution of the parasites is worldwide. Veterinary interest in the species is largely related to rare migration of ingested tetrathyridia into the abdominal cavity of domestic dogs and occasionally cats.[12] The subsequent prolific asexual reproduction of metacestodes and the ensuing severe granulomatous peritonitis has been termed canine peritoneal larval cestodiasis (CPLC).[2] In rare cases, parasites extend into abdominal organs and into the thoracic cavity.[11] It is not known whether CPLC truly represents aberrant migration of tetrathyridia through the intestinal wall after ingestion of the second intermediate host, or if it represents aberrant use of the dog as a secondary intermediate host after accidental ingestion of the first intermediate host.[2]

Diagnosis and treatment of CPLC can be challenging. Clinical signs are vague and include lethargy, weight loss, vomiting and ascites.[4] Occasionally subclinical cases are identified during routine ovariohysterectomy or castration.[2] In two reported cases, scrotal swelling was among the initial presenting complaints.[10,13] Diagnostic procedures include radiology, showing changes indicative of diffuse peritonitis, and ultrasonography.[12] Cytologic examination of the ascites fluid or aspiration of affected organs often reveals intact tetrathyridia, acephalic forms or calcareous corpuscles.[3,9] Diagnosis of infection by *Mesocestoides* spp. can be confirmed by morphologic identification of tetrathyridia or by PCR.[2] Recommended treatment involves

| COMMON VETERINARY CESTODE SPECIES | | |
|---|---|---|
| **ADULT** | **LARVA** | **SPECIES WITH ASSOCIATED PATHOLOGY** |
| *Spirometra spp.* | *Sparganum (Plerocercoid)* | Dog, Cat |
| *Mesocestoides spp.* | *Tetrathyridium* | Dog, Cat, NHPs |
| *Rodentolepis nana, R. microstoma, Hymenolepis diminuta* | *Cysticercus* | Rodent |
| *Taenia taeniaformis* | *Cysticercus fasciolaris* | Rodent |
| *Taenia pisiformis* | *Cysticercus pisiformis* | Rabbit, Dog |
| *Taenia hydatigena* | *Cysticercus tenuicollis* | Ruminants, Swine |
| *Taenia ovis* | *Cysticercus ovis* | Sheep |
| *Taenia saginata* | *Cysticercus bovis* | Cattle |
| *Taenia solium* | *Cysticercus cellulosae* | Swine |
| *Taenia multiceps* | *Coenurus cerebralis* | Sheep, Goat |
| *Moniezia spp., Thysaniezia giardi, Stilesia globipunctata* | *Cysticercus* | Ruminant |
| *Anoplocephala perfoliata* | *Cysticercus* | Horse |
| *Diphyllobothrium spp.* | *Cysticercus* | Fish-eating carnivore |
| *Diplydium caninum* | *Cysticercus* | Dog, Cat |
| *Echinococcus granulosus* | *Hydatid cysts* | Many |
| *Echinococcus multilocularis* | *Hydatid cysts* | Many |

peritoneal lavage and long term treatment with fenbendazole[4] although other drugs, such as praziquantel, have also been used.[8] Prognosis after treatment depends upon the severity of infection at the time of diagnosis and upon how aggressively therapy is instituted.[2] At least some dogs experience recrudescence months after therapy is discontinued, although reinfection cannot be ruled out.[1] The dog in this report had a massive peritoneal infection and was treated aggressively with lavage and 30 days of fenbendazole therapy. Four months after initial diagnosis he presented with vomiting and radiographic evidence of intestinal obstruction. Partial necropsy after euthanasia revealed massive abdominal adhesions, but no samples for histopathology were collected; whether adhesions

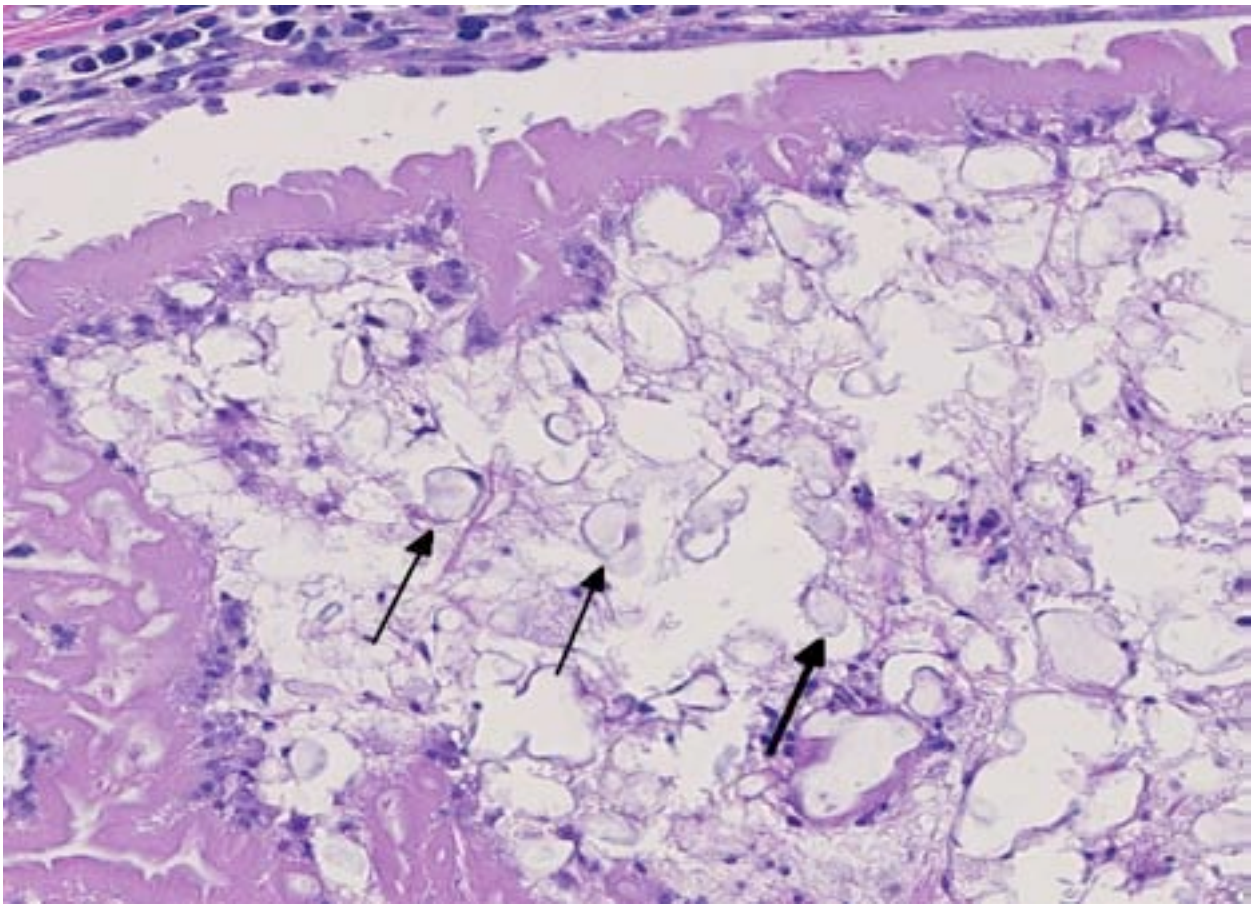

*3-4. Testis dog: Degenerating cestodes have a thick, smooth tegument, subjacent layer of somatic cells, a spongy parenchymatous body cavity, with numerous calcareous corpuscles (arrows). (HE 284X)*

represented complications of healing peritonitis or recurrence of cestodiasis was not determined.

Although PCR to confirm *Mesocestoides* infection was not performed in this case, histologic lesions were consistent with previously reported cases. Characteristics of cestodes include a thick cuticle, acoelomate body and numerous calcareous corpuscles.[6] Although most of the metacestodes were degenerate, examination of multiple sections failed to reveal definitive scolices or suckers; it is likely, therefore that most of the organisms in this dog were the acephalic forms. Both tetrathyridia and acephalic forms have been described in cases of CPLC.[4]

**JPC Morphologic Diagnosis:** Testes, vaginal tunic: Larval cestodes, multiple, with mild granulomatous periorchitis.

**Conference Comment:** With the poor preservation of the larval cestodes in most sections, conference participants struggled to assign a specific etiologic diagnosis to this case. The presence of calcareous corpuscles indicates that the parasites are cestodes, few species of which are present specifically in the vaginal tunics, an extension of the peritoneum. R. *Spirometra* spp. is a cestode which may encyst in the peritoneal cavity of carnivores. Its larval form, sparganum, is also solid-bodied and only differentiated from the tetrathyridium of *Mesocestoides* spp. by its lack of suckers or scolex.[6] Obtaining definitive evidence of suckers or a scolex requires serial sections through a well-preserved organism, thus we favored the diagnosis of proliferating larval cestodes in this example.

The class of flatworms (*Platyhelminthes*) referred to as cestodes are more commonly known as tapeworms, and infect nearly every vertebrate species. Cestodes typically inhabit the gastrointestinal tract, to include the ducts of the liver and pancreas. They are generally of minor significance to the animal though they may reach

spectacular size in some species (Consider the 60-foot long, *Diphyllobothrium latum* of man!). All tapeworms utilize at least two hosts to complete their lifecycle, and as the contributor concisely describes, some such as *Mesocestoides* spp. require more.

Adult cestodes are segmented into proglottids and both larvae and adults often contain suckers or hooks. All contain calcareous corpuscles which are of unknown function but most helpful in initially classifying the organism as a cestode. In this case, the corpuscles are shrunken and surrounded by a clear space which is likely a commonly observed artifact of fixations. *Spirometra* falls into the category with *Diphyllobothrium* of Pseudophyllideans. *Mesocestoides* are grouped with other common veterinary parasites such as *Taenia, Hymenolepis,* and *Echinococcus* in the Cyclophyllidean category characterized by four anterior suckers and muscles separating medullary and cortical regions.[6]

Since nearly all adult tapeworms are parasites of the digestive tract, those observed in tissue sections are usually larva. Along with the discussed sparganum and tetrathyridium larvae, most other larval forms have specific nomenclature. Pairing the appropriate larval and adult tapeworm species together can be an overwhelming challenge, though a focus on the following cestodes may cover those of greatest importance in veterinary pathology.

**Contributing Institution:** Department of Veterinary Microbiology and Pathology
College of Veterinary Medicine
Washington State University
Pullman, WA 99164-7040
www.vetmed.wsu.edu

**References:**

1. Barsanti JA. Mesocestoides infections: Recurrence or reinfection? *JAVMA*. 1999;214:478.
2. Boyce W, Shender L, Shultz L, et al. Survival analysis of dogs diagnosed with canine peritoneal larval cestodiasis (*Mesocestoides* spp.) *Vet Parasitol.* 2011;180:256-261.
3. Caruso KJ, James MP, Paulson RL, et al. Cytologic diagnosis of peritoneal cestodiasis in dogs caused by *Mesocestoides* sp. *Vet Clin Path*. 2003;32:50-60.
4. Crosbie PR, Boyce WM, Platzer EG, et al. Diagnostic procedures and treatment of eleven dogs with peritoneal infections caused by *Mesocestoides* spp. *JAVMA*. 1998;213:1578-1583.
5. Fuentes MV, Galan-Puchades MT, Malone JB. A new case report of human *Mesocestoides* infection in the United States. *Am J Trop Med Hyg*. 2003;68:566-567.
6. Gardiner CH, Boynton SL. An Atlas of Metazoan Parasites in Animal Tissues. Armed Forces Institute of Pathology/ American Registry of Pathology. Washington, DC. 2006:50-55.
7. Padgett KA, Boyce WM. Life history studies in two molecular strains of *Mesocestoides* (Cestoda: Mesocestoidae): Identification of sylvatic hosts and infectivity of immature life stages. *J Parasitol.* 2004;90:108-113.
8. Papini R, Matteini A, Bandinelli P, et al. Effectiveness of praziquantel for treatment of peritoneal larval cestodiasis in dogs: A case report. *Vet Parasitol.* 2010;170:158-161.
9. Patten PK, Rich LF, Zaks K, et al. Cestode infection in 2 dogs: Cytologic findings in liver and a mesenteric lymph node. *Vet Clin Path.* 2013;42:103-108.
10. Rodriguez F, Herraez P, Espinosa de los Monteros A, et al. Testicular necrosis caused by *Mesocestoides* in a dog. *Vet Rec*. 2003;153:275-276.
11. Topli N, Yildiz K, Tunay R. Massive cystic tetrthyridiosis in a dog. *J Small Animal Med.* 2004;45:410-412.
12. Venco L, Kramer L, Pagliaro L, et al. Ultrasonographic features of peritoneal cestodiasis caused by *Mesocestoides sp* in a dog and in a cat. *Vet Radiol & Ultrasound*. 2005;46:417-422.
13. Zeman DH, Cheney JM, Waldrup KA. Scrotal cestodiasis in a dog. *Cornell Vet*. 1988;78:273-279.

**CASE IV:** F1409682 (JPC 4048672)

**Signalment:** Adult female intact chicken (*Gallus gallus domesticus*), breed unknown.

**History:** 4-week history of respiratory illness in the flock, affecting up to 35 birds. Clinical signs include coughing and sneezing in a subset of birds. This patient was found deceased.

**Gross Pathology:** A brown hen was submitted for necropsy in poor body condition with a prominent keel due to marked atrophy of the pectoral muscles. There is a minimal amount of internal body fat stores and subcutaneous fat is not present. The kidneys are diffusely enlarged up to 3x normal, mottled pale to red in color, soft and friable, and bulge slightly upon cut section.

**Laboratory Results:** Tracheal swab Avian Influenza real-time PCR Negative

Tracheal swab Infectious Bronchitis Virus real-time PCR Negative

Kidney Infectious Bronchitis Virus real-time PCR Negative

**Histopathologic Description:** Diffusely throughout the renal parenchyma, there is widespread degeneration and necrosis of the renal tubular epithelium characterized by swollen cells with vacuolated cytoplasm and swollen nuclei (degeneration) or loss of cellular detail, eosinophilic cellular debris and pyknotic nuclei (necrosis). Tubules have segmental loss of epithelium with epithelial attenuation across bare basement membrane. Multifocally, small numbers of tubular epithelial cells contain increased amounts of basophilic cytoplasm, have anisokaryosis and rare mitotic figures (regeneration). Renal tubules are often ectatic, dilated up to 3x normal and contain numerous epithelial cell casts, moderate numbers of heterophils, occasional granular casts and/or amorphous, eosinophilic material (protein). The interstitium is expanded by coalescing aggregates of lymphocytes, plasma cells, and occasional heterophils. This inflammatory infiltrate is accompanied by mild to moderate amounts of

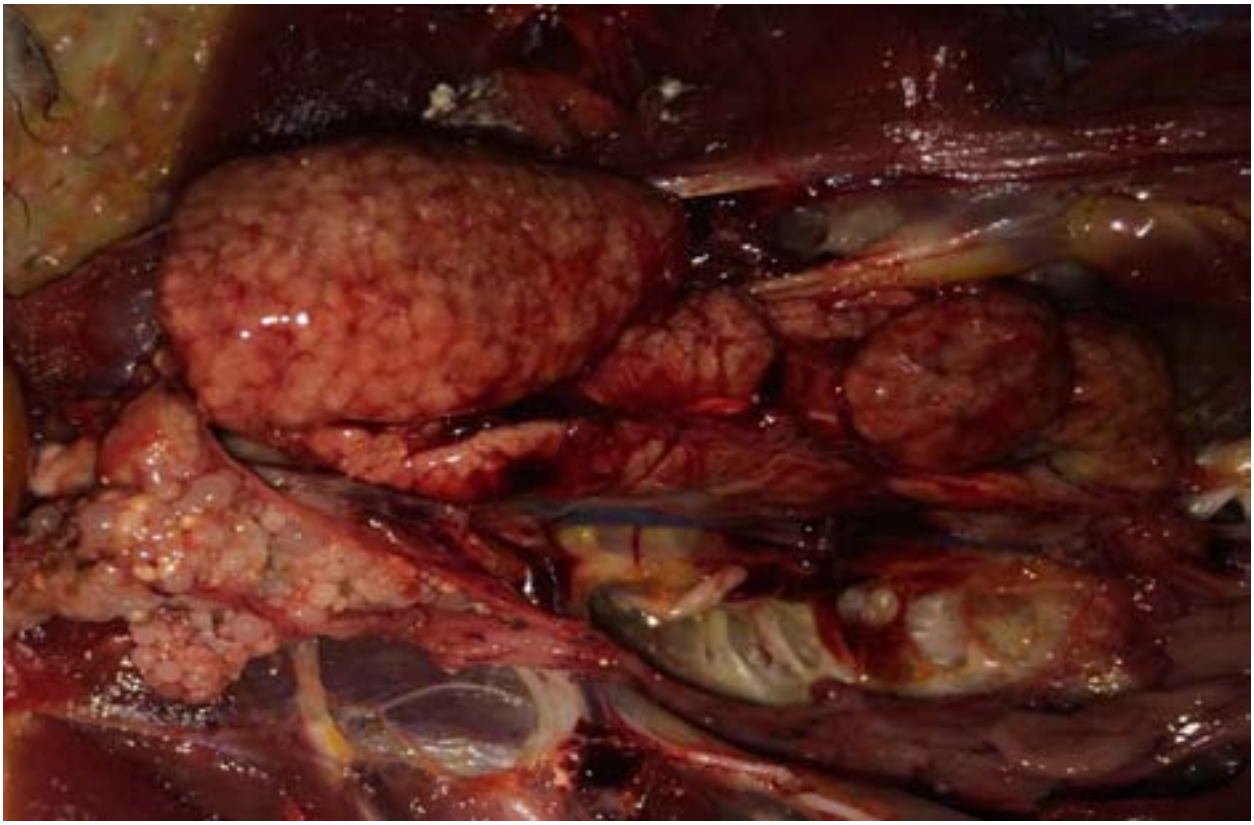

*4-1. Kidneys, chicken: The kidneys are diffusely enlarged up to 3x normal, mottled pale to red in color, soft and friable. (Photo courtesy of: Department of Microbiology, Immunology, and Pathology, College of Veterinary Medicine and Biomedical Sciences, Colorado State University, http://csu-cvmbs.colostate.edu/academics/mip/Pages/default.aspx)*

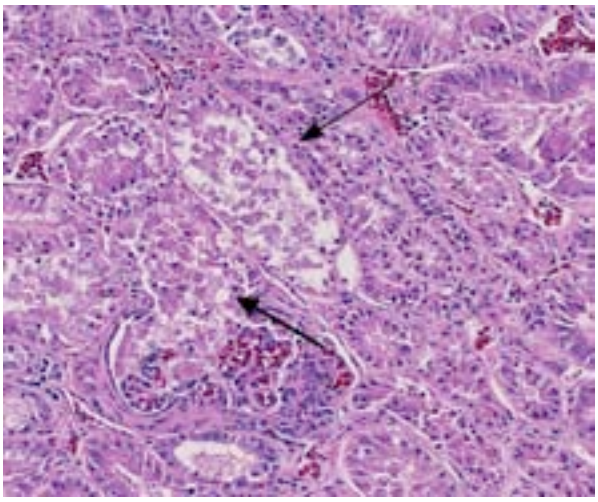

*4-2. Kidney, chicken: There are clusters of necrotic tubules scattered throughout the kidney. (HE 240X)*

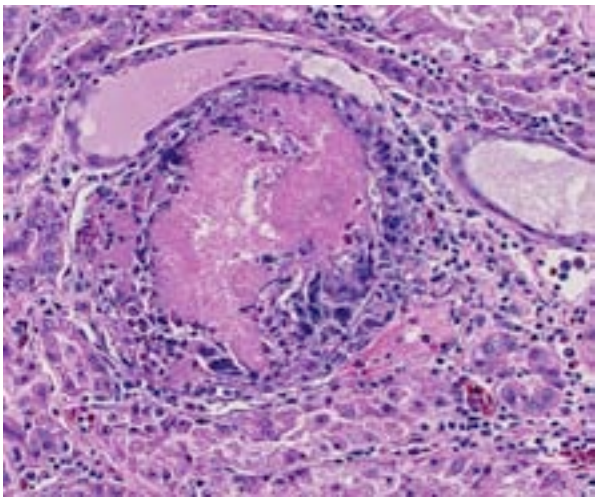

*4-3. Kidney, chicken: Rare gouty tophi, surrounded by foreign body macrophages, are scattered throughout the kidney. (HE 256X)*

edema and fibrosis. Additionally, renal tubules and glomeruli within the cortex are multifocally expanded and replaced by sharp, radiating, eosinophilic crystalline deposits that range in size from 50-150 microns in diameter and are surrounded by moderate numbers of degenerate heterophils and macrophages (urate tophi). Rarely, the parietal epithelium of Bowman's capsule is mildly hypertrophic, characterized by plump, cuboidal epithelial cells that protrude into the glomerular space.

**Contributor's Morphologic Diagnosis:** Kidney: Tubulointerstitial nephritis, diffuse, lymphoplasmacytic and heterophilic, chronic, severe with tubular necrosis, degeneration and regeneration, urate tophi, cellular casts and tubuloproteinosis.

**Contributor's Comment:** Tubulonephritis in chickens typically occurs as a result of infection with either the nephrogenic strain of infectious bronchitis virus or avian nephritis virus. Infectious bronchitis virus (IBV) is a coronavirus with a non-segmented, positive-sense, single-stranded RNA genome that infects all ages of chickens and results in major economic losses for the poultry industry.[3,5] Clinical manifestations of IBV infection include respiratory disease, reproductive disorders, and nephritis, with the latter presenting as a progression from respiratory illness to clinical signs of renal failure such as excessive water intake, rapid weight loss and diarrhea.[4] Infection with the nephrogenic strain of IBV initially results in viral replication in the trachea, followed by spread to the kidney and infection of the renal tubular epithelium.[1,2,5] Histologic lesions include interstitial polymorphonuclear inflammation, renal tubular degeneration and necrosis, and uric acid precipitation, with tubular regeneration occurring in surviving birds.[1,2,5] Detection of IBV infection is required for a definitive diagnosis, and is most commonly achieved by virus isolation, reverse-transcriptase polymerase chain reaction (RT-PCR), or serology.[3] In this case, RT-PCR was performed directly on a tracheal swab and on RNA extracted from kidney, with negative results. However, as previously demonstrated, IBV antigen is detected up to day 13 post-inoculation by immunohistochemistry, but not after, suggesting clearance of the virus.[1,2] The 4-week span of respiratory illness with progression to nephritis in this case may have allowed sufficient time for clearance of IBV from the trachea and kidney prior to sampling, thus resulting in a negative result on RT-PCR. Furthermore, if the primers used in the RT-PCR assay are not from conserved regions across all IBV strains, false negatives may occur.[3] Tracheal or renal clinical samples may also can contain non-specific inhibitors of the polymerase used in PCR, resulting in decreased sensitivity.[3] Together, these points highlight the difficult challenge of obtaining a definitive diagnosis of IBV infection, even in the presence of strongly supportive clinical signs and histopathologic findings. The clinical history of respiratory illness in this flock, together with the gross and histologic lesions observed in this adult chicken, are consistent with nephrogenic IBV infection. These findings

underscore the importance of recognizing distinct clinical signs and histopathological lesions so that an accurate diagnosis is made, allowing for the institution of appropriate flock management.

Alternatively, avian nephritis virus (ANV) represents another possible differential for the renal lesions observed in this case. Avian nephritis virus is a non-enveloped astrovirus with a single stranded, positive sense RNA genome that affects young poultry and results in degeneration of the renal tubules and interstitial inflammation, with formation of lymphoid follicles in later stages.[6,8,9] Virus isolation, serology, and/or RT-PCR are the most common laboratory methods of detecting ANV and a positive result is required for definitive diagnosis.[10] Although renal lesions in this case may be consistent with ANV infection, this virus is not documented to cause respiratory disease, such as that observed in this bird and the rest of the flock. Additionally, lymphoid follicles seen in chronic cases of ANV infection were not observed in the kidney of this case, despite 4-week duration of disease.

**JPC Morphologic Diagnosis:** 1. Kidney, tubules: Degeneration, necrosis, and regeneration, multifocal, moderate, with intratubular protein. 2. Kidney, cortex: Gouty tophi, multiple.

**Conference Comment:** The contributor provides an overview of the two most likely etiologic differentials in this case, and conference participants, whom are not privy to the provided clinical history, added avian influenza and Newcastle disease as well. Herpesvirus and polyomavirus may each also cause tubular necrosis in avian species, however, intranuclear inclusions would be prominent in both instances.[4]

Much of the conference discussion was focused on whether the gouty tophi and the described concentric amorphous structures, interpreted by most to be protein, were associated with the infection. Urates are actively excreted by renal tubular epithelium, so it stands to reason that loss of tubular epithelium can lead to urate accumulation and subsequent tophi formation. Additionally, a sick bird as described in this case would likely be dehydrated which will further exacerbate urate deposition. The gouty tophi formation was minimal in most sections, thus not likely a significant contributor to the tubular lesions as observed in cases of true renal gout.

As exemplified here, definitive diagnosis with even the ultra-sensitive PCR is challenging with infectious bronchitis virus, the most likely cause of disease in this case. This virus is unique among coronaviruses in that it replicates, mutates and recombines rapidly resulting in the creation of an extensive number of serotypes. These pose a challenge to poultry producers and veterinarians, as vaccines do not provide cross-protection for different serotypes, necessitating the need to develop specific vaccines to the identified serotype associated with an outbreak. Even the vaccines themselves have been associated with the emergence of new strains capable of causing disease. The most significant protein for virus detection is the club-shaped glycoprotein known as spike. Spike mediates cell attachment, fusion and target specificity. It is composed of two subunits: S1, which makes up the outer portion; and S2, which anchors it to the viral envelope. The S1 protein is the common target for RT-PCR and can be used to predict levels of cross-protection between different serotypes of IBV, thus making it the focus of research and vaccine development for this enduring disease.[7]

**Contributing Institution:** Department of Microbiology, Immunology, and Pathology
College of Veterinary Medicine and Biomedical Sciences
Colorado State University
http://csu-cvmbs.colostate.edu/academics/mip/Pages/default.aspx

**References:**

1. Chen BY, et al. Histopathology and immunohistochemistry of renal lesions due to infectious bronchitis virus in chicks. *Avian Pathology*. 1996;25(2):269-283.
2. Chen BY, Itakura C. Histopathology and immunohistochemistry of renal lesions due to avian infectious bronchitis virus in chicks uninoculated and previously inoculated with highly virulent infectious bursal disease virus. *Avian pathology*. 1997;26(3):607-624.
3. De Wit JJ. Detection of infectious bronchitis virus. *Avian pathology*. 2000;29(2):71-93.
4. Fletcher OJ, Abdul-Aziz T, Barnes HJ. Urinary system. In: Fletcher OJ, ed. *Avian Histopathology.* 3rd ed. Madison, WI: American Association of Avian Pathologists; 2008:241-242.
5. Ignjatović J, Sapats S. Avian infectious bronchitis virus. Revue scientifique et technique

(International Office of Epizootics). 2000;19(2): 493-508.
6. Imada T, Yamaguchi S, Mase M, Tsukamoto K, Kubo M, Morooka A. Avian nephritis virus (ANV) as a new member of the family Astroviridae and construction of infectious ANV cDNA. *Journal of Virology*. 2000;74(18): 8487-8493.
7. Jackwood MW. Review of infectious bronchitis virus around the world. *Avian Diseases*. 2012;56:634-641.
8. Narita M, Ohta K, Kawamura H, Shirai J, Nakamura K, Abe F. Pathogenesis of renal dysfunction in chicks experimentally induced by avian nephritis virus. *Avian Pathology*. 1990;19(3):571-582.
9. Shirai, J, Nakamura K, Narita M, Furuta K, Kawamura H. Avian nephritis virus infection of chicks: Virology, pathology, and serology. *Avian Diseases*. 1989;34(3):558-565.
10. Todd D, Trudgett J, McNeilly F, McBride N, Donnelly B, Smyth VJ, et al. Development and application of an RT-PCR test for detecting avian nephritis virus. *Avian Pathology*. 2010;39(3): 207-213.

**Joint Pathology Center**
**Veterinary Pathology Services**

*Conference Coordinator*
**Matthew C. Reed, DVM**
**Captain, Veterinary Corps, U.S. Army**
**Veterinary Pathology Services**
**Joint Pathology Center**

## WEDNESDAY SLIDE CONFERENCE 2014-2015

# Conference 4

**24 September 2014**

**Conference Moderator:**
Bruce Williams, DVM, Diplomate ACVP
Chief, Online Resources, Veterinary Pathology Services
Joint Pathology Center
Forest Glen Annex, Bldg. 161
2460 Linden Lane
Silver Spring, MD 20910

**CASE I:** 13110510 (JPC 4048566).

**Signalment:** Tissue from an 8-year-old intact female Miniature Rex rabbit (*Oryctolagus cuniculus*).

**History:** Tissue samples were received on routine biopsy service. History submitted by referring veterinarian indicated relatively acute onset of multiple cutaneous masses distributed "all over" patient's body.

[Follow-up by phone conversation: The referring veterinarian was contacted by phone 6 months after biopsy submission. The veterinarian reported that all masses that had abruptly appeared regressed and were completely gone by 2-3 months. The veterinarian reported that the rabbit was currently healthy.]

**Gross Pathology:** Two biopsies of consisting of haired skin were received. Each contained a nodular, well-demarcated firm mass that was solid

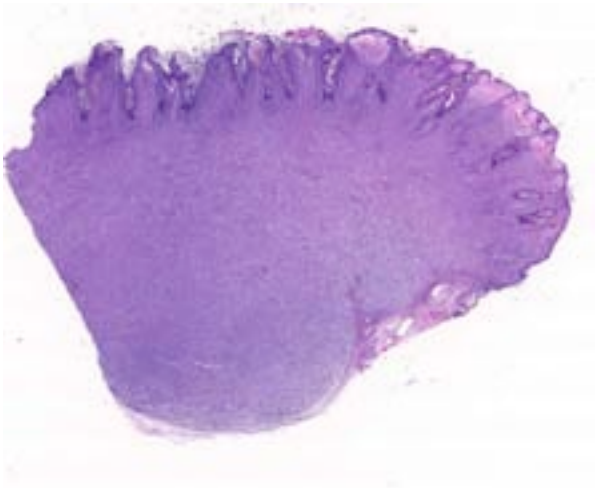

*1-1. Haired skin, rabbit: The dermis is expanded by a densely cellular neoplasm which elevates the overlying hyperplastic epithelium. (HE 0.63X)*

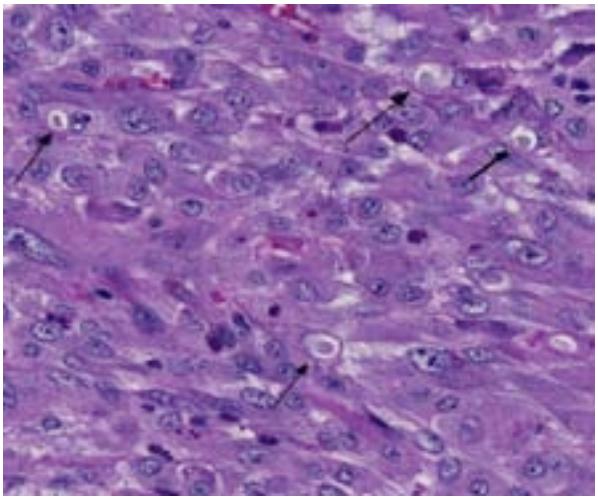

*1-2. Haired skin, rabbit: The neoplasm within the dermis is composed of densely packed hypertrophic fibroblasts which occasionally contain intracytoplasmic poxviral inclusions. (HE 256X)*

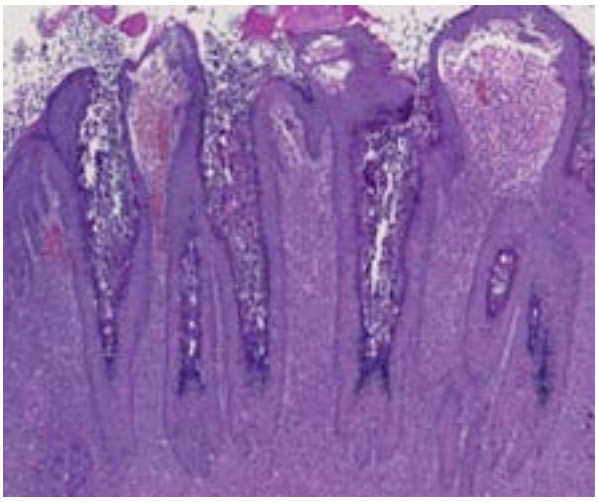

*1-3. Haired skin, rabbit: The epithelium overlying the neoplasm is markedly hyperplastic with abundant hyperkeratosis. (HE 35X)*

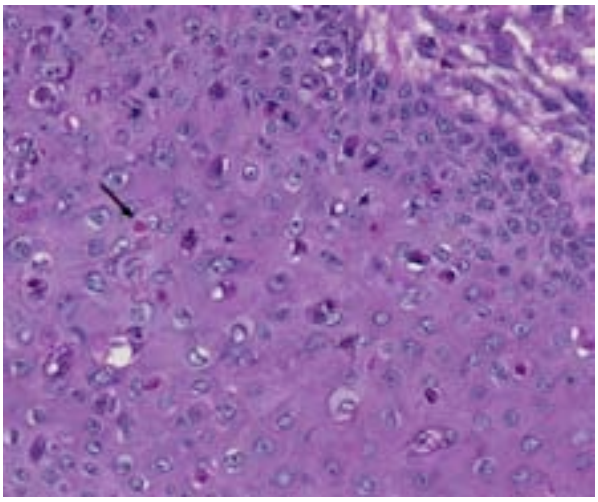

*1-4. Haired skin, rabbit: The hyperplastic epithelium contains ballooning degeneration and necrosis of individual hepatocytes as well as intracytoplasmic poxviral inclusions. (HE 256X)*

and homogeneous white/tan on cross section. The masses were 2.2cm and 3cm in diameter.

**Laboratory Results:** Not provided.

**Histopathologic Description:** Tissue samples are from haired skin or skin from mucocutaneous junction. Lesions are similar in each. The dermis is expanded by a raised, well-demarcated, non-encapsulated neoplastic mass. The mass is comprised of densely-cellular, primarily spindled to polyhedral cells arranged in streams or short, haphazardly-placed bundles or fascicles. The neoplastic cells have large nuclei exhibiting moderate anisokaryosis and prominent, often multiple, nucleoli. The cells have moderate amounts of amphophilic cytoplasm with rare, intracytoplasmic, round, eosinophilic inclusion bodies. There are 2 mitotic figures seen in 10 random high power fields examined. The epidermis overlying the mass is variably hyperplastic with regional orthokeratosis and occasional serocellular crusts. Innumerable epidermal cells at nearly all levels (strata) are rounded with either grey-smudged or vacuolated cytoplasm that includes single, conspicuous, roughly round, 5-12 µm in diameter, bright eosinophilic inclusion bodies. Inconsistent lesions across sections include regional edema, acute necrosis of individual neoplastic cells, scattered and variably intense heterophilic infiltrates and surface ulceration.

**Contributor's Morphologic Diagnosis:** Haired skin and mucocutaneous junctions, multiple sites: Fibromatosis with intracytoplasmic inclusion bodies.

**Contributor's Comment:** Shope fibroma virus (SFV) belongs to the *Leporipoxvirus* genus of the *Poxviridae* family of viruses. The natural host is the Eastern cottontail (*Sylvilagus floridanus*) rabbit; however, this is expanded to also include other rabbits, hares and squirrels.[5,12] The SFV genome has been completely sequenced and compared with the myxoma virus (MYX), which is a closely related virus that causes myxomatosis in rabbits.[12] These viruses are similar enough that live-attenuated SFV is administered as a vaccine providing cross-immunity towards myxomatosis.[5]

The lesions caused by SFV in rabbits were first described by Dr. R.E. Shope, a physician and virologist, in 1932.[8,9] SFV is transmitted to rabbits through biting insect and arthropod vectors such as mosquitoes and fleas.[1,5] Tumors can arise from each bite site, resulting in one to several masses appearing on the patient.[5] Lesions are most often located on the head and legs.[5] The disease exhibits seasonality with most cases reported in the fall (September-November).[5] Lesions typically reach maximum size between 7-12 days after inoculation, which can account for the relatively rapid onset noticed by owners as in this case. Afterwards, lesions will regress over 1-1.5 months leaving the host immune.[5] Infection by SFV in neonatal or very young rapids can lead to fatal infections with disease resembling myxomatosis.[1,5]

Von Bomhard et al. performed a retrospective study on cutaneous lesions in rabbits, separating lesions into virus-induced and non-virus-induced tumors.[11] Shope fibroma was the most common virally induced tumor followed by Shope papilloma (*Papovavirus*). Overall, trichoblastomas and collagenous hamartomas were the most common cutaneous tumors reported from this study. Interestingly, this study reported a sex predilection for mesenchymal tumors in rabbits, with mesenchymal proliferations occurring significantly more in male rabbits than females.

**JPC Diagnosis:** Haired skin: Atypical fibroblastic proliferation.

**Conference Comment:** This case presents a beautiful example of the characteristic poxvirus intracytoplasmic inclusions and delivers an opportunity for some introspective criticism and a revisionist morphologic diagnosis by the JPC. Historically, we have favored the diagnosis of "atypical mesenchymal proliferation" for Shope fibromas and myxomas, both the result of *Leporipoxvirus* infection in rabbits. While technically accurate, it fails to identify fibroblasts as the cellular origin which is well described in multiple sources and implied within its common name "Shope fibroma".[3,6]

The fibroblast proliferation is unusual among the poxviruses, which are generally epitheliotropic in nature. Viral replication within epithelial cells causes "ballooning degeneration" and necrosis, with sites of replication observable histologically as small, basophilic, intracytoplasmic inclusions designated as *type* B inclusions or Guarnieri bodies, while the larger eosinophilic inclusions as observed in this rabbit are those of *type* A which occur later in the replication cycle.[7]

Specific to the members of the *Leporipoxvirus* family (Shope fibroma virus, squirrel fibroma virus and myxoma virus), the proliferation of fibroblasts expanding the dermis is the more prominent histologic lesion. In SFV, poxviral inclusions are also found in these mesenchymal cells as observed in this case. In contrast, myxoma virus infections induce a more mucinous matrix separating fibroblasts which lack viral inclusions (but are seen in overlying epithelial cells).[6] Poxviruses are known to express proteins with similar mechanisms of action as epidermal growth factor[2], and it is logical to conclude members of the *Leporipoxvirus* family may similarly produce fibroblast growth factors, though this has not been demonstrated as research on these niche viruses is limited.

Through the discovery that pretreatment with RANTES (CCL5) to cells in culture could inhibit infection of myxoma virus, researchers uncovered its affinity for the chemokine receptor CCR5, in addition to CCR1 and CXCR4.[4] This is a noteworthy feature of HIV and SIV infections, in which individuals have been identified with a natural resistance to infection due to a mutation in the CCR5 gene.[10] These chemokine receptors are specific to white blood cells, which alludes to the immunosuppressive nature of HIV infections.[9] What this means, if anything, for poxviruses and specifically the behavior of the *Leporipoxvirus* family is still undetermined.

**Contributing Institution:** Department of Veterinary Pathobiology
Center for Veterinary Health Sciences
Oklahoma State University
www.cvm.okstate.edu

**References:**

1. Dalmat HT. Arthropod transmission of rabbit fibromatosis (Shope). *J Hyg.* 1959;57:1-30.
2. Ginn PE, Mansell JL, Rakich PM. Skin and appendages. In: Maxie MG ed. *Jubb, Kennedy, and Palmer's Pathology of Domestic Animals.* 5th ed. Vol. 1. Philadelphia, PA: Elsevier Saunders; 2007:664-674.
3. Jones TC, Hunt RD, King NW. *Veterinary Pathology.* Baltimore, MD: Lippincott Williams & Wilkins; 1997:208-209.
4. Lalani AS, Masters J, Zeng W, et al. Use of chemokine receptors by poxviruses. *Science.* 1999;286:1968-1971.
5. Meredith AL. Viral skin diseases of the rabbit. *Vet Clin North Am Exot Anim Pract.* 2013;16:705-714.
6. Percy DH, Barthold S. *Pathology of Laboratory Rodents and Rabbits.* 3rd ed. Ames, IA: Blackwell Publishing; 2007:257-258.
7. Pfeffer M, Meyer H. Poxvirus diagnostics. In: Mercer AA, Schmidt A, Weber O, eds. *Poxviruses*. Basel, Switzerland: Birkhäuser Verlag; 2007:359.
8. Pulley LT, Shively JN. Naturally occurring infectious fibroma in the domestic rabbit. *Vet Pathol.* 1973;10:509-519.

9. Shope RE. A transmissible tumor-like condition in rabbits. *J Exp Med.* 1932;56:793-802.
10. Silva E, Stumpf MP. HIV and the CCR5-32 resistance allele. *Micro Let.* 2004;214(1):1-12.
11. Von Bomhard W, Goldschmidt MH, Shofer FS, Perl L, Rosenthal KL, Mauldin EA. Cutaneous neoplasms in pet rabbits: a retrospective study. *Vet Pathol.* 2007;44:579-588.
12. Willer DO, McFadden G, Evans DH. The complete genome sequence of shope (rabbit) fibroma virus. *Virology*. 1999;264:319-343.

**CASE II:** WSC #1 (JPC 4048439).

**Signalment:** <1 month-old, female white-tailed deer fawn, *Odocoileus virginianus.*

**History:** This young fawn was found weak and emaciated in the summer on a farm in Connecticut. Due to concerns about the appearance of its skin, it was shot and submitted for necropsy.

**Gross Pathology:** The fawn was in poor body condition with absence of subcutaneous and visceral fat stores. There were extensive areas of alopecia and multiple red dermal abrasions on all four legs. Innumerable, firm, 1-2 mm thick, brown crusts that entrapped hair across multiple follicles were disseminated on the skin surface of the entire body, particularly on the dorsum and dorsolateral aspects of the trunk and on the face.

**Laboratory Results:** None.

**Histopathologic Description:** Haired skin: Covering an epidermis that is frequently ulcerated are thick crusts spanning multiple hair follicles and composed of layers of keratin with retained nuclei (parakeratosis), abundant hyaline eosinophilic (proteinaceous) material, accumulations of degenerate neutrophils (intracorneal pustules) and necrotic debris, entrapped hairs and small areas of hemorrhage. Throughout the crusts and extending into inflamed and frequently ruptured hair follicles (furunculosis) are innumerable tangled, branching, 1-2 µm wide filamentous structures composed of parallel rows of coccoid bodies. More amorphous colonies of coccoid bacteria are also present. In the remaining epidermis there is mild diffuse acanthosis and areas of spongiosis that also involve the follicular epithelium. Large numbers of neutrophils fill follicular lumina, disrupt follicular epithelium and extend into the surrounding dermis from areas of ulceration and furunculosis. Also present in the dermis are smaller numbers of macrophages, lymphocytes and plasma cells.

Gram Stain (not submitted): The filamentous and coccoid forms of bacteria stain gram-positive.

**Contributor's Morphologic Diagnosis:** Skin: Severe, exudative, crusting and neutrophilic dermatitis and folliculitis with ulceration, furunculosis, parakeratosis, and filamentous and coccoid bacteria, consistent with *Dermatophilus congolensis.*

**Contributor's Comment:** The gross appearance and histopathologic findings in this deer fawn were typical of dermatophilosis, caused by the Gram-positive actinomycete *Dermatophilus congolensis*. Although *D. congolensis* has a worldwide distribution, disease has historically been more common in tropical and subtropical climates, especially during prolonged periods of rain.[2,5] Dermatophilosis, also termed cutaneous

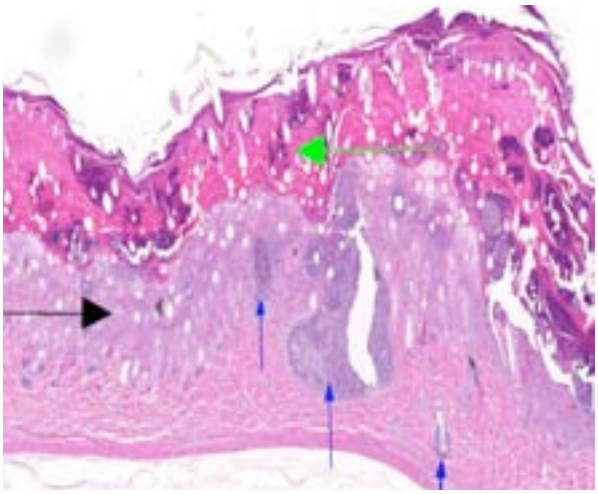

*2-1. Haired skin, fawn: The epidermis is covered by a lamellated serocellular crust with numerous collections of degenerate neutrophils (pustules – green arrow). The subjacent epidermis is multifocally hyperplastic (black arrow), numerous hair follicles are surrounded or effaced by aggregates of degenerate neutrophils (furunculosis – blue arrows). (HE 6.3X)*

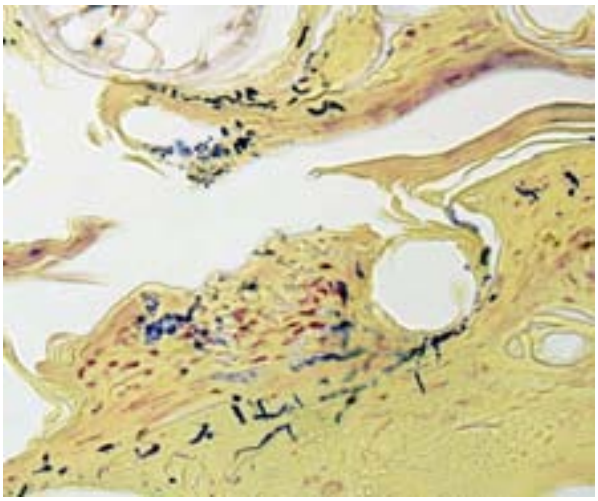

*2-2. Haired skin, fawn: The serocellular crust contain numerous filamentous chains of gram-positive zoospores, consistent with Dermatophilus congolensis. (Brown-Hopps 320X)*

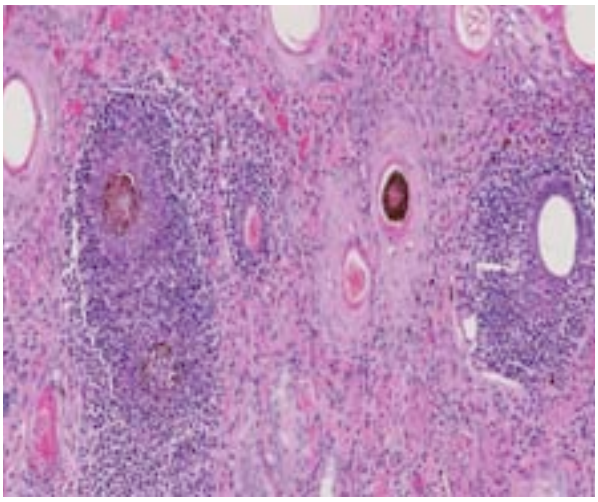

*2-3. Haired skin, fawn: Hair follicles are multifocally effaced by numerous neutrophils and fewer histiocytes infiltrating along the external root sheath. (HE 280X)*

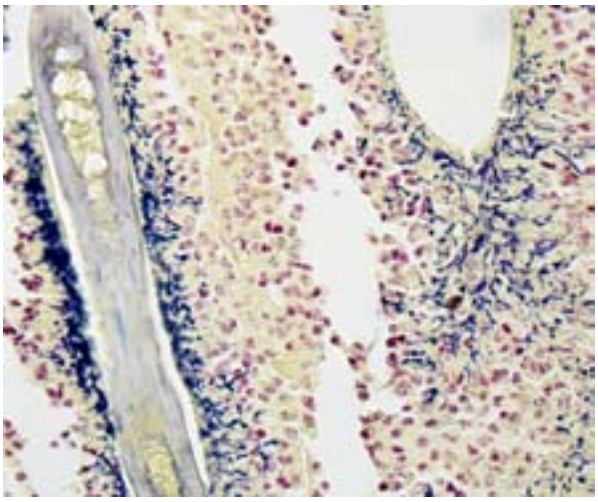

*2-4. Haired skin, fawn: Hair follicles contain numerous radiating filamentous chains of gram-positive zoospores, consistent with Dermatophilus congolensis. (Brown-Hopps 400X)*

streptothricosis, cutaneous actinomycosis, rain scald, rain rot, lumpy wool, and strawberry foot rot, has been reported in many species. Among domestic animals, it is most commonly seen in cattle, sheep, and goats, with horses less frequently affected.[1-3] The disease is also zoonotic, and spread from white-tailed deer to humans has been described.[3]

The first reports in white-tailed deer were from the New York state region in the 1970s, along with an isolated case in a fawn from South Carolina.[3,5] A recent survey of bacterial and parasitic dermatologic diseases in white-tailed deer from 1975-2012 found a 0.7% incidence (19/2569) of dermatophilosis.[4] At 21.6% of the cases, this was second only to demodicosis in frequency of bacterial or parasitic skin disease among deer in the Southeastern United States.[4] As in initial reports in twin fawns,[5] lesions most commonly involved the head/face and limbs and consisted of exudation and crusting, alopecia, ulcers and erosions.[4] In the current case, the lesions were particularly severe on the face but were also generalized. It has been hypothesized that a predilection for the rostrum in fawns could be due to transmission from an infected dam during nursing.[5] Dermatophilosis has been found in fawns as young as 2 weeks old,[5] and the study by Nemeth et al. found significantly more juveniles affected (63%) than adults.[4] Debilitation and emaciation in the fawn in this case were attributed to the severity of the dermatophilosis, which has been reported as a cause of death in other affected fawns.[3,4]

The diagnosis of dermatophilosis in this case was based on the presence of thick lamellated crusts in association with characteristic filaments of parallel rows of Gram-positive coccoid bodies ("railroad track" configuration) formed from transverse and longitudinal septation.[2] A combination of skin damage and prolonged moisture are generally required for establishment and spread of infection, as the organism is minimally invasive in intact epidermis, and wet conditions are needed for activation of coccoid bodies into motile zoospores.[2] Ectoparasites can be a cause of trauma and may also act as mechanical vectors to spread the infection.[2] Although usually confined to the epidermis and outer root sheaths of hair follicles, there are rare reports of deeper skin or lymph node involvement.[1,2] Ulceration and furunculosis were prominent features in the current case, but there was no evidence of spread to lymph nodes or other tissues.

**JPC Diagnosis:** Haired skin: Epidermitis and folliculitis, suppurative, diffuse, severe, with epithelial hyperplasia, parakeratotic hyperkeratosis, and numerous filamentous bacteria.

**Conference Comment:** The contributor gives an exceptional overview of dermatophilosis, a distinctive disease most often observed in production animals. Buried within the pathogenesis of infection with this gram-positive, actinomycete bacterium is a glimpse of the skin's effectiveness in providing a barrier to disease. The

combination of hair, surface lipid, and stratum corneum equate to an insurmountable barricade for *Dermatophilus* in the normal state. However, with even minor disruptions of the host's defenses combined with the moist conditions required to activate the zoospores, the bacteria incite a fulminant infection which contributes to significant meat, milk and wool production loss throughout the world.[2]

*Dermatophilus* produces exoenzymes and has an affinity for a low carbon dioxide environment which facilitates its colonization and tissue-specificity for the epidermis. The host responds to infection with cornification of keratinocytes and invasion of neutrophils effectively walling off the bacteria from the dermis. The progenitor cells of the follicular epithelium then propagate, forming a new layer of epidermis.[2] Subsequent invasion of this new layer followed by repetitive and unsuccessful defense responses of the host creates the thick laminar and parakeratotic crusts with entrapped hair follicles which are so characteristic to this bacterial infection and nicely exemplified in this case.

**Contributing Institution:** Department of Pathobiology and Veterinary Science
Connecticut Veterinary Medical Diagnostic Laboratory
College of Agriculture, Health and Natural Resources
University of Connecticut
http://www.pathobiology.uconn.edu/

**References:**

1. Byrne BA, Rand CL, McElliott VR, Samitz EM, Brault SA. Atypical *Dermatophilus congolensis* infection in a three-year-old pony. *J Vet Diagn Invest*. 2010;22:141-143.
2. Ginn PE, Mansell JEKL, Rakich PM. Skin and appendages. In: Maxie MG, ed. *Jubb, Kennedy, and Palmer's Pathology of Domestic Animals*. Vol. 1. 5th ed. Edinburgh, UK: Elsevier Limited; 2007:681-682.
3. Gordon MA, Salkin IF, Stone WB. *Dermatophilus* dermatitis enzootic in deer in New York state and vicinity. *J Wildl Dis*. 1977;13(2): 184-190.
4. Nemeth NM, Ruder MG, Gerhold RW, et al. Demodectic mange, dermatophilosis, and other parasitic and bacterial dermatologic diseases in free-ranging white-tailed deer (*Odocoileus virginianus*) in the United States from 1975 to 2012. *Vet Pathol*. 2014;51(3):633-640.
5. Roscoe DE, Lund RC, Gordin MA, Salkin IF. Spontaneous dermatophilosis in twin white-tailed deer fawns. *J Wildl Dis*. 1972;11(3):398-401.

**CASE III:** 09-163 (JPC 4017918).

**Signalment:** 2-year-old male Labrador retriever dog weighing 16 kg *(Canis familiaris)*.

**History:** This patient was one of two Labrador retriever dogs from the same litter that were noted to have persistently pale mucous membranes and a grade I/VI systolic heart murmur. Serial complete blood counts revealed a chronic, moderate to severe, macrocytic, and strongly regenerative anemia. Extensive diagnostic workup to rule out conditions leading to a strongly regenerative anemia was performed, including those causing acquired intermittent or chronic hemolytic anemia (immune-mediated, infectious, toxic), or blood loss anemia, all of which were negative. Additional studies led to the diagnosis of hereditary erythrocytic pyruvate kinase (PK) deficiency.

Over the next several months this dog developed mildly icteric mucous membranes with progression of the heart murmur to IV/VI, although otherwise remained clinically well despite persistent anemia and few crises. Three days prior to death he became icteric and lethargic and started vomiting. His clinical condition deteriorated rapidly, and aspiration pneumonia was strongly suspected. Due to a grave prognosis he was humanely euthanized.

**Gross Pathology:** The subcutaneous tissues, mucous membranes and fat were diffusely discolored yellow. The femoral bone marrow cavities were filled with dense bone matrix and small amounts of bone marrow, which sank in water.

Approximately 200 ml of yellow-red serosanguineous fluid with fibrin tags was present within the abdominal cavity. The liver weighed 1070 g (6.7% of body weight), was moderately enlarged and firm, with a dark red-brown granular capsular surface and multifocal 1- 2 mm in diameter circular firm tan foci within the parenchyma. The hepatic lymph nodes were prominent with normal architecture. The spleen was dark pink and enlarged, measuring 26 x 9 x 2.5 cm. On the capsular surface, there were multifocal 2-3 mm blue to green plaques (siderofibrotic plaques). There was 100 ml of red serosaguineous fluid in the thoracic cavity. The sternal lymph nodes were prominent with normal architecture. There was 20 ml of red serosaguineous fluid within the pericardium, and the heart weighed 180 g (1.1% of body weight). The ventral portions of the right cranial, middle and caudal lung lobes were red brown and firm. The left cranial lung lobe contained a 4-5 cm long depressed firm tan streak on the serosal surface. The right middle lung lobe sank in formalin.

**Laboratory Results:** Serial CBCs: PCV/Hct persistently ranging from 15-20%, with reticulocyte counts >170 K/uL.

- Direct antiglobulin (Coombs') test: Negative
- Erythrocytic osmotic fragility testing: Normal
- **Postmortem liver iron (ICP/MS): 37,300 ppm dry weight** (reference range canine: 350-1200 ppm dry weight, 100-300 ppm wet weight). Most published reference ranges are reported on a wet weight basis, dry weight results are expected to be 3.5 – 4 X higher than wet weight.
- DNA-based screening test for known PK mutations in Basenjis, Beagles and West Highland White terriers (8): Negative
- **DNA sequencing and mutation results: Homozygous single base missense mutation of *PK-LR* gene** (8)
-

**Histopathologic Description:** Liver: Multifocally within the hepatic parenchyma, portal areas are moderately to markedly expanded by increased numbers of macrophages that contain abundant dense dark brown to black globular pigment (hemosiderin), increased bile duct profiles, and bands of loose fibrous connective tissue that occasionally bridge adjacent portal areas, and less frequently, centrilobular regions. Fibrous connective tissue multifocally surrounds and individualizes periportal hepatocytes, which often contain intracytoplasmic finely granular dark brown to black pigment. Hepatocytes in the surrounding lobules also contain variable amount of a similar cytoplasmic pigment. Hepatic lobules are irregular in size and there are multifocal nodules of regeneration. Frequently within sinusoids and portals areas there are scattered aggregates of

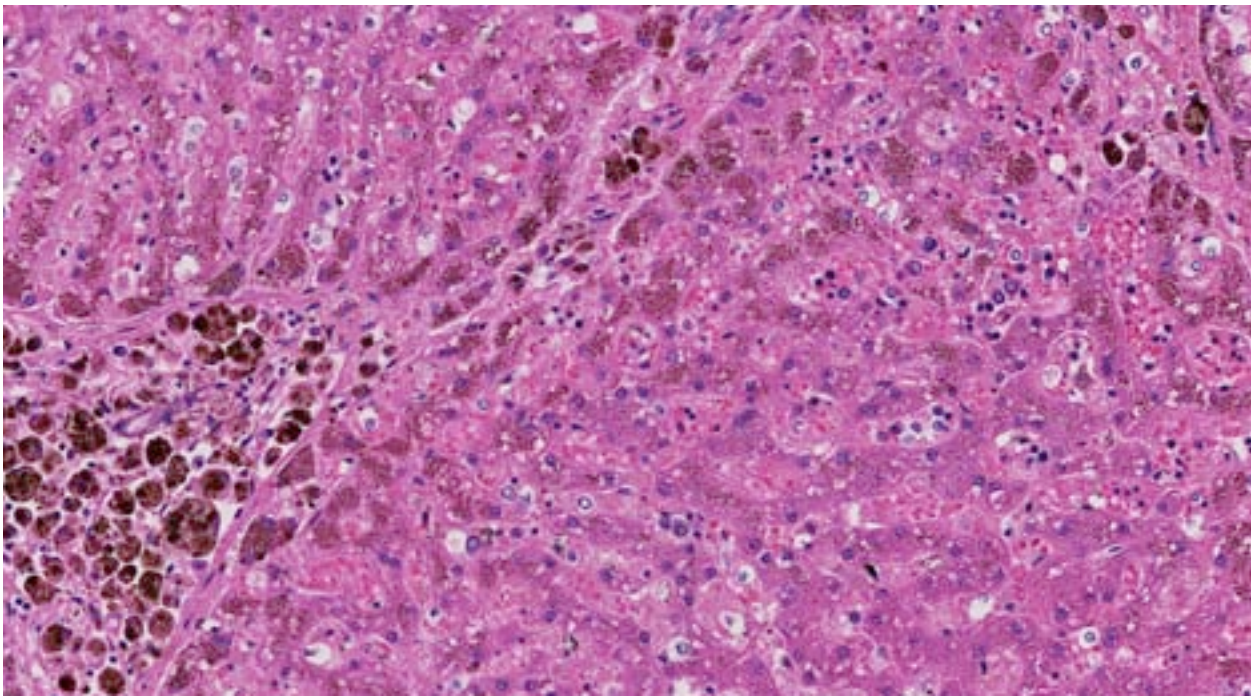

*3-1. Liver, dog: Hepatocytes, most prominent in periportal areas accumulate brown pigment, which is also present within large amounts of macrophages in portal areas (left). (HE 188X)*

primarily erythroid and fewer myeloid precursors (extramedullary hematopoiesis), as well as rare individual hepatocytes which are shrunken with hypereosinophilic cytoplasm and pyknotic nuclei (necrotic). Occasionally within connective tissue in portal areas and within blood vessel walls there is granular to globular basophilic material (mineral). Multifocally on the capsular surface and extending into the underlying hepatic parenchyma, there are regionally extensive areas of fibrosis with increased bile duct profiles (post-necrotic scarring).

Liver (Perl's iron, Figures 1A and 1B): Globular pigment within hepatocyte, macrophage and Kupffer cell cytoplasm in portal areas and extending into adjacent hepatic lobules stains positively, confirming the presence of iron.

Lymph node (hepatic, Figure 2): Multifocally, medullary cords are moderately expanded by large numbers of macrophages that contain abundant dense dark brown to black globular pigment (hemosiderin), intracytoplasmic fragments of erythrocytes (erythrophagocytosis) and scattered foci of extramedullary hematopoiesis. In these regions, connective tissue and blood vessel walls often contains mineral. A mild drainage reaction is present.

**Contributor's Morphologic Diagnosis:** Liver: Moderate multifocal chronic periportal and hepatocellular hemosiderosis, portal-portal and portal-central bridging fibrosis with nodular regeneration and bile duct hyperplasia (secondary hemochromatosis, cirrhosis); extramedullary hematopoiesis, connective tissue mineralization and post-necrotic scarring.

**Contributor's Comment:** Iron overload disorders are defined as either increased deposition of iron in parenchymal organs without clinical manifestations (hemosiderosis) or by organ dysfunction secondary to iron-induced injury (hemochromatosis).[11,16] Hemochromatosis was first described in humans in the 19th century based on the classical clinical presentation of bronze pigmentation of the skin, cirrhosis and diabetes mellitus.[14] It is common in humans and some species of birds, but rare in domestic animals.[17] Primary or hereditary hemochromatosis is due to autosomal recessive disorders in iron metabolism. In humans, most are associated with HFE gene mutations. The most common is caused by a single mutation in *HFE* gene; however, other gene mutations have also been described.[1,2,14] A hereditary form of hemochromatosis has also been described in Salers cattle and is similar to what is seen in humans.[10] Hereditary

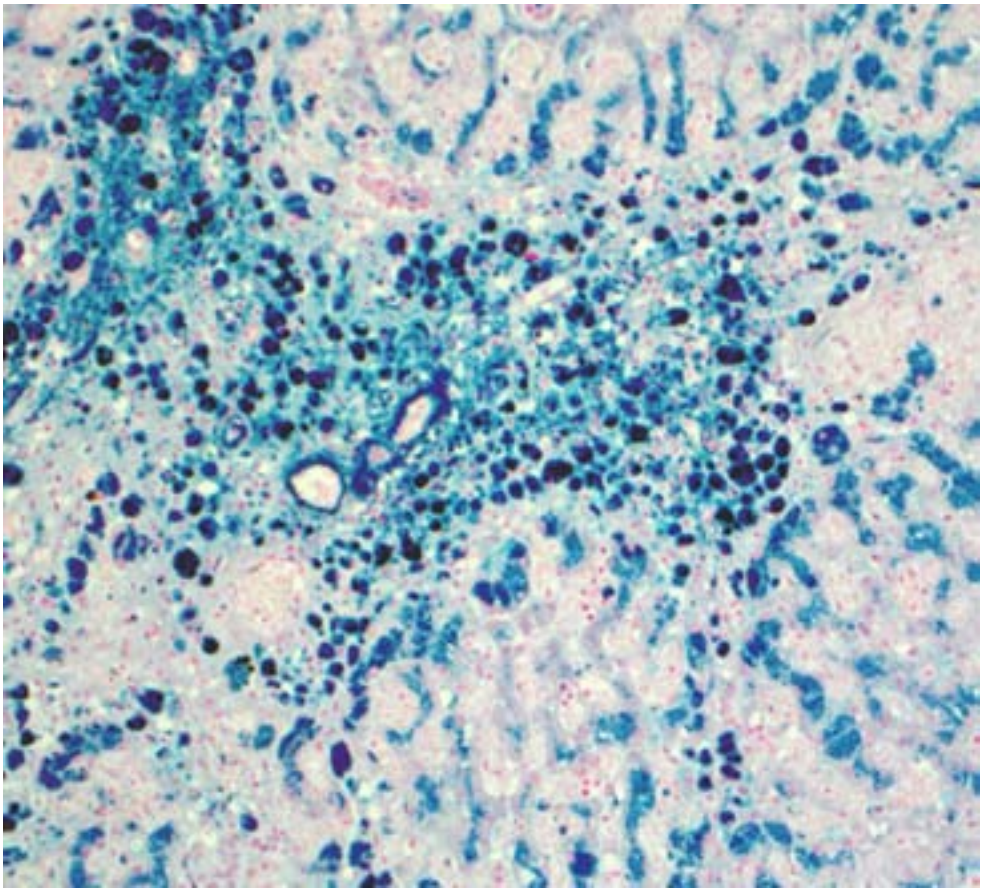

*3-2. Liver, dog: A Perl's iron stain shows accumulation of dark blue granules of hemosiderin within siderophages and blue tint of ferretin within hepatocytes. (HE 200X) (Photo courtesy of: University of Pennsylvania, School of Veterinary Medicine, Laboratory of Pathology and Toxicology and Section of Medical Genetics*

hemochromatosis is more common in humans than secondary; however, causes of secondary include hemolytic anemias +/- chronic transfusions (thalassemia major, sickle cell anemia, and others), dietary iron overload, chronic liver diseases (hepatitis C and B, alcohol-induced liver disease, porphyria cutanea tarda, and fatty liver disease), and other miscellaneous causes.[3,18] In domestic animals, secondary hemochromatosis is rarely seen and has been attributed to repeat blood transfusions, excessive dietary iron, parenteral iron supplementation, primary liver disease and hereditary erythroenzymopathies.[6,10,11,14,16,17]

In the dog of this report, the hemochromatosis is most likely due to the chronic severe hemolytic anemia caused by hereditary PK deficiency.[8] Pyruvate kinase deficiency is an autosomal recessive trait described most commonly in Basenjis, Beagles and West Highland White and Cairn terriers. Affected dogs present with decreased exercise tolerance, tachycardia, systolic heart murmur, pale mucous membranes and splenomegaly.[4,9] In the past the diagnosis was confirmed by measuring erythrocytic enzyme activity. This can be problematic, as erythrocytes of affected dogs lack the normal adult R-PK isoenzyme, but persistently express the $M_2$-PK isoenzyme, which is present in many fetal and adult tissues.[9,17] Testing for known *PK -LR* gene mutations is simpler and now available for Basenjis, Beagles, West Highland White and Cairn terriers, and Pugs.[7,8,15] The Labrador in this report did not have any of the known mutations but was homozygous for a single base substitution in exon 7 of the *PK-LR* gene; this mutation renders the protein dysfunctional.[8]

Pyruvate kinase is primarily responsible for catalyzing the last step in anaerobic glycolysis. A lack of this enzyme greatly impairs ATP-generation in affected erythrocytes, resulting in decreased lifespan and an extravascular hemolytic anemia which is strongly regenerative, with a marked peripheral reticulocytosis.[9] In normal healthy Basenjis, the apparent erythrocyte half-life is approximately 10-28 days, but only 5.8 days in affected dogs.[6] It is estimated that this rapid erythrocyte turnover results in a plasma iron turnover rate that is twice normal. Prolonged and progressive iron overload frequently results in hemosiderosis and may lead to bridging portal fibrosis (cirrhosis) and thus hemochromatosis in the liver of affected dogs.[6,11,12]

Tissue is damaged by excessive uptake of iron as non-transferrin bound iron (NTBI), which, if it accumulates at sufficient concentrations, results in free radical production, iron-induced lipid peroxidation and organelle dysfunction, such as mitochondrial death.[13,14] The organs most commonly affected due to excessive cytoplasmic iron deposition include the liver and pancreas, but can also occur in lymphoid organs, as well as myocardial and skeletal muscles.[10,14,16] Fibrosis and cirrhosis develop in people at a threshold level of approximately 22,000 ppm per dry weight matter (6600 wet weight), which is 12 x normal.[10] The postmortem liver iron level in this dog was 31 x the normal upper reference range limit for dogs, resulting in the changes observed within the hepatic parenchyma.

The lesions associated with hemochromatosis occur when there is loss of equilibrium in systemic iron homeostasis, which is a fine balance between absorption and loss. Control of intestinal iron absorption is tightly regulated by multiple genes and proteins, as there is apparently no regulated mechanism for hepatic or renal excretion of iron in mammals, which occurs only through loss of body secretions, desquamation of intestinal and epidermal cells, or bleeding.[13] Absorption occurs in the duodenum and proximal jejunum across the basolateral membrane of enterocytes where it is taken up as two forms: heme iron from the digestive breakdown of hemoglobin and myoglobin, and non-heme iron released from vegetarian food sources. One of two proteins then sequester the iron to keep it non-reactive: ferritin, which stores iron in cells and is the precursor to hemosiderin, or transferrin, which is the principal iron carrying protein in plasma that distributes iron among tissues for use in biosynthesis of hemoglobin and other iron-containing proteins, and transports to hepatocytes for storage or to tissue macrophages that phagocytize senescent erythrocytes and recycle iron.[1,11,13]

Much recent work has shown that the liver plays a central role in sensing iron needs, which is modulated in part by hepcidin, an acute phase protein which is produced in the liver and secreted into the circulation.[1,3] It is thought that hepcidin responds to two independent signals, iron level and inflammatory status.[13] Hepcidin is upregulated when increased plasma iron levels are sensed, and inhibits export of iron by enterocytes and iron laden macrophages, thus participating in a negative feedback mechanism of regulation.[11,13] It functions by binding to the iron export protein ferroportin, and induces its degradation.[5] Macrophage-based cytokines IL-6, IL-1 and tumor necrosis factor-α also stimulate hepatocellular synthesis of hepcidin.[13] This mechanism is proposed to limit the availability of iron to infectious agents and tumor cells, which require iron to proliferate.[13] Decreased hepcidin expression in dogs with induced iron deficiency has recently been validated, and this work provides incentive for further investigation of gene and protein expression of this and other iron regulating molecules in the dog.[5]

**JPC Diagnosis:** Hepatocytes: Siderosis, periportal, diffuse, severe, with periportal hepatocellular loss and bridging fibrosis.

**Conference Comment:** As elaborately summarized by the contributor, there are serious consequences to a mutation of the rate-limiting step of the anaerobic glycolytic pathway. Erythrocytes, which lack mitochondria, are solely dependent on this pathway for ATP production and thus are most severely affected. However, with the compensatory extramedullary hematopoiesis that can occur following the rapid turnover of erythrocytes, it is ultimately the accumulation of iron within the liver which causes the clinical deterioration observed in this case.

Osteosclerosis with the loss of marrow observed grossly in this case is consistent with other reports in dogs and does not occur in people or cats with PK deficiencies.[8] Mutations resulting in a deficiency of the enzyme phosphofructokinase, another protein in the glycolytic pathway, has also been described in dogs. It causes a persistent hemolytic anemia with occasional episodes of intravascular hemolysis due to alkalemia from hyperventilation, such as occurs during strenuous exercise. This also leads to hepatic hemosiderosis and can affect the skeletal muscle, however, osteosclerosis and liver failure has not been observed in these cases.[9]

**Contributing Institution:** University of Pennsylvania, School of Veterinary Medicine Laboratory of Pathology and Toxicology and Section of Medical Genetics

**References:**

1. Andrews N. Forging field: the golden age of iron biology. *Blood*. 2008;112:219-231.
2. Feder JV, Gnirke A, Thomas W, et al. A novel MHC class I – like gene is mutated in patients with hereditary haemochromatosis. *Nat Genet*. 1996;13:399-408.
3. Fleming RE, Ponka P. Iron overload in human disease. *N Engl J Med*. 2012;366:348-359.
4. Fry MM, McGavin MD. Bone marrow, blood cells and system. In: McGavin MD, Zachary JF, eds. *Pathologic Basis of Veterinary Disease*. 4th ed. St. Louis, MO: Mosby Inc.; 2007:790.
5. Fry MM, Kirk CA, Liggett JL, Daniel GB, Baek SJ, Gouffon JS, et al. Changes in hepatic gene expression in dogs with experimentally induced nutritional iron deficiency. *Vet Clin Path*. 2009;38:13-19.
6. Giger U, Noble NA. Determination of erythrocyte pyruvate kinase deficiency in Basenjis with chronic hemolytic anemia. *J Am Vet Med Assoc*. 1991;198:1755-1761.
7. Giger U. Erythrocyte phosphofructokinase and pyruvate kinase deficiencies. In: Feldman BF, Zinkl JG, Jain NC. *Schalm's Veterinary Hematology*. Baltimore, MD: Lippincott Williams and Wilkins; 2000:1020-1025.
8. Inal Gultekin G, Raj K, Foureman P, Lehman K, Manhart K, Abdulmalik O, et al. Erythrocyte pyruvate kinase mutations causing hemolytic anemia, osterosclerosis and secondary hemochromatosis. *J Vet Intern Med*. [in press, 2012]
9. Harvey JW. Pathogenesis, laboratory diagnosis, and clinical of erythrocyte enzyme deficiencies in dogs, cats and horses. *Vet Clin Pathol*. 2006:35;144-156.
10. House JK, Smith BP, Maas J, Lane VM, Anderson BC, Graham TW, et al. Hemochromatosis in Salers cattle. *J Vet Med*. 1994;8:105-11.
11. McCown JL, Specht AJ. Iron homeostasis and disorders in dogs and cats: a review. *JAAHA*. 2011;47(3):151-160.
12. Naigamwalla DZ, Webb JA, Giger U. Iron deficiency anemia. *Can Vet J*. 2012;53:250–25.
13. Nairz M, Weiss G. Molecular and clinical aspects of iron homeostasis: from anemia to hemochromatosis. *The Mid Europ J of Med*. 2006;118:442-462.
14. Pietrangelo A. Hereditary hemochromatosis-a new look at an old disease. *N Engl J Med*. 2004:350;2383-2397.
15. Skelly BJ, Wallace M, Rajpurohit YR, Wang P, Giger U. Identification of a 6 base pair insertion in West Highland white terriers with erythrocyte pyruvate kinase deficiency. *Am J Vet Res*. 1999:60;1169-1172.
16. Sprague WS, Hackett TB, Johnson JS, Swardson-Olver CJ. Hemochromatosis secondary to repeated blood transfusions in a dog. *Vet Pathol*. 2003:40;334-337.
17. Stalker MJ, Hayes MA. Liver and biliary system. In: Maxie MG, ed. *Jubb, Kennedy and Palmer's Pathology of Domestic Animals*. 5th ed. Vol. 2. Philadelphia, PA: Elsevier Saunders; 2007:308-9.
18. Tavill AS. Diagnosis and management of hemochromatosis. *Hepatology*. 2001;33(5): 1321-1328.

**CASE IV:** 10727798 (JPC 3166453).

**Signalment:** 10-year-old spayed female mixed breed dog (*Canis familiaris*).

**History:** Patient was initially being evaluated for a left mandibular mass. On additional imaging studies, other tumors were found in the left cranial lung lobe and left adrenal gland. The patient then underwent thoracotomy for partial lung lobectomy and the specimen was submitted for histopathological examination. Two weeks later, the dog underwent laparotomy for excision of the left adrenal gland, and an additional mass was noted in the right medial hepatic lobe. The patient never recovered from anesthesia after laparotomy and developed acute hemoabdomen and hematemesis. Samples from the hepatic mass and the left adrenal gland were submitted for histopathologic examination.

**Gross Pathologic Findings:** The sample from the left cranial lung lobe contained a 7 mm diameter, well demarcated subpleural nodule at the distal border of the lobe (Fig.1). On cut section, this nodule was firm and pale tan. Approximately 3mm cranial to this nodule there was an irregular and poorly demarcated area of parenchymal cavitation immediately adjacent to the inked (yellow) surgical margin.

**Histopathologic Description:** A section of lung contains an unencapsulated and well-demarcated peripheral subpleural mass. This mass is solid and composed of two distinct cellular populations, characterized by large scattered acinar-like structures and peripheral papilliferous projections (adenocarcinomatous component), amongst tightly packed cords of cells (small cell component), which diffusely obscure a background of fine fibrovascular stroma. The acinar-like structures are lined by a monolayer of tall columnar epithelium with abundant well-delineated acidophilic cytoplasm. The nuclei are round to ovoid and have sparse finely stippled chromatin with small conspicuous nucleoli. There is loss of nuclear polarity. Anisocytosis and anisokaryosis are moderate, up to 2 fold, with 0-1 mitotic figures per high power field (40X). The cells between the acinar structures are smaller, round to polygonal and have moderate to poorly delimited light acidophilic to clear cytoplasm. The nuclei are round to ovoid and have sparse finely stippled chromatin with large conspicuous nucleoli. Anisocytosis and anisokaryosis are moderate to marked, up to 3 fold, with 8-10 mitotic figures per high power field (40X). There is extensive coalescing necrosis of the mass. Abundant neutrophils, macrophages, sloughed neoplastic cells and basophilic mucus fill the lumen of the neoplastic acini. Small numbers of neutrophils, fewer eosinophils, lymphocytes and rare plasma cells infiltrate the mass. The inked surgical margin is clean but narrow and measures less than 1 mm thick. The pulmonary parenchyma adjacent to the mass is moderately atelectatic and displays extensive hemorrhage within alveolar spaces.


*4-1. Lung, dog: The left cranial lung lobe contained a 7 mm diameter, well demarcated subpleural nodule at the distal border of the lobe. (Photo courtesy of: The Animal Medical Center, 510 East 62nd St. New York, NY- www.amcny.org)*

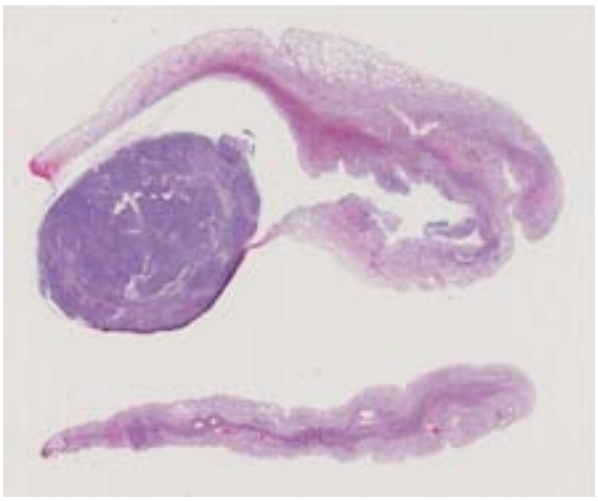

*4-2. Lung, dog: Subgross of the neoplastic nodule. (HE 6.3X)*

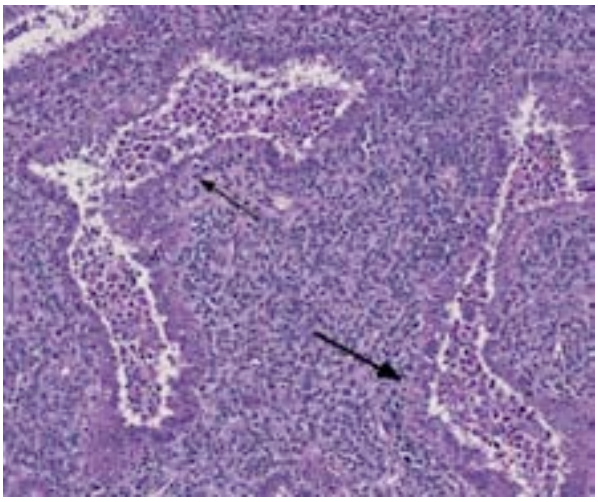

*4-3. Lung, dog: The neoplasm is composed of acini lined by neoplastic columnar epithelial cells (arrows), which are separated by neoplastic polygonal epithelial cells arranged on a moderate fibrous stroma. (HE 100X)*

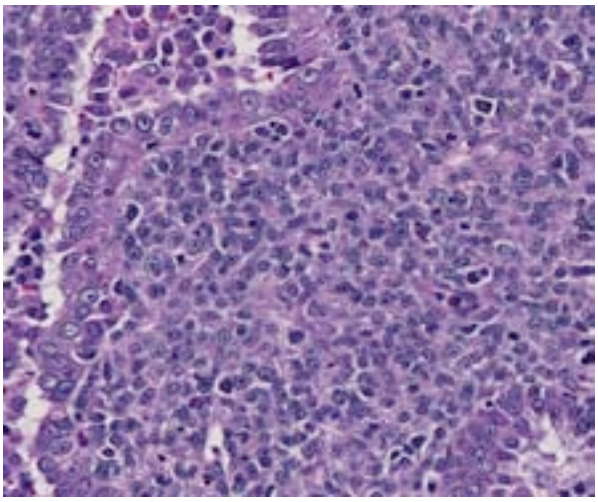

*4-4. Lung, dog: Higher magnification of neoplastic cells, with acini recapitulating primitive airways. (HE 320X)*

With immunohistochemistry, the adenocarcinomatous component of the tumor was strongly positive for pancytokeratin markers AE1 and AE3. Although pancytokeratin expression was negative for the vast majority of the small cell component, scattered individual cells displayed strong cytoplasmic expression for both markers. Neither the adenocarcinomatous or small cell component expressed synaptophysin, chromogranin or neuron specific enolase (NSE). Small numbers of scattered cells throughout the tumors expressed CD20 and CD18 and were interpreted in combination with the H&E section as leukocytes (secondary inflammation).

Histopathologic examination of the left mandibular mass (not provided) was consistent with a salivary gland adenocarcinoma. Sections from the left adrenal gland (not provided) revealed a malignant pheochromocytoma. The hepatic nodule from the right medial lobe (not provided) displayed the same morphology as observed in the pulmonary nodule and was interpreted as a focus of metastasis from the pulmonary neoplasm.

**Contributor's Morphologic Diagnosis:** Lung (left cranial lobe): Combined pulmonary carcinoma.

**Contributor's Comment:** The dog in the present case had three distinct unrelated neoplasms in different organs with no overt clinical evidence of metastatic disease, except for a hepatic nodule, which was later interpreted as a focus of metastasis from the primary pulmonary mass. The cause for initial presentation to our hospital was a left parotid salivary adenocarcinoma, and when a pulmonary nodule was found in subsequent imaging studies, the immediate clinical suspicion was of metastatic disease from the parotid gland to the lungs. Surprisingly, the pulmonary nodule exhibited unique dual microscopic morphology (an adenocarcinomatous and a small-cell component), not observed in the salivary gland mass, and was diagnosed as a combined pulmonary carcinoma.

Combined tumors are neoplasms that display more than one cellular morphology and microscopic architecture, often composed of cells with remarkably different histological, histochemical and immunohistochemical properties.[8] One example of combined tumor in humans is combined pulmonary carcinomas, which have been reported to exhibit combinations of up to 4 distinct morphologies (squamous cell carcinoma, small-cell/neuroendocrine carcinoma, blastoma and adenocarcinoma).[9] Additionally, extra-pulmonary combined tumors with a small cell/ neuroendocrine component associated with a component of squamous cell carcinoma or adenocarcinoma appear to be relatively common in the rare group of small cell carcinomas in people, and have been reported in the esophagus, prostate gland and colon.[10] Aside from combined pulmonary carcinoma of dogs and cats, other examples of combined tumors in domestic animals include carcinosarcomas of mammary

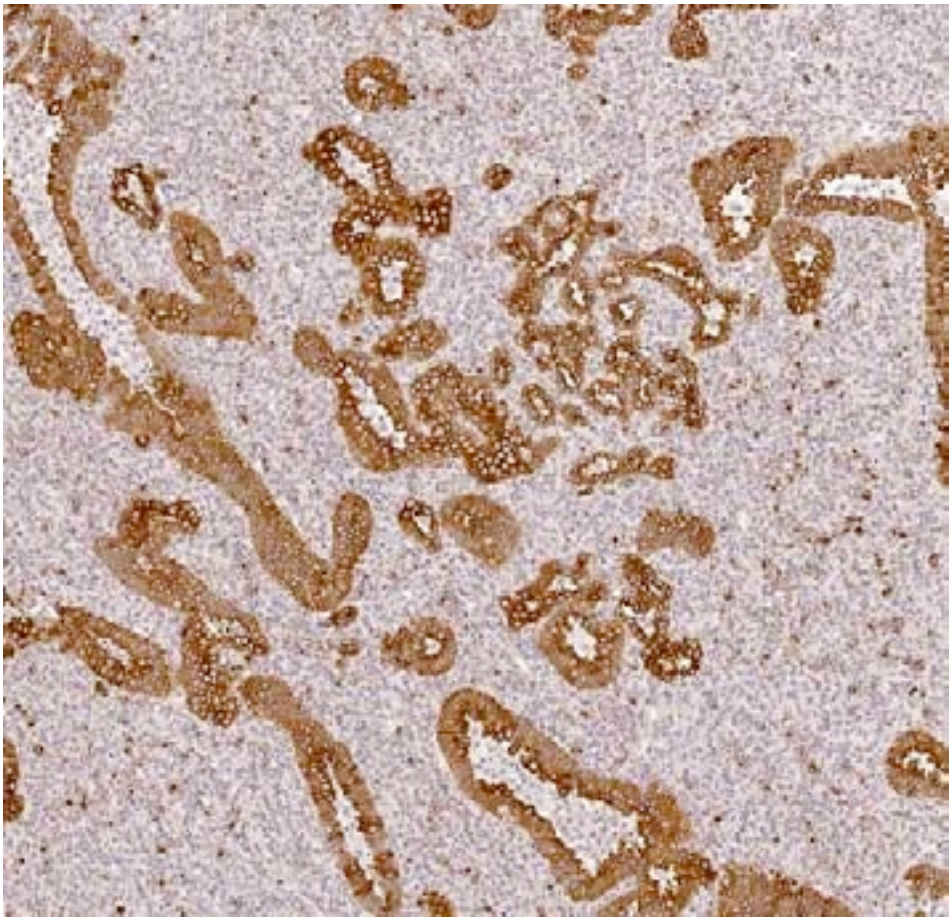

*4-5. Lung, dog: Neoplastic cells lining airways stain strongly positive for cytokeratin; polygonal cells multifocally stain positively as well. (Anti-cytokeratin 100X)*

gland and combined hepatocellular-cholangiocellular carcinoma.[13]

Overall, primary pulmonary neoplasms are exceedingly common in people and uncommon in dogs.[1] The prevalence of primary lung cancer in the overall canine population has been reported to be of 1% of all diagnosed canine neoplasia.[1,3,12] The most accepted veterinary classification of pulmonary neoplasms to date includes adenomas and papillomas, bronchial gland carcinoma, squamous cell carcinoma, adenocarcinomas of papillary, acinar, solid and mixed types, bronchioloalveolar carcinoma, adenosquamous carcinoma, small and large cell carcinomas, neuroendocrine carcinoma, pulmonary blastoma and combined carcinoma.[4,14] Adenocarcinomas appear to be the most common type of lung cancer in domestic animals.[3] In contrast to the veterinary classification, in people, combined carcinoma is classified as a subvariant of small cell carcinomas, since it has been shown that the small cell component in those tumors has neuroendrocrine properties. The importance of proper tumor classification in this instance lies in the fact that prognostic outcome and therapeutic management largely depend on the leading histomorphological tumor type.[6] The same has not been proven in the rare cases of combined pulmonary tumors of domestic animals[4], where the small cell component has failed to express the most common neuroendocrine immunohistochemical markers, such as chromogranin, synaptophysin and neuron-specific enolase (as in the present case), and accurate definition of histogenesis of this component remains unavailable. To date, the histogenesis of the small cell component of combined pulmonary tumors of domestic animals has only been morphologically and immunohistochemically characterized as a pulmonary basaloid cell. The difficulty in further analyzing these tumors at the molecular level in domestic animals is most likely due to the rarity of the tumor, which has only been reported in cats and less commonly dogs.[4]

Despite the high prevalence of lung cancer in people, combined pulmonary tumors are also rare in this population. In a recent retrospective study of 1,158 pulmonary surgical specimens of people, combined carcinomas represented 1.8% of all pulmonary tumors.[5] Nevertheless, a few studies in human specimens have been able to provide further insight on what seems to be the most intriguing and fascinating aspect of this rare neoplastic entity; the nature of its capability to produce such phenotypically distinct components.

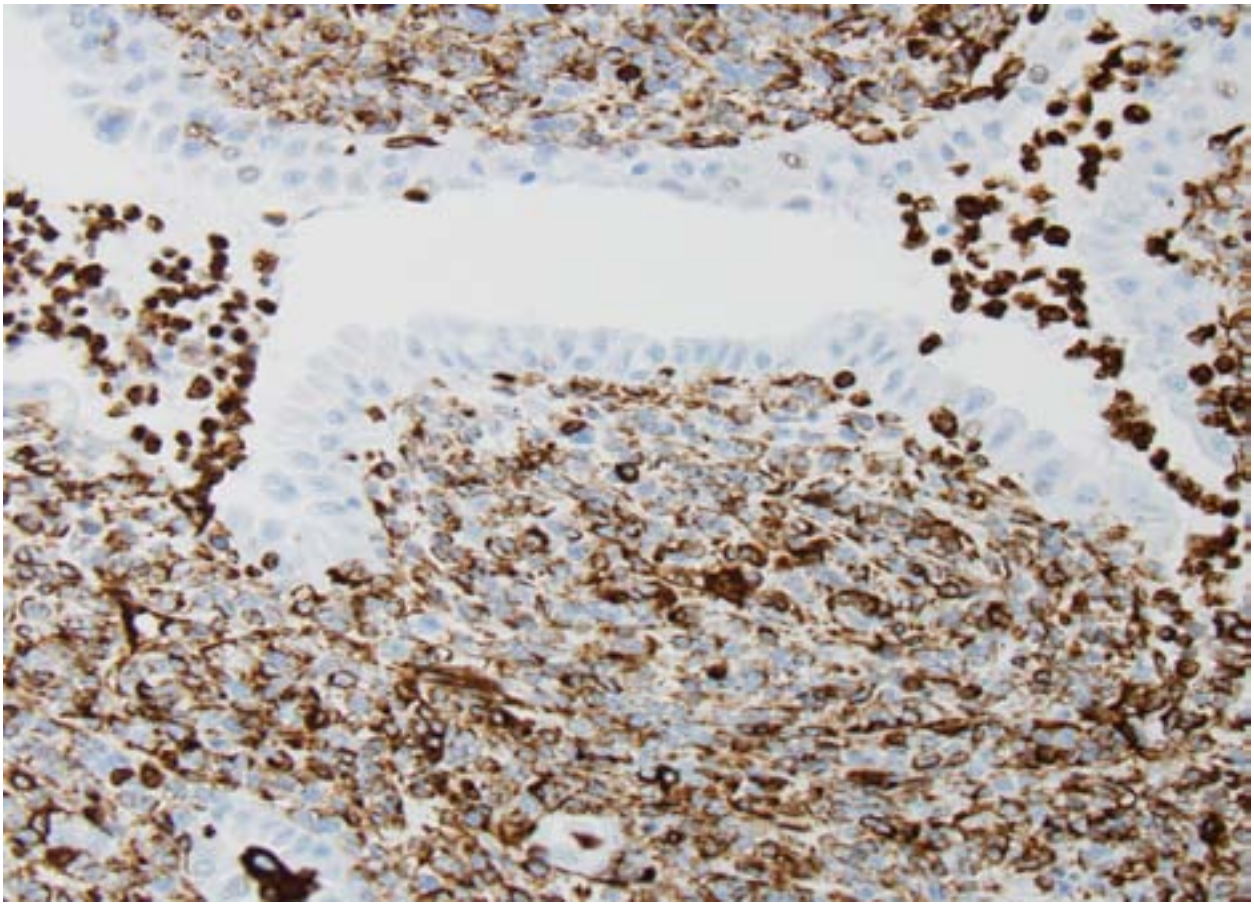

*4-6. Lung, dog: Neoplastic polygonal cells stain strongly positive for vimentin. (Anti-vimentin 280X)*

The main questions raised around this entity are whether the different components of the tumors are genetically related and why and how differentiation towards such different cellular components occurs.[5,8,9,11] Answer to these questions may shed light on the histogenesis and biologic behavior of the tumor cells. Clonality assays and study of LOH (loss of heterozygosity) have been employed to aid in answering these questions; however, so far, the results raise more questions than definitive results.

To date, a few studies have shown monoclonality and identical genetic alterations in the specific chromosomes analyzed in a few of these tumors, raising the hypothesis that the different cellular components of the tumors are likely derived from a common precursor cell and driven by the same carcinogens.[5,8,9,11] In these cases, it remains to be understood why cells with a common genetic profile display such distinct morphology, histochemical and immunohistochemical properties. It can be hypothesized that during malignant transformation, some of the progeny cells derived from a common precursor cell may convert to a different morphology under influence of different environmental stimuli. Alternatively, the clonal neoplastic cell may retain the ability to differentiate toward other morphologic phenotypes in response to different stimuli.[8]

In contrary to those results, one study has shown a few combined tumors with different genetic profiles, despite such close morphologic relationship of the different cellular components. In those cases, it was hypothesized that the different groups of cells (small cell component with squamous cell differentiation and a separate adenocarcinomatous component) may have undergone separate progression from a pluripotent single clone in a very early stage, resulting in distinct genetic abnormalities that may have developed in a later phase of the tumor progression.[11] Further clonality and LOH studies on this rare neoplastic entity are still necessary and would help to provide additional insight in the field of stem cells, tumor biology and oncologic pathology.

The concomitant development of multiple different neoplasms in this dog (salivary gland adenocarcinoma, combined pulmonary carcinoma and pheochromocytoma) is also an interesting point of discussion beyond the scope of this brief review.

**JPC Diagnosis:** Lung: Combined pulmonary carcinoma.

**Conference Comment:** This case provides an exceptional example of a rarely reported tumor in dogs and cats. As the contributor elucidates, the histogenesis of this neoplasm is not definitive which offers an interesting opportunity for discussion and speculation surrounding this case. The additional clinical findings of two other distinct neoplasms and liver metastasis in this dog further adds to the discussion with regard to tumor suppressors and malignant transformation.

As previously outlined, the reactivity of cytokeratin within both cell populations is characteristic to this diagnosis. The conference discussion, however, was focused on the finding of diffuse immunoreactivity among the small cell population with vimentin leading some to consider the diagnosis of carcinosarcoma for this case. Carcinosarcomas usually have areas of osseous or chondrous metaplasia within the mesenchymal cell population[4]; and the small cell component in this case does not have spindle cell morphology, thus our agreement with the contributor's diagnosis.

Participants noted the primitive morphology and loss of polarity within the small cell component. This led to a discussion on the epithelial-mesenchymal transition (EMT) as being a possible cause for the change in cellular morphology as well as the expression of vimentin, which would be consistent with the presence of metastasis observed in this case.

The EMT is a well-defined process of transformation during which neoplastic cells acquire the ability to invade and disseminate. Included in this transformation is a conversion from a polygonal to spindle morphology along with the repression of E-cadherin expression.[7] Loss of E-cadherin, a key cellular adhesion molecule, eliminates the cellular restraint mechanism within the tissue of origin thereby permitting dissemination. This transformation has been characterized histologically by increased expression of vimentin, which also has been found to correlate with grading criteria in some neoplasms.[15] While there have been studies examining cytokeratin and vimentin expression in canine pulmonary tumors, a correlation with histologic grade has not been demonstrated.[2]

**Contributing Institution**: The Animal Medical Center
510 East 62nd St.
New York, NY
www.amcny.org

**References:**

1. Buendia AJ, Sanchez A, Martinez CM, Navarro JA. Immunohistochemical characterization of a pulmonary large-cell carcinoma in a dog. *Vet Pathol*. 2008;45:484-485.
2. Burgess HJ, Kerr ME. Cytokeratin and vimentin co-expression in 21 canine pulmonary epithelial neoplasms. *J Vet Diagn*. 2009;21:815-820.
3. Castellano MC, Massonez AR, Idiart JR. Primary pulmonary adenocarcinoma metastatic to the uvea, brain, and adrenal gland in a dog. *J Vet Med A*. 2006;53:194-197.
4. Dungworth DL, Hauser B, Hahn FF, Wilson DW, Haenichen T, Harkema JR. *Histological Classification of Tumors of the Respiratory System of Domestic Animals*. 2nd ed. Vol VI. Washington, DC: Armed Forces Institute of Pathology, American Registry of Pathology. 1999.
5. Fellegara G, D'adda T, Pilato FP, Froio E, Ampollini L, Rusca M, et al. Genetics of a combined lung small cell carcinoma and large cell neuroendocrine carcinoma with adenocarcinoma. *Virchows Arch*. 2008;453:107-115.
6. Hahn FF, Muggenburg BA, Griffith WC. Primary lung neoplasia in a Beagle colony. *Vet Pathol*. 1996;33:633-638.
7. Hanahan D, Weinberg RA. Hallmarks of cancer: the next generation. *Cell*. 2011;144:646-674.
8. Huang J, Behrens C, Wistuba II, Gazdar AF, Jagirdar J. Clonality of combined tumors. *Arch Pathol Lab Med*. 2002;126:437-441.
9. Iezumi K, Masugana A, Kadofuku T, Iwamoto S, Masuda M, Suzuki S, et al. Combined small cell carcinoma with pulmonary blastoma and adenocarcinoma. Case report and clonality analysis. *Pathol Res Pract*. 2006;202:895-899.

10. Junker K, Wiethege T, Muller KM. Pathology of small-cell lung cancer. *J Cancer Res Clin Oncol*. 2000;126:361-368.
11. Murase T, Takino H, Shimizu S, Inagaki H, Tateyama H, Takahashi E, et al. Clonality analysis of different histological components in combined small cell and non-small cell carcinoma of the lung. *Hum Pathol*. 2003;34(11):1178-1184.
12. Polton GA, Brearley MJ, Powell SM, Burton CA. Impact of primary tumor stage on survival in dogs with solitary lung tumors. *J Small An Pract*. 2008;49:66-71.
13. Shiga A, Shirota K, Enomoto M. Combined hepatocellular and cholangiocellular carcinoma in a dog. *J Vet Med Sci*. 2001;63(4):483-486.
14. Wilson DW, Dungworth DL. Tumors of the respiratory tract. In: Meuten DJ, ed. *Tumors in Domestic Animals*. 4th ed. Ames, IA: Iowa State Press; 2002:365-399.
15. Zhao Y, Yan Q, Long X, Chen X, Wang Y. Vimentin affects the mobility and invasiveness of prostate cancer cells. *Cell Biochem Funct*. 2008;26:571-577.

**Joint Pathology Center**
**Veterinary Pathology Services**

*Conference Coordinator*
**Matthew C. Reed, DVM**
**Captain, Veterinary Corps, U.S. Army**
**Veterinary Pathology Services**
**Joint Pathology Center**

## WEDNESDAY SLIDE CONFERENCE 2014-2015

# Conference 5

**1 October 2014**

**Conference Moderator:**
LTC Shelley Honnold, DVM, Diplomate ACVP
Chief, Pathology Division
USAMRIID
1425 Porter Street
Fort Detrick, MD 21702

---

**CASE I:** W356-13 (JPC 4034430).

**Signalment:** 1-year-old male neutered Border Collie, dog, *Canis familiaris.*

**History:** The dog was presented at the Veterinary Hospital of the University of Melbourne with acute progressive severe respiratory distress. The dog had been diagnosed by the referring veterinarian with immune-mediated haemolytic anaemia (IMHA) two months prior to presentation and then treated with very high doses of immunosuppressants (prednisolone, cyclopsporine, azathioprine) and aspirin.

At presentation the dog had generalized heart sounds; radiographs showed a diffuse, mixed, predominantly interstitial pattern in all lung lobes. Transtracheal wash revealed neutrophilic

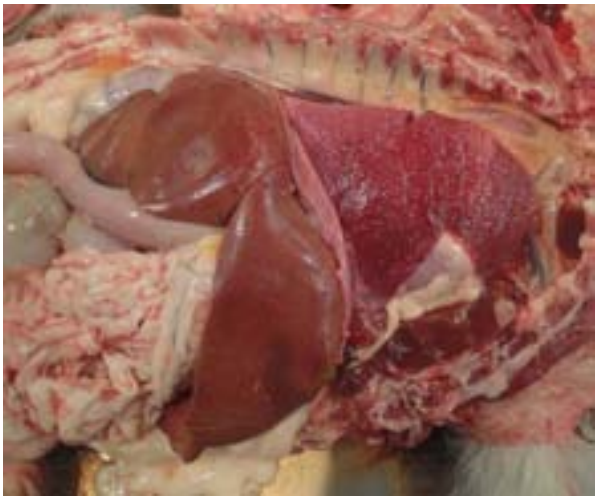

*1-1. In situ photograph, dog: Lung lobes are diffusely dark red with numerous randomly distributed cream-colored nodules. The liver is enlarged and tan with rounded borders. (Photo courtesy of: Faculty of Veterinary Science, University of Melbourne www.vet.unimelb.edu.au)*

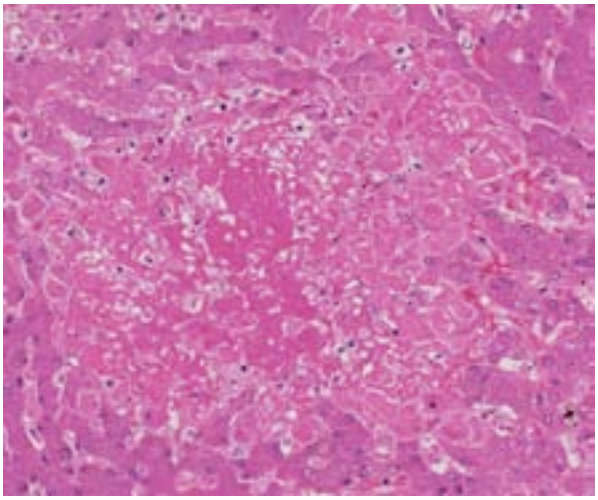

*1-2. Liver, dog: Foci of coagulative necrosis are randomly scattered throughout the section. (HE 172X)*

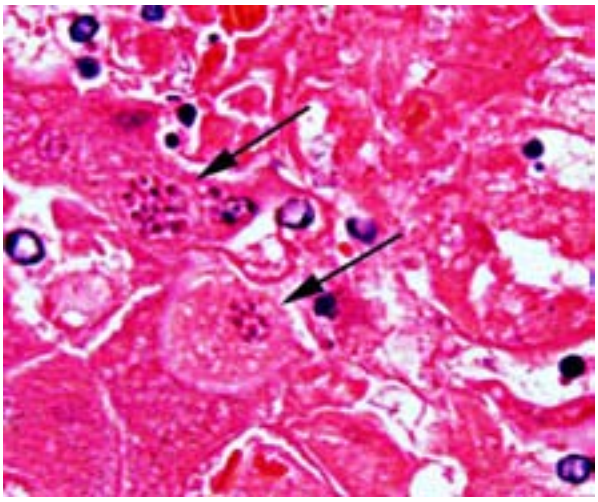

*1-3. Liver, dog: At the edges of necrotic foci, hepatocytes contain intracytoplasmic cysts with numerous 2-4 µm zoites. (HE 600X)*

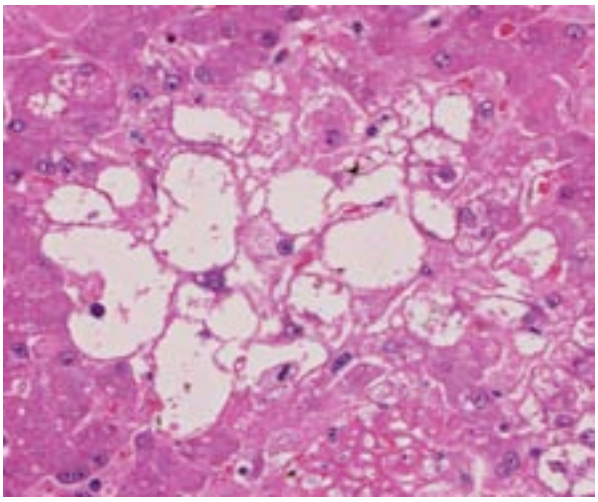

*1-4. Liver, dog: Multifocally, centrilobular and midzonal hepatocytes are swollen with coalescing clear vacuoles (glycogenosis) characteristic of steroid hepatopathy. (HE 292X)*

inflammation with protozoa. The dog deteriorated progressively and spontaneously arrested.

**Gross Pathology:** All lung lobes were diffuse dark red and had numerous randomly distributed cream-coloured nodules varying from 1-4 mm in diameter which extended throughout the lung parenchyma. The liver was enlarged with rounded borders and diffuse tan discolouration displaying fine red surface stippling.

**Laboratory Results:** IFAT (plasma): Positive for *Toxoplasma* sp. (titre 1:128), negative for *Neospora* sp. Immunohistochemistry was positive for *Toxoplasma* sp.

**Histopathologic Description:** Liver: Throughout the hepatic parenchyma there are multifocal randomly distributed areas of hepatocellular necrosis, characterized by loss of tissue architecture and replacement by eosinophilic cellular and karyorrhectic debris. In the necrotic areas, or peripheral to these, there are numerous, often clustered, tachyzoites approximately 2 µm in diameter with an indistinct internal structure that occasionally appears to have a bilobed nucleus. Multifocally groups of hepatocytes are swollen with clear, finely granular cytoplasm and peripherally displaced nucleus.

**Contributor's Morphologic Diagnosis:** Multifocal hepatocellular necrosis, subacute, severe, with intra-lesional protozoal organisms; multifocal hepatocellular vacuolar degeneration, moderate, chronic.

**Contributor's Comment:** *Toxoplasma gondii* is a coccidian protozoan that is found throughout the world and infects an extensive range of intermediate hosts in which it causes both clinical and more commonly, subclinical disease. Domestic and wild felids are the only known definitive hosts and also serve as intermediate hosts.[1]

Infection occurs by ingestion of sporulated oocysts excreted in the feces of felids, by ingestion of tissues of intermediate hosts that contain encysted bradyzoites or tachyzoites, and less frequently by vertical transmission. Once ingested, sporozoites excyst and multiply in the intestinal epithelial cells as tachyzoites. Tachyzoites can either disseminate and infect cells throughout the body resulting in the necrosis and less commonly non-suppurative inflammation characteristic of toxoplasmosis, or encyst in tissues as bradyzoites. Following ingestion of tissue cysts by an intermediate host, bradyzoites will excyst, become tachyzoites, and the cycle continues.[1] Necrosis is caused by rupture of infected cell membranes by rapidly dividing tachyzoites. Inflammation is typically not associated with the cysts and can be minimal in association with the tachyzoites.[2] Tissue cysts are presumed to persist throughout the life of the host. Even though a high percentage of animals are serologically positive for toxoplasmosis, only a few animals develop clinical disease. Immunosuppression commonly causes reactivation of latent infections caused by *T. gondii* and is usually characterized by

involvement of the central nervous system, occasionally the lungs and infrequently other organs, including the skin.[4]

The tachyzoites, bradizoites and tissue cysts of *Neospora caninum* and *Toxoplasma gondii* appear essentially identical by standard light microscopy. Immunohistochemistry and PCR are commonly used to confirm the diagnosis. Even though IHC using polyclonal antibodies against *T. gondii* is considered sensitive, positive results might not be conclusive, due to moderately low specificity of polyclonal antibodies that can cross-react between *T. gondii* and *N. caninum.*[5]

Ultrastructure is also used to distinguish between *T.gondii and N.caninum.* Some of the most prominent ultrastructural differences occur in the number, appearance and location of rhoptries, looped-back rhoptries, micronemes, dense granules, small dense granules and micropores. The tissue cysts of both parasites are basically similar, being surrounded by a cyst wall and not compartmentalised by septa. The cyst wall of N. *caninum* is usually irregular and substantially thicker (<0.5 mm), than those of *T. gondii* which are typically smooth and 0.5 mm thick.[6]

**JPC Diagnosis:** 1. Liver: Hepatitis, necrotizing, random, multifocal, moderate, with edema and intrahepatocytic, intrahistiocytic, and extracellular zoites.
2. Liver, hepatocytes: Glycogenosis, centrilobular and midzonal, multifocal, moderate.

**Conference Comment:** While most often associated with abortion in domestic animals, this case of *Toxoplasma gondii* serves as a reminder of its ubiquitous nature. All homeothermic animals are susceptible to infection, and the organism may be present in a wide range of organ systems.[2] Infection is also often associated with immunosuppression, as demonstrated in this case. Of note, marsupials are thought to be particularly susceptible to both *Toxoplasma* and *Neospora.*[3]

*Toxoplasmosis* is a significant contributor to abortion in domestic animals due to both cotyledonary and caruncular necrosis of the placenta. Other characteristic lesions include interstitial pneumonia, lymphadenitis, myocarditis, nonsuppurative meningitis, ophthalmitis and hepatic necrosis.[2]

*T. gondii* is an obligate intracellular parasite, and its growth and replication only occur in target cells and eventually cause cell death. At the core of its infectivity is the ability to cross barrier systems, including intestinal mucosa, the blood-brain barrier, the blood-retina barrier and the placenta. This process involves parasite motility, likely in the tachyzoite stage, and interactions between parasite adhesins and target cell receptors. The cellular binding occurs via the parasite surface proteins SAGs, which are expressed in abundance on tachyzoites, and SAG1 receptors in addition to laminin and lectin on target cells.[7]

The contributor accurately details the distinguishing characteristics between *Toxoplasma* and *Neospora* on electron microscopy. Both parasites induce similar lesions and appear identical with histopathology; however, *Toxoplasma* is always found within a parasitophorous vacuole while *Neospora* may not be. Other organisms which may be found within parasitophorous vacuoles include *Sarcocystis*, though these are primarily in skeletal or cardiac muscle.[2]

The glycogenosis noted in the hepatocytes is secondary to the administration of exogenous corticosteroids. Glycogenosis may be histologically differentiated from lipidosis as the vacuoles seen in glycogenosis are coalescing rather than discrete. In most cases, steroid-induced gluconeogenesis causes increases in both hepatocellular lipid and glycogen, but glycogensosis is often the predominant histologic change.

We favor the use of two morphologic diagnoses in this case, one for the protozoal infection and one for the glycogenosis, as they are part of two distinct, albeit related processes.

**Contributing Institution:** Faculty of Veterinary Science, University of Melbourne www.vet.unimelb.edu.au

**References:**
1. Dubey JP, Lindsay DS, Lappin MR. *Toxoplasmosis* and other intestinal coccidial infections in cats and dogs. *Vet Clin North Am Small Anim Pract*. 2009;39:1009–1034.
2. Brown CC, Baker DC, Barker IK. Alimentary system. In: Maxie MG, ed. *Jubb, Kennedy and*

*Palmer's Pathology of Domestic Animals.* 5th ed. Vol. 2. Philadelphia, PA: Elsevier Saunders; 2007:271-273.
3. Mayberry C, Maloney SK, Mitchell J, Mawson PR, Bencini R. Reproductive implications of exposure to *Toxoplasma gondii* and *Neospora caninum* in western grey kangaroos (*Macropus fuliginosus ocydromus)*. 2014;50(2):364-368.
4. Rodrigues Hoffman A, Cadieu J, Kiupel M, Lim A, Bolin SR, Mansell J. Cutaneous toxoplasmosis in two dogs. *J Vet Diagn Invest*. 2012;24:636-640.
5. Kaufmann H, Yamage M, Roditi I, et al. Discrimination of *Neospora caninum* from Toxoplasma gondii and other apicomplexan parasites by hybridization and PCR. *Mol Cell Probes*. 1996;10:289–29.
6. Speer CA, Dubey JP, McAllister MM, Blixt JA. Comparative ultrastructure of tachyzoites, bradyzoites, and tissue cysts of *Neospora caninum* and Toxoplasma gondii. *Int J Parasitol*. 1999;29:1509-1519.
7. Zachary JF. Mechanisms of microbial infections. In: Zachary JF, McGavin MD, eds. *Pathologic Basis of Veterinary Disease.* 5th ed. St. Louis, MO: Elsevier Mosby; 2012:239-240.

**CASE II**: 10536 (JPC 4048507).

**Signalment:** 9-year-old, spayed female Persian cat, *Felis catus.*

**History:** The cat developed a soft dermal nodule in the right thoracic region; the overlying skin was unremarkable. The cat was brought to the referring veterinarian due to rapid (2-week) enlargement of the nodule with ulceration (Fig. 1) 8 months after initial presentation. Cytology of the material was characterized by abundant necrotic debris, foamy reactive macrophages, degenerated neutrophils and occasional fragments of fungal hyphae. The nodule was surgically excised and processed for histology and electron microscopy. The histopathology revealed a pyogranulomatos inflammation centered on PAS positive fungal hyphae. After 3 years, the cat is still free of disease without any additional therapy. An electron micrograph at 12,000x magnification is provided.

**Gross Pathology:** Nodular lesion in dorso-lateral thorax with draining tracts oozing sero-sanguineous material

**Laboratory Results:** No fungal isolation was attempted by the referring veterinarian. CBC and urine analysis were unremarkable.

**Electron Microscopy Description:** Dermis, 12,000 magnification. On the electron micrograph, there are longitudinal and transverse sections of fungal hyphae within the cytoplasm of a reactive macrophage. On the right-hand top corner, two nuclei with slightly irregularly infolded nuclear envelopes, a prominent nucleolus, randomly scattered dispersed chromatin and multifocal aggregates of marginated chromatin are evident. The cytoplasm is abundant and contains mitochondria, stacks of rough endoplasmic reticulum and free ribosomes (binucleated macrophage).

*2-1. Presentation, cat: The cat presented with a nodular lesion in the dorsolateral thorax with a draining tract and a serosanguineous exudate. (Photo courtesy of: DIVET - Department of Veterinary Science and Public Health, http://www.divet.unimi.it/ecm/home)*

The fungal hyphae are septate and characterized by a thick homogeneously moderately electrondense fibrillar cell wall with an underlying thin, highly electron-dense plasma membrane enclosing moderate amount of granular, moderately electron-dense cytoplasm. The latter contains few elongated to round mitochondria, moderate numbers of round single-membrane bound electron lucent vacuoles, scattered ribosomes and rare myelin figures. Two nuclei with central to paracentral prominent nucleoli and a nuclear envelope are present. Fungal structures are surrounded by a variably thick, moderately to highly electron-dense, fibrillar material (accumulation of immunoglobulins – Splendore-Hoeppli reaction), multifocally radiating from the hyphal surface.

**Contributor's Morphologic Diagnosis:** Macrophagic (granulomatous) dermatitis with fungal hyphae and Splendore-Hoeppli formation consistent with pseudomycetoma.

**Contributor's Comment:** Fungal organisms are eukaryotes with structurally defined cell, cytoplasm and nucleus. According to ultrastructural descriptions, most fungal cells contain free ribosomes, mitochondria, vesicles involved in endocytosis and exocytosis and lipid. The fungal vacuole is similar to the plant vacuole has enzymatic functions. Nuclei are smaller than those of vertebrate cells with a defined nuclear membrane and a nucleolus. DNA is largely located in the nucleolus.[6]

Specifically, electron microscopy of *M. canis* has been well described.[17] *M. canis* hyphae have a cell wall consisting of an outer thin, electron-dense layer and an inner and broader fibrillar electron-lucid layer. Septa are produced from the inner and broader fibrillar electron-lucid layer and are characterized by septal pores. The plasma membrane is a thin, electron-dense delimiting membrane contiguous with the inner surface of

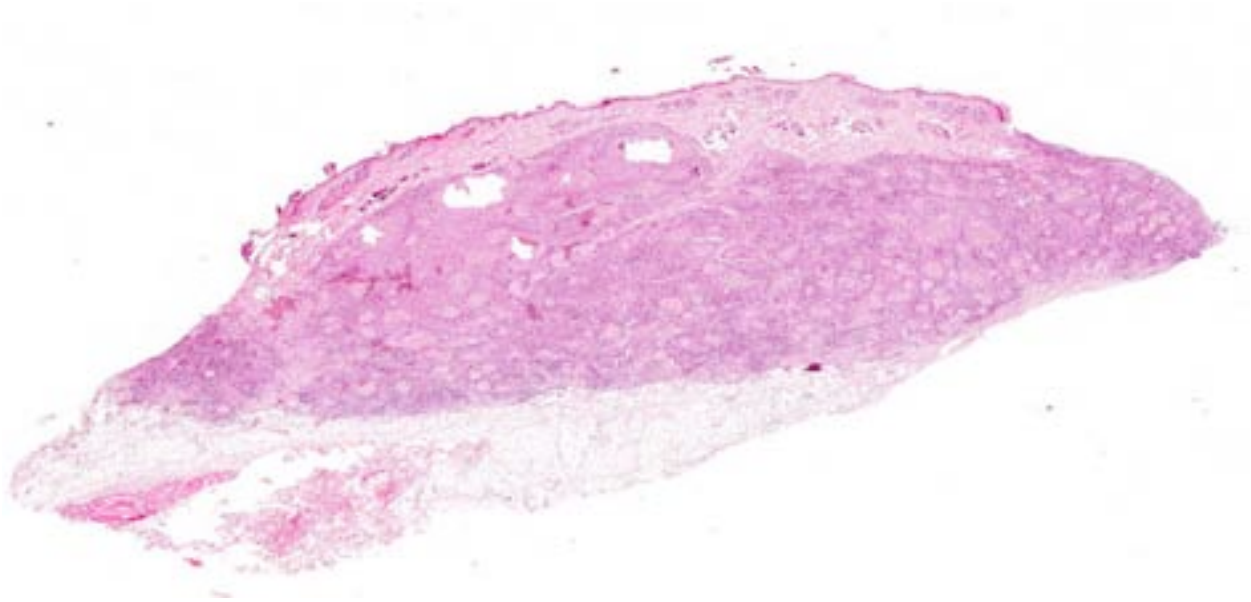

*2-2. Haired skin, cat: The dermis is expanded by coalescing poorly formed pyogranulomas. (HE 6.3X)*

the cell wall. In the cytoplasm, a large central vacuole surrounded by an electron-dense tonoplast enclosing electron-lucent flocculent material is visible. Mitochondria having no polarity are scattered throughout the cytoplasm of the hyphae and can be filamentous or spherical. Mitochondria have double membrane and extensive cristae that might extend across the organelles. Hyphae have sparse narrow tubular endoplasmic reticulum and a large tonoplast. Glycogen is abundant and often clumped and lipid inclusions are also present. Single membrane bound vesicles with central bodies are also present at the margins of the hyphae. Hyphae are often bi- to multinucleated (as in the image provided). The nuclear membrane has a double envelope with intervening nuclear pores. Additional features are the presence of single membrane bound vesicles with central bodies with high electron opacity.

Clinical, gross and microscopic findings were representative of a deep dermatophyte infection consistent with feline dermatophytic pseudomycetoma. The disease associated with *Microsporum canis* has been described also in dogs,[1,8] horses[12] and humans.[2,7,10,14] Dermatophytic pseudomycetomas are uncommon to rare, deep cutaneous to subcutaneous fungal infections that produce tissue grains or granules. These tissue grains are composed of fungal aggregates embedded in amorphous eosinophilic material representing antigen–antibody complexes (Splendore–Hoeppli reaction).

Feline pseudomycetomas have been reported mostly in Persian cats.[3,4,5,8,9,11,15] Sporadic cases have been reported in Himalayan, Domestic Shorthair, and in Maine Coon cats.[8,11,13,16] Genetic predisposition has been hypothesized to play a role in the development of these lesions since the Persian breed seems predisposed also to conventional dermatophytosis.[8] Age and gender predilections have not been observed.

The frequent localization of the lesions in the dorsal trunk, most commonly in outdoor cats, suggests a traumatic implantation of organisms from hair follicles with dermatophytic colonization by biting or fighting.[8] Some authors hypothesize that mycelial elements reach the dermis from spontaneously ruptured hair follicles in association with dermatophyte infection. Once in the dermis, fungi aggregate and induce a granulomatous reaction. Positive dermatophyte cultures from normal-appearing areas distant from the dermatophytic pseudomycetoma indicate that affected cats may previously have been inapparent carriers. Inapparent carriage of *Microsporum canis* is common in Persian and Himalayan cats.[5,8]

Grossly, dermatophytic pseudomycetomas are characterized by one or more subcutaneous nodules that occur most commonly over the dorsal trunk or tail base.[5,8,9,11] Lesions are firm,

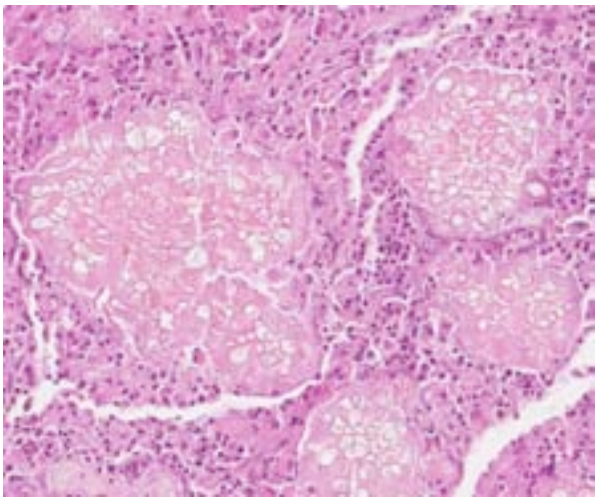

*2-3. Haired skin, cat: The pyogranulomas are centered on aggregates of fungal hyphae with thick, nonparallel walls, rare irregular non-dichotomous branching, and up to 25 µ m diameter bulbous swellings embedded in an amorphous eosinophilic material (Splendore-Hoeppli reaction). (HE 192X)*

*2-4. Haired skin, cat: Ultrastructural examination of fungal hyphae demonstrates several cross sections of a thick lamellar cell wall enclosing granular cytoplasm with moderate numbers of mitochondria and vacuoles and transverse septations. The hyphae are surrounded by electron-dense fibrillar Splendore-Hoeppli material. (EM X12,000)*

irregularly shaped nodules that gradually enlarge and coalesce in the dermis or the underlying subcutaneous tissue. Lesions may fistulate and discharge a seropurulent to necrotic material. Systemic clinical signs are uncommon, but lymphadenomegaly may be present. Intra-abdominal dermatophytic granulomatous peritonitis sharing many features with pseudomycetoma has been reported in Persian cats.[3,15,18]

Although dermatophytic pseudomycetoma fulfils most of the criteria for true mycetomas (nodular inflammation with fibrosis, fistulae draining from deep tissue, presence of tissue grains), fewer hyphal elements are present, and the lesions apparently lack the cement substance that holds true mycetoma grains together.[8]

Microscopically, lesions are located mostly in the dermis where aggregates of grey, refractile and highly pleomorphic fungal hyphae are characteristically found. These are tangled and delicate, and contain numerous large, clear, bulbous, thick-walled dilatations, resembling spores. Smaller swellings within the hyphae create a vacuolated or bubbly appearance to these structures. The fungal aggregates are imbedded in amorphous eosinophilic material to form large tissue grains, or granules that are also visible grossly. Splendore–Hoeppli reaction is brightly eosinophilic and locates around the periphery of organized aggregates of organisms. Granules are cuffed by and intermingled with large macrophages, giant cells, and variable, sometimes numerous neutrophils. Macrophages have abundant, granular cytoplasm. In some cases, fragments of hyphae are present within individual macrophages beyond the boundaries of tissue grains or granules. Reactive fibroblasts and collagen may surround or dissect the lesions often creating lobules composed of multiple granules and their attendant inflammation.[8,11]

Cytology has proven useful in the diagnosis of pseudomycetoma.[9,13,19] However, histopathology and fungal culture of biopsy specimens are required for a definitive and specific diagnosis. Organisms can be stained with periodic acid-Schiff, Gomori methenamine silver, Grocott stains and Fonata-Masson.[8,10] *Microsporum canis* has been isolated in typical cases of dermatophytic pseudomycetomas where fungal culture has been performed.[8] PCR from paraffin embedded tissues is also useful for *M. canis* identification and has been utilized in cases of feline, canine and equine lesions.[12] Immunohistochemistry using rabbit anti-*Microsporum canis* antiserum identified this agent also in two canine cases.[1]

Dermatophyte pseudomycetomas are considered difficult to manage clinically and the prognosis is considered poor in cats.[3,4,8] The lesions often recur after surgical excision alone[5] although in this case no recurrence was observed. There are contrasting reports regarding poor[4] or successful response of feline pseudomycetomas following terbinafine treatment.[13] Little response to

griseofulvin, ketoconazole or itraconazole has also been reported.[5,13,18] However, a combination of surgical excision with adjunctive long term medical therapy has recently been reported to be successful.[5,18]

Clinical differential diagnoses should include cryptococcosis and other systemic mycoses, sporotrichosis, cutaneous infections of other opportunistic fungi, and neoplasia. The marked breed predilection for Persian cats is helpful in increasing the index of suspicion for dermatophytic pseudomycetoma. Histologically, most of the systemic and opportunistic fungi affecting cats and dogs are smaller and more uniform in appearance and do not form granules or grains in tissue.[8] *Trichophyton mentagrophytes* has been reported to cause dermatophytic granulomatous inflammation in cats but the lesions do not have the typical histologic features of dermatophytic pseudomycetoma, and are characterized by a more diffuse tissue reaction with associated heavy colonization of the keratin of hair follicles and epidermis.

**JPC Diagnosis:** Haired skin: Dermatitis and panniculitis, granulomatous, focally extensive, severe, with Splendore-Hoeppli and numerous fungal hyphae.

**Conference Comment:** The presentation of this case provides a challenging perspective on an otherwise routine histopathologic diagnosis. Provided only the EM image, many participants were able to recognize a fungal hyphae within the cytoplasm of a macrophage; however, when given the accompanied glass slide during the conference, the characteristic granules of a pseudomycetoma due to *Microsporum canis* infection were readily identified.

The contributor provides an eloquent discussion on this entity, highlighting the characteristic ultrastructural, histopathologic and gross findings while adeptly discussing clinical presentation, management and appropriate differentials worthy of consideration.

**Contributing Institution:** DIVET Department of Veterinary Science and Public Health
http://www.divet.unimi.it/ecm/home

**References:**

1. Abramo F, Vercelli A, Mancianti F. Two cases of dermatophytic pseudomycetoma in the dog: an immunohistochemical study. *Vet Dermatol*. 2001;12:203-207.
2. Berg JC, Hamacher KL, Roberts GD. Pseudomycetoma caused by Microsporum canis in an immunosuppressed patient: a case report and review of the literature. *J Cutan Pathol*. 2007;34:431-434.
3. Black SS, Abernethy TE, Tyler JW, Thomas MW, Garma-Aviña A, Jensen HE. Intra-abdominal dermatophytic pseudomycetoma in a Persian cat. *J Vet Intern Med*. 2001;15:245-248.
4. Bond R, Pocknell AM, Tozet CE. Pseudomycetoma caused by Microsporum canis in a Persian cat: lack of response to oral terbinafine. *J Small Anim Pract.* 2001;42:557–560.
5. Chang SC, Liao JW, Shyu CL, Hsu WL, Wong ML. Dermatophytic pseudomycetomas in four cats. *Vet Dermatol*. 2011;22:181-7.
6. Cheville NF. Ultrastructural pathology. Algae, fungi and other eukaryotes. In: An introduction to interpretation. 1st ed. Ames, IA: Iowa State University Press; 1994:761-787.
7. Colwell AS, Kwaan MR, Orgill DP. Dermatophytic pseudomycetoma of the scalp. *Plast Reconstr Surg*. 2004;113:1072-1073.
8. Gross TL, Ihrke PJ, Walder EJ, Affolter VK. Infectious nodular and diffuse granulomatous and pyogranulomatous disease of the dermis. In: Skin Diseases of the Dog and Cat, Clinical and Histopathologic Diagnosis. 2nd ed. Oxford, UK: Blackwell Science Publishing; 2005:288-291.
9. Kano R, Edamura K, Yumikura H, Maruyama H, Asano K, Tanaka S, et al. Confirmed case of feline mycetoma due to Microsporum canis. *Mycoses*. 2009;52:80-83.
10. Kramer SC, Ryan M, Bourbeau P, Tyler WB, Elston DM. Fontana-positive grains in mycetoma caused by Microsporum canis. *Pediatr Dermatol*. 2006;23:473-475.
11. Miller RI. Nodular granulomatous fungal skin diseases of cats in the United Kingdom: a retrospective review. *Vet Dermatol*. 2010;21:130-5.
12. Nardoni S, Franceschi A, Mancianti F. Identification of *Microsporum canis* from dermatophytic pseudomycetoma in paraffin-embedded veterinary specimens using a common PCR protocol. *Mycoses*. 2007;50:215-217.
13. Nuttall TJ, German AJ, Holden SL, Hopkinson C, McEwan NA. Successful resolution

of dermatophyte mycetoma following terbinafine treatment in two cats. *Vet Dermatol*. 2008;19:405-410.
14. Rinaldi MG, Lamazor EA, Roeser EH, Wegner CJ. Mycetoma or pseudomycetoma? A distinctive mycosis caused by dermatophytes. *Mycopathologia*. 1983;81:41-48.
15. Stanley SW, Fischetti AJ, Jensen HE. Imaging diagnosis sublumbar pseudomycetoma in a Persian cat. *Vet Radiol Ultrasound*. 2008;49:176-178.
16. Thian A, Woodgyer AJ, Holloway SA. Dysgonic strain of Microsporum canis pseudomycetoma in a domestic long-hair cat. *Aust Vet J*. 2008;86:324-328.
17. Werner HJ, Jolly HW Jr, Spurlock BO. Electron microscope observations on the fine structure of Microsporum canis. *J Invest Dermatol*. 1966;46:130-134.
18. Zafrany A, Ben-Oz J, Segev G, Milgram J, Zemer O, Jensen HE, et al. Successful treatment of an intra-pelvic fungal pseudomycetoma causing constipation and hypercalcaemia in a Persian cat. *Feline Med Surg*. 2014;16:369-72.
19. Zimmerman K, Feldman B, Robertson J, Herring ES, Manning T. Dermal mass aspirate from a Persian cat. *Vet Clin Pathol*. 2003;32:213-217.

**CASE III**: D13-55496 (JPC 4048072).

**Signalment:** 12-year-old intact male Pug, dog (*Canis familiaris*).

**History:** The dog had a recent history of an oral melanoma, edema (not further specified), and cavitary effusion (not further specified). The dog had multiple biopsies of the oral mass that was on the left mandible, which was confirmed to be malignant melanoma. The mass with incomplete margins was removed along with teeth 304-308. The dog was ultimately euthanized.

**Gross Pathology:** The entire body of the dog was submitted in a state of fair to good postmortem preservation. The dog was in a good body condition with a moderate amount of subcutaneous and intraabdominal adipose tissue. There were no visible teeth in the 300 arcade (lower left) within the mandible. There was a locally invasive 5.5 cm x 4 cm x 5.5 cm firm, tan to white, multilobular mass encompassing the left side of the oral cavity involving both the mandible and maxilla. The mass surrounding the mandible extended caudally from the rostral aspect of the body of the mandible to the ramus, slightly across the midline in the caudal intermandibular region, and dorsally surrounding the caudal most aspect of the maxilla including the remaining maxillary molar (presumably tooth 210). The mass completely surrounded the mandible; however, it was not attached to the mandible. The left mandible was markedly thinned with a complete, mid-body, transverse fracture present. On cut section, the mass was tan to white and semifirm with a tan, soft, gelatinous central region and occasional cavities that oozed a small amount of yellow to green, semi-viscous, opaque material.

The lungs were diffusely mottled, tan to dark red and crepitant. There were multifocal, round, tan, slightly raised nodules ranging from pinpoint to 4 mm diameter throughout all lung lobes, but affecting less than 1% of the pulmonary parenchyma. One pedunculated tan nodule was present on the right caudal lobe. On cut section the pulmonary nodules were tan.

**Laboratory Results:** There were no ancillary tests performed.

**Histopathologic Description:** Compressing the adjacent salivary gland and submucosa as well as infiltrating and dissecting between the adjacent skeletal muscle and collagen bundles, and occasionally infiltrating the basal epithelial layer (junctional activity – variable by section), there is a densely cellular, multilobular, poorly demarcated, unencapsulated, infiltrative neoplasm composed of two populations of cells. One population of cells is arranged in cords, trabeculae, and packets and supported by a fine fibrovascular stroma. The neoplastic cells are polygonal to columnar with variably distinct cell borders, a moderate amount of eosinophilic cytoplasm, and one round to oval nucleus with finely

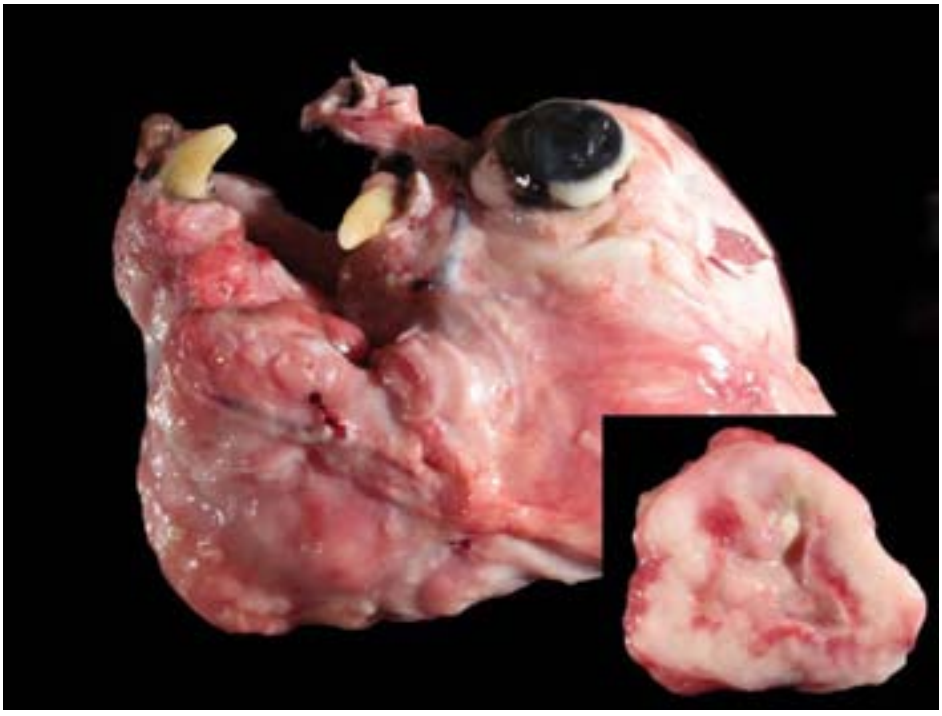

*3-1. Head, dog: There was a locally invasive, 5.5 cm x 4 cm x 5.5 cm firm, tan to white, multilobular mass encompassing the left side of the oral cavity involving both the mandible and maxilla. Inset: Cut section of the mass. (Photo courtesy of: Veterinary Diagnostic Laboratory, University of Minnesota, www.vdl@umn.edu)*

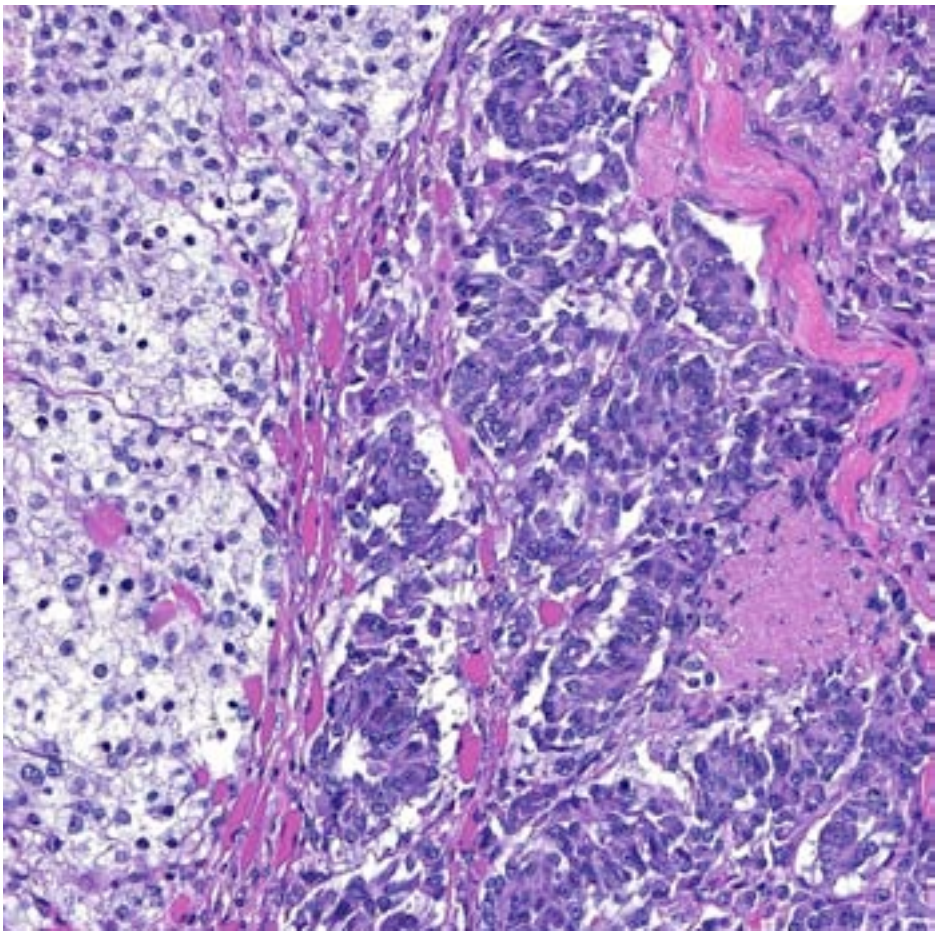

*3-2. Soft tissue, jaw: Melanocytes within the neoplasm have two distinct appearances with one population being polygonal with abundant clear cytoplasm (left) and a second being spindled with abundant granular basophilic cytoplasm. (HE 240X)*

stippled chromatin and one to three prominent nucleoli. The second population of cells is arranged in tightly arranged packets and supported by a fine fibrovascular stroma. The neoplastic cells are polygonal with indistinct cell borders, a large amount of clear to lightly eosinophilic, vacuolated cytoplasm, and one round to oval nucleus with finely stippled chromatin and one to two variably prominent nucleoli. Overall the neoplastic cells exhibit a moderate degree of anisocytosis and anisokaryosis with a mitotic rate of approximately 35 in 10 high power fields (400x). Multifocally within the neoplasm, the stroma is brightly eosinophilic and hyalinized. Multifocally, there are variably sized regions of coagulative to lytic necrosis characterized by eosinophilic and basophilic karyorrhectic cellular debris and a pale eosinophilic background with faded cellular outlines and nuclear details. Along the periphery of the neoplasm and admixed within the regions of necrosis, there are moderate numbers of degenerate and non-degenerate neutrophils, nuclear streaming, a small amount of deeply basophilic granular material (mineral), and small numbers of mixed bacterial colonies. The bacterial colonies are characterized as basophilic cocci and eosinophilic short rods. Scattered throughout the neoplasm are moderate numbers of individual apoptotic/necrotic cells with pyknotic nuclei and karyorrhectic debris. Throughout the neoplasm, numerous small and medium caliber blood vessels are expanded by moderate numbers of erythrocytes (congestion). Multifocally throughout the neoplasm, there are small to moderate aggregates of extravasated erythrocytes (hemorrhage). Along the periphery of the neoplasm and extending into the surrounding collagen bundles, there are small aggregates of lymphocytes and plasma cells. Within the adjacent muscle, there is myofiber degeneration and necrosis characterized by myofiber loss, variation in myofiber size, and loss of cross-striations. Within these same regions along the periphery of the neoplasm, there is moderate collagenolysis characterized by a loss of organization, collagen bundle fragmentation, loss of eosinophilia and increased basophilia. There are multifocal areas of pigmentary incontinence. Multifocally there is a loss of the overlying oral epithelium (ulceration).

Immunohistochemistry for Melan-A, S100, chromogranin A, and synaptophysin were prepared at the University of Minnesota Veterinary Diagnostic Laboratory. Less than 2%

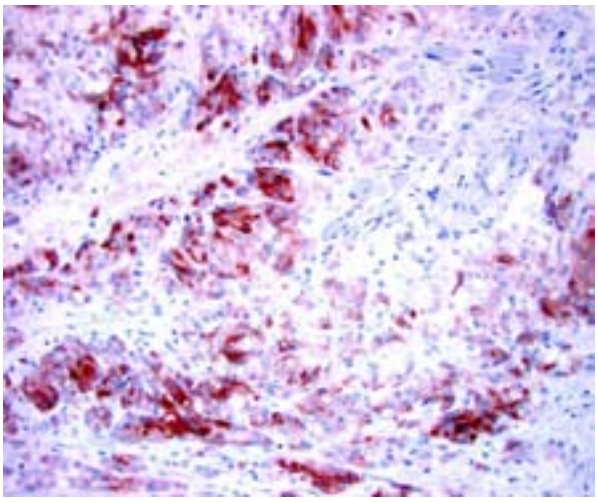

*3-3. Soft tissue, jaw: Neoplastic cells are weak to moderately immunopositive for melanA. (Photo courtesy of: Veterinary Diagnostic Laboratory, University of Minnesota, www.vdl@umn.edu)*

of neoplastic cells within the periphery of each lobule had strong intracytoplasmic immunopositivity and less than 10% of the neoplastic cells throughout the mass had weak to moderate intracytoplasmic immunopositivity for Melan-A. Approximately 50% of the neoplastic cells had weak intracytoplasmic immunopositivity for Chromogranin A. The neoplastic cells were immunonegative for S100 and Synaptophysin.

**Contributor's Morphologic Diagnosis:** Oral cavity, amelanotic melanoma with neuroendocrine differentiation, focally extensive (with metastasis to lungs and left mandibular pathologic fracture).

**Contributor's Comment:** The two main types of melanocytic tumors are melanocytoma and malignant melanoma.[8] These tumors are derived from melanocytes that originate as melanoblasts from neural crest ectoderm.[8] Melanocytomas are the benign neoplasm of melanocytes and are most often heavily pigmented.[8] As the name suggests, malignant melanoma is the malignant tumor of melanocytic origin and is often used synonymously with melanoma. Melanocytic tumors can be found in multiple locations; however, the integument (cutaneous) and oral cavity are common sites. Cutaneous tumors in dogs are often benign. The cutaneous form of melanoma is commonly seen in gray horses and swine.[3]

In dogs, malignant melanomas are the most common oral tumor and have variable breed and gender predilection.[3,7-9] These tumors are often heavily pigmented and grossly appear black; however, in some cases, these tumors are variably pigmented or completely unpigmented (amelanotic), and appear grossly white.[3,7,8] The degree of pigmentation does not indicate biologic behavior or aid in prognosis.[3,8] Malignant melanomas often metastasize, with the regional lymph nodes being the most common site, but also commonly spread to distant sites (ex. lung) through the blood and lymphatics.[3,9] Histologically, the cell morphology of malignant melanomas can range from round/polyhedral/epithelioid cells to spindloid cells to mixed (a combination of the two)[3,8]; however, one defining histologic feature of the these tumors is often junctional activity[4], which can be seen as tumor infiltration crossing between the basal epithelium of the mucosa and the submucosa.

Most often, well-differentiated round/polygonal/epithelioid cell melanocytic tumors with abundant pigmentation are easily diagnosed; however, amelanotic and spindloid appearing tumors are quite often diagnostically challenging. Special stains [Fontana-Masson, 3,4-dihydroxyphenylalanine (DOPA)], immunohistochemistry, and/or electron microscopy can be used to aid in the diagnosis of amelanotic tumors.[1,3,5,7,8,10] Amelanotic melanomas are generally immunopositive for tryrosinase-related proteins 1 and 2 (TRP-1 and TRP-2), Melan-A, melanocytic antigen PNL2, HMB-45, microphthalmia transcription factor (MiTF), S100, tyrosine hydroxylase, tyrosinase, and vimentin[3,5,7-10]; however, according to Smedley et al. PNL2, Melan-A, TRP-1 and TRP-2 as a group provide the most diagnostic information for canine oral amelanotic melanomas.

In human medicine, melanocytic tumors are often further classified allowing for integration of morphology, location, and biologic behavior; however, this classification system is not currently applied in veterinary medicine.[8] According to Eyden et al., while not currently a subclassification of malignant melanoma, neuroendocrine differentiation is a rarely seen variant. The three currently reported human cases of this variant had predominantly epithelioid cell morphology, variable pigmentation, and immunopositivity either in the primary tumor or metastases for both melanocytic and neuroendocrine markers. Ultrastructurally, the

assessed cases (2 of 3) revealed neuroendocrine granules and no melanosomes.[6] Although electron microscopy was not performed on the current case, the cell morphology, architecture, and immunophenotype are consistent with an amelanotic melanoma with neuroendocrine differentiation; which has currently not been reported in dogs.

**JPC Diagnosis:** Fibrovascular tissue adjacent to salivary gland: Malignant amelanotic melanoma.

**Conference Comment:** Melanomas are often referred to as "the great imitator" because of their ability to display a variety of cytologic features thanks to their common embryologic roots with both neural and epithelial tissues. This case nicely illustrates the point, due to variation is cellular appearance across various regions of the neoplasm. In some sections, there is a portion of the neoplasm which exhibits junctional activity, a feature which lends additional credence to the morphologic diagnosis on HE section. The list of other neoplasms that share this characteristic with melanomas is short, usually limited to histiocytomas and epitheliotropic (T-cell) lymphomas.

Nuclear atypia and mitotic activity is directly correlated with prognostic behavior in melanomas at all locations. Immunohistochemistry has recently been evaluated as an additional prognostic tool. Ki67, a protein expressed only in growth and mitotic phases of the cell cycle, is considered a measure of tumor growth fraction and its expression has been correlated with outcome in canine melanomas comparable to nuclear atypia and mitotic index.[2] Additionally, immunodetection of RACK1, a protein expressed at high levels in melanocytes, may be a specific marker aiding in not only identifying melanomas but also offering progonostic value as its expression is also consistently correlated with nuclear atypia and mitotic index.[4]

**Contributing Institution:** Veterinary Diagnostic Laboratory
University of Minnesota
www.vdl@umn.edu

**References:**

1 Banerjee SS, Harris M. Morphological and immunophenotypic variations in malignant melanoma. *Histopathology*. 2000;36:387-402.

2. Bergin IL, Smedley RC, Esplin DG, Spangler WL, Kiupel M. Prognostic evaluation of Ki67 threshold value in canine oral melanoma. *Vet Pathol*. 2011;48(1):41-53.

3. Brown CC, Baker DC, Barker IK. Alimentary system. In: Maxie MG, ed. *Jubb, Kennedy, and Palmer's Pathology of Domestic Animals*. 5th ed. Toronto: Saunders/Elsevier; 2007:29-30.

4. Campagne C, Jule S, Alleaume C, et. al. Canine melanoma diagnosis: RACK1 as a potential biologic marker. *Vet Pathol*. 2013;50(6): 1083-1090.

5. Choi C, Kusewitt DF. Comparison of Tyrosinase-related Protein-2, S-100, and Melan A Immunoreactivity in Canine Amelanotic Melanomas. *Vet Pathol*. 2003;40:713-718.

6. Eyden B, Pandit D, Banerjee SS. Malignant melanoma with neuroendocrine differentiation: clinical, histological, immunohistochemical and ultrastructural features of three cases. *Histopathology*. 2005;47:402-409.

7. Gelberg HB. Alimentary system and the peritoneum, omentum, mesentery, and peritoneal cavity. In: Zachary JF, McGavin MD, eds. *Pathologic Basis of Veterinary Disease.* 5th ed. St. Louis, MO: Elsevier; 2012:329.

8. Head KW, Cullen JM, Dubielzig RR, et al. *Histological Classification of Tumors of the Alimentary System of Domestic Animals*. Schulman FY, ed. 2nd series, Vol.10. Washington, DC: AFIP, CL Davis foundation, and WHO; 2003:33-35.

9. Ramos-Vara JA, Beissenherz ME, Miller MA, et al. Retrospective study of 338 canine oral melanomas with clinical, histologic, and immunohistochemical review of 129 cases. *Vet Pathol*. 2000;37:597-608.

10. Smedley RC, Lamoureux J, Sledge DG, Kiupel M. Immunohistochemical Diagnosis of Canine Oral Amelanotic Melanocytic Neoplasms. *Vet Pathol*. 2011;48(1):32-40.

**CASE IV:** N12-119 (JPC 4032704).

**Signalment:** 3-year-old male Australian shepherd (*Canis lupus familiaris*), canine.

**History:** A three-year-old male Australian Shepherd presented to the University of Florida Emergency Service for coughing, right hind-limb lameness, and a fever which did not respond to antibiotic therapy. He was adopted two months prior to presentation from a breeder in Illinois with no history of prior illness. He lives at home on a farm with several other adult dogs. They are primarily outdoor dogs and have free access to two acres. Two weeks prior to presentation, the patient became febrile and started coughing. He was placed on Baytril, chloramphenicol and prednisone, however his cough did not resolve. He was then taken to a specialist and prescribed fluconazole. Physical examination revealed harsh lung sounds bilaterally, right hind limb lameness with no neurological deficits, enlarged right popliteal lymph node, dry non-productive cough, and elevated temperature (temp 104.3). Thoracic radiographs were obtained and revealed diffuse miliary interstitial pulmonary pattern bilaterally. Owner elected for humane euthanasia.

**Gross Pathology:** LUNGS: The lungs are diffusely mottled light tan to dark red and contain too–numerous-to-count light tan, irregular, firm, granulomatous nodules in all lung fields. The granulomas range in size from 0.2 x 0.1 x 0.1cm to 5.0 x 2.5 x 2.5cm (left caudal lung lobe). The granulomas are slightly raised above the parenchymal surface and extend throughout all cut surfaces. There are only 2-3 of these larger than 5 mm diameter. The remaining parenchyma is diffusely dark red, wet, and heavy. All sections float low in formalin.

**Laboratory Results:** None.

**Histopathologic Description:** Lung: The alveolar capillaries are diffusely congested and there is lightly eosinophilic, homogenous material within 95% of the alveolar air spaces (alveolar edema). Approximately 40% of the lung parenchyma is effaced by pyogranulomatous inflammation. The interstitium is disrupted by numerous large, multifocal to coalescing pyogranulomas that are composed of a central area of necrotic debris and degenerate neutrophils, surrounded by a layer of macrophages and occasional multinucleated giant cells admixed with and surrounded by abundant degenerate neutrophils. Within the granulomas are numerous

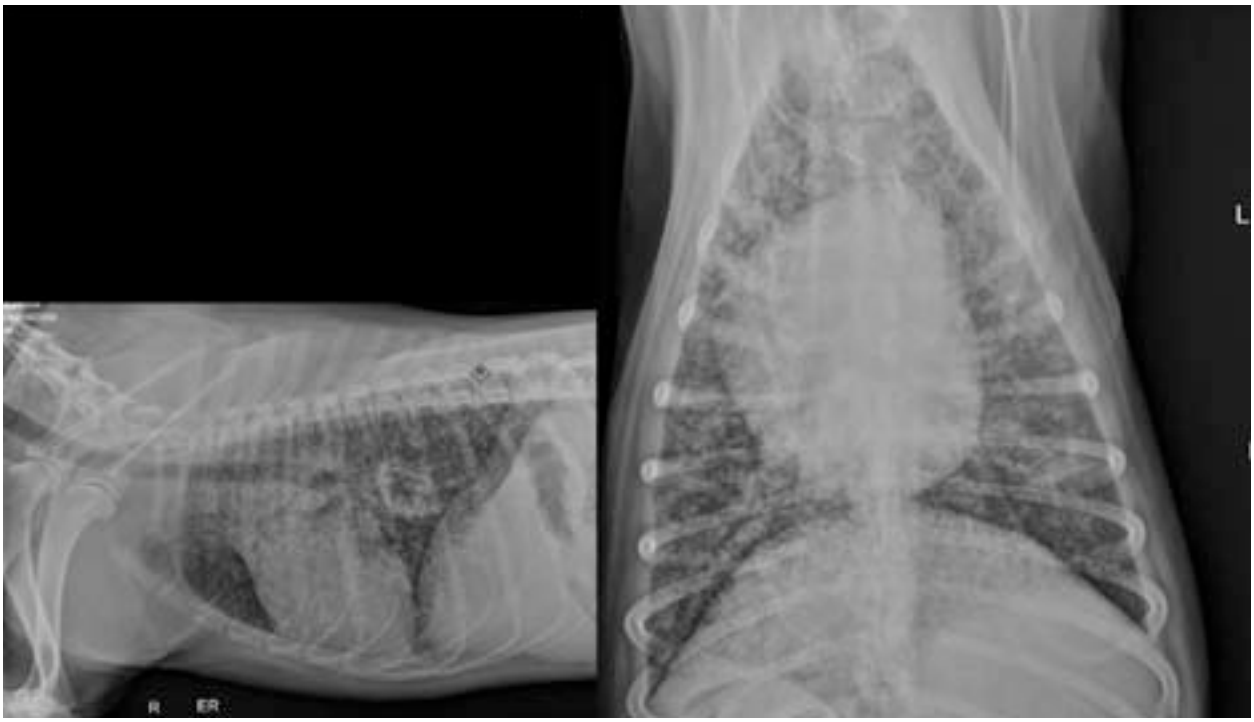

*4-1. Thoracic radiographs, dog: Lateral and ventrodorsal radiographs reveal a diffuse military pattern throughout all lung fields. (Photo courtesy of: University of Florida College of Veterinary Medicine, Department of Infectious Disease and Pathology)*

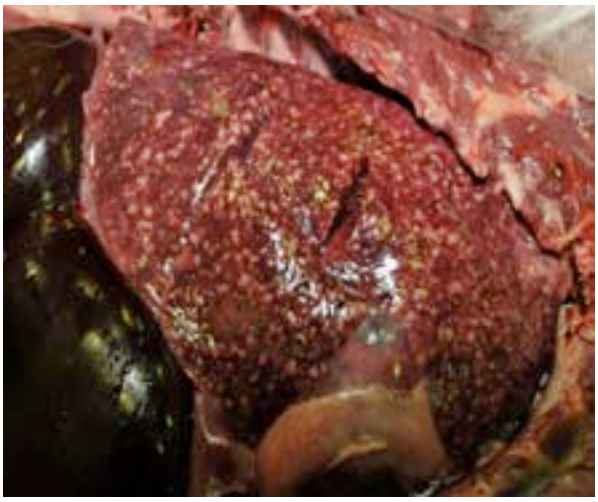

*4-2. Lung, dog: Lungs are diffusely mottled light tan to dark red and contain innumerable less than 5mm granulomas in all lung fields. (Photo courtesy of: University of Florida College of Veterinary Medicine, Department of Infectious Disease and Pathology)*

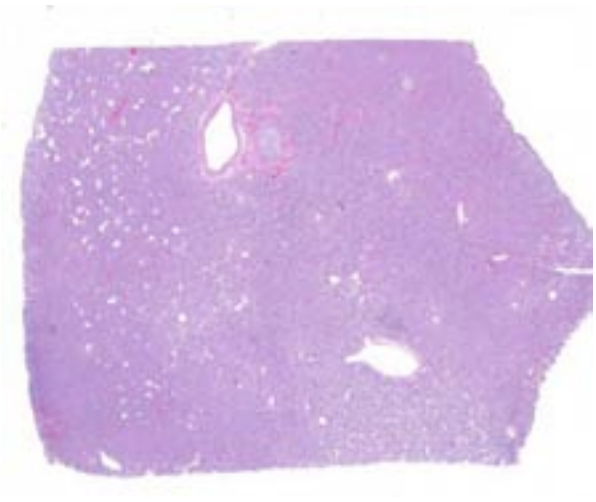

*4-3. Lung, dog: There is diffuse consolidation of the section, to include airways of all sizes. (HE 6.3X)*

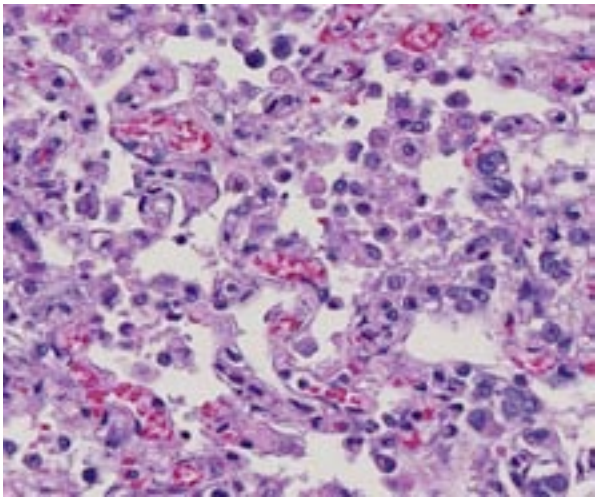

*4-4. Lung, dog: Alveolar septa and alveolar spaces are expanded by large numbers of foamy and rarely multinucleated macrophages, and is multifocal type II pneumocytes hyperplasia. (HE 400X)*

intracellular and extracellular 8-15 µm diameter argyrophilic round yeast with a 2-3 µm thick clear to basophilic, refractile capsule and a central, basophilic, granular nucleus (GMS stain). Yeasts frequently exhibit broad-based budding. There is mild to moderate, multifocal perivascular edema surrounding large vessels.

**Contributor's Morphologic Diagnoses:** 1. Granulomatous interstitial pneumonia, chronic, diffuse, severe, with fungal organisms consistent with *Blastomyces dermatitidis*, lung.
2. Granulomatous lymphadenitis, multifocal, severe, with fungal organisms consistent with *Blastomyces dermatitidis,* cranial mediastinal, tracheobronchial, and right popliteal lymph nodes.

**Contributor's Comment:** *Blastomyces dermatitis* is a dimorphic, saprophytic fungus most commonly associated with the Mississippi and Ohio River valleys.[6] The primary route of infection is inhalation, with young male dogs of hunting and working breeds most commonly affected.[3] Clinical signs follow physiologic dysfunction of the affected tissue and infection is frequently associated with underlying immunosuppression.[3] Although *Blastomyces dermatitidis* does infect both dogs and humans and is therefore considered zoonotic, infection is thought to originate from inhalation of spores from the soil.[6] No cases of direct transmission from animals to humans reported have been reported; however, dogs are up to 10 times more likely to acquire infections and are considered a sentinel species.[4] Due to its aggressive pathologic nature and potential of infection by inhalation, culture of the organism is not recommended due to the risk of transmission to staff.[5]

Infection begins with the inhalation of mycelial fungal conidia from contaminated soil. Following inhalation, conidia undergo nonspecific phagocytosis and killing mediated by polymorphonuclear leukocytes (PMN), monocytes, and alveolar macrophages. The infection is most commonly self-limiting; however, in select cases the primary infection is not eliminated and conidia are converted to the yeast phase at body temperature.[3] The yeasts are encapsulated by a thick cell wall and are more resistant to phagocytosis and killing. Local

replication occurs via asexual budding and systemic dissemination via hematogenous and lymphatic routes is common.[2] Dissemination to multiple organ systems has been reported including cutaneous, ocular, CNS and bone.[2]

Although 85% of fungal pneumonia is reported to be attributed to blastomycosis, other differentials for fungal pneumonia should be considered and include: *Histoplasma capsulatum*, *Coccidioides immitis*, *Cryptococcus neoformans* and *Aspergillosis*. Differentiation and definitive diagnosis is best determined by the combination of geographic location, clinical presentation and histopathologic findings.[6]

**JPC Diagnosis:** Lung: Pneumonia, interstitial, granulomatous, diffuse, severe, with patchy type II pneumocyte hyperplasia.

**Conference Comment:** Despite examining multiple sections, repeating fungal stains and consulting with the JPC Department of Infectious Disease, we were unable to definitively demonstrate the double-contoured, broad-based budding yeast of *Blastomyces* in the submitted slides. The clinical history, gross findings and histologic lesions are all consistent with *Blastomycosis*; thus we don't dispute the contributor's diagnosis and rather attribute it to the variation that comes with cutting hundreds of slides.

*Blastomycosis* is one of the dimorphic fungi, whose transition from the mycelial form, known as conidia, to the yeast form is thermally dependent and takes place in tissue where temperature exceeds 37ºC. Conidia are readily phagocytosed by neutrophils and macrophages while yeast are more resistant, thus this conversion enables its pathogenicity. Also facilitating infection is the appropriately-named surface protein BAD-1 which mediates adhesion to host cells and modulates the inflammatory response by suppression of TNF-α production.[3]

While the lung is the most commonly affected site, *Blastomyces dermatitidis* can cause a disseminated infection where lesions are commonly found in lymph nodes, eyes, skin, subcutaneous tissues, bones and joints.[3] It is also one of the listed causative agents of granulomatous disease associated with hypercalcemia. The mechanism behind hypercalcemia has not been proven; however, it is suspected the population of macrophages produce 1,25 dihydroxycholecalciferol. Also known as calcitriol, it is the active form of vitamin D which increases calcium uptake from the gastrointestinal tract.[5]

**Contributing Institution**: University of Florida College of Veterinary Medicine
Department of Infectious Disease and Pathology

**References:**

1. Arceneaux KA, Taboada J, Hosgood G. Blastomycosis in dogs: 115 cases (1980-1995). *J Amer Vet Med Assoc*. 1998;213(5):658-664.
2. Bateman BS. Disseminated blastomycosis in a German shepherd dog. *Can Vet J.* 2002;43(7): 550–552.
3. Caswell J. Respiratory system. In: Maxie MG, ed. *Jubb, Kennedy, and Palmer's Pathology of Domestic Animals*. 5th ed. Vol. 2. Philadelphia, PA: Saunders Elsevier; 2007:641-642.
4. Cote E, Barr SC, Allen C, Eaglefeather E. Blastomycosis in six dogs in New York state. *J Am Vet Med Assoc.* 1974;210:502-504.
5. Ferguson DC, Hoenig M. Endocrine system. In: Latimer KS, ed. *Duncan & Prasse's Veterinary Laboratory Medicine Clinical Pathology*. 5th ed. Oxford, UK: Wiley-Blackwell; 2011:301.
6. Legendre A. Blastomycosis. In: Greene CE, ed. *Infectious Diseases of the Dog and Cat*. 3rd ed. St. Louis, MO: Saunders; 2006:569-576.

**Joint Pathology Center**
**Veterinary Pathology Services**
**Wednesday Slide Conference**
**2014-2015**
**Conference 6**
**October 8, 2014**

**Conference Moderator:**
Jennifer Chapman, DVM, Diplomate ACVP

---

**CASE I:** NHP 14-22 (JPC 4048655).

**Signalment:** 10-year-old intact male rhesus macaque, *(Macaca mulatta)*.

**History:** This animal was part of a study at an outside research institution that was looking at neural recordings. The day after the first recording was made from the deep brainstem, vestibular signs were noted. The animal was treated and improved. About a month later a recording was made from the contralateral side of the brain stem. The next day, the animal was reported to be weak with conscious proprioceptive deficits. Over the next few days, the animal deteriorated and developed respiratory distress. Elective euthanasia was performed and lung and brain tissue were subsequently submitted for histologic evaluation.

**Gross Pathology:** The lungs are multifocally mottled dark red. The brain exhibits dark brown discoloration and cavitation around the 4th ventricle and near the hippocampal formation unilaterally.

**Laboratory Results:** N/A

**Contributor's Histopathologic Description:** Lung: In a section of lung, there are variably-sized aggregates of large foamy macrophages, lymphocytes, plasma cells, fewer neutrophils and scattered multinucleated giant cells typically centered on mildly to moderately ectatic bronchioles and less often alveoli and small to medium-caliber vessels. Inflammation infiltrates and expands the walls of affected bronchioles. These bronchioles are lined by severely attenuated to denuded epithelium and multiple coagula of fibrin, foamy macrophages, mature and degenerate neutrophils and multinucleated giant cells. Macrophages and giant cells often contain variable amounts of birefringent golden brown granular intracytoplasmic pigment. Smooth muscle and lymphoid tissue surrounding airways are multifocally and mildly to moderately hyperplastic. Within affected bronchioles and inflammation surrounding alveoli are variable numbers of partial to complete sections of 300-500 µm diameter arthropods characterized by a thin golden chitinous exoskeleton, jointed appendages, a body cavity with striated musculature, and digestive and reproductive tracts (consistent with *Pneumonyssus simicola*). Some of these airways are close to the pleural surface and inflammation extends into and through the pleura, forming a nearly diffuse coagulum of fibrin, foamy macrophages, multinucleate giant cells and few lymphocytes and plasma cells on the pleural surface. The tunicae media and intima of few scattered medium-caliber vessels in the section are diffusely and severely expanded by large foamy macrophages and multinucleated giant cells, narrowing the lumen. The tunicae intima and media of other vessels are obscured by deeply eosinophilic fibrillar material and scattered foamy

macrophages and multinucleated giant cells. Other scattered smaller caliber vessels are effaced by aggregates of fibrin, macrophages, lymphocytes and plasma cells. The adventitia of affected vessels is expanded by lymphocytes and fewer plasma cells. In less affected areas of the lung, there is multifocal moderate emphysema and the interstitium is multifocally and mildly expanded by infiltrates of macrophages and lymphocytes. There are scattered areas of mild hemorrhage.

**Contributor's Morphologic Diagnosis:** 1. Bronchiolitis, alveolitis and pleuritis, necrotizing, histiocytic, lymphoplasmacytic, multifocal, severe, chronic with bronchiolectasis, smooth muscle hyperplasia, lymphoid hyperplasia and intraluminal arthropods (*Pneumonyssus simicola*).
2. Vasculitis, multifocal, necrotizing to histiocytic, severe, chronic with multinucleated giant cells; lung.

**Contributor's Comment:** While *Pneumonyssus simicola*, the lung mite of macaques, is no longer a routine finding in colony-housed animals, pulmonary acariasis occurs in up to 100% of wild rhesus monkeys and is still seen in research colonies that include wild-caught or imported animals.[1,2,4,6] In all affected macaques, *P. simicola* infection is usually subclinical, but can result in clinical respiratory signs and other complications including pneumothorax and pulmonary arteritis.[4,6] Arteritis characterized by fibrinoid degeneration, macrophages and multinucleate giant cells is present in this case, and the pleural inflammatory reaction and acute onset of respiratory distress suggest an acute pneumothorax was possible prior to euthanasia.

The exact lifecycle has not been fully elucidated, but adult mites are obligate endoparasites and adults feed on host erythrocytes, lymph and epithelial cells in the lung. Transmission requires close association with infected animals as it is likely through direct contact.

Gross lesions are generally multifocal, round, yellow to tan cystic foci up to several millimeters in diameter within the lung parenchyma. Mites occasionally can be visualized in the center of these lesions with the aid of a dissecting scope. Histopathologic findings typically include granulomatous and eosinophilic inflammation centered on the terminal air passages, pigment-laden macrophages, bronchiectasis, alveolar emphysema, bronchiolar smooth muscle hyperplasia and interstitial fibrosis.[1,4-6] Female mites are most commonly seen in the airways and can be up to approximately 700 μm long with a thin chitinous exoskeleton, jointed appendages and a body cavity with a digestive tract and reproductive tract.[3-5] The characteristic birefringent crystalline pigment, regarded as a metabolite of the female mite, can be present in sections of tissue that lack mites and can be used to make a presumptive diagnosis.

While *P. simicola* is most frequently described in rhesus macaques, it has also been reported in other macaque species and a baboon.[3] Pulmonary acariasis is not limited to nonhuman primates; there are numerous species of mites that can be found in nasal passages and lungs of other animals including but not limited to *Rhinophaga* sp. in non-human primates, *Pneumonyssoides caninum* in dogs, *Entonyssus* sp. and *Entophionyssus* sp. in snakes, *Cephenemyia* sp. in wild cervids, *Cytodites nudus* in poultry, and *Sternostoma tracheacolum* in Gouldian finches.

**JPC Morphologic Diagnosis:** 1. Lung: Bronchiolitis, granulomatous and necrotizing, chronic, multifocal, severe, with bronchiolar smooth muscle hyperplasia, bronchiolectasis and intrabronchiolar arthropods and mite pigment.
2. Pleura: Serositis, granulomatous, multifocal, moderate, with epithelial hyperplasia.

3. Subpleural vasculature, smooth muscle: Hyperplasia, diffuse, mild to moderate.

**Conference Comment:** This is an exceptional example of pulmonary acariasis with well preserved sections of adults, eggs and often mite fragments within multinucleated giant cells scattered throughout conducting airways and occasionally within alveoli. Bronchiolar walls are often replaced by fibrin and abundant granulomatous inflammation. We observed fibrinoid change in widely scattered vessel in several slides, but it was not constant over the distributed sections, so we have elected not include it in our diagnosis.

The term acariasis equates with a mite infection and is derived from the Order *Acari* in which all mites are classified. While most mite infections are localized to the skin, there are at least ten species of lung mites which infect the lungs of Old World monkeys, all of the genus *Pneumonyssus*.[7]

Conference participants debated on possible causes of the evident granulomatous inflammation with multinucleated cells lining the outside of the pleura in this case. Most agreed with the contributor's suspicions of a secondary pneumothorax, possibly a sequela of ruptured mite houses. Additional Gram, fungal and acid-fast stains did not elucidate any additional infectious organisms. Without definitive causal evidence, we elected to separate out the diagnoses of serositis and the prominent smooth muscle hyperplasia of subpleural vessels.

As nicely described by the contributor, mite pigment is present in abundance in many sections. This is a golden brown to black pigment usually found within macrophages. This pigment does not contain carbon or melanin, but rather is iron-positive and likely the result of breakdown and excretion of the host's blood proteins.[7]

**Contributing Institution:** Memorial Sloan-Kettering Cancer Center
1275 York Ave
New York, NY 10065

**References:**

1. Abbott DP, Majeed SK. A survey of parasitic lesions in wild-caught, laboratory-maintained primates: (rhesus, cynomolgus, and baboon). *Veterinary Pathology*. 1984;21(2):198-207.
2. Andrade, MCR, Marchevsky, RS. Histopathologic findings of pulmonary acariasis in a rhesus monkeys breeding unit. [Aspectos histopatológicos da acaríase pulmonar em uma criação de maca-cos rhesus.] Revista Brasileira de Parasitologia Veterinária. 2007;16(4):229-234.
3. Cogswell F. Parasites of non-human primates. In: Baker DG, ed. *Flynn's Parasites of Laboratory Animals*. 2nd ed. Ames, Iowa: Blackwell Publishing; 2007:716-717.
4. Innes JR, Colton MW, Yevich PP, Smith CL. Lung mites; pulmonary acariasis as an enzootic disease caused by Pneumonyssus simicola in imported monkeys. *The American Journal of Pathology*. 1954;30(4):813-35.
5. Ogata T, Imai H, Coulston F. Pulmonary acariasis in rhesus monkeys: electron microscopy study. *Experimental and Molecular Pathology*. 1971;15(2):137-47.
6. Osborn K, Lowenstein L. Respiratory diseases. In: Bennett B, Abee C, Henrickson R, eds. *Nonhuman Primates in Biomedical Research: Diseases*. 1st ed. Vol. 2. San Diego, CA: Academic Press; 1998:302-303.

7. Strait K, Else JG, Eberhard ML. Parasitic diseases of nonhuman primates. In: Abee CR, Mansfield K, Tardiff S, Morris T, eds. *Nonhuman Primates in Biomedical Research: Diseases.* 2nd ed. Vol. 2. San Diego, CA: Academic Press; 2012:268-270.

---

**CASE II**: 13-26805 (JPC 4049055).

**Signalment:** 6-year-old castrated male Mastiff, dog, *(Canis lupis familiaris).*

**History:** Melena and weight loss (duration not indicated). A colonic mass was identified when the patient was placed under general anesthesia and colonoscopy was attempted. The mass was removed per rectum and submitted for histologic examination.

**Gross Pathology:** Received a 1.5 x 4.0 tan tissue. The surgical border could not be identified at the time of sectioning.

**Laboratory Results:** The neuronal ganglion cells stained positively with the neuron specific enolase (NSE; see Fig. 1), while Luxol fast blue staining failed to reveal the presence of myelin. Immunohistochemical staining for S-100 and glial fibrillary acidic protein (GFAP) and electron microscopy were not pursued.

**Histopathologic Description:** The section of the colonic mass is extensively ulcerated with accompanying marked collections of neutrophils, small lymphocytes, plasma cells and hemosiderophages that are also occur as a diffuse infiltrate in the lamina propria. Singleton and small groupings of neuronal ganglion cells are present throughout the lamina propria. The neuronal ganglion cells are polygonal with distinct cell borders and a moderate nuclear to cytoplasmic ratio. The nucleus is eccentric, round to oval with a finely stippled chromatin pattern and a single, prominent, round nucleus. The cytoplasm is moderate and there is a finely stippled to fibrillar pale pink material (Nissl substance) placed eccentrically in the cytoplasm. There are accompanying haphazard to parallel arrays of spindled cells and thin collagen fibers within the lamina propria that extend through the muscularis mucosa, interpreted to be a schwannian stroma. The cell borders are indistinct and the nuclear to cytoplasmic ratio is high. The nucleus is centric, oval to oblong with a finely stippled chromatin pattern and one to three, small nucleoli. The cytoplasm is scant and pink. Mitoses and cellular features of malignancy are not present in the neuronal ganglion cells and schwannian stroma. Profiles of submucosal plexuses are increased in number and size. The muscularis mucosa and serosa are not present in the sections examined.

**Contributor's Morphologic Diagnosis:** Diffuse colonic ganglioneuromatosis with accompanying ulcerative, moderate, mixed inflammatory cell colitis.

**Contributor's Comment:** The presence of a diffuse infiltrate of ectopic neuronal ganglion cells, a schwannian stroma and hypertrophied and hyperplastic enteric plexuses coupled with the location of the mass warranted a diagnosis of diffuse colonic ganglioneuromatosis (GN) in this dog.

GN is a rare disorder characterized by the abnormal, intramural to transmural, multinodular to diffuse, proliferation of nerve fibers and ganglion cells in a segment of the intestine.[1,12] The affected segment of bowel is thickened and the lumen can be dilated or narrowed. Human GN can occur anywhere in the gastrointestinal tract but most reported cases involve the colon and rectum.[1,12] Human GN may present as an acute gastrointestinal obstruction or motility disorder or incidentally, during investigations for other gastrointestinal diseases.[1,12] Human hereditary intestinal GN commonly occurs in association with multiple endocrine neoplasia type IIb (MEN-IIb), neurofibromatosis 1 (NF1; von Recklinghausen's disease) and Cowden's disease.[1,4,12] The pathogenesis of human GN remains undetermined. Surgical resection is recommended in human GN when lesions are confined to one section of the intestine.[4] When surgical resection is not an option, symptomatic management is advocated (may include one or more of the following: adjustments, laxatives or enemas, fiber supplementation and gastrointestinal motility modifiers).[4]

In the veterinary literature, reports of GN have been limited to juvenile and adult dogs, a horse and a steer.[3,5,9,10,12] Affected animals may present with gastrointestinal signs (e.g. vomiting, diarrhea or constipation, hematochezia, melena, tenesmus and abdominal pain) or they can be asymptomatic.[3,5,9,10,12] Abdominal ultrasonography may reveal thickening of the affected segment of the intestine and loss of the normal layers of the intestinal wall.[3,7] Histopathologic examination of full-thickness biopsies from the surgically resected affected segment of the intestine is needed to establish the diagnosis. Immunohistochemistry for neuron specific enolase, S-100 and glial fibrillary acidic protein (GFAP) will aid in establishing the diagnosis.[3,5,9,10,12] There are too few reports in the veterinary literature to comment on the prognosis or behaviour. In two of the reports the affected dogs were euthanized due to the development of a postoperative septic peritonitis.[3,5] There is a single report of a successful outcome following surgical resection in a dog with small intestinal GN.[3]

The pathogenesis of GN in animals is also unknown. It has yet to be established if the genetic mutations that have been identified in human GN occur in animal cases of GN. There is a single report in the veterinary literature in which a duplication of phosphatase and tensin homologue deleted on chromosome 10 (*PTEN)* was demonstrated, using a quantitative multiplex polymerase chain reaction, in a Great Dane puppy with concurrent colorectal hamartomatous polyposis and GN, implying a similar pathogenesis to human Cowden's disease.[3,4,12]

GN should be included as a differential diagnosis in dogs with intestinal thickening and gastrointestinal signs.

**JPC Morphologic Diagnosis:** 1. Colon: Ganglioneuroma. 2. Colon: Colitis, atrophic and lymphoplasmacytic, chronic, focal, severe.

**Conference Comment:** Without evidence of multiple sites of origin and given the well-demarcated lesion in sections with adjacent normal tissue, we prefer the diagnosis of ganglioneuroma in this case. Gastrointestinal pathology specialists at JPC were also consulted and concurred with our diagnosis; however, they commented that the extent of neural tissue within the submucosa is more prominent than is typical in similar cases in people. Although we believe the inflammation and abnormal glandular orientation is secondary to the neoplasm, we elected to separate out these changes in a second diagnosis.

Ganglioneuromas are characterized by exuberant proliferation of all elements of the intestinal ganglia, to include nerve fibers, ganglion cells and supporting cells.[1,7] This is in contrast to less differentiated but related tumors of ganglia origin, neuroblastomas. Neuroblastomas are composed of more primitive-appearing sheets of poorly defined cells with dark nuclei often forming pseudorosettes and lack the more mature ganglion cells of ganglioneuromas. The "schwannian stroma" as nicely described by the contributor and evident with immunohistochemistry for GFAP, organized fascicles of neuritic processes and fibroblasts are all histologic prerequisites for a diagnosis of ganglioneuroma.[8]

Cases may be localized to a mucosal or myenteric plexus, but are more often transmural; this case likely involves both.[1] Conference participants were reminded of the distinct locations within the intestinal wall of Auerbach's plexus (between the inner circular and outer longitudinal layers of muscularis externa) and Meissner's plexus (periphery of the submucosa). They are the sites of synapsis between preganglionic and postganglionic parasympathetic nerves necessary for autonomic control of the intestinal tract.[2]

The association of ganglioneuromas and multiple tumors of all three embryologic layers in Cowden syndrome in people and their correlation with PTEN mutations lend credence to the importance of a normally functioning PI3K/AKT signaling pathway in maintaining homestasis. This tyrosine kinase pathway, initiated by the binding of growth factors, consists of a series of phosphorylation events ultimately resulting in the inhibition of apoptosis (via phosphorylation of BAD, a BCL-2 family sensor & MDM2, direct inhibitor of p53) and enhancement of cell growth and survival (via TSC1/TSC2 inactivation and subsequent mTOR activation). PTEN applies the brakes at the beginning of this cascade where it blocks phosphorylation of $PIP_2$ into $PIP_3$ by PI3K.[11] Correlating the PTEN mutation with ganglioneuromatosis in animals has so far been limited to a single report in one dog as previously mentioned by the contributor.[3]

**Contributing Institution:** Prairie Diagnostic Services (PDS) and Department of Veterinary Pathology
Western College of Veterinary Medicine
52 Campus Drive
University of Saskatchewan
Saskatoon, Saskatchewan, S7N 5B4
Canada
Websites: www.pdsinc.ca and www.usask.ca/wcvm/vetpath

**References:**

1. d'Amore ESG, Manivel JC, Pettinato G, Neihans GA, Snover DC. Intestinal ganglioneuromatosis: mucosal and transmural types. A clinicopathological and immunohistochemical study of six cases. *Human Pathol*. 1991;22:276-286.
2. Bacha WJ, Bacha LM. *Color Atlas of Veterinary Histology*. 2nd ed. Philadelphia, PA: Lippincott Williams & Wilkins; 2000:146.
3. Bemelmans I, Küry S, Albaric O, Hordeaux J, Bertrand L Nguyen F, et al. Colorectal hamartomatous polyposis and ganglioneuromatosis in a dog. *Vet Path*. 2011;48:1012-1015.

4. Cohen MS, Phay JE, Albinson C, DeBenedetti MK, Skinner MA. Gastrointestinal manifestations of multiple endocrine neoplasia type. *Ann Surg*. 2002;235:648-654.
5. Cole DE, Migaki G, Leipold HW. Colonic ganglioneuromatosis in a steer. *Vet Pathol*. 1990;27:461-462.
6. Fairley RA, McEntee MF. Colorectal ganglioneuromatosis in a young female dog (Lhasa Apso). *Vet Pathol*. 1990;27:206-207.
7. Hazell KLA, Reeves MP, Swift IM. Small intestinal ganglioneuromatosis in a dog. *Austr Vet J*. 2011;89:15-18.
8. Maitra A. Diseases of infancy and childhood. In: Kumar V, Abbas AK, Fausto N, Aster JC, eds. *Robbins and Cotran Pathologic Basis of Disease.* 8th ed. Philadelphia, PA: Elsevier; 2010:475-476.
9. Paris JK, McCandlish AP, Schwarz T, Simpson JW, Smith SH. Small intestinal ganglioneuromatosis in a dog. *J Comp Path*. 2013;148:323-328.
10. Port BF, Starts RW, Payne HR, Edwards JF. Colonic ganglioneuromatosis in a horse. *Vet Path*. 2007;44:207-210.
11. Stricker TP, Kumar V. Neoplasia. In: Kumar V, Abbas AK, Fausto N, Aster JC, eds. *Robbins and Cotran Pathologic Basis of Disease.* 8th ed. Philadelphia, PA: Elsevier; 2010:294.
12. Thway K, Fisher C. Diffuse ganglioneuromatosis in small intestine associated with neurofibromatosis type 1. *Ann Diagn Path*. 2009;13:50-54.

---

**CASE III**: 14-19 (JPC 4048513).

**Signalment:** Adult male rhesus macaque, *(Macaca mulatta)*.

**History:** This SIV infected adult male Rhesus macaque had a several month history of severe icterus and subsequent terminal malaise, the pathogenesis of which was undetermined. It was sacrificed at its study endpoint and submitted for necropsy evaluation.

**Gross Pathology:** The pancreas was described as markedly enlarged and firm, with mottled areas of hemorrhage and an accentuated lobular pattern. Some patchy regions of normal appearing parenchyma remained.

**Laboratory Results:** None

**Histopathologic Description:** H&E sections of grossly abnormal pancreas are examined. There is massive, near diffuse necrosis of most lobules, with many demonstrating extensive hemorrhage, severe infiltrates of degenerative neutrophils and prominent acinar cell necrosis, with pyknosis, karyorrhexis and karyolysis. Some sections contain small adjacent and adhered portions of splenic parenchyma, in which there is moderate eosinophilic hyaline amyloid type material centrally within white pulp areas. In many necrotic lobules, remaining identifiable acinar cells contain extremely large basophilic or amphophilic intranuclear inclusion bodies, generally filling and expanding the entire nucleus and sometimes appearing to fuse with cytoplasmic contents, creating nucleocytoplasmic blurring (smudge cells). On highest light microscopy magnification, some of these inclusion structures have a fine interlaced or lattice type pattern visible. Inclusions are noted less frequently in remaining pancreatic ductal epithelium as well.

In addition, some lobules not completely necrotic demonstrate prominent regenerative hyperplasia with some atypia. Islet cell structures were infrequently observed and when visible, did not have evidence of primary viral cytopathic effect.

Although the organ was extensively effaced by this necrotizing process, there were small, patchy remaining areas of relatively normal appearing parenchyma (not generally seen in sections distributed). In some sections, overlying pancreatic capsule was markedly thickened and fibrotic, with infrequent fibrous adhesive tags.

**Contributor's Morphologic Diagnosis:** Pancreatitis, necrotizing and hemorrhagic, focally extensive to near diffuse, severe, with large basophilic and amphophilic intranuclear inclusion bodies and regions of marked regenerative hyperplasia (some sections).

**Contributor's Comment:** The microscopic findings are consistent morphologically with the entity of Adenoviral pancreatitis. This spontaneously occurring condition was originally described from a single case in the early 1970's[5] and further reported in the literature as additional individual entities or small clusters on subsequent occasions.[2,3,9,11,12] The paucity of both total cases described as well as absence from retrospective surveys suggests that although this is clearly a defined and consistent entity, it is not a commonly occurring one. An association between retroviral infection and adenoviral pancreatitis has been noted,[6,11] although SIV or other immunosuppressive agents do not appear to be a necessary condition for infection. Most cases are diagnosed based on visualization of characteristic inclusion bodies and the presence of typical adenoviral ultrastructural morphology. In two cases where viral culture has been performed, Adenovirus types 23 and 31 have been isolated.[11,12] Disease has been reported in both juvenile and adult animals, although, unlike this case, the clinical course is typically short, with a rapid (1-2 week) demise, often accompanied by severe bloody diarrhea.[3] Classical signs of acute pancreatitis as described in humans and domestic animal species such as abdominal pain and vomiting are not described. As in previously reported cases of this distinct clinical entity, viral inclusion bodies were not noted outside of the pancreas.[3,5,9,11] However, in several cases of fatal adenoviral pneumonia in non-human primates, intranuclear inclusion bodies were also occasionally observed in bile duct and pancreatic duct epithelium.[10] The presenting jaundiced condition seen in this animal was thought to be due to compression and obstruction of the common bile duct due to pancreatic parenchymal swelling and necrosis. Concurrent hepatic histological findings included prominent canalicular and ductal bile stasis, biliary ductal hyperplasia and mild cholecystitis. Inclusion bodies or other viral cytopathic effects were not noted in hepatocytes or biliary epithelium in this case.

Adenovirus has been isolated from a wide variety of tissues from healthy monkeys[6] and consensus suggests that these viruses usually exist in a latent state, only rarely causing disease,[3] although fatal adenoviral pneumonia has been encountered in a wide range of simian primates.[10] The immunofluorescent-demonstrated presence of duodenal adenovirus antigen was documented in two cases of monkeys with adenoviral pancreatitis and this, along with the common concurrent presence of clinical enteric disease suggests that pancreatic infection may occur from GI ascension through pancreatic ducts.[3] Adenovirus enteritis has been documented in SIV infected Rhesus monkeys.[6]

Necrotizing pancreatitis in animals is not typically associated with an infectious pathogenesis. Foals have been reported to have naturally occurring adenoviral pancreatitis, although this

appears as part of a widespread infection with primary lung and other tissue involvement.[13] Experimental pancreatitis has been induced in mice with a wide variety of viruses including Encephalomyocarditis virus (EMC), Reovirus, Coxsackie B virus, Foot and Mouth Disease virus, Venezuelan Equine Encephalomyelitis virus and others.[5,7] Economou & Zissis and others have enumerated infectious causes of acute pancreatitis in humans,[1,4] including multiple viruses such as Mumps, Coxsackie B virus and Hepatitis B virus, although it appears that many of these associations are based on antibody titer presence, clinical presentation and the exclusion of other known causes.

**JPC Morphologic Diagnosis:** Pancreas: Pancreatitis, necrotizing, diffuse, severe, with marked acinar atrophy and loss, and numerous intranuclear viral inclusions.

**Conference Comment:** In the most common adenoviral diseases of veterinary importance, including the equine adenovirus-1 (intestinal epithelial cells of SCID foals), canine adenovirus-2 (alveolar macrophages of dogs with kennel cough), canine adenovirus-1 (hepatocytes and endothelial cells of unvaccinated puppies), and adenoviral infection of macaques (pancreatic acinar cells of nonhuman primates), the characteristic intranuclear amphophilic inclusions are readily recognized and often associated with prior immune suppression. Adenoviruses occur worldwide and are generally species specific, although transmission between closely-related species can occur, including zoonotic transmission between monkeys and people.[14] Approximately 50 adenoviral serotypes have been identified in nonhuman primates.

Adenoviruses eject DNA from the viral capsid and into the nucleus, where subsequent DNA and protein synthesis create the distinctive inclusions and ultimately result in death of the cell. Ultrastructurally, the inclusions are composed of prominent paracrystalline arrays of virions and unassembled capsid proteins. Respiratory and gastrointestinal epithelial cells are the most common targets of viral replication; however, the epithelial cells of the conjunctiva, cornea, urinary bladder, and kidney, in addition to hepatocytes and pancreatic acinar cells, can also be infected. Although adenoviral inclusions are generally quite distinctive, they can resemble those of cytomegalovirus (herpesvirus) and SV40 (polyomavirus), which also cause significant cytomegaly and nucleomegaly.[14]

**Contributing Institution:** Division of Laboratory Animal Resources
University of Pittsburgh
http://www.dlar.pitt.edu/
http://pitt.edu/

**References:**

1. Adler JB, Mazzotta SA, Barkin JS. Pancreatitis caused by measles, mumps and rubella vaccine (Case report). *Pancreas*. 1991;6:489-490.
2. Baskin GB, Murphey-Corb, M, Watson A, Martin LN. Necropsy findings in Rhesus monkeys experimentally infected with cultured Simian Immunodeficiency Virus (SIV)/Delta. *Vet Pathol*. 1988;25:456-467.
3. Baskin GB, Soike KF. Adenovirus Enteritis in SIV-infected Rhesus monkeys. *Journal of Infectious Diseases.* 1989;160(5):905-906.
4. Boyce JT, Giddens WE, Valerio M. Simian adenoviral pneumonia. *Am J of Path*. 1978;91(2):259-276.

5. Chandler FW, Callaway CS, Adams SR. Pancreatitis associated Adenovirus in a Rhesus monkey. *Vet Pathol*. 1974;11:165-171.
6. Chandler FW, McClure HM. Adenoviral Pancreatitis in Rhesus monkeys: current knowledge. *Vet Pathol*. 1982;19(Supp. 7):171-180.
7. Craighead JE, Kanich RE, Kessler JB. Lesions of the Islets of Langerhans in Encephalomyocarditis virus infected mice with diabetes mellitus-like disease. *Am J of Path*. 1974;74(2):287-294.
8. Daniel MD, Desrosiers RC, Letvin NL, King NW, Schmidt DK, Sehgal P, Hunt RD. Simian models for AIDS. *Cancer Detection and Prevention Supplement.* 1987;1:501-507.
9. Daniel MD, Letvin NL, Sehgal PK, Desrosiers RC, Hunt RD, Waldron LM. Induction of AIDS-like disease in macaque monkeys with T-Cell tropic retrovirus STLV-III. *Science*. 1985;230:71.
10. Economou M, Zissis M. Infectious cases of acute pancreatitis. *Annals of Gastroenterology*. 2000;13(2):98-101.
11. Martin BJ, Dysko RC, Chrisp CE. Pancreatitis associated with Simian Adenovirus 23 in a Rhesus monkey. *Laboratory Animal Science*. 1991;41(4):382-384.
12. McClure HM, Chandler FW, Hierholzer JC. Necrotizing pancreatitis due to Simian Adenovirus Type 31 in a Rhesus monkey. *Arch Pathol Lab Med*. 1978;102:150-153.
13. McChesney AE, England JJ, Adcock JL, Stackhouse LL, Chow TL. Adenoviral infection in suckling Arabian foals. *Vet Pathol*. 1970;7:547-565.
14. Wachtman L, Mansfield K. Viral diseases of nonhuman primates. In: Abee CR, Mansfield K, Tardif S, Morris T, eds. *Nonhuman Primates in Biomedical Research: Diseases*. Vol. 2. 2nd ed. San Diego, CA: Academic Press; 2012:28-30.

---

**CASE IV:** N2013-584 (JPC 4048812).

**Signalment:** Adult female bushy-tailed jird, *(Sekeetamys calurus)*.

**History:** A total of 9 bushy-tailed jirds (8 adult and 1 immature; 6 females and 3 males) were found dead within 2 days and without premonitory signs. Three were too autolyzed for further assessment. All the animals came from the same enclosure.

**Gross Pathology:** Affecting over 80% of the liver parenchyma are coalescing, well demarcated, circular, flat, tan to pale red areas (necrosis). The rest of the parenchyma is mottled red to maroon. Similar foci are scattered throughout the splenic parenchyma. The wall of the large intestine is thickened up to 0.1 cm, pale yellow, has a shiny serosa and contains moderate amounts of green pasty digesta. There are prominent, well demarcated, 0.4 cm in diameter, tan to pale pink lymphoid aggregates that bulge into the serosa. The jird is in fair body condition with small to moderate amounts of subcutaneous and abdominal adipose tissue.

**Laboratory Results:** Aerobic culture, liver: Many *Listeria* spp.
Anaerobic culture, liver: No anaerobes isolated.
Lung or liver from 3 other jirds were sent for aerobic culture and revealed many *Listeria* spp. in two, and many *Listeria monocytogenes* in one.

**Histopathologic Description:** Liver: Multifocally affecting over 60% of the hepatic parenchyma are randomly scattered, well demarcated, 200 – 500 µm in diameter, coalescing areas of lytic necrosis with large numbers of intralesional, gram positive short bacilli. Bacteria are intra- and extracellular. In most of the sections portal areas are severely affected. The areas of necrosis are characterized by loss of tissue architecture with accumulation of eosinophilic amorphous material, few degenerated neutrophils and cellular and karyorrhectic debris. Necrotic hepatocytes are characterized by shrunken and/or fragmented hypereosinophilic cytoplasm and pyknosis, karyorrhexis or karyolysis. On the periphery of the areas of necrosis hepatocyes often contain multiple 2 – 7 µm in diameter round, clear vacuoles (lipid) and are moderately swollen (degeneration). In blood vessels adjacent or within affected areas there are increased numbers of neutrophils and eosinophilic strand-like material (fibrin) admixed with red blood cells. Multifocally in some of the sections are small areas of sinusoidal and central vein congestion.

Other significant histologic findings (not present in the slide provided) include:

Spleen: Splenitis, necrotizing, acute, multifocal severe with intralesional short bacilli
Lymph nodes, mesenteric and mandibular: Lymphadenitis, necrotizing, acute, diffuse, severe
Intestine: Enterocolitis, necrotizing, acute, multifocal to transmural, severe
Bone marrow: Myelitis, necrotizing, acute, multifocal, moderate
Gram stain: Bacteria are Gram positive.

**Contributor's Morphologic Diagnosis:** Liver: Hepatitis, necrotizing, acute, random, multifocal, severe with intralesional Gram positive short bacilli (*Listeria* spp.).

**Contributor's Comment:** Gross, histological and microbiological findings in this case are consistent with septicemic listeriosis. Listeriosis is caused by *Listeria monocytogenes* (LM), a Gram-positive, facultative anaerobic bacillus that is ubiquitous in the environment and can multiply in diverse environmental conditions.[8] As an example of LM ubiquity, it can be grown in a temperature range from 4° to 45° C and at a pH range of 5 to 9.[8] This pathogen has been diagnosed in a variety of domestic and non-domestic mammals,[7,10] reptiles[5] and birds.[1,2]

LM has more than 11 serotypes and almost all domestic animal infections are caused by serotypes 1/2a, 1/2b and 4b.[8] It is an intracellular pathogen of macrophages, neutrophils and epithelial cells.[8] Mobile genetic elements in *Listeria* spp. include pathogenicity islands (LIPI-1 and LIPI-2) and plasmids.[6] LIPI-1 encodes for a cluster of virulence factors including hemolysins (such as listeriolysin O)[11,13] and actin-polymerase factors, necessary for the intracellular survival and spread of the organism.[6] LIPI-2 is specific for *Listeria ivanovii* and thought to be responsible for restriction of its host specificity to ruminants and for its lack of typical tropism for the central nervous system observed in LM.[6] Other important virulence factors of LM include the internalins, surface proteins which internalize with E-cadherin to overcome the intestinal, placental and blood-brain barriers.[8]

The three recognized syndromes in domestic animals, that seldom overlap, are infection of the pregnant uterus with abortion, septicemia with miliary visceral abscesses, and encephalitis.[8] In rodents and small mammals the septicemic form predominates.[9] In our jirds, out of the 6 cases in which histology was performed, the organs most commonly affected were liver (6/6), spleen (6/6), large intestine (5/6), small intestine (4/6), lymph nodes (3/4), bone marrow (2/6), lung (1/6) and brain (1/6). Septicemic listeriosis is characterized by multisystemic bacterial

colonization with multifocal areas of necrosis or microabscess formation.[8] In our case, the lesions were very acute and only small numbers of neutrophils were recognized within the lesions and adjacent blood vessels. Jirds are gerbil-like rodents[12] that belong to the family *Gerbillinae*. Gerbils are used as models for *Listeria monocytogenes* infection and naturally succumb to the disease.[4]

LM is a zoonotic pathogen that can be transmitted through alimentary sources (food-borne) and direct contact.[11] Food-borne transmission of the bacterium was suspected in our jirds, but food was not available for testing. This disease has been previously reported in bushy tailed jirds and the source of infection was similarly not elucidated in that mortality event.[12] Diagnosis was reached by histopathology and microbiology. Gram stains confirmed the presence of gram-positive bacteria in the lesions. Other diagnostic methods that could be of use include immunohistochemistry and PCR.

**JPC Morphologic Diagnosis:** Liver: Hepatitis, necrotizing, random, multifocal, severe, with numerous bacilli.

**Conference Comment:** The contributor presents a classic disease entity in its septicemic form and discusses its ubiquitous and hardy nature in addition to describing its molecular interactions with host target cells as highlighted in recent literature. *Listeria* spp. has a unique affinity for the brain stem, and thus is perhaps most commonly associated with its encephalitic form which is almost solely observed in adult ruminants, usually subsequent to consumption of improperly stored silage.[13] Ingestion of the bacteria and its exposure to the host through damaged oral mucosa permits its colonization and ultimate localization to the brainstem via retrograde axonal transport along the trigeminal nerve.[9] It is these cases that present with the typical "circling" behavior and have the characteristic "microabscesses" histologically within the brainstem.

The pathogenicity island LIPI-1 encodes the bacterial surface protein *surface protein actA* which is vital for *Listeria*'s ability to colonize. Once the bacterial population reaches a sufficient size within a single cell, it propels into adjacent cells via actin polymerization of this protein and forms membrane protrusions known as pseudopods. The pseudopods penetrate into adjacent cells forming double-membrane endocytotic phagocytic vesicles which are subsequently lysed by the virulence factor listerolysin-O among others.[13] Transfer of the pseudopod into adjacent cells is facilitated by expression of phosphatidylserine, the well-known surface phospholipid important in both the coagulation cascade and efferocytosis. Effectively, *Listeria* spp. exploits efferocytosis to promote its dissemination. Therefore, a likely target of effective antimicrobial therapy may be phosphatidylserine or its binding receptor for this and other similar bacterial pathogens.[3]

**Contributing Institution:** Wildlife Conservation Society
Zoological Health Program
Department of Pathology
www.wcs.org

**References:**

1. Akanbi OB, Breithaupt A, Polster U, et al. Systemic listeriosis in caged canaries (Serinus canarius). *Avian Pathol*. 2008;37(3):329-332.
2. Crespo R, Garner MM, Hopkins SG, Shah DH. Outbreak of Listeria monocytogenes in an urban poultry flock. *BMC Veterinary Research*. 2013;9:204.
3. Czuczman MA, Fattouh R, Van Rijn JM, et al. Listeria monocytogenes exploits efferocytosis to promote cell-to-cell spread. *Nature*. 2014;509(7499):230-234.
4. Disson O, Nikitas G, Grayo S, Dussurget O, Cossart P, Lecuit M. Modeling human listeriosis in natural and genetically engineered animals. *Nature Protocols*. 2009;4(6):799-810.
5. Girling SJ, Fraser MA. Listeria monocytogenes septicaemia in an inland bearded dragon (Pogona vitticeps). *Journal of Herpetological Medicine and Surgery*. 2004;14:6-9.
6. Gyles C, Boerlin P. Horizontally transferred genetic elements and their role in pathogenesis of bacterial disease. *Vet Pathol*. 2014;51:328-340.
7. Langohr IM, Ramos-Vara JA, Wu CC, Froderman SF. Listeric meningoencephalomyelitis in a cougar (Felis concolor): Characterization by histopathologic, immunohistochemical and molecular methods. *Vet Pathol*. 2006;43(3):381-383.
8. Maxie GM, Youssef S. Nervous system. In: Maxie MG, ed. *Jubb, Kennedy and Palmer's Pathology of Domestic Animals*. 5th ed. Vol. 1. Philadelphia, PA: Saunders Elsevier; 2007:405–408.
9. Morner T. Listeriosis. In: Williams ES, Baker IK, eds. *Infectious Diseases of Wild Mammals*. 3rd ed. Ames, IA: Iowa State University Press. 2001:502.
10. Nichols M, Takacs N, Ragsdale J, Levenson D, Marques C, Roache K, et al. Listeria monocytogenes infection in a sugar glider (Petaurus breviceps)- New Mexico, 2011. *Zoonoses Public Health*. 2014: doi: 10.1111/zph.12134.
11. Oliver HF, Wiedmann M, Boor KJ. Environmental reservoir and transmission into the mammarlian host. In: Goldfine H, Shen H, eds. *Listeria Monocytogenes: Pathogenesis and Host Response*. 1st ed. New York, NY: Springer; 2007:111.
12. Tappe JP, Chandler FW, Westrom WK, Liu S, Dolensek EP. Listeriosis in seven bushy-tailed jirds. *J Am Vet Med Assoc*. 1984;185(11):1367-1370.
13. Zachary JF. Mechanisms of microbial infections. In: Zachary JF, McGavin MD, eds. *Pathologic Basis of Veterinary Disease*. 5th ed. St. Louis, MO: Elsevier; 2012:192-195.

**Joint Pathology Center**
**Veterinary Pathology Services**

*Conference Coordinator*
**Matthew C. Reed, DVM**
**Captain, Veterinary Corps, U.S. Army**
**Veterinary Pathology Services**
**Joint Pathology Center**

## WEDNESDAY SLIDE CONFERENCE 2014-2015

# Conference 7

**22 October 2014**

**Conference Moderator:**
COL Todd O. Johnson, DVM, Diplomate ACVP
Program Chair, Veterinary Pathology Services
Joint Pathology Center
Forest Glen Annex, Bldg 161
2460 Linden Lane
Silver Spring, MD 20910

**CASE I:** B13-962 (JPC 4049563).

**Signalment:** 10-year-old spayed female Welsh corgi dog, *Canis familiaris.*

**History:** The dog presented in 2011 for a 6-week history of hematuria. Urine culture was negative and no signs of uroliths were seen on radiographs. Ultrasound revealed two, 1.7 mm, mineralized foci in the left renal pelvis, but the kidneys were normal in shape and size. No further workup was performed at that time. The dog presented again in July 2013 with continued hematuria. On ultrasound, the left renal cortex had a 2.2 cm, round, heterogeneous mass with multiple, internal, anechoic regions.

**Gross Pathology:** The renal cortex was extensively disrupted by coalescing, dark red, blood-filled nodules ranging from 0.7 x 0.5 x 0.2 cm to 2.5 x 2 x 2 cm.

*1-1. Kidney, Welsh corgi: The cortex is expanded by large, ectatic, thin-walled vessels which efface renal parenchyma. (HE 6.3X)*

**Histopathologic Description:** Kidney: The renal interstitium is markedly expanded by many, severely dilated, blood-filled vascular spaces lined by mature endothelial cells surrounded by abundant fibrous tissue. Some vascular spaces contain thrombi with fibrin arranged as lines of Zahn separated by red and white blood cells that are occasionally attached to the vascular wall by fibrous tissue. The intervening and adjacent renal parenchyma is markedly atrophic with replacement of many nephrons by fibrosis, many lymphocytes and plasma cells, and variable hemorrhage. Remaining tubules

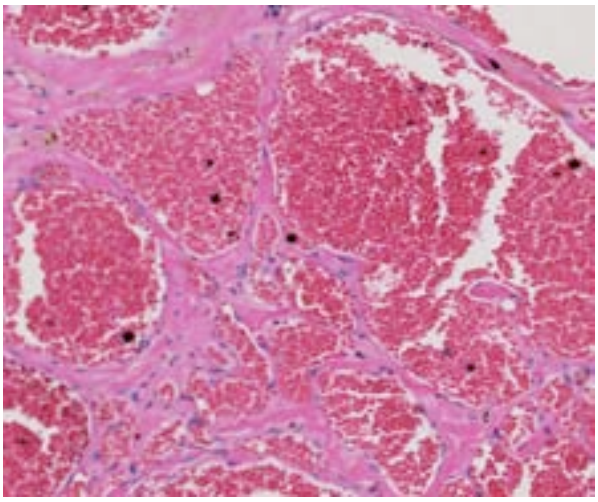

*1-2. Kidney, Welsh corgi: Vessels are thin-walled and separated by a moderate fibrous stroma. (HE 144X)*

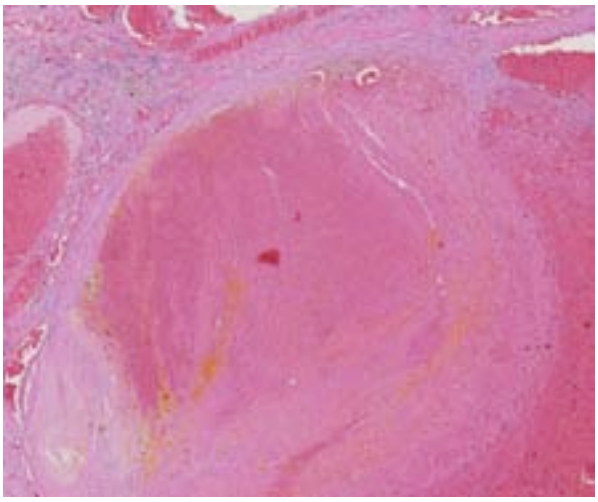

*1-3. Kidney, Welsh corgi: Larger vessels are partially occluded with fibrinous thrombi which contain lines of Zahn. (HE 35X)*

and glomeruli in these areas are often atrophic or sclerotic, respectively. Some tubules contain proteinaceous fluid. The renal pelvis contains degenerating erythrocytes and brown, granular pigment. The more distant renal parenchyma is unremarkable apart from congestion.

**Contributor's Morphologic Diagnosis:** Kidney: Renal telangiectasia.

**Contributor's Comment:** Renal telangiectasia is a rare, non-neoplastic proliferation of blood vessels.[3] It has been described in the Welsh corgi as a familial disease, and similar lesions have been described in cattle, dogs, cats, mink and ferrets.[2] Affected corgis typically present for hematuria and may have bilateral lesions or additional lesions in other tissues, such as the liver, duodenum, brain, vertebrae, subcutaneous tissue, and spleen.[3,4] In this case, no contralateral or extra-renal lesions were identified by abdominal ultrasound or at surgery. The primary clinical differential in this case was renal hemangiosarcoma. Renal telangiectasia is differentiated histologically from hemangiosarcoma by the fact that the vascular spaces are lined by a bland, mature endothelium without mitotic activity or cellular atypia.[4]

**JPC Morphologic Diagnosis:** Kidney: Vascular malformation with multifocal thrombosis.

**Conference Comment:** Conference participants discussed three optional diagnoses for this case: telangiectasia, hemangioma or vascular hamartoma. The familial lesion of renal telangiectasia in Pembroke Welsh corgis as described in the literature characteristically arises bilaterally with frequent occurrences in other organs. The clinical history in this case suggests the lesion is isolated to one kidney; however, the lesion lacks the well-circumscribed appearance of a hemangioma. The signalment and clinical signs do not correlate well with a hamartoma, which implies a congenital proliferation. The diagnosis of vascular malformation reflects these inconsistencies and participants' inability to arrive at a consensus.

The pattern of presentation in corgis interestingly resembles a familial condition in people known as hereditary hemorrhagic telangiectasia (HHT). Also known as Osler-Weber-Rendu disease, this autosomal dominant disorder occurs at a rate of 1 in 5,000 people and manifests as telangiectasia of the oral mucosa and arteriovenous malformations in the lungs, liver and less often brain. Three mutations have been identified in HHT, all with protein products influencing the TGF-β superfamily.[5]

TGF-β is a growth inhibitor of most epithelial cells but a potent stimulator of fibroblasts. Its binding to cell-surface receptors leads to phosphorylation of SMAD transcription factors, specifically Co-SMAD & R-SMAD. When phosphorylated, these factors overcome SMAD-7 inhibition, thereby promoting transcription and activation of fibroblasts. Additionally and likely pertaining to these vascular lesions, TGF-β is strongly implicated in the stabilization of nascent blood vessels, following their sprouting and

migration through the finely orchestrated events coordinated by VEGF and the Notch pathway.[1]

This inheritable condition has serious consequences in people due to their predisposition for hemorrhages and thrombosis. The understanding of disease pathogenesis has also shed new light on the specific molecular interactions of angiogenesis, one of the hallmarks of cancer. The authors speculated on the value of Pembroke Welsh corgis serving as an animal model for vascular malformations over 30 years ago.[3] While knockout mice have been developed which reproduce these lesions, this naturally occurring canine model may offer further valuable insight in piecing together the complex interactions of angiogenesis and its role in vascular malformations and neoplasia.

**Contributing Institution:** Tufts Cummings School of Veterinary Medicine
Department of Biomedical Sciences
200 Westboro Road
North Grafton, MA 01536
http://vet.tufts.edu/dbs/

**References:**

1. Kumar V, Abbas AK, Fausto N, Aster JC. Tissue renewal, regeneration and repair. In: Kumar V, Abbas AK, Fausto N, Aster JC, eds. *Robbins and Cotran Pathologic Basis of Disease*. 8th ed. Philadelphia, PA: Elsevier Saunders; 20010:89, 100-101.
2. Maxie MG, Newman SJ. Urinary system. In: Maxie MG, ed. *Jubb, Kennedy and Palmer's Pathology of Domestic Animals*. 5th ed. Vol 2. Philadelphia, PA: Elsevier Saunders; 2007:495.
3. Meuten DJ. Tumors of the urinary system. In: *Tumors in Domestic Animals*. 4th ed. Ames, IA; Iowa State Press; 2002:524.
4. Moore FM, Thornton GW. Telangiectasia of Pembroke Welsh corgi dogs. *Vet Pathol*. 1983;20(2):203-8.
5. Shovlin CL. Hereditary haemorrhagic telangiectasia: pathophysiology, diagnosis and treatment. *Blood Reviews*. 2010;24:203-219.

**CASE II**: 1259066 (JPC 4048671).

**Signalment:** 6-year-old spayed female Vizsla dog, *Canis familiaris.*

**History:** The patient had a 6-month history of minor incontinence followed by a 3-month history of recurrent UTI's, which were treated by the referring veterinarian with estradiol cypionate and antibiotics respectively (consecutive ampicillin, chloramphenicol, cephalexin, and metronidazole). The patient had a 1-month history of ataxia and progressively more frequent vomiting. She presented to Urgent Care Service on 7/27 for worsening neurologic signs, anorexia, lethargy, and PU/PD. Radiographs obtained were inconclusive. The patient was referred for neurology consult, recommended MRI, and remained for inpatient diagnostic testing and treatment for 5 days.

During diagnostic workup, there was mild C5-C6 disc protrusion noted on cervical myelogram. On post-contrast T1 weighted MR images, there was meningeal enhancement spinal cord through C1 and ventral to the brain stem and pons, as well as faint contrast enhancement in the cerebellum. On cerebellomedullary cistern cerebrospinal fluid aspirate cytology there was a severe mixed pleocytosis. *Neospora* and *Toxoplasma* PCR and serology, *Cryptococcus* latex agglutination, and bacterial cultures were all negative. Thoracic radiographs were unremarkable. Serum biochemistry findings were mild hyperglobulinemia and moderately elevated ALT and AST.

Therapeutic interventions included clindamycin, fluconazole, cytoarabine, and prednisolone at an immunosuppressive dose. The tentative clinical diagnosis was meningoencephalitis of unknown origin with concern about fungal disease or GME. The dog was discharged from the hospital 5 days after admission. During the following 2 weeks, the patient re-presented for weight loss, muscle wasting, and progressive ataxia leading to tetraparesis. The patient arrested shortly after presentation to urgent care in lateral recumbency and respiratory distress.

**Gross Pathology:** At necropsy, the dog was in very poor body condition (BCS = 2/9). Her mucous membranes and non-haired pinnae were markedly pale and eyes were recessed. In the kidneys, there were numerous miliary, pale tan, 1 to 2 mm diameter foci on the capsular surface that often extended in multifocal rays into the medullas. Similar minute nodules and streaks were throughout the myocardium. In the brain and spinal cord, there was moderate purulent subdural exudate (meningoencephalitis). The liver was diffusely friable, and moderately enlarged with rounded edges. The small and large intestines were segmentally reddened and thickened with multifocal irregular mucosal ulcerations. Multiple lymph nodes are moderately expanded by irregular firm to caseated foci. The adrenal cortices were mildly bilaterally thin (atrophy, consistent with steroid administration).

*2-1. Kidney, dog: Linear hypercellular foci replace cortical and medullary parenchyma. (HE 7X)*

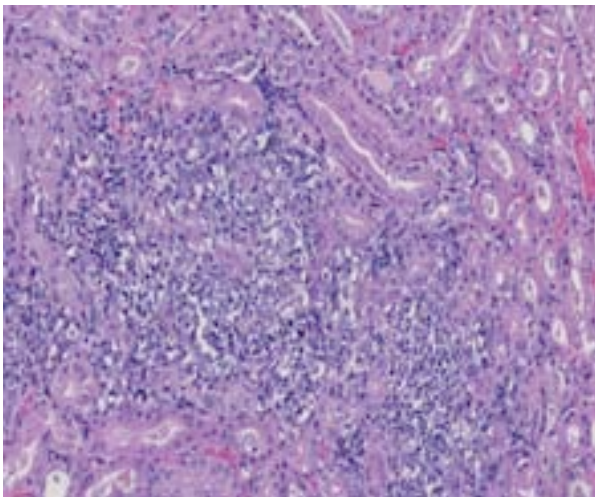

*2-2. Kidney, dog: The interstitium is infiltrated and tubules are replaced by large numbers of macrophages, lymphocytes and plasma cells. Algal sporangia are often seen within macrophages (arrows). (HE 228X)*

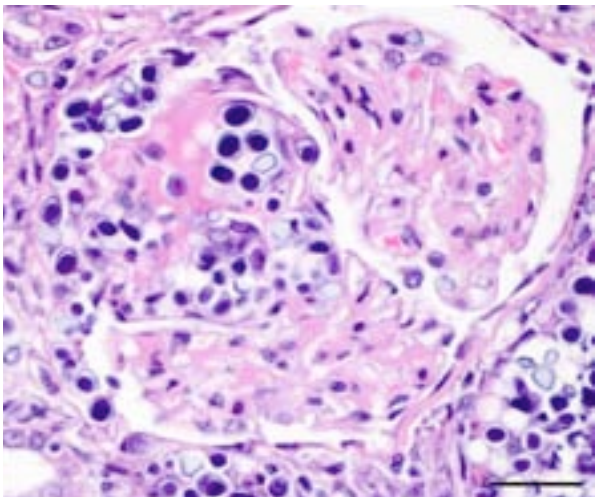

*2-3. Kidney, dog: Sporangia are occasionally seen within glomerular mesangium and Bowman's space. (HE 400X) (Photo courtesy of: Colorado State University, Department of Microbiology Immunology and Pathology: http://csu-cvmbs.colostate.edu/academics/mip/Pages/default.aspx)*

**Laboratory Results:** Myocardial impression smears were taken at the time of necropsy. There were numerous round unicellular organisms with refractile cell walls, basophilic cytoplasm, and internal septation.

**Histopathologic Description:** Kidney: Effacing the renal cortex and medulla are numerous large irregular foci of necrotic tubules and obliterated interstitium with moderately to markedly increased numbers of macrophages, plasma cells, fewer lymphocytes, and admixed neutrophils. Foci extend radially along tubules, effacing up to 1 mm wide tracts through the medulla and cortex. There are numerous unicellular, round to ovoid, 6 to 20 micrometer diameter organisms with pale staining to chromophobic refractile double-layer cell walls. The sporangia (theca) contain single round to ovoid, or multiple wedge-shaped, granular basophilic endospores with small dark basophilic nuclei. There are numerous poorly staining to clear empty theca. Inflammatory cells dissect through the moderately compressed renal interstitium surrounding and infiltrating dense clusters of organisms. Multifocal tubules and Bowman's capsules are distended by organisms, mixed inflammatory cells and karyorrhectic debris. Affected glomeruli are variably shrunken and hypereosinophilic with fibrin deposition and pyknotic to karyorrhectic nuclei. Tubules, with attenuated and necrotic epithelium, are segmentally obliterated and progressively lost, both within and adjacent to the lesion. There is moderate multifocal perilesional congestion.

Of additional interest, sections of liver are provided, demonstrating organisms in sinusoids, multifocal hepatocellular necrosis, dystrophic mineralization, hydropic degeneration, and occasional portal tracts effaced by *Prototheca* sporangia and granulomatous inflammation. Hepatic lesions are variable and clusters of organisms are not captured in all sections.

In tissues not included for conference material, multifocal to coalescing perivascular and random granulomatous inflammation with organisms is present throughout the gastrointestinal tract, pancreas, mesentery, lymph nodes, lung, myocardium, and meninges.

**Contributor's Morphologic Diagnosis:** Kidney: Nephritis, interstitial, granulomatous to lymphohistiocytic, multifocal, chronic, moderate to marked with tubular necrosis and loss, and with myriad intralesional algal organisms (consistent with *Prototheca* sp.).

**Contributor's Comment:** *Prototheca* spp. are saprophytic, achlorophyllous algae, closely related to *Chlorella* spp., with worldwide distribution.[7] This opportunistic pathogen is a spherical, 3 to 30 micron diameter, unicellular organism with a 0.5 micron thick poorly-staining refractile cell wall. In the sporangium, there are individual round, or up to 20 irregularly shaped, basophilic endospores produced by asexual cytoplasmic cleavage.[4,7,8] *Prototheca* and *Chlorella* are histologically indistinguishable on H&E-stained sections.[4] For both genera, endospores are Gram-positive and sporangia stain positively by Gomori methenamine silver (GMS). Differentiation is possible on fresh specimens and periodic acid-Schiff (PAS)-stained sections.[4,5,11,12] In gross fresh specimens and wet-mounts *Chlorella*-infected tissue and organisms are green, due to chlorophyll. Additionally, on PAS-stained sections, cytoplasmic starch of *Chlorella* spp. is visible as distinct globules that are strongly PAS-positive and diastase sensitive. The PAS-positive, diastase-resistant endospores of *Prototheca* spp. do not exhibit distinct cytoplasmic globules.[5,8] For an excellent example of PAS-positive starch globules in *Chlorella* spp. readers are referred to images published by Haenichen et al.[5] Morphologic differentiation between species of *Prototheca* is documented, but immunolabeling and 18S rRNA sequence analysis are also available.[8]

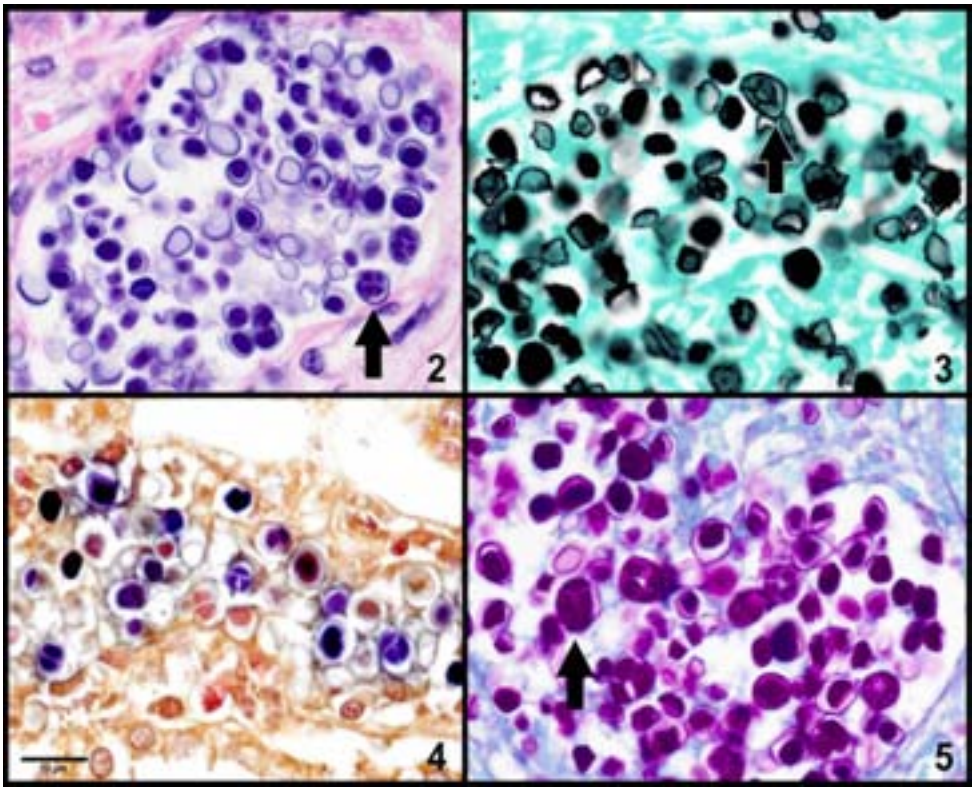


*2-4. Kidney, dog: Upper left: Within sporangia, endospores are in varying stages of division (arrow). (HE 600X). Upper right: Dark GMS-positive staining is present on the surfaces of sporangia and endospores (arrow). Inside endospores GMS staining is often minimal (GMS 600X). Lower left: Characteristic gram-positive staining endospores are admixed with gram-negative theca. (Gram 600X) Lower right: Both sporangia and endospores are diffusely PAS-positive. In contrast to the symmetric 'cartwheel' appearance of morula-like structures of P. wickerhamii, the asymmetric arrangement of endospores (arrow) is a feature of P. zopfii.[7] (PAS 600X) (Photo courtesy of: Colorado State University, Department of Microbiology Immunology and Pathology: http://csu-cvmbs.colostate.edu/academics/mip/Pages/default.aspx)*

Ubiquitous in moist environments, *Prototheca* spp. are found in slime flux of trees, a variety of freshwater environments, soil, animal waste lagoons, and in great abundance in sewage.[7,9] Despite their relative ubiquity, disease in mammals is rare. The two known pathogenic species are *Prototheca zopfii* and *P. wickerhamii*. Previously reported mammalian species infected include cattle, dogs, cats, and humans.[4] In cattle, *P. zopfii* is reported to cause severe mastitis, due to ascending infection from environmental contamination.[6] In humans, three clinical forms of protothecosis are recognized: systemic infection, bursitis, and cutaneous lesions most commonly.[8] In cats, only the cutaneous form is reported, and presumed to be due to trauma. In dogs, systemic dissemination is most commonly reported. Organs frequently infected include the intestinal tract, liver, kidney, heart, eyes, and central nervous system.[4]

The specific pathogenesis of disseminated canine protothecosis is not well studied, largely due to the limited number of cases. Infection is thought to occur by ingestion, and penetration of the colonic mucosa, at which point severe hemorrhagic colitis and diarrhea are often the first clinical findings.[4] Much less frequently, neurologic disease is the first reported finding.[7] Systemic infection occurs through hematogenous and lymphatic dissemination to multiple organs, where colonization, necrosis, and granulomatous inflammation are associated with myocardial collapse, acute renal failure, hepatic failure, blindness due to chorioretinitis and uveitis with retinal detachment, as well as varying presentations of neurologic disease.[2,4,7] Protothecosis is associated with therapeutic or pathologic immune system impairment in both dogs and humans.[7,8] With or without immunosuppression, there may be numerous organisms in tissue sections with relatively mild inflammation. Greater numbers of ruptured, empty theca are associated with much more severe pyogranulomatous reactions.[1]

Many aspects of this case are fairly characteristic for systemic canine protothecosis, including reported immunosuppression. However, the diagnosis made at necropsy was unexpected, due to the local arid climate, and rarity of protothecosis in such environments. Travel history was more thoroughly investigated after necropsy findings, and the dog was reportedly in the Southeastern US from late December to early January.

**JPC Morphologic Diagnosis:** 1. Kidney: Nephritis, granulomatous, multifocal, moderate, with mild glomerulonephritis and numerous endosporulating algae.
2. Liver, hepatocytes: Degeneration and necrosis, multifocal, random, mild, with mineralization.
3. Liver, hepatocytes: Glycogenosis, multifocal, mild.

**Conference Comment:** The contributor does an exceptional job comparing and contrasting *Prototheca* and *Chlorella* in histologic sections in addition to detailing the clinical presentation of these rarely reported infections. Conference participants were impressed with the tremendous quantity of organisms present within the kidneys and relatively few inflammatory cells leaving some to speculate on the severity of immunosuppression in this case. The most frequently identified causes of immunosuppression in protothecosis infections in people are steroid administration, neoplasia, diabetes mellitus and acquired immunodeficiency syndrome, however, similar associations have not been made in dogs.[10]

Protothecosis is typically observed as disseminated disease in dogs while it is also reported in cows, but as an important cause of mastitis. *P. zopfii* is most often associated with disseminated disease while *P. wickerhamii* usually associated with cutaneous infections.[3] The disseminated presentation in this case and the timeline of travel, development of urinary symptoms and subsequent neurologic signs would make for an interesting diagnostic exercise in detecting an immunosuppressive disorder and acquired *Prototheca* infection and correlating it with development of clinical signs.

*Prototheca* is one of the few pathogens which uniquely reproduce by endosporulation. The infective unit of these endosporulators is the endospore, which when implanted in tissues, grow into much larger sporangia. As a part of the maturation process of sporangia, endospores are produced and discharged effectively reinitiating the cycle. The other endosporulators of veterinary significance include: *Rhinosporidium seeberi, Chlorella* sp., *Coccidioides immitis,* and *Batrachochytrium dendrobatidis*.

In this case, the hepatocellular glycogenosis was attricuted to the immunosuppressive doses of corticosteroids noted in the clinical history. The cause for the random hepatocellular necrosis and mineralization was not evident.

**Contributing Institution**: Colorado State University
Department of Microbiology Immunology and Pathology
http://csu-cvmbs.colostate.edu/academics/mip/Pages/default.aspx

**References:**
1. Cheville NF, MacDonald J, Richard J. Ultrastructure of Prototheca zopfii in bovine granulomatous mastitis. *Vet Pathol*. 1984;21:341–348.
2. The Uvea: Canine ocular protothecosis. In: Dubielzig RR, ed. *Veterinary Ocular Pathology, A Comparative Review.* Philadelphia, PA: WB Saunders; 2010:278.
3. Ginn PE, Mansell JL, Rakich PM. Skin and appendages. In: Maxie MG, ed. *Jubb, Kennedy, and Palmer's Pathologic Basis of Veterinary Disease*. 5th ed. Vol. 1. Philadelphia, PA: Elsevier Saunders;2007:711-712.
4. Greene CE, Rakich PM, Latimer KS. Protothecosis. In: Greene CE, ed. *Infectious Diseases of the Dog and Cat*. 3rd ed. Philadelphia, PA: WB Saunders; 2006:659–665.
5. Haenichen T, Facher E, Wanner G, Hermanns W. Cutaneous chlorellosis in a gazelle (*Gazella dorcas*). *Vet Pathol*. 2002;39(3):386–389.
6. Jánosi S, Ratz F, Szigeti G, Kulcsar M, Kerényi J, Laukó T, et al. Review of the microbiological, pathological, and clinical aspects of bovine mastitis caused by the alga *Prototheca zopfii*. *Veterinary Quarterly*. 2001;23(2):58-61.
7. Lane LV, Meinkoth JH, Brunker J, Smith SK II, Snider TA, Thomas J, et al. Disseminated protothecosis diagnosed by evaluation of CSF in a dog. *Vet Clin Pathol*. 2012;41(1):147–152.
8. Lass-Flörl C, Mayr A. Human Protothecosis. *Clin Microbiol Rev*. 2007;20(2):230–242.
9. Pore RS, Barnett EA, Barnes WC, Walker JD. Prototheca ecology. *Mycopathologia*. 1983;81:49–62.
10. Pressler BM. Prothecosis and chlorellosis. In: Greene CE, ed. *Infectious Diseases of the Dog and Cat*. 4th ed. St. Louis, MO: Elsevier Saunders; 2012:696-701.
11. Retovsky R, Klasterska I. Study of the growth and development of *Chlorella* populations in the culture as a whole: Basophilia and oxido-

reduction relationships in *Chlorella* cells. *Folia Microbiologica*. 1961;6:127–135.
12. Taniyama H, Okamoto F, Kurosawa T, Furuoka H, Kaji Y, Okada H, et al. Disseminated protothecosis caused by *Prototheca zopfii* in a cow. *Vet Pathol*. 1994;31(1):123–125.

**CASE III**: 14-10 (JPC 4048510).

**Signalment:** 3-month-old female Yorkshire Cross pig, *Sus scrofa domesticus.*

**History:** This piglet was received at 1 month old and began receiving weekly carbon-14 injections via the ear vein with ketamine/xylazine sedation approximately one week after arrival. She was found down and extremely weak two months after arrival while other animals in same group had no clinical symptoms. The investigator elected euthanasia and a gross necropsy was performed.

**Gross Pathology:** On postmortem examination, connective tissues throughout the body are edematous and bright yellow. The liver has multifocal to coalescing pinpoint to 3 mm dark red foci, is enlarged, and flabby.

**Laboratory Results:** Clinical chemistry reveals severely icteric serum, high potassium, ALT, ALP, and amylase. The CBC shows a stress leukogram. Postmortem testing of hepatic selenium concentrations reveal levels as inadequate.

**Histopathologic Description:** Liver: Within all lobules examined, there is massive centrilobular to diffuse hepatocellular necrosis and hemorrhage. Hepatocytes in these areas are often completely lost and replaced by hemorrhage. In other area, hepatocytes are hypereosinophilic and individualized, with pyknotic or absent nuclei and are often surrounded by cellular debris, neutrophils, and fibrin. Portal areas contain mildly increased numbers of lymphocytes, reactive fibroblasts, and neutrophils, with rare pyknotic cells.

Skeletal muscle: Diffusely throughout the tissue, there is random individual myocyte degeneration characterized by sarcoplasmic hypereosinophilia and swelling, loss of cross-striations, fragmentation, pyknosis, karyorrhexis and karyolysis.

**Contributor's Morphologic Diagnosis:** 1. Liver: Necrosis, acute, centrilobular to massive, hemorrhagic, Yorkshire cross, pig. 2. Skeletal muscle: Degeneration and necrosis, acute, multifocal, mild to moderate, Yorkshire cross, pig.

**Contributor's Comment:** Additional histopathologic findings included moderate multifocal fat necrosis of the mesentery, and minimal multifocal myocardial necrosis. Vitamin E/selenium deficiency was highly suspected due to the gross and histopathologic findings. Postmortem hepatic selenium concentrations were inadequate. Blood samples from the remaining three pigs in the cohort were also tested. A blood sample from one pig was marginal and the other two pigs were adequate. Vitamin E and selenium was supplemented and no clinical symptoms ensued in any of the remaining animals. The pigs had been fed a commercial pig diet and it is still unclear how this deficiency occurred. Unfortunately, there was no remaining feed from the suspect lot available for testing. There were no other reports of problems with other lots of this

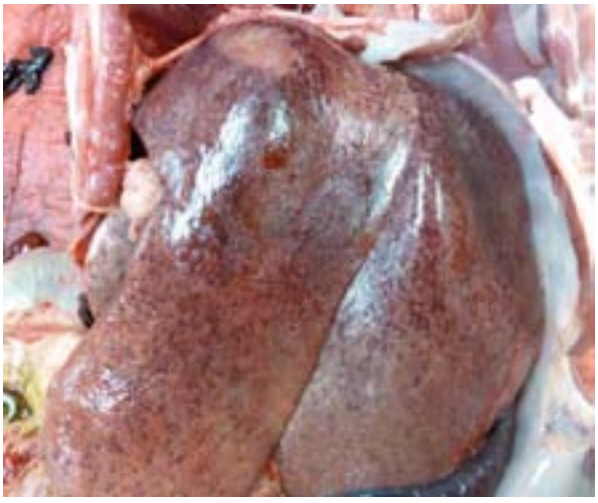

*3-1. Liver, piglet: The liver has multifocal to coalescing pinpoint to 3 mm dark red foci, is enlarged, and flabby. (Photo courtesy of: Division of Laboratory Animal Resources, University of Pittsburgh, http://www.dlar.pitt.edu/, http://pitt.edu/)*

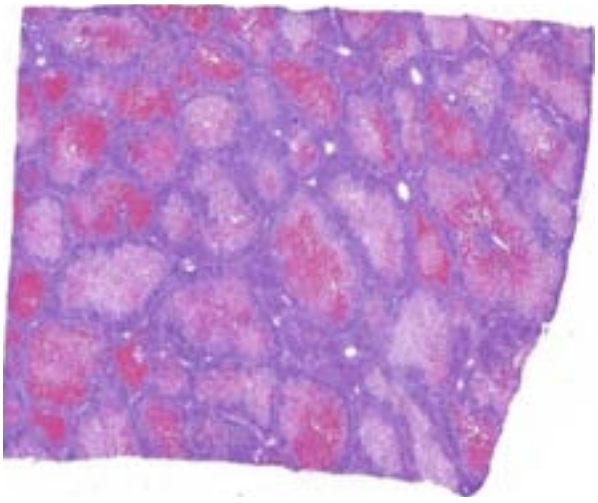

*3-2. Liver, piglet: At subgross magnification, centrilobular and midzonal portions of each lobule exhibits necrosis and hemorrhage. (HE 0.63X)*

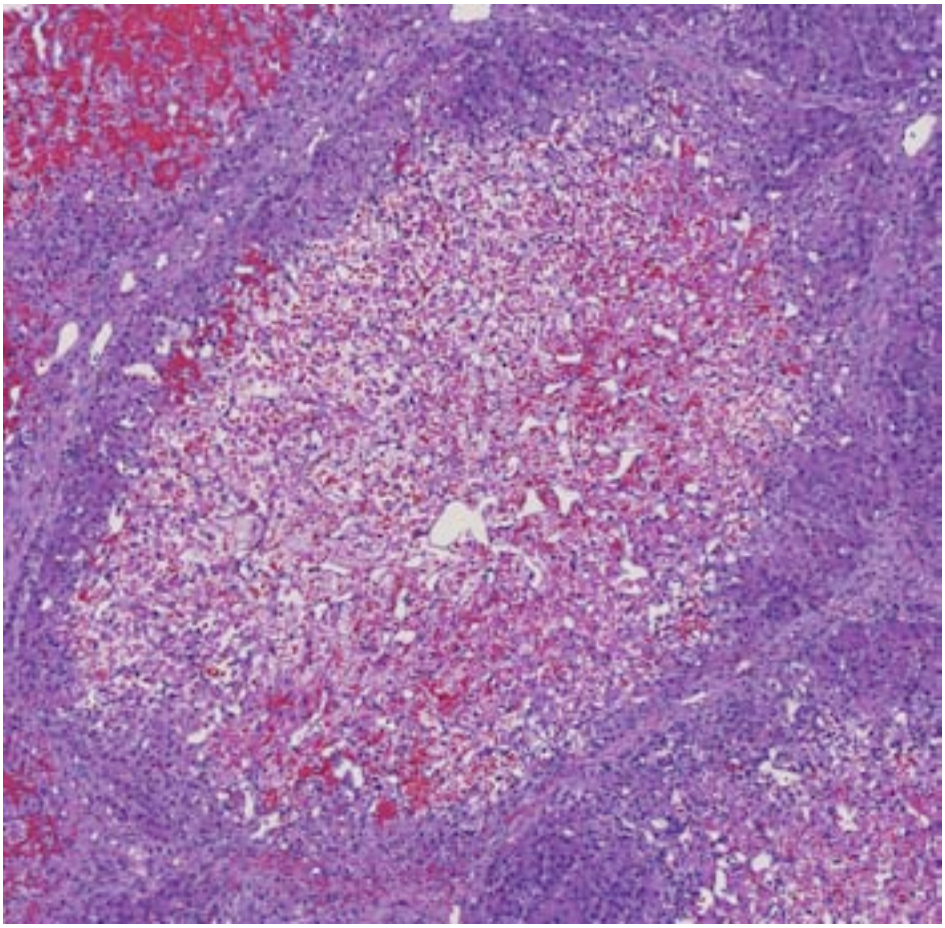

*3-3. Liver, piglet: There is diffuse centrilobular and midzonal coagulative necrosis with maintenance of sinusoidal architecture and multifocal hemorrhage. Periportal hepatocytes are spared. (HE 144X)*

feed to the vendor. One possibility is that this adult diet had inadequate concentrations of vitamin E and/or selenium for such a young piglet.

In the pig, the most obvious effect of Vitamin E/ Selenium deficiency is sudden death, typically in young, fast growing weaners. Two principle presentations seen at post mortem examination are mulberry heart disease (MHD) and hepatosis dietetia (HD). Selenium is an integral part of the membrane enzyme glutathione peroxidase, reducing toxic lipid peroxidases to hydroxyl acids.[5] Vitamin E is an antioxidant and acts synergistically with selenium to protect membranes from high concentrations of lipoperoxidases.[5]

HD is characterized by hemorrhagic centrilobular to massive hepatic necrosis. Animals that survive the acute disease can develop lesions of parenchymal collapse and post necrotic scarring.[1,6] The most severe injuries are often present dorsally in the diaphragmatic liver lobes.[6] The pathogenesis of HD is not completely understood, but it is thought to be caused by a deficiency in vitamin E and/or selenium.[1] Affected animals respond to vitamin E or selenium supplementation, although, interestingly, it is difficult to experimentally induce this condition by feeding diets deficient in vitamin E and selenium.[1] It is thought that oxidative injury leads to hepatocyte necrosis since vitamin E and selenium-containing enzymes are antagonists of free radical formation and are therefore important in maintaining the stability and integrity of cellular membranes.[1,6] Experimental observations have revealed the need for concurrent deficiencies of sulfur-containing amino acids, tocopherols, and trace amounts of selenium for hepatic necrosis to develop.[6] Yellow staining of the adipose tissue is a common gross finding[6] as was seen in this case. The gallbladder may be edematous.[5] In relapsing cases, animals may be jaundice and hemorrhagic diathesis may occur with the primary manifestation of hemorrhage into or surrounding the joints.[6]

MHD (dietary microangiopathy of pigs) is characterized by fibrinoid necrosis and thrombosis of small vessels resulting in microhemorrhages.[8] The resulting hemorrhages lead to a “mulberry-like” discoloration of the epicardial surface, particularly of the right atrium.[5,8] Hydropericardium is also a common finding. There is often widespread fibrinoid necrosis of small arteries and arterioles with endothelial damage and fibrin thrombi, particularly in the

capillaries of the myocardium.[5,8] Typically, the following microscopic lesions are observed in a heart affected by MHD: interstitial hemorrhage associated with swollen cardiac myofibers that have lost cross striations, are hypereosinophilic, and have pyknotic nuclei.[4] In this entity, selenium concentrations within the liver and heart are often within normal limits.[5] Supplementation of selenium appears to decrease the incidence of HD, but not MHD. Therefore, vitamin E is considered to play a central role in the development of MHD.[5] An additional lesion that can be found in animals surviving greater than 24 hours is bilaterally symmetric softening of the cerebral white matter.[5]

Aside from the disease entities in pigs, vitamin E/selenium deficiency results in a broad spectrum of diseases in a variety of animal species and humans, including but not limited to: myopathy, steatitis, liver necrosis, and encephalomalacia because of increased oxidative stress on cells.[2]

**JPC Morphologic Diagnosis:** 1. Liver, hepatocytes: Necrosis, centrilobular and midzonal, diffuse, severe, with hemorrhage and periportal hepatocellular lipidosis.
2. Skeletal muscle: Degeneration and necrosis, multifocal, marked.

**Conference Comment:** Massive hepatic necrosis implies necrosis of the entire hepatic acinus – centrilobular, midzonal, and periportal hepatocytes. Selenium and/or vitamin E deficiency is classically associated with massive hepatic necrosis, a disease in pigs known as "hepatosis dietetica". Conference participants discussed the finding of intact, often regenerating periportal hepatocytes in this case and how it relates to the pathogenesis of massive necrosis. It was hypothesized this lesion may represent an early state of disease prior to full expression of massive necrosis. In addition to vitamin E and selenium deficiencies, other differentials for hepatic necrosis worthy of consideration include blue-green algae, *Amanita* (mushrooms), *Cestrum diurnum, Xanthium* sp. (cocklebur), iron dextran, aflatoxin, fumonisin B1, sporidesmin and pyrrolizidine alkaloids.[5] In horses, serum sickness is characterized by a near diffuse hepatic necrosis with only a narrow rim of usually vacuolated hepatocytes surrounding periportal regions.[1]

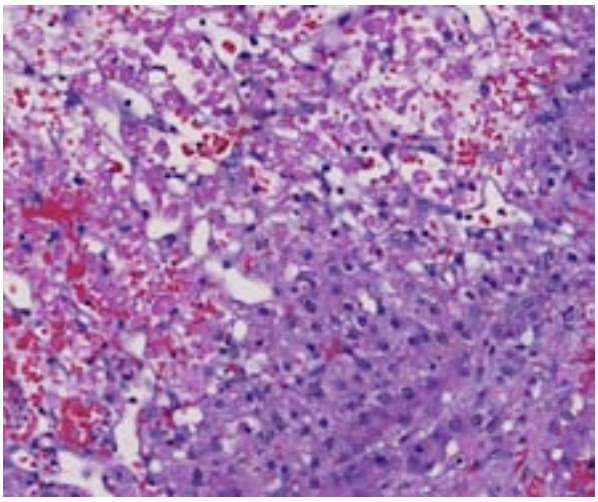

*3-4. Liver, piglet: The junction of midzonal and periportal hepatocytes contain demonstrates coagulative necrosis of midzonal hepatocytes (upper left) and mild lipid accumulation (degeneration) of periportal hepatocytes (lower right). (HE 320X)*

When hepatic necrosis is observed in conjunction with rhabdomyocyte necrosis, vitamin E and/or selenium deficiency should be considered most likely. Selenium deficiency does not only occur in managed feed situations, but also in pasture-raised livestock. Selenium is normally present in soil and taken up by growing plants, however, in areas such as the Pacific Northwest, the soil is naturally deficient. Poor quality forages are also deficient in vitamin E, thus both must be supplemented in some situations.[7] Deficiencies of either result in the body's reduced capacity to scavenge free radicals.

Free radicals are molecules with unpaired electrons rendering them highly reactive as they look to unload or oxidize that electron. They are generated as a normal product of mitochondrial respiration, absorption of radiant energy, enzymatic metabolism of drugs or chemicals, transition metals (Fenton reaction), nitric oxide production and by activated leukocytes during inflammation. Free radicals are very effective at killing cells, both those of pathogens and the normal host. Three reactions most relevant to free radical-induced cellular injury are lipid peroxidation of membranes, oxidation of proteins and DNA damage.[3] Antioxidants serve to protect the host by counteracting this oxidation. The importance of antioxidants in maintaining equilibrium is exemplified by the multitude of lesions associated with vitamin E and selenium deficiencies and nicely illustrated in this case.

**Contributing Institution**: Division of Laboratory Animal Resources
University of Pittsburgh
http://www.dlar.pitt.edu/
http://pitt.edu/

**References:**

1. Cullen JM, Brown DL. Hepatobiliary system and exocrine pancreas. In: McGavin DM, Zachary JF, eds. *Pathologic Basis of Veterinary Disease*. 5th ed. Philadelphia, PA: Elsevier Mosby; 2012:446-448.
2. Kane AB, Kumar V. Environmental and nutritional pathology. In: Kumar V, Abbas AK, Fausto N, Aster JC, eds. *Robbins and Cotran Pathologic Basis of Disease.* 7th ed. Philadelphia, PA: Elsevier Saunders; 2005:455-456, 461.
3. Kumar V, Abbas AK, Fausto N, Aster JC. Cellular responses to stress and toxic insults: adaptation, injury and death. In: Kumar V, Abbas AK, Fausto N, Aster JC, eds. *Robbins and Cotran Pathologic Basis of Disease.* 8th ed. Philadelphia, PA: Elsevier Saunders; 2010:20-23.
4. Pallarés FJ, Yaeger MJ, Janke BH, Fernández G, Halbur PG. Vitamin E and selenium concentrations in livers of pigs diagnosed with mulberry heart disease. *J Vet Diagn Invest*. 2002;14:412–414.
5. Robinson WF, Maxie MG. The cardiovascular system. In: Maxie MG, ed. *Jubb, Kennedy, and Palmer's Pathology of Domestic Animals*. 5th ed. Vol 3. Philadelphia, PA: Elsevier Saunders; 2007:37-40.
6. Stalker MJ, Hayes MA. The liver and biliary system. In: Maxie MG, ed. *Jubb, Kennedy, and Palmer's Pathology of Domestic Animals*. 5th ed. Vol 2. Philadelphia, PA: Elsevier Saunders; 2007:322-323, 368-373.
7. Valentine BA, McGavin MD. Skeletal muscle. In: McGavin MD, Zachary JF, eds. *Pathologic Basis of Veterinary Disease.* 5th ed. St. Louis, MO: Elsevier Mosby; 2012:900.
8. Van Vleet JF, Ferrans VJ. Cardiovascular system. In: McGavin MD, Zachary JF, eds. *Pathologic Basis of Veterinary Disease.* 5th ed. St. Louis, MO: Elsevier Mosby; 2012:581.

**CASE IV:** O 339/11 (JPC 4019381).

**Signalment:** 1-day-old male cross breed piglet, *Sus scrofa.*

**History:** The piglet was born weak with skin lesions. It died after a day. The rest of the litter was healthy and without skin lesions.

**Gross Pathology:** The skin on the back was dry with cracks creating a tiger-like pattern. Severe hyperkeratosis, hyperemia and cracks were seen on abdomen, legs, ears and nose. The hooves were unaffected. Very sparse amount of coagulated milk was found in the stomach. Internal organs were without pathological findings.

**Laboratory Results:** None performed.

**Histopathologic Description:** Haired skin: The epidermis shows severe hyperplasia with compact lamellar orthokeratosis and parakeratosis with multifocal infiltration of bacteria (mixed population) and foreign material. Most of the slides show suprabasilar cleft formations. There is moderate to severe vacuolation of keratinocytes in stratum spinosum and stratum granulosum. Multifocally, there is loss of stratum granulosum. Hair follicles are unaffected and no inflammation in dermis is found.

**Contributor's Morphologic Diagnosis:** Haired skin, epidermal hyperplasia with marked ortho- and parakeratosis, vacuolation of keratinocytes in stratum spinosum and stratum granulosum and suprabasilar clefting, consistent with ichthyosis.

**Contributor's Comment:** A few cases of ichthyosis have been reported in cattle, dogs, pigs, chickens, laboratory mice and llama.[4] Most of the cases are from cattle.[1-3,7,9] In humans several different kinds of ichthyosis and syndromes including ichthyosis are reported.[8] In the veterinary literature five different types of human ichthyosis are described: ichthyosis vulgaris, x-linked ichthyosis, epidermolytic hyperkeratosis, lamellar ichthyosis and harlequin ichthyosis.[4] The main findings in the different human types are as follows:

- Ichthyosis vulgaris: Orthokeratotic hyperkeratosis and a decreased or absent granular layer.
- X-linked ichthyosis: Orthokeratotic hyperkeratosis with normal or hyperplastic granular layer.
- Epidermolytic hyperkeratosis: Orthokeratotic and parakeratotic hyperkeratosis, vacuolation of keratinocytes in the upper stratum spinosum and stratum granulosum and a markedly thickened granular layer.

*4-1. Haired skin, 1-day-old piglet: Diffusely, the skin was dry with cracks creating a tiger-like pattern. (Photo courtesy of: Department of BVF, Division of Pathology, Pharmacology & Toxicology, SLU (Swedish University of Agricultural Sciences), Box 7028, SE-750 07 Uppsala, Sweden. http://www.bvf.slu.se)*

*4-2. Haired skin, 1-day-old piglet: Closeup of the skin seen in 4-1. Severe hyperkeratosis is present on closer examination, with fissuring, clefting, and peeling back of the cornified scale. (Photo courtesy of: Department of BVF, Division of Pathology, Pharmacology & Toxicology, SLU (Swedish University of Agricultural Sciences), Box 7028, SE-750 07 Uppsala, Sweden. http://www.bvf.slu.se)*

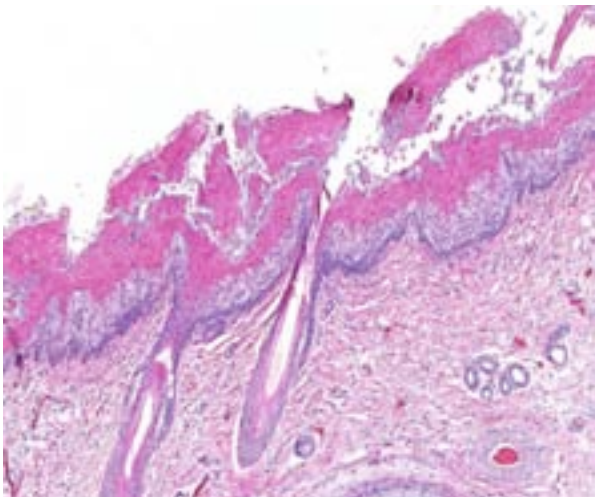

*4-3. Haired skin, 1-day-old piglet: The epidermis is covered by a parakeratotic cornified scale up to 400 µm thick, which does not extend into hair follicles. (HE 63X)*

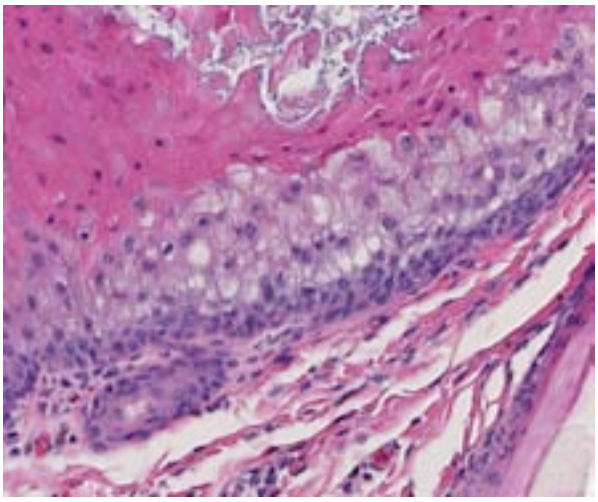

*4-4. Haired skin, 1-day-old piglet: The granular layer of the epidermis is absent. There is moderate intracellular swelling of the cells of the stratum spinosum and mild hyperplasia and disorganization of the basal layer. (HE 253X)*

- Lamellar ichthyosis: Compact orthokeratotic hyperkeratosis and mild acanthosis.
- Harlequin ichthyosis: Thick compact stratum corneum with follicular hyperkeratosis and variable appearance of the stratum granulosum.

In cattle, two forms of ichthyosis are described: ichthyosis fetalis and ichthyosis congenita.[4] In ichthyosis fetalis morphological findings are similar to harlequin ichthyosis. Ichthyosis congenita has a prominent laminated orthokeratotic hyperkeratosis of the epidermis and superficial portion of hair follicles. In dogs, nonepidermolytic and epidermolytic classifications are used.[5] It has been concluded that well characterized cases of ichthyosis in animals do not correlate well with the human classification system.[4]

In this case, the lesions are somewhat similar to epidermolytic hyperkeratosis with orthokeratotic and parakeratotic hyperkeratosis and vacuolation of keratinocytes in the upper stratum spinosum and stratum granulosum, but lack the markedly thickened granular layer that is present in epidermolytic hyperkeratosis. Also lesions consistent with ichthyosis vulgaris (orthokeratotic hyperkeratosis and decreased or absent granular layer) are present. Furthermore, similarities with ichthyosis congenita are seen; however, there is no involvement of the hair follicles in the present case.

Due to the different morphologic findings in the present case and the current human classification systems our conclusion is that the disease is best regarded as ichthyosis with no further classification.

**JPC Morphologic Diagnosis:** Skin: Hyperkeratosis, lamellar, parakeratotic, diffuse, marked, with acanthosis and spongiosis.

**Conference Comment:** As is customary at the JPC, conference participants are deprived of clinical history and signalment with WSC cases to maintain relevance for board preparation. Thus, without knowing the age of this pig, participants discussed their differentials for parakeratotic hyperkeratosis in this case and in other species.

The contributor outlines ichthyosis and its variable presentation among domestic animals as the cause of hyperkeratosis in this case. Another condition associated with hyperkeratosis in swine is zinc-responsive dermatosis, which occurs in 2-4 month-old piglets and is a secondary zinc deficiency due to the presence of phytic acid in plant protein rations that affects its availability. Zinc-responsive dermatoses are more commonly identified in dogs as one of three distinct varieties: reduced absorption in Arctic breeds, generic dog food, and lethal acrodermatitis of Bull Terriers. Thallium toxicity is another historical cause in many species and vitamin A-

responsive dermatoses have been described in Cocker Spaniels as causing hyperkeratosis. Superficial necrolytic dermatitis in dogs and people characteristically exhibits parakeratosis along with laminar epidermal edema and basilar hyperplasia. This is also called hepatocutaneous syndrome due to its correlation with liver dysfunction and subsequent deranged glucose and amino acid metabolism inducing hypoaminoacidemia. Canine morbillivirus and pemphigus foliaceous both induce hyperkeratosis of the footpads in dogs.[4]

Congenital ichthyosis occurs in domestic animals as a heterogenous syndrome of autosomal recessive inheritance. Collectively, they are called autosomal recessive congenital ichthyoses (ARCIs) and their pathophysiology involves abnormal synthesis and/or secretion of lipid within the stratum corneum. Recently, specific genetic mutations have been linked to certain cornification disorders affecting particular breeds of dogs. ARCI in Golden Retrievers is associated with PNPLA1 mutations, in Jack Russell terriers an insertion in TGM1 has been described, and most recently an upstream insertion of NIPAL4 (ICHTHYIN) was identified in American bulldogs.[6]

**Contributing Institution**: Department of BVF
Division of Pathology
Pharmacology & Toxicology
SLU (Swedish University of Agricultural Sciences)
Box 7028, SE-750 07
Uppsala, Sweden
http://www.bvf.slu.se

**References:**

1. Baker JR, Ward WR. Ichthyosis in domestic animals: a review of the literature and a case report. *Br Vet J.* 1985;141:1-8.
2. Chittick EJ, Olivry T, Dalldorf F, et al. Harlequin Ichthyosis in two Greater Kudu (Tragelaphus strepsiceros). *Vet Pathol*. 2002;39:751-756.
3. Cho JK, Son JM, Lee DS, et al. Harlequin Ichthyosis in a Han Woo Calf. *J Vet Med Sci* 2007;69(5):553-555.
4. Ginn PE, Mansell JL, Rakich PM. Skin and appendages. In: Maxie MG, ed. *Jubb, Kennedy and Palmer's Pathology of Domestic Animals.* 5th ed. Vol 1. Phildadelphia, PA: Elsevier Saunders; 2007:576-578, 628-648.
5. Gross TL, Ihrke PJ, Walder EJ, Affolter VK. Diseases with abnormal cornification. In: *Skin Diseases of the Dog and Cat: Clinical and Histopathologic Diagnosis*. 2nd ed. Oxford: Blackwell Publishing; 2005;174-179.
6. Mauldin EA, Wang P, Evans E, et al. Autosomal recessive congenital ichthyosis in American bulldogs is associated with NIPAL4 (ICHTHYIN) deficiency. *Vet Pathol.* 2014 Oct 16. pii: 0300985814551425. [Epub ahead of print]
7. Molteni L, Dardano S, Parma P, et al. Ichthyosis in Chianina cattle. *Vet Rec*. 2006;158:412-414.
8. Oji V, Traupe H. Ichthyosis: differential diagnosis and molecular genetics. *Eur J Dermatol* 2006;16(4):349-59.
9. Testoni S, Zappulli V, Gentile A. Ichthyosis in two Cianina calves. *Dtsch Tierarztl Wochenschr*. 2006;113(9):351-4.

**Joint Pathology Center**
**Veterinary Pathology Services**

# WEDNESDAY SLIDE CONFERENCE 2014-2015

## Conference 8

**25 March 2015**

**Guest Moderator:**
Julie B. Engiles, VMD, DACVP
Department of Pathobiology
University of Pennsylvania, Murphy Laboratory

---

**CASE I:** 65647 (JPC 4048575).

**Signalment:** 9-year-old spayed female DSH feline, *Felis catus*.

**History:** Three-month history of progressively worsening left hind limb lameness. On external examination, a large, firm mass was noted on the left proximal tibia. Radiographs of the limb revealed a focally extensive area of osteolysis with periosteal elevation along the proximal tibia. The left rear leg was amputated mid-femur and the entire limb was submitted for histopathological analysis.

**Gross Pathology:** Submitted for histopathology was the entire left hind limb that had been amputated at the level of the middle femur. Dissection revealed a pronounced thickening of the proximal tibia with irregular and lytic areas of periosteum and cortical bone.

**Laboratory Results:** N/A

**Histopathologic Description:** Examined is a section of bone and surrounding soft tissue (tendon, muscle) where the bone is markedly expanded and focally replaced by a poorly demarcated, non-encapsulated, densely cellular mass. Neoplastic cells fill greater than 50% of the marrow spaces, surrounding and replacing trabeculae, multifocally replacing the cortex and extending into the periosteum. Neoplastic cells are arranged in sheets and streams, supported by a fine fibrovascular stroma. Cells are pleomorphic; most cells are polygonal to stellate with poorly defined cell borders, moderate eosinophilic fibrillar cytoplasm, eccentric ovoid nuclei, finely stippled chromatin, and a single amphophilic prominent nucleolus. There is moderate anisocytosis and anisokaryosis. There are numerous scattered binucleate and multinucleate giant cells, sometimes containing >20 nuclei, often adjacent to osteoid matrix. Mitotic figures are rare with 1 or fewer per 10 hpf. Neoplastic cells appear to produce a dense fibrillar to homogenous eosinophilic matrix (osteoid). There are extensive multifocal to coalescing regions of cartilaginous differentiation. Scattered throughout and adjacent to the neoplasm there is bone lysis, necrotic bone, and mild multifocal to coalescing areas of hemorrhage. The cortical bone is discontinuous, interrupted by clusters of neoplastic cells surrounded by abundant fibrous connective tissue (scirrhous reaction). Multifocally, there is periosteal proliferation of reactive bone (exostosis) and few perivascular infiltrates of lymphocytes, plasma cells, and fewer

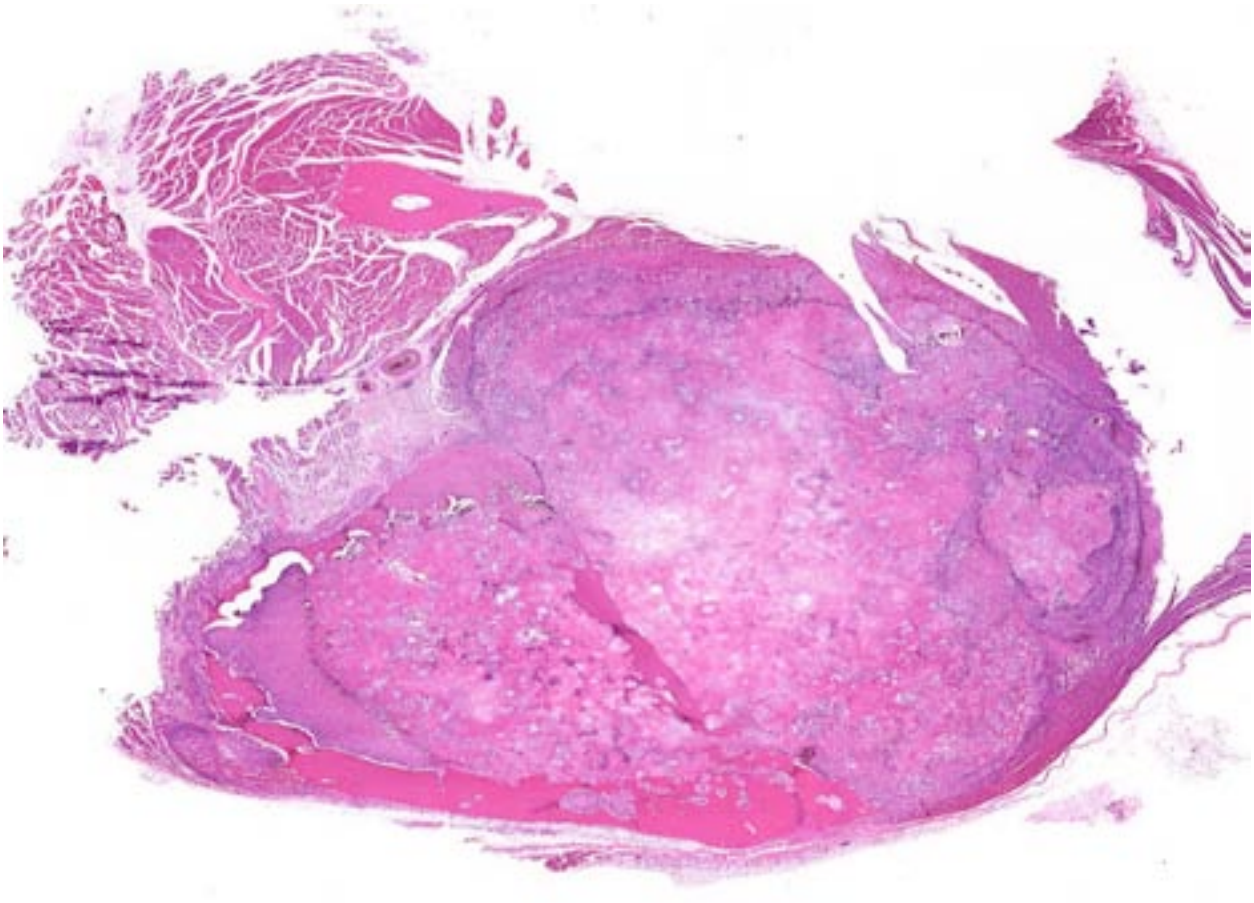

*1-1. Tibia, cat: The tibial diaphysis is markedly expanded and replaced by an infiltrative neoplasm producing extensive osteoid. The tibial cortex is largely replaced, except at the lower left. The fibula is present at upper left. (HE 6.3X)*

macrophages that extend into the adjacent soft tissue.

**Contributor's Morphologic Diagnosis:** Bone, proximal tibia: Osteosarcoma.

**Contributor's Comment:** Primary bone tumors are an uncommon finding in the feline patient with reported incidence of 3.1 to 3.9 per 100,000 cases.[5] Of the primary bone tumors, osteosarcomas (OS) account for 70 to 80 percent of findings.[3] Differing from canine OS, which exhibits a biphasic impact distribution, feline OS tends to impact middle age to older cats (average age 8-10 years).[3] Tumor locations can be divided into axial, appendicular, and extraskeletal. Extraskeletal sites have been noted to occur sporadically in multiple tissues and anatomical locations with a propensity for occurring in locations commonly associated with vaccine administration. The most common skeletal locations for feline OS include distal femur and proximal humerus and tibia and overall hind limbs are more commonly impacted. Further differing from canine OS, feline OS exhibits a low rate of (5-10%) of pulmonary metastasis.[5] Radiographic features of osteosarcoma in cats are variable with the aggressive periosteal proliferation often noted in canine OS being less prevalent.[4]

Cats with appendicular or extra skeletal forms of OS tend to survive longer when compared to those with axial forms. In a study published by Dimopoulou, survival prognosis for cats with osteosarcoma was related to histologic grade and mitotic index.

Spugnini, reported similar findings with median survival of 49 months for cats following amputation alone with appendicular OS, compared with a median survival time of only 5.5 months for cats with axial skeletal OS. If the tumor permits removal, surgery alone may be curative with extended survival time for those undergoing advanced adjunctive therapies. The

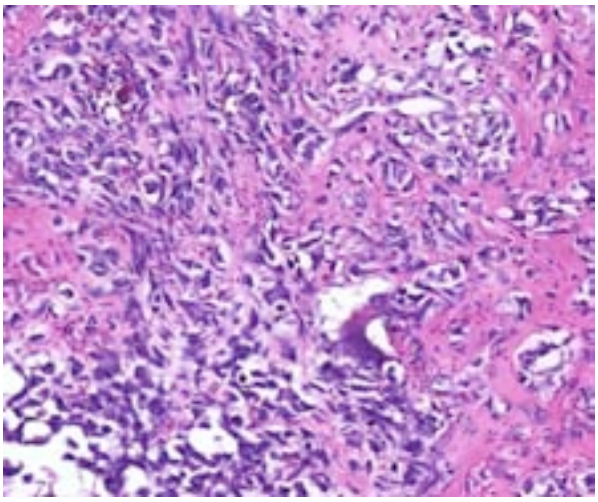

*1-2. Tibia, cat: Neoplastic cells are spindled to stellate, and produce (and eventually incorporated within) abundant osteoid. Rare giant cells (center) are scattered throughout the neoplasm. (HE 220X)*

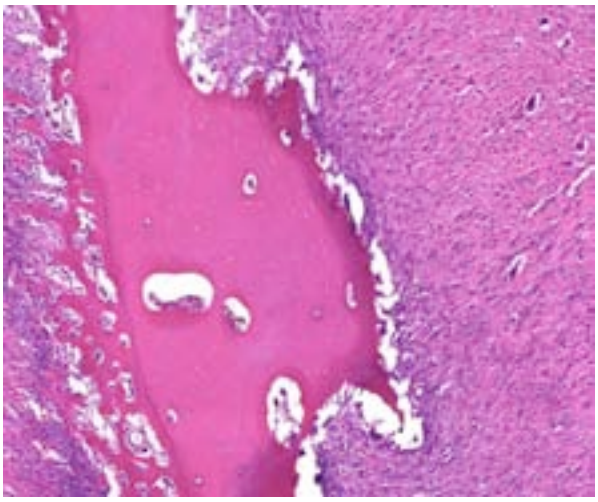

*1-3. Tibia, cat: The advancing front of the neoplasm results in resorption of overlying lamellar bone. There is periosteal new bone growth at the outer edge (at left), trying in vain to reinforce the rapidly disappearing cortex. (HE 61X)*

histologic grade in this case was relatively low (rare mitotic figures, low to moderate tumor cell density, abundant tumor matrix, minimal to mild necrosis, moderate pleomorphism) and is suggestive of a fair to guarded prognosis. Although amputation is often curative, neoplastic cells were noted rarely in blood vessels within the section in this case. Interestingly, tumor invasion into vessels was not found to be a significant prognosticator in one retrospective study of feline osteosarcoma.[3] No long-term follow up is available for this patient.

This tumor was made up of predominantly osteoblast-like neoplastic cells with numerous clusters of multinucleate giant cells scattered amongst a prominent matrix of osteoid, mature bone, and cartilage. Scattered multinucleate giant cells are not uncommon in feline osteosarcoma, though a giant cell variant osteosarcoma such as this one, with numerous giant cells, is unusual. The origin of multinucleated giant cells in OS is poorly understood and both osteoclast and osteoblast origins have been postulated. In a report by Negrin[8], both osteoclast and osteoblast immune staining features were noted in a feline OS of the calvarium. Osteoclast like features included TRAP, vimentin, and S-100 positive staining with cytokeratin-negative staining. An osteoblast like feature includes MHC II–negative reaction.[8] No prognostic significance has been related to the giant cell variant osteosarcoma seen in cats.

**JPC Diagnosis:** Bone, tibia: Osteosarcoma.

**Conference Comment:** Osteosarcomas (OSA) are commonly described as malignant long bone tumors of large breed dogs, with the distal radius, distal tibia, and proximal humerus being the most common sites of occurrence[1] and are much more common than their feline counterpart. The differences between OSA of dogs and cats have been highlighted by the contributor. Conference participants discussed the particulars of obtaining a definitive diagnosis of OSA. In many cases, diagnosis is often complicated by a small sample submission and the fact that these neoplasms are often heterogenous and admixed with reactive bone which may result from a proliferative response due to nonneoplastic mechanisms. Bone reacts to local and systemic stimuli through systematic and regimented processes, regardless of etiologic stimulus (e.g. fracture, benign or malignant neoplasm or infectious disease). This case nicely illustrates this point, as in some areas, woven bone is overtly neoplastic and characterized by large, atypical, irregularly clustered osteoblasts haphazardly oriented to disorganized bone trabeculae, or embedded within lacy deposits of osteoid. The disorganized areas of bone are intermixed with "reactive" or reparative woven bone characterized by plump osteoblasts coalescing around, and oriented perpendicular to the longitudinal axis of woven bone trabeculae, thus demonstrating a structural uniformity distinguishable from neoplastic bone islands. However, in small samples without clinical or

radiographic context, distinguishing osteosarcoma from reactive bone can prove problematic. As stated in the WHO tumor fascicles "practice and experience cannot be supplanted," in the case of interpreting proliferative bony and reactive periosteal lesions.[9]

The variety of histologic presentations of OSA has led to the description of nine separate subclassifications in a recent paper.[7] Subclassifying these tumors is also hindered by their heterogeneic nature as often several histologic subtypes are evident within a single neoplasm; however, their subclassification, with the exception of the aggressive telangiectatic variant, does not appear prognostically significant.[7] Histologic grade, on the other hand, is often cited as offering considerable prognostic value, though only mitotic index was identified specifically in cats.[3] Evidence has accumulated in the literature supporting the hypothesis that cyclooxgenase-2 (COX-2) is involved in the pathogenesis of osteosarcoma, and recently prostaglandin $E_2$ was pinpointed as the downstream culprit of interest, lending credence to the use of COX-2 inhibitors in chemotherapy regimens and suggesting selective inhibition of $PGE_2$ may be equally effective.[6]

**Contributing Institution:** http://www.hopkinsmedicine.org/mcp/index.html

**References:**

1. Carlson CS, Weisbrode SE. Bones, joints, tendons and ligaments. Zachary JF, McGavin MD, eds. *Pathologic Basis of Veterinary Disease*. 5th ed. St. Louis, MO: Elsevier Mosby; 2012:959.
2. Culp WT, Olea-Popelka F, Sefton J, et al. Evaluation of outcome and prognostic factors for dogs living greater than one year after diagnosis of osteosarcoma: 90 cases (1997-2008). *J Am Vet Med Assoc.* 2014;245(10):1141-1146.
3. Dimopoulou M, Kirpensteijn J, Moens H, Kik M. Histologic prognosticators in feline osteosarcoma: a comparison with phenotypically similar canine osteosarcoma. *Vet Surg*. 2008;37(5):466-71.
4. Frankel CS, Young TL, Alvarez-Berger F, Spencer CP. What Is Your Diagnosis? *Journal of the American Veterinary Medical Association*. 2013;243(3):329-331
5. Heldmann E, Anderson MA, Wagner-Mann C. Feline Osteosarcoma: 145 Cases (1990–1995). *J Am Anim Hosp Assoc*. 2000;36:518–21.
6. Millanta F, Asproni P, Cancedda S, Vignoli M, Bacci B, Poli A. Immunohistochemical expression of COX-2, mPGES and EP2 receptor in normal and reactive canine bone and in canine osteosarcoma. *J Comp Pathol*. 2012;147(2-3): 153-160.
7. Nagamine E, Hirayama K, Matsuda K, et al. Diversity of histologic patterns and expression of cytoskeletal proteins in canine skeletal osteosarcoma. *Vet Pathol.* 2015 Mar 13. pii: 0300985815574006. [Epub ahead of print]
8. Negrin A, Bernardini M, Diana A, Castagnaro M. Giant cell osteosarcoma in the calvarium of a cat. *Vet Pathol*. 2006;43:179.
9. Slayter MV, Boosinger TR, Inskeep W, Pool RR, Dammrich K, Larsen S. *Histologic Classification of Bone and Joint Tumors of Domestic Animals*. 2nd series. Vol. I. Washington, D.C.: Armed Forces Institute of Pathology/ American Registry of Pathology; 1994:9-11.

**CASE II**: RE-13-121 (JPC 4048075).

**Signalment:** 4-month-old male Newfoundland dog, *Canis lupus familiaris.*

**History:** This dog had a history of being slow to get up and having trouble with the rear legs. The onset and duration of these clinical signs was not reported and could not be obtained. The referring veterinarian (rDVM) reported that the dog had swollen and thickened elbows and that the right elbow was worse than the left. The right elbow was possibly luxated. The dog also had severe pain in the hips and at the base of the tail. Additional clinical findings were not reported. Radiographs were reported to show white stippling due to decreased endochondral bone formation in all epiphyses of the limbs. The vertebrae were also affected. The owner elected euthanasia and declined a full necropsy. The rDVM removed the right front leg at the level of the scapula and the right rear leg at the level of the proximal femur and submitted them for examination. No other information could be obtained regarding status of littermates, diet, age of onset, etc.

**Gross Pathology:** The right front limb, including the scapula, and the entire right rear limb were submitted fresh. The soft tissues were removed so that the bones could be examined and sectioned. The articular surfaces of all bones were smooth with a characteristic mottled white appearance. The apophyses were the most affected. The trochlea of the humerus appeared thickened and flared. On cut section, the epiphyses contained increased amounts of cartilaginous tissue which was most evident and extensive in the humeral condyles and the apophyses of other bones; these regions also had much smaller ossification centers than less affected bones. Occasionally, the metaphyseal physes were irregular and there were tongues of cartilage that extended from the physis into the metaphysis. Small islands of cartilage were also present in the metaphysis.

**Laboratory Results:** None.

**Histopathologic Description:** Multiple longitudinal sections of bone, including the proximal and distal femur, the proximal and distal tibia, the proximal and distal humerus, and the proximal radius were decalcified and examined microscopically. The slide submitted contains a section of the distal femur. The articular-epiphyseal (AE) complex and areas of persistent epiphyseal cartilage are highly irregular with various staining patterns. There are multifocal to coalescing areas of eosinophilic cartilage alternating with increased amounts of basophilic hyaline cartilage creating a mosaic type appearance. The eosinophilic regions of cartilage are indicative of loss of proteoglycans suggesting degeneration. There are two adjacent irregular spaces within the hyaline cartilage that contain fragments of basophilic debris. The cartilage is irregularly organized and there are separate multifocal islands of cartilage within the epiphysis that are undergoing ossification. Some of these islands extend to, and merge with, the

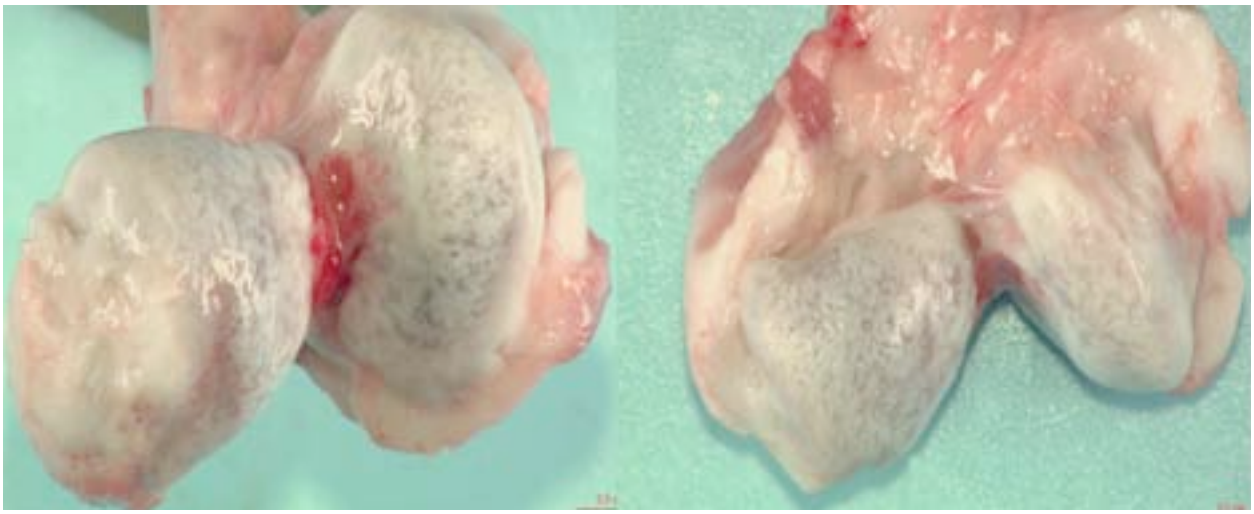

*2-1. Humerus, cranial and caudal views of the condyle, dog: The trochlea are thickened and widely flared. The articular surface has the same mottled white appearance as shown for the femur. (Photo courtesy of: Michigan State University, Diagnostic Center for Population and Animal Health, www.animalhealth.msu.edu)*

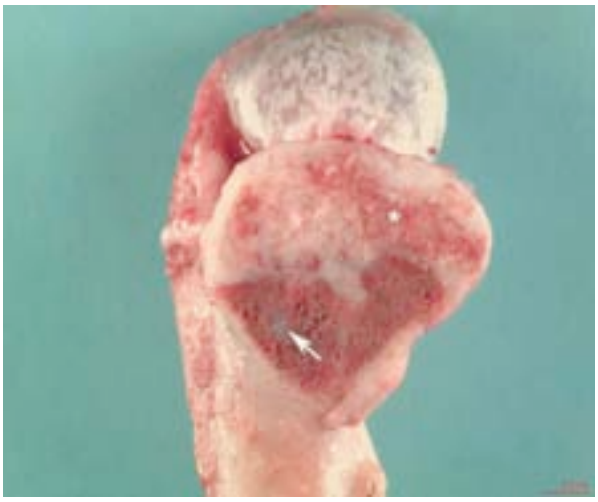

*2-2. Humerus, trochlea (sagittal section), dog: There is a marked increase in cartilaginous tissue in the epiphysis with a smaller than normal ossification center (*). The metaphyseal physis is irregular with a tongue of cartilage extending into the metaphysis. There is also a separate island of cartilage present in the metaphysis (arrow). (Photo courtesy of: Michigan State University, Diagnostic Center for Population and Animal Health, www.animalhealth.msu.edu)*

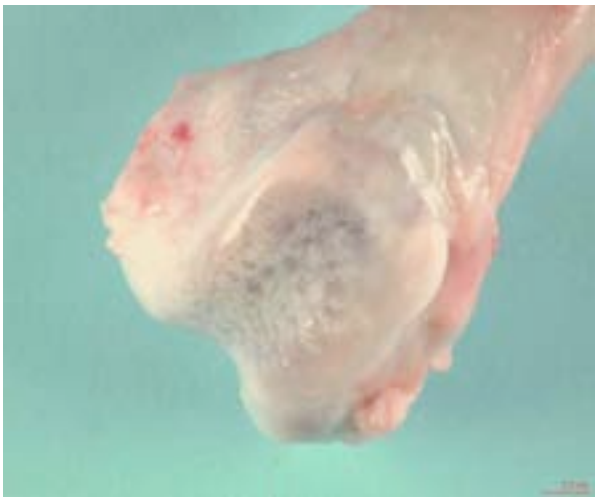

*2-3. Femur, trochlea, dog: The articular surface has a mottled white appearance. (Photo courtesy of: Michigan State University, Diagnostic Center for Population and Animal Health, www.animalhealth.msu.edu)*

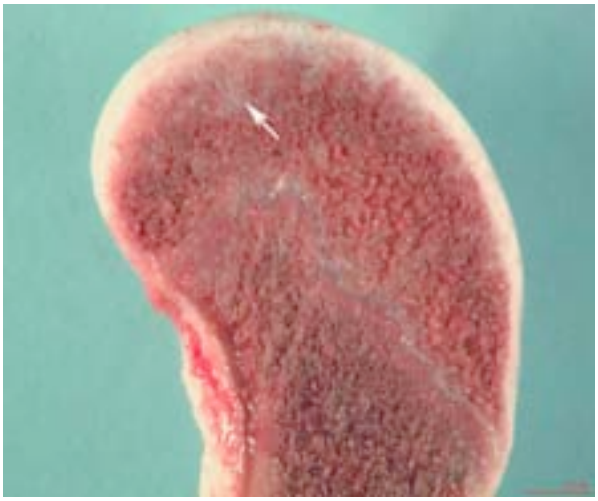

*2-4. Femur, medial condyle (sagittal section), dog: There is increased epiphyseal cartilage (arrow) and a mildly irregular metaphyseal physis. (Photo courtesy of: Michigan State University, Diagnostic Center for Population and Animal Health, www.animalhealth.msu.edu)*

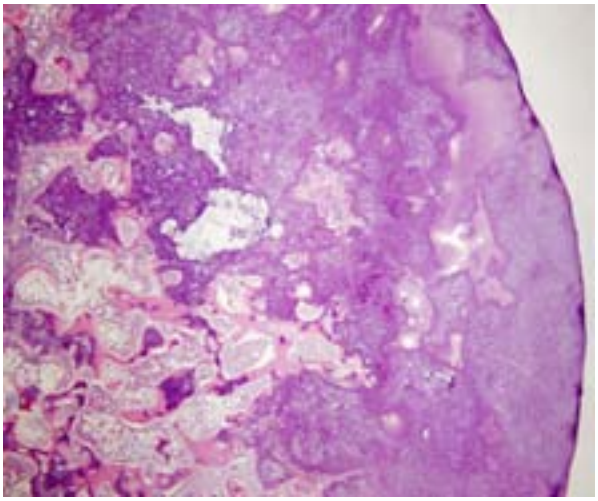

*2-5. Femur, medial condyle (sagittal section), dog: The articular-epiphyseal (AE) complex and areas of persistent epiphyseal cartilage are highly irregular with various staining patterns. There are multifocal to coalescing areas of eosinophilic cartilage alternating with increased amounts of basophilic hyaline cartilage creating a mosaic type appearance. (HE 2X) (Photo courtesy of: Michigan State University, Diagnostic Center for Population and Animal Health, www.animalhealth.msu.edu)*

metaphyseal growth plate. There appears to be reduced ingrowth of vascular channels along the edges of the reduced ossification centers. The metaphyseal growth plate (not present in all submitted sections) varies from normal regions to multifocal irregular areas characterized by disorganization of the three cartilage zones (resting, proliferating and hypertrophic) as well as multifocal extensions of cartilage tongues into the metaphysis. In some of these irregular regions, islands of cartilage within the epiphysis merge with the metaphyseal growth plate causing marked disorganization.

Similar lesions of varying degrees were noted in all of the other bones examined histologically. In some bones the metaphyseal physes were more affected than in others, especially in the proximal radius and trochlea of the distal humerus.

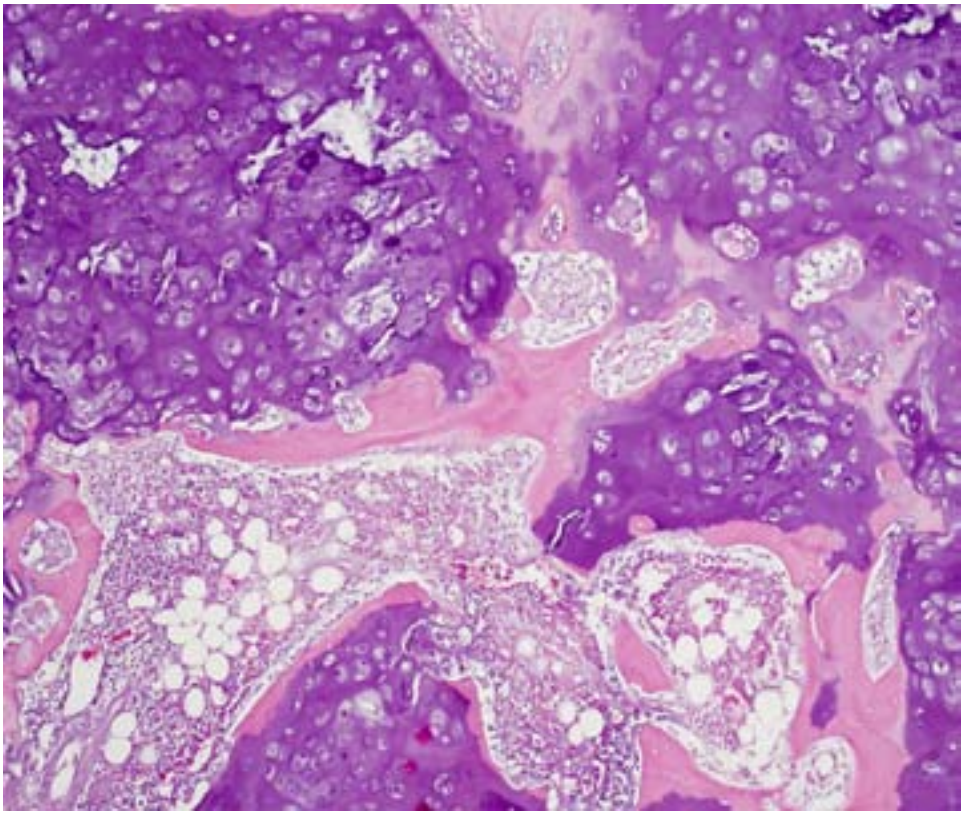

*2-6. Femur, medial condyle (sagittal section), dog: There is reduced ingrowth of vascular channels along the edges of the reduced ossification centers in the epiphysis. (HE 10X) (Photo courtesy of: Michigan State University, Diagnostic Center for Population and Animal Health, www.animalhealth.msu.edu)*

**Contributor's Morphologic Diagnosis:** Distal femur: Severe epiphyseal dysplasia and mild metaphyseal dysplasia.

**Contributor's Comment:** A variety of inherited osteochondrodysplasia have been described in dogs and some are considered normal characteristics of certain breeds. Those that cause disease may be present at birth or develop later in life, especially as weight-bearing increases.[5] Many bone dysplasias are breed specific, such as chondrodysplasias in the Alaskan Malamute, the Norwegian Elkhound, the English Pointer, and in the Great Pyrenees.[5] In these types of chondrodysplasias, the main lesions are in the metaphyseal growth plates and are generally associated with dwarfism or short stature.[5] The growth plates are disorganized with tongues of cartilage often extending into the metaphysis.[5] There are specific differences among breeds in terms of which zones of cartilage, and which bones, are most affected. Pseudoachondroplastic dysplasia of miniature poodles is another type of dysplasia that was originally termed epiphyseal dysplasia. Affected dogs are smaller than their littermates.[5] Enlarged costochondral junctions, long costal cartilages, shortened vertebrate, and abnormal formation of the trachea and nasal septum have been described.[1] The limb bones often have enlarged epiphyses that are sometimes flared over the metaphyses.[1] The cartilage matrix is described as sparse with a lack of basophilia.[1] Chondrocytes have variable size and sometimes are clumped in large lacunae.[1] Radiographic findings show irregular multifocal development of ossification centers that create a stippled appearance.[1] Decreased sulfation of glycosaminoglycans despite normal collagen synthesis is proposed as a cause of these lesions.[1] Osteochondrodysplasia in the Scottish Deerhound is characterized by growth plates that are irregular in width and physeal-metaphyseal junctions that are uneven.[1] There is also a syndrome in Labrador Retrievers and Samoyeds that involves both ocular and skeletal dysplasia.[1] An autosomal recessive inheritance has been suggested for most of these breed specific conditions.[1]

Multiple epiphyseal dysplasia (MED) has been reported rarely in single dog case reports and in two case series. One case series included a litter of Beagle puppies[5] and the other included 19 dogs of various breeds.[6] MED has been described in dogs as a rare condition that involves a deficiency in ossification of the epiphyses of the long bones and vertebrate, the cuboidal bones, and the apophyses.[6] An autosomal recessive mode of inheritance has been suggested.[6] This is in contrast to the disease in humans which most commonly has a dominant pattern of inheritance. However, recessive forms of the disease in

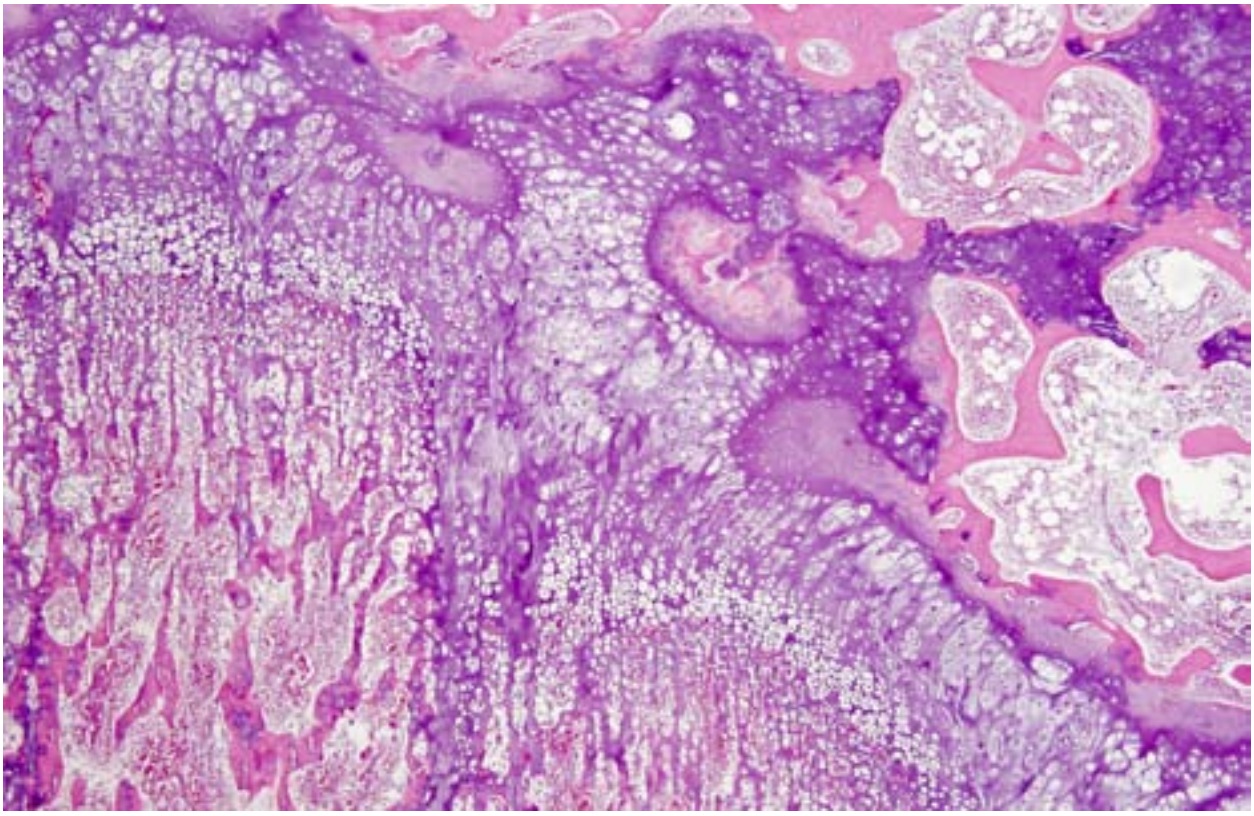

*2-7. Femur, medial condyle (sagittal section), dog: An island of epiphyseal cartilage merges with the metaphyseal growth plate causing marked disorganization in this region. There is also extension of a cartilage tongue into the metaphysis. (HE 4X) (Photo courtesy of: Michigan State University, Diagnostic Center for Population and Animal Health, www.animalhealth.msu.edu)*

humans have been reported and have been linked to a mutation in the gene encoding the oligomeric cartilage matrix protein on chromosome 19 as well as mutations in genes encoding type IX collagen (COL9A2) and matrilin-3.[1] These mutations lead to an anomaly in the matrix of hyaline, articular, and physeal cartilage.[1] In dogs, specific causative mutations have not yet been identified and it has been suggested that environmental factors such as toxins, drugs, and nutritional deficiencies may aid penetrance.[6]

In the case series of 19 affected dogs, dogs were normal at birth, lesions were noted on radiographs as early as 8-weeks-old, mild clinical signs were reported at 2 to 3 months of age, and most dogs had severe lameness by 5 to 8 months of age.[6] Radiographic findings in that case series were reportedly similar to those described in dogs with congenital hypothyroidism.[6] Thyroid testing could not be performed in the present case. Radiographic findings include: a delay in ossification of the epiphyses, apophyses, and cuboidal bones of the appendicular skeleton, the patella, the fabellae, and the epiphyses of the vertebrae; normal appearing metaphyses and diaphyses of the long bones and vertebrae which also seemed normal in length; continued abnormal appearing epiphyses throughout the growth phase but bone formation proceeded from the normal ossification centers and the size of ossification centers increased with age; and a stippled appearance to the distal epiphysis of the tibia.[1]

The shoulder, stifle, and hip joints have been reported to be the most severely affected in dogs, likely due to greater weight bearing on these joints.[6] Reported gross lesions in dogs with MED include: a whitish appearance to all epiphyses, including those in the vertebrate, and in the apophyses and cuboidal bones; occasional loose fragments of cartilage in some joints; and smaller ossification centers noted in sagittal sections.[6] Histologic findings described in affected dogs include: smaller than normal ossification centers with poorly developed bone tissue and an irregular poorly developed hypertrophic zone in the epiphyses; decreased ingrowth of vascular channels at the periphery of ossification centers

and few vacuoles in the adjacent chondroid tissue; cartilaginous tissue in the epiphyses with uneven staining, pale areas, and many lacunae with large, often vacuolated chondrocytes with round dark nuclei; and few or no blood vessels within the epiphyseal cartilage.[6] Flocculent accumulation of chondroitin sulfate and glycoprotein in chondrocyte lacunae is described as the initial lesion.[1] Adjacent lacunae then coalesce and liquefy to form cysts and their contents mineralize.[1]

As the epiphyses of multiple long bones were the most severely affected in the current case, a diagnosis of MED was made. The gross and histologic findings were similar to those described in other reports of MED.[1,5,6] Other differentials considered for this case included pseudoachondroplasia and spondyloepiphyseal dysplasia. The former condition has been described in humans and Miniature Poodles and the latter has been described in humans. These dysplasias are characterized by lesions in both the physes and metaphases, thus resulting in severe dwarfism.[5,1] In this case, the metaphyseal lesions were generally mild to moderate in most bones and dwarfism was not evident. In the 19 dog case series, some dogs had moderate lesions in the metaphyses, and the authors stated that MED should not be excluded in dogs with these lesions.[5] Nonetheless, another form, or multiple forms, of dysplasia cannot be entirely ruled out in the current case. As there is currently no treatment that can relieve the pain in affected dogs, euthanasia is recommended.[6]

**JPC Diagnosis:** Bone, distal femur: Epiphyseal/metaphyseal dysplasia (epiphyseal/metaphyseal (osteo) chondrodysplasia).

**Conference Comment:** This is an interesting and complex entity in which pinpointing causation to a specific genetic anomaly has not been successful. The clinical, radiographic and morphologic abnormalities associated with skeletal dysplasias are heterogeneous with over 200 described disorders, and can be broadly divided into connective tissue disorders that disrupt formation of bone (osteodysplasia) or cartilage and endochondral ossification (chondrodysplasia).[3] The nomenclature is confusing and often terms such as dysplasia (processes involving generalized defects caused by intrinsic alterations), dysostosis (processes limited to a specific bone or bone segment), and dystrophy (defects caused by an extrinsic process) are often used interchangeably.[1] Often the term osteochondrodysplasia is applied when morphologically both cartilage and endochondral bone is altered; however, given the complexity of bone development, in some disorders, tissues other than bone are affected, as this case in chondrodysplasia of the Alaskan Malamute. Several animal models of chondrodysplasia have been established.[8] In humans, several causative genes have been identified, which include cartilage matrix proteins (e.g. *COL2A1*, *COMP*), transcription factors (e.g. *Hox* and *Pax* genes) growth factor receptors (e.g. I), and chondrocyte maturation/hypertrophy factors (e.g. PTH/PTHrP, CBFA1).[3] Recently, single gene mutations associated with specific disorders have been identified, such as the chondrodysplastic "breed-standard" phenotypes of nineteen breeds of domestic dogs.[4] The underlying genetic mechanism presented in this case has not been determined.

Relevant to the discussion is the acquired atypical expression of FGF4 which manifests as the characteristic skeletal breed traits among chondrodysplastic breeds such as dachshunds and bassett hounds.[4] FGF4 induces the expression of sprouty genes which interfere with ubiquitin mediated degradation of FGF receptors, causing their overactivation.[4] The receptor FGFR3 is a negative regulator of bone growth, thus chondrocyte proliferation is downregulated in these breeds leading to their short stature.[2] In contrast, spider lamb chondrodysplasia is caused by inhibition of FGFR3 leading to uncontrolled chondrocyte proliferation, resulting in the long, splayed legs of black-faced lambs.[2]

For this case conference participants preferred a morphologic diagnosis of epiphyseal and metaphyseal chondrodysplasia to identify the histologic abnormalities of chondrocytes/cartilage matrix and disruption of normal ossification within both the epiphysis and metaphysis visible in most sections. However, the more general term "osteochondrodysplasia" would be appropriate as well. However, conference participants recognize the difficulty involved in characterizing these complex abnormalities, and note the contributor's diagnosis of MED correlates with previous case reports in dogs and people with the distinctive

stippling of the epiphyses evident grossly, radiographically and histologically.[6]

The contributor provides an in-depth discussion on MED while contrasting other breed-specific osteochondrodysplasias. The diversity in causes and presentations of both osseous and chondrous dysplasias reveal the intricate and complex nature of osteogenesis both during development and in repair from injurious stimuli.

**Contributing Institution:** Michigan State University, Diagnostic Center for Population and Animal Health, www.animalhealth.msu.edu

**References:**

1. Borrego E, Farrinton DM, Downey FJ. Advances in bone dysplasias. *Rev Esp Cir Ortop Traumatol.* 2014;58(3):171-181.
2. Carlson CS, Weisbrode SE. Bones, joints, tendons, and ligaments. In: Zachary JF, McGavin MD, eds. *Pathologic Basis of Veterinary Disease*. 5th ed. St. Louis, MO: Elsevier Mosby; 2012:941-942.
3. Newman B, Wallis GA. Skeletal dysplasias caused by a disruption of skeletal patterning and endochondral ossification." *Clinical Genetics*. 2003;63(4):241-251.
4. Parker HG, VonHoldt BM, Quignon P, et al. *Science*. 2009;325(5943):995-998.
5. Thompson K. Bones and joints. In: Maxie MG, ed. *Jubb, Kennedy, and Palmer's Pathology of Domestic Animals*. 5th ed. Vol. 2. St. Louis, MO: Elsevier Limited; 2007:30-33.
6. Rasmussen PG. Multiple epiphyseal dysplasia in a litter of Beagle puppies. *J Small Anim. Pract.* 1971;12:91-96.
7. Rørvik AM, Teige J, Ottesen N, Lingaas F. Clinical, radiographic, and pathogic abnormalities in dogs with multiple epiphyseal dysplasia: 19 cases (1991-2005). *JAVMA*. 2008;233(4): 600-606.
8. Terpin T, Roach MR. Chondrodysplasia in the Alaskan Malamute: involvement of arteries, as well as bone and blood. *Am J Vet Res*. 1981;42(11):1865-1873.

**CASE III**: EHO-5 ZNFE960 (JPC 4050817).

**Signalment:** 12-week-old male Sprague-Dawley rat, *Rattus norvegicus.*

**History:** While under anesthesia, this animal underwent blast over-pressure at 120 kPa, traumatic fracture of the right rear limb with a drop weight apparatus, soft tissue crush injury at 20 psi for 1 minute and a trans-femoral amputation. The animal was maintained on an appropriate sustained-release pain control regimen and humane euthanasia was performed 7 days post injury. The right rear limb was disarticulated from the hip joint and submitted for routine processing. All animal care was done in accordance with the WRAIR/NMRC institutional animal care and use committee's guidelines.

**Gross Pathology:** Not available.

**Laboratory Results:** N/A

**Histopathologic Description:** Femur and associated soft tissues: There is a mid-diaphyseal, blunt, angled, traumatic fracture of the femur with loss of the distal bone fragment. At the distal end of the bone fragment, there is a small hematoma composed of erythrocytes admixed with aggregates of disorganized fibrin. The hematoma is surrounded by densely packed proliferating mesenchymal cells (callus) which contain numerous perpendicularly oriented arterioles, fragments of woven bone, collagen, and few scattered multinucleate cells (osteoclasts). There is subperiosteal new woven bone composed of irregular and random to densely organized collagen fibers which widens from proximal to distal as it extends towards the fracture site and forms a small region of hyaline cartilage adjacent to the fracture. Woven bone is hypercellular with increased numbers of osteoblasts, enlarged osteocytes, and fewer osteoclasts. Within the callus, there is a small osteophyte embedded within dense connective tissue. Multifocally, the surrounding myofibers are variably characterized by: pallor, swelling, and vacuolization (degeneration); sarcoplasmic hypereosinophilia, loss of cross-striations, fragmentation, and pyknosis (necrosis); or sarcoplasmic basophilia with nuclear internalization with rowing of nuclei,

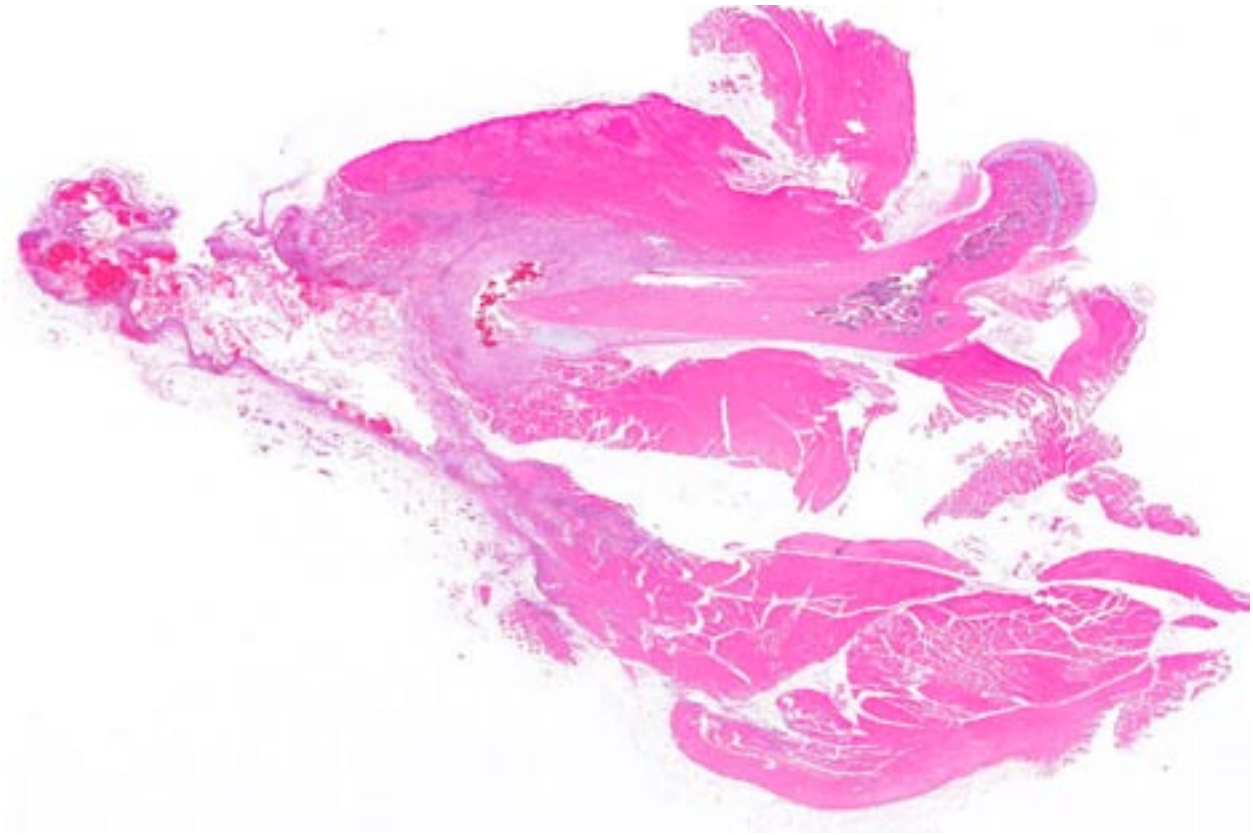

*3-1. Femur, rat: There is a mid-shaft, angled femoral fracture with removal of the distal fragment. (HE 6.3X)*

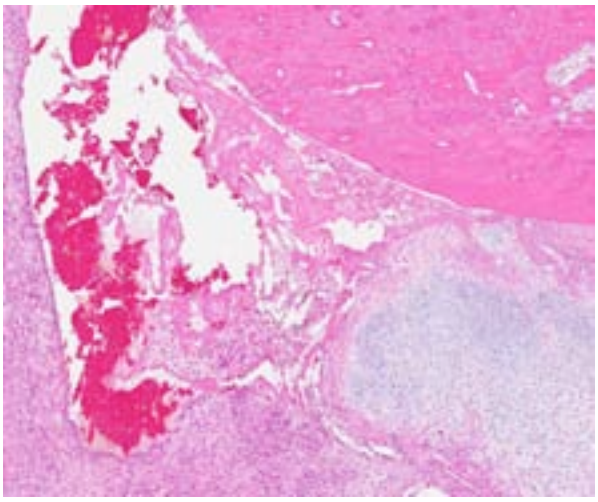

*3-2. Femur, rat: At the distal end of the fracture site, there is a hematoma with hemorrhage and loosely polymerized fibrin strands. (34X)*

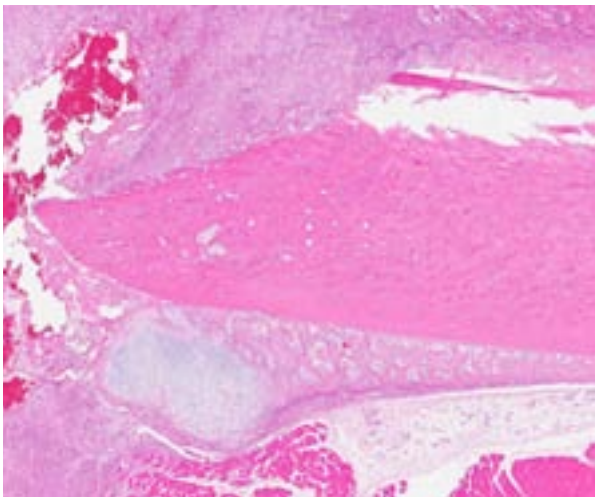

*3-3. Femur, rat: The distal end of the fragment is surrounded by a thick band of proliferating mesenchymal cells (callus). The periosteum (right) is elevated by proliferating trabeculae of woven bone, and a focal area of cartilage is present at the distal end. (HE 45X)*

and large nuclei with large nucleoli (regeneration). Multifocally, myofibers are separated, surrounded and replaced by loose connective tissue, fibrin, edema, and hemorrhage. Distal to the fracture, there is a focally extensive area of inflammation forming a pseudocyst around a pocket of fibrin, hemorrhage, edema, and eosinophilic cellular and karyorrhectic debris (necrosis). Multifocally, there are clusters of histiocytes, neutrophils, lymphocytes and plasma cells at the periphery. Multifocally there is scattered golden yellow pigment (hemosiderin) within the callus and within surrounding connective tissues.

**Contributor's Morphologic Diagnosis:** Femur and associated soft tissues: Fracture, mid-diaphyseal, with subperiosteal new bone growth, cartilage growth, and callus formation, with adjacent myofiber necrosis, degeneration, and regeneration.

**Contributor's Comment:** Unlike most other tissues, bone is capable of repair by regeneration rather than scar formation.[3] The first stage of fracture repair is formation of a hematoma.[3] The hematoma is rapidly replaced by mesenchymal cells from the medullary cavity, endosteum, and periosteum to form a callus which is initially composed of loose connective tissue.[3] Next, primitive mesenchymal cells in the fracture gap differentiate into chondroblasts and replace the loose connective tissue with chondroid matrix.[3] The fracture site is revascularized and cartilage is replaced by trabeculae of woven bone.[3] The final phase, which may take months or years, involves the replacement of woven bone in the callus with mature lamellar bone.[3] This coincides with modeling of the callus to restore the bone to its original shape and strength.[3] In adults, persistence of medullary trabeculae and thickening of the periosteal bone surface are likely to persist at the healed fracture site, whereas in younger animals, the fracture may completely resolve.[3]

Three critical constituents are required for formation of bone: (1) the presence of collagen, (2) the availability of phosphate (and calcium), and (3) removal or absence of inhibitors of mineralization, such as pyrophosphate.[1] The bony biochemical milieu is complex and involves the interplay between soluble factors, extracellular matrix proteins and enzymes, and biomechanical forces that influence the modeling of bone.[1-3] This discussion will focus on the signaling molecules involved in bone homeostasis.

Signaling Molecules. Signaling molecules include hormones, cytokines and growth factors.[1,3]

Hormones. Parathyroid hormone and calcitonin are hormones that function to maintain a stable serum calcium concentration.[1,3] Estrogens and androgens are important regulators of skeletal growth and maturation.[3] The anabolic effect of estrogen is quite complex, but it appears to act indirectly by modulating other factors such as interleukin 6 (IL-6) and transforming growth factor beta (TGF-).[1] A significant effect of

estrogens appears to be inhibiting bone resorption.[3] Estrogen depletion induced by ovariectomy in a rat model markedly increases the synthesis of IL-6 by osteoblasts or their precursors in the bone marrow stroma.[3] Androgens also exert anabolic effects on bone either directly or after aromatization to estrogen.[1] Androgens tend to increase periosteal bone formation and radial growth, whereas estrogens decrease it, thus accounting for some of the differences noted between the sexes.[1] Thyroxine is essential for skeletal tissue formation, and if deficient leads to cretinism characterized by short stature and developmental abnormalities.[1,3] Growth hormone (GH) is secreted throughout life, but is highest in childhood and peaks during puberty.[1] While several hormones influence longitudinal bone growth, GH is generally regarded as the most important.[1]

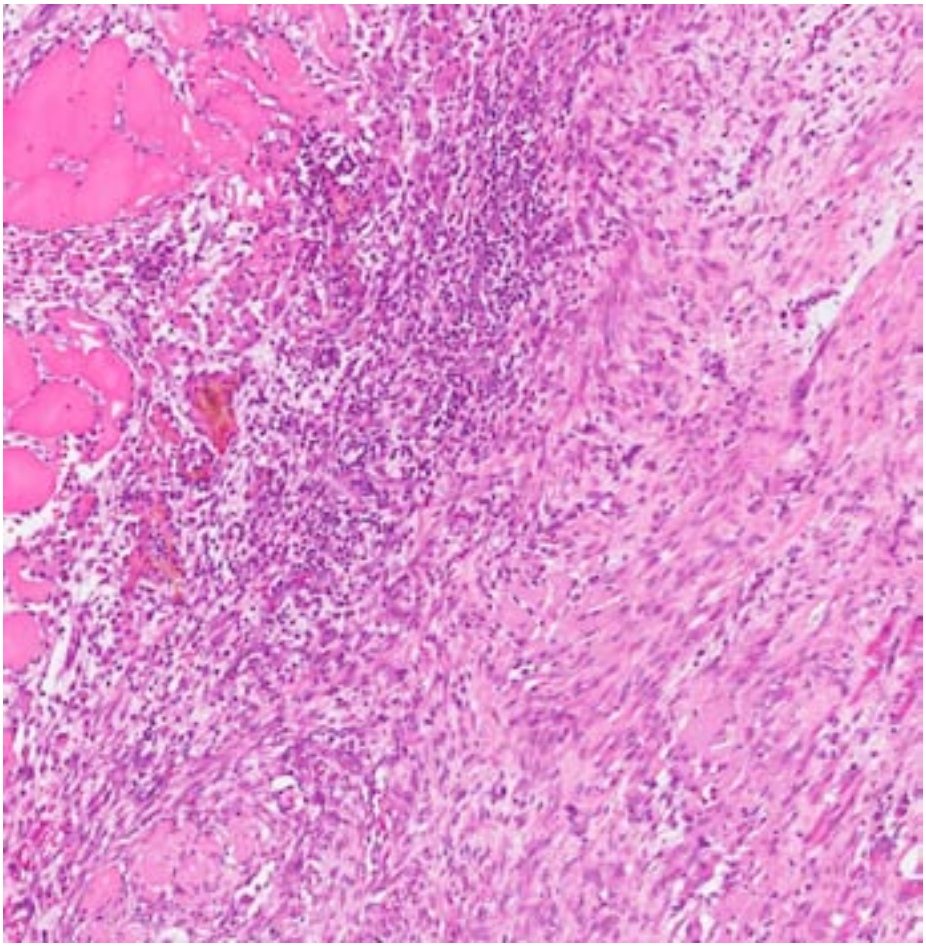

*3-4. Femur, rat: The callus transitions into abundant granulation tissue which infiltrates the adjacent atrophic skeletal muscle. (HE 218X)*

Cytokines. Cytokines include interleukins, interferons, lymphokines, prostaglandins, and other polypeptides involved in host defense and homeostasis.[1] Interleukins are pro-inflammatory cytokines that are involved in bone resorption and remodeling.[1] Cytokines such as IL-6 and IL-11 appear to play a crucial role in the recruitment, proliferation, and differentiation of osteoclast progenitors that eventually lead to reduced bone mass in estrogen deficiency.[2] Prostaglandins are a subclass of eicosanoids that are enzymatically derived from fatty acids and act as potent messengers in regulation of vascular tone, inflammation, and cell growth.[1] However, they also have been shown to be an important mediator of local bone resorption.[1,3]

Growth Factors. The principal function of growth factors is regulation of cellular growth and function.[1] The actions of the TGF- superfamily, the bone morphogenetic protein (BMP) family, insulin-like growth factor (IGF), fibroblast growth factor-2 (FGF-2), epidermal growth factor (EGF), platelet-derived growth factor (PDGF), and vascular endothelial growth factor (VEGF) have all been shown to influence bone metabolism.[1]

Transforming Growth Factor− (TGF−). TGF− has powerful effects on both osteoclasts and osteoblasts, and probably plays a key role in bone remodeling.[3] Expression of TGF− is especially high during active matrix secretion.[1] In vivo rat models have shown that osteoblast and osteoclast TGF-s (especially TGF−1) increase during fracture healing.[1] Functionally, TGF−1 has several effects that are synergistically conducive to matrix production and ossification.[1] First, TGF−1 recruits the appropriate cells for bone

formation and remodeling such as osteoprogenitor cells and fibroblasts.[1] During bone healing, TGF−1 initially inhibits activation of osteoclasts, which is permissive for net bone formation.[1,3] Later, TGF−1 is an indirect promotor of osteoclast activation.[1,3] This is crucial when osteoclasts are required not only to remodel bone, but to liberate protein-bound enzymes within the extracellular matrix.[1] In addition to recruiting cells, TGF−s are a potent promotor of collagen production without which ossification cannot occur.[1,3]

Bone Morphogenic Proteins. BMPs are a family of growth factors which belong to the TGF−superfamily.[1,3] Like their parent TGF−s, the BMP signaling molecules regulate myriad cellular processes, including proliferation, differentiation, and growth.[1,3] In the context of bone formation, at low concentrations they promote chemotaxis and cellular proliferation.[1] At high concentrations, they favor cellular differentiation and bone formation.[1] BMPs are believed to stimulate production of osteoprotegerin (OPG) which is an osteoblast-secreted decoy receptor that specifically binds to osteoclast differentiation factor and inhibits osteoclast maturation.[1] BMPs are the most osteoinductive growth factors described.[1] BMP−specific antagonists, such as noggin and chordin, have also been identified.[3]

Insulin-like Growth Factor-1, Fibroblast Growth Factor-2, and Epidermal Growth Factor. In vivo and in vitro data suggest that insulin-like growth factor-1 (IGF-1) stimulates osteoprogenitor cell mitosis and differentiation, thereby increasing the number of functionally mature osteoblasts.[1] FGFs act in concert with heparin sulfate−containing proteoglycans to modulate cell migration, angiogenesis, bone development and repair, and epithelial-mesenchymal interactions.[1] FGF-2 is the most abundant ligand and has been shown to stimulate osteoblast proliferation and enhance bone formation.[1] FGF-2 expression is elevated during fracture healing.[1] Exogenously applied FGF-2 accelerates osteogenesis in critical-size bone defects and fracture sites.[1] EGF has been shown to stimulate bone resorption and upregulate production of matrix metalloproteinases, thus promoting remodeling.[1]

Platelet-Derived Growth Factor and Vascular Endothelial Growth Factor. PDGF is best known for its role in angiogenesis, but also is instrumental in embryological development and postnatal cellular migration and proliferation.[1] As its name suggestions, PDGF is secreted systemically by platelets.[1] In bone, its cellular origin is unknown.[1] Functionally, PDGF exerts one of the strongest chemotactic effects on osteoblasts and stem cell precursors.[1] Furthermore, PDGF is a potent activator of osteoclasts, fibroblasts, and endothelial cells.[1] PDGF is a potent stimulator of new bone formation, but also promotes bone resorption.[3] The VEGFs are involved in both angiogenesis and vasculogenesis.[1] VEGF increases endothelial cell and endothelial progenitor cell chemotaxis and mitogenesis, promoting new vessel formation.[1] In bone, osteoblasts secrete VEGF and express VEGF receptors.[1] Further, osteoclasts also express VEGF receptors, and VEGF chemotactically recruits osteoclasts to remodeling zones.[1] Following fracture or osteotomy, vascular disruption of nutrient arteries, release of lysosomal enzymes from necrotic bone edges and soft tissues, and vasoconstriction of periosteal and medullary arteries result in the formation of a hypoxic interfragmental zone of injury.[1] These stimuli serve collectively as a catalyst for new blood vessel formation.[1] VEGF-mediated angiogenesis has been demonstrated to be an absolute requirement for successful bone induction in fracture zones.[1]

**JPC Diagnosis:** Bone, femur: Severely displaced (traumatic amputation), simple, mid-diaphyseal femoral fracture with organizing hematoma, subacute subperiosteal woven bone and cartilaginous callus, adjacent myofiber degeneration, necrosis, and regeneration.

**Conference Comment:** Appropriate fracture healing requires alteration in expression of several thousand genes.[2] The contributor provided a comprehensive overview of the most well known signaling molecules which play a prominent role, and this case is an opportunity to observe the process histologically.

Indirect, or secondary, fracture healing occurs most commonly, and consists of endochondral and intramembranous bone healing in situations of weight-bearing fractures with a small degree of motion. Excessive motion or load results in delayed healing or non-union. No anatomical reduction is required with these types of fractures;

however, some fixation techniques may initiate it if they induce subtle motion at the fracture site.[2]

Direct fracture healing does not occur as a natural process, but rather following anatomical reduction and stable fixation. It is the desired end state of surgical fracture repair, as the direct remodeling of lamellar bone, Haversian canals and blood vessels may lead to complete healing within months, while indirect healing often occurs for years before the bone is completely remodeled from a fracture callus to lamellar bone.[2] This process also alters the electrical potential of bone, and recent studies have demonstrated that measured electrical potentials may correlate with prognosis of adequate fracture repair.[4]

**Contributing Institution:** Walter Reed Army Institute of Research, 503 Robert Grant Avenue, Silver Spring, MD 20910-7500
http://wrair-www.army.mil/

**References:**

1. Allori AC, Sailon AM, Warren SM. Biological basis of bone formation, remodeling, and repair-part I: biochemical signaling molecules. *Tissue Eng Part B*. 2008;14(3):259-73.
2. Marsell R, Einhorn TA. The biology of fracture healing. *Injury*. 2011;42(6):551-555.
3. Thompson, K. Bones and joints. In: Maxie MG, ed. *Jubb, Kennedy and Palmer's Pathology of Domestic Animals*, Vol 1. 5th ed. Philadelphia, PA: Elsevier Limited; 2007;1-23.
4. Zigman T, Davila S, Dobric I. Intraoperative measurement of bone electrical potential: a piece in the puzzle of understanding fracture healing. *Injury*. 2013;44 Suppl 3:S16-19.

**CASE IV:** HB6280 (JPC 4033562).

**Signalment:** 8-month-old female thoroughbred horse, *Equus caballus.*

**History:** The mare showed sudden renal failure and no response to treatment. Anorexia and severe uremia were continuing and the animal was euthanized.

**Gross Pathology:** After formalin fixation, the surfaces of the both kidneys were slightly irregular and the cortex showed whitish to tan on the cut sections. No significant gross lesion was observed in other organs.

**Laboratory Results:** Blood test revealed high BUN 206.7 mg/dl (normal: 9.0-20.0) and CRE: 9.69 mg/dl (normal: 0.9-1.8). Serology (antibody titer) and PCR showed no evidence of *Leptospira sp*. infection.

**Histopathologic Description:** Diffuse and global, partially segmental glomerular sclerosis and enlarged glomeruli with mild to moderate proliferation of mesangial cells are remarkable. Irregularly dilated tubules are predominant in renal cortex, and papillary projections of tubular epithelium into the lumens are occasional. Immature small tubules with indistinct luminal structures and dysplastic tubules with enlarged clear nuclei are frequent. Protein cast formation, deposition of oxalate crystal and hyaline droplet degeneration are rarely in tubules/tubular epithelium. Diffuse and mild fibrosis is in interstitial tissues with mild lymphoplasmacytic infiltration, sometimes along with concentric fibrosis around renal tubules and/or Bowman's capsules and deposition of eosinophilic homogenous material. Small to mid-sized arterioles are increasing in the cortex. Rarely, abnormal large muscular arteries are in subcapsular cortex (not in all slides). Pale basophilic myxoid material depositions are rare in the interstitium.

**Contributor's Morphologic Diagnosis:** Kidney: Equine renal dysplasia.

**Contributor's Comment:** Based on the histopathological findings, renal dysplasia was considered most likely in the present case. Abnormal proliferation of arterioles in the renal cortex also supports a developmental anomaly of the kidneys in this mare. Variously affected glomeruli with hypercellularity and sclerosing changes suggest that the primary lesions are not located in glomeruli. However, regenerative tubules with juvenile epithelial cells, interstitial fibrosis and mild to moderate mesangial proliferation suggest a differential diagnosis of tubular nephritis following renal injury, such as toxicosis or leptospire infection. The present case was negative for leptospires. Further, plant toxicosis is unlikely because no other case of toxicosis was found in the ranch.

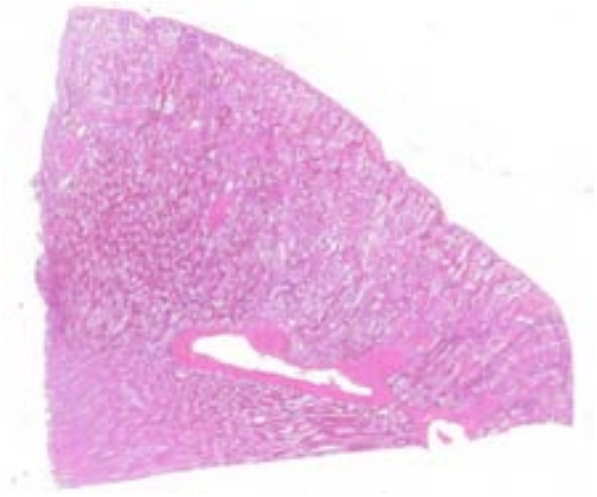

*4-1. Kidney, 8-month-old thoroughbred foal: There is diffuse distortion of renal architecture with dilstation of tubules and markedly enlarged and tortuous renal vasculature.*

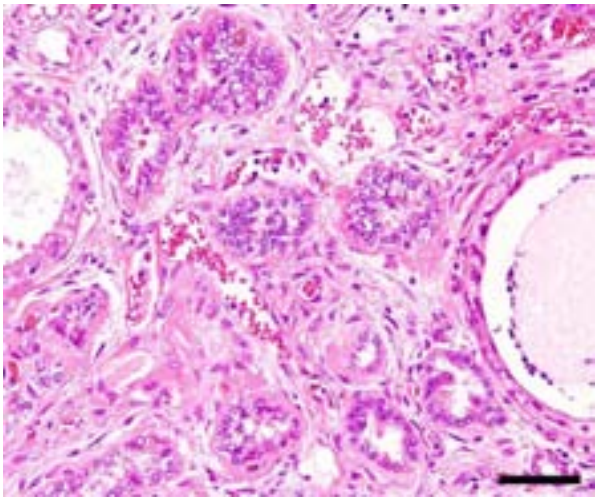

*4-2. Kidney, foal: Immature renal tubules with atypical epithelial cells and incomplete luminal structures. HE. Bar=50μm. (Photo courtesy of: Laboratory of Comparative Pathology, Graduate School of Veterinary Medicine, Hokkaido University, Sapporo, 060-0818, JAPAN http://www.hokudai.ac.jp/veteri))*

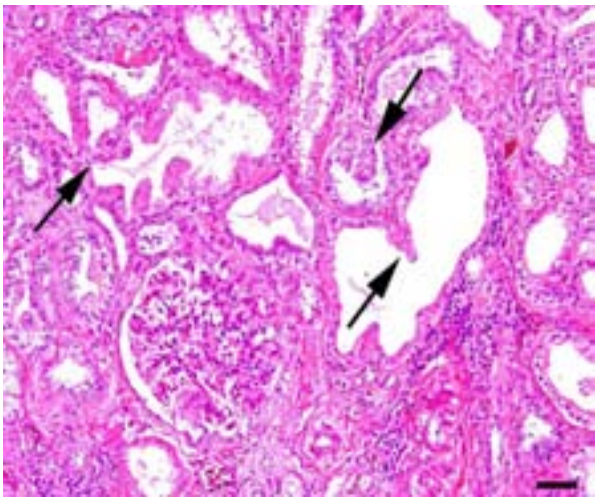

*4-3. Kidney, foal: Papillary projections (arrows) into the lumen of tubules. HE. Bar=50µm (Photo courtesy of: Laboratory of Comparative Pathology, Graduate School of Veterinary Medicine, Hokkaido University, Sapporo, 060-0818, JAPAN http://www.hokudai.ac.jp/veteri))*

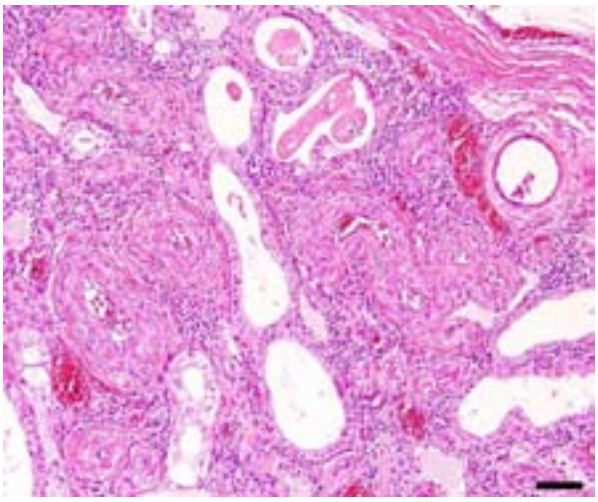

*4-4. Kidney, foal: Many arterioles are present in renal cortex. Dilation of tubules is also noted. HE. Bar=50µm. (Photo courtesy of: Laboratory of Comparative Pathology, Graduate School of Veterinary Medicine ,Hokkaido University, Sapporo, 060-0818, JAPAN http://www.hokudai.ac.jp/veteri))*

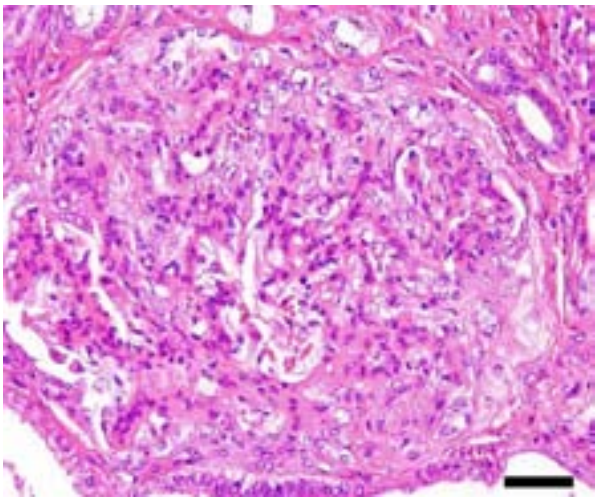

*4-5. Kidney, foal: Enlarged glomerulus with proliferation of mesangial cells and adhesion with Bowman's capsule. (Photo courtesy of: Laboratory of Comparative Pathology, Graduate School of Veterinary Medicine, Hokkaido University, Sapporo, 060-0818, JAPAN http://www.hokudai.ac.jp/veteri))*

Renal dysplasia is a rare congenital disease of developmental uni- or bilateral kidney anomaly reported in various animals.[4] Renal dysplasia in dogs is well documented; however, equine renal dysplasia is also reported. The size of the affected kidney shows small and irregular surface with demonstration of immature histological structures like undifferentiated stromal tissues, immature renal tubules and glomeruli. Primitive ductal structures and cartilage and/or bone formation are sometimes found.

The major histological findings reported in equine renal dysplasia are papillary proliferation of tubular epithelium, immature tubules and islands of interstitial fibrosis.[1,2,7] Renal artery dysplasia is also described in one adult horse with chronic renal failure[1] and also in humans. The histopathological changes in the present case are very complicated; however, some of them, including oxalate deposition, appear to be secondary changes following renal failures. The various proposed pathogeneses of renal dysplasia, like abnormal metanephrons or vascular malformation, may be putative but clear mechanisms are still unknown.

**JPC Diagnosis:** Kidney: Dysplasia characterized by hypercellular glomeruli, glomerulosclerosis, tubular epithelial hyperplasia, hypertrophic arterioles and arteries, and interstitial myxoid matrix.

**Conference Comment:** Equine renal dysplasia is rarely reported in the horse and often has a variable histopathologic presentation. Many of the well-defined, characteristic histologic features observed in dogs, including persistent metanephric ducts, primitive mesenchyme and cartilaginous or osseous tissue, are not present in this case. Yet the clinical history and glomerular changes are consistent with the diagnosis. Some reports of equine renal dysplasia describe renal cysts, fetal glomeruli, and tubules lined by cuboidal epithelium, while others have identified normal kidney size with normal appearance and number of glomeruli but with hypoplastic nephron tubules.[5,9] Conference participants were

intrigued with the aberrant arterioles and large muscular arteries present throughout the renal cortex, and speculated whether these may have played a primary role in the development of other pathologic changes in this case. Interestingly, these aberrant vascular features have been reported in human cases of segmental or complete renal dysplasia.[8] Segmental hypoplasia with renal vascular anomalies (Ask-Upmark kidney) has also been described in young Boxer dogs.[3]

A related, possibly equivalent, condition to renal dysplasia is referred to as progressive juvenile nephropathy and is associated with specific dog breeds including Lhasa Apso, Shih Tzu, and the golden retriever. These conditions share several features with dysplasia though typical presentation depends on the breed. Often a glomerulopathy resembling membranoproliferative glomerulonephritis is present and may progress to glomerulosclerosis. Overall gross and microscopic features are comparable to those of chronic renal disease with renal fibrosis in aging dogs, but this condition affects dogs under 2 years of age.[6]

**Contributing Institution:** Laboratory of Comparative Pathology, Graduate School of Veterinary Medicine, Hokkaido University, Sapporo, 060-0818, JAPAN
http://www.hokudai.ac.jp/veteri

**References:**

1. Anderson WI, Picut CA, King JM et al. Renal dysplasia in a Standard Colt. *Vet Pathol*. 1988;25:179-180.
2. Gull T, Schmitz DG, Bahr A et al. Renal hypoplasia and dysplasia in an American miniature foal. *Vet Rec*. 2001;149:199-203.
3. Kolbjørnsen, Ø, Heggelund M, Jansen JH. End-stage kidney disease probably due to reflux nephropathy with segmental hypoplasia (Ask-Upmark kidney) in young Boxer dogs in Norway. A retrospective study. *Veterinary Pathology Online*. 2008;45.4:467-474.
4. Maxie MG, Newmann SJ. Urinary system. In: Maxie MG, ed. *Jubb, Kennedy, and Palmer's Pathology of Domestic Animals*. Vol. 2. 5th ed. Philadelphia, PA: Elsevier Saunders; 2007:439-442.
5. Medina-Torres CE, Hewson J, Stampfli S, Stalker MJ. Bilateral diffuse cystic renal dysplasia in a 9-day-old thoroughbred filly. *Can Vet J*. 2014;55(2):141-146.
6. Newman SJ. The urinary system. In: Zachary JF, McGavin MD, eds. *Pathologic Basis of Veterinary Disease*. 5th ed. St. Louis, MO: Elsevier Saunders; 2012:618,655-656.
7. Rosen N, Amstel SR, Nesbit JW et al. Renal dysplasia in two adult horses: clinical and pathological aspects. *Vet Rec*. 1993;132:269-270.
8. Rosenfeld JB, et al. Unilateral renal hypoplasia with hypertension (Ask-Upmark kidney). *BMJ*. 1973;2.5860:217-219.
9. Zicker SC, Marty GD, Carlson GP, Madigan JE, Smith JM, Goetzman BW. Bilateral renal dysplasia with nephron hypoplasia in a foal. *J Am Vet Med Assoc*. 1990;196(12):2001-2005.

**Joint Pathology Center**
**Veterinary Pathology Services**

*Conference Coordinator*
**Matthew C. Reed, DVM**
**Captain, Veterinary Corps, U.S. Army**
**Veterinary Pathology Services**
**Joint Pathology Center**

## WEDNESDAY SLIDE CONFERENCE 2014-2015

# Conference 9

**9 November 2014**

**Conference Moderator:**
Michael Garner, DVM, DACVP
Northwest ZooPath
654 W Main St.
Monroe, WA 98272

---

**CASE I:** AFIP-2 (JPC 4004343).

**Signalment:** Male white-tailed deer, age unknown, *Odocoileus virginianus*.

**History:** The animal has been submitted to necropsy with a history of CNS signs ("Disoriented, weak, antlers caught in shrub").

**Gross Pathology:** The gross pathology of the deer examined revealed inadequate body fat and 2.5 cm abscess filled with pus in the center of the left half of the cerebrum. No other gross lesions have been observed in the other organs of the deer examined.

**Laboratory Results:** The antigen ELISA for CWD was negative, *A. pyogenes* and *P. multocida* were isolated from the brain, and the result of fecal float showed rare strongyle-type ova and *Strongyloides*. No other ancillary tests have been performed on other organs.

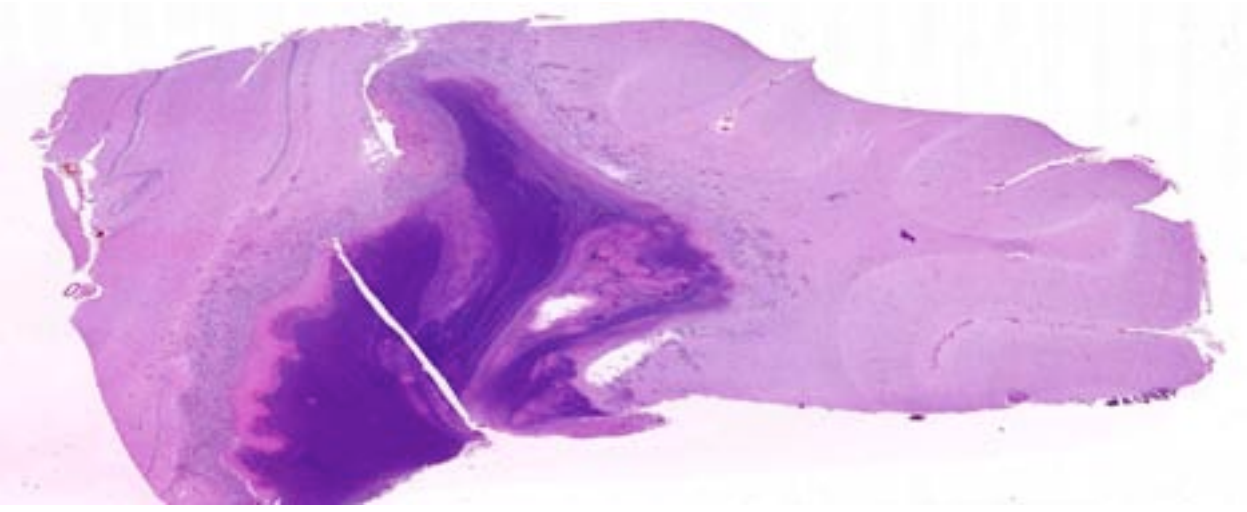

*1-1. Cerebrum, deer: Centrally within the section, there is a focal, well-demarcated cellular infiltrate. (HE 6.3X)*

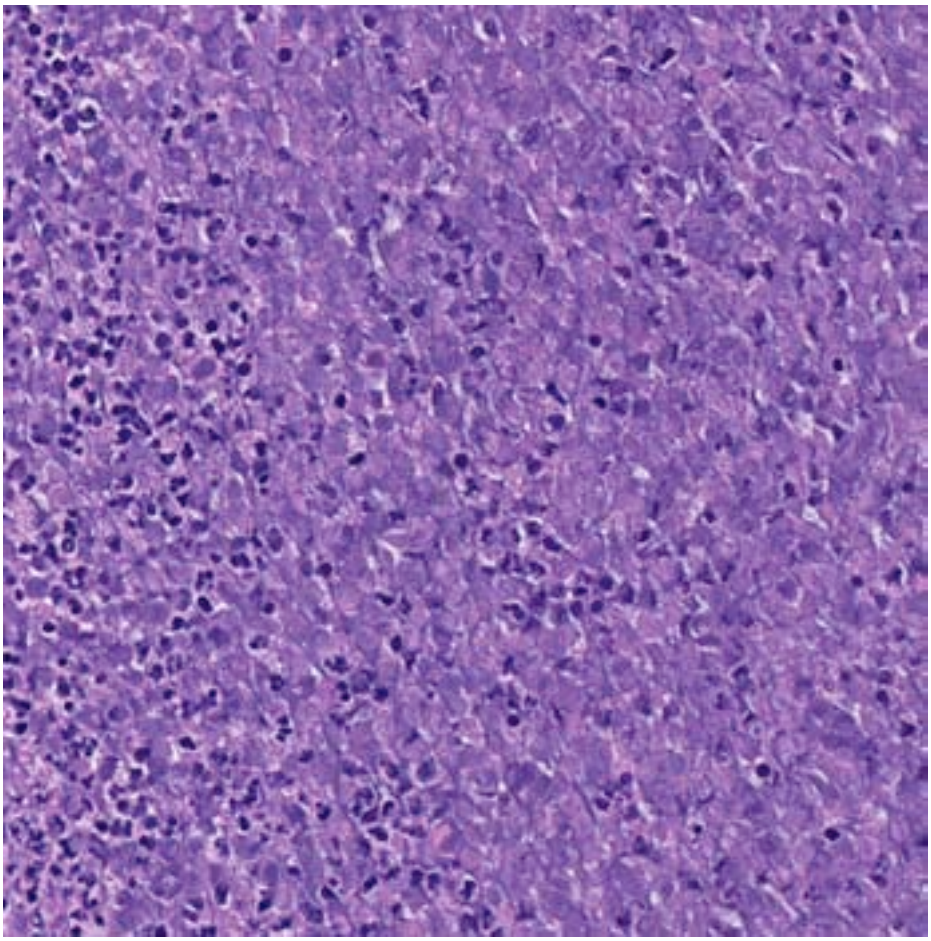

*1-2. Cerebrum, deer: The cellular infiltrate is composed of degenerate neutrophils and abundant cellular debris, consistent with an abscess. (HE 196X)*

**Histopathologic Description:** Brain (cerebrum): There is locally extensive necrosis of the nervous tissue containing cellular debris with bacterial colonization. The necrotic area is surrounded by a wide zone of inflammatory cells, mainly composed of neutrophils with fewer lymphocytes and macrophages. There is diffuse intravascular lymphocytic cuffing.

**Contributor's Morphologic Diagnosis:** Encephalitis, locally extensive, necrotizing, subacute with granulation tissue (capsule) formation and bacterial colonization.

**Contributor's Comment:** Brain abscess-related mortality is a growing concern of deer managers and biologists across the country. Brain abscesses are caused by a variety of bacteria (primarily *Arcanobacterium pyogenes*) that naturally inhabit the skin of deer, as well as other animals.[1,2,3,5] These bacteria typically enter the brain through lesions and skin abrasions associated with the antler pedicle (where the antler protrudes from the skull) or junctions between cranial bones that are referred to as "sutures". Mortality generally occurs from fall (following velvet shedding) through spring (shortly after antler casting). Thus, the period when bucks are developing antlers or when antlers have hardened is when they are most susceptible to this disease.[1]

Certain buck behaviors, such as aggressive sparring and fighting, can cause damage to the antler pedicle and/or other parts of the skull that can predispose them to brain abscesses.[1]

Different studies, from 1996-2008, showed that the intracranial abscesses were diagnosed as the cause of death or illness in white-tailed deer examined by the diagnostic laboratories across portions of the United States and Canada. The bacterium *Arcanobacterium pyogenes* was the primary cause of infection.[1,2,3,5]

The clinical signs include several behavioral characteristics associated with the neurological system, such as "circling" or loss of coordination. Often times, deer can become emaciated, which is characterized by excessive weight loss or having a "deteriorated" appearance. Bucks also may have a puss-like substance located around the antler pedicle that leaks through openings in the skull. It is not known whether this disease can be transmitted between deer or other animals through direct contact or other sources. Also, it is important to note that deer with brain abscesses are not recommended for consumption.[1]

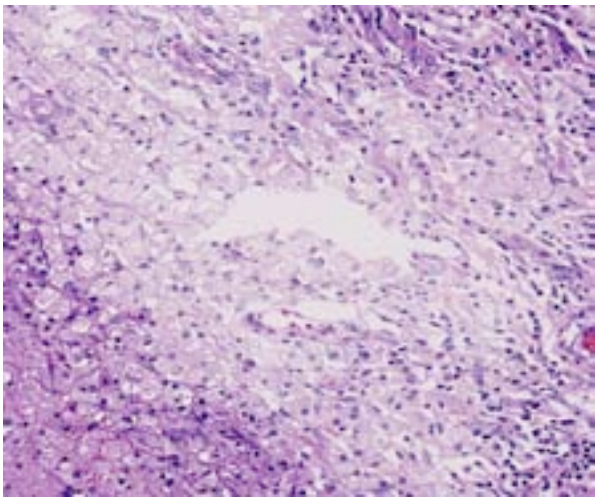

*1-3. Cerebrum, deer: Cerebral abscesses lack a capsule due to the lack of fibroblasts in the brain; there are areas of liquefactive necrosis infiltrated by large numbers of Gitter cells in the adjacent white matter. (HE 256X)*

The clinical, gross examination and ancillary tests findings were compatible with the previous studies.

Note: Multiple blocks were used for the slides submission; therefore, not all the participants will get the same copy of the slides.

**JPC Diagnosis:** Brain, midbrain: Abscess, focally extensive, with gliosis, spongiosis, nonsuppurative perivascular cuffing, and numerous colonies of bacilli.

**Conference Comment:** The contributor highlights the disease pathogenesis in this case as associated with antler development and biologic behavior in this species. A second possible pathogenesis discussed by conference participants is a hematogenous route, likely subsequent to oral infection. Oral mucosal damage or severe dental disease could potentially lead to bacterial emboli seeding in the brain and inducing a lesion such as is observed in this case.

For a deer exhibiting neurologic symptoms, the differential of *Listeria monocytogenes* must also be considered. Lesions of listeriosis are typically smaller (microabscesses) and confined to the brainstem.

There is an increasing trend for hunters and property owners to allow bucks to reach a more mature age before harvesting to improve herd health and antler quality.[1] Associated with the trend is the unintended consequence of increased numbers of brain abscesses occurring in mature males. Recently, a study of 26 collared bucks over 2.5 years old identified brain abscess as the cause of death in 35% of cases, likely related to the increased competition among mature bucks.[5]

*Arcanobacterium pyogenes* is the most commonly cultured isolate from brain abscess, being the only isolate in almost 50% of cases.[2] The bacterium has been through a series of name changes, and has recently been reclassified as *Trueperella pyogenes* based on DNA sequencing and mass spectrometry.[4]

**Contributing Institution:** Animal Disease Research and Diagnostic Laboratory-Veterinary & Biomedical Sciences Department
South Dakota State University
http://www.sdstate.edu/vs/

**References:**

1. Basinger R. Brain Abscesses – A potential thorn in the side of intensive deer management programs. *Westervelt Wildlife Service.* 2009;9:26–31.
2. Baumann CD, Davidson WR, Roscoe DE, Beheler-Amass K. Intracranial abscessation in white-tailed deer of North America. *J Wildl Dis.* 2001;37(4):661–70.
3. Hattel AL, Shaw DP, Love BC, Wagner DC, Drake TR, Brooks JW. A retrospective study of mortality in Pennsylvania captive white-tailed deer (*Odocoileus virginianus*): 2000–2003. *J Vet Diagn Invest.* 2004;16:515–521.
4. Hijazin M, Hassan AA, Alber J, et al. Evaluation of matrix-associated laser desorption ionization-time of flight mass spectrometry (MALDI-TOF MS) for species identification of bacteria of genera Arcanobacterium and Trueperella. *Vet Microbiol.* 2012;157(1-2): 243-245.
5. Karns GR, Lancia RA, Deperno CS, Conner MC, Stoskopf MK. Intracranial abscessation as a natural mortality factor for adult male white-tailed deer (*Odocoileus virginianus*) in Kent County, Maryland, USA. *J Wildl Dis.* 2009;45(1):196–200.

**CASE II**: 66400 (JPC 4048574).

**Signalment:** 8 year-old female African black-footed penguin.

**History:** This penguin has a history of intermittent seizures, mild anemia, severe leukocytosis and hyperglobulinemia. Recently the penguin presented with increasing frequency of seizures, acute facial swelling, lethargy, inappetance and weight loss (BCS 3/9). The penguin was treated with supportive care as well as doxycycline, enrofloxacin, itraconazole, terbinafine, and amphotericin B for suspected aspergillosis and avian malaria. The penguin did not respond to therapy and ultimately died.

**Gross Pathology:** The animal is in poor body condition and there are minimal subcutaneous fat stores. A focally extensive, 5 x 5 cm focus of wet, gelatinous subcutaneous tissue (edema) is noted over the keel. Upon opening the coelomic cavity, approximately 100 ml of transudate primarily located within the pleura surrounding the heart and potentially cranial air sacs is noted. The heart is pale red with numerous tan streaks present throughout the myocardium. At the base of the heart on the endocardium there are multifocal to coalescing areas of petechial hemorrhage. Atrioventricular and semilunar valves are unremarkable.

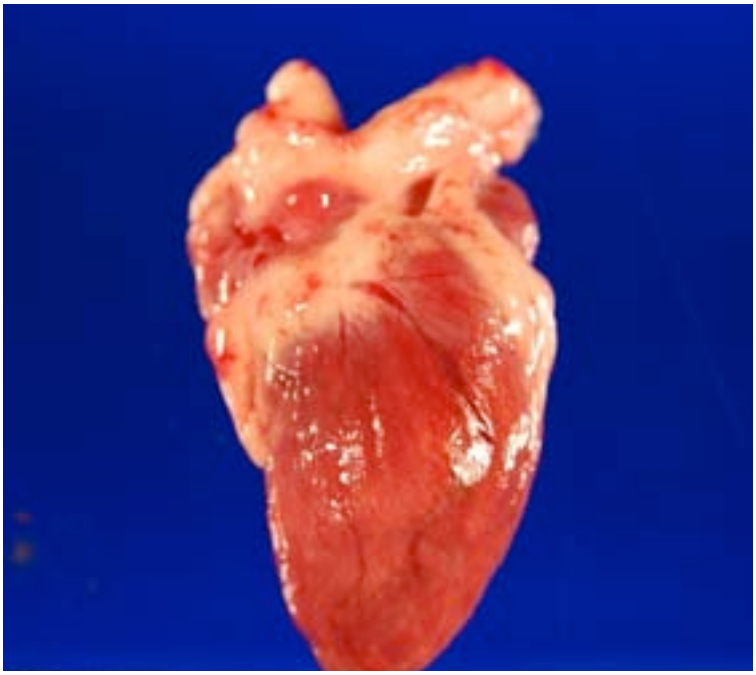

*2-1. Heart, penguin: The myocardium contains numerous pale streaks, and petechiae are distributed randomly at the heart base. (Photo courtesy of: Department of Molecular and Comparative Pathobiology, Johns Hopkins University, 733 N. Broadway, Suite 811, Baltimore, MD 21205)*

**Histopathology:** Multifocal areas of degeneration, necrosis and inflammation centered on capillaries disrupt approximately 20 – 30% of the left and right ventricular myocardium. Areas of degeneration and necrosis are characterized by pale cardiomyocytes with extensive vacuolation of the sarcoplasm (degeneration), loss of cross striations, fragmented, hypereosinophilic fibers, pyknotic nuclei, scattered karyorrhectic nuclear debris (necrosis) and occasional degenerate heterophils. Multifocally, surrounding blood vessels are infiltrated by moderate numbers of macrophages, lymphocytes, plasma cells, and heterophils. Multifocally, within these areas of inflammation, there are numerous endothelial cells displaying abundant vacuolated cytoplasm often expanded by oval to round, 15 – 25 µm thin wall (1 µm) cysts (schizont) containing between 15 – 30 1 – 2 µ m, round, basophilic apicomplexans (merozoites). Some sections contain a focal, 1 – 2 mm, intravascular aggregate of basophilic to granular material surrounded by layers of fibroblasts, myoepithelial cells, fibrin, and scattered erythrocytes (thrombus), which occludes 80% of a medium caliber artery. Scattered lymphocytes are present within the endocardium. Multifocally separating muscle fascicles and in between blood vessels there are moderate amounts of edema, scattered hemorrhage and numerous small foci of fibrin localized in and around necrotic endothelial cells.

**Morphologic Diagnosis:** Heart, myocarditis, necrotizing, chronic, multifocal, moderate with lymphohistiocytic and heterophilic infiltrate, fibrin deposition, edema, hemorrhage, thrombosis and intra-endothelial, extra-erythrotic schizonts.

**Contributor's Comments:** Avian malaria is caused by single celled, intracellular parasite of the *Hemosporidia* phylum, which includes *Haemoproteus*, *Paraemoproteus*, *Leucocytozoon*, *Plasmodium*, and *Hepatocystis*.[1] *Plasmodium* spp. are one of the main hemoparasites affecting

captive bird species, including penguins. Development and transmission of *Plasmodium* species occur in mosquitoes of genera *Culex, Aedes*, and rarely *Anopheles*. Often wild bird species are able to control disease and serve as reservoirs for infection, however, symptomatic birds can present with a range of clinical symptoms including hemolysis and anemia. Most of the clinical symptoms are attributed as a result of severe anemia including anorexia, depression, vomiting, and dyspnea, which may all occur hours before death. Outbreaks in North America have been seen in anseriforms (ducks, geese, and swans), Passeriformes (perching birds, robins, blue jays, and etc.), and columbiforms (doves and pigeons).[7]

Avian malaria associated with *Plasmodium sp.* is a major cause of avian morbidity and mortality in zoos worldwide, most notably captive penguin populations. Several *Plasmodium* sp. have been implicated as causative agents of avian malaria in captive penguins, including *P. relictum*, *P. enlongatum*, *P. tejerai*, and *P. juxtanuclear*.[2,4,8,11,12] *Plasmodium* sp. have a complex life cycle involving both asexual and sexual reproductive stages, which take place in the host and vector. When an infected female mosquito takes a blood meal, sporozoites are released into the host's peripheral circulation. The sporozoites then invade cells of the reticuloendothelial system where they multiply and grow within parasitophorous vacuoles to produce schizonts, which can contain up to 10,000 – 30, 000 merozites (in the case of *Plasmodium falciparum*). Most commonly this development is in the liver, but they will also develop in other tissues such as the kidney, lungs, CNS, spleen, and heart. The schizonts produce thousands of merozoites, which are released into host cell-derived merosomes that are protected from host immunity. At this point individual merozoites are released into the circulation and infect erythrocytes. In the erythrocyte they develop into trophozoites (the feeding or ring stage).While feeding on hemoglobin they release hemoglobin pigments (hemozoin) which are a by-product of hemoglobin metabolism and a feature of the erythrocyte life cycle stage that can be appreciated on histopathology of the liver and lungs. Trophozoites then develop into a schizonts containing between 8-32 merozoites, which once released into the circulation can reinfect more erythrocytes recapitulating this stage of the infectious life cycle. After several cycles of invading erythrocytes, some of the merozoites transform into microgametocytes and macrogametocytes. Once a mosquito ingests erythrocytes containing these gametes, they further develop and fuse forming oocysts that yield the infective sporozoites.[1,6,7,10]

The extra-erythrocytic pathway of replication predominates in penguins, explaining the generally low levels of parasitemia seen on blood smears.[4,11,12] Previous studies demonstrated the utility of leukocyte counts as another predictive factor of parasitism to combine with blood smear evaluation. In cases with detectable parasitemia, the severity of leukocytosis was often a predictive factor in disease severity.[11] In this animal, the relative leukocyte count was greater than 75,000 WBC/uL. Immune suppression associated with stress, other infectious agents, or immaturity have been consistently demonstrated to be a contributing factor in *Plasmodium* disease

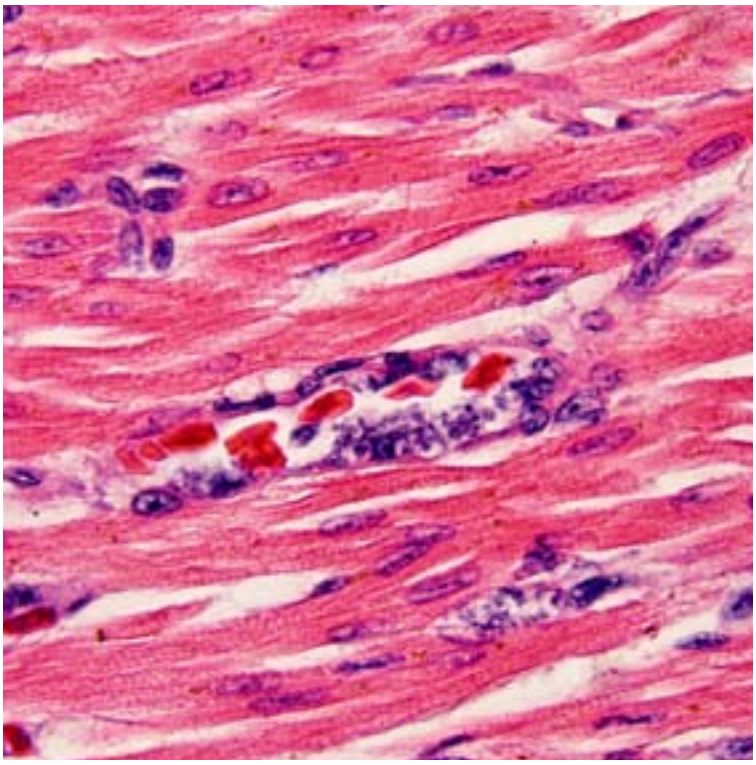

*2-2. Heart, penguin: Numerous capillary endothelial cells are distended, partially occluding the lumen, by a single intracytoplasmic 20 µm schizont containing numerous round basophilic merozoitse, consistent with Plasmodium sp. (HE 600X)*

progression in captive penguins.[3] Penguin mortality is closely associated with the presence of disseminated extra-erythrocytic replication, including in the liver, lung, heart, kidney, and CNS.[4,8,11]

This penguin came from a colony previously known to be infected with both *Plasmodium relictum* and *P. elongatum*. Historically, disease surveillance of this colony via blood smear analysis has often yielded low to undetectable blood parasite levels, yet, necropsy of a small numbers of these animals over a 15-year period reveal that some of the animals suffered from severe multi-organ disease attributed to extra-erythrocytic replication of *Plasmodium sp*. Similar to previous cases, intra-endothelial protozoa with morphology consistent with *Plasmodium sp.* schizonts were noted in the liver, lung, spleen, kidney, meninges, brain, and heart. Repeated episodes of seizures in this animal are attributed to the development of meningoencephalitis. Interestingly, focal arterial thrombosis was noted in several sections of the heart from this animal. Coagulopathies in humans infected with *Plasmodium falciparum* are thought to be associated with the ability of parasitized erythrocytes to activate the coagulation cascade through recognition of numerous receptors and pathways.[5] Based on this finding it is a possibility that a similar phenomenon may exist with avian malaria.

**JPC Diagnosis:** Heart: Intraendothelial protozoa, etiology consistent with *Plasmodium* spp., with myofiber necrosis and edema.

**Conference Comment:** *Plasmodium* spp. has a complex, two-stage life cycle of which the contributor does an exceptional job of describing. Exoerythrocytic stages typically occur in the liver and spleen initially, while endothelial cell infection becomes especially prominent within the lung in more advanced cases. Tissue sections in this case represent the described exoerythrocytic stage where meronts are found within endothelial cells of the heart. Anemia is not usually a feature of this disease in penguins as erythrocyte infection rate is usually low while massive endothelial exoerythrocytic schizogony is quite characteristic.[1,4]

In the penguin alone, schizonts, merozoites and gametocytes may be detected simultaneosly. Schizonts are smaller than the host nucleus and there is little cytoplasm present. The merozoite stage is directly adjacent to the erythrocyte nucleus, also with little or no cytoplasm. Gametocytes are variably shaped, from irregular to spherical, and occasionally displace the host cell nucleus.[8]

**Contributing Institution:** Department of Molecular and Comparative Pathobiology
Johns Hopkins University
733 N. Broadway, Suite 811
Baltimore, MD 21205

**References**

1. Bermudez AJ. Miscellaneous and sporadic protozoal infections. In: Calnek BW, ed. Diseases of Poultry. 11th ed. Ames, Iowa: Iowa State Press; 2003:1010-1015.
2. Bueno MG, Lopez RP, de Menezes RM, Costa-Nascimento Mde J, Lima GF, et al. Identification of Plasmodium relictum causing mortality in penguins (Spheniscus magellanicus) from São Paulo Zoo, Brazil. *Vet Parasitol*. 2010;11:173(1-2):123-7.
3. Cranfield MR, Graczyk TK, Beall FB, Ialeggio DM, Shaw ML, Skjoldager ML. Subclinical avian malaria infections in African black-footed penguins (Spheniscus demersus) and induction of parasite recrudescence. *J Wildl Dis*. 1994;30(3): 372-6.
4. Fix AS, Waterhouse C, Greiner EC, Stoskopf MK. Plasmodium relictum as a cause of avian malaria in wild-caught magellanic penguins (Spheniscus magellanicus). *J Wildl Dis*. 1988;24(4):610-9.
5. Francischetti IMB, Seydel KB, Montiero RQ. Blood coagulation, inflammation, and malaria. *Microcirculation*. 2008;15(2):81-107.
6. Gardiner CH, Fayer R, Dubey JP. An Atlas of Protozoan Parasites in Animal Tissues. 2nd ed. Washingtn, DC: Armed Forces Institute of Pathology; 1998:65-66.
7. Greiner EC, Ritchie BW. Parasites. In: Ritchie BW, Harrison GJ, Harrison LR , eds. Avian Medicine: Principles and Application. Lake Worth, FL; Wingers Publishing, Inc. 1994:1019-1021.
8. Grim KC, Van der Merwe E, Sullivan M, Parsons N, McCutchan TF, Cranfield M. Plasmodium Juxtanucleare associated with mortality in black-footed penguins (Spheniscus demersus) admitted to a rehabilitation center. *J Zoo Wildl Med*. 2003;34(3):250-5.

9. Jones TC, Hunt RD, King NW. *Veterinary Pathology*. 6th ed. Baltimore, MD: Williams and Wilkins; 1996:590-593.
10. Olivier S, Mota M, Matuschewski K, Prudêncio M. Interactions of the malaria parasite with its host. Current opinion in microbiology. Volume 11. 2008;(4):352–359.
11. Stoskopf MK, Beier J. Avian malaria in African Black-Footed Penguins. *JAVMA*. 1972;175(9):944-7.
12. Vanstreels RE, Kolesnikovas CK, Sandri S, Silveira P, Belo NO, Ferreira Junior FC, et al. Outbreak of avian malaria associated to multiple species of Plasmodium in magellanic penguins undergoing rehabilitation in southern Brazil. PLoS One. 2014;15;9(4):e94994.

**CASE III**: L13 14765 (JPC 4041399).

**Signalment:** 2-year-old male inland bearded dragon, *Pogona vitticeps*.

**History:** A 2-year-old male bearded dragon was living in a glass terrarium with sand substrate, UVB light, and a basking bulb as a classroom pet. The animal presented with a 3-week history of multifocal raised nodules on its dorsum, ventrum, and head; several of which were exfoliating upon manual examination revealing areas of ulceration. Impression smears obtained from ulcerations on the dorsum, ventrum, neck, and above the left eye were suggestive of fungal infection with evidence of granulomatous inflammation. The owner elected euthanasia due to poor prognosis of medical treatment efficacy.

**Gross Pathology:** Post mortem examination identified bilaterally symmetrical, circular, oval areas of yellow discoloration on the ventral abdomen that each measured 3.5x3 cm, extending onto the proximal limbs, ventral neck, and head. Multifocally, there were also raised, irregular, firm lesions with thickened epidermis in the left periorbital region (1.5x1.5 cm), on the left caudal mandible (3x2.5x1 cm), on the right dorsal neck (2,5x2 cm), and on the right body wall caudal to the thoracic limb (2x1.5 cm). On cut surface, these raised lesions consisted of poorly defined, firm, whitish nodules, surrounded by pale yellow, soft tissue of gelatinous consistency. The skin also had multiple annular areas of ulceration: above the left eye (2x2 cm), left dorsum (2x2 cm), and ventrally between the thoracic limbs (1.5x1 cm). No other abnormalities were noted at necropsy.

**Laboratory Results:** Mycology culture: *Chrysosporium* sp. isolate.

PCR: *Nannizziopsis guarroi* based on DNA sequence analysis of the ITS and D1/D2 regions (performed at the University of Texas Health Sciences Center).

**Histopathologic Description:** Skin: Alterations in all sections of the examined raised skin lesions from different areas are similar and, thus, will be described collectively. There are extensive areas of ulceration flanked by epidermis with extensive chromatophore accumulation just beneath the epidermal basal lamina. The superficial epidermis has multifocal areas of degeneration, characterized by vacuoles filled with eosinophilic, proteinaceous cellular debris and overall loss of cellular stratification. At the interface of the ulcerated and intact epidermis, the stratum corneum is moderately thickened with no retention of nuclei (orthokeratotic hyperkeratosis). The dermis is moderately expanded by edema and inflammatory cell infiltrate, composed of heterophils and macrophages. Underlying the ulcerated regions, the dermis is markedly expanded by multifocal to coalescing granulomas within dense fibrous connective tissue. Granulomas are composed of necrotic centers, surrounded by concentrically arranged epithelioid

*3-1. Scaled skin, bearded dragon: There are multiple firm areas of epidermal hyperplasia in the left periorbital region. (Photo courtesy of: Department of Pathobiological Sciences, School of Veterinary Medicine, Louisiana State University, http://www1.vetmed.lsu.edu//PBS/index.html)*

*3-2. Scaled skin, bearded dragon: There are bilaterally symmetrical, irregularly round areas of yellow discoloration on the ventral abdomen which measure 3.5x3 cm each. (Photo courtesy of: Department of Pathobiological Sciences, School of Veterinary Medicine, Louisiana State University, http://www1.vetmed.lsu.edu//PBS/index.html)*

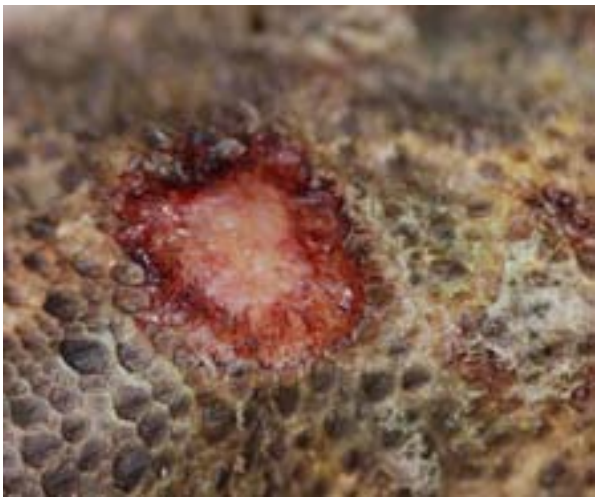

*3-3. Scaled skin, bearded dragon: There was an annual area of ulceration on the left dorsum. (Photo courtesy of: Department of Pathobiological Sciences, School of Veterinary Medicine, Louisiana State University, http://www1.vetmed.lsu.edu//PBS/index.html)*

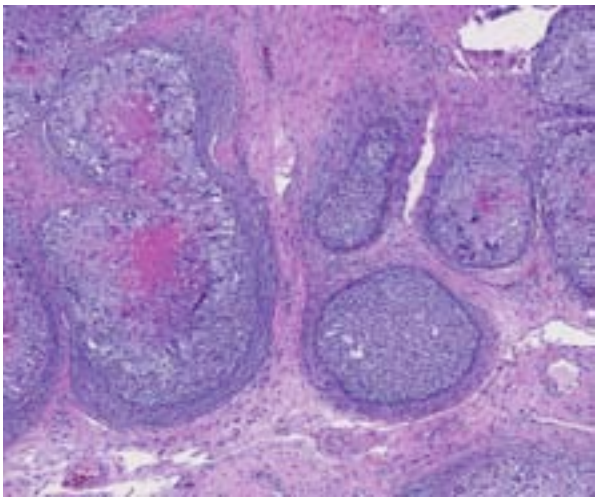

*3-4. Scaled skin, bearded dragon: Underneath the ulcerated epidermis, there are numerous discrete granulomas within the dermis. (HE 47X)*

macrophages interspersed with heterophils and multinucleated giant cells, and encapsulated by fibroblasts. The dense connective tissue surrounding and separating the granulomas is markedly infiltrated by heterophils, macrophages, lymphocytes, and plasma cells. Overlying the granulomas and replacing the epidermis is extensive necrotic cellular debris admixed with hemorrhage, aggregates of dark yellow-to-brown pigment, and dense tufts of arthroconidia and hyphae embedded within dense layers of keratin. Occasional fungal organisms, similar to those described previously, are also identified within the granulomas and loosely within the dermal connective tissue. The subcutis contains mild inflammatory cellular infiltrates, consisting of heterophils, lymphocytes, plasma cells, and mast cells, with random foci of necrosis.

In sections of the ventral abdomen, deep layers of the epidermis contain multifocal, round, expansile aggregates of myriad fungal spores and hyphae. Fungal aggregates are primarily encased in dense keratin, and other times they are found clustered within the superficial stratum corneum. Fungal organisms are similar to those described above in the raised skin lesions. Commonly, arthroconidia are identified among the hyphae as well as free within the nearby epidermis. Epidermal changes surrounding the fungal aggregates include moderate dilation of intercellular spaces (spongiosis), ballooning degeneration, and mild transmigration of heterophils. Segmentally, in close proximity to the fungal organisms, the stratum corneum displays moderate orthokeratotic hyperkeratosis. In the underlying dermis, there is moderate infiltrate composed mainly of heterophils, lymphocytes, plasma cells and macrophages.

**Contributor's Morphologic Diagnosis:** Skin: Proliferative and ulcerative dermatitis, granulomatous, multifocal, chronic, severe, with myriad intralesional segmented hyphae and arthroconidia.

**Contributor's Comment:** While the majority of fungal organisms affecting reptiles are believed to be opportunistic, *Nannizziopsis* sp. have been suggested as obligate fungal pathogens of reptiles. An infectious model with veiled chameleons fulfilled Koch's postulate in transmitting what is now known to be *Nannizziopsis dermatitidis* via application of the fungus to intact and abraded skin, with subsequent development of the lesions observed naturally. *N. dermatitidis*. was also determined to be infectious via direct contact and/or through fomite transmission in the same study.[3]

The *Nannizziopsis* species seen most commonly in bearded dragons and green iguanas is *N. guarroi*.[1,2] The disease is often called Yellow Fungus Disease by hobbyists because the crusts found on bearded dragons tend to have yellow discoloration. Thus, crust formation, color change and necrosis are commonly seen in these cases. Lesions tend to be multifocal and may include the head, oral cavity, limbs, ventrum and dorsum. The infection is often aggressive, with extension into

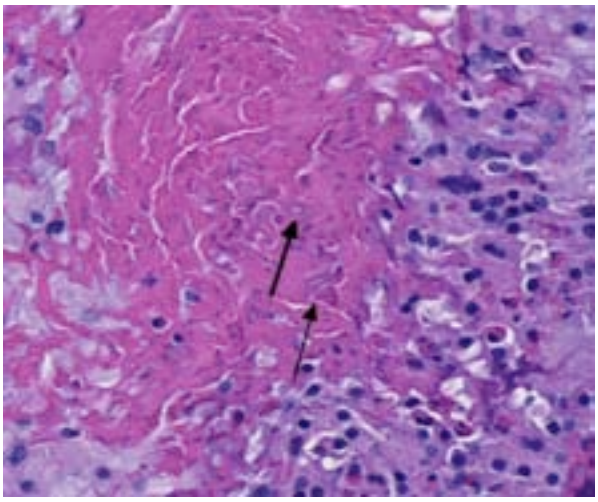

*3-5. Scaled skin, bearded dragon: Cross- and tangential sections of arthroconidia and pauciseptate fungal hyphae (arrows) may be seen within granulomas. (HE 356X)*

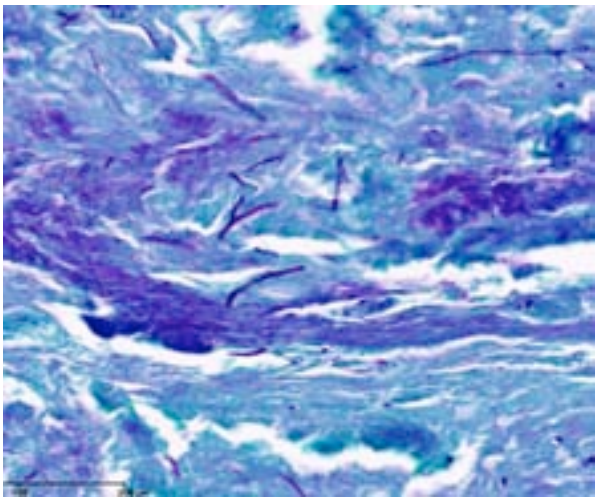

*3-6. Scaled skin, bearded dragon: A PAS stain on the overlying keratin crust demonstrates the morphology of numerous fungal hyphae and occasional arthroconidia. (Photo courtesy of: Department of Pathobiological Sciences, School of Veterinary Medicine, Louisiana State University, http://www1.vetmed.lsu.edu//PBS/index.html)*

the subcutaneous tissues, muscles, and bones.[3] In some cases there is also systemic spread to the lungs and liver after local cutaneous invasion.[3]

This inland bearded dragon had multifocal raised nodules on the skin, with multiple areas of ulceration and an irregular oval area of yellow discoloration on the ventral head, neck and abdomen, with no evidence of extension into underlying muscle and/or bone. Microscopically the raised nodules consisted of granulomatous proliferative dermatitis. Additionally, there was superficial ulceration with myriad intralesional segmented hyphae and arthroconidia, which by mycological culture and PCR were identified as *Nannizziopsis guarroi*.

Recently, morphologically similar isolates formerly referred to as members of the "CANV" complex, have been properly identified into three genera: *Nannizziopsis, Paranannizziopsis*, and *Ophidiomyces*, which are not particularly closely related within the Onygenales. The genus *Nannizziopsis* was split into 8 unique species: *N. vriesii, N. dermatitidis, N. crocodili, N. barbata, N. guarroi, N. infrequens, N. hominis*, and *N. obscura*. Benefits of this classification scheme include clarification of the range of susceptible hosts for each fungal species, monitoring trends of infection, determination of the prevalence of specific species in the environment, ability to evaluate species-specific antifungal efficacy, and development of specific strategies for disease prevention.[4]

*N. guarroi* is a keratinophilic ascomycetous fungus that has been associated with several cases of granulomatous dermatitis in toxicoferan squamates. Due to the inherent stress that may accompany classroom pets related to frequent handling and/or taunting, the role of stress cannot be ruled out in the susceptibility to the fungal infection in this case. *N. guarroi* do not grow at 40 °*C* and hospitalizing reptiles at increased temperatures during treatment may help the patient eliminate the fungus. Additionally, laboratories may be underreporting *N. guarroi* infections if culture protocols call for temperatures in excess of 37 °*C (false negatives), stressing the importance of communication with laboratories in suspected N. guarroi cases*.[2]

**JPC Diagnosis:** Skin: Ulcerative crusting dermatitis, with granulomatous inflammation and intralesional fungal elements, etiology consistent with *Nannizziopsis* guarroi.

**Conference Comment:** *N. guarroi* dermatomycosis is a contagious disease that can have severe consequences for reptile collections. Hyphal proliferation occurs initially within the superficial dead epidermal layers.[3] As with many skin diseases in reptiles, the scale fold becomes an excellent media for infection as keratin becomes impacted. From here, hyphae penetrate downward pushing through the basement membrane. The fungal invasion can continue beyond the dermis into the subjacent musculature.[3] Necrotizing

cutaneous infections can progress to systemic disease and may become fatal.[2]

Fungi have used a nomenclature inconsistent with the rest of biology. There are separate genus and species names for asexual anamorph stages and sexual teleomorph stages of the same organism, resulting in multiple species names and paraphyletic taxa. In 2011, it was decided by the Nomenclature Section meeting of the International Botanical Congress that teleomorph names should be used (Hawksworth, 2011). This is problematic for medicine, as nearly all names of systemic fungi routinely used are anamorph names (e.g. *Cryptococcus, Blastomyces, Histoplasma, Aspergillus*, etc.). The anamorph genus *Chrysosporium* is widespread across the tree of the fungal order Onygenales, and contains organisms in more than 15 teleomorph genera, including *Nannizziopsis*. Many *Chrysosporium* sp. infecting reptiles have been morphologically misidentified as "*Chrysosporium* anamorph of *Nannizziopsis vriesii* (CANV)"

Recent publications have identified *Nannizziopsis guarroi* as the most common cause of yellow skin disease in bearded dragons.[1,5] This correlates with PCR findings in this case, and further illustrates the inaccuracy of the term CANV for this entity.

*Special thanks to Dr. Jim Wellehan, Asst. Professor at the University of Florida College of Veterinary Medicine for his contributions to this case*

**Contributing Institution**: Department of Pathobiological Sciences
School of Veterinary Medicine
Louisiana State University
http://www1.vetmed.lsu.edu//PBS/index.html

**References:**

1. Abarca ML, Castella G, Martorell J, Cabanes FJ. *Chrysosporium guarroi* sp. nov. a new emerging pathogen of pet green iguanas (*Iguana iguana)*. *Med Mycol*. 2010;48:365-372.
2. Abarca ML, Martorell J, Castellá G, Ramis A, Cabañes FJ. Der- matomycosis in a pet inland bearded dragon (*Pogona vitticeps*) caused by a Chrysosporium species related to Nannizziopsis vriesii. *Vet. Dermatol*. 2009;20:295–299.
3. Hawksworth DL. A new dawn for the naming of fungi: impacts of decisions made in Melbourne in July 2011 on the future publication and regulation of fungal names. *MycoKeys*. 2011;1: 7–20.
4. Paré JA, et al. Pathogenicity of the *Chrysosporium Anamorph* of *Nannizziopsis vriesii* for veiled chameleons (*Chamaeleo calyptratus*). *Medical Mycology*. 2006;44:25-31.
5. Sigler L, et al. Molecular characterization of reptile pathogens currently known as members of *Chrysosporium* anamorph of *Nannizziopsis vriesii* complex and relationship with some human-associated isolates. *Journal of Clinical Microbiology*. 2013;51:3338-3357.
6. Stchigel AM, Sutton DA, Cano-Lira JF, et al. Phylogeny of chrysosporia infecting reptiles: proposal of new family *Nannizziopsiaceae* and five new species. *Persoonia*. 2013;31:86-100.

**CASE IV:** S11-1330 (JPC 4019410).

**Signalment:** Adult male giant ditch frog, *Leptodactylus fallax*.

**History:** The frogs lived in the Zürich zoo and were put in quarantine for one week because of renovation of their terrarium. After putting the frogs back in the compound, some frogs suddenly died. These were sent to the Institute of Veterinary Pathology of Zürich for examination.

**Gross Pathology:** Nutrient status: The frog was severely emaciated.

Integument: The skin on the ventrum, as well as proximally on the hind legs, was diffusely reddened and, mainly on the ventrum, severely eroded. The right forelimb, distal from the elbow, was swollen and had a focal poorly demarcated thickening (1-2 mm) measuring 1 x 0.4 cm dorsally; this involved the subcutis and the underlying musculature which was diffusely discolored yellow (with multifocal yellow crumbly material deposits).

Coelomic cavity: the liver was interspersed with multiple, round, variably sized (0.5-2 mm in diameter) yellowish soft masses that had sometimes a creamy center. All other organs were macroscopically unremarkable.

**Laboratory Results:** Ziehl-Neelsen staining: No acid fast bacteria were visible.

PAS staining: The fungal structures were positive but the brownish color obliterated the PAS staining.

A fungal culture was not performed and the PCR of paraffin embedded liver was negative for any fungus.

A parasitologic analysis of the feces was negative.

The bacteriological analysis of the coeloma (swab) demonstrated a mild content of *Pseudomonas aeruginosa*, *Serratia marcescens*, *Enterobacter* sp., and *Acinetobacter* sp., all considered most likely as contaminants.

**Histopathologic Description:** Liver: Randomly distributed there are multiple 1 mm diameter granulomas consisting of central eosinophilic granular material (focal caseous necrosis) surrounded by macrophages and proliferating

*4-1. Skin and coelom, frog: There is multifocal hyperemia and erosion of the skin of the abdomen and legs, as well as disseminated granulomas throughout the liver. (Photo courtesy of: University of Zürich, Institute for Veterinary Pathology, Vetsuisse Faculty, Winterthurerstrasse 268, CH-8057 Zürich, Switzerland)*

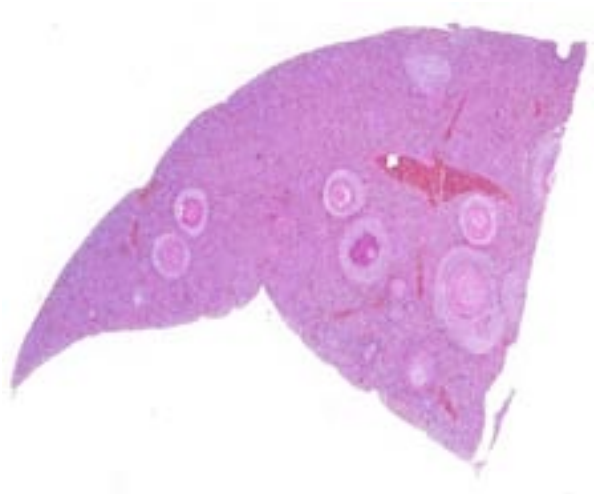

*4-2. Liver, frog: There are numerous discrete granulomas scattered randomly throughout the section. (HE 6.3X)*

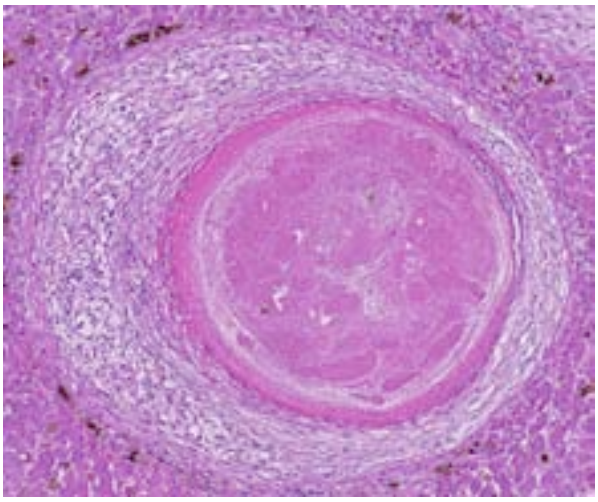

*4-3. Liver, frog: Higher magnification of one of the hepatic granulomas. (HE 80X)*

fibroblasts, forming a thin irregular to thick fibrous wall. Within the granulomas, multinucleated giant cells of the foreign body type (with all nuclei aligned circular at the border of the cells) and of the Langhans type (with randomly arranged nuclei), as well as lymphocytes, are visible. Mainly in the necrotic areas, but also in lesser numbers randomly distributed in the surrounding fibrous wall, there are roundish structures (10-15 µm in ø) that are sometimes centrally septated (binary fission) and sometimes grouped in clusters of 2-5. The wall of these structures is brownish-gold with a total thickness of about 1 µm (structures interpreted as fungal sclerotic cells = Medlar bodies). Hyphal structures were not found.

Kidneys (not submitted): Granulomas as described above were found.

Skeletal musculature (not submitted): Multifocally extensive muscular degeneration is present, characterized by loss of cross striations and hypereosinophilia of the cytoplasm. Within the degenerate musculature, small clusters of sclerotic bodies are present embedded within extensive granulomas.

Skin (not submitted): Multifocal extensive and deep ulcerations are observed with embedded pigmented fungi in small amounts.

**Contributor's Morphologic Diagnosis:**

Liver: Hepatitis severe, multifocal, (necrotizing and) granulomatous, with presence of fungal pigmented sclerotic bodies and multinucleated giant cells (foreign and Langhans type)

Kidney, coeloma and musculature: Interstitial nephritis, coelomitis and myositis, severe, multifocal, (necrotizing) and granulomatous, with presence of fungal pigmented sclerotic bodies and multinucleated giant cells (foreign and Langhans type)

Skin: Dermatitis, severe, ulcerative and necrotizing, multifocal to confluent, with presence of pigmented fungal structures and secondary severe bacterial colonisation

Musculature: Hyaline muscle fiber degeneration, dystrophic calcification and necrosis, mild to moderate and multifocal

**Contributor's Comment:** Chromoblastomycosis is a worldwide distributed zoonotic skin disease that most commonly presents in the tropical regions and is caused by several dematiaceous (pigmented) saprophytic fungi belonging to the division of the ascomycota. The most important etiologic agents for this disease are *Fonsecae* (*F. pedrosoi and F. compacta*), *Phialophora verrucosa* and *Cladosporium carionii*. *Fonseca pedrosoi* is the most common agent found in the tropical forests (Amazon) and in temperate regions in Latin America; *Cladophialophora*

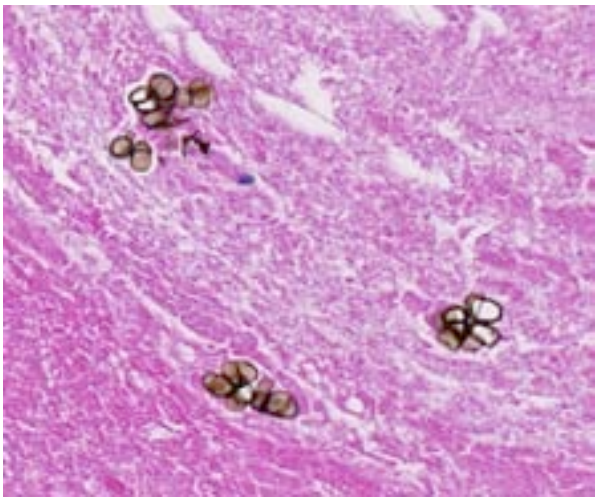

*4-4. Liver, frog: Within the necrotic center of the granuloma, there are clusters of pigmented sclerotic bodies which are septate as a result of ongoing binary fission. (HE 80X)*

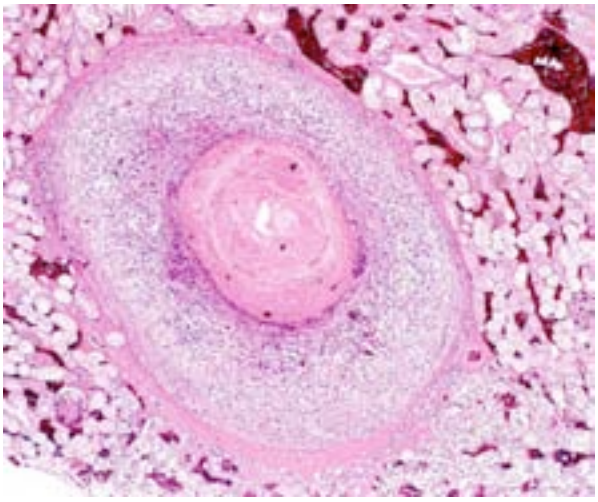

*4-5. Kidney, frog: Granuloma within the kidney. (Photo courtesy of: University of Zürich, Institute for Veterinary Pathology, Vetsuisse Faculty, Winterthurerstrasse 268, CH-8057 Zürich, Switzerland)*

*carrionii* is the most common agent in dry countries and desert regions (Australia, South Africa and Cuba).[1]

These ubiquitous fungi are mainly inoculated by trauma. In warm blooded animals (most often humans and rarely other mammals like cats, horses and dogs), the subcutaneous skin is focally affected, growing slowly to warts or verrucous plaques; only seldom and very late in the disease they may disseminate into lymphatics and blood vessels. The most important complications are damage of the lymphatic system and malignant transformation of the epidermis in the affected regions. The pathogenesis of this disease in cold blooded animals differs from the mammalian cases and is usually systemic, involving mainly skin and internal organs; it has been observed mainly in frogs[6] and toads[2,7] but is also present in other amphibians and in reptiles like marine radiate tortoises.[8] Predisposing factors include any kind of stress in animals as, for example, removal from their natural habitat or competition for food with subsequent bite wounds.

Macroscopically, usually ulcerating and non-ulcerating gray to yellow nodules (up to 5mm) are present in the skin (mainly belly, head and legs) and other organs such as liver, kidneys, heart, lungs, body fat, ovaries, brain, spleen, bone marrow. Histologically, these nodules present as granulomas, with central coagulative to caseous necrosis, many multinucleated giant cells, epithelioid cells and dark brown roundish and thick walled fungal structures, also called sclerotic cells, or Medlar bodies, that frequently undergo equatorial septation (replication by binary fission) and lie extracellularly in small clusters or are phagocytosed by giant cells; more seldom, septated hyphae and pseudohyphae are found. In some cases (e.g. the madagascan radiate tortoise[7]), the lesion presents histologically as an abscess with a central core of heterophils and many dark brown sclerotic bodies surrounded by giant cells, lymphocytes and fibroblasts.

The detection of septate sclerotic bodies is pathognomonic for chromoblastomycosis. A phaeohyphomycosis, also caused by dematiaceous fungi, can be excluded morphologically because they form broad septate hyphae.

Different therapy protocols exist in humans depending on the fungal agent, location and extent of the lesion. In amphibians and reptiles, the best protocol seems to be amputation. It is only possible if performed during early stages when the infection is limited to the skin; other treatments like antifungal drugs have been reported to be ineffective.[2,6] Because of its zoonotic potential, careful handling of affected animals is advised.

**JPC Diagnosis:** Liver: Granulomas, multiple, with sclerotic bodies.

**Conference Comment:** This is a nice case of one of the darkly pigmented dematiaceous fungi which, in most cases, derive their characteristic appearance from the production of melanin.[3]

Melanin is used by many pathogens as a virulence factor aiding in colonization and evasion of the immune system by virtue of its antioxidant properties and ability to disrupt antibody-mediated phagocytosis, counteract antifungal agents and bind iron.[5]

Other dematiaceous fungi include those which cause phaeohyphomycosis. These typically exist in tissue as hyphae rather than the distinct sclerotic bodies of chromoblastomycosis species. Sclerotic bodies are the result of cell division by binary fission, in contrast to most fungal pathogens that replicate through budding.[3]

Important differentials to consider for granulomas in frogs include *Mycobacterium marinum* and *Brucella* spp., as both may have some overlap with histopathology. Chromoblastomycosis is a relatively common condition in amphibians and can result in severe systemic disease and frequently death, with the most often targeted organs being the skin, liver, lungs and kidneys. Encephalitis and meningitis has also been reported in these species.[2] Chromoblastomycosis can cause outbreaks in stressed colonies and strict quarantine guidelines must be adhered to due to its transmissibility between animals and humans.[6]

**Contributing Institution:** University of Zürich
Institute for Veterinary Pathology, Vetsuisse Faculty
Winterthurerstrasse 268, CH-8057
Zürich, Switzerland

**References:**

1. Ahmeen M. Managing chromoblastomycosis. *Tropical Doctor*. 2010;40:65-67.
2. Bube A, Burkhardt E, Weiss R. Spontaneous Chromoblastomycosis in the Marine Toad (*Bufo marinus*). *Journal of Comparative Pathology*. 1992;106:73-77.
3. Dixon DM, Polak-Wyss A. The medically important dematiaceous fungi and their identification. *Mycoses*. 1991;34(1-2):1-18.
4. Guedes Salgado Claudio. Fungal x host interactions in chromoblastomycosis, what we have learned from animal models what is yet to be solved. *Virulence*. 2010;I(I):3-5.
5. McAdam AJ, Milner DA, Sharpe, AH. Infectious diseases. In: Kumar V, Abbas AK, Aster JC, eds. *Robbins and Cotran Pathologic Basis of Disease*. 8th ed. Philadelphia, PA: Elsevier Saunders; 2015:388.
6. Miller E, Montali R, Ramsay E. Rideout B. Disseminated Chromoblastomycosis in a colony of ornate-horned frogs (*Ceratophirs Ornata*). *Journal of Zoo and Wildlife Medicine*. 1992;23(4): 433-438.
7. Velasquez LF, Restrepo MA. Chromomycosis in the toad (*Bufo marinus*) and a comparison of the ethiologic agent with fungi causing human chromomycosis. *Sabouradia*. 1975;13:1-9.
8. Verseput MP. Chromoblastomycosis in a Madagascan Radiate Tortoise, Geochelone Radiata. *The Journal of Herpetological Association of Africa*. 1990;38(1):14-15.

**Joint Pathology Center**
**Veterinary Pathology Services**

*Conference Coordinator*
**Matthew C. Reed, DVM**
**Captain, Veterinary Corps, U.S. Army**
**Veterinary Pathology Services**
**Joint Pathology Center**

## WEDNESDAY SLIDE CONFERENCE 2014-2015

# Conference 10

**29 October 2014**

**Conference Moderator:**
MAJ Brian Smith, DVM, DACVP
Chief, Resident Training
Veterinary Pathology Service
Joint Pathology Center
606 Stephen Sitter Ave
Silver Spring, MD 20910

**CASE I:** V14-14710 (JPC 4049286).

**Signalment:** Adult male Maine Coon cat, *Felis catus.*

**History:** The cat was found dead in the home by a relative taking care of the cat for a hospitalized man.

**Gross Pathology:** The right front foot and the right antebrachium were swollen approximately 2 times their original size. There were open wounds on the cranial aspect of the right carpus with dried exudate on the hair adjacent to the wounds. The subcutis of the right front foot and right antebrachium were edematous and bright red up to the right elbow. The right prescapular lymph node was enlarged 5-6 times its normal size and the right axillary lymph node was enlarged 2-3

*1-1. Lung, cat: At necropsy, the right antebrachium and paw were swollen to twice normal size with multiple open cutaneous wounds. (Photo courtesy of: New Mexico Department of Agriculture Veterinary Diagnostic Services, http://www.nmda.nmsu.edu/vds/).*

*1-2. Lung, cat: The lungs contained multiple randomly distributed firm targetoid foci. (Photo courtesy of: New Mexico Department of Agriculture Veterinary Diagnostic Services, http://www.nmda.nmsu.edu/vds/).*

*1-3. Lung, cat: At subgross examination, 75% of the alveolar spaces are filled with a cellular exudate. (HE 6.3X)*

times its normal size. Both of the lymph nodes were mottled tan and bright red with foci of necrosis within the lymph node on cross section. The lungs contained multiple random firm targetoid foci that had a tan center surrounded by a red ring, which was further surrounded by a tan ring. These foci were randomly distributed in all of the lung lobes. There was one pinpoint tan focus on the capsule of the spleen.

**Laboratory Results:** *Yersinia pestis* was isolated from a swab of the wound on the right front leg, the right axillary lymph node, the lung, the liver, and the spleen.

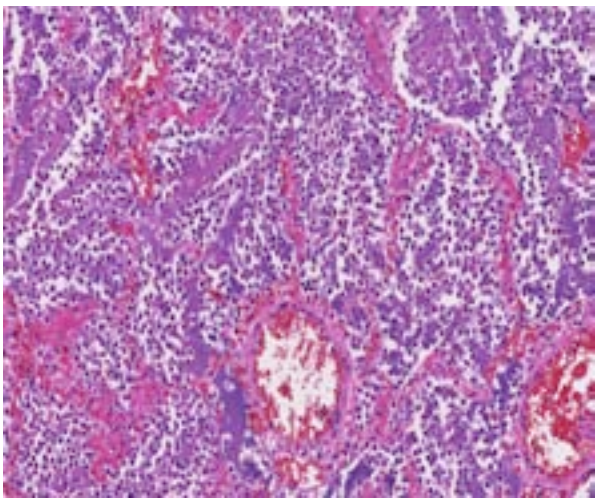

*1-4. Lung, cat: Alveoli contain numerous viable and degenerate neutrophils and large basophilic colonies of bacilli, a characteristic finding associated with Yersinia pestis. (HE 168X)*

**Histopathologic Description:** The lung contains multiple large foci of necrosis filled with necrotic debris, myriad coccobacilli, and degenerate neutrophils. The necrotic areas often contain an arteriole with a necrotic tunica media that is infiltrated by neutrophils. The affected arterioles are surrounded by myriad coccobacilli, and occasionally contain fibrin thrombi. The foci of necrosis are surrounded by a concentric variably thick layer of numerous neutrophils, fibrin, hemorrhage, and myriad bacteria. The alveoli of the lung between the foci of necrosis contain small variable numbers of coccobacilli and intact and degenerate neutrophils that occasionally become dense enough to coalesce into foci of necrosis. There are rare small arterioles and alveolar capillaries that contain emboli of coccobacilli.

**Contributor's Morphologic Diagnosis:** Multifocal to coalescing necrotizing suppurative pneumonia with myriad intralesional coccobacilli, necrotizing vasculitis, fibrin thrombi, and bacterial emboli; etiology, *Yersinia pestis.*

**Contributor's Comment:** *Yersinia pestis* is a gram-negative coccobacillus that is the causative agent of plague.[5,8-10,13] Plague occurs worldwide, but it tends to occur in endemic regions on different continents.[5,13] These endemic regions have similar geographic characteristics in that they are cool, semiarid climates near deserts with rodents that have short life spans and high reproductive material.[5] These endemic regions

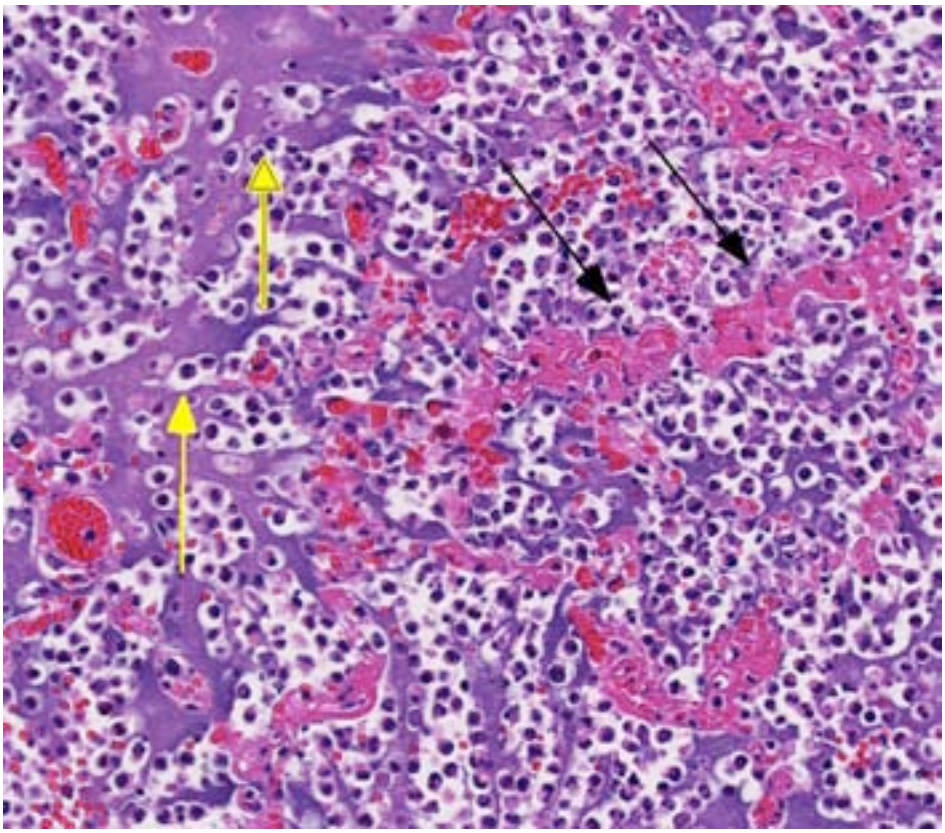

*1-5. Lung, cat: Infiltrated areas exhibit multifocal septal necrosis, with either interruption and loss of septa (yellow arrows) or marked expansion and replacement by fibrin and cellular debris (black arrows.) (HE 168X)*

often have year-round flea activity. In the states of Arizona, Colorado, New Mexico, and Utah (the Four Corners area of the United States), the endemic areas of plague tend to be those locations with elevations up to 2300 meters (7546 feet) and have a piñon pine-juniper habitat or a ponderosa pine habitat. The incidence of plague cases in humans and animals is influenced by annual precipitation, as increased soil moisture favors flea survival and vegetation growth on which rodents feed. In addition, there is evidence that *Yersinia pestis* can survive and remain virulent in soil up to 40 weeks.[2]

*Yersinia pestis* is propagated in a flea-mammal (usually rodents) life cycle.[5,13] A flea capable of transmitting *Y. pestis* first must take a blood meal from a mammal that is septicemic with *Y. pestis*. The bacterium proliferates within the flea's proventriculus, eventually obstructing the flea's gastrointestinal tract. The gastrointestinal obstruction causes the flea to regurgitate *Y. pestis* into a mammalian host when the flea is taking subsequent blood meals. Although this is the accepted paradigm for flea transmission of plague, other methods of propagation have also been proposed.[6] Of the domestic species, cats are most susceptible to infection and disease, but dogs may also become infected and occasionally develop disease.[5,11] Cats are also more likely to transmit plague to people than dogs.[7,12] However, the cat flea, *Ctenocephalides felis*, is not an effective transmitter of *Y. pestis*.

Once *Y. pestis* is injected into a mammalian host by the flea, it expresses several virulence factors that help it to evade the mammalian host immune system.[5,9,10] Two virulence factors that help *Y. pestis* survive in the mammalian host are Yersinia outer coat proteins (YOPS) and a capsule consisting of fraction 1 protein (fraction 1 antigen). YOPS are injected into the host's phagocytic cells via a type III secretory system to inhibit the inflammatory response by reorganizing the host cell cytoskeleton and inhibiting NF-κB suppressing cytokine production. YOPS can also be injected into endothelial cells, decreasing the expression of adhesion proteins on the cell surface. The capsule of *Y. pestis* is antiphagocytic and helps the bacterium to survive intracellularly when it is phagocytosed by a mammalian phagocyte, particularly monocytes and macrophages. The survival of *Y. pestis* within phagocytes helps it to be distributed from the initial site of infection to the regional lymph nodes and into the circulation.

The pathology of plague is similar in both cats and people.[5,10,13] The site of injection of *Y. pestis* at the flea bite can develop dermatitis and cellulitis, such as in this case, or more commonly has minimal inflammation. The most common presenting lesion is a swollen lymph node

(bubonic plague) that may become necrotic and abscess. *Y. pestis* can then spread lymphogenously to other lymph nodes or hematogenously to other organs, particularly the organs that contain large numbers of resident macrophages (septicemic plague). In addition to the flea-mammal transmission, *Y. pestis* can be transmitted through the inhalation of aerolized *Y. pestis* (pneumonic plague) or through the ingestion of a *Y. pestis* infected rodent. Inhalation and ingestion of *Y. pestis* often results in a shorter incubation period of 1-3 days versus the 2-6 days incubation period after a flea bite due to the fact that the inhaled and ingested *Y. pestis* usually has already developed a capsule allowing the bacterium to spread more quickly in the host.[5]

**JPC Diagnosis:** Lung: Pneumonia, embolic, fibrinosuppurative and necrotizing, with vasculitis and numerous large colonies of coccbacilli.

**Conference Comment:** This is a great case illustrating the characteristic appearance of the gram-negative coccobacilli *Yersinia pestis* in tissue section, which is readily distinguishable from other large colony-forming bacteria such as *Actinomyces, Actinobacillus, Corynebacterium, Staphylococcus and Streptococcus* spp. Other species of *Yersinia* (*Y. pseudotuberculosis* and *Y. enterocolitica*) more typically affect the gastrointestinal tract of domestic animals, but also have the same histologic appearance as is present in this case, which are often referred to as "microcolonies".[3]

Plague is an endemic disease within the southwestern U.S., with prairie dogs being considered highly susceptible and important for disease transmission. A colony of Gunnison's prairie dogs has been identified as resistant to infection.[4] Only a minority of these animals mount an antibody response in the face of an outbreak, alluding to the role of the innate immune system as being responsible for conferring resistance to disease. Several proteins of the innate immune response, including VCAM-1, CXCL-1, and vWF, are upregulated in these animals following *Yersinia* exposure.[4]

Conference participants reviewed a vital component of the innate immune system: the pattern recognition receptors known as toll-like receptors (TLR). TLRs recognize pathogen-associated molecular patterns, or PAMPs, which

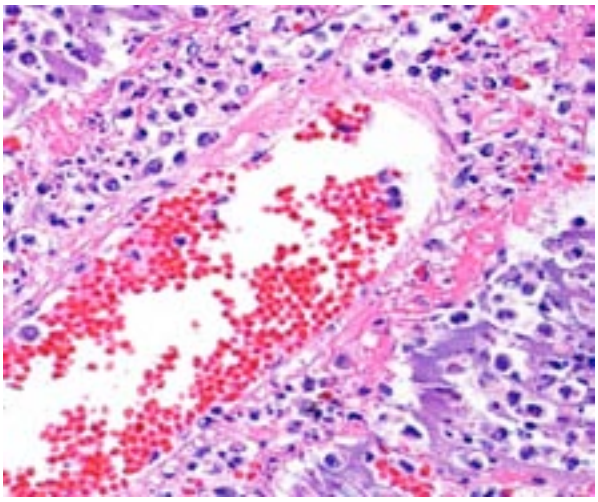

*1-6. Lung, cat: Multifocally, the walls of pulmonary veins are expanded with neutrophils, cellular debris and edema (vasculitis). (HE 360X)*

are exogenous microbial products and include LPS, lipoteichoic acid, and peptidoglycans. This recognition of a microbe ultimately results in NF-κB activation which upregulates transcription of proteins important to the immune response. All TLRs except for two mediate NF-κB activation via MyD88 signaling, and thus are MyD88-dependent. TLR 4 has the ability to engage MyD88 or bypass it with TRAM and TRIF, resulting in type 1 IFN formation and release. TLR 3 operates exclusively through TRIF, and thus is MyD88-independent. TLRs can be characterized by which specific PAMPs they detect in addition to whether they're located in the cell membrane or within the membrane of the endosome.[1] Understanding the specifics of TLR-signaling is often an important factor in elucidating disease pathogenesis and the corresponding immune response to a particular pathogen.

The contributor highlighted two important virulence factors of *Yersinia* spp., YOPS and fraction 1 antigen. YOPS are bacterial toxins which are injected into the cell. Three specific proteins (YopE, YopH, YopT) block phagocytosis by inactivating molecules that regulate actin polymerization. YopJ blocks inflammatory cytokine production by inhibiting LPS signaling pathways.[10]

**Contributing Institution:** New Mexico Department of Agriculture Veterinary Diagnostic Services
http://www.nmda.nmsu.edu/vds/

**References:**

1. Ackermann MR. Inflammation and healing. In: Zachary JF, McGavin MD, eds. *Pathologic Basis of Veterinary Disease.* 5th ed. St. Louis, MO: Elsevier Mosby; 2012:111-113.
2. Ayyadurai S, Houhamdi L, Lepidi H, Nappez C, Raoult D, Drancourt M. Long-term persistence of virulent *Yersinia pestis* in soil. *Microbiology*. 2008;154:2865-2871.
3. Brown CC, Baker DC, Barker IK. Alimentary system. In: Maxie MG, ed. *Jubb, Kennedy, and Palmer's Pathologic Basis of Veterinary Disease*. 5th ed. Vol. 2. Philadelphia, PA: Elsevier Saunders; 2007:204-205.
4. Busch JD, Van Andel R, Stone NE, et al. The innate immune response may be important for surviving plague in wild Gunnison's prairie dogs. *J Wildl Dis.* 2013;49(4):920-931.
5. Chomel BB. Plague. In: Greene CE, ed. *Infectious Diseases of the Dog and Cat*. 4th ed. St. Louis, MO: Elsevier; 2012:469-476.
6. Eisen RJ, Bearden SW, Wilder AP, et al. Early-phase transmission of *Yersinia pestis* by unblocked fleas as a mechanism explaining rapidly spreading plague epizootics. *PNAS.* 2006;103:15380-5.
7. Gage KL, Dennis DT, Orloski K A, et al. Cases of cat-associated plague in the western US, 1977-1998. *Clin Infec Dis* 2000;30:893-900.
8. Hirsh DC. Enterobacteriaceae: *Yersinia*. In: Hirsh DC, MacLachlan NJ, Walker RL, eds. *Veterinary Microbiology*. 2nd ed. Ames, IA: Blackwell; 2004:75-80.
9. Li B, Yang R. Interaction between *Yersinia pestis* and the host immune system. *Infect Immun*. 2005;76(5):1804-1811.
10. McAdam AJ, Sharpe AH. Infectious diseases. In: Kumar V, Abbas AK, Fausto N, Aster JC, eds. *Robbins and Cotran Pathologic Basis of Disease*. 8th ed. Philadelphia, PA: Saunders: 2010:331-398
11. Nichols MC, Ettestad PJ, VinHatton ES, et al. *Yersinia pestis* infection in dogs: 62 cases (2003-2011). *J Am Vet Med Assoc.* 2014;244(10): 1176-1180.
12. Pennisi MG, Egberink H, Hartmann K, et al. *Yersinia pestis* infection in cats: ABCD guidelines on prevention and management. *J Feline Med Surg*. 2013;15:582-584.
13. Perry RD, Fetherston JD. *Yersinia pestis* – etiologic agent of plague. *Clin Microbiol Rev*. 1997;10(1):35-66.

**CASE II**: S1342/13 (JPC 4050932).

**Signalment:** 26-year-old thoroughbred gelding horse, *Equus caballus.*

**History:** The horse was presented to the veterinary clinic with a 14-day history of fever, hematuria and intermittent colic. The referring veterinarian initially treated the animal unsuccessfully with antibiotics due to a suspected cystitis. Urine analysis at the clinic confirmed the initial diagnosis of hematuria. A neoplastic process in the left kidney was suspected after rectal palpation.

Ultrasonographically there was an irregular cavitated mass located cranially of the kidneys of about 30 cm in diameter. Renal parenchyma was only partially recognizable by ultrasound. The urinary bladder was unremarkable. Blood analysis revealed marked azotemia, elevated creatinine, hyperproteinemia with hyperglobulinemia and hyperfibrinogenemia.

Due to the clinical symptoms, the age of the gelding and additional orthopedic problems (founder) as well as a poor prognosis due to the suspected renal neoplasia, the animal was euthanized and submitted for necropsy.

**Gross Pathology:** At necropsy both kidneys were severely enlarged and firm. The parenchyma contained multiple yellowish-white firm nodules of about 5-15 cm in diameter. The renal pelvis of both kidneys was filled with few milliliters of serosanguineous fluid. The urinary bladder contained pure blood.

**Laboratory Results:**

| | |
|---|---|
| Creatinine µmol/l) | 260 µmol/l (ref. 69-155 |
| Urea mmol/l) | 11.41 mmol/l (3.18-7.31 |
| Serum protein | 90.7 g/l (58-74 g/l) |
| Albumine | 26.1 g/l (29.93-37.88 g/l) |
| Globuline | 64.6 g/l (23.07-42.09 g/l) |
| Fibrinogen | 5.14 g/l (1.25-3.29 g/l) |

**Histopathologic Description:** Lymph node and adipose tissue: Affecting approximately 60 % of the section there is a 15 x 10 mm granulomatous and fibrous nodular lesion. The inflammatory infiltrate is interspersed between large amounts of fibrous tissue, and consists of epithelioid cells, occasional multinucleated giant cells of foreign body (haphazardly arranged nuclei) and Langhans (peripherally arranged nuclei) type as well as many plasma cells, fewer lymphocytes and occasional eosinophils. Free within fibrous tissue, surrounded or engulfed by macrophages are multiple cross and tangential sections of nematode parasites. The parasites are 250-300 µm in length and 15-20 µm in diameter and show a thin, smooth cuticle.

Sometimes a dorsoflexed uterus, occasionally with uninucleated eggs, and a rhabditiform esophagus with

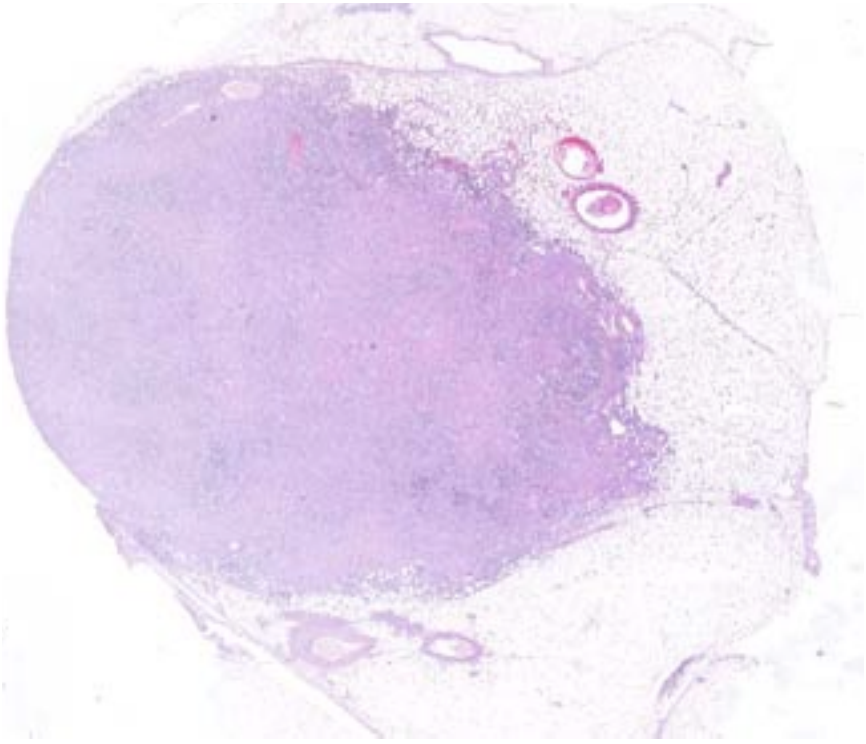

*2-1. Lymph node, horse: Nodal architecture is diffusely effaced. (HE 6.3X)*

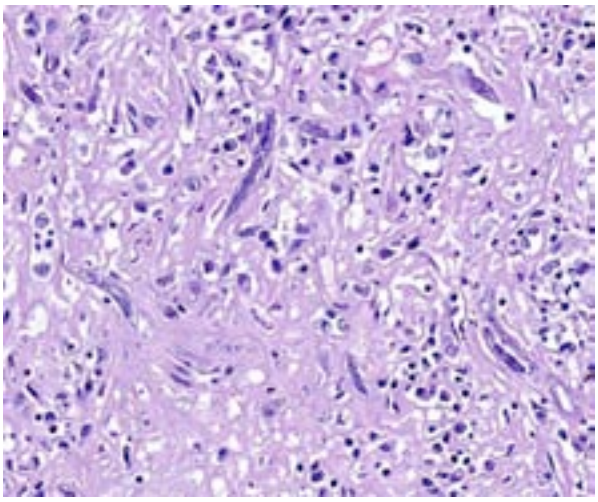

*2-2. Lymph node, horse: The lymph node is replaced by fibrous connective tissue, granulomatous inflammation and numerous cross- and tangential section of nematode parasites measuring 15-20 µm in diameter. (HE 252X)*

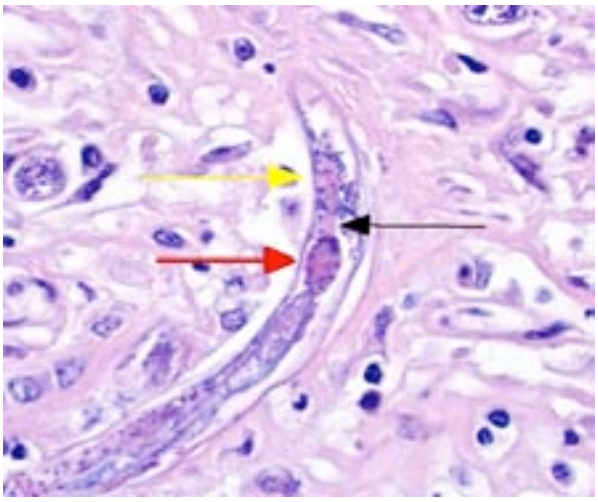

*2-3. Lymph node, horse: Nematode parasites, upon serendipitous section, possess a characteristic rhabditiform esophagus with a corpus (yellow arrow), isthmus (black arrow), and bulb (red arrow) characteristic of Halicephalobus gingivalis. (HE 400X)*

corpus, isthmus and bulb can be seen. Eggs, measuring about 15 x 20 µm are occasionally observed free within the inflamed tissue. Multifocally, smaller forms of the parasites with rhabditiform esophagus and internal granular structures can be found (larvae). Parasites are multifocally surrounded by areas of lytic necrosis characterized by replacement of tissue with nuclear and cellular debris. Intralesional vessels are dilated (hyperemia) and in one location parasites, surrounded by inflammatory cells, are found within a medium sized artery. At the margins of the granuloma are moderate numbers of macrophages containing a yellow-brown globular pigment (hemosiderin).

**Contributor's Morphologic Diagnosis:** Lymphadenitis and steatitis, granulomatous and eosinphilic, focal, moderate with intralesional adult and larval rhabditoid nematodes, etiology consistent with *Halicephalobus gingivalis.*

**Contributor's Comment:** *Halicephalobus gingivalis* (syn. *Micronema deletrix, Halicephalobus deletrix*) is a free-living soil saprophyte worm belonging to the nematode order *Rhabditida,* family *Panagrolaimidae,* and has the ability to produce extensive tissue damage because of its migratory behaviour.[1,2,6] Equine cases of this parasitosis were reported in Europe, North and South America, Japan, Egypt and South Korea.[8] One case of a halicephalobosis in a zebra can be found in the literature.[7] Rare fatalities in man have also been described.[12]

It has been shown that only female worms and larvae induce lesions. In the kidneys, the parasite causes multifocal to coalescing granulomas containing numerous larval and adult rhabditiform nematodes and occasional embryonated eggs. Macroscopically, these granulomas often resemble neoplasms.[9]

The nematodes are 15-20 µm in diameter, 250-430 µm in length and have a thin, smooth cuticle. They possess a platymyarian-meromyarian musculature, a pseudocoelom and a rhabditiform esophagus composed of a corpus, isthmus and bulb. The intestinal tract is lined by uninucleate, low cuboidal cells and a single genital tube/uterus containing one egg/ova.[5]

Other important lesions in horses are severe encephalitis and myelitis,[1,6,10] orchitis,[4] osteomyelitis[13] and posthitis.[11] Sometimes disseminated disease can develop.[7]

There are different hypotheses regarding the life cycle and the way of transmission of the nematode. Oral ingestion, inhalation or wound infections with nematode stages are suggested.[2] In one case vertical transmission on the colostral way from the dam to the foal was described.[10,15]

Successful surgical therapies of cases with localized lesions are recorded, but it is possible that the parasites may survive within the granulomas; however, in the CNS the parasites can survive because anthelmintics do not easily cross the blood-brain barrier.[3]

In cases of renal halicephalobosis, also the case in the presented horse, azotemia and renal failure as well as hematuria can be observed. Parasitic lesions in tissues other than kidney and lymph node were not detectable in our case.

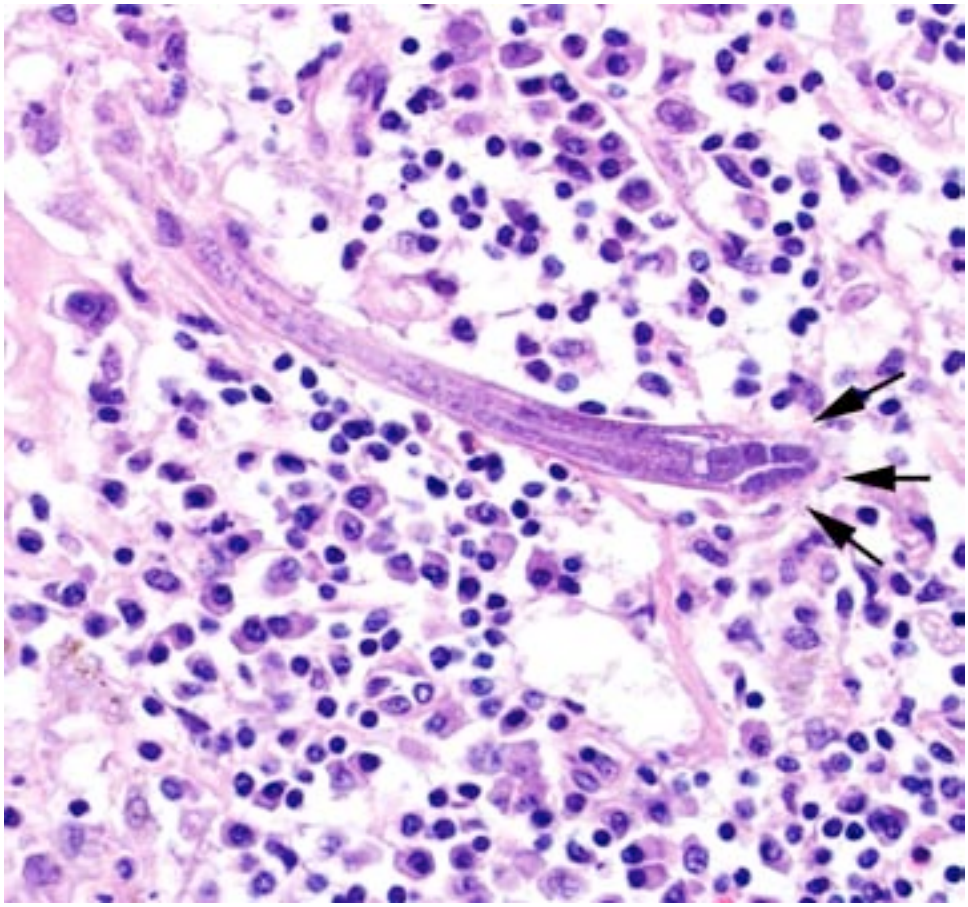

*2-4. Lymph node, horse: Nematode parasites also possess a dorsoflexed uterus arrows. (HE 400X)*

**JPC Diagnosis:** Lymph nodes: Lymphadenitis, granulomatous, chronic, diffuse, severe, with nematode adults, larva and eggs.

**Conference Comment:** *Halicephalobus gingivalis* has a very characteristic appearance on histologic sections though it is often difficult to the histologic attributes described adroitly by the contributor. This case, however, presents a unique opportunity to observe all of its morphologic features with all three life stages found in abundance and in good preservation.

There are a number of migrating nematodes capable of inducing disease in the equine. While *H. gingivalis* is readily distinguishable, infections of *Strongylus vulgaris, Strongylus equinus, Angiostrongylus cantonensis, Setaria* spp., and *Draschia megastoma* can all manifest into a variety of clinical presentations to include neurologic signs and thus may be worthy of consideration.[8] *H. gingivalis* has more affinity for the kidneys, lymph nodes and central nervous system; therefore infected animals most often present with renal signs as in this case or neurologic symptoms such as ataxia, circling, loss of balance, and head tremors.[2]

There are nine species of *Halicephalobus,* though only *H. gingivalis* is known to cause disease in animals.[2] Its pathogenesis is largely unproven, including routes of infection. Hematogenous spread is widely accepted and supported by the presence of larva within arteries in this case. It is interesting, however, why it has predilection for certain tissues and often spares organs such as the liver and spleen. Only adult females, larval stages, and eggs have been identified in tissue sections, indicating the likelihood of parthenogenetic reproduction.[2,7] Many details of the pathogenesis of this rarely reported parasitic infection remain undetermined.

**Contributing Institution:**
Institut fuer Veterinaer-Pathologie, Justus-Liebig-Universitaet Giessen
Frankfurter Str. 96, 35392 Giessen, Germany
http://www.uni-giessen.de/cms/fbz/fb10/institute_klinikum/institute/pathologie

**References:**
1. Akagami M, Shibahara T, Yoshiga T, Tanaka N, Yaguchi Y, Onuki T, et al. Granulomatous

nephritis and meningoencephalomyelitis caused by Halicephalobus gingivalis in a pony gelding. *J Vet Med Sci*. 2007;69:1187-1190.
2. Bryant UK, Lyons ET, Bain FT, Hong CB. Halicephalobus gingivalis-associated meningoencephalitis in a Thoroughbred foal. *J Vet Diagn Invest*. 2006;18:612-615.
3. Ferguson R, van Dreumel T, Keystone JS, Manning A, Malatestinic A, Caswell JL, et al. Unsuccessful treatment of a horse with mandibular granulomatous osteomyelitis due to Halicephalobus gingivalis. *Can Vet J*. 2008;49:1099-1103.
4. Foster RA, Ladds PW. Male genital system. In: Maxie MG, ed., *Jubb, Kennedy, and Palmer's Pathology of Domestic Animals*. 5th ed. Philadelphia, PA: Elsevier Limited; 2007;(3):587.
5. Gardiner CH, Poynton SL. An Atlas of Metazoan Parasites in Animal Tissue. Washington, DC: Registry of Veterinary Pathology/ Armed Force Institute of Pathology. 1999, revised 2006.
6. Hermosilla C, Coumbe KM, Habershon-Butcher J, Schöniger S. Fatal equine meningoencephalitis in the United Kingdom caused by the panagrolaimid nematode Halicephalobus gingivalis: case report and review of the literature. *Equine Vet J*. 2011;43:759-763.
7. Isaza R, Schiller CA, Stover J, Smith PJ, Greiner EC. Halicephalobus gingivalis (Nematoda) infection in a Grevy's zebra (Equus grevyi). *J Zoo Wildl Med*. 2000;31:77-81.
8. Jung JY, Lee KH, Rhyoo MY, Byun JW, Bae YC, Choi E, et al. Meningoencephalitis caused by Halicephalobus gingivalis in a thoroughbred gelding. *J Vet Med Sci*. 2014;76:281-284.
9. Maxie MG, Newman SJ. Urinary system. In: Maxie MG, ed. *Jubb, Kennedy, and Palmer's Pathology of Domestic Animals*. 5th ed. Philadelphia, PA: Elsevier Limited; 2007;(2):498.
10. Maxie MG, Youssef S. Nervous system. In: Maxie MG, ed. *Jubb, Kennedy, and Palmer's Pathology of Domestic Animals*. 5th ed. Philadelphia, PA: Elsevier Limited; 2007;(1): 437-444.
11. Muller S, Grzybowski M, Sager H, Bornand V, Brehm W. A nodular granulomatous posthitis caused by Halicephalobus sp. in a horse. *Vet Dermatol*. 2008;19:44-48.
12. Papadi B, Boudreaux C, Tucker JA, Mathison B, Bishop H, Eberhard ME. Halicephalobus gingivalis: a rare cause of fatal meningoencephalomyelitis in humans. *Am J Trop Med Hyg*. 2013;88:1062-1064.
13. Teifke JP, Schmidt E, Traenckner CM, Bauer C. [Halicephalobus (Syn. Micronema) deletrix as a cause of granulomatous gingivitis and osteomyelitis in a horse]. *Tieraerztl Prax Ausg G Grosstiere Nutztiere*. 1998;26:157-161.
14. Wilkins PA, Wacholder S, Nolan TJ, Bolin DC, Hunt P, Bernard W, et al. Evidence for transmission of Halicephalobus deletrix (H. gingivalis) from dam to foal. *J Vet Intern Med*. 2001;15:412-417.

**CASE III**: N10-103 (JPC 3166502).

**Signalment:** 16-month-old intact mixed breed male cat, *Felis catus.*

**History:** The animal was a rescue shelter cat current on all vaccinations. The animal presented with dyspnea and strider upon exercise. Radiographs of the lungs revealed a diffuse interstitial pattern.

**Gross Pathologic Findings:** The carcass demonstrated an adequate nutritional plane. There was a red watery discharge from both nostrils. Upon reflecting the skin, the subcutaneous tissues were noted to stick to the prosector's gloves. The lungs did not collapse upon opening the thoracic cavity. They were moist and diffusely mottled gray to pink. Approximately 3mls of a pink watery fluid was in the chest cavity. The heart was enlarged and occupied three and a half intercostal spaces. A small amount of fluid oozed form a cut surface of the lungs.

**Laboratory Results:**

**Clinical Pathology:**

WBC:10.8 K/ul

NEU:3.47 32.2%N

LYM:5.69 52.9%L

MONO: 0.026 0.239%M

EOS 1.57 14.6%E

BASO 0.002 0.020 %B

**Histopathologic Description:** There is moderate to marked hyperplasia and hypertrophy of the tunica muscularis of pulmonary arteries. The smooth muscle of bronchioles and alveolar ducts is also prominent. The epithelial linings of many bronchi are sloughed and there are increased numbers of bronchial glands. Small to moderate numbers of lymphocytes, plasma cells and macrophages infiltrate bronchial and bronchiolar walls, peribronchial connective tissue, and adjacent periarterial tissue. Peribronchial stroma is expanded by small clear spaces (edema).

**Contributor's Morphologic Diagnosis:** Bronchitis and bronchiolitis, chronic, multifocal, moderate, with alveolar ductal and arterial smooth muscle hyperplasia, and peribronchial glandular hyperplasia, lung.

**Contributor's Comment:** Based on the microscopic lesions, a diagnosis of feline asthma syndrome (FAS) was made. This syndrome is characterized by episodes of coughing, wheezing and or dyspnea which are due to the bronchoconstriction secondary to hyperactivity of airway smooth muscle.[1] It has been referred to as allergic bronchitis or allergic pneumonia. Though the exact cause is unknown, it is associated with a type I immediate hypersensitivity reaction to inhaled antigens. Inhaled cat litter dust, aerosol sprays and cigarette smoke as well as infectious causes have been associated with this syndrome.[3] This disease is rarely the primary cause of death

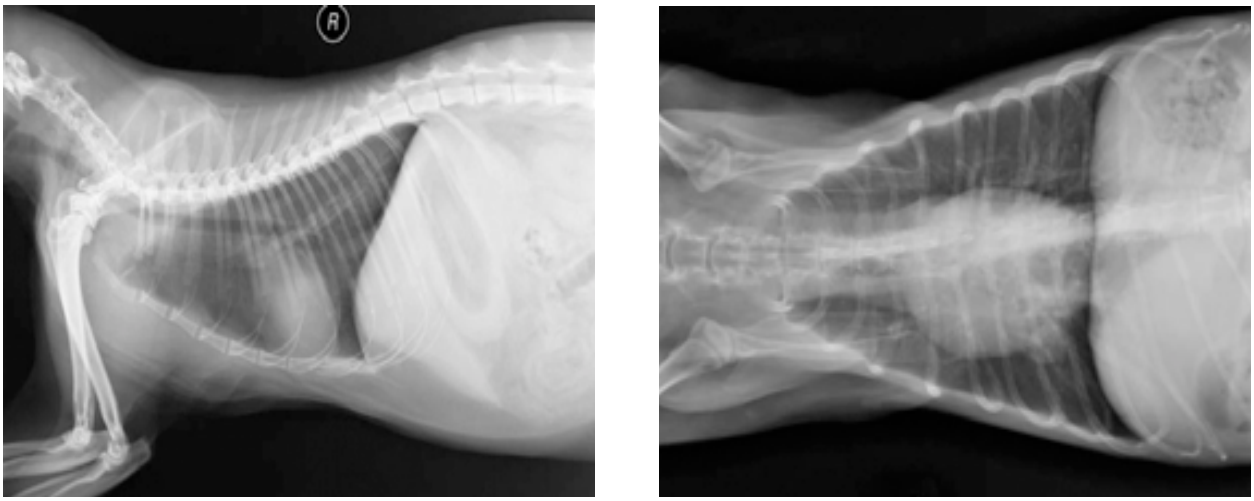

*3-1. Lung, cat: Lateral and dorsoventral views demonstrate a marked diffuse interstitial pattern in all lung lobes. (Photo courtesy of: Tuskegee University, School of Veterinary Medicine, Department of Pathobiology, Clinical Anatomy Building, Tuskegee, AL 36088)*

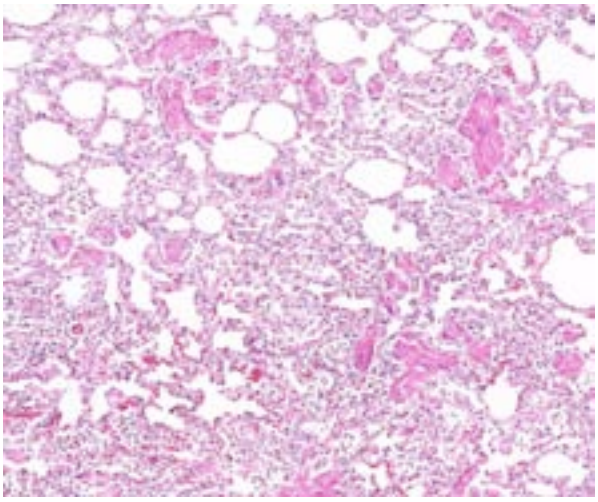

*3-2. Lung, cat: There is diffuse hyperplasia of smooth muscle surrounding terminal airways, and alveolar septa are expanded, and alveoli filed by a cellular infiltrate. (HE 96X)*

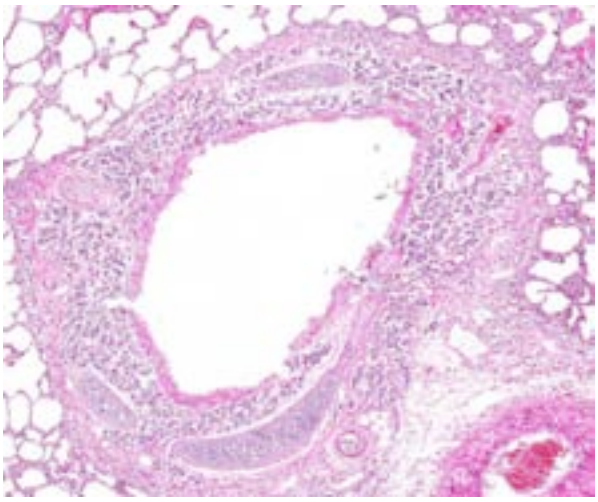

*3-3. Lung, cat: There is diffuse hyperplasia of submucosal glands around airways. (HE 36X)*

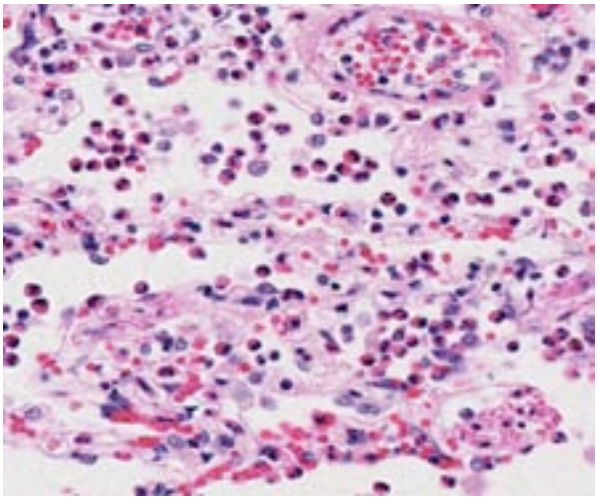

*3-4. Lung, cat: Higher magnification of expanded alveolar septa and alveoli containing numerous eosinophils. (HE 356X)*

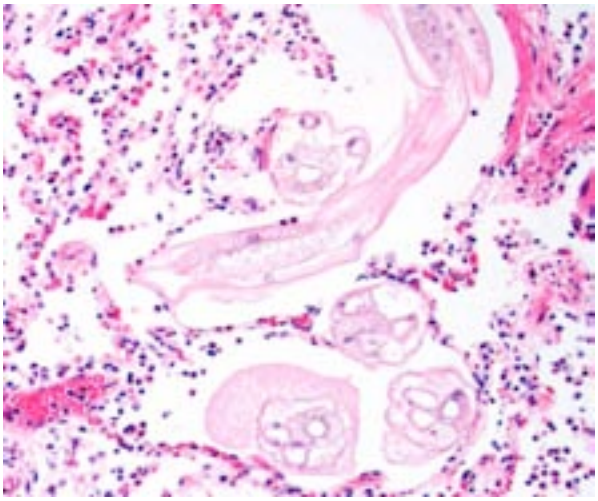

*3-5. Lung, cat: Within the section, there are cross- and tangential sections of a strongyle nematode with a smooth cuticle, pseudocoelom, coelomyarian-polymyarian musculature, and an intestine lined by multinucleated cells. Definitive speciation cannot be completed on this single section. (HE 280X)*

except when a secondary bacterial pneumonia occurs.

In the early stages of this disease there is a mild eosinophilic inflammatory infiltrate with mucosal edema.[3] As seen in this case, eosinophils are not always the prominent cell type. In the more advanced stages the characteristic lesions include bronchial gland hyperplasia along with smooth muscle hypertrophy of arteries and airways.

**JPC Diagnosis:** Lung: Pneumonia, eosinophilic, chronic, multifocal, moderate with bronchiolar and smooth muscle hyperplasia, and intrabronchiolar adult nematodes.

**Conference Comment:** This is an interesting case, not in its classic or dramatic presentation of a lesion as often observed in WSC cases, but rather in its subtlety, effectively delivering a real-world diagnostic challenge to all conference participants. The contributor's diagnosis of feline asthma is based on the presence of smooth muscle and peribronchial gland hyperplasia as corresponding with the animal's clinical signs, as well as a diffuse mild eosinophilic infiltrate, primarily within alveoli. However, a number of

slides contain tangential sections of degenerate adult nematodes which were not described by the contributor, and which we believe are a primary component of this clinical presentation. The level of degeneration precludes definitive diagnosis; however, a large, multinucleated intestine is present in some nematode sections and when coupled with the vague coelomyarian musculature, strongly suggests a metastrongyle. *Aelurostrongylus abstrusus* is considered a ubiquitous nematode of domestic cats and thus the most likely species of metastrongyle in this case.[3] Another possibility is the feline parasite *Ollulanus tricuspis,* a trichostrongyle which could have been regurgitated and aspirated into the lung parenchyma.

The changes seen in this case correlate best with a late-stage chronic infection with *A. abstrusus* in cats. In one study, 24 weeks following infection, eggs and larvae were completely absent and adult nematodes present in only 3 of nearly 100 examined histologic sections.[2] Smooth muscle and peribronchial gland hyperplasia are typical findings in these cases, though it is worth mentioning this is often considered a normal finding in healthy cats with no evidence of parasitism.[1]

*A. abstrusus* is common in cats, with an array of corresponding clinical signs from asymptomatic to chronic coughing and tachypnea. In characteristic lesions, there are nodules formed by masses of eggs and larvae in alveoli and terminal bronchioles with few adult worms. Eosinophils and neutrophils predominate early, with more mononuclear cells and giant cells occurring later. Typically, chronic cases devoid of larvae and eggs have remaining epithelialized alveoli and septa thickened by fibrous tissue and smooth muscle.[1] The infection is usually self-limiting[3] and given the mild extent of pathology in most slides, it is possible there were unidentified contributing factors to the clinical presentation described in this case.

**Contributing Institution:**
tgraham@tuskegee.edu

**References:**

1. Caswell JL, Williams KW. Respiratory system. In: Maxie MG, ed. *Jubb, Kennedy, Palmer's Pathology of Domestic Animals*. 5th ed. Vol. 2. Philadelphia, PA: Elsevier Saunders; 2007:557, 649-650.
2. Hamilton JM. Experimental lungworm disease of the cat. *J Comp Pathol.* 1966;76:147-157.
3. Lacorcia L, Gasser RB, Anderson GA, Beveridge I. Comparison of bronchioalveolar lavage fluid examination and other diagnostic techniques with the Baermann technique for detection of naturally occurring *Aelurostrongylus abstrusus* infection in cats. *JAVMA.* 2009;235(1): 43-49.

**CASE IV:** 14-8745 (JPC 4052875).

**Signalment:** 9-day-old piglet, *Sus scrofa domesticus*.

**History:** This piglet is from a unit with ongoing diarrhea problems.

**Gross Pathological Findings:** The carcasses were thin and rough-haired. One of two pigs had milk in the stomach. The small intestines were thin-walled and fluid-filled. Spiral colons contained watery feces.

**Histopathologic Description:** Jejunum and ileum have severe atrophic enteritis. There is villus fusion and epithelial attenuation.

**Contributor's Morphologic Diagnoses:** Severe atrophic enteritis with villus fusion and epithelial attenuation.

**Laboratory Results:** Porcine epidemic diarrhea virus, confirmed with PCR. Immunohistochemistry stains are positive also.

**Contributor's Comment:** Porcine epidemic diarrhea virus (PEDV) was first identified in England in 1971 and was then confirmed in the United States in the spring of 2013.[2] As of the summer of 2014, the virus has spread to 30 states and has resulted in the loss of millions of pigs. The disease causes severe diarrhea and vomiting in all ages of pigs with mortality in suckling pigs of 90-95%. The original US isolates were nearly identical to Chinese isolates from 2012. It is not known how PEDV arrived in the US. PEDV is a member of the genus *Alphacoronavirus* together with transmissible gastroenteritis virus (TGEV).

The pathology of PEDV has been described in gnotobiotic pigs.[3] The lesions were similar to those observed in conventional pigs infected with PEDV.

**JPC Diagnosis:** Small intestine: Enteritis, necrotizing, with villous blunting and fusion, and crypt hyperplasia.

**Conference Comment:** For an industry that excels in implementing biosecurity practices, the rapid spread of porcine epidemic diarrhea virus proves a major source of concern for our ability to control infectious diseases. In April 2013, hog confinement facilities with closed-herd strategies and shower-in, shower-out facilities broke out with explosive diarrhea and vomiting in suckling pigs. This led to a mortality rate approaching a staggering 95% within 3 days of the onset of clinical signs. Multiple facilities separated by hundreds of miles began to experience the same symptoms and a diarrhea epidemic ensued. Within months, the majority of states in the continental U.S. were reporting cases of PEDV.[2]

PEDV is an *Alphacoronavirus* that contains an enveloped, single-stranded positive-sense RNA genome.[2] It was first discovered in the UK in 1971 and continued to cause sporadic outbreaks in Europe and Asia for decades.[2] Though it is similar in structure and pathogenesis as TGE, its genome

*4-1. Jejunum, 9-day-old piglet: Villi are diffusely and severely shortened. (HE 6.3X)*

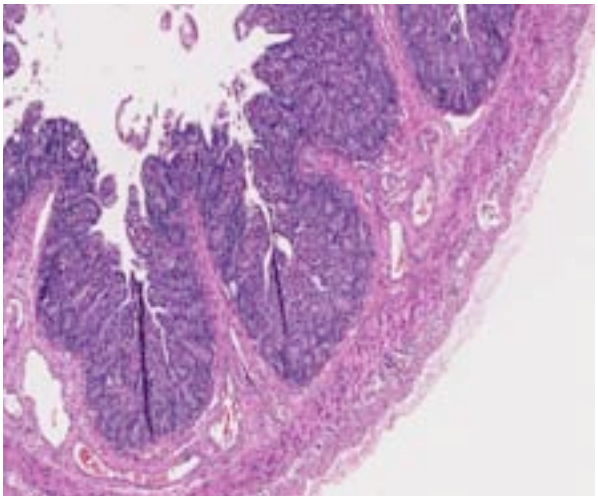

*4-2. Jejunum, 9-day-old piglet: Villar epithelium lining shortened villi is multifocally attenuated and lost. (HE 6.3X)*

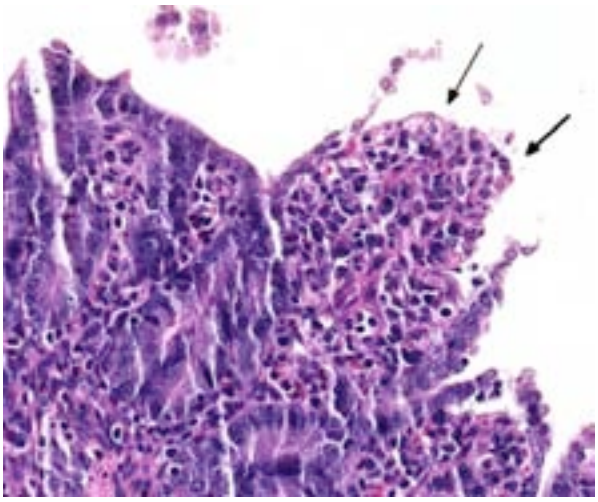

*4-3. Jejunum, 9-day-old piglet: Immunohistochemical labeling for porcine epidemic diarrhea coronavirus antigen is diffuse and restricted to villar epithelium. (HE 6.3X)*

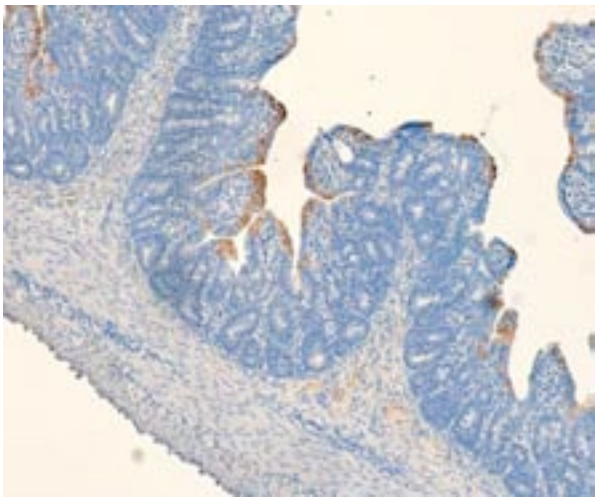

*4-4. Treatment of affected sections of intestine with anti-PED antibodies demonstrates positive staining within villar tip enterocytes. (anti-PED coronavirus, 200X)*

is more closely related to bat *Alphacoronaviruses*.[8] The virus targets intestinal epithelial cells of nursing pigs; however, infection of alveolar macrophages has also been demonstrated.[7] Typical microscopic findings include severe atrophic enteritis throughout the small intestine and viral shedding can precede and continue beyond the observation of clinical signs.[5] In this case, slides from multiple blocks were submitted and among them, the lesions varied from mild blunting and fusion of villi with moderate crypt hyperplasia to severe necrosis. There are also sections with mild loss of lymphocytes in Peyer's patches. Syncytial cell formation was evident throughout the more severely affected lesions.

There has been much attention on the possible mechanisms of virus transmission. Transportation equipment and contaminated feedstuffs are the most often cited culprits, as this may explain the sporadic, simultaneous outbreaks in facilities separated by hundreds of miles.[3] Transmission between animals is largely fecal-oral, but airborne transmission is also suspected.[1]

PEDV contains a transmembrane envelope glycoprotein virulence factor called spike, which is responsible for binding and fusion to host epithelial cells and macrophages. Spike contains two domains, S1 and S2, and the S1 domain is the primary target of vaccines due to its specific high-affinity binding to cell receptors.[6] The first licensed vaccine for PEDV was released in the U.S. in 2014, and now there are several on the market. Incidence rate has been dropping recently and, while the disease has killed over seven million pigs in just the last year, it appears the peak of this devastating epidemic has already passed.

**Contributing Institution:** Animal Disease Research and Diagnostic Laboratory
South Dakota State University
Brookings, South Dakota 57007

**References:**

1. Alonso C, Goede DP, Morrison RB, et al. Evidence of infectivity of airborne porcine epidemic diarrhea virus and detection of airborne viral RNA at long distances from infected herds. *Vet Res*. 2014;45:73.
2. Stevenson GW, et al. Emergence of porcine epidemic diarrhea virus in the United States: clinical signs, lesions, and viral genomic sequences. *J of Vet Diagn Invest.* 2013;25(5):649–654.
3. Jung K, et al. Pathology of US porcine epidemic diarrhea virus strain PC21A in gnotobiotic pigs. *Emerg Infect Dis.* 2014;20(4): 662-665.
4. Lowe J, Gauger P Harmon K, et al. Role of transportation in spread of porcine epidemic diarrhea virus infection, United States. *Emerg Infect Dis*. 2014;20(5):872-874.
5. Madson DM, Magstadt DR, Arruda PH, et al. Pathogenesis of porcine epidemic diarrhea virus isolate (US/Iowa/18984/2013) in 3-week-old weaned pigs. *Vet Microbiol.* 2014 Sep 22. pii: S0378-1135(14)00425-8. [Epub ahead of print]

6. Oh J, Lee KW, Choi HW, Lee C. Immunogenicity and protective efficacy of recombinant S1 domain of the porcine epidemic diarrhea virus spike protein. *Arch Virol*. 2014;159(11):2977-2987.
7. Park JE, Shin HJ. Porcine epidemic diarrhea virus infects and replicates in porcine alveolar macrophages. *Virus Res.* 2014;191:143-152.
8. Vlasova AN, Marthaler D, Wang Q, et al. Distinct characteristics and complex evolution of PEDV strains, North America, May 2013-February 2014. *Emerg Infect Dis*. 2014;20(10): 1620-1628.

**Joint Pathology Center**
**Veterinary Pathology Services**

*Conference Coordinator*
**Matthew C. Reed, DVM**
**Captain, Veterinary Corps, U.S. Army**
**Veterinary Pathology Services**
**Joint Pathology Center**

## WEDNESDAY SLIDE CONFERENCE 2014-2015

# Conference 11

**3 December 2014**

**Conference Moderators:**

Chris Gardiner, DVM, Ph.D
Consultant for Veterinary Parasitology
Head, JCIDS Capability Document Cell
2377 Greely Road
Fort Sam Houston, TX 78234-7731

Keith Harris, DVM, DACVP
Professor and Department Head
College of Veterinary Medicine
University of Georgia
501 DW Brooks Drive
Athens, GA 30602

**CASE I:** 10N0217 (JPC 3166543).

**Signalment:** 1-year-old male Thoroughbred equine*, Equus ferus caballus.*

**History:** Submitted was a 299 kg yearling Thoroughbred colt that lived on pasture with about ten other yearlings. He presented on emergency to the Equine Surgery Service at the Veterinary Medical Teaching Hospital (VMTH) at UC Davis on 28 Jan 2010 for colic of approximately 3 hours duration. The colt was initially found down and rolling in his pasture. His pasture mates were also yearlings. One

*1-1. Colon, horse: 14 cm of the apex of the cecum was present within the lumen of the right ventral colon. (Photo courtesy of: Department of Pathology, Microbiology and Immunology, 5323 Vet Med 3A, School of Veterinary Medicine, University of California Davis, Davis, CA 95616, http://www.vetmed.ucdavis.edu/pmi/).*

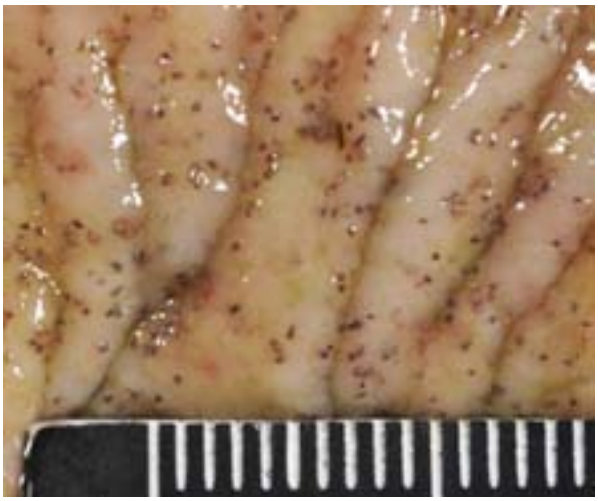

*1-2. Colon, horse: The mucosal surface of the large colons (ventral>dorsal) and cecum was thickened (up to 1.5 cm in width), and finely corrugated. Innumerable, pinpoint to 0.1 cm diameter, dark flecks cover the mucosal surface and visualized by the dissecting scope, correspond to encysted larval worms. (Photo courtesy of: Department of Pathology, Microbiology and Immunology, 5323 Vet Med 3A, School of Veterinary Medicine, University of California Davis, Davis, CA 95616, http://www.vetmed.ucdavis.edu/pmi/).*

*1-3. Colon, horse: At subgross examination, the colonic mucosa is diffusely hypercellular and irregularly thickened; submucosal capillaries are markedly congested and the submucosa is edematous. (HE 6.3X)*

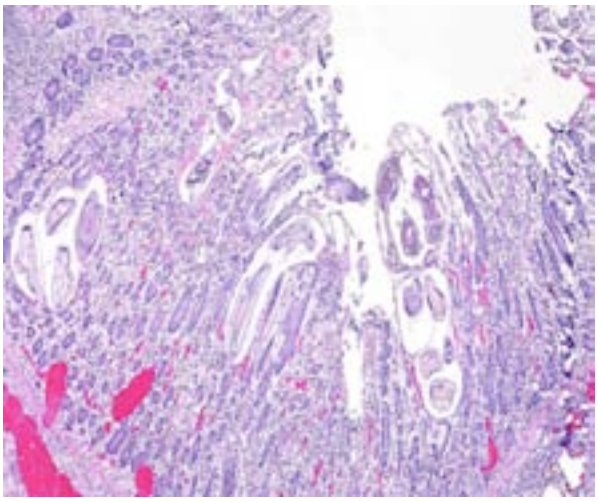

*1-4. Colon, horse: Cross section of numerous coiled nematode larva are present within the mucosa. (HE 52X)*

pasture mate had presented with colic on the previous day and the others were clinically normal. The colt and pasture mates were fed a sweet feed and alfalfa twice daily. He was dewormed on 1 Dec 09 with ivermectin, and then on 1 Jan 10 with fenbendazole.

On presentation at the teaching hospital, the colt was depressed to obtunded. He continually attempted to lie down and exhibited severe discomfort regardless of analgesia administration. Mucous membranes were hyperemic and tacky, and the horse was tachypnic. Reduced borborygmi were ausculted in dorsal left quadrant, with excessive borborygmi in all other quadrants. Dried feces were pasted to the perianal area. Serum chemistry abnormalities included albumin 1.7 g/dL (reference: 2.7-4.2 g/dL), total protein 4.8 g/dL (reference 5.8-8.7 g/dL), neutrophils 17,313 /uL (reference: 2600-6800 / uL), fibrinogen 700 mg/dL (reference: 100-400 mg/dL).

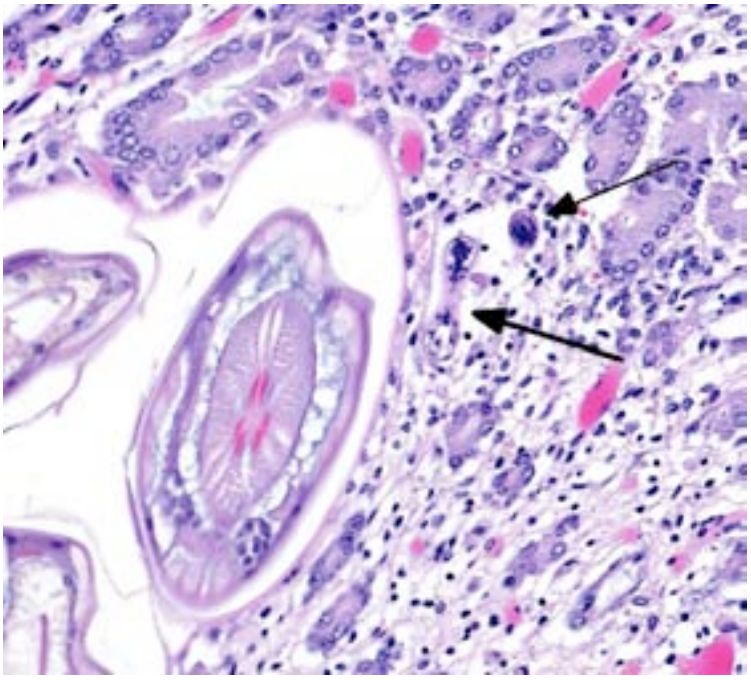

*1-5. Colon, horse: Both L4 stage small strongyle larvae (with most internal organs except a reproductive tract, as well as much smaller, less developed L3 larvae are present within the mucosa. (HE 172X)*

Nasogastric intubation resulted in no net reflux. Cloudy fluid was obtained via abdominocentesis and characterized by 19,880 total nucleated cells (89% neutrophils) and a lactate of 5.5 mg/dL. Due to unrelenting pain, immediate surgery was recommended and preparations were begun, but euthanasia was ultimately selected due to financial concerns.

**Gross Pathologic Findings:** The colt was in good post mortem and body condition. The oral mucosa was generally dull red, with a distinctive darker red-purple line along the gingiva of the maxillary incisors. The sclera of both eyes were injected. The haircoat was dirty and patches of hair were matted with mud. Approximately 5 L of yellow, cloudy fluid filled the

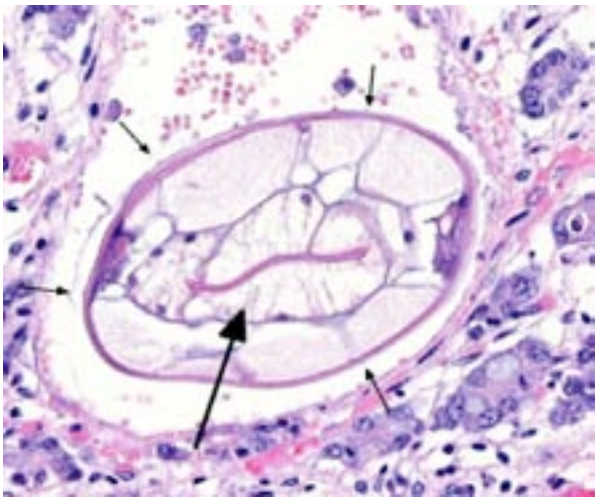

*1-6. Colon, horse: Cyathostome L4 larvae have a 5 µm cuticle with longitudinal ridges small arrows, high polymyarian-coelomyarian musculature, prominent lateral cords, and a large gastrointestinal tract lined by few multinucleated cells. (HE 292X)*

peritoneal cavity. The serosal surface of the large colon was gray-purple and the colic arteries and veins were prominent and distended. The mesenteric lymph nodes associated with the large colon, most notably along the intercolonic mesothelium, were turgid, dark red, and embedded in edematous connective tissue. The large colon and cecum contained abundant green, liquid fluid ingesta with fewer than 100 free floating tapeworms. The mucosal surface of the large colon (ventral>dorsal) and cecum was thickened (up to 1.5 cm in width), pale pink to tan, and finely corrugated. Innumerable, pinpoint to 0.1 cm diameter, dark flecks cover the mucosal surface ("salt and pepper colon") and visualized by the dissecting scope, correspond to encysted larval worms. The apex of the cecum was inverted, extending proximally from the apical tip, with approximately 14 cm present beyond the ceco-colic junction and within the lumen of the right ventral colon. The base of the cecum was gas distended. The serosal surface of the intussusceptum was deep dark red, dull, and friable, and the associated mucosal surface was diffusely dark red, thickened to 1 cm, and oozed serosanguinous fluid on cut section. The lumen of the cecum near this intussusception within the base contained thick, mucoid, yellow material. The stomach contained abundant semi-dry, packed feed.

**Laboratory Results:** Cecal contents submitted for parasitology analysis revealed two endoparasites via flotation: filariform nematode larvae, consistent with the 3rd/4th stage of cyathostome larvae and adult *Anoplocephala* sp. tapeworms. No ova were found on flotation.

**Histopathologic Description:** Multiple sections of large intestinal mucosa were examined in which abundant cyathostome larvae were present. The majority of the cysts were embedded within the tubular glands of the mucosa, where curled single larvae resided in dilated glandular crypts either freely or surrounded by a thin fibrous capsule. Occasionally, the cysts penetrated beneath the basement membrane and submucosa where the larvae were surrounded with a more prominent fibrous capsule, and a variably dense circumferential band of inflammation. The lamina propria was expanded by edema, congested submucosal blood vessels, and an inflammatory infiltrate comprised of neutrophils, plasma cells, lymphocytes, and histiocytes. The number of eosinophils varied among sections of the colon. Multifocally, the superficial mucosal epithelium was eroded, and luminal contents included acellular eosinophilic material. Submucosal arteries had moderate medial hyperplasia and scattered foci of intimal mineralization ("intimal bodies").

**Contributor's Morphologic Diagnosis:**
1. Cecum: Apical cecal intussusception with acute infarction.
2. Large colon and cecum: Mucosal larval cyathostomiasis.
3. Peritoneum: Moderate peritoneal effusion.

**Contributor's Comment:** The *Cyathostominae*, or small strongyles, are a subfamily of the class *Nematoda* that include four main genera. It is the larvae, typically, that are clinically significant, mainly in equid hosts.[2] Larval stages (L3) migrate into the deep mucosa or submucosa of the large bowel (mainly cecum and ventral colon) from the gut lumen and enter the glands to molt and develop, before emerging into the lumen to molt again and mature. If larvae undergo a period of arrested development, most anthelmentics are ineffective.[4] If arrested larvae synchronously emerge from these cysts (hypobiosis), edema, rupture of the muscularis mucosa and ulceration of the overlying mucosa may occur. Alternatively, larvae can complete development in the cecum and colon lumen, and shed eggs into the feces.[2]

It is postulated that cyathostomes have become resistant to certain anthelmintic drugs.[4] A combination of lack of penetration of anthelmintics during the encysted stage along with current inconsistent deworming practices practiced by horse owners and managers has likely led to these new resistant populations, which in turn has led to an increase in incidence of infection over the last 10 years.[4,5] As a result, cyathostomes are considered the primary parasitic pathogen of horses.[6]

Cyathostomiasis has been associated with non-specific clinical signs of colic and chronic diarrhea, and more specifically with cecocecal intussusceptions.[6] Disrupted intestinal motility, which has been experimentally induced by infection with cyathostomes,[6] could contribute to both diarrhea and/or cecocecal intussusception. Given the large number of potential motility disorders in the horse, it is puzzling that cecocolic intussusception is commonly associated with only a limited number of etiologies. Some blood chemistry and hematology aberrations that have been associated with cyathostomiasis include neutrophilia and hypoalbuminemia.[6] Histopathological changes associated with cyathostome larvae infection of the colonic mucosa include a fibroblastic reaction to penetrating larvae, which results in distension and distortion of the glands as the larvae grow. Goblet cell hyperplasia and hypertrophy and a modest, predominantly lymphocytic, inflammatory infiltrate are associated with the encysted larvae.[6]

This colt had numerous clinical signs, hematologic changes, and post mortem findings characteristic of cyathostomiasis. The striking cecocolic intussusception was the probable source of colic and unrelenting pain that ultimately led to euthanasia. An additional sign supportive of intestinal dysmotility was pasting of feces in the perianal area, suggestive of diarrhea. Changes suggestive of cyathostomiasis in blood work parameters were found, including hypoalbuminemia and neutrophilia. Post mortem exam revealed abundant larvae encysted in the mucosa, with mucosal changes described above that are characteristic of cyathostomiasis.

**JPC Diagnosis:** Colon: Colitis, histiocytic and lymphoplasmacytic, diffuse, moderate, with numerous mucosal small strongyle larvae.

**Conference Comment:** This is an excellent case illustrating the severe reaction and associated clinical gastrointestinal problems which may ensue following a mass emergence from hypobiosis of the most pathogenically significant nematode of horses. The contributor highlights the important aspects of the *Cyathostome* spp. lifecycle and how it relates to anthelmintic resistance, an increasing problem among many domestic animals and their parasitic inhabitants. Conference participants agreed that the histologic lesions in this case are more acute than chronic, with little evidence of fibrosis and only 3rd stage and 4th stage larvae identified. This is consistent with a simultaneous, massive eruption of larvae in spite of recent anthelmintic treatment just over two weeks prior to presentation.

Adult small strongyles are essentially nonpathogenic; rather, it is the mass emergence of previously arrested larvae in a short period of time which causes clinical disease. The development of arrested larvae more often occurs from late winter to early summer, and the host and/or environmental factors which influence it are poorly understood.[1] Some evidence suggests the presence of luminal worms provide negative feedback to mucosal larvae,[6] which may correlate with their emergence after anthelmintic treatment and elimination of adults, as likely occurred in this case. Interestingly, arrested development of larvae has been documented for periods extending over two years.[6]

Histologic classification of nematodes is often possible when organisms are well preserved like in the current case. The characteristic large intestine with few multinucleated cells is readily identifiable and is indicative of one of three strongyle subgroups. Cyathostomes are part of the subgroup *Trichostrongylus,* and all are found with platymyarian musculature and longitudinal ridges along their external cuticle.[3] The ridges are faintly visible on some cross sections in this case as small and evenly-spaced. True strongyles also have platymyarian musculature, thick smooth cuticle and often vacuolated lateral chords. The third group, *Metastrongylus,* are the only strongyles with coelomyarian musculature.[3] Also important to speciation in this example is the presence of numerous organisms, as small strongyles often occur in large numbers.

Conference participants discussed the absence of fibrin thrombi within vessels in the affected area and how that relates to intestinal diseases of displacement such as an intussusception, which often do not cause endothelial damage. This is in contrast to infectious diseases such as *Clostridium* spp. or *Salmonella* spp., where fibrin thrombi are commonly observed.

**Contributing Institution:** Department of Pathology, Microbiology and Immunology, 5323 Vet Med 3A, School of Veterinary Medicine, University of California Davis, Davis, CA 95616
http://www.vetmed.ucdavis.edu/pmi/

**References:**

1. Brown CC, Baker DC, Barker IK. Alimentary system. In: Maxie MG, ed. *Jubb, Kennedy, and Palmer's Pathology of Domestic Animals*. 5th ed. Vol. 2. Philadelphia, PA: Elsevier Saunders; 2007:248-249.
2. Corning S. Equine cytahostomins: a review of biology, clinical significance and therapy. *Parasites & Vectors*. 2009:2 (Suppl 2):S1-6.
3. Gardiner CH, Poynton SL. *An Atlas of Metazoan Parasites in Animal Tissues*. Washington, DC: American Registry of Pathology; 1999:22.
4. Peregrine AS, McEwen B, Bienzle D, Koch TG, Weese JS. Larval cyathostominosis in horses in Ontario: An emerging disease? *Can Vet J*. 2006;47:80-82.
5. Kaplan RM, Klei TR, Lyons ET, Lester G, Courtney CH, French DD, et al. Prevalence of anthelmintic resistant cyathostomes on horse farms. *JAVMA*. 2004;225:903-910.
6. Love S, Murphy D, Mellor D. Pathogenicity of cyathostome infection. *Vet Parasitol*. 1999;85:113–121.

**CASE II**: 070181-41/41A (JPC 4032316).

**Signalment:** Adult male cynomolgus macaque, *Macaca fascicularis*.

**History:** This macaque was part of an experimental study to investigate the efficacy of a vaccine against *Yersinia pestis* (*Y. pestis*). This animal was administered the vaccine and was later challenged with aerosolized *Y. pestis*; the challenge dose of bacteria that was used has been previously shown to cause 100% mortality in unvaccinated control animals.

This monkey survived the bacterial challenge and was euthanized at the end of the experiment. The carcass was then submitted for a complete necropsy.

This experiment and the necropsy were performed under biosafety level 3 (BSL-3) biocontainment conditions. This research was conducted under an IACUC approved protocol in compliance with the Animal Welfare Act, PHS Policy, and other federal statutes and regulations relating to animals and experiments involving animals. The facility where this research was conducted is accredited by the Association for Assessment and Accreditation of Laboratory Animal Care, International and adheres to principles stated in the Guide for the Care and Use of Laboratory Animals, National Research Council, 2011.

This research was sponsored by the Joint Science and Technology Office (JSTO), [Project No. R.R.0001_07_RD_B].

**Gross Pathology:** There were no gross lesions attributable to *Y. pestis* infection. Within the omentum, there were three C-shaped pseudosegmented vermiform parasites, each measuring approximately 1 cm in length and 3 mm in diameter.

**Laboratory Results:** Samples of lung, liver and spleen were collected at necropsy for bacterial culture; these were negative for *Y. pestis*.

**Histopathologic Description:** Adipose tissue (omentum): At the peripheral margin of the tissue there is a coiled, encysted metazoan parasite measuring approximately 9 mm in length and 2 mm in widest diameter. The cyst wall consists of an eosinophilic to basophilic, 5-10 µm thick, hyaline membranous layer with multifocal undulations; this layer also contains multiple approximately 10 µm wide pore-like openings lined by refractile eosinophilic material. Adjacent to the cyst wall there is a 25-50 µm thick layer of well-vascularized fibrous connective tissue. Occasional infiltrates of low numbers of lymphocytes and plasma cells are located in the adjacent adipose tissue. Features of the metazoan parasite include: 1) a 3-5 µm thick cuticle containing multiple 8-10 µ m wide pore-like openings lined by eosinophilic refractive material;

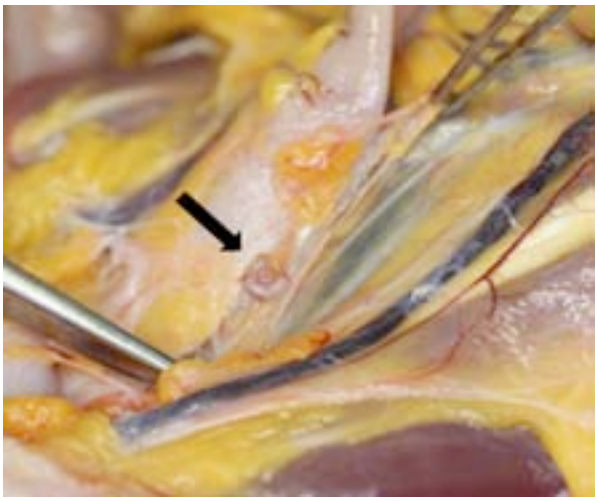

*2-1. Omentum, cynomolgus macaque: Gross photograph showing an encysted, C-shaped, vermiform parasite (arrow) in the omentum of a cynomolgus macaque. (Photo courtesy of: US Army Medical Research Institute of Infectious Diseases: Pathology Division; Fort Detrick, MD http://www.usamriid.army.mil/)*

*2-2. Omentum, cynomolgus macaque: Gross photograph of another encysted parasite in the omentum of the same macaque. Transverse indentations in the parasite's body (arrows) produce a pseudosegmented appearance. (Photo courtesy of: US Army Medical Research Institute of Infectious Diseases: Pathology Division; Fort Detrick, MD http://www.usamriid.army.mil/)*

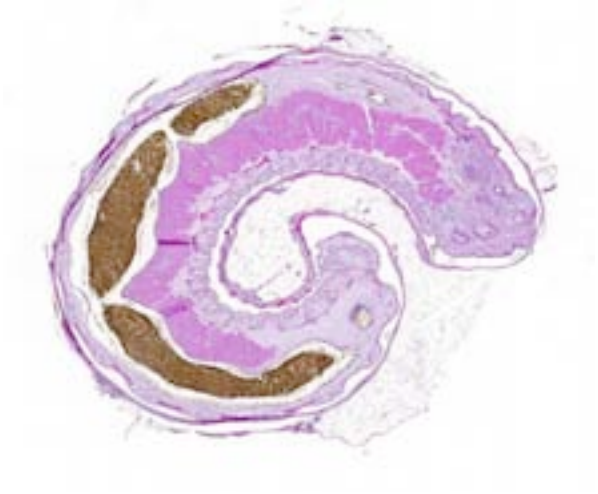

*2-3. Omentum, cynomolgus macaque: Subgross image of pentastome nymph encysted within a thin rim of adipose tissue. (HE 6.3X)*

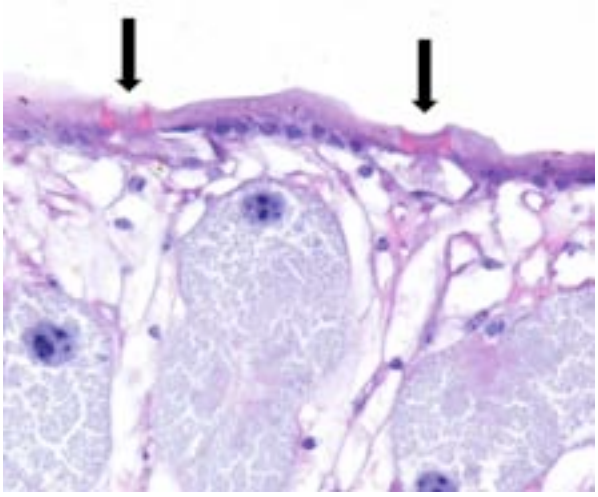

*2-4. Omentum, cynomolgus macaque: The cuticle has sclerotized pores (arrows) lined by eosinophilic refractile material (this material is composed of sclerotin). (HE 600X) (Photo courtesy of: US Army Medical Research Institute of Infectious Diseases: Pathology Division; Fort Detrick, MD http://www.usamriid.army.mil/)*


*2-5. Omentum, cynomolgus macaque: The fibrovascular wall surrounding the parasite is lined by a shed parasite cuticle which is identifiable by the presence of sclerotized pores. (HE 600X) (Photo courtesy of: US Army Medical Research Institute of Infectious Diseases: Pathology Division; Fort Detrick, MD http://www.usamriid.army.mil/)*

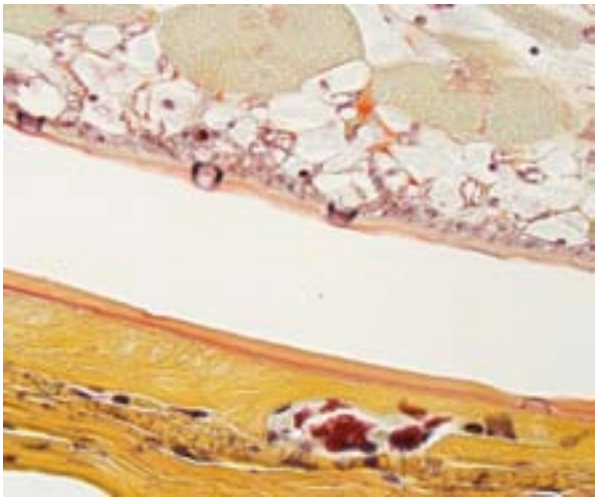

*2-6. Omentum, cynomolgus macaque: A Movat's pentachrome stain easily demonstrates the presence of sclerotized pores (arrows) in the cuticle of the parasite (above) and shed cuticle (below) by staining them a deep brown-black. (Movat's pentachrome, 600X)*

2) multiple annular bands of cuticle and underlying body wall (Figure 5); 3) skeletal muscle; 4) a multicellular digestive tract containing gray-brown granular material within the lumen; and 5) aggregates of large (up to 150 µm diameter) round to oval uninucleate cells containing eosinophilic finely granular cytoplasm that are located adjacent to the digestive tract. In some sections, one end of the parasite (i.e. the head) has 1 to 3 yellow refractile U-shaped to sickle-shaped structures, consistent with cephalic hooks.

**Contributor's Morphologic Diagnosis:** Omentum; encysted pentastome nymph, with fibrosis and minimal multifocal lymphoplasmacytic inflammation.

**Contributor's Comment:** The parasites encysted in the omentum of this monkey are incidental findings. Based on the gross morphology and microscopic features of these parasites, they are pentastome nymphs. Characteristic gross morphology includes the "C-shape" and the cuticular annulations which give it

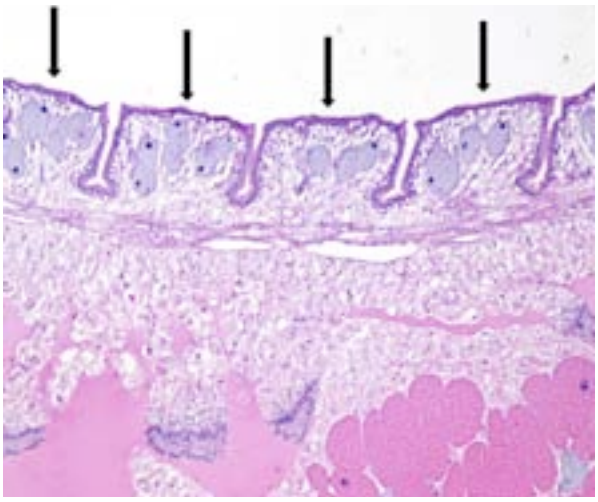

*2-7. Omentum, cynomolgus macaque: The cuticle and underlying body wall form annular bands (arrows); these are called cuticular annulations and produce the gross appearance of pseudosegmention. (HE 100X). (Photo courtesy of: US Army Medical Research Institute of Infectious Diseases: Pathology Division; Fort Detrick, MD http://www.usamriid.army.mil/)*

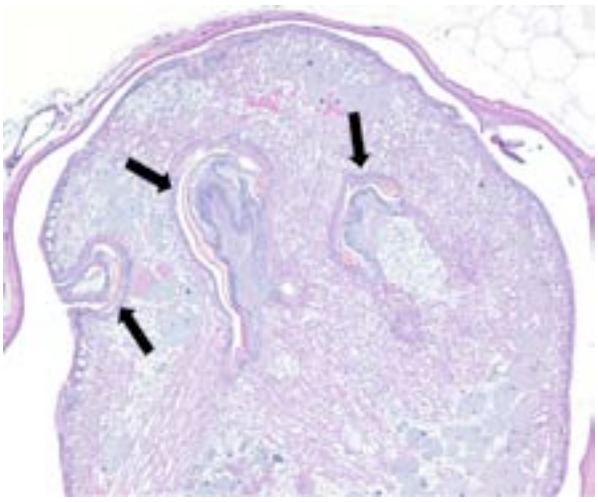

*2-8. Omentum, cynomolgus macaque: The parasite's anterior end has three yellow, refractile cephalic hooks (arrows). (HE 100X) (Photo courtesy of: US Army Medical Research Institute of Infectious Diseases: Pathology Division; Fort Detrick, MD http://www.usamriid.army.mil/)*

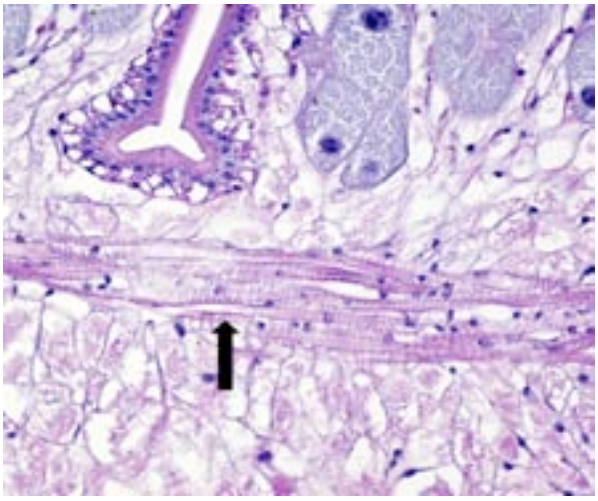

*2-9. Omentum, cynomolgus macaque: There is striated, skeletal muscle (arrow) subjacent to the cuticular annulations. (HE 400X) (Photo courtesy of: US Army Medical Research Institute of Infectious Diseases: Pathology Division; Fort Detrick, MD http://www.usamriid.army.mil/)*

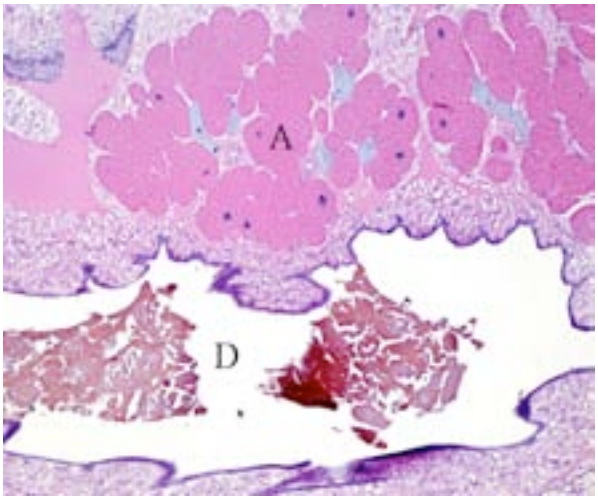


*2-10. Omentum, cynomolgus macaque: The pentastome's digestive tract (D) contains intraluminal blood pigments. Adjacent to the digestive tract are aggregates of large eosinophilic cells that from acidophilic glands (A). (HE 600X) (Photo courtesy of: US Army Medical Research Institute of Infectious Diseases: Pathology Division; Fort Detrick, MD http://www.usamriid.army.mil/)*

a pseudosegmented appearance.[1,6,7] Microscopic features of pentastomes include: a cuticle with sclerotized openings; cephalic hooks; striated muscle; and a digestive tract bordered by deeply eosinophilic "acidophilic glands".[1,3]

Pentastomes are a unique group of animals, all of which are parasites. The adult parasites inhabit the respiratory tract of vertebrates. More than 100 species have been described and for approximately 90% of these, the definitive host is a carnivorous reptile.[4] However, there is one species, *Linguatula serrata*, where the adult parasites live in the nasal passages of dogs and other carnivores. Adults in the genus *Linguatula* have a shape that resembles a mammalian tongue; this is the basis for the genus name and for the common term of "tongue worms" for pentastomes in general.

Each pentastome has two pairs of cephalic hooks adjacent to its mouth. These hooks are used to assist in attachment and burrowing. Early researchers mistook these hooks to be four

additional mouths; this error is the basis for the name of this group of parasites (i.e., penta stoma).[3]

Although a few pentastome species have a direct life cycle, the great majority of species utilize intermediate hosts.[4] Adult females lay eggs containing legged larvae that resemble mites.[1] The larvated eggs are passed into the environment either directly in respiratory secretions or are swallowed and passed in feces. Intermediate hosts become infected by ingestion of food or water contaminated with the eggs. Eggs hatch in the intestinal tract of the intermediate host and the larvae burrow through the intestinal wall. The larvae then develop into nymphs and encyst in the viscera and/or serous membranes of the intermediate host. After the intermediate host is consumed by the definitive host, the nymphs migrate to the respiratory tract of the final host and develop into adults.

A wide variety of animals (including humans) can serve as intermediate hosts for pentastomes. It is very difficult to accurately identify a pentastome species based solely on the morphology of nymphs.[5] In a report about the massive pentastome nymph infection of a stray dog from the southern United States, the species of pentastome was identified as *Porocephalus crotali* using a combination of gross parasite morphology and DNA analysis.[2]

The species of pentastome present in this monkey was not identified. However, the definitive host is most likely a snake or crocodilian that inhabited the native environment of this macaque. In a recent report about a massive pentastome infection of a cynomolgus macaque imported from China, the pentastome nymphs were identified as *Armillifer agkistrodontis* by DNA analysis.[5] *Armillifer agkitrodontis* adults occur in the lungs of pit vipers in SE Asia and the usual intermediate hosts are small rodents that serve as the prey base for the snakes; the monkey described in the case report was thought to be an accidental, dead-end host.[5]

The parasites present in this WSC case submission elicited mild fibrosis and very little inflammation by its primate host; this is typical, even in cases of massive pentastome infections.[2,5] However, fatal peritonitis has occasionally been associated with nymph penetration of the intestinal wall.[6] Dead nymphs cause intense inflammation and may eventually become mineralized.

In humans, three types of histologic lesions caused by pentastomid nymphs have been described.[7] The first lesion consists of an encysted and viable nymph surrounded by little to no inflammation (as in this monkey). In the second type of lesion, a dead nymph is surrounded by granulomatous and usually eosinophilic inflammation, encapsulated by concentric rings of fibrosis. In the third type of lesion, known as the granulomatous scar or cuticle granuloma, fibrous tissue surrounds a central mass of amorphous and/or mineralized material consisting of remnants of the long-dead parasite.

The cuticle of a pentastome often remains long after the rest of the dead parasite has degenerated. Finding parts of a cuticle with sclerotized openings within a focus of inflammation proves that the lesion was caused by a pentastome because no other parasites have sclerotized openings.[3] Visualization of the sclerotized openings can be greatly enhanced with a Movat pentachrome or Masson's trichrome stain.[3,7] In this case, the cyst wall also has sclerotized openings. This means that the wall is composed of a molted cuticle from the parasite.

The taxonomic classification of pentastomes was a subject of debate for many years. It has been long thought that they should be classified as arthropods or arthropod-like animals. Based on more recent DNA analyses, it is now generally accepted that pentastomes constitute a unique subclass (i.e., Pentastomida) of crustacean arthropods and are most closely related to the crustacean subclass Branchiura -- species of which are ectoparasites of fish and are commonly known as "fish lice".[4]

**Acknowledgement:** The author wishes to thank Dr. Kathleen Cashman for providing photography assistance and the gross photographs.

**Note:** Opinions, interpretations, conclusions, and recommendations are those of the author and are not necessarily endorsed by the U.S. Army.

**JPC Diagnosis:** Omentum: Encapsulated pentastome nymph.

**Conference Comment:** The contributor eloquently discusses the history, life cycle and clinical implications of pentastome infections. Routine sectioning and submission for histopathology of an encysted pentastome is likely a rare event due to its gross diagnosis, making this case a rare opportunity to see the organism in such exquisite detail. As mentioned, the observation of sclerotized openings are specific for pentastomes and of diagnostic importance in cases which lack intact specimens and appear as otherwise nonspecific inflammation. These become distinctly dark and readily identifiable with a Movat pentachrome stain, and portions of cuticle can remain in tissue for long after the rest of the parasite has died and been reabsorbed.[3]

Conference participants discussed the peculiarity of consistently observing the shed cuticle, or exuvia, lining the cystic cavity which encloses the pentastome. The exuvia is never observed floating freely, but rather always tightly adhered to tissue forming the cyst wall. This exuvia is from a previous nymph, and as nymphal stages undergo multiple molts before becoming a mature adult, it is possible the exuvia becomes a protective barrier from the immune defenses of the host. This is supported by the finding that intact cysts with viable nymphs are usually found with little or no adjacent cellular infiltration of the host tissue as antigenic compounds are largely sequestered.[7]

**Contributing Institution:** US Army Medical Research Institute of Infectious Diseases, Pathology Division, Fort Detrick, MD
http://www.usamriid.army.mil/

**References:**

1. Bowman DW, Lynn RC, Eberhard ML, Alcaraz A. *Georgis' Parasitology for Veterinarians*. 8th ed. St. Louis, MO: Saunders; 2003.
2. Brookins MD, Wellehan JFX, Roberts JF, et al. Massive visceral pentastomiasis caused by *Porocephalus crotali* in a dog. *Vet Path*. 2009;46:460-463.
3. Gardiner CH, Poynton SL. *An Atlas of Metazoan Parasites in Animal Tissues*. Washington, DC; Armed Forces Institute of Pathology; 2006.
4. Lavrov DV, Brown WM, Boore JL. Phylogenetic position of the Pentastomida and (pan)crustacean relationships. *Proc R Soc Lond B*. 2004;271:537-544.
5. Matz-Rensing K, Lampe K, Rohde G, Kaup F-J. Massive visceral pentastomiasis in a long-tailed macaque – an incidental finding. *J Med Primatol*. 2012;41(3):210-213.
6. Strait K, Else JG, Eberhard ML. Parasitic diseases of nonhuman primates. In: Abee CR, Mansfield K, Tardif S, Morris T, eds. *Nonhuman Primates in Biomedical Research Volume 2: Diseases*. 2nd ed. Boston, MA: Academic Press; 2012:271-272.
7. Tappe D, Büttner DW. Diagnosis of human visceral pentastomiasis. *PLoS Negl Trop Dis*. 2009; 3(2):e320. doi:10.1371/journal.pntd.0000320

**CASE III**: NCI/MPU 2012-2 (JPC 4019853).

**Signalment:** Adult woodchuck, *Marmota monax.*

**History:** The tissue derives from a woodchuck killed and field dressed by a hunter in early summer in the state of Maryland. An approximately 4 cm diameter mass was identified in the muscles of the shoulder. The hunter saw similar masses in multiple woodchucks throughout the spring.

**Gross Pathology:** The excised nodule is approximately 4 cm in diameter and encased in thick, fibrous connective tissue. On cut section, numerous fluid-filled cysts ranging from 5 to 20 mm in diameter are separated by a variably thick fibrous stroma. Cysts contain multiple, 0.5-1 mm diameter, white cysticerci that are variably attached to the inner cyst wall or are floating within the cyst fluid.

**Histopathologic Description:** A large, multilocular mass effaces and distorts skeletal muscle. The mass is composed of cystic cavities that contain multiple cysticerci and are surrounded by thick bands of fibrous connective tissue and inflammatory infiltrates. In some areas, there is complete loss of the cyst wall (cyst rupture) with neutrophils, eosinophils, macrophages, multinucleated giant cells, and lymphocytes infiltrating degenerate cysticerci with loss of distinct architecture and variable parenchymal mineralization. Cysticerci measure up to 1 mm in diameter and have a thick tegument that surrounds a large bladder and an inverted neck. They lack a pseudocoleom, a digestive tract, and reproductive organs. The parenchyma of the neck contains numerous calcareous corpuscles, excretory ducts, and an inverted scolex covered by a thick tegument and associated with large muscular suckers. Rostellar hooks are present in few cross-sections. The surrounding mature fibrous connective tissue is infiltrated by many neutrophils, eosinophils, macrophages, and fewer lymphocytes and plasma cells admixed with necrotic cell debris. Surrounding skeletal muscle fibers are in varying stages of degeneration, ranging from swollen, hypereosinophilic myocytes to myocytes with fragmented, flocculent sarcoplasm that lack cross-striations. Few myocytes in the surrounding skeletal muscle are distended by intracytoplasmic apicomplexan cysts containing myriad bradyzoites that measure approximately 5 µm in diameter (*Sarcocyst spp*., presumptive). Postmortem bacterial overgrowth is prominent.

**Contributor's Morphologic Diagnosis:** 1. Skeletal muscle: Cysticercosis with eosinophilic, granulomatous myositis, fibrosis, and myodegeneration.
2. Skeletal muscle: Sarcocytosis.

**Contributor's Comment:** Cysticercosis has been reported several times in woodchucks, most

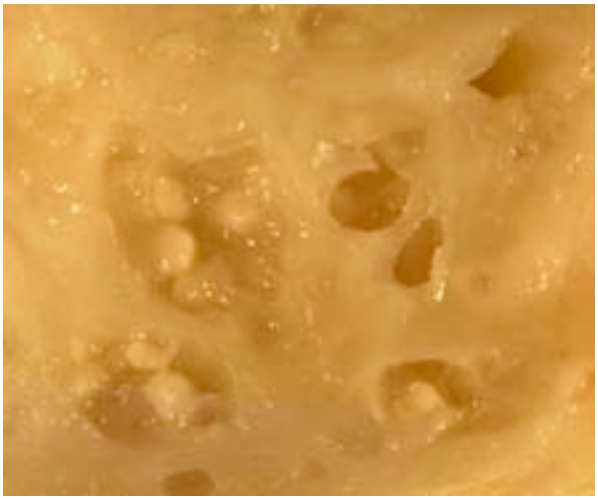

*3-1. Skeletal muscle, woodchuck: Cut section of the fixed mass taken with a stereomicroscope showing multiple cystic cavities containing numerous small, white cysticerci. (Photo courtesy of: Comparative Molecular Pathology Unit, Laboratory of Cancer Biology and Genetics, Center for Cancer Research, National Cancer Institute; http://ccr.cancer.gov/staff/staff.asp?profileid=8472)*

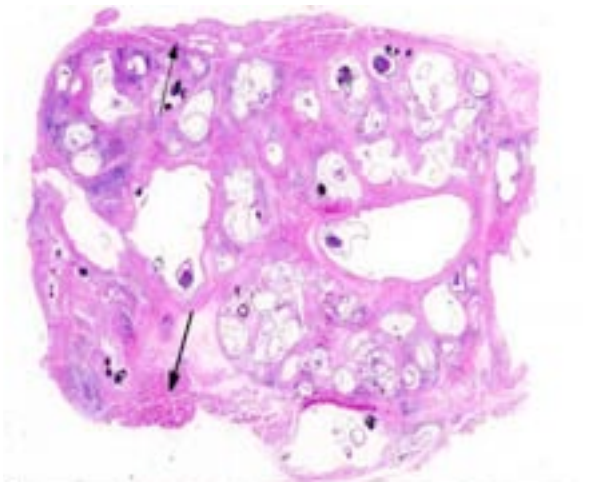

*3-2. Skeletal muscle, woodchuck: This section of skeletal muscle contains an unusual concentration of cysticerci. A small amount of atrophic skeletal muscle is present at the top and bottom of the section (arrows). (HE 6.3X)*

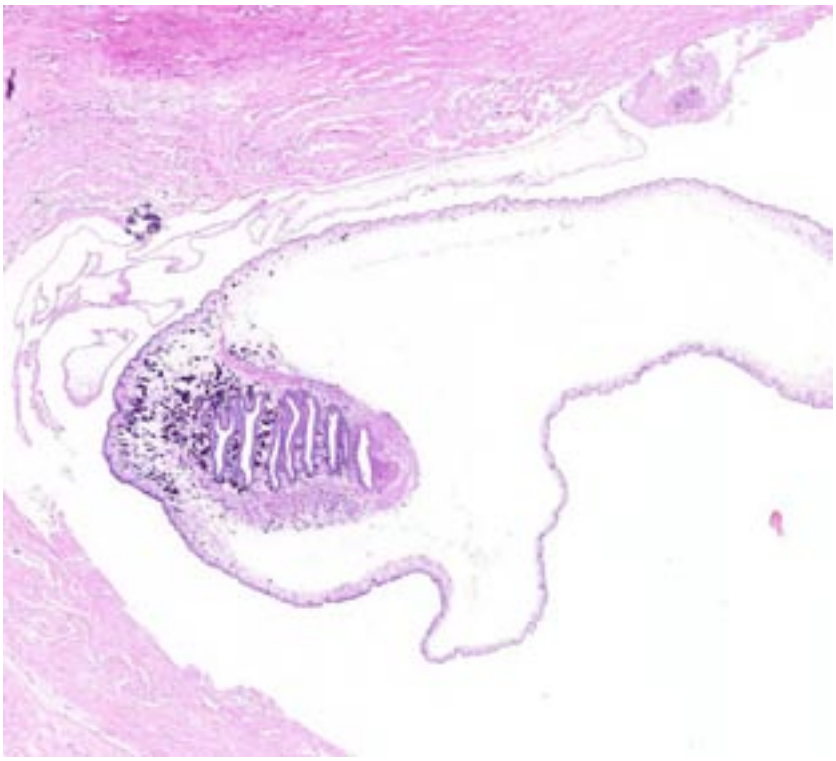

*3-3. Skeletal muscle, woodchuck: Within each of the fibrous cysts is a cysticercus with a large bladder and an inverted scolex. (HE 34X)*

commonly due to infection with *Taenia crassiceps*. The axillary subcutis is most commonly affected, though other subcutaneous regions may also be affected as well as the peritoneal cavity, thoracic cavity, nasal sinuses, liver, lung, and brain.[1,3,5]

Feral woodchucks may bear heavy cysticerci burdens that may be particularly prominent after emergence from hibernation.[2] Laboratory woodchucks may also develop cysticercosis, especially if the animals are of wild-caught origin.[1,5]

The species of tapeworm affecting this woodchuck is not definitively known. Previously reported cases of woodchuck cysticercosis were consistent with *T. crassiceps* larvae; the fox was considered the likely definitive host in these cases.[1-3,5] Morphologic features of this parasite are consistent with *T. crassiceps* and include an anterior scolex with four suckers, an apical rostellum that contains large and small rostellar hooks, and a posterior bladder.[1,4,5]
The inflammatory response in this case is relatively mild and composed of a mixed population of inflammatory cells. Inflammation is more intense in areas of cyst rupture. Previous reports of the inflammatory reaction woodchuck cysticercosis describe a similarly mild response with more prominent lymphocytic infiltrates and a similar variability in the degree of reactive fibrosis.[1]

**JPC Diagnosis:** Skeletal muscle: Multiple cysticerci with fibrosis and moderate histiocytic and atrophic rhabdomyositis.

**Conference Comment:** The interesting aspect of this case is its unique presentation. As is consistent with previously reported cases highlighted by the contributor, the cysticerci were found in a focal aggregrate in the skeletal muscle of the shoulder.

There are two orders in the phylum *Platyhelminthes* which comprise tapeworms.[4] The order of pseudophyllideans grows into much larger adults, such as *Diphyllobothrium* spp., and never shed their proglottids. This is contrast to the order of cyclophyllideans, as observed in this case, which shed gravid proglottids each containing thousands of infectious eggs. The cyclophyllideans are more readily transmissible and as a result, are the most significant cause of

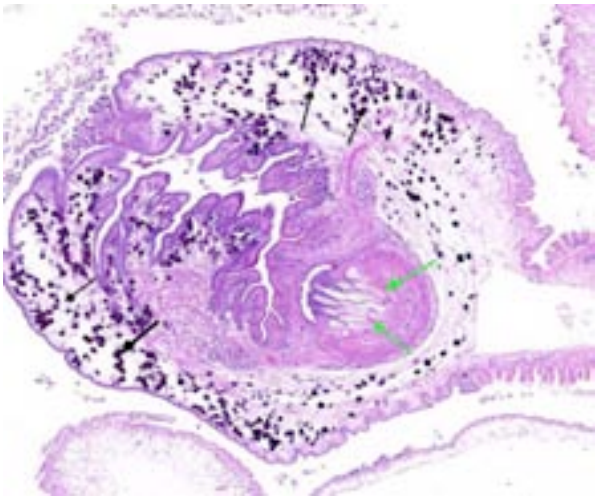

*3-4. Skeletal muscle, woodchuck: Cestodes contain an armed rostellum with several hooks (green arrows), a parenchymatous body cavity and numerous brown-black calcareous corpuscles (black arrows). (HE 47X)*

CNS disease in people in South America.[6] When the eggs are ingested, the larvae migrate into various tissues resulting in significant pathology. Conference participants speculated on what drove these larvae to all migrate to the same location in this woodchuck.

We agree with the contributor that, although *T. cracisseps* is the most often reported and most likely species in this case, the presence of an anterior scolex with four suckers and a posterior bladder is only indicative of the type of larval cestodes known as a cysticercus and cannot be differentiated further. However, some references indicate the possibility of species identification based on the length of small and large hooks in the rostellum.[3] Other groups of larval cestodes include the cysticercoids which have a tiny bladder and a scolex surrounded by parenchymous arms, coenurus which has more than one scolex, and hydatid cysts with a bladder and numerous small protoscolices each with a scolex and suckers. Solid-bodied cestodes are plerocercoids (lack suckers) or tetrathyridium (has suckers).[4]

**Contributing Institution:** Comparative Molecular Pathology Unit, Laboratory of Cancer Biology and Genetics, Center for Cancer Research, National Cancer Institute; http://ccr.cancer.gov/staff/staff.asp?profileid=8472

**References:**

1. Anderson WI, Scott DW, Hornbuckle WE, King JM, Tennant BC. Taenia crassiceps infection in the woodchuck: a retrospective study of 13 cases. *Vet Dermatol*. 1990;1:85-92.
2. Beaudoin RL, Davis DE, Murrell KD. Antibodies to larval Taenia crassiceps in hibernating woodchucks, *Marmota monax*. *Exp Parasitol*. 1969;24(1):42-6.
3. Brojer CM, Peregrine AS, Barker IK, Carreno RA, Post C. Cerebral Cysticercosis in a Woodchuck (*Marmota monax*). *Journal of Wildlife Diseases*. 2002;38(3):621–624.
4. Gardiner CH, Poynton SL. Morphologic characteristics of cestodes in tissue section. In: An Atlas of Metazoan Parasites in Animal Tissues/ American Registry of Pathology. Washington, D.C. 1999:50-55.
5. Shiga J, Aoymana H, Yamamoto K, Imai S, Saeki H, Sasaki N, Koshimizu K. A case report of cysticercosis caused by Cysticercus longicollis, a larval form of Taenia crassiceps in a woodchuck (*Marmota monax*). *Jikken Dobutsu*. 1987;36(2): 213-7.
http://www.cdc.gov/parasites/cysticercosis. Center for Disease Control. April 16, 2014.

**CASE IV:** 2 (JPC 4048512).

**Signalment:** Juvenile female Springer Spaniel, *Canis familiaris*.

**History:** This was a stray dog found dead on February 2014 and sent for necropsy to evaluate the circumstances of death.

**Gross Pathology:** Mucosae were icteric and severely anemic. In the abdominal cavity, liver was enlarged and fibrotic with severe passive congestion. Abdominal aorta was severely focally dilated (aneurysm) and yellow (jaundice). Elevated numbers of trichurids (whipworms) were observed in the rectum and cecum. In the thoracic cavity, severe pneumomediastinum and pneumothorax was observed. Moderate hemothorax was also present.

Severe, diffuse pleural thickening and fibrinous pleuritis affected all lung lobes. Severe diffuse pulmonary edema and fibrino-necrotizing pneumonia were present. Multifocal areas of necrotizing and gangrenous pneumonia with colliquative necrosis were evidenced on cut section of lung lobes.

Mild pericardial effusion and severe right ventricular and atrial dilation were observed.

**Laboratory Results:** Parasitologic isolation of adult nematodes from lung specimens identified the parasites as *Angiostrongylus vasorum*. Parasitologic examination of intestinal nematodes identified the species as *Trichuris vulpis*.

**Histopathologic Description:** Lung: Approximately 80-90% of the pulmonary parenchyma (severity of extension varies among tissue sections) is affected by severe degenerative and inflammatory changes involving pulmonary arteries, pulmonary interstitium and to a lesser extent alveolar spaces.

Occasionally, in arterial lumens or embedded in the endoluminal fibrin thrombi there are variable numbers of transverse and longitudinal sections of both viable and degenerated/necrotic adult nematodes associated in some instances with larvae, occasionally with deep basophilic granular material (dystrophic mineralization). Intravascular adult nematodes are approximately 450-550 µm in length and 200-250 µm in diameter, with a smooth eosinophilic 4-5 µm thick cuticle, coelomyarian musculature and a pseudocoelom, in which are detectable tracts of the gastrointestinal tract with an intestine lined by multinucleated cells and of the reproductive male and female tracts, the latter with intrauterine embryonated eggs.

Pulmonary arteries multifocally are occluded by laminated meshwork of pale eosinophilic finely beaded to fibrillar material adherent to the endothelium (fibrin thrombi), occasionally characterized by ingrowth of endothelial cells, smooth muscle cells, fibroblasts and slit-like

*4-1. Lung, dog: Cut sections of lung contained multifocal areas of necrotizing and gangrenous pneumonia with colliquative necrosis. (Photo courtesy of: C DIVET- School of Veterinary Medicine, Milano – Italy, http://www.anapatvet.unimi.it/)*

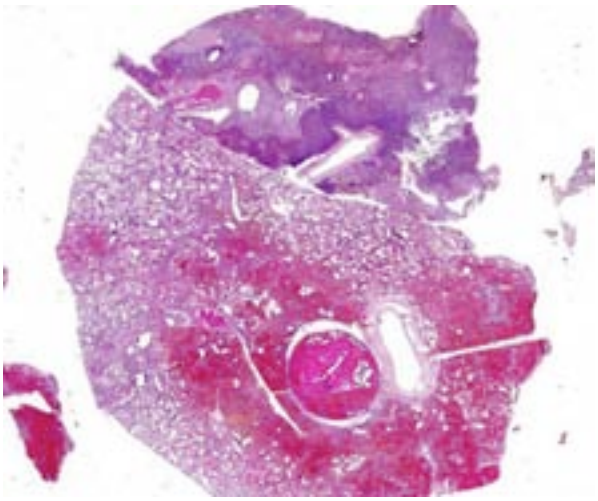

*4-2. Lung, dog: Subgross of submitted slides. The one at top has a large area of suppuration and necrosis, likely second to an infarct. The larger section at the bottom has a large thrombosed artery and extensive hemorrhage. (HE 6.3X)*

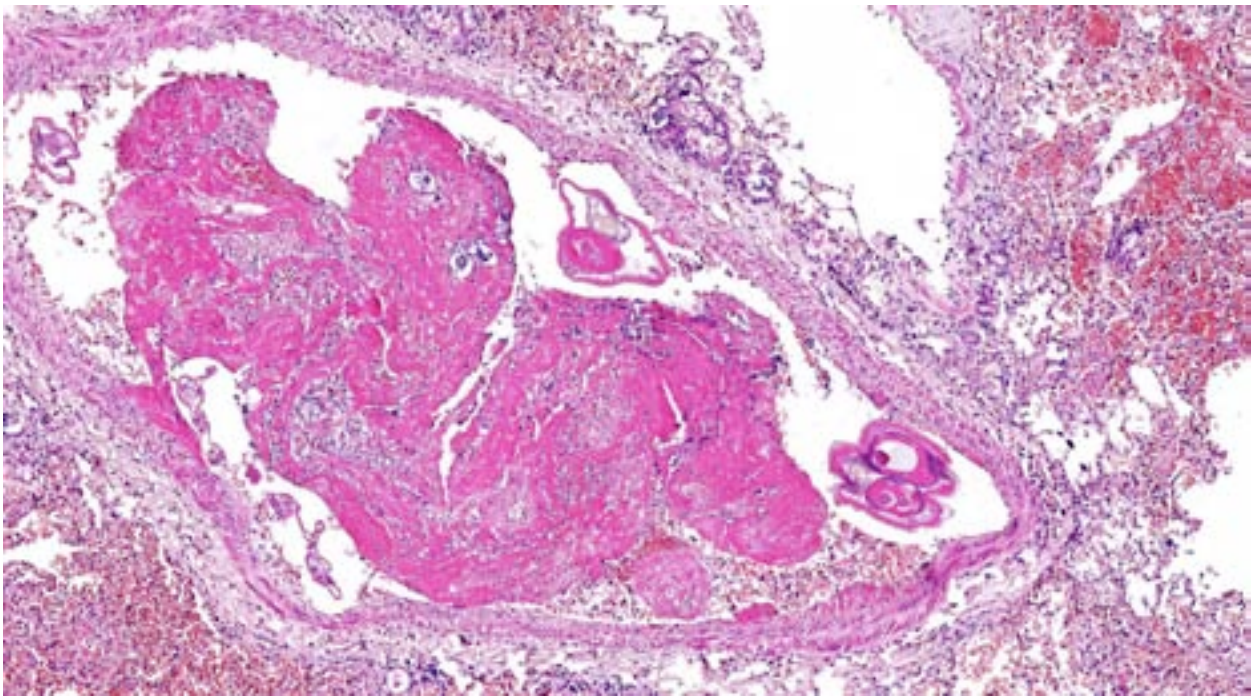

*4-3. Lung, dog: Thrombosed artery with numerous cross- and tangential sections of Angiostrongylus vasorum. (HE 60X)*

clefts (capillary channels; thrombus organization and recanalization) and extravasated erythrocytes (hemorrhages). Some arterial lumens contain necrotic debris and moderate numbers of both viable and degenerated (karyorrhectic) neutrophils (thrombus dissolution). Multifocally, arteries have medial hypertrophy/hyperplasia with intima bulging within the vascular lumen (luminal narrowing) and endothelium lined by plump reactive endothelial cells (proliferative endoarteritis). The walls of pulmonary arteries are multifocally expanded by extravasated erythrocytes (intramural hemorrhages) or by bright eosinophilic amorphous material (fibrinoid necrosis), in which are embedded degenerated neutrophils (leukocytoclastic vasculitis) with disruption of the wall.

Multifocally expanding alveolar septa, peribronchial interstitium and filling alveolar lumens there are nematode eggs and larvae, or more rarely on adult nematodes. Eggs are round to oval, 40-50 µm in diameter, filled with eosinophilic granular material and containing a single basophilic often eccentric, 10 µm in diameter nucleus (nonembryonated eggs) or are oval, 150x50 µm and are multinucleated (embryonated eggs). Larvae are 150x50 µm and are composed of numerous, round, 4-6 µm in diameter, basophilic nuclei with scant eosinophilic cytoplasm and a smooth 1 µm wide amphophilic cuticle.

Larvae and eggs are occasionally free in the alveoli but more frequently are surrounded by inflammatory cells composed by a prevalence of epithelioid macrophages, foamy reactive macrophages, occasionally containing golden granular material (hemosiderin), and by lesser numbers of multinucleated giant cells with up to 7 haphazardly arranged nuclei (foreign body-type) and rare eosinophils and granulocytes. Granulomas are multifocally surrounded by dense fibrous tissue.

Multifocally the lung is characterized by locally extensive areas of coagulative necrosis (pulmonary infarcts) associated often with hemorrhages and/or hematoidin (chronic hemorrhages). Alveoli not affected by the inflammatory process are characterized by edema, rupture of alveolar septa and blunted clubbed ends (alveolar compensatory emphysema) or atelectasis. Diffusely, alveolar capillaries are engorged by erythrocytes (alveolar septa hyperemia).

In some of the examined slides are also detectable:

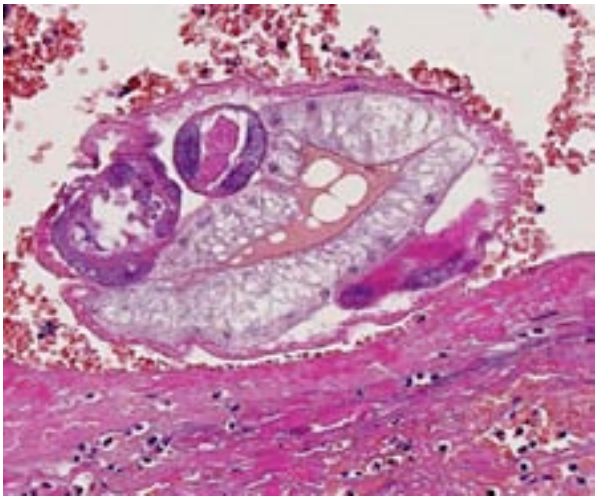

*4-4. Lung, dog: Cross section of an adult female A. vasorum within a thrombosed arteriole. The parasite has low coelomyarian-polymyarian musculature and three sections of the genital tract surrounding a large central intestine with few multinucleated intestinal cells. (HE 140X)*

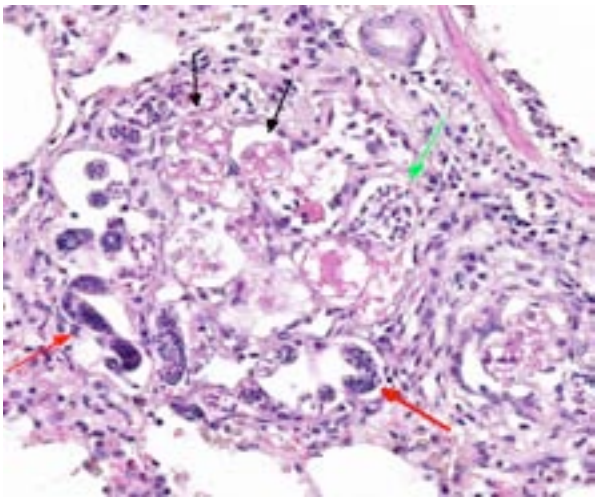

*4-5. Lung, dog: In areas of granulomatous inflammation, alveoli contain variable numbers of nematode larvae (red arrows), and morulated (green arrows) and embryonated (larvated) eggs (black arrows). (HE 192X)*

-intrabronchial and intrabronchiolar nematode larvae, admixed with sloughed epithelial cells and a moderate amount of eosinophilic cellular and karyorrhectic necrotic debris;
-bronchioles lined by a multifocally ulcerated epithelium, with denuded lamina propria;
-thickening of the pleura, expanded up to 8-10 times normal by collagen bundles (fibrosis);
-alveolar septa lined by plump type II pneumocytes (type II pneumocytes hyperplasia).

**Contributor's Morphologic Diagnosis:** 1. Pulmonary multifocal to locally extensive necrosis (pulmonary infarcts) and hemorrhage with multifocal occlusive arterial thrombosis with variable numbers of adult nematodes, larvae and eggs and multifocal moderate subacute proliferative endoarteritis. 2. Multifocal to coalescing severe chronic granulomatous and eosinophilic pneumonia, with intralesional nematode adult, larvae and eggs, with multifocal severe subacute pulmonary coagulative necrosis (infarcts), hemorrhages and hemosiderosis

**Contributor's Comment:** The cause of death in this case was ascribed to severe massive pulmonary thromboembolism (acute and chronic) with pulmonary infarction, locally extensive necrotizing and gangrenous pneumonia, all findings associated with vascular occlusion by *A. vasorum* adults.

In the first part of 2014 (February, March, April), an increased number of dogs (at least one every week) were referred for necropsy at our institution and were diagnosed with massive pulmonary nematodiasis, with parasitological identification of *A. vasorum*. Italy is considered one of the European countries where this nematode is spreading rapidly.[7] Northern Italy this year has been, for the most part, a warm winter with mild temperatures that have caused an increased survival/vitality rate of intermediate hosts and larvae of *A. vasorum*.

An increased emergence of canine heartworms and lungworms has been reported in Europe. This increase may have many drives including global warming, changes in vector epidemiology and movement of animal populations.[19] Survival rates of *A. vasorum* L1 larvae have been demonstrated to be influenced by temperatures and temperatures over 10° celsius influencing positively larval development into infective L3 stage larvae.[8,9] Also, larval burdens within slugs are highly dependent on temperatures.[9]

Additional risk factors in dogs include age (higher risk in younger dogs), season (more cases earlier in the calendar year), and worming history (lower risk if given milbemycin oxime in the past 12 weeks).[13] No history was available in this dog; however, young age and the time of year (February) were compatible with these observations.

*Angiostrongylus vasorum,* French heartworm, is a metastrongyloid parasite found in the pulmonary

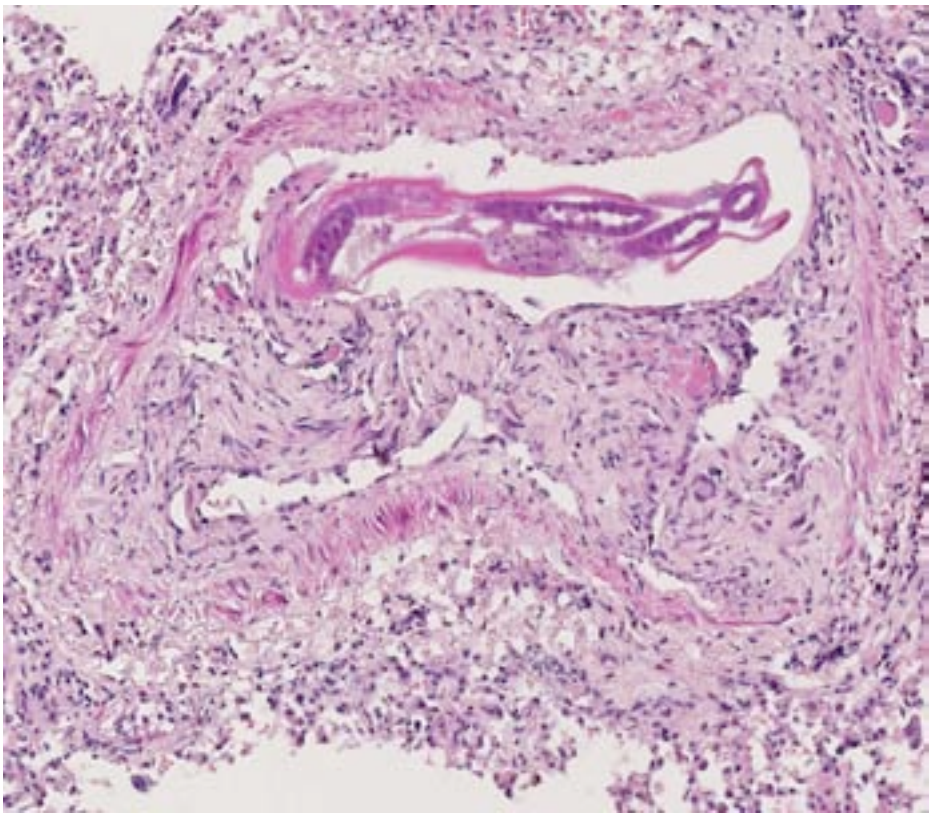

*4-6. Lung, dog: The intima of small arterioles exhibits marked fibrosis and formation of slit-like channels, and has small amounts of brightly eosinophilic extruded fibrin (villar endarteritis, fibrinoid vasculitis recanalization, as a result of the presence of adult nematodes. (HE 102X)*

arteries and right ventricle of wild and domestic canids and various other animal species.[5,19] The natural definitive hosts are foxes. The geographic distribution of the parasite includes various countries of Europe, Africa, South America, and North America. In North America, autochthonous *A. vasorum* infection occurs only in the Canadian province of Newfoundland-Labrador.[5] Angiostrongylosis is considered an emerging disease in dogs in Europe[19] and North America.[5] At present, angiostrongylosis is considered endemic in parts of France, southwestern England, Ireland, Denmark, Italy, Spain, Germany, Hungary, Finland, Switzerland, and Turkey, in South America in Brazil and Colombia, and in Uganda.[2] However, in the last decade, a relatively new endemic focus of *A. vasorum* infection has emerged in eastern Canada, in the provinces of Newfoundland and Labrador.[2] The reasons of increased emergence are little known but many drivers such as global warming, changes in vector epidemiology and movements in animal populations may be taken into account.

*A. vasorum* is a nematode of the superfamily Metastrongyloidea, family angiostrongylidae. The life cycle of *A. vasorum* is indirect. Adults inhabit the pulmonary arteries and right ventricle of dogs and foxes.[3,7] Red foxes and other species of wild foxes serve as natural definitive hosts and are an important reservoir of infection for dogs.[7] Natural infection has also rarely been reported in other species including badgers, wolves and coyotes.[3,7] Gastropods such as snails and slugs but, also amphibians such as frogs may serve as intermediate hosts. Gastropods become infected with L1 when foraging on infected feces or on contaminated plant material. In the intermediate host, the larvae mature and develop into second-stage and third-stage larvae (L2 and L3). The final host, usually a fox or dog, becomes infected by eating an intermediate host containing L3. The slug or snail is digested within the stomach or intestine of the canid, releasing L3 that penetrate the gastrointestinal tract wall, migrate to visceral lymph nodes, and eventually develop into immature adults. The juvenile worms migrate via portal circulation to the liver, caudal vena cava, the right atrium, right ventricle, and pulmonary arteries where they reach maturity approximately 33 to 35 days post-infection. The prepatent period for *A. vasorum* is approximately 38 to 57 days.[2, 5]

Clinical signs associated with angiostrongylosis may be diverse and a range of signs is described in the above reports. However, two prevalent clinical syndromes predominate; respiratory disease caused by the inflammatory response to eggs and migrating larvae, and hemorrhagic diatheses manifesting as local or diffuse haemorrhages.[4,15] Clinical features include

cardiorespiratory (63%), coagulopathic (71%) and other (63%) signs. Cough, dyspnea and tachypnea have been reported as the most common cardiorespiratory abnormalities. Of animals with evidence of coagulopathy, excessive hemorrhage from wounds, airway hemorrhages, epistaxis, hematomas, haemarthrosis, and hematuria have been reported.[4,15] Vague signs of exercise intolerance, lethargy and weakness may be present.[15]

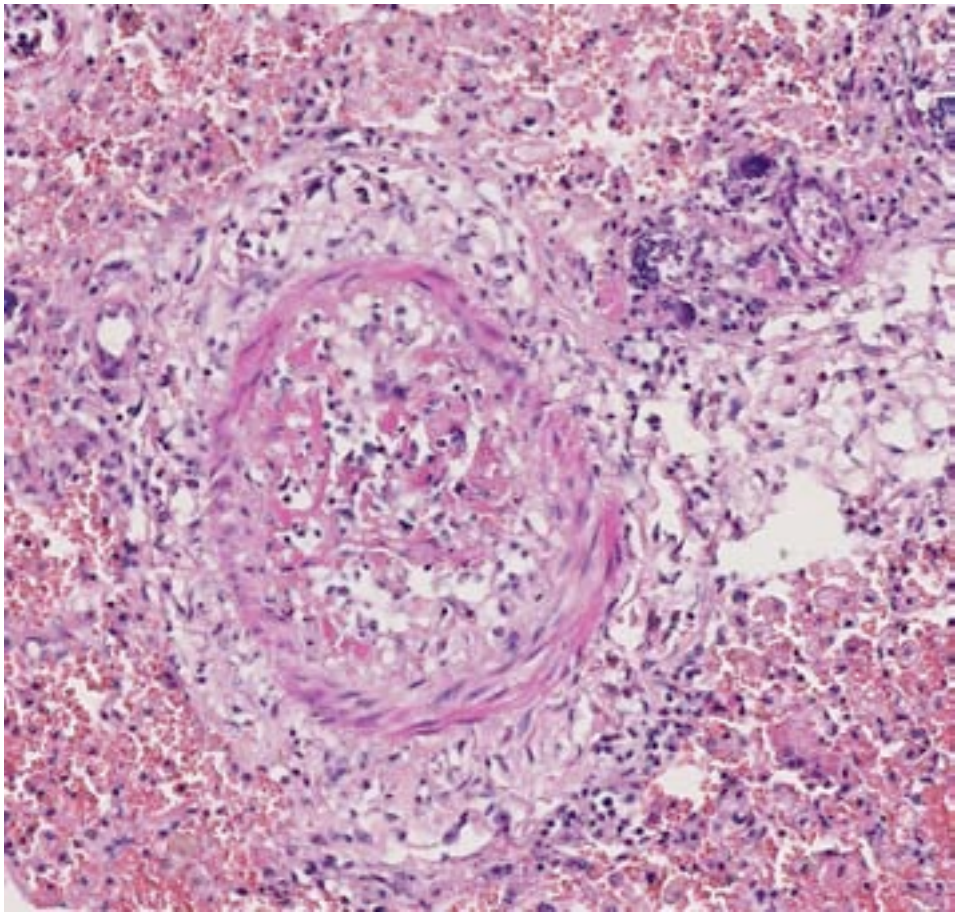

*4-7. Lung, dog: Another recanalized arteriole with ongoing fibrinoid change. (HE 154X)*

Most cases develop chronic heart failure, but acute interstitial pneumonia occurs in heavily infected dogs. Pulmonary arterial hypertension seems to develop rarely despite the severe lung lesions in chronic cases.[14] Other uncommon manifestations include disseminated intravascular coagulation, uveitis in response to aberrant migration to the anterior chamber of the eye,[3] hemothorax[16] and hemoabdomen.[22]

Acute neurological signs caused by hemorrhages in the central nervous system (brain and/or spinal cord) have been reported.[6,10,11,21] In these cases, results of coagulation assays are inconsistent for certain authors[11] while others find consistently coagulopathy and associated pulmonary hemorrhages.[6,10]

Neurological signs reflect the site of lesions and may include seizures, various cranial nerve deficits, vestibular signs, proprioceptive deficits, ataxia and paraplegia.[6,10,11,21] Thoracic radiographs (n = 19) identified abnormalities in 100% of cases.[15] A variety of changes were observed, the most typical being a patchy alveolar-interstitial pattern affecting the dorso-caudal lung fields.[4]

Dogs may exhibit increased total white blood cell counts with transient neutrophilia and eosinophilia. An increase in serum globulins and a decrease in serum fructosamine have also been found.[23] Variably severe anemia (hematocrit $\leq$ 0.20 L/L) and thrombocytopenia characterize dogs with hemorrhagic diatheses. Prolonged prothrombin time and/or activated partial thromboplastin and BMB values have been observed.[4]

The mechanism behind the coagulation defects is poorly understood but most authors have suggested that antigenic factors secreted by the parasites cause excessive intravascular coagulation and a consumptive coagulopathy.[4] Dogs with neurological signs may demonstrate high concentrations of protein and evidence of erythrophagia in the cerebrospinal fluid.[23]

Lesions during the prepatent period are mild. Adult, 14-21 mm long worms are present in the pulmonary arteries, and the lungs contain a few 1-2 mm red nodules, consisting of aggregates of eosinophils and mononuclear cells.[3] More severe lesions develop at the time of patency, including proliferative endoarteritis in response to the adult worms in the pulmonary arteries, and granulomatous to pyogranulomatous pneumonia as a consequence of embolized eggs and larvae.[2,3] Arterial lesions include thrombosis, thickening of the tunica intima by fibromuscular tissue, medial hypertrophy, and lymphoplasmacytic aggregates in the adventitia.[2,3,6,17] Pulmonary lesions consist of red or golden-brown, nodular or confluent areas of hemorrhage, edema, and firmness at the periphery of the lung.[2,3] Histologically, coalescing granulomas formed by macrophages and giant cells are centered on parasite eggs and larvae in the lung are present with variable association with necrosis, neutrophils and eosinophils.[2,3,6,17] There is mild proliferation of type II pneumocytes, alveolar hemorrhage, hemosiderin-laden macrophages, and arteriolar thrombosis.[2,3,17] Fibrosis and recanalization of arterial thrombi develop as the lesion ages. Similar granulomas developing around dead or degenerating worms have been reported in brain, kidney, and various tissues.[3] Foci of granulomatous interstitial pneumonia can often be found when worm remnants may no longer be identified. Central nervous system hemorrhages have also been observed.[2] Definitive ante-mortem diagnosis is by detection of L(1) in feces, sputum, or bronchoalveolar lavage samples. Baermann fecal examination is the most reliable method for fecal detection.[5] However, a false negative result can occur due to the typical erratic/sporadic fecal larval shedding pattern of *A. vasorum*.[5,6] Furthermore, this method has been reported to have low sensitivity. Only recently has an increased repertoire of techniques for *A. vasorum* infection diagnosis been reported, such as detection of L1 in broncho-alveolar lavage fluid and the development of a sandwich ELISA to detect circulating antibodies and worm excretory/secretory antigens.[18,20]

Diagnosis has been achieved by testing fecal samples and blood of foxes and domestic dogs by PCR.[1,12] Definitive diagnosis requires extraction of intact adults from the lungs, as the histologic appearance is similar to *Andersonstrongylus milksi*. *Angiostrongylus* can be differentiated from *Dirofilaria* by examination of intact adults, or by histologic examination. *Angiostrongylus* has thin coelomyarian musculature, a large, strongyloid intestine composed of few multinucleate cells, and eggs in the uterus. The females have a "barber-pole" appearance due to the helically arranged red gut and white ovaries. The larvae in the lungs are wider and more developed than the microfilariae of *Dirofilaria*. In contrast, *Dirofilaria* has well-developed coelomyarian musculature, a smaller intestine, and a uterus containing microfilariae.[3]

Current treatment options include moxidectin, milbemycin oxime, and fenbendazole.[5] However, killing the worms with an anthelmintic may incite severe response.[3,10,11]

**JPC Diagnosis:** Lung: Pneumonia, interstitial, granulomatous, chronic, multifocal, marked, with severe arterial hypertrophy, villar endarteritis, thrombosis, and numerous nematode adults, larvae and eggs.

**Conference Comment:** With the multitude of lesions present, this case provides an exercise in delivering a thorough histopathologic description. In addition, the contributor's exhaustive review of pathogenesis highlights the important elements of this emerging disease. The details of this case serve as a reminder of resilience of these parasites despite effective anthelmintics and adequate medical infrastructure.

**Contributing Institution:** DIVET- School of Veterinary Medicine**,** Milano - Italy
http://www.anapatvet.unimi.it/

**References**

1. Al-Sabi M, Deplazes P, Webster P, Willesen J, Davidson R, Kapel C. PCR detection of *Angiostrongylus vasorum* in faecal samples of dogs and foxes. *Parasitol Res*. 2010;107:135-140.
2. Bourque A, Conboy G, Miller L, Whitney H. Pathological findings in dogs naturally infected with *Angiostrongylus vasorum* in Newfoundland and Labrador, Canada. *J Vet Diagn Invest*. 2008;20:11-20.
3. Casewell J, Williams K. Respiratory System. St. Louis, MO: Elsevier; 2007:2:648.
4. Chapman PS, Boag AK, Guitian J, Boswood A. *Angiostrongylus vasorum* infection in 23 dogs (1999-2002). *J Small Anim Pract*. 2004;45:435.

5. Conboy G. Canine angiostrongylosis: the French heartworm: an emerging threat in North America. *Vet Parasitol*. 2011;176:382-389.
6. Denk D, Matiasek K, Just FT, Hermanns W, Baiker K, Herbach N, et al. Disseminated angiostrongylosis with fatal cerebral haemorrhages in two dogs in Germany: A clinical case study. *Vet Parasitol*. 2009;160:100-108.
7. Eleni C, Grifoni G, Di Egidio A, Meoli R, De Liberato C. Pathological findings of *Angiostrongylus vasorum* infection in red foxes (Vulpes vulpes) from Central Italy, with the first report of a disseminated infection in this host species. *Parasitol Res*. 2014;113:1247-50.
8. Ferdushy T, Hasan MT. Survival of first stage larvae (L1) of *Angiostrongylus vasorum* under various conditions of temperature and humidity. *Parasitol Res*. 2010;107:1323-1327.
9. Ferdushy T, Kapel CM, Webster P, Al-Sabi MN, Grønvold JR. The effect of temperature and host age on the infectivity and development of *Angiostrongylus vasorum* in the slug Arion lusitanicus. *Parasitol Res*. 2010;107:147-151.
10. Garosi L, Platt SR, MCConnell JF, Wray JD, Smoth KC. Intracranial haemorrhage associated with *Angiostrongylus vasorum* infection in three dogs. *J Small Anim Pract*. 2005;46:93-99.
11. Gredal H, Willesen JL, Jensen HE, Nielsen OL, Kristensen AT, Koch J, et al. Acute neurological signs as the predominant clinical manifestation in four dogs with *Angiostrongylus vasorum* infections in Denmark. *Acta Vet Scan*. 2011;53:43-51.
12. Jefferies R, Morgan E, Shaw S. A SYBR green real-time PCR assay for the detection of the nematode *Angiostrongylus vasorum* in definitive and intermediate hosts. *Vet Parasitol*. 2009;166:112-118.
13. Morgan ER, Jefferies R, van Otterdijk L, McEniry RB, Allen F, Bakewell M, et al. *Angiostrongylus vasorum* infection in dogs: Presentation and risk factors. *Vet Parasitol*. 2010;173:255-261.
14. Nicolle AP, Chetboul V, Tessier-Vetzel D, Sampedrano C, Aletti E, Pouchelon J-L. Severe pulmonary arterial hypertension due to *Angiostrongylosus vasorum* in a dog. *Can Vet J*. 2006;4:792-795.
15. O'Neill E, Acke E, Tobin E, McCarthy G. Immune-mediated thrombocytopenia associated with *Angiostrongylus vasorum* infection in a Jack Russell Terrier. *Irish Vet J*. 2010;63:434-440.
16. Sasanelli M, Paradies P, Otranto D, Lia RP, De Caprariis D. Haemothorax associated with *Angiostrongylus vasorum* infection in a dog. *J Small Anim Pract*. 2008;49:417-420.
17. Schnyder M, Fahrion A, Riond B, Ossent P, Webster P, Kranjc A, et al. Clinical, laboratory and pathological findings in dogs experimentally infected with *Angiostrongylus vasorum*. *Parasitol Res*. 2010;107:1471-1480.
18. Schucan A, Schnyder M, Tanner I, Barutzki D, Deplazes P. Detection of specific antibodies in dogs infected with *Angiostrongylus vasorum* . *Vet Parasitol*. 2012;185:216-224.
19. Traversa D, Di Cesare A. Canine and feline cardiopulmonary parasitic nematodes in Europe: emerging and underestimated. *Parasit Vectors 3*. 2010;62-84.
20. Verzberger-Epshtein I, Markham R, Sheppard J, Stryhn H, Whitney H. Serologic detection of *Angiostrongylus vasorum* infection in dogs. *Vet Parasitol*. 2008;151:53-60.
21. Wessmann A, Lu D, Lamb C, Smyth B, Mantis P, Chandler K, et al. Brain and spinal cord haemorrhages associated with *Angiostrongylus vasorum* infection in four dogs. *Vet Rec*. 2006;158:858-863.
22. Willesen JL, Bjornvad CR, Koch J. Acute haemoabdomen associated with *Angiostrongylus vasorum* infection in a dog: a case report. *Irish Vet J*. 2008;61:591-593.
23. Willesen JL, Jensen AL, Kristensen AT, Koch J. Haematologicaland biochemical changes in dogs naturally infected with *Angiostrongylus vasorum* before and after treatment. *Vet J*. 2009;180:106-111.

**Joint Pathology Center**
**Veterinary Pathology Services**

*Conference Coordinator*
**Matthew C. Reed, DVM**
**Captain, Veterinary Corps, U.S. Army**
**Veterinary Pathology Services**
**Joint Pathology Center**

## WEDNESDAY SLIDE CONFERENCE 2014-2015

# Conference 12

**10 December 2014**

**Conference Moderators:**
Elizabeth Mauldin, DVM, DACVP, DACVD
Associate Professor, Dermatopathology
Laboratory of Pathology and Toxicology
School of Veterinary Medicine
3900 Delancey Street
Philadelphia, PA 19104-6051

**CASE I:** 1734-10 (JPC 4003079).

**Signalment:** 3-month-old female Holstein-Friesian calf, *Bos Taurus.*

**History:** In the flock there was a history of diarrhea, emaciation and pneumonia. This calf died and was submitted for necropsy.

**Gross Pathologic Findings:** The calf was emaciated (weight 37.5 kg), with serous atrophy of the pericardial adipose tissue. There were multiple gingival ulcers located where the teeth had contact with the buccal mucosa, an acute diffuse purulent rhinitis and a marked bronchopneumonia of the cranioventral lung areas. Predominantly at the head and neck, the skin showed multifocal well demarcated areas characterized by alopecia, crusts and thickened epidermis.

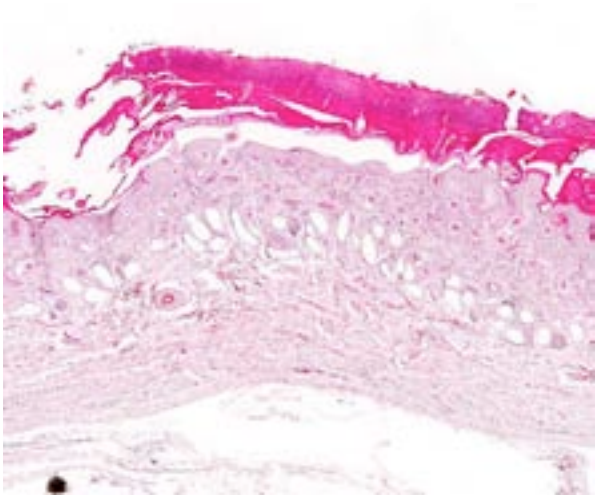

*1-1. Haired skin, calf: There is a thick serocellular crust covering a focally extensive area of the epidermis. (HE 6X)*

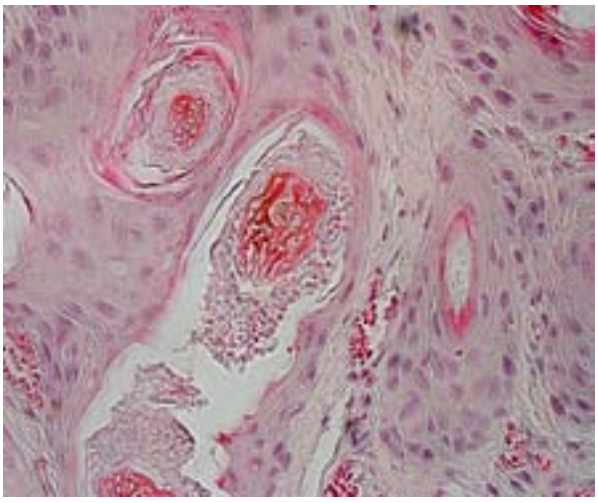

*1-2. Haired skin, calf: There are numerous 2-3 µ m arthrospores surrounding the hair shaft and hyphae within the medulla of the hair shaft itself, seen primarily in negative relief. (HE 400X)*

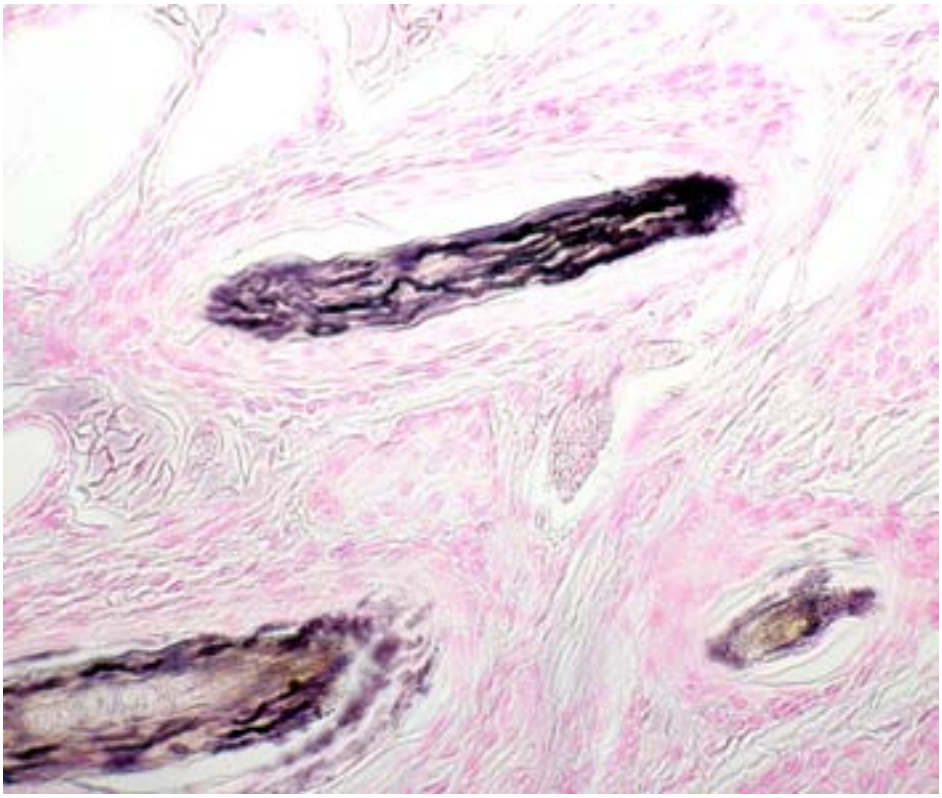

*1-3. Haired skin, calf: A silver stain demonstrates the fungal hyphae within the hair shafts. (Photo courtesy of: Institut fuer Veterinaer-Pathologie, Justus-Liebig-Universitaet Giessen, Frankfurter Str. 96, 35392 Giessen, Germany http://www.uni-giessen.de/cms/fbz/fb10/institute_klinikum/institute/pathologie) (Grocott, 400X)*

**Laboratory Results:** No specific pathogens were identified. Skin was not examined microbiologically.

**Histopathologic Description:** Haired skin: Multifocally affecting the epidermis and dermis, there is an eosinophilic inflammation. The epidermis is covered by thick serocellular crusts composed of lamellated eosinophilic material (keratin), karyorrhectic and cellular debris (degenerated eosinophils and neutrophils) and an eosinophilic homogenous material (exudate). The epidermis is mildly thickened (hyperplasia) and shows an orthokeratotic hyperkeratosis. On the epidermal surface and between the keratin lamellae of the stratum corneum, there are multiple cross and tangential sections of adult arthropod parasites measuring up to 1 mm in diameter. They are round to oval, have a chitinous exoskeleton with occasional spines, striated musculature and jointed appendages (scab mites).

Within dilated hair follicles and around free hair shafts in epidermal crusts are numerous 2-3 µm sized basophilic arthrospores and hyphae with thin parallel walls and indistinct branching and septation (*Trichophyton sp.*). Often, hair follicles are additionally mildly expanded by clumped keratin (infundibular hyperkeratosis). Around blood vessels in the upper dermis is a mild inflammatory infiltrate composed of eosinophils, of lymphocytes and as well as of lesser neutrophils and macrophages. Sweat glands are mildly dilated.

**Contributor's Morphologic Diagnosis:** Haired skin: Dermatitis, perivascular, eosinophilic, mild, with superficial crusting, epidermal and follicular hyperkeratosis with dermatophytes and mites, etiology consistent with *Trichophyton verrucosum* and *Psoroptes ovis*. (Dermatophytosis and psoroptic mange)

**Contributor's Comment:** In the bovine, predominantly *Trichophyton verrucosum* causes ringworm. Other isolates (*T. mentagrophytes, T. equinum, Microsporum gypseum, M. canis, M. nanum*) may also play a role in bovine skin disease. Outbreaks are often associated with crowding with a seasonal increase of cases in fall and winter. Lesions have a typical anatomical distribution: the skin of head and neck. Clinical signs are pruritic and alopecic well-demarcated thickened skin lesions with scales and crusts.[1,3,4]

Transmission occurs through contact while arthrospores may survive in the environment for more than a year. Dermatophytes colonize the superficial dermis and hair follicles and they are adapted to digesting keratin.[4,5] Histologically, dermatophytes are more easily detectable using PAS method or Grocott stain. Septated hyphae are detectable between the keratin of the stratum corneum and within the hair shafts. There is

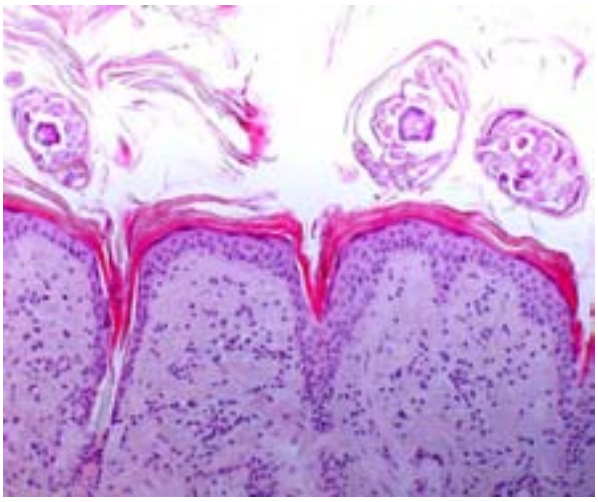

*1-4. Haired skin, calf: Cross-sections of several arthropod parasties (consistent with mites) are present superficially to adjacent, less affected skin. Unfortunately, it is not possible to speciate the mite in tissue section. (Photo courtesy of: Institut fuer Veterinaer-Pathologie, Justus-Liebig-Universitaet Giessen, Frankfurter Str. 96, 35392 Giessen, Germany http://www.uni-giessen.de/cms/fbz/fb10/institute_klinikum/institute/pathologie) (Grocott, 400X)*

regularly a mild acanthosis and hyperkeratosis. Inflammatory changes are often mild.[1] Vaccination is effective for prophylaxis and treatment of bovine ringworm.[6]

Scab mites cause a highly pruritic dermatitis and psoroptic mange is like demodicosis of high economic importance in bovine species. In some countries it is a reportable disease.[1,3] *Psoroptes ovis* is the assumed species of mites responsible for psoroptic mange in cattle.[8] Mites can survive for about 7-12 weeks outside the host. Transmission results directly by contact or indirectly by vectors (e.g. bedding, contaminated objects like feed fences or cow brushes). Psoroptes mites complete their life cycle on the skin. In contrast to *Sarcoptes sp.*, they do not invade the epidermis.[7]

Lesions in cattle can be detected at the skin of the head, neck, back, inguinal and sacral areas and may become generalized. They are characterized by alopecia, crusts, scales and exudation. Due to severe pruritus, excoriations and secondary bacterial infections may blur the picture. In more severe cases the skin shows increased thickness with diffuse alopecia and deep folds.[1,3,7]

In accordance with the clinical symptoms, histologically there is superficial perivascular dermatitis with eosinophils, lymphocytes, macrophages and mast cells. Due to an assumed hypersensitivity reaction there is often spongiosis and marked dermal edema. In chronic cases, hyperplasia of the epidermis can be observed.[1] Mites could be identified microscopically within skin scrapings or biopsies, but not with certainty.[7]

Sarcoptic mange is a differential diagnosis for the lesions in the present case. However, in the present case, the mites are detectable on the surface and between superficial keratin lamellae whereas *Sarcoptes* mites dig deeper. On the other hand there were no burrows filled with eggs and/or larvae within the layers of the epidermis, which are typical for *Sarcoptes* but not seen in *Psoroptes* infestation.[1]

In the present case, a combined infection with dermatophytes and mites occurred. The nutritional stage and concurrent debilitating diseases may have influenced the development of both infections. Both diseases, mange and dermatophytosis, are differentials for each other, and it has to be considered, that dermatophytosis is a zoonotic disease. In contrast to *Sarcoptes* mites *Psoroptes* mites are believed to be non-pathogenic for humans.[1]

**JPC Diagnosis:** Haired skin: Hyperplasia, epidermal, diffuse, moderate, with diffuse hyperkeratosis, serocellular crusts and numerous intrafollicular dermatophyte arthrospores, hyphae, and rare extraepidermal adult mites and eggs.

**Conference Comment:** Conference participants debated whether the rare mites observed in this case were associated with any of the identified lesions. As noted by the contributor, they are located superficially, sometimes exterior to the stratum corneum, are at a distance from the crust formation, and no burrows or larvae are present in the slides examined. We eventually elected to include the presence of mites within one diagnosis which implies their association with the cutaneous lesion, however, we cannot definitively prove their causality.

Dermatophytosis is more common in young animals and often associated with immunosuppression, which is supported in this case by the simultaneous symptoms of respiratory disease and oral ulcers. Notably, other than the neutrophils within the crusts, there is minimal inflammation present despite the fungal proliferation within nearly every hair shaft. Avoiding immune detection and subsequent

provocation of an inflammatory response is instrumental to survival for these pathogens. The arthrospores are always along the periphery of the hair while hyphae are confined within the hair shaft.[3] The organisms never penetrate Adamson's fringe into the mitotic region of the follicle, and fungal growth is terminated along with growth of the hair. Dead telogen hairs, known as "club hairs", are resistant to infection. Resolution of clinical signs typically occurs spontaneously within a few months.[3] This is in contrast to other fungal infections which invade the subcutaneous tissue, incite a tremendous inflammatory response, and often necessitate surgical excision such as pseudomycetomas, phaeohyphomycosis and sporotrichosis.[2]

**Contributing Institution:** Institut fuer Veterinaer-Pathologie, Justus-Liebig-Universitaet Giessen**,** Frankfurter Str. 96, 35392 Giessen, Germany**,** http://www.uni-giessen.de/cms/fbz/fb10/institute_klinikum/institute/pathologie

**References:**

1. Ginn PE, Mansell JEKL, Rakich PM. Skin and appendages. In: Maxie MG, ed. *Jubb, Kennedy, and Palmer's Pathology of Domestic Animals.* 5th ed. Vol 1. Philadelphia, PA: Elsevier Limited; 2007:553-781.
2. Hargis AM, Ginn PE. The integument. In: Zachary JF, McGavin MD, eds. *Pathologic Basis of Veterinary Disease*. 5th ed. St. Louis, MO: Elsevier Mosby; 2012:1038-1039.
3. Scott DW. *Large Animal Dermatology*. Philadelphia, PA: WB Saunders Company; 1988:174-182.
4. Chermette R, Ferreiro L, Guillot J. Dermatophytoses in animals. *Mycopathologia.* 2008;166(5-6):385-405.
5. Bond R. Superficial veterinary mycoses. *Clin Dermatol*. 2010;28(2):226-236.
6. Lund A, Deboer DJ. Immunoprophylaxis of dermatophytosis in animals. Mycopathologia. 2008;166(5-6):407-424.
7. Rommel M, Eckert J, Kutzer E, Körting W, Schnieder T. Veterinärmedizinische Parasitologie. 5th ed. Berlin: Parey; 2000.
8. Bates PG. Inter- and intra-specific variation within the genus Psoroptes (Acari: Psoroptidae). *Vet Parasitol.* 1999;83(3-4):201-217.

**CASE II**: 05-2655A/B (JPC 3139939).

**Signalment:** 3-month and 14-month-old unknown gender Nigerian dwarf goats, *Capra hircus*.

**History:** In a herd of 30 Nigerian dwarf goats, 10 have had bilateral crusty skin lesions on the face, perineum and distal limbs for up to 7 months.

**Gross Pathologic Findings:** The skin around the eyes and mouth of both goats is symmetrically alopecic, erythematous and covered by scales and dry crusts.

**Laboratory Results:** None.

**Histopathologic Description:** Examined is one section of a punch biopsy of haired skin. The surface and follicular epidermis is acanthotic and hypergranular with areas of spongiosis and superficial erosions. The stratum corneum is diffusely thickened with parakeratosis and orthokeratosis layered with degenerative neutrophils admixed with amphophilic amorphous material (serum). Multifocal epidermal papillations are covered by parakeratotic caps expanded by intracorneal lakes of serum admixed with degenerative neutrophils. In some sections the surface or follicular epithelium is focally infiltrated by well-demarcated, intraepithelial aggregates of neutrophils surrounded by macrophages. In the superficial to deep dermis, abundant vascular profiles are lined by plump endothelial cells and surrounded by moderate to high numbers of eosinophils, lymphocytes and plasma cells, which extend into the interstitium. Lymphocytes exocytose through the surface of follicular epithelium. Follicular lumens occasionally contain small clusters of neutrophils and eosinophils.

Periodic acid-Schiff and Gomori methenamine silver stains revealed no fungi.

**Contributor's Morphologic Diagnosis:** Skin: Hyperkeratosis, parakeratotic and orthokeratotic, severe, diffuse with acanthosis and spongiosis; Dermatitis, perivascular to interstitial, eosinophilic and lymphoplasmacytic, multifocal to coalescing, moderate, chronic with transmural folliculitis, lymphocytic exocytosis and intraepithelial eosinophilic pustules, consistent with zinc responsive dermatosis.

**Contributor's Comment:** The section examined exemplifies the histological lesions of zinc-responsive dermatosis, which are similar in all ruminants, and include hyperkeratosis, predominantly parakeratotic, that extends into the follicular ostia and forms parakeratotic spires, epidermal hyperplasia, perivascular eosinophilic infiltrates and lymphocytic exocytosis. Inflammation and pustular dermatitis (not represented on all slides) reflect a secondary bacterial disease, self-trauma and, possibly, *Malassezia* infection. Staphylococcal dermatitis has been a reported complication of zinc responsive dermatosis in goats.[5] Zinc-responsive dermatosis in production animals is usually caused by excess dietary calcium or copper, which causes zinc malabsorption.[7] Zinc regulates apoptosis and DNA repair through activation of p53 gene, nuclear factor κβ and activator protein.[3] Zinc also reduces oxidative damage and regulates caspase activity by maintaining intracellular metalloprotease concentrations. Tissues with high cell turnover, like the skin, lymphoid and reproductive organs are most susceptible to disease due to zinc deficiency.[2]

Gross lesions of zinc-responsive dermatosis are similar in all species and include hyperkeratosis, alopecia and erythema. The distribution is generally, but not always, symmetrical and can involve the periocular and perioral skin, the pinnae and the nasal planum. In large animals the distal legs and coronary bands may develop crusts and fissures. In pigs, the ventral abdomen may be

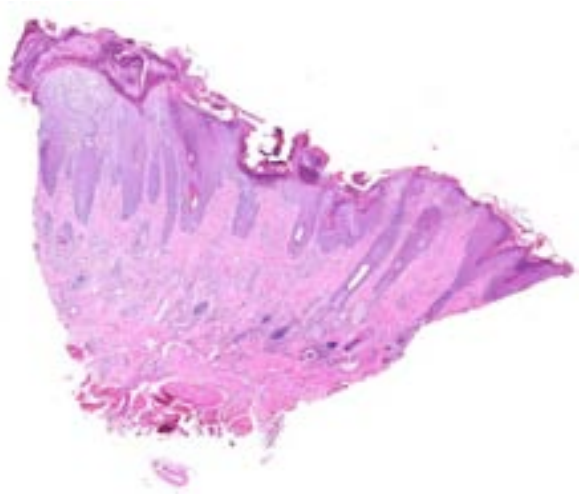

*2-1. Haired skin, goat: At subgross, there is marked epidermal hyperplasia with formation of thick, anastomosing rete ridges. There is a thick serocellular crust overlying the hyperplastic epidermis, and moderate perivascular inflammation within the underlying dermis. (HE 6.3X)*

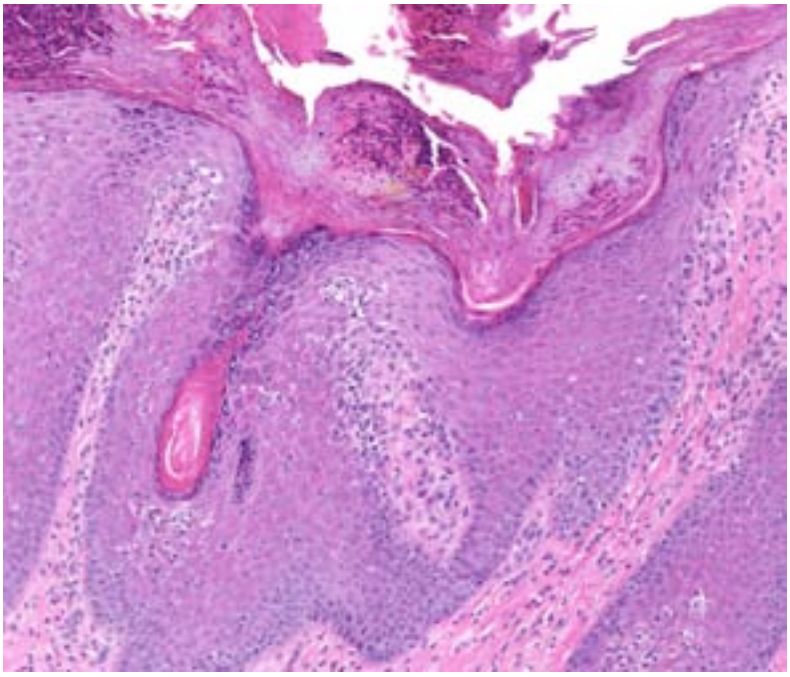

*2-2. Haired skin, goat: The serocellular crust is composed of a combination of para- and orthokeratotic hyperkeratosis which extends into the follicular ostia, as well as focal pustules. (HE 112X)*

affected. Low or low normal serum alkaline phosphatase levels have been described in ruminants, and serum zinc levels, as a rule, do not correlate with gross or histological lesions.[7]

Zinc deficiency in domestic animals is classified as hereditary or dietary. Hereditary zinc deficiency occurs in three forms: 1) lethal trait A46 in Black Pied Danish and Friesian calves; 2) lethal acrodermatitis in bull terriers (hypothetically due to zinc deficiency); and 3) inherited zinc responsive dermatosis in Northern breed dogs. Lethal acrodermatitis in bull terriers is not responsive to zinc supplementation, and its association with zinc deficiency is based largely on clinical similarities to inherited zinc deficient dermatoses in cattle and humans. Dietary zinc deficiency is the predominant form in production animals and large breed puppies.

The most severe inherited forms are lethal trait A 46 or bovine hereditary zinc deficiency in Black Pied Danish and Freisian calves and lethal acrodermatitis in bull terrier pups. These diseases are clinically similar to acrodermatitis enteropathica in humans, caused by a defect in the SLC39A4 gene that encodes the Zip4 protein, a zinc transporter protein distributed along the apical border of duodenal and jejunal enterocytes. Similar mutations in the bovine ortholog of SLC39A4 have been identified in affected calves.[7] In bull terriers the disease is not genetically characterized, but the pathogenesis of the disease has recently been attributed to increased oxidative stress secondary to hepatocelluar metabolic dysfunction. Symptoms begin in the first few weeks of life, and can include acrodermatitis, generalized alopecia, growth retardation, diarrhea, small or absent thymus, defective T-lymphocyte function, and chronic infections. Without treatment affected humans and animals invariably succumb to secondary infection. Humans and calves are responsive to oral zinc supplementation. The disease is currently untreatable in bull terriers.[10]

Northern breed dogs, Siberian huskies and Alaskan malamutes, are genetically predisposed to a more benign inherited zinc responsive dermatosis, known as syndrome I. Onset of symptoms can occur in dogs of any age, but most commonly affects juveniles.[9] Lesions are distributed most commonly on the periorbital skin, pinna and nasal planum and are histologically similar to those reported in other inherited zinc dermatopathies, though less severe.

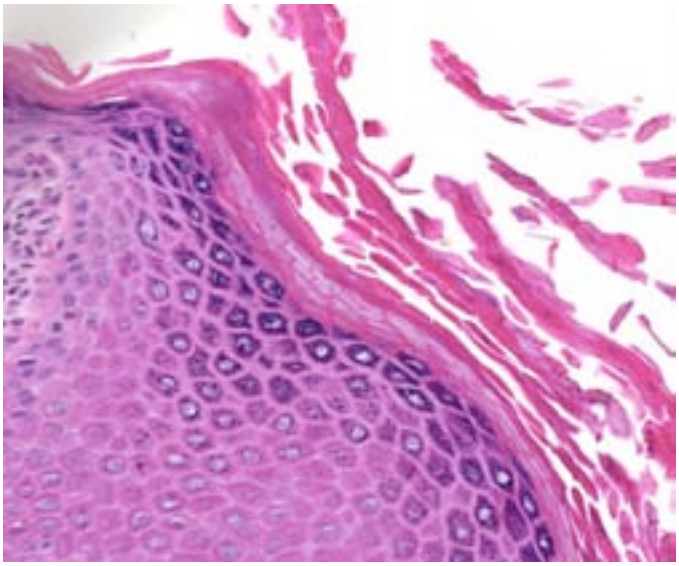

*2-3. Haired skin, goat: Areas in which there is a stratum granulosum are covered by orthokeratotic hyperkeratosis, recapitulating normal epidermal maturation. (HE 220X)*

A dietary form of zinc responsive dermatosis, known as Syndrome II, occurs in growing large breed puppies with increase metabolic demands.[1]

Zinc deficiency in production animals is generally attributed to high dietary concentrations of calcium and copper, which block zinc absorption. Cereal grains contain high concentrations of phytates and phytic acids (inositol hexaphosphate) which chelate zinc; however, this mechanism of zinc deficiency is considered less important in ruminants due to production of phytases by rumen microflora. Excessive levels of oxalates, cadmium, iron, molybdenum and orthophosphates in the diet have also implicated zinc malabsorption. Conversely, zinc availability is enhanced by vitamin C, lactose and citrate.[5,8]

Despite the etiogenesis, histologic lesions of zinc-responsive dermatosis are similar in most species, allowing for moderate variations in severity. The differentials commonly include dermatophytosis, demodicosis, pemphigus foliaceus (dogs, cats, horses, goats) and other nutritional dermatopathies.

**JPC Diagnosis:** Haired skin: Hyperplasia, epidermal, diffuse, moderate, with acanthosis and hyperkeratosis, lymphocytic and neutrophilic dermatitis, and intracorneal pustules.

**Conference Comment:** The histopathology and clinical history are suggestive of zinc-responsive dermatosis in this case; however, the conference moderator noted that in the absence of serum or hair zinc levels, response to therapy must be demonstrated for definitive causation. Serum or hair zinc levels can be diagnostic when decreased; however, studies have demonstrated similar zinc concentrations between clinical animals and healthy animals from nearby farms.[7] Additionally, comparing metallothionein immunoreactivity of squamous epithelial cells to normal controls may be indicative of low zinc levels and possibly helpful in obtaining a definitive diagnosis.[6] Besides zinc deficiency, typical differential diagnoses for parakeratotic hyperkeratosis include thallium toxicity, hepatocutaneous syndrome, glucagonoma, autoimmune diseases, dermatophytosis, demodicosis, and superficial bacterial infections.

The contributor elaborates on the various manifestations of zinc-responsive dermatoses, including both hereditary and dietary. The pathogenic mechanisms underlying the development of cutaneous lesions in zinc deficiency is largely unclear. Zinc has a prominent role in the influence of molecular conformation, stability and activity in addition to its antioxidant effects which support the hypothesis of oxidative stress inducing these cutaneous lesions.[6] The heat shock protein 72 (Hsp72) is synthesized in response to damaged cellular proteins and functions to prevent their aggregration. It is found at increased concentrations in the nucleus of keratinocytes in canine zinc-responsive dermatoses[6], further demonstrating the increased susceptibility to protein damage of squamous epithelial cells when zinc levels are low.

**Contributing Institution:** Cornell University**,** College of Veterinary Medicine**,** Department of Biomedical Sciences**,** Division of Anatomic Pathology**,** S2118 Schurman Hall**,** Ithaca, NY 18453-6401

**References:**

1. Colombini S, Dunstan RW. Zinc-responsive dermatosis in northern-breed dogs: 17 cases (1990-1996). *J Am Vet Med Assoc*. 1997;211:451-453.
2. Cummings JE, Kovacic JP. The ubiquitous role of zinc in health and disease. *J Vet Emerg Crit Care. 2009;*19:215-240.
3. Grider A, Mouat MF, Mauldin EA, Casal ML. Analysis of the liver soluble proteome from bull terriers affected with inherited lethal acrodermatitis. *Molecular Genetics and Metabolism*. 2007;92:249-257.
4. Krametter-Froetscher R, Hauser S, Baumgartner W. Zinc-responsive dermatosis in goats suggestive of hereditary malabsorption: two field cases. *Vet Dermatol*. 2005;16:269-275.
5. Nelson DR, Wolff WA, Blodgett DJ, Luecke B, Ely RW, Zachary JF. Zinc deficiency in sheep and goats: three field cases. *J Am Vet Med Assoc*. 1984;184:1480-1485.
6. Romanucci M, Bongiovanni L, Russo A. Oxidative stress in the pathogenesis of canine zinc-responsive dermatosis. *Vet Dermatol*. 2010;22(1):31-38.
7. Scott, DW. *Large Animal Dermatology*. Philadelphia, PA: W.B. Saunders Company; 1988:487.
8. Singer LJ, Herron A, Altman N. Zinc responsive dermatopathy in goats: two field cases. *Contemp Top Lab Anim Sci*. 2000;39:32-35.

9. White SD, Bourdeau P, Rosychuk RA, Cohen B, Bonenberger T, Fieseler KV, et al. Zinc-responsive dermatosis in dogs: 41 cases and literature review. *Vet Dermatol*. 2001;12:101-109.

10. Yuzbasiyan-Gurkan V, Bartlett E. Identification of a unique splice site variant in SLC39A4 in bovine hereditary zinc deficiency, lethal trait A46: An animal model of acrodermatitis enteropathica. *Genomics*. 2006;88:521-6.

**CASE III**: 13-1614/6 (JPC 4048849).

**Signalment:** 3-year-old adult female bovine limousine breed, *Bos Taurus.*

**History:** A 3-year-old female limousine was referred to the Veterinary School of Lyon for clinical signs of 1 month duration. Cow shows persistent severe hyperthermia, bilateral keratitis, conjunctivitis, mucopurulent nasal discharge, ulcerative lesions on muzzle and in oral cavity, hooves and horn junctions, and emaciation. There are also sheep on the farm.

**Gross Pathologic Findings:** The main gross lesions at necropsy were:

- Multifocal severe ulcerative dermatitis with crusts on muzzle, hooves and one horn
- Multifocal to diffuse exudative dermatitis with skin thickening and matted hairs
- Ulcerative gingivitis and loss of lingual papillae
- Numerous ulcers on esophageal mucosa
- Prescapular lymph node hypertrophy
- Bilateral mucopurulent rhinitis
- Marked congestive laryngitis

**Laboratory Results:** PCR: positive for Ovine herpes virus 2 (OvHv-2).

**Histopathological Description:** Haired skin: More than 90% of epidermis and superficial dermis is necrotic and replaced by crusts containing colonies of cocci and degenerate neutrophils. In viable adjacent epidermis (only in some slides) or in the follicular wall there are pustules containing necrotic or apoptotic keratinocytes and degenerate neutrophils. There are also hemorrhages and perivascular infiltration by numerous lymphoid cells admixed with plasma cells and viable and variable number of degenerate neutrophils. In the deep dermis, some vascular walls are expanded by fibrin, edema, and admixed with cellular and karyorrhectic debris (necrotizing vasculitis). Multifocally, vessel lumena were partially or completely occluded by fibrin thrombi.

**Contributor's Morphological Diagnosis:** Haired skin: Severe necrotizing and ulcerative dermatitis, necrotizing vasculitis with fibrin thrombi, lymphocytic périvasculitis and vasculitis, consistent with malignant catarrhal fever, limousine breed, bovine.

**Contributor's Comment:** Malignant catarrhal fever (MCF) is an infectious disease of domestic cattle, some wild ruminants and occasionally pigs. The disease is characterized by lymphoproliferation, vasculitis and erosive-ulcerative mucosal and cutaneous lesions. It is generally sporadic although severe herd outbreaks

*3-1. Haired skin, ox: There are extensive areas of exudative dermatitis with thickening of the skin and matted hair. (Photo courtesy of: Anatomie Pathologique, Vetagro Sup, Campus veterinaire, 1, Avenue Bourgelat, 69280 Marcy l'etoile, France)*

*3-2. Haired skin, ox: The coronary band is ulcerated. (Photo courtesy of: Anatomie Pathologique, Vetagro Sup, Campus veterinaire, 1, Avenue Bourgelat, 69280 Marcy l'etoile, France)*

*3-3. Hoof, ox: There is sloughing of the hoof. (Photo courtesy of: Anatomie Pathologique, Vetagro Sup, Campus veterinaire, 1, Avenue Bourgelat, 69280 Marcy l'etoile, France)*

have been reported. Mortality in susceptible species approaches 100%. MCF is caused by cross species infection with members of the MCF virus group of ruminant rhadinoviruses (genus *Rhadinovirus* subfamily Gammaherpesvirinae).[2] Economically important outbreaks of MCF are due to 2 of the 10 viruses of the MCF virus group: ovine herpesvirus 2 (OvHV-2 and alcelaphine herpes virus I (AIHV-I).[3]

The pathogenesis, clinical signs and lesions are similar whatever the agent inducing MCF. MCF is characterized by marked T lymphocyte hyperplasia. A population of large granular lymphocytes appears to be infected and transformed by rhadinovirus infection, and OHV-2 genome has been detected in CD8+ T cells. These cells are probably cytotoxic T lymphocytes or T-suppressor cells but the mechanism by which they mediate the lesions of MCF is unclear.

Animals probably encounter these viruses through inhalation and ingestion of fomites from oronasal-pharyngeal-ocular fluids from reservoirs animals that are actively shedding virus.[3]

Disease is not contagious among affected cattle, which are thought to be dead end hosts

There is a great variation in the presenting clinical syndromes which are potentially pansystemic.[2]

Gross cutaneous lesions especially in sheep-associated MCF are common. Affected areas include the thorax, abdomen inguinal regions, perineum, udder and occasionally the head. Sometimes the cutaneous changes begin in about the base of hooves and horn. In our cases, cutaneous lesions were severe in hooves and coronary band and the cow has lost all epidermal parts of one horn.

The characteristic histological changes are found in lymphoid tissue and in the adventitia and walls of medium sized vessels, especially arteries. They are characterized by perivascular accumulation of mainly mononuclear cells and fibrinoid necrotizing vasculitis. These changes may be focal or segmental and may involve the full thickness of the wall or be confined more or less to one layer.

Differentiation of acute severe mucosal disease is sometimes difficult but MCF affects more organs and there is lymphoid hyperplasia whereas lymphoid tissue in BVDV infection is expected to be atrophic. Other differential diagnosis include: bluetongue, vesicular stomatitis, foot and mouth disease, and photosensitization.[3]

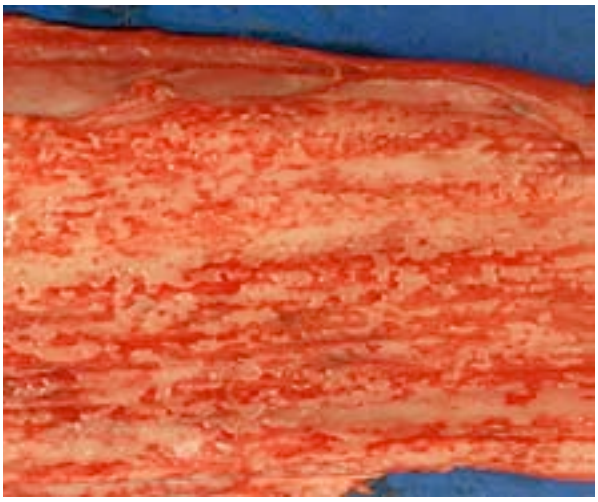

*3-4. Esophagus, ox: There are extensive areas of ulceration on the esophageal mucosa. (Photo courtesy of: Anatomie Pathologique, Vetagro Sup, Campus veterinaire, 1, Avenue Bourgelat, 69280 Marcy l'etoile, France)*

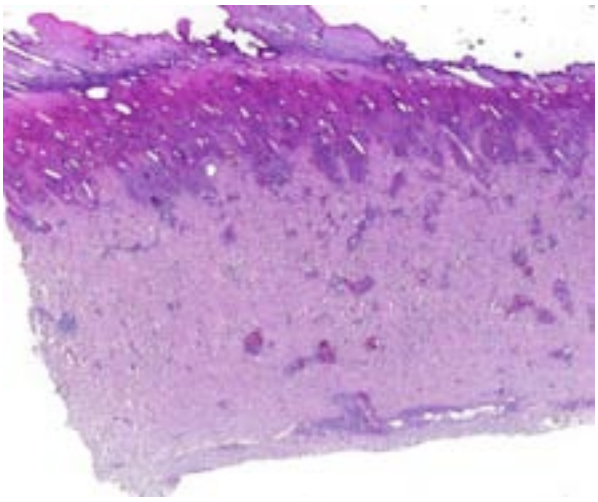

*3-5. Haired skin, ox: There is diffuse severe necrosis of the epidermis, and vessels within the dermis are emphasized by an outlining cellular infiltrate and necrotic debris. (HE 2X)*

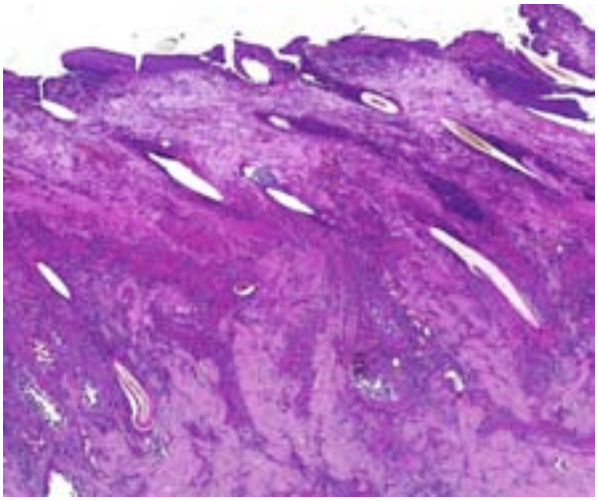

*3-6. Haired skin, ox: The epidermis is diffusely necrotic – hair follicles and adnexa are infiltrated by numerous degenerate neutrophils. There is not a single viable cell left in this whole field! (HE 38X)*

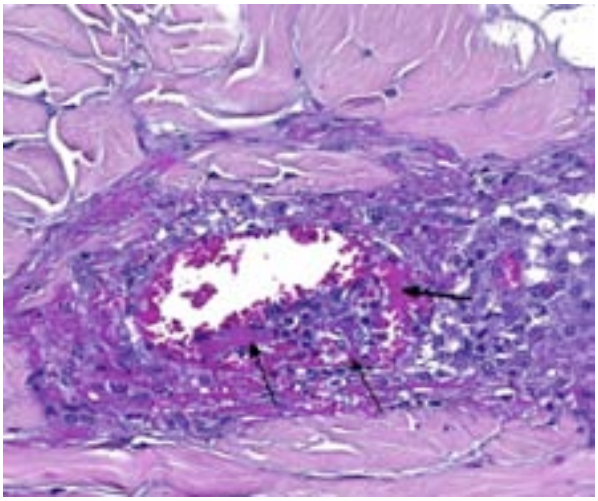

*3-7. Haired skin, dermis, ox: Vessel walls are expanded by numerous viable and degenerate lymphocytes and fewer neutrophils, edema, and extravasated brightly eosinophilic protein (arrows) (fibrinoid necrosis). Hemorrhage and protein-rich edema fluid, as well as moderate numbers of lymphocytes infiltrate the surrounding perivascular dermis. (HE 328X)*

In our case definitive diagnosis was made by histology and positive OVHV-2 PCR results. This method is sensitive and specific.

Clinical MCF is divided into four variable and overlapping categories:[5]

·Peracute form: Severe oral and nasal mucosal inflammation, hemorrhagic gastroenteritis

·Intestinal form: Pyrexia, diarrhea, hyperemic oral and nasal mucosa with profuse catarrhal and mucopurulent discharge, generalized lymphadenopathy

·Head-and-eye form (most common): Pyrexia, copious serous to mucopurulent ocular and nasal secretions, encrusted muzzle with occluded nostrils, dyspnea and open-mouthed breathing, oral mucosal hyperemia with erosions, sloughed buccal mucosal tips; Ocular lesions: Ophthalmia, photophobia, palpebral conjunctival hyperemia and edema, corneal opacity, +/- hypopyon

·Mild form: mild oral and nasal mucosal erosions

**JPC Diagnosis:** Haired skin: Vasculitis, necrotizing, multifocal, severe, with thrombosis,

and diffuse epidermal and adnexal necrosis (infarct).

**Conference Comment:** This is a unique look at a disease more familiarly causing the gastrointestinal trifecta of arteritis, lymphoid proliferation and mucosal necrosis.[3] The degree of necrosis in this case is so dramatic, one conference participant accurately declared, "There is not a single living epithelial cell!" The hallmark of MCF in cattle is severe lymphocytic arteritis-periarteritis with necrosis of the tunica media[3] which is beautifully demonstrated in this example.

OVHV-2 can be a contentiously complicating infectious disease for producers, as owners of sheep can move flocks in and out of a facility without consequence while an adjacent closed-herd of cattle or bison suffers severe outbreaks. In endemic areas, nearly all sheep are infected during their first year of life and rarely develop clinical disease; which is in stark contrast to infection in cattle where the clinical course typically ends in death or euthanasia. Even in cases where outbreaks of systemic vasculitis occur in a sheep flock and positive detection of viral antigen is confirmed, OVHV-2 can only be considered with suspicion. The detection of ORF25, a viral-encoded protein of OVHV-2, would be more persuasive in such instances.[3]

All gammaherpesviruses have a tropism for T or B lymphocytes, and members of the MCF viruses preferentially target T cells.[3] Infected CD8+ T lymphocytes spread the virus systemically and incite production and recruitment of proinflammatory cytokines which lead to the tremendous lesions observed.[4] In sheep, only aerosol challenges result in infection, where initial replication occurs within type II pneumocytes. Intravenous, intraperitoneal, and transplacental inoculations do not result in infection while infected colostrums may rarely result in infection.[3]

The contributor mentioned important differentials to consider in cases which present with acute mucosal disease. The endemicity of MCF, BVDV, and now bluetongue among cattle in Europe make obtaining a definitive diagnosis of special importance. Studies have characterized MCF and BVDV as being more clinically similar; however, cattle with bluetongue more often have a better appetite, demeanor and facial appearance and do not have bilateral lymph node enlargement.[1]

**Contributing Institution:** Anatomie Pathologique, Vetagro Sup, Campus vétérinaire, 1 Avenue Bourgelat, 69280 Marcy l'etoile, France

**References:**

1. Bexiga R, Guyot H, Saegerman C, et. al. Clinical differentiation of malignant catarrhal fever, mucosal disease and bluetongue. *Vet Rec*. 2007;161:858-859.
2. Brown CC, Baker DC and Barker IK. Alimentary system. In: Maxie MG, ed. *Jubb, Kennedy and Palmer's Pathology of Domestic Animals*. Vol 2. 5th ed. Philadelphia, PA: Elsevier Saunders; 2007:152-158.
3. O'Toole D, Li H. The pathology of malignant catarrhal fever with an emphasis on Ovine Herpesvirus 2. *Veterinary Pathology*. 2014;51(2): 437-452.
4. Zachary JF. Mechanisms of Microbial Infections in Pathologic Basis of Disease. Fifth edition. 2012:219.
5. Joint pathology VSPO U-V02 - Malignant catarrhal fever (MCF) - kidney, haired skin – steer.

**CASE IV:** RP19229 (JPC 4048505).

**Signalment:** Adult male wild house mouse, *Mus musculus*.

**History:** Found dead.

**Gross Pathology:** The mouse was 17.5 g and had minimal to no adipose stores. There were multiple hairless patches along the dorsum and face. Bilaterally, the margins of the pinnae were irregular and lacerated. The right pinna contained a 5 x 3 x 3 mm tan, multinodular skin mass. There were similar 1 mm diameter tan nodules within the hairless patches of the dorsum and face. The thoracic cavity contained a moderate amount of dark red hemorrhage.

**Laboratory Results:** None.

**Histopathologic Description:** Hair follicles of the face, pinnae, and dorsum are multifocally dilated and contain abundant arthropods (mites) embedded in hyperkeratotic and hyperplastic follicular epithelium. Arthropods are 80 - 110 microns in diameter with a chitinous exoskeleton, multiple jointed appendages, skeletal muscle, and a reproductive tract containing basophilic material. Similar mites are embedded in hyperkeratotic surface epithelium. There are multifocal 40 - 60 micron diameter basophilic eggs. Rare sections contain subcutaneous inflammation characterized by lymphocytes, plasma cells, and neutrophils and hemorrhage. Rarely, follicles also contain clusters of 3 - 5 micron round to oval structures that are periodic acid-Schiff positive (yeasts).

**Contributor's Morphologic Diagnosis:** Haired skin (face, pinnae, and dorsum): Severe follicular plugging, hyperkeratosis, and hyperplasia with intrafollicular and superficial epidermal mites (etiology: *Psorergates simplex*).

**Contributor's Comment:** The gross and histologic presentation in this case is typical of the follicular mite, *Psorergates simplex*. The characteristic gross lesion caused by this mite is numerous 2 mm tan to white cystic dermal nodules.[1,2,4,5] The nodules, also described as nests and pouches,[3] are most obvious when the skin is reflected back during postmortem examination.[1,2,4] Lesions most commonly occur in the loose skin of the neck, back, trunk, shoulders, and abdomen, but can occur anywhere, including the face and legs. The cysts resemble comedones and histologically are characterized by dilated follicles plugged with abundant mites and keratin debris.[1,5] Inflammation is usually minimal but will occur around ruptured follicles (furunculosis). The presence of mites in hair follicles of the pinnae, as was seen in this case, is a less common presentation.[1] Nodules can occur on either or both sides of the pinna and may need to be differentiated from notoedric ear mange,[1] in which the lesion tends to be more superficial and proliferative with mites embedded in the stratum corneum.[4] *Notoedres* sp. are also larger mites (250 - 400 microns long), whereas *P. simplex* are 90 - 150 microns long.[1]

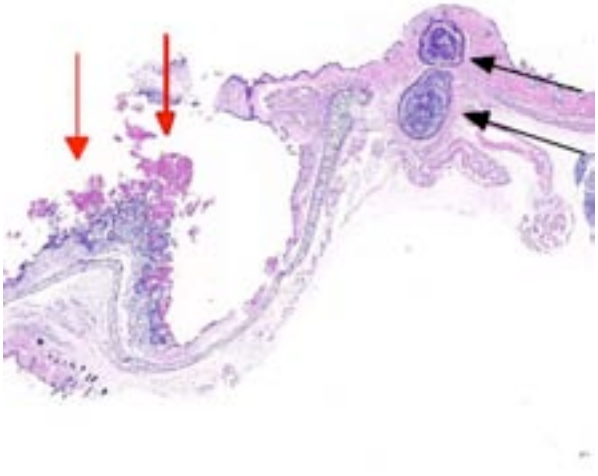

*4-1. Haired skin and ear canal, mouse: There are two large dilated hair follicles containing abundant keratin debris (comedones) (black arrows) subjacent to the base of the ear, and a marked area of crusting within the external ear canal (red arrows). (HE 7X)*

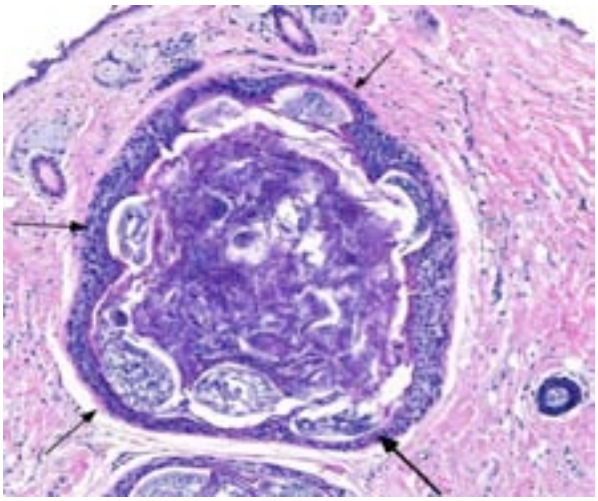

*4-2. Haired skin, mouse: There are numerous cross sections of arthropod parasites (mites) lining the wall of the comedone. (HE 7X)*

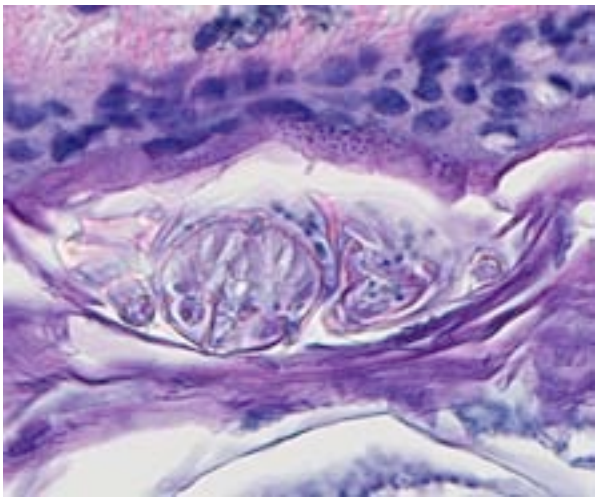

*4-3. Haired skin, mouse: The cross sections of the mites contain a chitinous exoskeleton, obvious jointed appendages, and striated muscle. (HE 400X)*

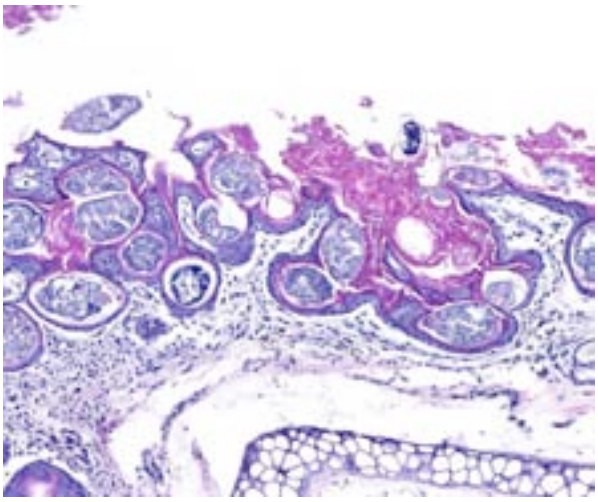

*4-4. External ear canal, mouse: There is a focal area of epidermal hyperplasia and hyperkeratosis within the dorsal ear canal with numerous intraepithelial and intrafollicular mites. (HE 125X)*

Infection with *P. simplex* is uncommon in wild and pet mice and rare to absent in laboratory mice. The complete life cycle of *P. simplex* is unknown.[1,5] The mites are transmitted by direct contact[1] and gravid females enter the hair follicles to form nests which expand the follicles by internal pressure.[1,2] All stages of the mite life cycle (eggs, larvae, nymphs, and adults) can be found within hair follicles.[1,5]

Death of this wild house mouse was attributed to a suspected traumatic event which caused dermal hemorrhage and hemothorax. The mites were an incidental finding. We receive few wild mice at our laboratory but in our experience *P. simplex* is uncommon. Rare yeasts in the follicles are most consistent with *Malassezia* sp. and most likely represent a secondary infection.

**JPC Diagnosis:** 1. Haired skin: Comedones, multiple, with infundibular adult mites and eggs. 2. Haired skin: Infundibular fungal arthrospores (presumptive) and hyphae. 3. Pinna: Otitis externa, hyperkeratotic and lymphohistiocytic, diffuse, moderate, with infundibular adult mites and eggs.

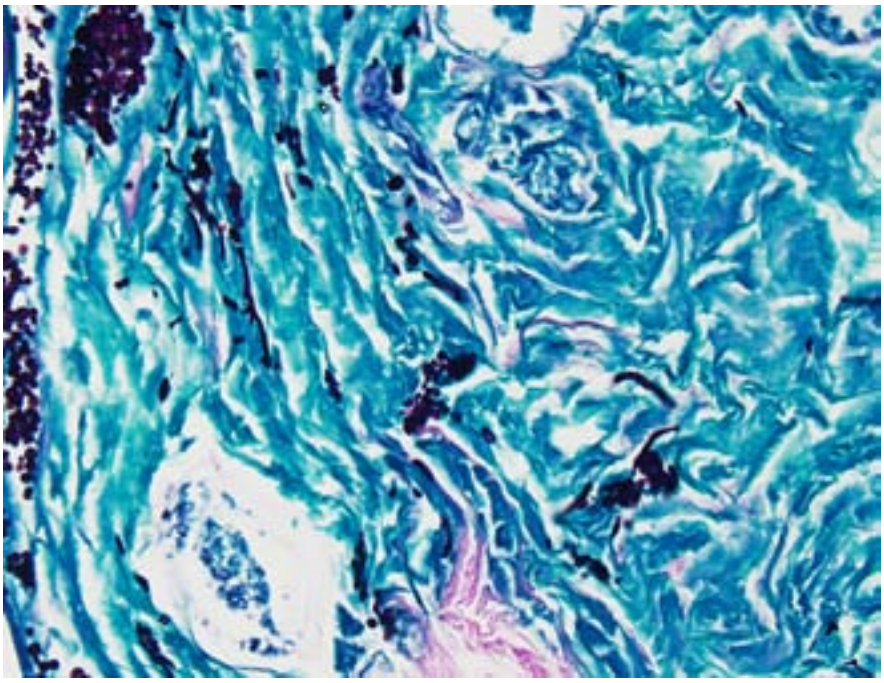

*4-5. Hair follicles, mouse: Centrally within the comedones, there are moderate numbers of yeasts and hyphae, which are likely incidental. (Periodic acid-Schiff, 400X)*

**Conference Comment:** For an institution with thousands of animals comprising hundreds of different species, this case serves as a reminder of the importance in monitoring the health of wildlife pests in addition to exhibit animal population. *Psorergates simplex* mites were once prevalent in laboratory mice but are now only readily recognized among wild and pet mice.[5] While little is

known regarding its pathogenesis, most skin mites of mice are directly transmissible which may pose a risk to some zoo inhabitants. Conference participants discussed the finding of some sections of mites which appeared to be larger (200-300 µ m) and found superficial to the epidermis in some slides. These larger mites often had a striated cuticle not observed among the intrafollicular mite sections, leading many to speculate on the presence of a second species. Several species of mites are relatively common in mice, including *Myobia musculi, Myocoptes musculinis*, and *Radfordia affinis*.[5] Additionally, the contributor mentions *Notoedres* sp. which are much larger and more superficial in histologic sections. Any of these are a possibility, as all lack distinguishing morphologic characteristics. In fact, of all genres of mites, only *Sarcoptes* sp. (with dorsal cuticular spines) and *Demodex* sp. (with elongated abdomen and closely apposed appendages) can be readily identified on histologic section by their morphology alone.[3] *Myobia* sp. are the most clinically significant mites which cause a hypersensitivity reaction while *Myocoptes* sp. is most common.[5]

We also observed the 3-5 µm spores present often in conjunction with mites in dilated follicles. These are PAS- and GMS-positive, which also revealed few fungal hyphae in the same location. Upon histochemical staining, we are unable to determine the specific species of this fungus though we do not believe this morphology is consistent with *Malassezia* sp.; their location within the follicles as well as hyphal formation is consistent with a dermatophyte. The lack of inflammation associated with the dilated follicles was curious, as neither the mites nor fungi seemed to elicit a response from the host. In some slides, sections of ear pinna were identified which appeared to be the only area where lymphocytes and macrophages were recruited. We elected to include a third diagnosis for this location, though it is worth mentioning the mites seemed to be concentrated in larger numbers in these sections.

**Contributing Institution:** Wildlife Disease Laboratories, Institute for Conservation Research, San Diego Zoo Global: http://www.sandiegozooglobal.org

**References:**

1. Baker DG. Parasites of Rats and Mice. In: *Flynn's Parasites of Laboratory Animals*. 2nd ed. Ames, IA: Blackwell Publishing Professional: 2007:366-367.
2. Flynn RJ, Jaroslow BN. Nidification of a mite (*Psorergates simplex* Tyrell, 1883: Myobiidae) in the skin of mice. *J Parasitology*. 1956;42:49-52.
3. Gardiner CH, Poynton SL. *An Atlas of Metazoan Parasites in Animal Tissues*. Washington, DC: Armed Forces Institute of Pathology; 1999:56-58.
4. Izdebska JN, Fryderyk S. New for the fauna of Poland species of *Psorergates* spp. with the data of occurrence of mites from Psorergatidae family (Acari, Prostigmata) in native mammals. *Annals Parasitology*. 2012;58:19-22.
5. Percy DH, Barthold SW. Mouse. In: *Pathology of Laboratory Rodents and Rabbits*. 3rd ed. Ames, IA: Blackwell Publishing Professional: 2008:85-87.

**Joint Pathology Center**
**Veterinary Pathology Services**

# WEDNESDAY SLIDE CONFERENCE 2014-2015

## Conference 13

**7 January 2015**

**Guest Moderator:**
Tim Walsh DVM, DACVP
National Zoological Park
Washington, DC

---

**CASE I:** 2008 Case#2 (JPC 3106257)

**Signalment:** Captive adult female green iguana, *Iguana iguana.*

**History:** Chronic ascites; suspected neoplastic or inflammatory infiltrate in the liver.

**Laboratory Results:** None provided.

**Gross Pathologic Findings:** The liver lobes were diffusely enlarged, pale and rubbery, with a slightly raised cobblestone appearance to the left lobe. There were numerous 0.3 to 1.5 cm in diameter, occasionally pendulous fluid-filled cysts containing pale yellow, clear fluid in the capsule along margins of the left lobe. Approximately 200 ml of blood-tinged, watery fluid was present in the coelomic cavity.

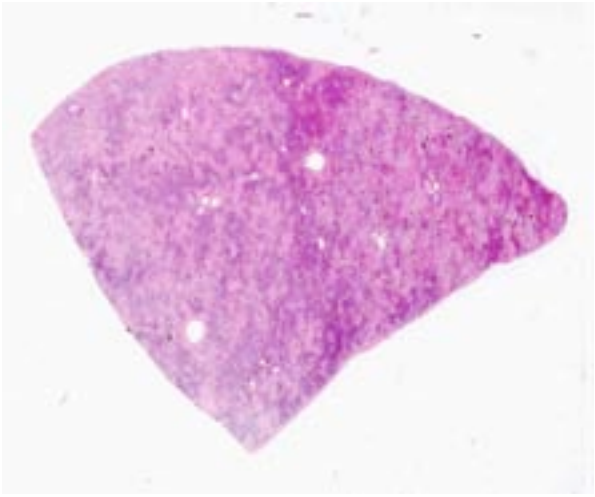

*1-1. Liver, iguana: The hepatic architecture is diffusely altered and replaced by a bright pink, hypocellular material. (HE 6X)*

**Histopathologic Description:** Liver: The normal liver architecture is almost completely replaced by coalescing, variably dense aggregates of ductules and tubules separated by variably broad trabeculae of fibrous connective tissue in which are scattered capillaries. Spared are several small patches of short cords of hepatocytes. Ductules are lined by a single layer of cuboidal cells with light eosinophilic cytoplasm and central round to oval nuclei having uniformly granular chromatin, with 1-2 nucleoli. Mild anisocytosis is present, and mitotic figures are not seen. Golden-brown, granular pigment is present in the cytoplasm of some ductal epithelial cells, scattered macrophages and hepatocytes (hemosiderin). Scattered throughout the parenchyma are small foci of ducts with shrunken, hypereosinophilic cells, pyknotic nuclei and karyorrhectic debris (necrosis). There are sparse perivascular infiltrates of lymphocytes and heterophils. Segments of the

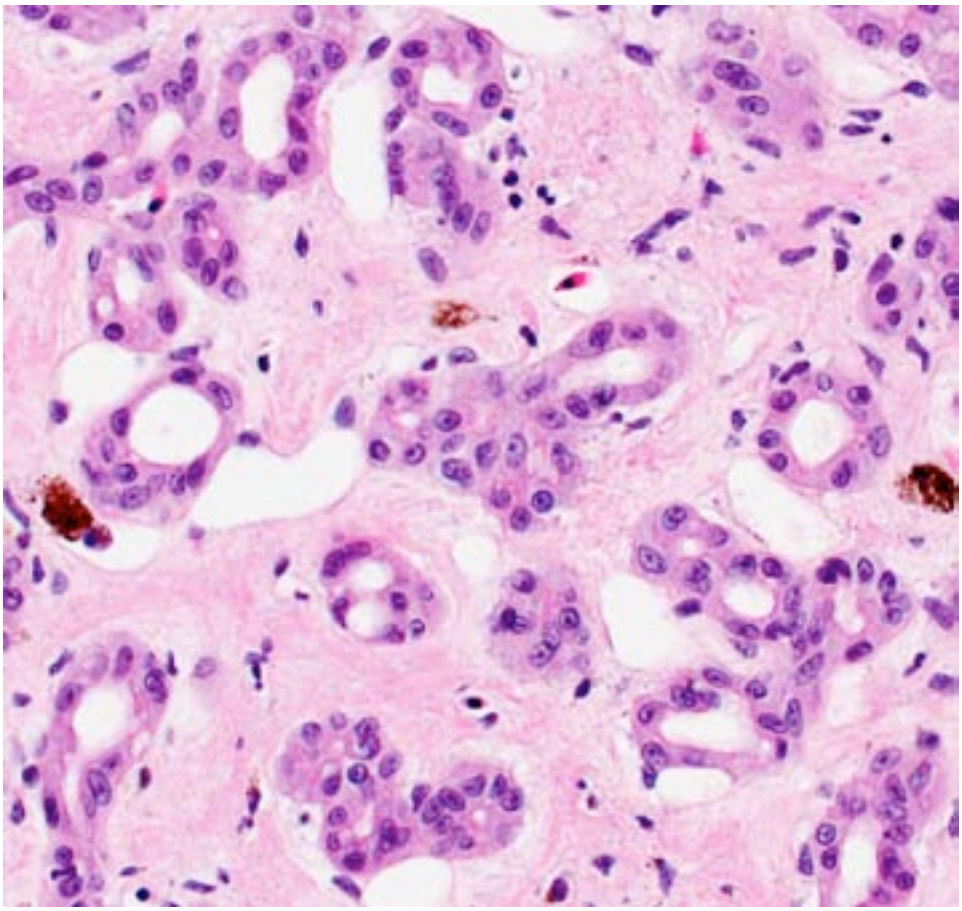

*1-2. Liver, iguana: At higher magnification, hepatocytes are diffusely replaced by proliferating bile ducts separated by a dense collagenous stroma. (HE 256X)*

capsule are mildly to moderately thickened by fibrous connective tissue.

**Contributor's Morphologic Diagnoses:** 1. Liver: Severe, diffuse, chronic, pseudocarcinomatous biliary hyperplasia with marked interstitial fibrosis.
2 Liver: Moderate biliary, hepatocellular and histiocytic iron accumulation.

**Contributor's Comment:** In this case, the diagnosis of pseudocarcinomatous biliary hyperplasia (PBH) met the criteria discussed for two previously reported cases in female green iguanas.[19] Histologically, well-differentiated biliary ductules replace the majority of normal liver parenchyma, sparing small islands and clusters of hepatic cords. Mild cellular atypia, the absence of mitotic figures, and lack of invasion of basement membranes by ductule epithelial cells make cholangiocarcinoma a less likely differential diagnosis.[6] In support of a benign process are the lack of gross or histologic evidence of metastasis, and the absence of a gross tumor.

Cholangiocarcinomas can have a massive or multilobular appearance, are often umbilicated and protrude from the liver capsule. Clinically, prolonged survival after initial diagnosis is also supportive of a diagnosis of PBH.

Pseudocarcinomatous biliary hyperplasia must also be differentiated from biliary hamartoma and cholangioma. In human and veterinary medicine, biliary hamartomas are rare and consist of ducts of varying caliber, unique cystic cavity formation and fibrosis.[15,17] In domestic animals, cholangiomas are usually solitary, well demarcated, round, cystic and solid masses, which grow by expansion and tend to bulge beyond the normal liver surface. In one retrospective study, 31% of all primary neoplasms in lizards affected the liver versus other organ systems,[16] with malignant biliary processes being the most frequent.

In veterinary medicine, biliary hyperplasia has been described in association with internal papillomatosis and chronic mycotoxicosis in avian species. Aflatoxins are excreted in the bile, causing periportal necrosis and inflammation in acute cases. With chronic exposure, there is bile duct hyperplasia and fibrosis, as described with chronic active hepatitis.[13] Severe biliary hyperplasia has been reported in an alpaca in association with parasitic ova of *Fasciola hepatica,*[8,14] and hepatic coccidiosis.[14] Experimental bile duct ligation or administration of alpha-naphthylisothiocyanate (ANIT), both producing obstructive cholestasis, or intravenous

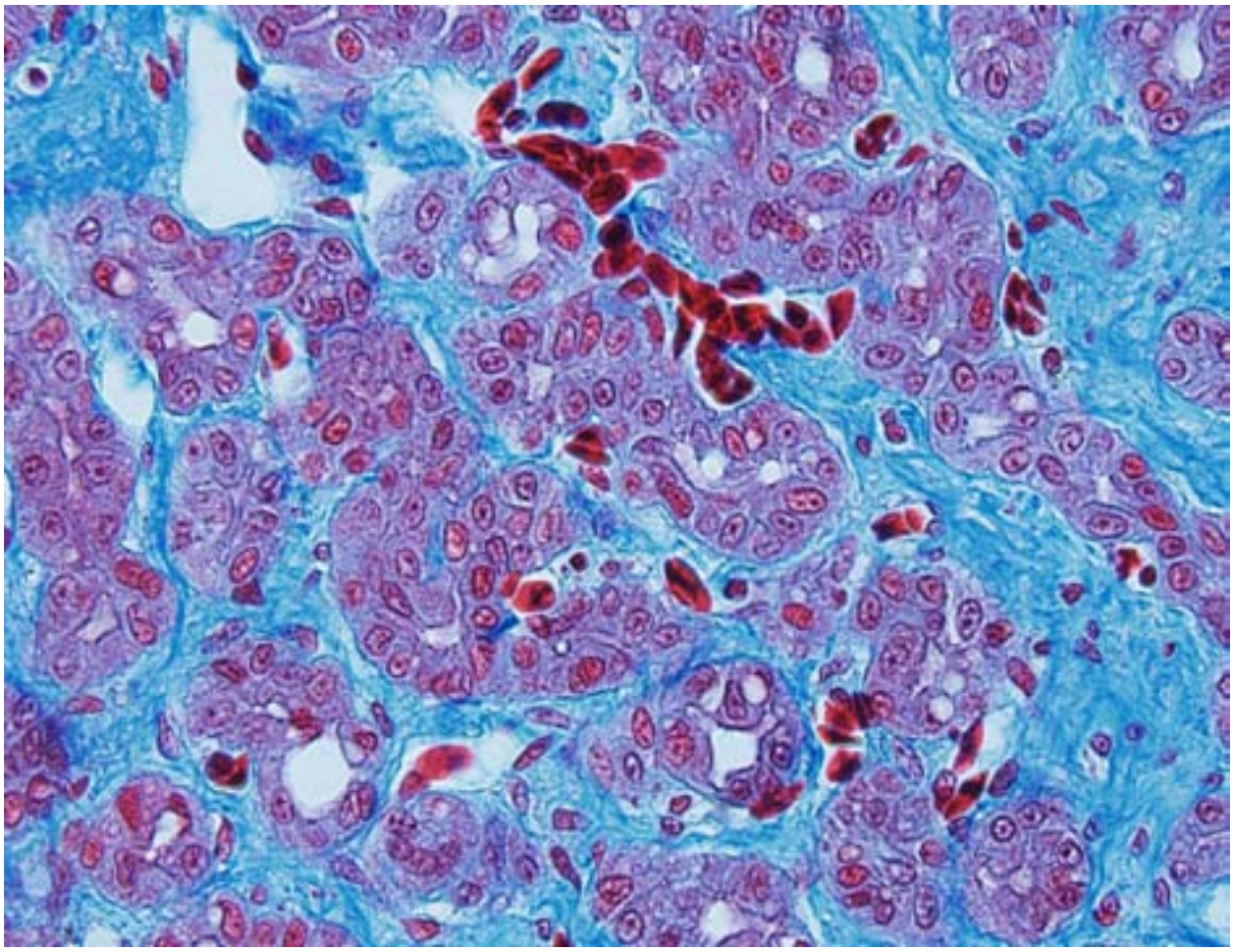

*1-3. Liver, iguana: The collagenous stroma stains densely blue with Masson's trichrome stain. (Masson's trichrome, 256X)*

estradiol glucuronide, which causes non-obstructive cholestasis, have been shown to cause biliary epithelial cell hyperplasia in male Sprague-Dawley rats.[10]

In human medicine, the term pseudocarcinomatous hyperplasia is used to refer to marked epidermal proliferation with down growth into the dermis, associated with chronic granulomatous conditions of the underlying dermis or with keratinocyte atypia.[9] It has been described as hyperplastic glandular or ductular epithelium with a cribriform pattern, mimicking carcinoma, in different neoplastic and inflammatory processes. These include granular cell tumors,[2] anaplastic large cell lymphoma,[12] chronic osteomyelitis of the jaw and limbs,[18] oral syphilis infection,[1] and chronic salpingitis.[3] Pseudocarcinomatous urothelial hyperplasia of the urinary bladder has been associated with prior irradiation or chemotherapy and, recently, in several cases without such predisposing treatment.[11] Hyperplasia of biliary ducts in humans has been associated with biliary atresia, where the pathological changes include hyperplasia of canaliculi, inflammation, cholestasis and interstitial fibrosis of portal zones.[20]

The pathogenesis of pseudocarcinomatous hyperplasia (of the skin) has been related to epidermal growth factor (EGF) and transforming growth factor (TGF) elaborated by the primary tumor (e.g. lymphoma) or inflammatory cells.[4] Both of these growth factors have the same specific membrane receptor (EGFr) which has tyrosine kinase activity. The activation of this receptor can be involved in epithelial hyperplasia, wound healing and tumorigenesis.[7]

**JPC Diagnosis:** Liver: Biliary hyperplasia, diffuse, severe, with fibrosis.

**Conference Comment:** This is a very unusual lesion, and sparked not only lively debate but a

number of post-conference special stains. This is a rarely reported case in iguanas, although previous WSC moderators consulted with on this case have suggested that the lesion occurs commonly. Conference participants discussed at length several aspects surrounding this case. The acini, which completely replace hepatic parenchyma in most sections, certainly appear to be biliary ducts and in our view, lack malignant characteristics as mentioned by the contributor. Conference participants noted that certain hepatocellular neoplasms can also form acinar structures, however, further testing for hepatocyte antigen and pancytokeratin were negative, which proves these are all biliary epithelial cells. Additional debate centered on the composition of the abundant eosinophilic fibrillar material between acini, which proved to be collagen, based on staining properties with Masson's trichrome and a lack of fluorescence with Congo red.

Biliary hyperplasia is a nonspecific response to a variety of liver insults,[5] many of which are mentioned by the contributor. It is typically regarded as a result of long-standing hepatic injury, particularly after diseases which result in the obstruction of normal bile drainage.[5] It may also develop secondary to portal inflammation and fibrosis.[14] Ductular reaction is a term utilized when the progenitor cells with potential to differentiate into either biliary epithelium or hepatocytes proliferate, as also may occur in severe hepatic injury.[5] See the conference comments from WSC 2011-12, conference 3, case 2 for a detailed discussion of ductular reaction and its pathogenesis.

Diffuse hepatic fibrosis also corresponds with repeated toxic hepatic injury; however, this typically is followed by nodular regeneration as observed in a cirrhotic liver. When a single event induces widespread hepatocellular necrosis, fibrosis and condensation of preexisting connective tissue often occurs in the absence of regeneration and is termed postnecrotic scarring.[5] This is because the normal reticulin network of type III collagen, hepatic stellate cells, and nerves which occupy the space of Disse collapses, allowing portal triads to converge, giving rise to irregular bands of scar tissue.[14] Postnecrotic fibrosis, which develops around hepatic venules, is termed periacinar fibrosis and occurs commonly in cases of chronic passive congestion or pyrrolizidine alkaloid toxicity.[14]

In this case, the gross description and histopathologic findings best correlate with a diffuse, chronic hepatic insult. The presence of ascites is consistent with two previously reported cases,[18] and it would be interesting to compare clinical pathologic findings in this case to those previously reported to assist in determining whether the abdominal fluid is related to the hepatic lesion.

**Contributing Institution:** Department of Pathobiology and Veterinary Science
University of Connecticut
Storrs, CT
http://www.patho.uconn.edu

**References:**

1. Barrett AW, Dorrego MV, Hodgson TA, Porter SR, Hopper C, Argiriadou AS, Speight PM. The histopathology of syphilis of the oral mucosa. *J Oral Pathol Med.* 2004;33:286-291.
2. Brannon RB, Anand PM. Oral granular cell tumors: An analysis of 10 new pediatric and adolescent cases and a review of the literature. *J Clin Pediatr Dent.* 2004;29(1):69-74.
3. Cheung ANY, Young RH, Scully RE. Pseudocarcinomatous hyperplasia of the fallopian tube associated with salpingitis. *Am J Surg Pathol*. 1994;8(11):1125-1130.
4. Courville P, Wechsler J, Thomine E, Vergier B, Fonck Y, Souteyrand P, Beylot-Barry M, Bagot M, Joly P, and The French Study Group On Cutaneous Lymphoma. *Brit J Dermatol*. 1999;140:421-426.
5. Cullen JM, Brown DL. Hepatobiliary system and exocrine pancreas. In: Zachary JF, McGavin MD, eds. *Pathologic Basis of Veterinary Disease*. 5th ed. St. Louis, MO: Elsevier Mosby; 2012:415-418.
6. Cullen JM, Popp JA. Tumors of the liver and gall bladder. In: Meuten DJ, ed. Tumors in Domestic Animals. 4th ed. Ames, IA: Blackwell Publishing; 2002:483-508.
7. De Boer WI, Houtsmuller AB, Izadifar V, Muscatelli-Groux B, Van Der Kwast TH, Chopin DK. Expression and functions of EGF, FGF and TGF beta-growth-factor family members and their receptors in invasive human transitional cell carcinoma cells. *Int J Cancer*. 1997;71:284-291.
8. Hamir AN, Smith BB. Severe biliary hyperplasia associated with liver fluke infection in an adult alpaca. *Vet Pathol*. 2002;39:592-594.
9. KawachiY, Taguchi S, Fijisawa Y, Furuta J, Nakamura Y, Ishii Y, et al. Epidermal

pseudocarcinomatous hyperplasia with underlying epidermal growth factor-producing cutaneous CD30-positive lymphoproliferative disorder. *J Eur Acad Derm Venereology*. 2008; Letter to the Editor.
10. Kossor DC, Meunier PC, Dulik DM, Leonard TB, Goldstein RS. Bile duct obstruction is not a prerequisite for type I biliary epithelial cell hyperplasia. *Tox and Appl Pharmacol*. 1998;152:327-338.
11. Lane Z, Epstein JI. Pseudocarcinomatous epithelial hyperplasia in the bladder unassociated with prior irradiation or chemotherapy. *Am J Surg Path*. 2008;32:92-97.
12. Lin J, Lee JY. Primary cutaneous CD30+ anaplastic large cell lymphoma with keratoacanthoma-like pseudocarcinomatous hyperplasia and marked eosinophilia and neutrophilia. *J Cutan Pathol*. 2004;32:458-461.
13. Schmidt RE, Reavill DR, Phalen DN. Liver. In: Pathology of Pet and Aviary Birds. 1st ed. Ames, IA: Blackwell Publishing; 2003:67-93.
14. Stalker MJ, Hayes MA. Liver and biliary system. In: Maxie MG, ed. Pathology of Domestic Animals. 5th ed. Philadelphia, PA: Elsevier Saunders; 2007:298-387.
15. Starost MF. Solitary biliary hamartoma with cholelithiasis in a domestic rabbit (*Oryctolagus cuniculus*). *Vet Pathol*. 2007;44:92-95.
16. Sykes IV JM, Trupkiewicz JG. Reptile neoplasia at the Philadelphia Zoological Garden 1901-2002. *J Zoo Wildlife Med*. 2006;37(1): 11-19.
17. Tohmé-Noun C, Cazals D, Noun R, Menassa L, Valla D, Vilgrain V. Multiple biliary hamartomas: magnetic resonance features with histopathologic correlation. *Eur Radiol*. 2008;18:493-499.
18. Warter A, Walter P, Meyer C, Barriére P, Galatir L, Wilk A. Mandibular pseudocarcinomatous hyperplasia. *Histopathology*. 2000;37:115-117.
19. Wilson GH, Fontenot DK, Brown CA, Kling MA, Stedman N, Greenacre CB. Pseudocarcinomatous biliary hyperplasia in two green iguanas, *Iguana iguana*. *J Herpetological Med & Surg*. 2004;14(4):12-18.
20. Zheng S, Luo Y, Xiao X. Analysis of the pathomorphology of the intra- and extrahepatic biliary system in biliary atresia. *Eur J Pediatr Surg*. 2008;18:98-102.

**CASE II**: 11-0047D (JPC 4007417)

**Signalment:** Southern hairy nosed wombat, *Lasiorhinus latifrons*.

**History:** Multiple free-ranging wild wombats reported by wombat conservation organization with alopecia, dermatitis and poor body condition. This wombat was in poor body condition and culled (bullet wound to the skull) for post mortem examination for a wombat health investigation study by the University of Adelaide.

**Gross Pathology:**

1. Moderate multifocal dorsal and lateral alopecia with mild seborrhoea and exudative dermatitis
2. Severe trauma to the head with comminuted fractures of the skull and jaw (as per method of euthanasia)
3. Poor body condition
4. Duodenal cestodiasis
5. Colonic helminthiasis

**Laboratory Results:** Not performed.

**Histopathologic Description:** Lung: Diffusely there is thickening and hypercellularity of alveolar septa by increased macrophages, rare neutrophils and eosinophils and increased fibrocollagenous connective tissue. There are increased intra-alveolar macrophages, which have moderate to abundant foamy cytoplasm. Free within alveolar lumina or more commonly within multinucleated alveolar macrophages there are many large spherical organisms (yeasts). Yeasts measure 22 - 35 µm in diameter, have a thin 1-2 µm thick lightly basophilic translucent capsule, and internally comprise indistinct basophilic granular material. There are increased Goblet cells in the epithelium of large bronchioles and adjacent airways are filled with foamy basophilic mucoid secretion. Occasionally, subepithelial connective tissues of bronchioles are infiltrated by aggregates of foamy macrophages forming small granulomas with intralesional yeasts. There are infrequent subepithelial infiltrates of lymphocytes, plasma cells, and eosinophils; and there is focal exocytosis of eosinophils into bronchiolar epithelium. In some sections of lung, alveoli are filled by hemorrhage and alveolar septal capillaries are congested.

**Contributor's Morphologic Diagnosis:** 1). Lung: Moderate histiocytic interstitial pneumonia and fibrosis with intralesional fungal elements (interpreted as *Emmonsia parva*).
2. Lung: Multifocal alveolar hemorrhage and congestion.

**Contributor's Comment:** Pulmonary adiaspiromycosis is caused by *Emmonsia crescens* or *E. parva*, dimorphic fungi which form thick-walled non-budding non-replicating adiaspores in tissue and elicit granulomatous inflammatory reactions in the host. *E. crescens* and *E. parva* are distinct but morphologically similar species; however, adiaspores of *E. crescens* generally form larger and sometimes multinucleated adiaspores (up to 500 µm in diameter), and *E. parva* monuonucleate adiaspores only 20-40 µm in diameter.[13] The two species also differ in their geographical distribution, *E. parva* being more common throughout central Asia, Africa and parts of the Americas, and *E. crescens* mainly observed in Europe and the UK.[2,8,15]

Pulmonary adiaspiromycosis is known primarily to occur in small rodents, carnivores and mustelids. In Australia, *E. parva* is described as the cause of pulmonary adiaspiromycosis in wombats on the basis of fungal morphology, although results of genetic characterization and confirmation of organism identity is yet to be reported.[11,12] In New Zealand, *E. crescens* is the reported cause of pulmonary adiaspiromycosis in the brushtail possum (*Trichosurus vulpecula*),[9] most likely secondary to co-habitation of the opossum with introduced British mammals (otter, stoat, weasel, mole, red fox and pine martin) in which *E. crescens* is widespread in the UK.[3] Adiaspiromycosis in humans is rare; most human infections are attributed to *E. crescens* although *E. parva* may be observed in AIDs patients.[5,6] Rarely, fatal human infections have been described.[2]

Wombats are large herbivorous burrowing marsupials native to Australia, of which there are three extant species: the southern hairy nosed wombat (*Lasiorhinus latifrons*), the northern hairy nosed wombat (*Lasiorhinus krefftii*), and the

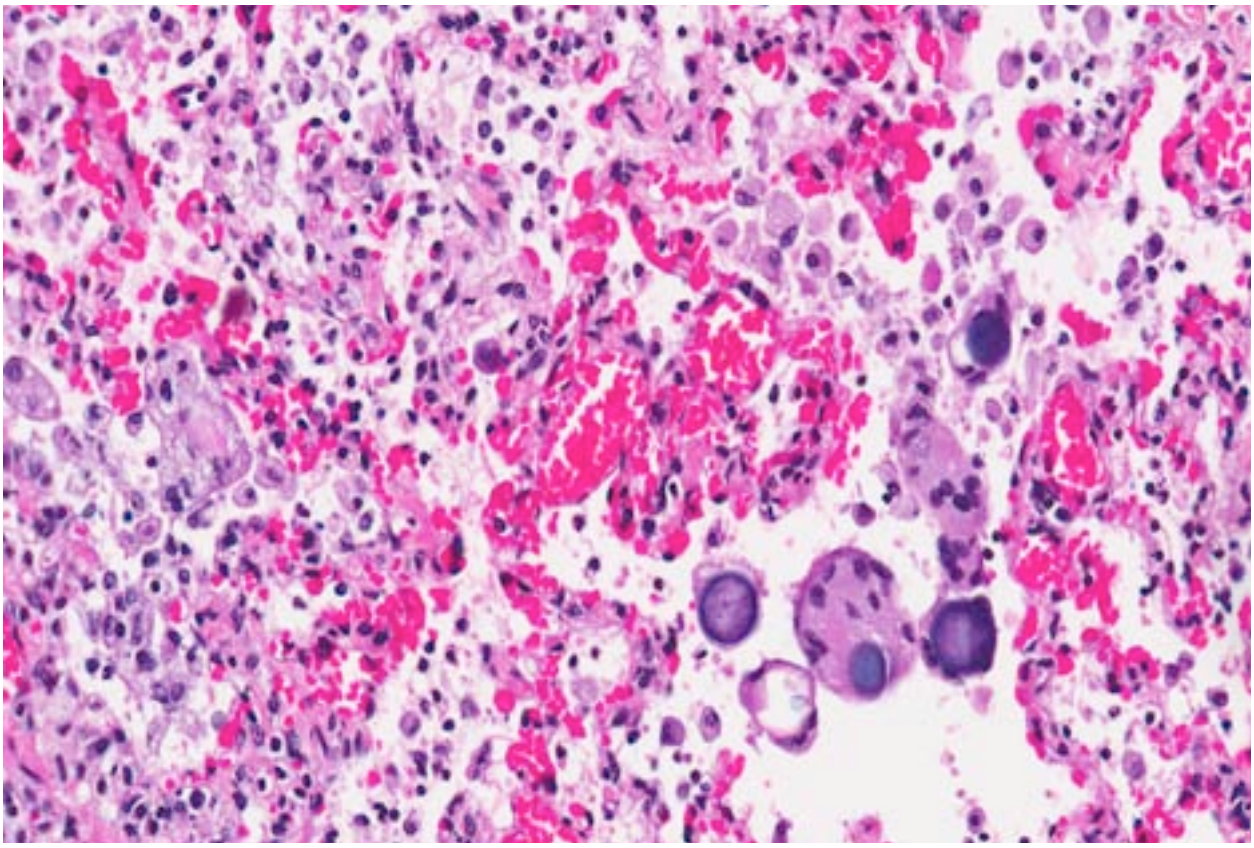

*2-1. Lung, wombat: Alveoli contain moderate numbers of foamy macrophages and neutrophils with fewer multinucleated giant cell macrophage admixed with fibrin and cellular debris. Multinucleated macrophages range up to 70 µm and contained basophilic adiaspores with a 2-3 µm clear hyaline wall. (HE 256X)*

common wombat (*Vombatus ursinis)*. The southern hairy nosed wombat is native to South Australia and it is estimated that up to 100,000 remain in the wild. The wombat presented in this case was culled and examined as part of a larger study examining skin disease and poor body condition in wombats in the Murrayland region of South Australia. Pulmonary adiaspiromycosis was observed in all wild wombats culled concurrently from this site. Gross lung lesions were not evident at post mortem. Previously reported gross findings in affected wombats have ranged from minimal change, to pale consolidation of ventral lung lobes with mucopurulent exudate in the bronchi and bronchioles.[11,12] The significance of pulmonary adiaspiromycosis in these wombats is uncertain; however, it may have contributed to poor body condition. Alternatively pulmonary fungal load and infection may have been exacerbated due to the presence of concurrent disease or immune suppression. Investigations into Southern hairy nosed wombat health in the region are continuing.

Aleuriospores of *Emmonsia* are ubiquitous and soil borne, and on inhalation form thick-walled non-replicating adiaspores in host tissues which continue to increase in size. Infection of wombats is thought to occur when they are pouch young, and a linear increase in *Emmonsia* spherule size with increasing wombat age has been observed.[11] The habitat and burrowing habits of the wombat is thought to render them prone to infections.[10] Southern hairy nosed wombats spend up to three-quarters of their time underground, and have small home ranges centered around their clay/ calcrete or calcrete warrens.[7]

*Emmonsia* adiaspores must be differentiated in tissue section from other dimorphic fungi forming yeasts in host tissues. Phylogenetic studies recently found isolates of *E. parva* to be closer to *Blastomyces dermatitidis* than *E. crescens*, and the authors further suggest that there may be little basis to maintain *Blastomyces* and *Emmonsia* as separate genera.[13] In tissue section, the yeasts may be distinguished as either budding yeasts (*B. dermatitidis* and *H. capsulatum)* or thick-walled,

or non-budding adiaspores (*Emmonsia*). *Emmonsia* adiaspores also resemble *Coccidoides immitis* in tissue section, with the exception that *Emmonsia* lacks internal spores.[14]

**JPC Diagnosis:** Lung: Pneumonia, interstitial, granulomatous, diffuse, mild to moderate, with occasional intrahistiocytic adiaspores.

**Conference Comment:** This is a unique look at a rarely observed, but morphologically distinct fungus. Lesions are restricted to the lungs in reported cases and there is a tremendously broad host range.[3] Until recently, *Emmonsia* spp. were classified with *Chrysoporium* spp. which shares many similarities; though molecular genetics has clearly differentiated the two genera.[1] Conference participants briefly discussed whether to classify the pneumonia in this case as interstitial, as the described pathogenesis with this entity involves inhalation of the infectious organisms which typically corresponds with bronchopneumonia. Though the changes in this case were minimal, which was curious in itself when compared with the described poor body condition, they were largely confined to the interstitium as adequately described by the contributor. Additionally, it was not clear whether there was hemorrhage and congestion in the participants' sections due to the collapsed and often distorted tissue so we elected not to include this in our diagnosis.

With *Blastomyces dermatitidis* being a close relative of *Emmonsia* spp., it is curious how dramatically different the extent of disease is between the two species. *Emmonsia* spp. is more typically self-limiting and often human patients receive only supportive therapy,[1] which provides a stark contrast to *B. dermatitidis* which incites a more dramatic granulomatous reaction and is capable of spreading systemically.[4] It is suspected that *Emmonsia* spp. lacks the virulence factors identified with *B. dermatitidis* and the other dimorphic fungi which are well known to cause significant respiratory and often systemic disease in animals.

**Contributing Institution:** School of Animal and Veterinary Sciences, University of Adelaide

**References:**

1. Anstead GM, Sutton DA, Graybill JR. Adiaspiromycosis causing respiratory failure and a review of human infections due to *Emmonsia* and *Chrysosporium* spp. *J Clin Microbiol*. 2012;50(4):1346-1354.
2. Barbas Filho JV, Amato MB, Deheinzelin D, Saldiva PH, de Carvalho CR. Respiratory failure caused by adiaspiromycosis. *Chest*. 1990;97:1171-1175.
3. Borman AM, Simpson VR, Palmer MD, Linton CJ, Johnson EM. Adiaspiromycosis due to Emmonsia crescens is widespread in native British mammals. *Mycopathologia*. 2009;168:153-163.
4. Caswell JL, Williams KJ. Respiratory system. In: Maxie MG, ed. *Jubb, Kennedy, and Palmer's Pathology of Domestic Animals*. 5th ed. Vol. 2. Philadelphia, PA: Elsevier Saunders; 2007:641-642.
5. Echavarria E, Cano EL, Restrepo A. Disseminated adiaspiromycosis in a patient with AIDS. *J Med Vet Mycol*. 1993;31:91-97.
6. England DM, Hochholzer L. Adiaspiromycosis: an unusual fungal infection of the lung. Report of 11 cases. *Am J Surg Pathol*. 1993;17:876-886.
7. Finlayson GR, Shimmin GA, Temple-Smith PD, Handasyde KA, Taggart DA. Burrow use and ranging behaviour of the southern hairy-nosed wombat (Lasiorhinus latifrons) in the Murraylands, South Australia. *Journal of Zoology*. 2005;265:189–200.
8. Hubalek Z. Emmonsiosis of wild rodents and insectivores in Czechland. *J Wildl Dis*. 1999;35:243-249.
9. Johnstone AC, Hussein HM, Woodgyer A. Adiaspiromycosis in suspected cases of pulmonary tuberculosis in the common brushtail possum (Trichosurus vulpecula). *N Z Vet J*. 1993;41:175-178.
10. Ladds P. Pathology of Australian Native Wildlife. 1 ed. Melbourne: CSIRO Publishing; 2009.
11. Mason RW, Gauhwin M. Adiaspiromycosis in south Australian hairy-nosed wombats (Lasiorhinus latifrons). *J Wildl Dis*. 1982;18:3-8.
12. Nimmo J, Krockenberger M, Smith EF. Pulmonary adiasporomycosis in a Victorian wombat. In: Australian Society of Veterinary Pathology Annual Meeting. Attwood, Victoria 2007:65-67.
13. Peterson SW, Sigler L. Molecular genetic variation in Emmonsia crescens and Emmonsia parva, etiologic agents of adiaspiromycosis, and their phylogenetic relationship to Blastomyces dermatitidis (Ajellomyces dermatitidis) and other

systemic fungal pathogens. *J Clin Microbiol*. 1998;36:2918-2925.
14. Sigler L. Agents of adiaspiromycosis. In: Ajello L, Hay R, eds. *Topley & Wilson's Microbiology and Microbial Infections*. 9th ed. Arnold, London, UK; 1999:571-583.
15. Sigler L. Ajellomyces crescens sp. nov., taxonomy of Emmonsia spp., and relatedness with Blastomyces dermatitidis (teleomorph Ajellomyces dermatitidis). *J Med Vet Mycol*. 1996;34:303-314.

**CASE III**: AFIP 14 0454-93 C (JPC 4049379)

**Signalment:** Male boa constrictor imperator, *Boa constrictor imperator*.

**History:** The boa was part of a reptile husbandry in which numerous animals were found to be in poor condition. Numerous petechiae were present on its ventral scales. Complete blood cell count revealed severe leukocytosis. These findings raised the suspicion for septicemia and, due to poor condition, the animal was euthanized. A necropsy was performed.

**Gross Pathology:** The animal was in poor body condition and showed severe cachexia. Numerous petechiae were present on ventral scales. The coelomic cavity contained about 15 mL of clear fluid. Serosa and organs were grossly unremarkable.

**Laboratory Results**: Antemortem blood cell count revealed severe leukocytosis with lymphocytosis (results not provided). Cytologic analysis was performed on coelomic effusion and revealed the presence of numerous bluish, homogenous, intracytoplasmic inclusions within leukocytes and red blood cells, leading to a diagnosis of Inclusion Body Disease (IBD). IBD was confirmed by PCR testing for IBD virus.

**Histopathologic Description:** The slide contains sections from the kidney, epididymis and nervous ganglia (including chromaffin cells). Numerous eosinophilic, round, variable-sized (2-10 µm) intracytoplasmic inclusion bodies are present in the renal tubular epithelium, neurons and chromaffin cells, and epididymal epithelial cells. These inclusions are consistent with inclusions of IBD.

In the kidney, almost all glomeruli show abundant collagen deposition within the mesangium (glomerulosclerosis). Some glomeruli show cystic atrophy. Rare lymphocytes and heterophils infiltrate the interstitium. Numerous intensely eosinophilic and tightly packed 2-µm granules are present in nephrocytes of the distal convoluted tubules (sexual segment) whereas epithelium of the proximal convoluted tubules contain coarsely granular brownish pigments (see discussion).

**Contributor's Morphologic Diagnosis:**

Kidney:

1) Numerous intracytoplasmic eosinophilic inclusions within renal tubular epithelium, consistent with inclusions of Inclusion Body Disease.
2) Glomerulosclerosis, diffuse, severe with rare glomerular cystic atrophy.
3) Numerous brownish cytoplasmic pigments of unknown significance within epithelium of the proximal convoluted tubules.

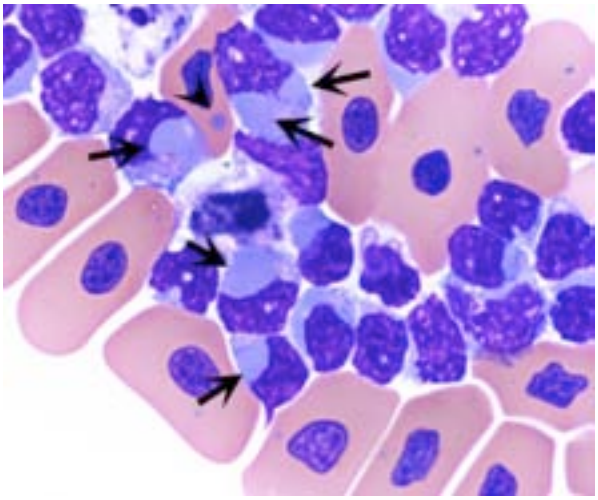

*3-1. Coelomic effusion, boa: Numerous leukocytes (arrows) and erythrocytes (arrowhead) contain homogenous bluish intracytoplasmic inclusions. (Photo courtesy of: Unité d'Histologie, Embryologie et Anatomie pathologique, Département des Sciences Biologiques et Pharmaceutiques, Ecole Nationale Vétérinaire d'Alfort, FRANCE: www.vet-alfort.fr)*

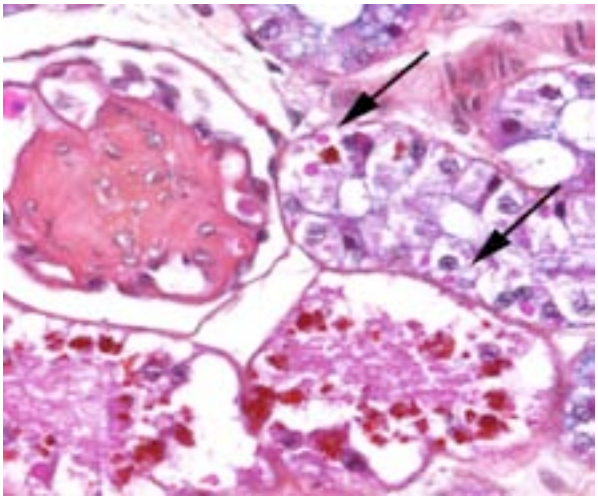

*3-2. Kidney, boa: Renal tubular epithelial cells contain one or more round, variably-sized eosinophilic intracytoplasmic inclusions (arrows). Many epithelial cells also contain large amounts of an unidentified reddish brown granular pigment. (HE 200X) (Photo courtesy of: Unité d'Histologie, Embryologie et Anatomie pathologique, Département des Sciences Biologiques et Pharmaceutiques, Ecole Nationale Vétérinaire d'Alfort, FRANCE: www.vet-alfort.fr)*

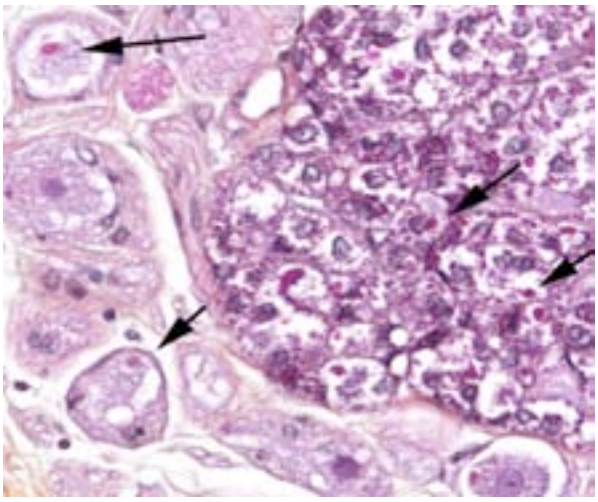

*3-3. Kidney, boa: Renal tubular epithelial cells contain one or more round, variably-sized eosinophilic intracytoplasmic inclusions (arrows). Many epithelial cells also contain large amounts of an unidentified reddish brown granular pigment. (HE 200X) (Photo courtesy of: Unité d'Histologie, Embryologie et Anatomie pathologique, Département des Sciences Biologiques et Pharmaceutiques, Ecole Nationale Vétérinaire d'Alfort, FRANCE: www.vet-alfort.fr)*

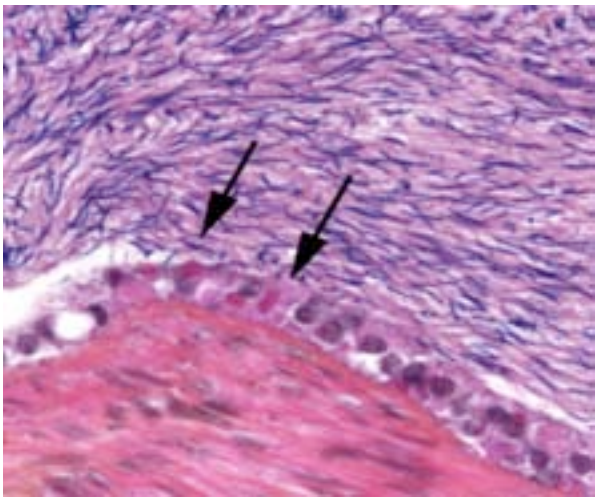

*3-4. Epididymis, boa: Epididymal lining epithelium contains one or more round, variably-sized eosinophilic intracytoplasmic inclusions (arrows). (HE 400X) (Photo courtesy of: Unité d'Histologie, Embryologie et Anatomie pathologique, Département des Sciences Biologiques et Pharmaceutiques, Ecole Nationale Vétérinaire d'Alfort, FRANCE: www.vet-alfort.fr)*

4) Epididymis: Numerous intracytoplasmic eosinophilic inclusions within epididymal epithelium, consistent with inclusions of Inclusion Body Disease.
5) Nervous ganglia: Numerous intracytoplasmic eosinophilic inclusions with neurons and chromaffin cells, consistent with inclusions of Inclusion Body Disease.

**Contributor's Comment:** Inclusion body disease (IBD) is a well-known, worldwide and fatal disease of boids (boas and pythons), first described 30 years ago.[14] The disease is characterized by the presence of eosinophilic intracytoplasmic inclusions in cells of numerous tissues. The etiology of IBD remained uncertain for years. The discovery of virus-like particles by transmission electron microscopy in affected tissues raised the suspicion for a viral etiology. These particles had a diameter of 110 nm and a hexagonal capsid, resembling C-type retroviral particles.[14] However, the exact etiology of IBD was recently proven to be arenaviruses.[2,9,15] The bloodsucking snake mite *Ophionyssus natricis* may be a vector for IBD virus.[14]

Arenaviruses are negative single-stranded RNA viruses. Their genome contains two elements: small (S) and large (L). The S segment encodes the viral nucleocapsid protein and the glycoprotein L segment encodes the RNA-dependent RNA polymerase and a small ring-domain-containing protein.[3] The genus arenavirus is the only genus of the *Arenaviridae* family and comprises 25 species according to the International Committee on Taxonomy of Viruses (ICTV, 2014). Two major lineages of arenaviruses are described based on genetic differences and geographical distribution: Old World arenaviruses and New World arenaviruses.[3,5]

In humans, arenaviruses cause hemorrhagic fevers (Lassa, Junin, Machupo, Guanarito, Sabia and Chapare viruses) and lymphocytic choriomeningitis (LCM) due to LCM virus. Asymptomatic infections also occur.[6]

The LCM virus can also produce congenital malformations and has been recently described as an important cause of fatal infection in organ transplantations recipients and immunocompetent patients.[6] LCM virus has a wide range of hosts: humans, hamsters, guinea pigs, cotton rats, chinchillas, canids and primates.[11] *Mus musculus* is considered the natural reservoir host. In New World primates of the *Callitrichidae* family (marmosets, tamarins), LCM virus causes callitrichid hepatitis.[11]

In boids, IBD does not manifest similarly between boas and pythons. Boas usually show intermittent regurgitation followed by anorexia. After a few weeks, neurologic signs appear and are characterized by head tremor, disorientation, ataxia, opisthotonos and behavioral changes.[14,16]

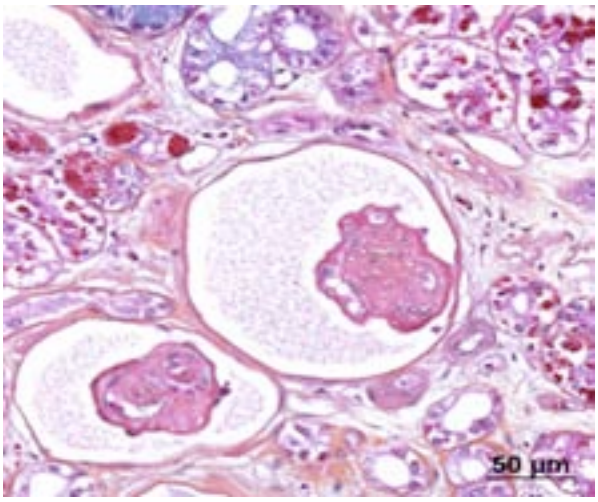


*3-5. Kidney, boa: Diffusely, glomeruli are sclerotic, and Bowman capsules are markedly dilated (glomerulocystic disease). (HE 400X) (Photo courtesy of: Unité d'Histologie, Embryologie et Anatomie pathologique, Département des Sciences Biologiques et Pharmaceutiques, Ecole Nationale Vétérinaire d'Alfort, FRANCE: www.vet-alfort.fr)*

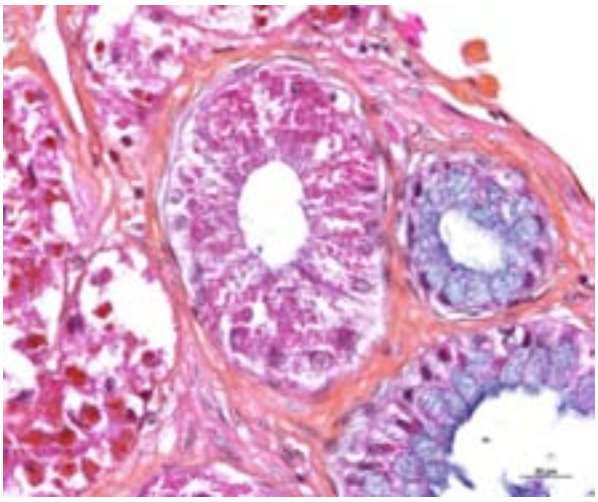

*3-6. Kidney, boa: Cells of the "sexual segment" of the distal convoluted tubules contain numerous small red protein droplets. (HE 400X) (Photo courtesy of: Unité d'Histologie, Embryologie et Anatomie pathologique, Département des Sciences Biologiques et Pharmaceutiques, Ecole Nationale Vétérinaire d'Alfort, FRANCE: www.vet-alfort.fr)*

Pneumonia and necrotizing stomatitis are common complications. After a few weeks or months of progression, death occurs.[13] Pythons do not display regurgitation but are often anorectic. Neurologic signs occur earlier in pythons than in boas, and are more severe. The progression is more rapid and death occurs after a few weeks.[4,14]

Historically, the diagnosis of IBD relied on the demonstration of characteristic eosinophilic intracytoplasmic inclusions on histological sections. In pythons, these inclusions are mostly found in the neurons of the central nervous system.[4] In boa constrictors, inclusions are commonly seen, in addition to neurons and glial cells of the central nervous system, in esophageal tonsils (epithelium and lymphoid cells), gastrointestinal and respiratory epithelia, hepatocytes, pancreatic acinar cells and renal tubular epithelium.[4] Inclusions can also be demonstrated on blood smears and/or impression smears of organs (liver and kidney). Such smears can be stained with Wright-Giemsa stain but H&E stain can also be used and appears more sensitive.[4] On blood smears, inclusions can be demonstrated in erythrocytes, lymphocytes and heterophils.[4] Tissues for diagnosis can be obtained from necropsy samples but antemortem diagnosis is also possible through esophageal tonsil, liver or renal biopsies.[4] As the number and distribution of inclusions is variable, with boas having more inclusions than pythons, diagnosis relying on identification of inclusion bodies is not a very sensitive method. Furthermore, inclusions can be found in other diseases.[4] With the recent discovery of IBD virus, a definitive and more sensitive diagnosis is now possible through PCR testing.

In this case, inclusion bodies were found in a large number of tissues as well as in cells from coelomic effusion, allowing antemortem diagnosis. PCR testing confirmed infection by IBD virus. In the kidney, renal epithelial cells also contained variable-sized acidophilic granules and brownish pigments. The acidophilic granules are typical to adult males of some snake and lizard species. They are present in the distal convoluted tubules, referred to as the "sexual segment". The content of the granules is extruded into the urinary wastes and is believed to represent pheromones that are useful for sexual courtship and mating.[1] The brownish pigments are of unknown origin and significance. They were negative for Prussian blue stain, Schmorl's stain and PAS stain.

**JPC Diagnosis:** 1. Epithelial cells of renal tubules, ureter, and epididymis and neurons: Intracytoplasmic protein droplets, numerous. 2. Kidney: Glomerulosclerosis, diffuse, moderate. 3. Kidney, tubular epithelium: Brown pigment of unspecified origin. 4. Kidney, tubular epithelium: Intracytoplasmic apicomplexans, few.

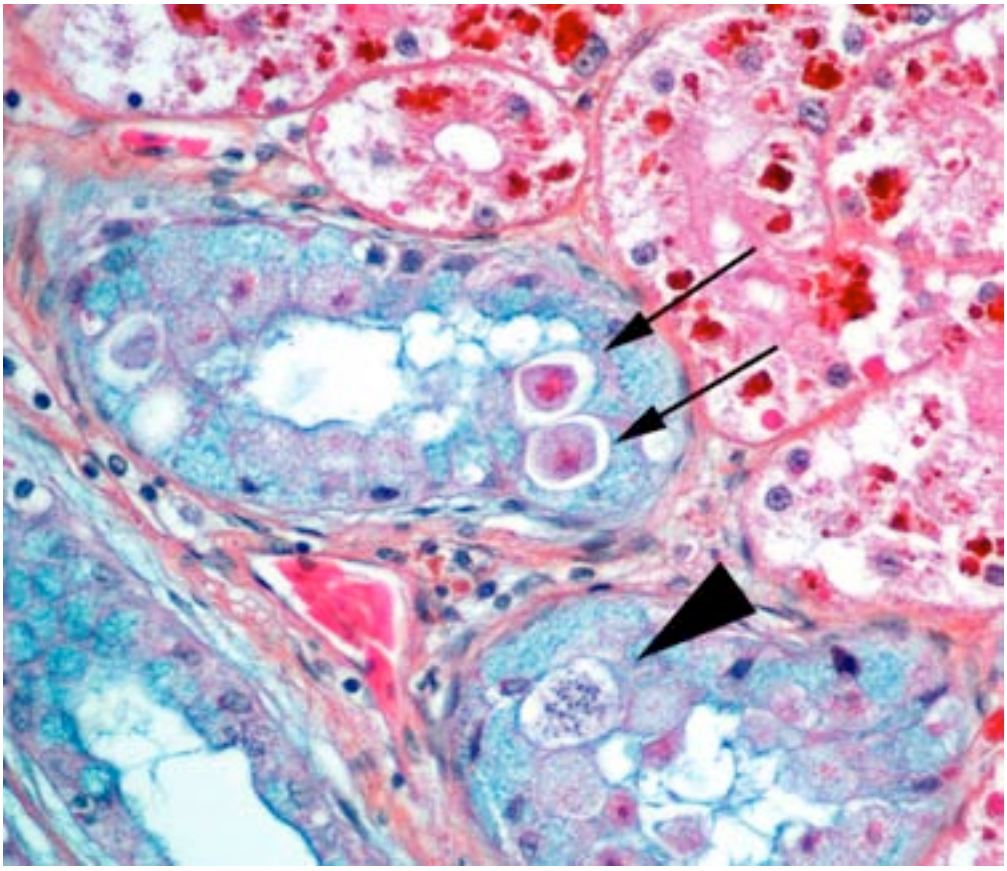

*3-7. Kidney, boa: Renal tubules contain rare intraepithelial structures resembling coccidian (arrow), including one schizont). (HE 400X)*

**Conference Comment:** This case generated a lot of discussion, largely on the source of the unspecified brown inclusions within renal epithelium which are quite dramatic in most sections. The discussed differentials included protein, iron, copper, hemoglobin, melanin or lipofuscin. Unfortunately the contributor's stains and our additional stains did not aid in their characterization.

The contributor highlights the recent identification of an arenavirus as the cause of IBD. The characteristic cytoplasmic inclusions associated with IBD are dramatic and found in many tissues usually in the absence of inflammation.[4] Typically, viral inclusions are the result of viral nucleic acid templates liberated in the cytoplasm which are utilized by the host cell to produce aberrant production of viral proteins. These proteins are often produced in excess and subsequently accumulate as inclusion bodies. While most viral inclusions are composed of excess viral proteins and membranes with viral particles, some consist of mature viral particles (virions) arranged in lattice formations.[7] IBD inclusions are nonviral, composed exclusively of 68-KDa protein deposited by ribosomes[10] which may have hindered prompt identification of the virus.

As discussed by the contributor, the observation of viral protein inclusions and brown pigment within the tubular epithelium was further complicated by the prominent acidophilic granules common in male reptiles. It is worth mentioning this snake was in its reproductive season at the time of necropsy as the granules are prominent and sperm production is abundant.

The presence of glomerulosclerosis is a common finding in older reptiles; and we chose to separate its diagnosis as most did not feel it was related to the viral infection. Glomerulosclerosis is characterized by shrunken and hyalinized mesangium, with an increase in fibrous connective tissue and a loss of capillaries. Tubular degeneration often occurs secondarily, as they receive their blood supply from the glomerular efferent arteriole which becomes compromised in these instances. Glomerulosclerosis is accelerated by inflammation, excessive dietary protein and increased glomerular capillary pressure.[12] Its widespread occurrence in reptiles is most often attributed to high protein diets.[8]

Rarely observed in a few sections and confined to one small area of renal tubules, there are few intraepithelial organisms closely resembling an

undetermined species of coccidia which gave us a fourth diagnosis to contribute.

**Contributing Institution:** Unité d'Histologie, Embryologie et Anatomie pathologique, Département des Sciences Biologiques et Pharmaceutiques
Ecole Nationale Vétérinaire d'Alfort, FRANCE: www.vet-alfort.fr

**References:**

1. Aughey E, Frye FL. Urinary System. In: *Comparative Veterinary Histology with Clinical Correlates*. 1st edition. London: CRC Press; 2001:137-148.
2. Bodewes R, Kik MJL, Raj VS, et al. Detection of novel divergent arenaviruses in boid snakes with inclusion body disease in The Netherlands. *J Gen Virol.* 2013;94:1206–10.
3. Buchmeier M, de la Torre J, Peters C. Arenaviridae. In: Knipe DM, Howley PM, eds. *Fields Virology*. 5th edition. New York, NY: Lippincott Williams & Wilkins; 2006:1791–828.
4. Chang L-W, Jacobson ER. Inclusion body disease. A worldwide infectious disease of Boid snakes: A review. *J Exotic Pet Med.* 2010;19:216–25.
5. Charrel RN, de Lamballerie X, Emonet S. Phylogeny of the genus Arenavirus. *Curr Opin Microbiol.* 2008;11:362–8.
6. Charrel RN, de Lamballerie X. Zoonotic aspects of arenavirus infections. *Vet Microbiol.* 2010;140:213–20.
7. Cheville NF. *Ultrastructural Pathology The Comparative Celullar Basis of Disease.* 2nd ed. Ames, IA: Blackwell Publishing; 2009:851.
8. Hernandez-Divers S, Innis CJ. Renal disease in reptiles: diagnosis and clinical management. In: Mader DR, ed. *Reptile Medicine and Surgery*. 2nd ed. St. Louis, MO: Saunders Elsevier; 2006:879.
9. Hetzel U, Sironen T, Laurinmäki P, et al. Isolation, identification, and characterization of novel arenaviruses, the etiological agents of boid inclusion body disease. *J Virol.* 2013;87:10918–35.
10. Jacobson ER. Viruses and viral diseases of reptiles. In: Jacobson ER, ed. *Infectious Diseases and Pathology of Reptiles*. Boca Raton, FL: CRC Press; 2007:410-412.
11. Montali RJ, Connolly BM, Armstrong DL, Scanga CA, Holmes KV. Pathology and immunohistochemistry of callitrichid hepatitis, an emerging disease of captive New World primates caused by lymphocytic choriomeningitis virus. *Am J Pathol.* 1995;147:1441–9.
12. Newman SJ. The urinary system. In: Zachary JF, McGavin MD, eds. *Pathologic Basis of Veterinary Disease.* St. Louis, MO: Elsevier Mosby; 2012:626-627.
13. Percy DH, Barthold SW. The mouse. In: *Pathology of Laboratory Rodents and Rabbits*. 3rd edition. Ames, Iowa: Wiley-Blackwell; 2007:3-124.
14. Schumacher J, Jacobson ER, Homer BL, Gaskin JM. Inclusion body disease in Boid snakes. *J Zoo Wildl Med.* 1994;25:511–24.
15. Stenglein MD, Sanders C, Kistler AL, et al. Identification, characterization, and in vitro culture of highly divergent arenaviruses from boa constrictors and annulated tree boas: candidate etiological agents for snake inclusion body disease. *MBio.* 2012;3:e00180–00112.
16. Vancraeynest D, Pasmans F, Martel A, et al. Inclusion body disease in snakes: a review and description of three cases in boa constrictors in Belgium. *Vet Rec.* 2006;158:757–60.

**CASE IV:** E 5496/12 (JPC 4033372)

**Signalment:** Snowy owl of unknown age and gender, *Bubo scandiacus.*

**History:** The snowy owl was found dead without any previous clinical signs.

**Gross Pathology:** Autopsy revealed numerous white spots of about 0.2 cm in diameter in the spleen and liver.

**Laboratory Results:** None.

**Histopathologic Description:** Small intestine: Multifocally, the mucosa and submucosa are replaced by large areas of coagulation necrosis characterized by loss of cellular detail, karyorrhexis, karyopyknosis, karyolysis and the presence of numerous heterophils (mostly degenerated, partially viable), extravasated erythrocytes (hemorrhage), and deposition of fine fibrillar, pale eosinophilic material (fibrin). Adjacent to the necrotic areas are moderate infiltrates composed of macrophages and fewer lymphocytes. Occasionally, the necrosis and inflammatory cells extend through the tunica muscularis and to the serosa with multifocal mild serosal inflammation as described above. There are multifocal crypt abscesses characterized by attenuated epithelium and intraluminal accumulation of cellular debris, sloughed epithelial cells, fibrin and few degenerate heterophils. In numerous epithelial cells, large (4-6 μm) intranuclear, eosinophilic inclusion bodies that almost fill the nucleus and marginate the chromatin are present. Some adventitial vessels show an increased number of erythrocytes (mild congestion).

**Contributor's Morphologic Diagnosis:** Small intestine: Enteritis, severe, acute, necrotizing and ulcerative, multifocal, with intranuclear eosinophilic inclusion bodies (Cowdry A type) consistent with strigid herpesvirus-1 infection.

Microscopic Findings of Tissues (not submitted): In the liver and spleen multifocal areas of acute necrosis with intralesional eosinophilic intranuclear inclusion bodies are present.

**Contributor's Comment:** Strigid herpesvirus-1 (StHV-1) belongs to the β-herpesvirinae[8] and is the cause of *hepatosplenitis infectiosa strigum*, a disease that affects only owls with a yellow or orange iris and was first described in 1936[7] and further classified in 1973.[1] It is closely related to falconid herpesvirus-1 (FHV-1) of falcons, eagles, and hawks, and columbid herpesvirus-1 (CoHV-1) of pigeons.[10] The three viruses were indistinguishable by serum neutralization and it was hypothesized they might represent the same virus.[8]

*4-1. Liver and spleen, snowy owl: The spleen and liver contain numerous necrotic foci ranging up to 0.2 cm in diameter. (Photo courtesy of: Department of Veterinary Pathology, Freie Universität Berlin, Germany, http://www.vetmed.fu-berlin.de/en/einrichtungen/institute/we12/index.html)*

Sequence analyses revealed an almost 100% sequence identity between FHV-1, CoHV-1, and StHV-1 whereas there were considerable differences to other avian herpesviruses.[8] These results further supported the hypothesis that owls and falcons might get infected by the consumption of pigeons

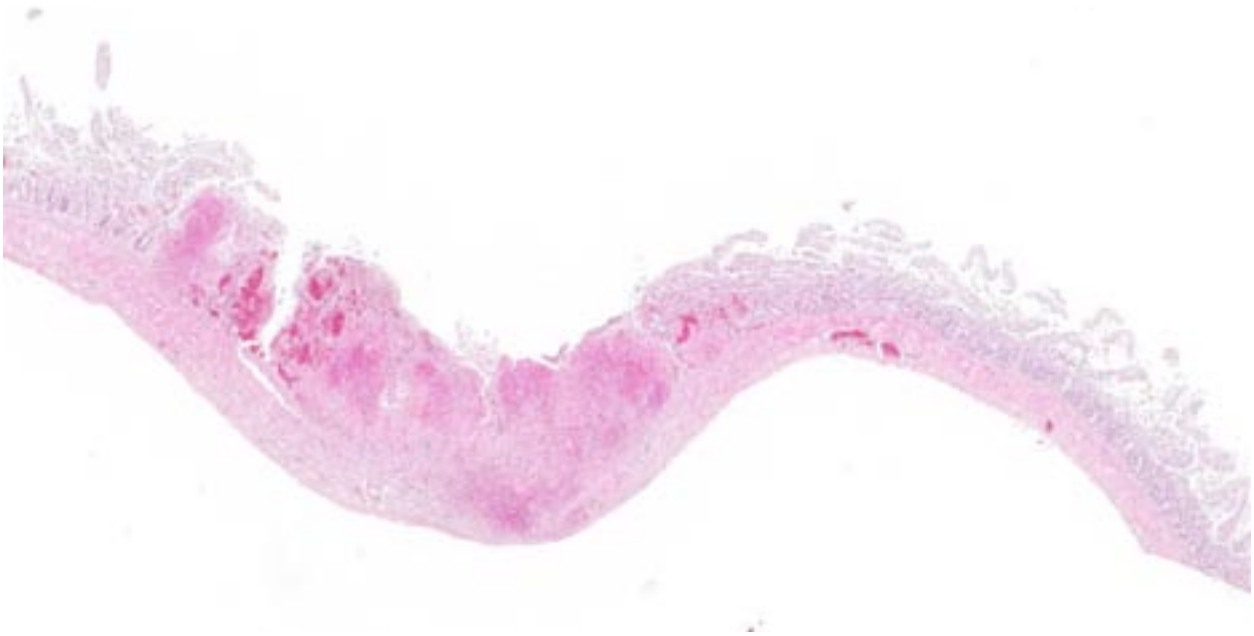

*4-2. Intestine, snowy owl: There are multifocal areas of transmural lytic necrosis scattered randomly along the section. (HE 15X)*

infected with CoHV-1.[6,8] Natural infections with StHV-1 have been observed in the eagle owl (*Bubo bubo L.*), long-eared owl (*Asio otus L.*) and snowy owl (*Bubo scandiacus*) as well as in great horned owls (*Bubo virginianus*) in the United States.[2,8]

The majority of infected owls are found dead without previous clinical signs. However, some show depression, anorexia, conjunctivitis, oral and pharyngeal ulcerations and respiratory symptoms as well as diarrhea.[2,6]

The main histologic feature of the disease is the presence of numerous necrotic foci in the liver, spleen and bone marrow.[6] Typically, in the liver, spleen and several additional organs, eosinophilic intranuclear inclusion bodies of Cowdry A type are present. Necrotic areas may appear in the pharynx and small intestine as well.[6]

**JPC Diagnosis:** Intestine: Enteritis, necrotizing, transmural, focally extensive, severe, with intranuclear viral inclusions.

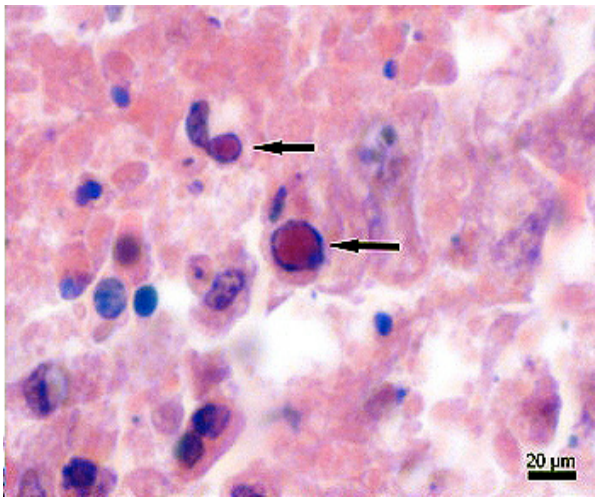


*4-3. Intestine, snowy owl: Degenerate enterocytes within the intestine contain intranuclear eosinophilic viral inclusions which peripheralize chromatin. (Photo courtesy of: Department of Veterinary Pathology, Freie Universität Berlin, Germany, http://www.vetmed.fu-berlin.de/en/einrichtungen/institute/we12/index.html)*

**Conference Comment:** Herpesvirus infection in birds of prey is caused by a member of the subfamily *Alphaherpesvirinae*. The debate over whether owls and falcons are infected by a closely-related but genetically distinct herpesvirus, so named strigid herpesvirus-1 and falconid herpesvirus-1, seems to have been resolved with recent unequivocal evidence demonstrating all raptors being infected by a single herpesvirus, columbid herpesvirus-1 (CoHV-1).[6,8,11] CoHV-1 is harbored, often subclinically, within adult rock pigeons yet causes significant lesions in raptors,[6] akin to other host-adapted herpes infections such as ovine herpesvirus-2 in sheep. In squabs (nestling pigeons), its infection may manifest as observed in raptor species: hepatic necrosis, splenic

necrosis, renal necrosis, and ulceration of the respiratory and gastrointestinal tracts.[2] Typically, raptors will prey on pigeons when more preferable options are scarce, as often occurs in the early spring, which offers a reasonable mode of viral transmission. The number of great horned owls infected with *Trichomonas gallinae*, a protozoan parasite also harbored in rock pigeons, has been documented to be elevated during this time of year further supporting this theory.[11]

Herpesviruses are well-known, ubiquitous infectious agents across the entire animal kingdom, with new strains being discovered regularly, often which pose significant health threats to the affected population. Recent publications have described herpesviral necrotizing stomatitis in Eastern box turtles (terrapene herpesvirus-1),[12] significant mortality in koi and common carp (cyprinid herpesvirus-3),[5] and a sarcoma inducing herpesvirus in baboons (Kaposi's Sarcoma-associated herpesvirus).[13] Adding further interest to the subject are the peculiarities of pathogenesis and disease transmission among some herpes pathogens, such as the seasonal-dependent neoplastic growth or viral shedding of ranid herpesvirus-1 in leopard frogs[3] and the recent proposal of chelonid herpesvirus-5 "superspreaders" causing outbreaks of fibropapillomatosis in marine turtles.[14]

Central to the success of all herpesviruses is the interplay between latency and lytic modes of infection. Latency is characterized by restricted viral gene expression permitting the virus to evade the host immune system. Upon reactivation, a cascade of gene expression is initiated enabling its spread between cells and between hosts. In all subfamilies of human herpesviruses, the latent to lytic switch has been found to occur through expression of one or more microRNAs (miRNA).[4] MiRNAs are noncoding, or transcribed but not translated, single stranded RNAs which inhibit translation of messenger RNA through the action of the RNA-induced silencing complex (RISC). In this way, they are able to control cell growth, differentiation and survival. Their characteristics are now well understood regarding development of cancer and their expression is conserved among all eukaryotes, including microorganisms such as the numerous herpesviruses discussed here.[9]

**Contributing Institution:** Department of Veterinary Pathology, Freie Universität Berlin, Germany, http://www.vetmed.fu-berlin.de/en/einrichtungen/institute/we12/index.html

**References:**

1. Bürki F, Burtscher H, Sibalin M. Herpesvirus strigis: a new avian herpesvirus. I. Biological properties. *Arch Gesamte Virusforsch*. 1973;43:14-24.
2. Burtscher H, Sibalin M. Herpesvirus strigis: host spectrum and distribution in infected owls. *J Wildl Dis*. 1975;11:164-9.
3. Carlson DL, Sauerbier W, Rollins-Smith LA, McKinnell RG. The presence of DNA sequences of the Lucke herpesvirus in normal and neoplastic kidney tissue of Rana pipiens. *J Comp Pathol.* 1994;110:349-355.
4. Frapper L. Regulation of herpesvirus reactivation by host miRNAs. *J Virol.* 2014 Dec 24 pii: JVI.03413-14 [Epub ahead of print].
5. Fujioka H, Yamasaki K, Furusawa K. Prevalence and characteristics of Cyprinid herpesvirus 3 (CyHV-3) infection in common carp (Cyprinus carpio L.) inhabiting three rivers in Kochi Prefecture, Japan. *Vet Microbiol.* 2014 Dec 11. Pii: S0378-1135(14)005574 [Epub ahead of print]
6. Gailbreath KL, Oaks JL. Herpesviral inclusion body disease in owls and falcons is caused by the pigeon herpesvirus (columbid herpesvirus 1). *J Wildl Dis*. 2008;44:427-33.
7. Green RG, Schillinger JE. A virus disease of owls. *Am J Pathol*. 1936;12:405-410.
8. Kaleta EF. Herpesviruses of birds - a review. *Avian Pathol*. 1990;19:193-211.
9. Kumar V, Abbas AK, Aster JC. *Robbins and Cotran Pathologic Basis of Disease.* 9th ed. Philadelphia, PA: Elsevier Saunders; 2015:320.
10. Potgieter LN, Kocan AA, Kocan KM. Isolation of a herpesvirus from an American kestrel with inclusion body disease. *J Wildl Dis*. 1979;15:143-9.
11. Rose N, Warren AL, Whiteside D, et al. *Columbid herpesvirus-1* mortality in great horned owls (*Bubo virginianus)* from Calgary, Alberta. *Can Vet J.* 2012;53(3):265-268.
12. Sim RR, Norton TM, Bronson E, et al. Identification of a novel herpesvirus in captive Eastern box turtles (Terrapene carolina carolina). *Vet Microbiol*. 2014 Dec 13. Pii: S0378-1135(14)005549. [Epub ahead of print]

13. Whitby D, Stossel A, Gamache C, et al. Novel Kaposi's sarcoma-associated herpesvirus homolog in baboons. *J Virol*. 2003;77(14): 8159-8165.
14. Work TM, Dagenais J, Balazs GH, Schettle N, Ackermann M. Dynamics of virus shedding and in situ confirmation of chelonid herpesvirus 5 in Hawaiian green turtles with fibropapillomatosis. *Vet Pathol.* 2014 Dec 1 DOI: 10.1177/03000985814560236 [Epub ahead of print].

**Joint Pathology Center**
**Veterinary Pathology Services**
**Wednesday Slide Conference**
**2014-2015**
**Conference 14**
**January 14, 2015**

---

**CASE I:** 12-0433 (JPC 4036190).

**Signalment:** 17-week-old female C57BL/6 mouse, *Mus musculus*.

**History:** 17-week-old female C57BL/6J mouse which was one of a cohort infected with a sublethal dose of murine cytomegalovirus (MCMV). Six days post-infection, this mouse and one other showed decreased activity; both were culled and submitted for post mortem.

**Gross Pathology:** The liver and kidneys were pale tan and pale red, respectively. There were multiple petechial and ecchymotic hemorrhages on the surfaces of the gall bladder, small intestine, and the urinary bladder. There were extensive petechial and ecchymotic hemorrhages affecting 30-40% of the total skin area and the paws. Both eyes were diffusely red-black, and there was a small amount of free blood in the pleural cavity.

**Laboratory Results:** N/A

**Histopathologic Description:** Liver – Throughout the hepatic parenchyma there are randomly scattered foci of hepatocellular loss, and the tissue is replaced with amorphous eosinophilic material, often with remnant cellular outlines, and with pyknotic/karyorrhectic nuclei (acute necrosis). Associated with these foci, many of the nuclei of hepatocytes and Kupffer cells contain large, often well-demarcated bodies of deeply eosinophilic material with margination and blebbing of chromatin (intranuclear inclusions). Occasionally, small, discrete eosinophilic inclusions are also present in the cytoplasm. In the remaining tissue, the hepatocytes are generally swollen with microvesicular vacuolation (hydropic change).

Spleen – The reticuloendothelial cells of the red pulp are extensively lost and replaced by amorphous eosinophilic material and nuclear debris with little trace of the normal splenic architecture (acute necrosis). The remaining reticuloendothelial cells contain intranuclear inclusions as seen in the liver. The white pulp is relatively preserved, although many lymphocytes in the periarteriolar lymphoid sheaths, individually and in clusters, have shrunken, pyknotic nuclei.

**Contributor's Morphologic Diagnosis:**

1. Liver – severe, acute, multifocal to coalescing hepatic necrosis with intranuclear and intracytoplasmic inclusions
2. Spleen –
    a. severe, acute, diffuse red pulp necrosis with intranuclear inclusions
    b. mild, acute, multifocal white pulp lymphoid necrosis

**Contributor's Comment:** This mouse was one of a cohort that had been infected with what was described as a sublethal dose of murine cytomegalovirus (MCMV). At day 6 post infection, this mouse and one other from the same cohort were less active than the others in the group, and these 2 were culled. Notwithstanding the description of the administered dose of virus, there were no gross or microscopic findings in either mouse other than those referable to acute MCMV infection.

Murine cytomegalovirus is a DNA virus in the family *Herpesviridae*, the subfamily *Betaherpesvirinae*, and the genus *Muromegalovirus*.[4] The betaherpesviruses are highly host specific viruses that infect humans, mice, rats and guinea pigs (and other mammals, though these are generally less well characterized). MCMV infections in mice have been extensively studied, largely because the course of infection in mice has several pertinent similarities to the course of Human Cytomegalovirus (HCMV) infection, making it a useful model to study the human disease. HCMV is a highly prevalent infection of humans worldwide, with seroprevalence in women of reproductive age varying from approximately 40% (US, much of western Europe, Australia) to >90% (Brazil, Chile, Italy, India, Turkey, Japan).[3] Infection rarely causes clinical signs in immunocompetent individuals. It is, however, a significant cause of morbidity in immunosuppressed individuals and is an important cause of disease (notably of hearing loss and neurological impairment) in children born to mothers who are first infected during pregnancy.[5]

As is typical of herpesviruses, MCMV causes lifelong, persistent infections with intermittent reactivation and virus shedding at times of host immunosuppression. After initial infection, MCMV replication occurs in salivary glands; excretion in saliva appears to be the primary means of transmission through grooming and biting activities. The virus then disseminates and severe infections may induce encephalitis, retinitis, pneumonia, hepatitis, myocarditis, adrenalitis and/or haemopoietic failure. Besides saliva, infective virus is also present in the tears, urine and seminal fluid of infected animals, though the occurrence of natural transmission by means of these secretions has not been well established. Viral DNA replication occurs in the nucleus of infected cells, while production of the capsid protein occurs in the cytoplasm. The capsid proteins are transported to the nucleus where viral packaging takes place; the packaged particles are then transported back to the cytoplasm where they acquire their primary envelope. A second enveloping stage is required before the virions are ready for release. Hence, infection is associated with both intranuclear and intracytoplasmic inclusions. The outcome of MCMV infection is highly dose-dependent – in mouse models of infection, mortality may change from 0% to 100% with only a four-fold increase in dose. Other determinants of susceptibility include strain (BALB/C are highly susceptible; C57BL/6 are resistant) and age of the host (young animals are highly susceptible).

Investigations into the variable susceptibility of mouse strains to MCMV infection has shown that innate immune function, in particular the effectiveness of the natural killer (NK) cell response, is the key determinant of an animal's capacity to resist the initial infection and to suppress viral replication. A host gene designated *Cmv1* has been identified which encodes a natural killer (NK) cell receptor that confers resistance to infection. This receptor, the ligand for which is Ly49H, recognizes MCMV directly and its stimulation induces NK cell expansion and activation.[8] NK cells suppress the infection by direct lysis of infected cells and by producing cytokines to mediate T-cell responses. Counteracting the host immune system are a number of

viral genes, the products of which modify the host immune response by inhibition of NK cell function, blocking of cytotoxic T-lymphocyte function, or inducing resistance to interferon or complement. T-lymphocytes, especially cytotoxic CD8+ cells, are activated by NK cell cytokines, and they play an important role in controlling the MCMV infection and in inducing the state of latency. CD4+ cells are involved to an extent in modulating the CD8+ response, but depletion of these cells does not alter the course of infection. Humoral immunity is relatively unimportant in controlling MCMV infection.

Latent virus in the mouse is identifiable in the salivary glands and in other tissues including lung, spleen, liver, kidney, heart, adrenal glands, and myeloid cells. The severity of reactivated infection may be related to the severity of the initial infection, that is, to the number of cells in which latent virus resides.

**JPC Diagnosis:** 1. Liver: Hepatitis, necrotizing, multifocal to coalescing, severe, with karyomegaly and intranuclear viral inclusions. 2. Spleen: Splenitis, necrotizing, multifocal to coalescing, severe, with lymphocytolysis, karyomegaly and intranuclear viral inclusions.

**Conference Comment:** This is a nice case of this appropriately-named betaherpesvirus, as it demonstrates the marked cytomegaly, karyomegaly and intranuclear inclusions so characteristic to cytomegalovirus infection. Its presentation within a mouse model is relevant to the human form of infection, and these models have aided in the characterization of physiologic mechanisms of immunity as nicely highlighted by the contributor. The degree of necrosis is especially prominent in the spleen in this case, with some conference participants speculating that only extramedullary hematopoietic cells are still viable in most sections.

Natural infections of cytomegalovirus are observed in primates and guinea pigs in addition to mice. Rhesus cytomegalovirus (macacine herpesvirus-3) is the most common opportunistic viral infection in rhesus macaques infected with SIV.[1] It causes multiorgan pathology, with interstitial pneumonia, encephalitis, gastroenteritis, and lymphadenitis being most common.[2] Viral infection is commonly associated with neutrophilic infiltrates, regardless of tissue, and when it occurs in conjunction with simian polyomavirus 40, mesenchymoproliferative enteropathy has been described.[9] Recently, peripheral nerve lesions such as facial neuritis have been identified in macaques, which are likely a bystander effect secondary to inflammation and infected macrophages.[1] In guinea pigs, lesions are largely regarded as incidental findings at necropsy and usually confined to the ductal epithelial cells of the salivary glands.[10]

The contributor details the importance of NK cells in resisting and controlling murine cytomegalovirus (MCMV) infection in mice. Of special interest is the ability of NK cells to clonally expand upon activation of the Ly49H receptor. This stimulated NK cell population persists for months following the resolution of infection, and when the animal is re-introduced to MCMV, a secondary expansion occurs, conferring resistance to re-infection, effectively demonstrating the generation of memory within this cell population.[6] This a well-known feature of T cells in the adaptive immune response, but NK cells are typically described as an important component of the innate immune response, especially concerning virus-infected and neoplastic cells. NK cell regulation occurs through cytokine expression (IL-2 and IL-15 stimulate proliferation, IL-12 activates killing) and inhibitory receptors which recognize the class I MHC molecules expressed by all healthy cells. Viral infection or neoplastic transformation often

reduces class I MHC expression in a cell, thereby activating NK cells to destroy it. Activated NK cells, which all express CD16 and CD56, also secrete IFN-γ which activates macrophages.[7] Interestingly, C57BL/6 (B6) mice are readily recognized as having resistance to MCMV due to Ly49H expression, and its infection in this case indicates a possible deficiency in one of the several factors critical for generation of memory NK cells in MCMV infection: IL-12, microRNA-155, and DNAM-1.[6]

Conference participants discussed their top differentials for necrotizing hepatitis in mice. Other viral infections include: mouse adenovirus-1 (intranuclear inclusions), mouse hepatitis virus (viral syncytia), mousepox (intracytoplasmic inclusions), and mammalian orthoreovirus (only in infant mice). Bacterial causes include *Helicobacter* spp., *Clostridium piliforme*, *Salmonella* spp., *Proteus mirabilis*, and *Listeria monocytogenes* as demonstrated in WSC 14-15 Conference 6.

**Contributing Institution:** Murdoch University Veterinary Hospital
http://www.murdoch.edu.au/

**References:**


1. Assaf BT, Knight HL, Miller AD. Rhesus cytomegalovirus (Macacine herpesvirus 3)-associated facial neuritis in simian immunodeficiency virus-infected rhesus macaques (Macaca mulatta). *Vet Pathol.* 2015;52(1):217-223.
2. Baskin GB. Disseminated cytomegalovirus infection in immunodeficient rhesus monkeys. *Am J Pathol.* 1987;129(2):345-352.
3. Cannon MJ, Schmid DS, Hyde TB. Review of cytomegalovirus seroprevalence and demographic characteristics associated with infection. *Rev Med Virol.* 2010:20(4):202-213.
4. Davison AJ, Eberle R, Ehlers B, Hayward GS, McGeoch DJ, Minson AC, et al. The order Herpesvirales. *Arch Virol.* 2009:154(1):171-177.
5. Fox JG. *The Mouse in Biomedical Research*. Amsterdam; Boston: Elsevier/Academic Press; 2007.
6. Kamimura Y, Lanier LL. Homestatic control of memory cell progenitors in the natural killer cell lineage. *Cell Rep*. 2015;10(2):280-291.
7. Kumar V, Abbas AK, Aster JC. Diseases of the immune system. In: Kumar V, Abbas AK, Aster JC, eds. *Robbins and Cotran Pathologic Basis of Disease.* 9th ed. Philadelphia, PA: Elsevier Saunders; 2015:192.
8. Lee SH, Kim KS, Fodil-Cornu N, Vidal SM, Biron CA. Activating receptors promote NK cell expansion for maintenance, IL-10 production, and CD8 T cell regulation during viral infection. *J Exp Med.* 2009:206(10):2235-2251.
9. Macri SC, Knight HL, Miller AD. Mesenchymoproliferative enteropathy associated with dual simian polyomavirus and rhesus cytomegalovirus infection in a simian immunodeficiency virus-infected rhesus macaque (Macaca mulatta). *Vet Pathol.* 2012;50(4):715-721.
10. Percy DH, Barthold SW. *Pathology of Laboratory Rodents and Rabbits*. 3rd ed. Ames, IA: Blackwell Publishing; 2007:222.


---

**CASE II**: R05-43 (JPC 3138067)

**Signalment:** Adult female goat.

**History:** During 2004 and 2005, a goat farm in Northern Taiwan accounted episodes of severe abortion. Two flocks of goats had been introduced from central and Southern Taiwan about half a year prior to the incidence.

**Gross Pathologic Findings:** At necropsy, the lungs of fetus were mottled, patchy, dark purple to dark grayish red. The placenta was diffusely dark-red with the presence of some yellow to red turbid exudates on the surface of the cotyledonary and intercotyledonary areas. No other gross lesions were found.

**Laboratory Results:**
1. The detection of *Coxiella burnetii* by PCR with the primer pair of Trans1/Trans2 (687 bp) (Houver et al., 1992) and by nested PCR with the primer pairs of OMP1/OMP2 (501 bp) and OMP3/OMP4 (438 bp) (Zhang GQ et al., 1998) was employed for the final diagnosis of this case.
2. Other laboratory tests including chlamydiosis by PCR, foot & mouth disease by ELISA, and bluetongue by ELISA were all negative. Bacterial culture of the fetal tissues was also negative.

**Histopathologic Description:** Microscopically, the placenta had multifocal to locally extensive necrosis in the superficial epithelium in both cotyledons and intercotyledonary areas. The trophoblasts were distended by small, approximately 1μm diameter, basophilic, intracytoplasmic organisms. The underlying stroma had mild to moderate lymphoplasmacytic infiltrates with evident perivascular lymphoplasmacytic aggregates. Macchiavello's staining revealed heavy intracytoplasmic load of positive microorganisms that were negative for Gram stain. In the fetus, mild to moderate inflammation consisting of lymphocytes, plasma cells, and epithelioid macrophages are frequently seen within in the parenchyma of liver, lungs, and kidney. Occasionally, non-suppurative meningoencephalitis and lymphocytic perivascular cuffing could also be observed.

**Contributor's Morphologic Diagnosis:** Placenta, chorioallantoic: Placentitis, necrotizing, acute, multifocal, moderate, with focal vasculitis and intracellular organisms.

**Contributor's Comment:** *Coxiella burnetii* is a ubiquitous zoonotic pathogen of Q fever, initially identified in Queensland, Australia, in 1935, after an outbreak of febrile illness among slaughterhouse workers. *Coxiella* was historically considered as a *Rickettsia*, but gene-sequence analysis now classifies it in the order *Legionellales*, family *Coxiellaceae*, genus *Coxiella*. It is an intracellular, small pleomorphic gram-negative bacterium, which completes its life cycle within the phagosomes of infected cells. Although possessing a membrane similar to that of the gram-negative bacteria, it is usually not stained by the Gram technique. According to Raoult et al. (2005), the survival and multiplication of *C. burnetii* in the acidophilic phagosomes prevent antibiotics from killing the bacteria. Increasing pH with lysosomotropic agents such as chloroquine restores the bactericidal activity of doxycycline. The agent has 2 distinct life cycle stages known as the large-cell variant (LCV) and small cell variant. The large-cell variant is the vegetative form of the bacteria seen in infected cells. The small-cell variant (SCV) may be metabolically inactive and is the extracellular and presumably with infectious form of the organism. The SCV form of *C. burnetii* is likely to be long-lived in the environment because of its resistance to osmotic stress, physical disruption, and chemical agents. Two phases of the bacterium have been described: the highly virulent phase I organisms are found in the infected

hosts and insect vectors. The phase II organisms are less virulent or devoid of virulence for mammalian hosts and are obtained through multiple passages of chicken embryos.

*Coxiella burnetii* is a potential bioterrorism and occupational hazardous agent. Q fever has been described worldwide except in Antarctica and New Zealand. Through the air-borne, it can be inhaled by humans. A single organism of *C. burnetii* may cause disease in a susceptible person. In animals, *C. burnetii* can infect many animal species, including domestic animals, birds, reptile, wildlife, and arthropods such as ticks. Cats and dogs may represent reservoirs of *C. burnetii*. Dogs may be infected by tick bites, by consumption of placentas or milk from infected ruminants, and by aerosol. The possibility of human Q fever acquired from infected dogs and cats has been reported. The infected animals are generally asymptomatic, but in mammals they may induce pneumonia, abortion, stillbirth, and delivery of weak lambs, calves or kids. The *Coxiella burnetii*-infected herds of cows have showed shedding the organisms within the milk for 13 months. The ewe can shed the organisms within the vaginal mucus for 71 days. People who may come into contact with infected animals are at the greatest risk, including farmers, slaughterhouse workers, laboratory workers, and veterinarians. In humans, *C. burnetii* causes highly variable clinical manifestations, ranging from acute to fatal chronic infections. However, about 60% of the human infections are asymptomatic seroconversions. Acute Q fever in humans displays mainly flu-like symptoms, atypical pneumonia or granulomatous hepatitis. Various rare clinical signs of meningoencephalitis, endocarditis, pericarditis, pancreatitis, and abortion have also been described. It is prudent for pregnant women to limit the contact with infected animals, especially with fetal fluids and unpasteurized milk.

In Taiwan, the first case of acute human *C. burnetii* infection was reported in 1993. Since 2005, samples have been routinely collected from goats, sheep, cattle, and wildlife for the study of the seroprevalence and histopathological changes of Q fever and the DNA sequence of *C. burnetii*. The results indicate that Q fever should be considered as a possible pathogen in association with the commonly observed abortion in goats, cattle, and wildlife in Taiwan. To our knowledge, this is the first diagnosis of *Coxiella burnetii* infection in Taiwan livestock.

**JPC Diagnosis:** Placenta, chorioallantois: Placentitis, necrotizing, subacute, multifocal, severe, with intraepithelial and intratrophoblastic coccobacilli.

**Conference Comment:** The contributor offers an excellent opportunity to identify, describe, and interpret lesions in an organ not often observed in histologic section. Conference participants spent some time discussing the components of the placenta and using the identification of individual layers and their orientation to infer a more specific location of these sections. The placenta is comprised of endometrium (the maternal component) and the fused chorioallantoic membranes (CAM, the fetal component). The indeciduate nature of ruminant placentas implies the maternal and fetal components are in contact but not intimately fused. Additionally, ruminants have cotyledonary placentation, meaning there are numerous but isolated areas where the CAM contributes to the placenta. In these areas, the CAM villi insert into pockets or crypts in the area of the endometrium known as caruncles. Specific to small ruminants, the caruncles have lost their epithelium, leaving 5 tissue layers which separate maternal and fetal blood: endothelium, connective tissue, and epithelium of the CAM, and endothelium and connective tissue of the endometrium.[1] Conference participants concluded there is no maternal tissue within these sections, and the presence of amnion and the CAM villi indicates these must have been

collected from the cotyledon. Additionally, there are prominent eosinophilic crystals (hemoglobin) within an area of the CAM epithelium indicating the likelihood of a junction between cotyledonary and intercotyledonary placenta, as this is the location where hemophagocytosis is often most prominent.

Although *Coxiella burnetti*'s zoonotic potential earns it the distinction of being an abortion agent of great importance, there are many other infectious causes of abortion outbreaks in ruminants which may induce similar placental lesions. Conference participants discussed other differentials for this case, including bacteria: *Chlamydophila abortus, Histophilus somni, Yersinia pseudotuberculosis, Salmonella* spp., *Trueperella pyogenes, Leptospira* spp., *Listeria monocytogenes, Campylobacter* spp., and *Brucella* spp., parasites: *Toxoplasma gondii, Neospora caninum, Sarcocystis* spp., and *Tritrichomonas foetus,* and viruses: *Border disease virus, Wesselsbron, Bluetongue, Bovine herpesvirus 1,* and several *Bunyaviruses.* Some are easily differentiated based on lesion distribution in the placenta, such as *T. gondii* and *Y. pseudotuberculosis* which both exclusively target the cotyledons.[9]

*C. burnetti* is known to infect many species and has recently been described as an emerging infectious disease in birds, in which it exhibits variable tissue tropism, with the most recent reports identifying myocarditis and hepatitis in a parrot.[10] Ectoparasites such as ticks are often cited as important vectors of transmission; however, intranasal inoculation was determined to be most effective in causing disease in pregnant goats.[8] Trophoblasts in the allantochorion of the placenta are the primary target of infection and replication of the bacteria; and their main excretion route from these infected goats is during delivery of the aborted fetus, as bacterial DNA was not detected in feces or vaginal mucus in a recent study.[8]

*C. burnetti* is considered highly infectious, though its inoculation does not necessarily translate into reproductive disease. A recent publication identified the organism in 75% of abortion submissions based on PCR, but when combined with histopathology and additional ancillary testing, *C. burnetti* was only determined to be the actual cause in 21% of those cases. The more commonly identified cause of abortions in this study was *T. gondii,* with *Campylobacter* spp. and *Chlamydophila* spp. also being more prevalent than the agent of Q fever.[4]

**Contributing Institution:** Division of Animal Medicine, Animal Technology Institute Taiwan

**References:**

1. Bacha WJ, Bacha LM. *Color Atlas of Veterinary Histology*. 2nd ed. Baltimore, MD: Lippincott Williams & Wilkins; 2000:222.
2. Berri M, Crochet D, Santiago S, Rodolakis A. Spread of *Coxiella burnetii* infection in a flock of sheep after an episode of Q fever. *Vet Rec.* 2005:157, 737-740.
3. Glazunova O, Roux V, Freylikman O, Sekeyova Z, Fournous G, Tyczka J, et al. *Coxiella burnetii* genotyping. *Emerg Infect Dis.* 2005;11, 1211-1217.
4. Hazlett MJ, McDowall R, DeLay J, et al. A prospective study of sheep and goat abortion using real-time polymerase chain reaction and cut point estimation shows Coxiella burnetii and Chlamydophila abortus infection concurrently with other major pathogens. *J Vet Diagn Invest.* 2013;25(3):359-368.
5. Lai CH, Huang CK, Chin C, Chung HC, Huang WS, Lin CW. Acute Q fever: An emergin and endemic disease in Southern Taiwan. *Scand J Infect Dis*. 2008;40:105-110.

6. Raoult D, Drancourt M, Vestris G. Bactericidal effect of doxycycline associated with lysosomtropic agents on Coxiella burnetii in P388D1 cells. *Antimicrob Agents Chemother*. 1990;34:1512-1514.
7. Raoult D, Marrie T, Mege J. Natural history and pathophysiology of Q fever. *Lancet Infect Dis* 2005;5:219-226.
8. Roest HJ, Gelderen BV, Dinkla A, et. al. Q fever in pregnant goats: pathogenesis and excretion of coxiella burnetii. PLoS One 2012;7(11):1-14.
9. Schlafer DH, Miller RB. Female genital system. In: Maxie MG, ed. *Jubb, Kennedy, and Palmer's Pathology of Domestic Animals*. Vol. 3. 5th ed. Philadelphia, PA: Elsevier Saunders; 2007:484-530.
10. Vapniarsky N, Barr BC, Murphy B. Systemic Coxiella-like infection with myocarditis and hepatitis in an eclectus parrot (Eclectus roratus). *Vet Pathol.* 2012;49(4):717-722.
11. Woldehiwet Z. Q fever (coxiellosis): epidemiology and pathogenesis. *Res Vet Sci.* 2004;77:93–100.

---

**CASE III**: Case 2 (JPC 4049887)

**Signalment:** 12-year-old intact male rhesus macaque, *Macaca mulatta.*

**History:** The animal was part of a closed laboratory setting with twenty-five sexually mature rhesus monkeys of different ages and sexes. They were housed in large group cages together in one room with a common air ventilation system. Some of the animals became suspicious with coughing and weight loss. A routine health check was done including a tuberculosis screen. The palpebral skin test of this monkey became positive, indicated by obvious swelling, drooping and erythema of the eyelid within 24 to 48 hours after application. Furthermore, blood testing using the PRIMAGAM®-test, revealed evidence for mycobacterial infection, and chest radiographs showed multiple small-sized shadows throughout the lung. Finally, the presence of mycobacteria within gastric lavage fluid could be demonstrated by microbiological culture and PCR. The animal was humanely euthanized because of animal welfare reasons.

**Gross Pathology:** At necropsy, the animal showed a poor body condition and main pathological findings were located within the respiratory tract. Multiple small firm nodules varying in size from pinpoint to several millimeters in diameter were visible within the lung, affecting mainly the right *lobus cranialis* and *caudalis*. These granulomatous nodules were yellow-white with some of them coalescing to a large necrotic area of 2,5 x 3,5 cm within the right cranial lobe. The tracheobronchial and hilar lymph nodes were moderately enlarged with caseous necrotic centres on cut surface. More than 40 granulomatous nodules of different size were found in the liver and further 15 granulomas were present in the spleen. One single small lesion was detectable within the testis.

**Laboratory Results:** *Mycobacterium tuberculosis* was isolated from aseptically obtained fresh pulmonary and liver tissue by culture and confirmed by PCR. Ziehl-Neelsen stain: negative.

**Histopathologic Description:** Throughout the lung parenchyma, there are multifocal to coalescing caseous granulomas, characterized by a central necrotic area of amorphous

eosinophilic debris surrounded by a small rim of epithelioid macrophages and few multinucleated giant cells with peripherally arranged nuclei (Langhans type). Mineralization of the necrotic centers is not observed. Granulomas are circumscribed by small amounts of fibrous connective tissue, accompanied by various numbers of lymphocytes and plasma cells. In the periphery of larger granulomas, small non-necrotizing granulomas merely composed of epithelioid macrophages and Langhans giant cells with a small outer rim of lymphocytes are present. Some of the larger granulomas break into major airways resulting in cavity formation together with ulceration of the bronchial epithelium and marked infiltration of neutrophilic granulocytes. Expanded bronchial airways contain necrotic debris admixed with several inflammatory cells. Pulmonary lesions were accompanied by varying degrees of alveolar edema and hemorrhage. The lymph node is characterized by moderate to severe follicular hyperplasia with focal solid granuloma formation, composed of epithelioid macrophages, Langhans giant cells and neutrophilic granulocytes.

**Contributor's Morphologic Diagnosis:** Lung: granulomatous pneumonia, chronic, severe, multifocal to coalescing, with cavity formation and necrosuppurative bronchitis, induced by *Mycobacterium (M.) tuberculosis,* rhesus macaque (*Macaca mulatta*), nonhuman primate. Pulmonary lymph node (not included in all slides): granulomatous lymphadenitis, subacute, moderate, focal, rhesus macaque (*Macaca mulatta*), nonhuman primate.

**Contributor's Comment:** Tuberculosis in Old World monkeys commonly results in a debilitating pulmonary disease. The most common sign is coughing and weight loss, which should be regarded as an indicator for the disease.[4] The clinical disease state is directly associated with the amount of gross alterations.

The primary lesion of simian tuberculosis is the typical tubercle. Lesions can vary from non-detectable lesions to widely disseminated characteristic granulomas. The granulomas are firm yellow-white or greyish nodules of different size. Palpable firm nodules may affect all major organs, but the lung is the most commonly affected organ system. Gross lesions also include large cavernous and coalescing lesions within the lung and tubercles may extend into the thoracic pleura or trachea. Alterations can be accompanied by enlarged tracheobronchial lymph nodes with focal or multifocal granulomas and loss of nodal architecture to various degrees. Advanced stages of the disease are characterized by secondary spread to spleen, kidney, liver and different lymph nodes.[4] Dissemination to spleen, liver, and other organs varies among monkeys and does not necessarily correlate with the severity of lung involvement.

Microscopic findings are dependent on duration and extension of the disease. The histopathological hallmark is the granuloma. In experimental studies, a wide spectrum of different granuloma types can be seen depending on the stage of disease.[6] Early stages of the disease are characterized by small granulomas consisting of circumscribed accumulations of epithelioid cells and few Langhans-type giant cells confined to the lung or the intestinal tract. Advanced stages of the disease are characterized by the classic tubercle formation. Tubercles are typical caseous granulomas of varying size containing a caseous center consisting of acellular necrotic debris or proteinaceous material. The central cores are surrounded by a mantle zone of epithelioid cells and a band of plasmacytic and lymphocytic cells interspersed with only a few Langhans-type giant cells. In contrast to other animal species, a fibrous capsule is usually not

found in nonhuman primates. Non-necrotizing granulomas are merely composed of epithelioid macrophages and Langhans-giant cells surrounded by lymphocytes. These solid granulomas exclusively occur in active TB. Fibrocalcific granulomas are composed of various combinations of fibrous connective tissue and mineral deposition. These lesions are generally observed in monkeys with latent infection. However, calcification is usually rare or lacking. Experimental studies show that only long-term non-progressive lesions tend to calcify.[3] The number of acid-fast bacilli within granulomatous lesions can vary considerably. Hence, it can be difficult to demonstrate the bacteria within histologic slides, like in the present cases. Therefore, the microscopic examination alone is not sufficient for the diagnosis of simian tuberculosis. A combination of different test methods based on serology, x-ray, histology and microbiology is advisable to accurately diagnose simian TB.[2,5]

**JPC Diagnosis:** Lung: Pyogranulomas, multifocal to coalescing, numerous.

**Conference Comment:** This is a classic case of the primate tuberculosis, in which the textbook pyogranulomas seem to entirely efface nearly every bronchiole. Not every slide includes the described lymph node, but of those which do, some have only lymphoid hyperplasia while others have a more prominent granulomatous infiltrate.

Along with the contributor, we also performed acid-fast stains on these sections and did not identify a single organism. This is often typical of tuberculoid granulomas, which are $T_H1$-driven lymphocytic responses to infection of *Mycobacterium* spp. The macrophages in these lesions are actually utilized by the bacteria to facilitate its spread, as their cellular uptake is promoted by the recognition of multiple membrane pathogen receptors including complement, mannose, surfactant protein, and CD14. Within the macrophage, they disrupt phagosome-lysosome fusion and are able to grow, replicate, and subsequently disseminate.[8]

Following this period of bacterial proliferation, typically about 3 weeks after infection in humans, $T_H1$ lymphocytes are produced following stimulation of TLR2 by mycobacterial ligands which ramp up production of IL-12. $T_H1$ cells produce IFN-γ in abundance, which are the critical mediators enabling macrophages to contain the infection. Additionally, IFN-γ orchestrates the formation of granulomas by inducing differentiation of macrophages into their epithelioid versions which aggregate and often fuse to form giant cells. The immune response, while effective as evidenced by the lack of bacteria present in the current case, comes at the cost of tissue destruction.[7]

Interestingly, a von Kossa stain demonstrated no mineral within the granulomas in this case. Central mineralization occurs commonly in stage III of granuloma formation (which occurs several weeks to a month following infection) and is characterized by a mineralized necrotic center with more organized zones of lymphocytes, fibroblasts and a fibrous connective tissue capsule.[1] Mineralization is not usually present in active infections. The lesions in this case also lack prominent fibrous capsules and the abundant neutrophils present with lack of mineralization suggest an earlier form of disease such as stage I or II. As the contributor mentioned, this presentation may be more common in primates, as mineralization is less often described in contrast to its common occurrence in cattle.[1]

**Contributing Institution:** German Primate Center
http://dpz.eu

**References:**
1. Ackermann MR. Inflammation and healing. In: Zachary JF, McGavin MD, eds. *Pathologic Basis of Veterinary Disease*. 5th ed. St. Louis, MO: Elsevier Mosby; 2012:122-124.
2. Bushmitz M, Lecu A, Verreck F, Preussing E, Rensing S, Mätz-Rensing K. Guidelines for the prevention and control of tuberculosis in non-human primates: recommendations of the European Primate Veterinary Association Working Group on Tuberculosis. *J Med Primato*l. 2009;38(1):59-69.
3. Capuano SV 3rd, Croix DA, Pawar S, et al. Experimental *Mycobacterium tuberculosis* infection of cynomolgus macaques closely resembles the various manifestations of human *M. tuberculosis* infection. *Infect Immun*. 2003;71(10):5831–5844.
4. Garcia MA, Bouley DM, Larson MJ, et al. Outbreak of *Mycobacterium bovis* in a conditioned colony of rhesus (*Macaca mulatta*) and cynomolgus (*Macaca fascicularis*) macaques. *Comp Med.* 2004a; 54(5):578-584.
5. Garcia MA, Yee J, Bouley DM, Moorhead R, Lerche NW. Diagnosis of tuberculosis in macaques using whole-blood in vitro interferon-gamma (PRIMAGAM) testing. *Comp Med*. 2004b;54(1):86-92.
6. Lin PL, Rodgers M, Smith L, et al. Quantitative comparison of active and latent tuberculosis in the cynomolgus macaque model. *Infect Immun.* 2009;77(10):4631-42.
7. McAdam AJ, Milner DA, Sharpe AH. Infectious diseases. In: Kumar V, Abbas AK, Aster JC, eds. *Robbins and Cotran Pathologic Basis of Disease*. 9th ed. Philadelphia, PA: Elsevier Saunders; 2015:371-378.
8. Zachary JF. Mechanisms of microbial infections. In: Zachary JF, McGavin MD, eds. *Pathologic Basis of Veterinary Disease*. 5th ed. St. Louis, MO: Elsevier Mosby; 2012:181-182.

---

**CASE IV:** 09A029 (JPC 3134289)

**Signalment:** 1.6 yr male Indian rhesus monkey, *Macaca mulatta.*

**History:** This animal was moved indoors from an outdoor corral one week prior to developing a head tilt, tremors, and anorexia overnight. It failed to respond to therapy.

**Gross Pathologic Findings:** Meninges were congested and cloudy. A 1 cm area of hemorrhage and malacia was observed in the right frontal lobe of the brain. Smaller petechial hemorrhages were noted bilaterally throughout the parenchyma.

**Laboratory Results:** CBC: 5.67 Rbc, 12.6 Hgb, 38.3 Hct, 20.1 WBC, 84.2 Seg, 0.5 Eo, 0.2 Eo, 0.2 Bso, 2.8 Mno, 12.3 Lym, 403000 Plt, 0 Rtc

Chem: 145 Na, 104 Cl, 6.8 Pro, 4 Alb, 2.8 Glob, 1.4 A/G, 9.9 Ca, 26 BUN, 83 Glu, 0.56 Crt, 4.1 Ph

Brain Culture: Alpha-hemolytic *streptococcus*

**Histopathologic Description:** The macroscopic cerebral hemorrhage represents a large zone of malacia filled with fibrin, hemorrhage, necrotic cellular debris and infiltrated with foamy histiocytes, lymphocytes, plasma cells and neutrophils. Some vessels contain fibrin thrombi and their walls are disrupted by eosinophilic fibrinoid material and degenerating neutrophils. Many vessels in the meninges and parenchyma are lined by plump endothelial cells and are cuffed by mixed leukocytes. Neutrophils predominate in and around vessels with necrotic walls. Adjacent neuropil is vacuolated and contains swollen degenerated neuron cell bodies and axonal degeneration (spheroid material).

**Contributor's Morphologic Diagnosis:** Subacute, severe necrohemorrhagic encephalomalacia with meningitis and vasculitis, alpha-hemolytic streptococcus.

**Contributor's Comment:** The most common human CNS infections are bacterial, although the incidence in the US (6 per 100,000) is considerably lower than in developing countries (300-400 per 100,000).[3] Vaccination has reduced the importance of *Haemophilus influenzae type b* but *Neisseria meningitides* and *Streptococcus pneumoniae* are still leading causes.[4] In our colony, the incident rate is more comparable to an unvaccinated population (82 per 100,000) with *S. pneumoniae,* the most common pathogen, while *Neisseria* and *Haemohilus* are not detected. *Alpha streptococcus* is a less frequent but equally devastating pathogen in young rhesus monkeys. *Alpha streptococcus*, sometimes called viridans streptococcus, can be differentiated from *S. pneumoniae* by resistance to the optochin disk, lack of bile solubility, and failure to grow on 6.5% NaCL. Although the viridans group is not known for factors that facilitate tissue invasion, the ability to bind to laminin may confer pathogenic ability to a select few in the normal flora of mucosal surfaces.[7] Predisposing conditions such as diabetes, cirrhosis, cancer and chronic sinusitis were not detected in this animal.

**JPC Diagnosis:** Brain, cerebrum: Encephalitis, necrotizing and hemorrhagic, multifocal, acute, severe.

**Conference Comment:** Conference participants enjoyed describing and discussing this case, although they could not arrive at a consensus on a pathogenesis of the vascular lesions. Most attributed a majority of the pathology to a primary infarct, as a pale central area surrounding an infarcted vessel is distinctly void of any neutrophils. Immediately surrounding the pale area are abundant neutrophils suggesting a blockage of the arterial supply prevented leukocyte migration to the necrotic center. The additional vascular lesions, observed occasionally as fibrinoid change within vessels or necrotizing vasculitis, may be due to toxin secretion from the cultured gram-positive bacteria or a more chronic hypersensitivity reaction. Regardless, necrotizing vasculitis and fibrin thrombi with subsequent ischemic necrosis does routinely occur in primates with streptococcal meningitis.[2]

*Streptococcus* spp. are gram-positive cocci that grow in pairs or long chains. There are over 50 recognized species, and all are divided into one of three groups based on their hemolytic properties.[7] The α-hemolytic group is comprised of *Streptococcus pneumonia*e, a common cause of pneumonia in adult people and meningitis in children, and some members of the viridians group.[4] The viridians group is largely composed of commensal bacteria, especially of the oral cavity. Some members of this group are nonhemolytic, thus not classified with the rest of the α-hemolytic group; however, characteristic to all viridians streptococci is their lack of Lancefield antigens. The β-hemolytic group all express Lancefield antigens and are typed accordingly.[7]

*Streptococcus pneumoniae* has been one of the most extensively studied of all the microorganisms, lending credit to its persistence in the crowded field of important pathogens. The identification of DNA was inferred from work performed on this bacterium, during which a "transforming principle" was described by the discovery that nonencapsulated strains could be converted into capsulated strains in 1928.[1] Other important discoveries derived from this pathogen include the efficacy of penicillin, the demonstration of antibody formation to polysaccharides, and the identification of regulatory T-lymphocytes.[1]

More recently, the two-component system (TCS) has been characterized as a key mechanism through which bacteria perceive and respond to their environment. The TCS model is composed of two proteins: a membrane-associated sensor histidine kinase (HK) and a cytoplasmic cognate response regulator (RR). The HK receives external stimuli and phosphorylates the RR which regulates gene expression or protein function. The importance of the TCS is not only in bacterial pathogenicity, but also in osmoregulation, chemotaxis, sporulation, and photosynthesis. These systems are absent from vertebrates, and thus have received attention as potential targets for antimicrobials.[5] Many specific TSCs have been identified in *Streptococcus* spp., and whether they lead to the generation of a new class of antimicrobials remains to be seen.

**Contributing Institution:** Department of Comparative Pathology
Tulane National Primate
www.tpc.tulane.edu

**References:**

1. AlonsoDeVelasco E, Verheul AM, Verhoef J, Snippe H. Streptococcus pneumonia: virulence factors, pathogenesis, and vaccines. *Microbiol Rev.* 1995:591-603.
2. Fahey MA, Westmoreland SV. Nervous system disorders of nonhuman primates and research models. In: Abee CR, Mansfield K, Tardiff S, Morris T, eds. *Nonhuman Primates in Biomedical Research Vol 2: Diseases*. 2nd ed. San Diego, CA: Academic Press; 2012:742-743.
3. Gray LD, Fedorko DP. Laboratory diagnosis of bacterial meningitis. *Clin Microbiol Rev*. 1992;5(2):130-145.
4. McAdam AJ, Milner DA, Sharpe AH. Infectious diseases. In: Kumar V, Abbas AK, Aster JC, eds. *Robbins and Cotran Pathologic Basis of Disease*. 9th ed. Philadelphia, PA: Elsevier Saunders; 2015:364.
5. Paterson GK, Blue CE, Mitchell TJ. Role of two-component systems in virulence of Streptococcus pneumoniae. *J Med Microbiol.* 2006;55:355-363.
6. Theodoridou MN, Vasilopoulou VA, Atsali EE, et al. Meningitis registry of hospitalized cases in children: epidemiological patterns of acute bacterial meningitis throughout a 32-year period. *BMC Infect Dis*. 2007;7(101):1-12.
7. Songer JG, Post KW. *Veterinary Microbiology Bacterial and Fungal Agents of Animal Disease*. St. Louis, MO: Elsevier Saunders; 2005:43-53.
8. Switalski LM, Murchison H, Timpl R, Curtiss III R, Hook M. Binding of laminin to oral and endocardial strains of viridans streptococci. *J Bacteriol*. 1987;169(3):1095-1101.

**Joint Pathology Center**
**Veterinary Pathology Services**
**Wednesday Slide Conference**
**2014-2015**
**Conference 15**
**January 21, 2015**

**Guest Moderator:**
Cory Brayton, DVM, DACVP
Johns Hopkins University

---

**CASE I:** L13-2372-2 (JPC 4032973).

**Signalment:** 4-month-old male BALB/c mouse, *Mus muculus*

**History:** This mouse received a single bolus of 400 µL PBS containing an unknown concentration of cultured murine trophoblastic cells via tail vein injection. The mouse died immediately and spontaneously after injection.

**Gross Pathology:** This mouse was presented dead in good body condition and fresh post mortem preservation. All organs and tissues were within normal gross limits.

**Histopathologic Description:** Multiple sections of lungs are examined, revealing diffusely scattered prominence of pulmonary alveolar capillaries, pulmonary arterioles, and small-caliber pulmonary arteries due to presence of moderate numbers of individually scattered and entrapped, intraluminal, 10-25 µm diameter, polygonal- to amorphously-shaped, deeply amphophilic, coarsely granular cells. The nuclei of these cells (when observable) are large and round- to ovoid-shaped with prominent single nucleoli. Additionally, pulmonary alveolar capillaries, pulmonary arterioles, and small-caliber pulmonary arteries are prominent due to presence of discrete to extensive, amorphous and/or meshwork-like rafts of finely granular, eosinophilic, weakly-PTAH-positive material (interpreted as peracute fibrin thrombi), which may or may not be intimately associated with the aforementioned cells.

**Contributor's Morphologic Diagnosis:** Lung, trophoblastic pulmonary embolism, disseminated, peracute, moderate with intravascular fibrin thrombi.

**Contributor's Comment:** An embolus refers to a detached, intravascular mass (solid, liquid, or gaseous) that is carried by and travels within the blood circulation. Embolism occurs when an embolus lodges within the circulation distant from the point of origin of the embolus. Embolism may result in partial or complete blockage of the circulation, and may potentially result in ischemic necrosis (infarction) of distal tissue. Thromboembolism refers to embolism that involves emboli derived from fragments of a thrombus.[6]

Nonthrombotic pulmonary embolism is defined as embolization of the pulmonary circulation by different cell types (adipocytes, hemopoietic, amniotic, trophoblastic, or tumor), bacteria, fungi, foreign material, or gas.[4] The pathogenesis of nonthrombotic pulmonary embolism is more complex and diverse than that associated with pure mechanical obstruction of pulmonary

embolism caused by vascular thrombi, and as such, often results in unusual or peculiar clinical signs.[4] However, many cases of nonthrombotic pulmonary embolism (regardless of cause) are associated with the development of severe peracute/acute inflammatory reactions in the pulmonary circulation, such as acute respiratory distress syndrome.[4]

Trophoblastic pulmonary embolism refers to embolization of the pulmonary circulation by trophoblastic cells derived from placental tissue.[4] Trophoblastic pulmonary embolism has been documented as a spontaneous condition in mammals with hemochorial placentation (where there is direct contact between fetal trophoblastic cells with the maternal circulation), primarily in humans and chinchillas.[3,4] In these species during pregnancy, syncytiotrophoblasts regularly desquamate from the placenta and into the maternal circulation.[3,4] The intravascular trophoblastic cells usually lodge in capillaries of the alveolar septae of the lung. Histologically, they appear as large (>50-100 μm diameter), round to deformable cells with abundant cytoplasm containing multiple, large (>25-50 μm diameter) nuclei.[3,4] The syncytiotrophoblasts are ultimately removed without consequence.[3,4] Trophoblastic pulmonary embolism is only associated with clinical disease is rare cases, and when it does occur, severe respiratory distress is the most common presentation. Positive antemortem clinical diagnosis is difficult. Most cases of trophoblastic pulmonary embolism diagnosed on microscopic examination of lung is usually incidental.[2,3]

In this case, this mouse was part of an experiment studying the interactions of trophoblasts with the circulation. The trophoblasts are smaller than those noted in spontaneous cases in humans or chinchillas. Their morphology is more similar to cytotrophoblasts rather than syncytiotrophoblasts, and might be explained by the cultured history of the cells. Regardless of morphology, the death of the animal immediately post-injection is most suggestive that rapid trophoblastic pulmonary embolism is the cause of death in this animal.

**JPC Diagnosis:** Lung, pulmonary arterioles and septal capillaries: Trophoblastic emboli, with multifocal fibrin thrombi.

**Conference Comment:** Conference participants discussed this interesting entity at length, including its correlation to the cause of death in this case. The contributor nicely highlights the different types of emboli and their manifestations in relation to systemic disease, to which trophoblastic emboli are typically described as incidental findings. They have been documented to cause fatalities in people, however.[1] The limited details provided regarding the circumstances of this case left participants to only speculate as to the cause of death in this mouse. The differentials of consideration were anaphylaxis, cerebral embolism, and volume overload. Additional details regarding the timing of death in relation to injection, whether other animals in the study were also affected, and whether similar lesions were observed in other tissues, would help in further elucidating the mystery. Most participants felt the pulmonary lesions were minimal and likely not significant enough to cause the animal's death.

While this condition is most often observed in humans and chinchillas, recently it has been described as a common finding in a colony of cotton rats used to study a variety of infectious agents, indicating the possibility of an alternative model of aberrant trophoblastic deportation in women.[4]

In a developing blastocyst, trophoblasts are the peripheral cells first located at a single pole. They eventually give rise to the embryonic portion of the placenta, by proliferating rapidly into

two distinct cell populations. The inner population is a monolayer of individual cells which are mitotically active and are known as cytotrophoblasts, while the thicker outer layer is composed of continuous multinucleated cells with no cytoplasmic demarcation and are called syncytiotrophoblasts. Cytotrophoblasts continue to proliferate, with the new cells joining the ranks of syncytiotrophoblasts. As syncytiotrophoblasts increase in number, they form vacuoles that coalesce into large spaces known as lacunae. The continued growth of the syncytium erodes the adjacent endometrium and eventually the maternal blood vessels, allowing maternal blood to fill the newly formed lacunae and nourish the developing embryo.[2] With such close association, it follows that syncytiotrophoblasts could be readily introduced into the maternal blood supply causing their embolization as observed in this case.

**Contributing institution:** Veterinary Service Center, Department of Comparative Medicine, Stanford School of Medicine (http://med.stanford.edu/compmed/)

**References:**


1. Delmis J, Pfeifer D, Ivanisevic M, Forko JI, Hlupic L. Sudden death from trophoblastic embolism in pregnancy. *Eur J Obstet Gynecol Reprod Biol*. 2000;92(2):225-227.
2. Gartner LP, Hiatt JL. *Color Textbook of Histology*. 2nd ed. Philadelphia, PA: W.B. Saunders Company; 2001:480-482.
3. Ilha MR, Bezerra Jr PS, Sanches AW, et al. Trophoblastic pulmonary embolism in chinchillas (*Chinchilla laniger*). *Ciencia Rural, Santa Maria*. 2000;30:903-904.
4. Jorens PG, Van Marck E, Snoeckx, et al. Nonthrombotic pulmonary embolism. *European Respiratory Journal*. 2009;34:452-474.
5. La Perle KM, Green MG, Niewiesk S. Trophoblast deportation to the lungs of cotton rats (*Sigmodon hispidus). Comp Med*. 2014;64(6):448-455.
6. Mitchell RN. Hemodynamic disorders, thromboembolic disease, and shock. In: Kumar V, Abbas AK, Fausto N. *Robbins and Coltran Pathologic Basis of Disease*. 7th ed. Philadelphia, PA: Elsevier Saunders; 2005:135-137.


---

**CASE II**: 13082899 (JPC 4056244).

**Signalment:** 20-25 week old NOD-SCID (NOD.CB17-Prkdcscid/J) Mice

**History:** Mice harboring orthotopic xenograft of cancer cell line for oncology research.

**Gross Pathology:** No gross abnormalities noted at necropsy.

**Histopathologic Description:** Irregular packets of pleomorphic cells with round to angular, hyperchromatic nuclei diffusely infiltrated the brain parenchyma. Most cells had very little cytoplasm. Few neoplastic cells were large, with abundant eosinophilic cytoplasm and multiple abnormal nuclei. There were several mitotic figures, apoptotic bodies, and degenerate neurons within each high power field (Figure 1). Neoplastic cells infiltrated the cerebral parenchyma without causing significant distortion of normal anatomic structures, hydrocephalus, or extensive necrosis. Capillaries were readily apparent among the neoplastic cells. There was typically bilateral involvement of the cerebral hemispheres and rare extension into the distal brainstem and cerebellum.

**Contributor's Morphologic Diagnosis:** Brain, gliomatosis cerebri

**Contributor's Comment:** The engrafted cell line was derived from resection of a human anaplastic oligoastrocytoma (oligoastrocytoma WHO Grade III).[6] The cell line, designated BT142, expresses a mutant form of isocitrate dehydrogenase. Isocitrate dehydrogenase 1 (IDH1) catalyzes the oxidative decarboxylation of isocitrate into α-ketoglutarate within the Krebs cycle. *In vivo,* missense mutations in IDH1 have been identified in a large percentage of gliomas and are thought to play an important role in the biology of these tumors. A loss of IDH1 function leads to inducible levels of hypoxia inducible factor-1 alpha (HIF-1α), an important gene in tumorigenesis. A gain of IDH1 function may also occur, leading to excessive production of 2-hydroxyglutarate.[10] The most common mutation, which is also carried in the BT142 cell line, is R132H, located within the isocitrate binding site.[1,4]

The cell line was orthotopically injected into the right cerebral cortex of the mice with a 30-gauge needle (per protocol approved by the Institutional Animal Care and Use Committee). In the contributor's experience, implantation of other cell lines into the brain by this technique result in a space occupying mass of cells within the cerebrum or adjacent meninges. Cell proliferation typically causes compression of adjacent brain structures and hydrocephalus, which results in clinical signs that can be monitored as a surrogate marker of xenograft growth and progression. The diffuse infiltrative pattern observed in this study, by contrast, failed to produce outward signs of neurologic involvement in the expected timeframe and there was concern that the orthotopic xenograft had failed.

While the pattern of infiltration was unique, the cellular morphology of the implanted BT142 cells were consistent with that described in similar experiments.[6] The diffuse, non-disruptive pattern of infiltration is characteristic of gliomatosis cerebri[3,9] in humans and dogs. This rare disorder is characterized by diffuse and widespread infiltration of the CNS by neoplastic glial cells with relative preservation of the glial architecture. Approximately 42% of cases of gliomatosis cerebri have been found to carry the IDH1 mutation.[2,5,8,10] In humans, IDH1 mutations can be associated with prolonged survival and better outcomes than tumors not positive for the IDH1 mutations.[5]

Gliomatosis cerebri is usually considered to be a malignant lesion corresponding to WHO grade III. These neoplasms are typically of astrocytic and oligodendroglial origin and in some cases positive IHC staining with GFAP is observed. Common symptoms in human cases include corticospinal tract deficits, dementia, headaches, mental and behavioral changes, and seizures. Signs and symptoms begin abruptly or progress slowly for weeks or months, with a long latency period before the development of clinical signs. There is no evidence of sex predisposition and all ages are affected with the peak incidence between 40 and 50 years of age.[9] Similarly, dogs generally present with a variety of clinical signs, including cranial nerve deficits, depression, circling, and reaction deficits.[9]

Human cases are pleomorphic, with cells ranging from well-differentiated protoplastic and fibrillary astrocytes to elongated, more poorly differentiated glial cells. Pleomorphism and anisocytosis are more marked in densely infiltrated areas of the brain, typically the cerebrum and brain stem.[9] White matter is more affected than gray matter and the cerebellum is generally less affected. The morphology of the neoplastic cells in dogs shows ovoid to slender nuclei with indistinct cytoplasm. While the cerebrum is often affected in dogs, the cerebellum is also often

affected, in contrast to human cases.[7] Both humans and dogs show neuronal satellitosis, subpial and subependymal accumlations, perivascular cuffing, and parallel arrangement of neoplastic cells within white matter tracts.[9]

**JPC Diagnosis:** Brain, cerebrum: Malignant glioma, anaplastic, consistent with xenograft of BT142 anaplastic oligoastrocytoma.

**Conference Comment:** Our diagnosis was determined following consultation with JPC human physician neuropathologists and evaluation of the immunohistochemical profile. If we were to be consistent with that used in the GORENI (referenced below) classification standard for this case, diffuse malignant astrocytoma would be the most appropriate classification. The morphologic appearance is consistent with the diagnosis provided by the contributor. Also, given the experimental history in this case, another suggested by our consultants (mixed malignant glioma, high grade) may also be appropriate.

Glioblastoma cerebri is a rarely reported neoplasm classified as a neuroepithelial tumor of unknown origin,[3] and the contributor mentions other sources describing it as astrocytic and oligodendroglial origin. Our GFAP stain revealed only reactive astrocytes; neoplastic cells were negative. There is currently not a consistently reliable immunohistochemical marker available for differentiating between astrocytes and oligodendroglial cells, which led some participants to view the diagnosis of the engrafted cell line, anaplastic oligoastrocytoma, with some suspicion though it is recognized in the WHO classification system. The submitted slides from this case represent two different mice, however both from the same study. There is some variation in appearance between a diffusely infiltrative pattern with preservation of normal architecture to some areas with more of a mass effect replacing the neuropil which led to further deliberation on arriving on a name for this tumor. Regardless of nomenclature, the anaplastic features of this neoplasm and extensive involvement through multiple cross sections of the brain indicate a high grade malignant process and many were amazed as to the apparent lack of clinical signs in this animal.

http://www.goreni.org/

**Contributing institution:** Eli Lilly and Company, Department of Pathology and Toxicology, Indianapolis, IN 46285. www.lilly.com

**References:**

1. Alexander BM, Mehta MP: Role of isocitrate dehydrogenase in glioma. *Expert Review of Neurotherapeutics* 2011:11(10)**:**1399-1409.
2. Desestret V, Ciccarino P, Ducray F, Criniere E, Boisselier B, Labussiere M, et al.: Prognostic stratification of gliomatosis cerebri by IDH1 R132H and INA expression. *J Neurooncol* 2011:105(2)**:**219-224.
3. Gruber A, Leschnik M, Kneissl S, Schmidt P: Gliomatosis cerebri in a dog. *J Vet Med A Physiol Pathol Clin Med* 2006:53(8)**:**435-438.
4. Gupta R, Webb-Myers R, Flanagan S, Buckland ME: Isocitrate dehydrogenase mutations in diffuse gliomas: clinical and aetiological implications. *J Clin Pathol* 2011:64(10)**:**835-844.

5. Kwon MJ, Kim ST, Kong DS, Lee D, Park S, Kang SY, et al.: Mutated IDH1 is a favorable prognostic factor for type 2 gliomatosis cerebri. *Brain Pathol* 2012:22(3)**:**307-317.
6. Luchman HA, Stechishin OD, Dang NH, Blough MD, Chesnelong C, Kelly JJ, et al.: An in vivo patient-derived model of endogenous IDH1-mutant glioma. *Neuro-Oncology* 2012:14(2)**:**184-191.
7. Martin-Vaquero P, da Costa RC, Wolk KE, Premanandan C, Oglesbee MJ: MRI features of gliomatosis cerebri in a dog. *Vet Radiol Ultrasound* 2012:53(2)**:**189-192.
8. Narasimhaiah D, Miquel C, Verhamme E, Desclee P, Cosnard G, Godfraind C: IDH1 mutation, a genetic alteration associated with adult gliomatosis cerebri. *Neuropathology* 2012:32(1)**:**30-37.
9. Porter B, de Lahunta A, Summers B: Gliomatosis cerebri in six dogs. *Vet Pathol* 2003:40(1)**:**97-102.
10. Seiz M, Tuettenberg J, Meyer J, Essig M, Schmieder K, Mawrin C, et al.: Detection of IDH1 mutations in gliomatosis cerebri, but only in tumors with additional solid component: evidence for molecular subtypes. *Acta Neuropathol* 2010:120(2)**:**261-267.

---

**CASE III**: 13-7233 (JPC 4049289).

**Signalment:** 22-month-old female Syrian hamster, *Mesocricetus auratus*

**History:** Control hamster from an experimental study

**Gross Pathology:** No significant gross lesions were seen.

**Laboratory Results:** None.

**Histopathologic Description:** Ovary: The normal ovarian architecture is effaced and compressed by an encapsulated and well differentiated neoplasm. The neoplasm is composed of polygonal neoplastic cells arranged in nests, sheets, and cords supported by moderate fibrovascular stroma. Neoplastic cells have variably distinct cell borders and moderate amounts of foamy to fibrillar eosinophilic cytoplasm. Nuclei are round to oval with finely stippled chromatin and 2-3 distinct nucleoli. Mitotic figures average 1-2 per HPF and neoplastic cells often undergoes individual cell necrosis. Cellular pleomorphism is characterized by mild anisokaryosis. The adjacent stroma, bursa, and adipose tissue are infiltrated by low to moderate numbers of neutrophils, macrophages, lymphocytes and low numbers of mast cells. The lumen of the oviduct and uterus have moderate numbers of neutrophils admixed with epithelial cells, cellular debris and amphophilic fibrillar material.

**Contributor's Morphologic Diagnosis:** Ovary: Granulosa cell tumor

**Contributor's Comment:** Granulosa cell tumors are the most common sex-cord stromal tumors reported in domestic animals and have been reported in horses, cows, and dogs, and laboratory animals such as non-human primates, mice, and rats.[15,10,6] They are usually unilateral and benign in mares.[14] Malignant granulosa cell tumors have been reported in cows, dogs, cats, and laboratory mice.[2,5,12,18] Clinical signs associated with granulosa cell tumor in mares include anestrus, stallion-like behavior, and nymphomania. In mares, neoplastic granulosa cells produce

inhibin a peptide hormone that may cause atrophy of the contralateral ovary.[15] Granulosa cell tumors are the most common ovarian tumors of Syrian hamsters.[8,13] Occurrence of both benign and malignant granulosa cell tumors in Syrian hamsters have been reported.[11]

In humans, granulosa cell tumors represent 2-5% of all ovarian tumors and usually have clinical features of hyperestrogenism.[16] Mutations in transcription factor FOXL2 is pathognomonic for adult-type granulosa cell tumors in humans.[17] Further, 17β-estradiol, inhibin, and mullerian inhibiting substance are considered to be reliable diagnostic and prognostic markers in humans.[8] While inhibin-α is a reliable marker in canine granulosa cell tumors[14] calretinin, GATA-4, and neuron-specific enolase are consistently expressed in non-human primate granulosa cell tumors.[3] No such markers have been reported in Syrian hamsters.

**JPC Diagnosis:** 1. Ovary: Granulosa cell tumor. 2. Oviduct: Salpingitis, suppurative, diffuse, moderate, with ductular ectasia.

**Conference Comment:** The common occurrence of granulosa cell tumors in hamsters and its histologic difference from those which occur in domestic animals makes this a noteworthy case. The common histologic patterns are follicular (microfollicular and macrofollicular), insular, trabecular, and diffuse. The distinctive microcavities containing eosinophilic material lined by a rosette arrangement of granulosa cells are known as "Call-Exner bodies" and occur most commonly in the microfollicular pattern.[7] This type of arrangement is observed in early stages of bovine neoplasms, but less common in other species.[15] These tumors have a very characteristic gross presentation, especially in the mare, composed of numerous cysts with areas of solid white or yellow content. The cystic cavities are often observed histologically lined by granulosa cells and surrounded by a variable population of thecal cells, and often identified as granulosa-theca cell tumors.[15] In our sections, the neoplasm is a densely cellular population of granulosa cells in nests and packets, with each outlined by a fine fibrous stroma. No cystic cavities or Call-Exner bodies are present in this particular case, which may be indicative of its species-specific differences.

The interesting aspect of sex cord-stromal tumors is their ability to produce a variety of hormones and induce corresponding clinical signs. The contributor mentioned those exhibited by mares, and recent publications have demonstrated increased levels of testosterone and inhibin can be useful in obtaining a presumptive diagnosis.[4] Additionally, anti-Müllerian hormone concentrations are elevated in mares and cows with these neoplasms.[1,4] Estrogen and progesterone may also be secreted, as cystic endometrial hyperplasia and pyometra are common in bitches with sex cord-stromal tumors.[15] In this case, we believe the oviduct and uterus are moderately distended, and there is suppurative inflammation in some sections within the oviduct. The relationship of these inflammatory changes with the ovarian neoplasm is unclear.

**Contributing institution:** http://web.mit.edu/comp-med

**References:**

1. Ball BA, Almeida J, Conley AJ. Determination of serum anti-Mullerian hormone concentrations for the diagnosis of granulose-cell tumours in mares. *Equine Vet J.* 2013;45(2):199-203.

2. Beamer WG, Hoppe PC, Whitten WK: Spontaneous Malignant Granulosa Cell Tumors in Ovaries of Young SWR Mice. *Cancer Res.* 1985:45(11 Part 2):5575-5581.
3. Durkes A, Garner M, Juan-Sallés C, Ramos-Vara J: Immunohistochemical Characterization of Nonhuman Primate Ovarian Sex Cord–Stromal Tumors. *Vet Pathol.* 2012:49(5):834-838.
4. Gee EK, Dicken M, Archer RM, Herdan CL, Pauwels FE, Drayton BM. Granulosa theca cell tumour in a pregnant mare: concentrations of inhibin and testosterone before and after surgery. *N Z Vet J*. 2012;60(2):160-163.
5. Gelberg HB, McEntee K: Feline Ovarian Neoplasms. *Vet Pathol*. 1985:22(6):572-576.
6. Gregson RL, Lewis DJ, Abbott DP: Spontaneous ovarian neoplasms of the laboratory rat. *Vet Pathol.* 1984:21(3):292-299.
7. Kennedy PC, Cullen JM, Edwards JF, et. al. *Histological Classification of Tumors of the Genital System of Domestic Animals*. 2nd series, Vol. 4. Washington, D.C.: Armed Forces Institute of Pathology; 1998:24-25.
8. Kondo H, Onuma M, Shibuya H, Sato T: Spontaneous tumors in domestic hamsters. *Vet Pathol.* 2008:45(5):674-680.
9. Kottarathil VD, Antony MA, Nair IR, Pavithran K: Recent advances in granulosa cell tumor ovary: a review. *Indian J Surg Oncol.* 2013:4(1):37-47.
10. Maclachlan NJ, Kennedy PC: Tumors of the Genital Systems, Sex-cord stromal tumors. In: Meuten DJ, ed. Tumors in Domestic Animals. 4 ed. Ames, IA: Iowa State Press; 2002: 550-551.
11. McInnes EF, Ernst H, Germann P-G: Spontaneous Neoplastic Lesions in Control Syrian Hamsters in 6-, 12-, and 24-Month Short-Term and Carcinogenicity Studies. *Toxicol Pathol.* 2012.
12. Patnaik AK, Greenlee PG: Canine Ovarian Neoplasms: A Clinicopathologic Study of 71 Cases, Including Histology of 12 Granulosa Cell Tumors. *Vet Pathol.*1987:24(6):509-514.
13. Pour P, Mohr U, Althoff J, Cardesa A, Kmoch N: Spontaneous tumors and common diseases in two colonies of Syrian hamsters. III. Urogenital system and endocrine glands. *J Natl Cancer Inst.* 1976:56(5):949-961.
14. Riccardi E, Greco V, Verganti S, Finazzi M: Immunohistochemical Diagnosis of Canine Ovarian Epithelial and Granulosa Cell Tumors. *J Vet Diagn Invest.* 2007:19(4):431-435.
15. Schlafer DH, Miller RB: Female genital system. In: Maxie MG, ed. *Jubb, Kennedy, and Palmer's Pathology of Domestic Animals*. St. Louis, MO: Saunders Elsevier; 2007: 450-451.
16. Schumer ST, Cannistra SA: Granulosa Cell Tumor of the Ovary. *J Clin Oncol.* 2003:21(6):1180-1189.
17. Shah SP, Köbel M, Senz J, Morin RD, Clarke BA, Wiegand KC, et al.: Mutation of FOXL2 in Granulosa-Cell Tumors of the Ovary. *N Engl J Med.* 2009:360(26):2719-2729.
18. Zachary JF, Haliburton JC: Malignant Granulosa Cell Tumor in an Angus Cow. *Vet. Pathol.*1983:20(4):506-509.

---

**CASE IV:** S12/1884 (JPC 4035414).

**Signalment:** A male, adult (exact age not known) European hedgehog (*Erinaceus europaeus*) from a wildlife park

**History:** The hedgehog was found in lateral position with tremors. There was a short improvement of the symptoms with medical treatment (Dexamethasone, Baytril and Levamisol). Euthanasia was performed because of vestibular ataxia four days later.

**Gross Pathology:** At necropsy, the hedgehog was in poor general body condition. There was severe lung edema and all lung lobes were mottled in dark and light red. There was no macroscopic lesion in the tympanic bullae or the brain.

**Laboratory Results:** PCR Result: *Cryptococcus neoformans var. gattii*

**Histopathologic Description:** Brain: Diffusely, the meninges, plexus choroideus, cerebrospinal fluid in the lateral ventricles, Virchow-Robbins space and surrounding brain tissue of the white and grey matter are massively thickened and infiltrated by intra- and extracellular fungal yeasts of 5-20 um in diameter, ovoid to spherical with a 1-2 um basophilic cell wall and a non-staining thick capsule observed as a clear circular halo up to 10 um in thickness. There is rare narrow-based budding. The yeasts are accompanied by a severe infiltrate of macrophages, lymphocytes, plasma cells, fewer eosinophils and neutrophils. Predominantly perivascular located and multifocal pallisading are large numbers of multinucleated giant cells of the foreign body type and Langhans cell type. They contain up to 20 nuclei and intracytoplasmic fungal yeast (phagocytosis). The meningeal and encephalic vessel walls, predominantly of the veins, are severely infiltrated by the above mentioned inflammatory cells, giant cells and yeasts and slightly homogenous and hypereosinophilic (vasculitis and fibrinoid degeneration). Multifocal in the inflammatory areas are moderate numbers of extravasated erythrocytes (hemorrhage). Within the grey and white matter, there is a severe, diffuse increase of glial cells (gliosis) predominantly astrocytes (astrocytosis) which have an elongated or glassy, rounded nuclei (activation), often surrounding neurons (satellitosis). At the white-grey matter junction, the neuropil is loosely arranged and vacuolated, mostly around the affected vessels (edema). Additionally, the epithelium of the ventricle is multifocally thickened and composed of two or three cell layers (hyperplasia).

**Contributor's Morphologic Diagnosis:**
Brain: granulomatous and lymphoplasmocytic meningoencephalitis and vasculitis, severe, diffuse, chronic with intralesional yeasts consistent with *Cryptococcus* sp.

**Contributor's Comment:** The disease cryptococcosis is caused by the genus *Cryptcoccus (C.)*, including over 37 species, the majority of which do not cause disease in mammals.[7] The disease-causing *Cryptococcus* sp. are referred to as the *C. neoformans – C. gattii species* complex, which includes *C. neoformans var. neoformans*, *C. neoformans var. grubii* and *C. gattii*.[7] The classification was originally based on serotype, determined by capsular antigens.[3,7] Nowadays, genotyping has replaced serologic typing and divided *Cryptococcus* in two different species, *C. neoformans* and *C. gattii,* and in molecular types VNI and VNII, (*C. neoformans var. grubii*, serotype A), VNIV (*C. neoformans var. neoformans*, serotype D), VNIII (hybrid serotype AD), VGI, VGII, VGIII and VGIV (*C.gatti*, serotype B and C).[3,7]

In our case, the PCR resulted as *Cryptococcus neoformans var. gattii.*

Cryptococcosis is the most common systemic mycotic disease of cats worldwide, but has been described in other domestic species (ferrets, horses, cattle, goats, sheep and llamas) and non-domestic species (parrots, elk, koalas and dolphins).[1,7] The disease is sporadic and the infection is neither contagious nor zoonotic.[1] To our knowledge, *Cryptococcus* has not been described in hedgehogs. This animal was kept in an open wildlife park environment. The immune status was unknown. Similar lesions containing yeasts were also found in the lung and kidney, the infection was considered as systemic. Clinical presentations of cryptococcosis are similar in all described animals; althought *C. gattii* appears to be more virulent and has a greater propensity to infect the CNS.[7] The route of entry is considered by inhalation of basidiospores (yeast cells).[1] CNS penetration is a consequence of the number of organisms inhaled, the virulence of the isolate and the ease of penetration of the nasal and frontal bones and the cribiform plate.[7] It is described that dogs, in comparison to cats, develop a marked inflammatory response, primarily mixed cellular or granulomatous, whereas cats develop a mild, primarily neutrophilic response.[9] In the present case of the hedgehog, there is a moderate to severe granulomatous meningoencephalitis, similar to the described lesions in dogs. Reports of cerebral cryptococcosis without respiratory involvement in domestic animals are scarce, though described in cats[6], horses[2] and in cows.[5]

Recent reports of CNS cryptococcosis include single reports in a bull from Brazil[8] and smaller series of animals as in dogs and cats from California.[9] A special variant of CNS cryptococcosis is the so called cryptococcoma, a single gelatinous pseudocyst in the CNS, often suggested as neoplasia with MRI.[9] The cyst is histologically composed of cryptococcal organisms surrounded by a pyogranulomatous inflammatory reaction and necrosis.[5,6] In people, neurocryptococcosis is linked to immunosuppression, often seen in HIV-infected patients. Whether the same is true in animals remains the subject of debate.[6]

Here, diagnosis was based on H&E histology, supported by special stains and a PCR investigation: The wall of the yeasts stained positive with Periodic acid Schiff (PAS) and Grocott and the capsule stained positive with Mayer's mucicarmine. PCR: *Cryptococcus neoformans var. gattii.*

Histological differential diagnoses based on similar morphology: *Blastomyces dermatitidis*, *Histoplasma capsulatum*, *Candida albicans*, *Sporothrix schenkii* and *Prototheca spp*.[5]

**JPC Diagnosis:** Cerebrum, meninges: Meningoencephalitis, granulomatous, multifocal to coalescing, moderate, with granulomatous ventriculitis and choroiditis, moderate hydrocephalus and numerous intrahistiocytic and extracellular yeasts.

**Conference Comment:** The contributor introduced recent literature discussing the updated nomenclature of this organism. *Cryptococcus gattii*, identified in this case, occurs in immunocompetent mammals and is thus considered a primary pathogen, while *C. neoformans* var. *neoformans* and *C. neoformans* var. *grubii* are often opportunistic pathogens linked with immunosuppression.[7] Although considered a primary pathogen, the sheer number of organisms present within the meninges and outnumbering the inflammatory cells in this case led conference participants to speculate whether the administration of steroids permitted this organism to proliferate further prior to necropsy. However, glucocorticoid therapy has successfully achieved favorable clinical responses in some cases of cryptococcosis.[9] Contrarily, it may be the yeast

capsule's ability to inhibit leukocyte recognition and chemotaxis that accounts for the lack of inflammation.[1] *Cryptococcus* spp. are readily identifiable by this large negatively-staining but carminophilic capsule, which also aids it in prevention of phagocytosis by macrophages and neutrophils. The organisms also utilize superoxide dismutase and catalase in addition to being one of the many species which produce melanin, all to provide protection from oxidative damage by host mechanisms. Utilizing dopamine as a substrate for melanin production may facilitate its affinity for the CNS.[7]

The thick polysaccharide capsule gives lesions a gross gelatinous appearance, and in the cerebrum these often characteristically develop into cystic spaces as mentioned by the contributor. This is most commonly observed in cats and occurs through a repetitive process of macrophage phagocytosis, cell lysis and subsequent chemotaxis of additional macrophages allowing an expansive accumulation of the polysaccharide capsule.[10] The pathogenesis of this infection is curious, and largely still unexplained as to why the variability in inflammatory responses and lesion development occurs. Findings such as large cryptococcomas being more commonly reported in immunocompetent patients[9], and the lack of increased susceptibility in cats with retrovirus infections[7] seem to be counterintuitive. Overall, cryptococcosis is a disease often associated with a poor prognosis, as median survival time (MST) for all cats was just 19 days in one study despite treatment with antifungal drugs.[9] But when excluding the rapidly deteriorating patients, or those which didn't survive the first three days following diagnosis, the MST is much longer with many cats surviving past the conclusion of the study.[9]

The presentation of *Cryptococcus* in a hedgehog is unique, and conference participants discussed other known diseases within this species as they are becoming increasingly popular as pets. Hedgehogs seem to have a high incidence of neoplasia, with its prevalence at necropsy being as high as 53%.[4] Another condition first described in the mid-1990's is a progressive paralysis called Wobbly hedgehog syndrome with an incidence of 10% in pet hedgehogs in North America.[4] This is characterized histologically as vacuolation of the white matter tracts without an inflammatory infiltrate,[4] similar to degenerative myelopathy which occurs commonly in German Shepherd Dogs.

**Contributing Institution:** Institute of Animal Pathology, University of Berne, Länggassstrasse 122, Postfach 8466, CH-3001 Bern, Switzerland
http://www.itpa.vetsuisse.unibe.ch/html

**References:**

1. Caswell JL, Williams KJ. The respiratory system In: Maxie, MG ed. Jubb, Kennedy and Palmer's Pathology of Domestic Animals. 5th ed. Edinburgh, Scotland: Elsevier; 2007:642-644.
2. Cho DY, Pace LW, Beadle RE. Cerebral crytococcosis in a horse. *Vet Pathol.* 1986;23:207-209.
3. Fragnello J, Dutra V, Schrank A, et al. Identification of genomic differences between *Cryptococcus neoformans and Cryptococcus gattii* by representational differences analysis (RDA). Med Mycol. 2009;47:584-591.
4. Gibson CJ, Parry NA, Jakowski RM, Eshar D. Anaplastic astrocytoma in the spinal cord of an African pygmy hedgehog (*Atelerix albiventris)*. *Vet Pathol.* 2008;45:934-938.

5. Magalhaes GM, Elsen Saut JP, Beninati T, et al. Cerebral cryptococcomas in a cow. J Comp Path. 2012;147:106-110.
6. Mandrioli L, Bettini G, Marcato, OS, et al. Central nervous system Cryptococcoma in a cat. *J Vet Med A*. 2002;49:526-530.
7. Lester SJ, Malik R, Bartlett KH, et al. Cryptococcosis: update and emergence of *Cryptococcus gattii*. *Vet Clin Pathol*. 2011;40:4-17.
8. Riet-Correa F, Krockenberger M, Dantas AFM, et al. Bovine cryptococcal meningoencephalitis. *J Vet Diagn Invest.* 2011;23:1056-1060.
9. Sykes JE, Sturges BK, Cannon MS, et al. Clinical signs, imagin features, neuropathology, and outcome in cats and dogs with central nervous system cryptococcosis from California. *J Vet Intern Med.* 2010;24:1427-1438.
10. Zachary JF. Mechanisms of microbial infections. In: Zachary JF, McGavin MD, eds. *Pathologic Basis of Veterinary Disease*. 5th ed. St. Louis, MO: Elsevier Mosby; 2012:237.

**Joint Pathology Center**
**Veterinary Pathology Services**
**Wednesday Slide Conference**
**2014-2015**
**Conference 16**
**January 28, 2015**

**Guest Moderator:**
Jeffrey C. Wolf, DVM, Diplomate ACVP
Experimental Pathology Laboratories, Inc.

---

**CASE I:** ITPA BERN 2011/1 (JPC 4002421).

**Signalment:** 2 cichlids (order *Perciformes)*, male, *Neolamprologus multifasciatus*

**History:** Two moribund cichlids with poor general body condition were submitted to the Center of Fish and Wildlife Medicine (FIWI) Berne, Switzerland.

**Gross Pathology:** The main macroscopic findings at necropsy were:
Eyes: unilateral corneal opacification (ca. 3mm in diameter) and exophthalmos
Skin: 2 ulcerations on the head (ca. 2cm and 1mm in diameter)
Gallbladder: congestion
Spleen: severely enlarged, with round margins, scattered white pinpoints through the parenchyma
Intestine: low amount of whitish pasty content

**Laboratory Results:** Parasitology: negative
Bacteriology: mixed flora with *Aeromonas sobria* in kidney, spleen, liver, skin

**Histopathologic Description: stomach, intestine, liver, spleen**

Stomach, focally extensively, the mucosa is replaced by moderate amounts of cell and nuclear debris (necrosis), large amounts of macrophages with abundant foamy cytoplasm, lymphocytes and plasma cells intermixed with multiple protozoan parasites. These parasites are pear-shaped, 4x10 µm, with one to two apical nuclei and two visible flagella on the other site (interpreted as *Cryptobia iubilans*). The same flagellates are also located in groups of up to 10 in the lamina propria, submucosa and serosa surrounded by aforementioned inflammatory cells and necrotic material. There is moderate proliferation of fibroblasts.

Multifocally to coalescing, the lamina propria, the submucosa and the serosa are severely thickened due to accumulation of large amounts of macrophages and lymphocytes, few plasma cells and eosinophil-like cells. Multifocally, mainly in the submucosa, granulomas are formed with central necrosis, marginating epithelioid macrophages, lymphocytes and fibroblasts.

In the adjacent perivisceral fat tissue and the spleen there are the same granulomas formed.

In one section of liver, multifocally in the bile ducts, there are elongated structures with a basophilic membrane, granulated cytoplasm and multiple internal oval to pear shaped structures, 2x4 µm, with one to two nuclei (myxozoan plasmodia).

**Contributor's Morphologic Diagnosis:** Stomach, ulcerative and granulomatous gastritis, focally extensive, severe with intralesional flagellates.

Mesenteric fat tissue, granulomatous steatitis, multifocal, moderate

Liver, myxozoan plasmodia in bile ducts

**Contributor's Comment:** Histological examination of the affected fish revealed various degrees of granulomatous gastritis and many granulomas involving different organs, including the kidney, spleen, liver, mesentery, mesenteric fat, swim bladder, eye, heart and gonads. The etiology of these lesions is consistent with the flagellate *Cryptobia iubilans,* which is an important parasite of cichlids that typically induces granulomatous disease, primarily involving the stomach.

The ovoid or elongated body, 19x5 µm, has an anterior flagellum 1.5 to 2 times body length extending from the flagellar pocket, which is shielded by a mobile anterolateral protrusion of the anterior end, the rostrum, appearing as a small lobe and evidently supported by the microtubules of the preoral ridge.[1] It tends to be more elongated in early infection and more oval, tear-drop shaped or round in chronic infections.[2]

In transmission electron microscopy the flagellates are present in vacuoles (parasitophorous vacuole) in host cells. They are members of the order *Kinetoplastida* based on the detection of a kinetoplast, paraxial rod (lattice-like structure along the axoneme in the flagellum), and a cytoskeleton composed of microtubules lying beneath the body surface.[2]

Granulomatous gastritis caused by *Cryptobia iubilans* has previously been reported in 15 species of Old World and New World cichlids. As differential diagnoses for granuloma formation, mycobacteriosis, fungal, rickettsial, other parasitic (amoeba, nematodes) infection or foreign bodies could be considered. In this case, Ziehl-Neelsen special stain for acid-fast bacteria was negative. Flagellates commonly found in the intestine of many cichlid species are members of the order *Diplomonadida*, family *Hexamitidae*, including *Spironucleus* spp and *Hexamita* spp. They are typically found in the lumen of the intestinal tract and do not incite a granulomatous response.[2]

Morbidity and mortality rates in an infected population of fish appear to be linked to many environmental and biological variables such as water quality, the presence of other parasites or bacteria, diet, species, and age of fish. There are no effective clinically proven treatments against *C. iubilans* infection.

In salmonids, the haemoflagellate *Cryptobia salmositica* causes a microcytic and hypochromic anaemia and the severity of the disease is directly related to the parasitemia.[3]

In salmonids susceptible to *Cryptobia salmositica,* a generalized inflammatory response with severe lesions in connective tissues and in the reticuloendothelial system, as well as

microlesions appearing in the liver, gills, and spleen at 1–2 weeks after infection, followed by endovasculitis with mononuclear cell and extravascular parasite infiltrations was described.[4]

**JPC Diagnosis:** Stomach: Gastritis, granulomatous, transmural, multifocal, severe, with numerous intracellular and extracellular flagellates.

**Conference Comment:** The multiple granulomas in the stomach are extensive and coalesce and replace over half the normal architecture in some sections. .In this case, the organisms are more readily apparent within the mucosal epithelium than within areas of inflammation. Often in severe infections that lead to death of the fish, no identifiable organisms are present at necropsy, as they have likely been killed and cleared by the inflammatory cells. It is akin to the pauci-bacterial lesions of *Mycobacteria* spp. in which much of the tissue destruction occurs due to the extensive inflammation long after the acid-fast organisms are removed from the tissue.

*Cryptobia* spp. infections in fish colonies have severe consequence for the aquarist, whose often only option to combat the disease is to depopulate, as there are no treatments yet clinically proven to be effective.[2] Relatively little is known about this recently reported parasite of African cichlids. While *C. iubilans* is considered to be pathogenic, some researchers consider it a facultative organism which capitalizes on stressful conditions such as poor water quality or other parasitism.[2] Granulomatous gastritis is the most commonly reported lesion, but granulomatous disease is often observed in multiple organ systems simultaneously. Within some sections in this case, granulomas are present in the spleen and liver, while pancreatic atrophy and testicular degeneration is also often apparent. The second parasite described by the contributor is a myxosporean, of which many have an evolved relationship with their host and thus do not result in disease. The myxozoan was not observed on most participants' slides.

**Contributing institution:** Institute of Animal Pathology, Center for Fish- and Wildlife medicine, University of Berne, Länggasstrasse 122, CH-3001, Berne, Switzerland
http://www.itpa.vetsuisse.unibe.ch/fiwi/

**References:**

1. Lom J and Dykova I. Protozoan Parasites of Fishes. 1992. Elsevier Science Publishers B.V. Amsterdam, Netherlands. pages 52-51.
2. Yanong RPE, Curtis E, Russo R, Francis Floyd R, Klinger R, Berzins I, Kelley K, Poynton SL. *Cryptobila iubilans* infection in juvenile discus. J Am Vet Med Assoc 2004; 224(10): 1644-1650
3. Woo PTK. *Cryptobia (Trypanoplasma) salmositica* and salmonid Cryptobiosis. J Fish Dis 2003; 26: 627–646
4. Woo PTK. Immunological and Therapeutic Strategies against Salmonid Cryptobiosis. J Biomed Biotech 2010; doi:10.1155/2010/341783

---

**CASE II**: 13-8143 (JPC 4034291).

**Signalment:** 20 whole barramundi fingerlings (*Lates calcerifer)* submitted. All approximately 60 days old and male. 5000 fingerlings at risk, 1-200 sick and 15-20 dead.

**History:** Following a recent large mortality event of up to 10,000 fish, the surviving fish were graded based on size. Three days prior to submission to the SVDL, a proportion of fingerlings began to lose interest in feed and die.

**Gross Pathology:** No visible gross lesions evident, other than mild darkening. Many showed flaring of mouth and gill covers

**Laboratory Results:** None

**Histopathologic Description:** Fish, gills; Bilaterally and diffusely, there is marked distortion of normal gill architecture with marked blunting and fusion of lamellae. Interlamellar, extensive epithelial hyperplasia is present in most filaments. Multifocally, discrete colonies of small, 0.5um punctate, basophilic organisms markedly expanded individual epithelial cells, surrounded by a clear halo and with margination of the epithelial cell nucleus.

**Contributor's Morphologic Diagnosis:** Gill; branchitis, proliferative, diffuse, marked with fusion and blunting of lamellae and discrete bacterial colonies.

**Contributor's Comment: "**Epitheliocystis" is an intracellular infection of gills, and less commonly skin, caused by a genetically diverse group of gram-negative organisms belonging to the order *Chlamydiales*.[12,6] First recognized as a bacterial disease and named in 1969,[8] epitheliocystis has been reported in over 50 freshwater and marine species of teleosts,[12] elasmobranchs[3] and chondrosteans.[7] It is characterized by enlarged host cells, each containing a granular basophilic inclusion of organisms. Infections occur in skin, mouth and gill epithelial cells, including pavement cells,[10] chloride cells, goblet cells,[5] mucous cells, macrophages and pillar cells.[12] The organism's preference for chloride cells has been hypothesized to be related to its demand for energy. In contrast, it has also been suggested that the increased number of mitochondria in infected pavement cells could result in incorrect identification of pavement cells as chloride cells. On HE-stained sections, infected cells are morphologically obscured by the inclusion and identity is based on location in the gill.[10] The wide range of target cell types could be due to the specific preferences of the many different epitheliocystis-causing organisms and variations between host species.

Epitheliocystis is often considered an incidental finding.[5,1] However the prevalence, associated pathology and resultant mortality are highly variable among fish species and geographical locations. Risk factors associated with epitheliocystis infections include a higher morbidity and mortality in cultured fish, with losses up to 100%,[12] and seasonal variation related to water temperature.[12,13] Incidental epitheliocystis has been reported in Australian cultured barramundi.[1,11] A recent study of epitheliocystis in striped trumpeter *Latris lineate*, indicated a significant elevation of serum osmolality and lysozyme activity in infected fish, and this correlated also with the densities of infected cells in individuals. These findings indicate a measurable pathophysiological effect of epitheliocystis on the host. [10]

The etiological agents of epitheliocystis have not successfully been cultured in vitro, despite using a range of media and cell lines,[9] thus limiting our knowledge of this disease.[12, 10] Molecular

studies have identified a large variety of causative agents, however not all of these have included *in situ* methods for confirming the agents relation to the intracellular inclusions.[15] Agents identified by 16S rDNA include *Candidatus Piscichlamydia salmonis* in Atlantic salmon (*Salmo salar*)[4] and *Candidatus Parilichlamydia carangidicola* in Yellowtail kingfish (*Seriola lalandi*)[14], with sequences consistent with rRNA of *Chlamydiales* isolated from epitheliocystis in leafy seadragon (*Phycodurus eques*),[11] silver perch (*Bidyanus bidyanus*),[11] grass carp (*Ctenopharyngodon idella*)[8] and barramundi (*Lates calcarifer*)[11]. Mixed infections occurring in the same fish species have also been reported.[13]

A review by Nowak and associates (2006) revealed the most reliable test for epitheliocystis is histology. In some cases it may also be seen grossly or on wet preparations, however these techniques are not as sensitive.[12]

**JPC Diagnosis:** 1. Gills: Lamellar epithelial hyperplasia and hypertrophy, with multifocal lamellar fusion and numerous coccobacilli.
2. Skin, branchial cavity: Epithelial hyperplasia, diffuse, mild, with extracellular protozoans.

**Conference Comment:** This is a nice case of epitheliocystis, as the distinctive granular appearance of the bacterial colonies are well represented. The gill lamellae are often blunted, fused and thickened by a mixture of inflammatory cells and epithelial hyperplasia. Most participants believed the epithelial component predominated which is reflected in our diagnosis.

The specific cause of epitheliocystis remains elusive, and these bacterial colonies can often be observed without any other apparent pathology. A true causal relationship has not necessarily been demonstrated. Adding interest to this case, there are numerous flagellated protozoans along the skin surface and occasionally within the branchial cavity. These are most consistent with *Ichthyobodo necator*, an important parasite of hatcheries which is capable of producing significant pathology of the skin, gills and fins. This parasite is found in both fresh water and marine species and have been known to induce T cell and IgT lymphocyte depletion in the skin under experimental conditions.[2] Whether its presence here is related to the gill pathology was a point of conjecture among conference participants and is left for speculation among our readers.

**Contributing institution:** www.dpi.nsw.gov.au

**References:**

1. Anderson, I.G., Prior, H.C. (1992) Subclinical epitheliocystis in barramundi, *Lates catcarifer*, reared in sea cages. *Australian Veterinary Journal* **69**(9): 226-227
2. Buchmann K. Impact and control of protozoan parasites in maricultured fishes. *Parasitology*. 2015;142:168-177.
3. Camus, A., Soto, E., Berliner, A., Clauss, T., Sanchez, S. (2013) Epitheliocystis hyperinfection in captive spotted eagle rays *Aetobatus narinari* associated with a novel *Chlamydiales* 16S rDNA signature sequence. *Diseases of Aquatic Organisms*, **104**: 13–21
4. Draghi, A., Popov, V.L., Kahl, M.M., Stanton, J.B., Brown, C.C., Tsongalis, G.J., West, A.B., Frasca, S. (2004) Characterization of "*Candidatus* Piscichlamydia salmonis" (Order *Chlamydiales*), a *Chlamydia*-Like Bacterium Associated With Epitheliocystis in Farmed Atlantic Salmon (*Salmo salar*). Journal of Clinical Microbiology, 42 (11) 5286–5297

5. Ferguson H.W., (Ed.) (2006) *Systemic Pathology of Fish*. Scotian Press, London, pg.53
6. Fryer, J.L., Lannan C.N. (1994) Rickettsial and Chlamydial Infections of Freshwater and Marine Fishes, Bivalves, and Crustaceans. *Zoological Studies* **33**(2): 95-107.
7. Groff, J.M., LaPatra, S.E., Munn, R.J., Anderson, M.L., Osburn, B. I. (1996) Epitheliocystis infection in cultured white sturgeon (*Acipenser transmontanus*): antigenic and ultrastructural similarities of the causative agent to the chlamydiae, *Journal of Veterinary Diagnostic Investigation*, **8**: 172-180
8. Hoffman G.I., Dunbar, C.E., Wolf, K., Zwillenberg, L.O. (1969) Epitheliocystis, a new infectious disease of bluegill (*Lepomis macrochirus*). *Antonie van Leevenhoek Journal of Microbiology and Serology* **35**, 146-158.
9. Kumar, G., Mayrhofer, R., Soliman, H., El-Matbouli, M. (2013) Novel *Chlamydiales* associated with epitheliocystis in grass carp (*Ctenopharyngodon idella*). Veterinary Record **172**: 47-49
10. Lai, C.C., Crosbie, P.B.B., Battaglene, S.C., Nowak, B.F. (2013) Effects of epitheliocystis on serum lysozyme activity and osmoregulation in cultured juvenile striped trumpeter, *Latris lineata* (Forster). Aquaculture **388**–391 99–104
11. Meijer, A., Roholl, P.J.M., Ossewaarde, J.M., Jones, B., Nowak, B.F. (2006) Molecular Evidence for Association of *Chlamydiales* Bacteria with Epitheliocystis in Leafy Seadragon (*Phycodurus eques*), Silver Perch (*Bidyanus bidyanus*), and Barramundi (*Lates calcarifer*). *Applied and Environmental Microbiology* **72** (1) 284–290
12. Nowak, B. F., LaPatra, S.E. (2006) Epitheliocystis in fish. *Journal of fish diseases* 2006 **29**, 573-588.
13. Schmidt-Posthaus, H., Polkinghorne, A., Nufer, L., Schifferli, A., Zimmermann, D.R., Segner, H., Steiner, P., Vaughan, L. (2012) A natural freshwater origin for two chlamydial species, *Candidatus* Piscichlamydia salmonis and *Candidatus* Clavochlamydia salmonicola, causing mixed infections in wild brown trout (*Salmo trutta*). *Environmental Microbiology* **14**(8), 2048–2057
14. Stride, M.C., Polkinghorne, A., Miller, T.L., Groff, J.M., LaPatra, S.E., Nowak, B. F. (2013) Molecular Characterization of "*Candidatus* Parilichlamydia carangidicola," a Novel *Chlamydia*-Like Epitheliocystis Agent in Yellowtail Kingfish, *Seriola lalandi* (Valenciennes), and the Proposal of a New Family, "*Candidatus* Parilichlamydiaceae" fam. nov. (Order *Chlamydiales*). *Applied and Environmental Microbiology* 79 (5)1590–1597
15. Toenshoff E. R., Kvellestad, A., Mitchell, S.O., Steinum, T., Falk, K., Colquhoun D.J., Horn, M. (2013) A Novel Betaproteobacterial Agent of Gill Epitheliocystis in Seawater Farmed Atlantic Salmon (*Salmo salar*). *PLoS ONE* **7**(3): e32696. doi:10.1371/journal.pone.0032696

---

**CASE III**: 50646 (JPC 4048506).

**Signalment:** Adult, male, African bullfrog (*Pyxicephalus adspersus*)

**History:** Found dead. Animal caretakers noted some redness near the cloaca.

**Gross Pathology:** There were no relevant gross findings.

**Laboratory Results:** none

**Histopathologic Description:** The epidermis ranges from multifocally to diffusely hyperplastic with a thick layer of hyperkeratosis. The basal layers are multifocally disorganized with loss of orientation. The stratum corneum frequently contains multiple stages of fungal organisms (all stages may not be present in all sections). There are 10 micron zoosporangia containing numerous 2-3 micron diameter basophilic zoospores, and 5-15 micron thalli. Zoosporangia rarely have a funnel or discharge tube. Thalli include various forms: uninucleate thalli, larger multinucleated thalli, and empty thalli with fine internal septations (colonial thalli). There is multifocal widespread necrosis of the epidermis. There are few granulocytes within dermal glands. Within the superficial epidermis there is multifocal secondary invasion by bacteria and fungal hyphae.

**Contributor's Morphologic Diagnosis:** Skin: Severe chronic multifocal hyperkeratosis, hyperplasia, dyskeratosis, and necrosis with intralesional fungal thalli and luminal zoospores, and superficial secondary bacteria and fungal hyphae (etiology: *Batrachochytrium dendrobatidis*)

**Contributor's Comment:** *Batrachochytrium dendrobatidis* (Bd) is a type of chytrid fungus that is pathogenic to a wide range of amphibian species and is an important contributor to amphibian morbidity and mortality as well as loss of diversity. Chytrids are a large phylum of fungal organisms that are predominantly involved with degradation of plant and animal matter, and, unlike Bd, most chytrids are not pathogenic.[5]

Bd only affects keratinizing stratified squamous epithelium, which includes the mouthparts in tadpoles and the skin in adults. Clinical signs are variable and may include anorexia, lethargy, reluctance to place the ventrum on substrate, or even loss of righting reflex. Gross lesions most commonly occur on the ventrum and feet. Lesions include excessive skin shedding (dysecdysis), skin discoloration, and roughening of the skin. In tadpoles, depigmentation of the jaw sheath is commonly seen. Lack of gross lesions does not rule out chytridiomycosis, as was seen in this case.[5]

Histopathologic lesions of Bd include hyperplastic and hyperkeratotic epithelium containing the distinctive thalli within the keratin layers. There are 3 morphologic types of thalli which can range from 7 - 20 microns in diameter. Zoosporangia are the mature form, which contain 2 - 3 micron diameter basophilic zoospores and occasionally a flask-shaped discharge tube. Other types of thalli include a uninucleate stage with homogenous basophilic cytoplasm, and a multinucleated thallus with stippled to microvacuolated cytoplasm. Empty thalli with fine internal septations (colonial thalli) are zoosporangia that have discharged their zoospores and are a common finding. In many cases the empty thalli may be the only indication of Bd. Periodic acid-Schiff may be helpful in highlighting empty thalli, which could be interpreted to be an artifact in hematoxylin and eosin stained sections. Rhizoids are thin, root-like extensions from thalli and may be visible in silver-stained sections. Inflammation is usually minimal to absent. Secondary bacterial, fungal, and oomycete infections are common.[5]

The life cycle of Bd is well described. The zoospore is the infective stage and is released from a mature zoosporangium through the discharge tube. Transmission of the infectious motile flagellated zoospores occurs via direct animal contact or contact with water or substrates contaminated by affected animals. The zoospores become encysted in a new keratinocyte to

develop into a thallus. Cleavage of the thallus results in the development of new zoospores within a zoosporangium. All stages can be found in the keratin layers of an infected animal.[5]

Infection with chytrid fungi lead to morbidity and mortality through the disruption of both innate and cell-mediated immunity and loss of the physiologic function of the skin. The normal skin flora, including *Janthinobacterium lividum,* produce the antifungal toxin, violacein, which may be important for innate immunity.[2] Cell-mediated immunity may also be affected by toxins released from the fungus that inhibit T and B lymphocyte proliferation and cause lymphocyte apoptosis.[1] The major contributing factor to death in affected animals is disruption of normal cutaneous function. The skin of frogs is important for water absorption, osmoregulation, and respiration. In experimental infections, frogs became hyponatremic, hypokalemic, hypomagnesemic, and hypochloremic compared to controls. Disruption of cutaneous electrolyte transport is considered responsible.[6] As in this animal, secondary fungal and bacterial infections leading to epidermal necrosis may also contribute to death.

Other methods for the diagnosis of chytridiomycosis include cytology and real-time polymerase chain reaction (PCR). Cytology may be useful in identification of thalli or zoospores in shed skin or a skin scraping; however, differentiation from yeasts and oomycetes can be difficult. Confirmation by histopathology or PCR may be necessary. PCR is most commonly used for screening animals in quarantine or prior to translocation, surveying captive and free-ranging populations, and confirming a positive result on wet mount or cytology. PCR is highly sensitive and may help identify subclinical cases.[5]

In addition to the lesion presented in this case, sections also demonstrate the Eberth-Kastschenko (EK) layer that is characteristic of many frog species. The EK layer is a deeply basophilic layer of calcium deposits within the dermis. The function of this layer is unclear but speculated to be involved with protection from dessication, storage and mobilization of calcium, or the interchange of substances between the animal's internal and external environment.[3]

**JPC Diagnosis:** Skin, epidermis: Necrosis, hyperplasia and hyperkeratosis, multifocal to coalescing, moderate, with numerous fungal thalli and zoospores.

**Conference Comment:** This is an excellent example of chytridiomycosis, the all-important fungus associated with the declining population of amphibians. The keratinized epidermal crust is especially fragile and easily lost during processing of amphibian skin, and yet it is required to make this diagnosis. *B. dendrobatidis* is only found within this layer, illustrating the importance of delicate tissue handling during necropsy and tissue trimming. The additional presence of fungal hyphae seems to be most associated with an area of coagulative epidermal necrosis, indicating these are likely secondary invaders and we elected not to include them into our morphologic diagnosis.

The contributor provided extensive detail regarding the clinical presentation and pathogenesis of this entity. The discussed electrolyte disturbances induced by the loss of skin function often results in death due to cardiac arrest.[4] Interestingly, some species appear to be resistant to infection, including the well-studied *Xenopus laevis* which has contributed significantly to the understanding of the immune system's role in evoking this resistance. The immunoglobulins IgG and IgY secreted within the mucus from the skin appear to play a prominent role in providing

protection. Their innate immune system also prevents colonization through the release of antimicrobial peptides, whose secretion is dramatically increased during periods of stress.[4]

**Contributing institution:** Wildlife Disease Laboratories, Institute for Conservation Research, San Diego Zoo Global; http://www.sandiegozooglobal.org

**References:**


1. Fites JS, Ramsey JP, Holden WM, et al. The invasive chytrid fungus of amphibians paralyzes lymphocyte response. *Science*. 2013;342:366-369.
2. Harris RN, Brucker RM, Walke JB, et al. Skin microbes on frogs prevent morbidity and mortality caused by a lethal skin fungus. *ISME J.* 2009;3:818-824.
3. Katchburian E, Anoniazzi MM, Jared C, et al. Mineralized dermal layer of the Brazilian tree-frog *Corythomantis greeningi*. *J Morphology*. 2001;248:56-63.
4. Pessier AP. Chytridiomycosis. In: *Current Therapy in Reptile Medicine and Surgery*. St. Louis, MO: Saunders:2014:255-270.
5. Ramsey JP, Reinart LK, Harper LK, Woodhams DC, Rollins-Smith LA. Immune defenses against *Batrachochytrium dendrobatidis*, a fungus linked to global amphibian declines in the South African clawed frog, *xenopus laevis*. *Infect Immun*. 2010;78(9):3981-3992.
6. Voyles J, Young S, Berger L, et al. Pathogenesis of chytridiomycosis, a cause of catastrophic amphibian declines. *Science.* 2009; 326:582-585.


---

**CASE IV:** 09N1672 T2 (JPC 3166542).

**Signalment:** 2.5-year-old male Lined Seahorse, *Hippocampus erectus*

**History:** This seahorse initially presented for a 3 week history of multiple bubbles on the tail. No changes in behavior or appetite were noted. The three other seahorses in the aquarium were unaffected. All four seahorses were kept in an indoor 40 gallon glass hexagonal tank with 60 lbs of live rock, crushed coral and sand substrate, and sea grass. The water temperature was kept at 67$^{o}$ F. Tap water was used to make salt water. Water quality was maintained by a large filter, protein skimmer and a 20-30% water change every 2 weeks. The aeration unit was a pump with a submerged airstone. The diet was composed of frozen shrimp. On physical exam, the seahorse had inappropriate orientation with its tail floating above the head. At the distal half of the tail, there were five randomly scattered regions where the skin was lifted above a gas-filled space (bubble). Two cavities were aspirated for culture and the rest were reduced with a #28 needle. Bacterial culture from one aspirate was negative and from the other aspirate, small numbers of mixed growth grew including fastidious gram-negative bacteria. No bacteria or protozoa were seen on skin scrapes. A diagnosis of internal gas bubble disease was made and the patient was discharged on ceftazadine (20mg/kg, IM, every three days). Two weeks after the initial presentation, the seahorse was reevaluated. At this time there were more and larger bubbles on the tail, the seahorse was floating upside down, and was no longer feeding. One of the other seahorses in the tank had begun to show similar signs. The seahorse and 3 cohorts were treated with ceftazadine (20mg/kg, IM, every three days). A week later the seahorse was euthanized at home by the owner.

**Gross pathologic findings:** The adult male

lined seahorse weighed 20.7 g, was in good post-mortem condition and had adequate adipose stores. Five subcutaneous gas-filled bubbles were present on the ventral aspect of the distal half of the tail, measuring (cranial to caudal): 0.4 x .03 x 0.2 cm, 0.6 x 0.5 x 0.4 cm, 0.5 x 0.4 x 0.3 cm, 0.5 x 0.5 x 0.4 cm, and 1.1 x 0.6 x 0.5 cm. The swim bladder was severely distended and displaced the esophagus and stomach ventrally and compressed the kidneys dorsally. The intestine was markedly distended and displaced the liver ventrally and to the left.

**Laboratory results:** No bacterial organisms were seen on direct smear nor cultured from a coelomic cavity swab or liver sample.

**Histopathologic description:** In the examined longitudinal section of the tip of the tail, multiple 1 to 5mm clear spaces surrounded by variable amount of inflammation expand and compress the dermis, subcutaneous tissue and skeletal muscle. The clear spaces are variably lined by flattened elongated cells (presumed fibroblasts) or a combination of histiocytes, lymphocytes and infrequent multinucleate giant cells. Most spaces are empty. Less than 10% of the spaces contain scattered, radiating aggregates of eosinophilic, thin (<1μm diameter) up to 10 μm in length, beaded, filamentous bacteria that are surrounded by a 2-5 cell-thick rim of macrophages. In the deep dermis and subcutis between the clear spaces, there are dense, similar inflammatory cells that surround dilated blood vessels and are intermixed with haphazardly arranged plump fibroblasts. Focally, the inflammation extends to a central fragment of vertebral bone that has an irregular, scalloped surface lined by osteoclasts (bone resorption). Multifocally the epidermis is hyperplastic.

**Contributor's morphologic diagnosis:**
1. Tail (dermis, subcutis, skeletal muscle): Multifocal gas bubbles with chronic granulomatous cellulitis, and focal boney remodeling.
2. Subcutis: Granulomatous cellulitis with intalesional gram-positive filamentous bacteria

**Contributor's Comment:** Gas bubble disease (GBD) is a traumatic condition that can generically be referred to as a gas entrapment disorder.[3] The obvious gross lesions, gas-filled bubbles in the tissue, give the entity its name. In Syngnathids and sea horses in particular, gas bubble disease is a classic and frequently recognized entity.[1,2] In a 2005 review of syngnathids in public aquaria, *H. procerus, H. ingens, H. subelongatus* and *H. fisheri* were reported to be unusually susceptible to developing gas bubble disease.[2] Though susceptibility is more likely defined by housing and husbandry conditions rather than species susceptibility, *H. fisheri* is considered not suited for long-term display in aquaria because its particular susceptibility may be due to a need for access to deeper waters in order to maintain homeostasis.[2] Common presentations include gas entrapment in the brood pouch of male seahorses, subcutaneous emphysema, over-inflation of the swim bladder, and/or abnormal swimming, body posture or loss of neutral buoyancy. Subcutaneous emphysema most commonly presents as grossly visible bubbles in the tail and along with brood pouch over-inflation, are the most frequently observed gas entrapment problems.[1,2] Treatment of this disorder includes direct aspiration of the bubbles and administration of a carbonic anhydrase inhibitor, acetazolamide, and/or an antibiotic, ceftazidime.[1] Some institutions have had temporary success in reducing gas bubbles by increasing the barometric pressure (dropping the seahorses to a depth of 4 meters).[1] To date, the association between gas super-saturation and/or infectious agents and the development of gas bubble disease in seahorses has not been proven.[1,2]

The rare published reports of the histopathologic correlates have described gas-filled pseudocysts surrounded by varying amounts of fibrosis and granulomatous to histiocytic inflammation.[2] (personal communication, A. Nyaoke) No infectious organisms, unlike in this case, were described in association with the lesions. In this case, we suggest that the filamentous bacteria were an opportunistic infection, potentially introduced during the needle-aspirate reduction of the gas filled spaces and may explain the success of using antibiotics as an adjunct therapy to gas-reducing methods. In support of this theory, the deeper gas filled spaces, such as those within the muscle, did not contain bacteria. The filamentous bacteria were not recovered on culture, likely due to sampling site (coelomic cavity and liver), and were gram-negative and Fites acid-fast negative.

In general, in teleost fish and other aquatic species, gas bubble disease is associated with supersaturation of the water with nitrogen or oxygen and can be caused by anything that alters the gas saturation of the water, such as leaks in the pump or valve systems, sudden temperature gradients, altitude changes during air transportation and/or rapid barometric changes most often associated with collection of specimens at depth.[3] The disease is particularly important in cultured fish and amphibians;[4,5] however, wild fish are occasionally affected with reported cases in several fresh and marine species.[3] Some of the cases in the wild have been associated with heavy macroalgal blooms that were considered responsible for excessive levels of dissolved gases and subsequent disease. Fish often die of GBD without overt clinical signs. Occlusion of the large branchial vessels by gas emboli with endothelial damage and thrombi formation is considered the principal cause of acute mortality.[3,6] When clinical signs are present in teleost fish, they range from bilateral exophthalmia, subcutaneous emphysema, gasping behavior, hemorrhages, and anomalous swimming or loss of neutral bouyancy.[3,5]

**JPC Diagnosis:** 1. Tail, skeletal muscle: Cavitary pseudocyst, consistent with gas bubbles in tissue. 2. Tail: Cellulitis, granulomatous, chronic, multifocal, with granulation tissue and numerous bacilli.

**Conference Comment:** This is an intriguing case that initiated the exchange of theories among conference participants regarding the origin of the cysts in this seahorse, as there seemed to be three varieties present. The first occurring most prominently are the empty lumens lined by a layer of inflammatory cells which most believed to be gas-filled pseudocysts within the subcutaneous tissue. Occasional cysts in most sections appeared to be lined by endothelial cells leading some to conclude they were gas-distended lymphatics. Finally, as the contributor mentioned, the inflammatory infiltrate surrounded filamentous bacteria and, in some sections, encompassed much of the cystic space lending credence to speculation these were either primary granulomas or secondary bacterial infections. The hypothesis proposed by the contributor is quite plausible given the history of aspiration in this case.

In rare slides, there is a section of bone likely representing the vertebrae of this animal. When present, the bone edges are scalloped and often lined by activated osteoclasts consistent with active bone remodeling. This seems to provide further evidence in support of a chronic bacterial infection, which may correlate with the initial positive bacterial culture of this area.

Considerable information has been derived from the lifecycle of seahorses following the development of commercial rearing facilities. They are peculiar creatures with the responsibility

of fertilization and incubation of the young taken on by the males following a monogamous relationship with a single female. In addition to vibriosis and mycobacteriosis, gas entrapment problems are a major health issue for seahorses in culture and their relationship with gas supersaturation and infectious agents is largely unresolved.[1]

**Contributing Institution:** Department of Pathology, Microbiology and Immunology
5323 Vet Med 3A
School of Veterinary Medicine
University of California Davis
Davis, CA 95616
http://www.vetmed.ucdavis.edu/pmi/

**References:**

1. Koldewey HM-S, K.M.: A global review of the seahorse aquaculture. Aquaculture **302:** 131-152, 2010
2. Koldewey H: Syngnathid Husbandry in Public Aquariums, London, 2005
3. Roberts JR: Fish Pathology, Third ed. Harcourt Publishers Limited, London, 2001
4. Saeed MO, al-Thobaiti SA: Gas bubble disease in farmed fish in Saudi Arabia. Vet Rec **140:** 682-684, 1997
5. Salas-Leiton E, Canovas-Conesa B, Zerolo R, Lopez-Barea J, Canavate JP, Alhama J: Proteomics of juvenile senegal sole (Solea senegalensis) affected by gas bubble disease in hyperoxygenated ponds. Mar Biotechnol (NY) **11:** 473-487, 2009
6. Speare DJ: Endothelial lesions associated with gas bubble disease in fish. J Comp Pathol **104:** 327-335, 1991

**Joint Pathology Center**
**Veterinary Pathology Services**

# WEDNESDAY SLIDE CONFERENCE 2014-2015

## Conference 17

**4 February 2015**

**Guest Moderator:**
Matthew Starost, DVM, PhD, DACVP
National Institutes of Health

---

**CASE I:** L13-16980 (JPC 4048155).

**Signalment:** 3-year-old female rat, *Rattus norvegicus.*

**History:** This pet rat presented for less than 12 hours of neurologic signs and urinary incontinence. On examination the rat had left head tilt with bilateral mydriasis and absent pupillary light reflexes. The body was also tilted to the left. Ventral to the right ear, there was a hyperemic swelling; when compressed, pus exuded from the ear canal. Over the next 12 hours the animal was treated with antibiotics but deteriorated and was euthanized.

**Gross Pathology:** There was a 1 x 1 x 0.3 cm swelling immediately ventral to the right pinna. On manipulation of the swelling, yellow, creamy exudate mixed with heterogeneous, firm, yellow and brown material oozed from the ear canal. The right tympanic bulla was enlarged and measured 10 x 9 x 4 mm, whereas the left tympanic bulla measured 7 x 3 x 3 mm. The right cerebral hemisphere was slightly swollen and there was thick, creamy, yellow-green, opaque exudate in the leptomeninges covering the rostral cerebellum.

**Laboratory Results:** Postmortem cultures yielded *Prevotella melaninogenica* from the ear, brain, and an acutely congested and edematous lung. *Enterococcus* sp. was also isolated from the ear. *Mycoplasma* culture on the same set of samples was negative.

**Histopathologic Description:** Skull (multiple levels): Bilaterally associated with ulceration of the external ear canal, extending into and multifocally effacing the tympanic cavities of the middle ears, and extending into the cranium on the right side, are innumerable degenerate neutrophils and fewer macrophages mixed with abundant cellular debris, edema, and fibrin (lytic necrosis). In the right external ear, there is fibropapillomatous epithelial proliferation, with abundant underlying granulation tissue that entraps squamous epithelial cells and debris. The right tympanic bulla is four times normal size and contains large amounts of keratin and multifocal inflammatory cell infiltrate as previously described. The cell infiltrate also fills the left tympanic cavity and bilaterally infiltrates the extensively ulcerated stratified squamous epithelium and the subepithelial tissue of the middle ears, accompanied by multifocal resorption and remodeling of the temporal bones. There is no evidence of the auditory ossicles on

*1-1. Right external ear canal, rat: On manipulation of the ear base, swelling, yellow, creamy exudate mixed with heterogeneous, firm, yellow and brown material oozed from the ear canal. (Photo courtesy of: Department of Pathobiological Sciences, School of Veterinary Medicine, Louisiana State University, http://www1.vetmed.lsu.edu//PBS/index.html)*

*1-2. Brain, rat: The right cerebral hemisphere was slightly swollen. Thick, creamy, yellow-green, opaque exudate covered the rostral cerebellum. (Photo courtesy of: Department of Pathobiological Sciences, School of Veterinary Medicine, Louisiana State University, http://www1.vetmed.lsu.edu//PBS/index.html)*

either side. Within the submucosal stroma of the middle ears, the infiltrate is predominantly lymphoplasmacytic. There is also goblet cell metaplasia/hyperplasia and multiple glands distended with amphophilic (mucous) secretion. The inflammation extends along and multifocally infiltrates degenerate trigeminal nerves, and results in necrosis of approximately 10% of the right cerebral hemisphere. Adjacent to the necrotic regions in the brain, multifocal areas of neuropil are rarefied (malacia). Multiple neurons are degenerate, with regional gliosis. Within the right lateral and the third ventricles of the brain, there are small numbers of neutrophils, macrophages, lymphocytes, and plasma cells. The midline of the cerebrum is slightly displaced to the left. Multifocally and primarily at the edges of the foci of necrosis in the tympanic cavities and in the brain there are colonies of gram-negative rod-shaped and gram-positive coccoid bacteria. The inflammatory process also involves the laryngeal submucosa and skeletal muscle, resulting in myofiber necrosis characterized by hyalinization and fragmentation. The intracranial bone marrow appears hypercellular, with moderate myeloid hyperplasia.

**Contributor's Morphologic Diagnosis:** Ears: Otitis externa and media, bilateral, proliferative, ulcerative, and necrosuppurative, chronic, severe, with intralesional mixed bacteria and extension to encephalitis.

**Contributor's Comment:** Otitis media (OM) is common in laboratory and pet rats. An otoscopic study of 80 Wistar laboratory rats housed in barrier versus non-barrier units showed incidences of spontaneous OM to be 5% and 20%, respectively.[13] The condition is likely underestimated in most laboratory and domestic mammals, with the notable exception of horses, in which OM is usually only associated with temporohyoid osteoarthropathy.[15] In developed countries, 80% of children will have an episode of otitis media by their third birthday, and 40% will have at least six episodes by age seven.[11]

Primary or secondary bacterial infection is virtually ubiquitous in otitis media, and bacterial ascension through the tympanic bulla or via the Eustachian tube are proven routes of entry. Evidence for hematogenous infection remains circumstantial. The progressive pathology of otitis media is well-described.[15] To reflect the clinical progression of OM, otolaryngology provides an instructive classification scheme: 1) Otitis Media with Effusion (OME) corresponds to asymptomatic persistent middle ear effusion, 2) Acute Otitis Media (AOM) is recurrent middle ear effusion with clinical signs, and 3) Chronic Suppurative Otitis Media (CSOM) refers to discharge through a perforated tympanic membrane for greater than 2 weeks.[11] Complications of OM include hearing impairment, vestibulopathy, extension to otitis interna, and meningoencephalitis. Globally

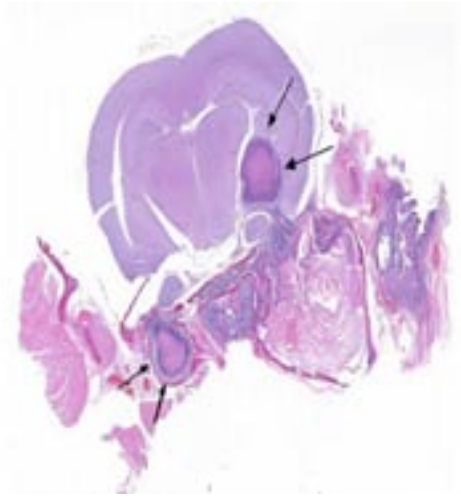

*1-3. Skull, rat: There was extensive remodeling and enlargement of the tympanic bullae. This alteration was most severe on the right side. Abscesses are seen within the left bulla and the right ventral hippocampus (arrows). (HE 400X) (Photo courtesy of: Department of Pathobiological Sciences, School of Veterinary Medicine, Louisiana State University, http://www1.vetmed.lsu.edu//PBS/index.html)*

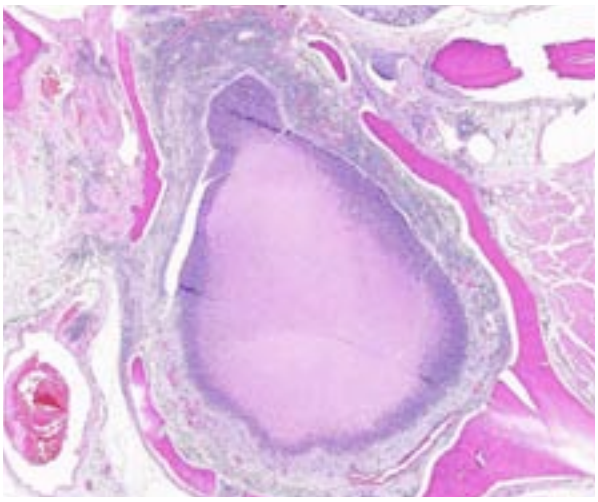

*1-4. Left tympanic bulla, rat: The inflammatory infiltrate results in remodeling and multifocal resorption of the temporal bone. (HE 200X) (Photo courtesy of: Department of Pathobiological Sciences, School of Veterinary Medicine, Louisiana State University, http://www1.vetmed.lsu.edu//PBS/index.html)*

21,000 people die annually due to OM-related complications.[7] The presence of stratified squamous epithelium, goblet cell metaplasia/ hyperplasia and mucus-producing submucosal glands in the middle ear is consistent with a chronic suppurative otitis media in this rat. Although not evident in the current case, concurrent otitis interna was strongly suspected due to extension of the inflammatory process into the brain.

Clinical signs of OM are ear pain, odor, head tilt, vestibular signs, scratching at the ear, and neurologic signs related to meningoencephalitis. Discharge/debris from and below the ear canal may be seen. Otoscopic examination may reveal an inflamed tympanic membrane, pus behind the membrane, or membrane rupture.[5] Clinical diagnosis can be aided by radiography, CT scan, cytology, and bacteriology.

Organisms commonly implicated in otitis media in rats are *Mycoplasma pulmonis*, *Streptococcus pneumonia*, *Pasteurella pneumotropica*, *Staphylococcus* sp., *Corynebacterium kutscheri*, and *Klebsiella* sp.[5] In this case *Mycoplasma* culture of the ear, brain, and lung was negative.

*Prevotella melaninogenica* (formerly *Bacteroides melaninogenicus*) is an anaerobic gram-negative bacillus. Of the anaerobic gram-negative bacilli involved in animal diseases, *Fusobacterium* is the most important genus, and other genera include *Bacteroides*, *Dichelobacter*, and *Porphyromonas*. *P. melaninogenica* is also classified as a "black pigmented bacterium" due to its production of black iron metabolites on blood-containing media; thus, the species name is a misnomer as melanin pigments are tyrosine-based. Virulence factors include hemolysin, neuraminidase, and collagenase.[3,12] *P. melaninogenica* is a component of the normal flora in the rumen and the human oral cavity, gut and vagina. It is mainly a periodontal pathogen but also considered to be an emerging pathogen in human OM.[1,10] A search of the current veterinary literature identified *P. melaninogenica* as a common pathogen in bovine footrot and bite wounds from dogs and cats, but no reports of otitis in rats were found.

**JPC Diagnosis:** 1. Brain: Meningoencephalitis, suppurative, focally extensive, with neural degeneration.
2. Middle ear: Cholesteatoma.
3. Middle ear: Otitis media, suppurative, focally extensive, with mucosal ulceration, squamous metaplasia, and bone remodeling.
4. Eustachian tube: Eustachitis, suppurative, diffuse, chronic-active.
5. Nasopharynx: Nasopharyngitis, suppurative, diffuse, with mucus metaplasia.
6. External ear canal: Otitis externa, ulcerative, focally extensive, chronic-active.

**Conference Comment:** The opportunity to observe an entire pathologic process in a single

section makes this a truly unique case. It is likely the initial insult was bacterial colonization within the nasopharynx that spread up the Eustachian tube to the middle ear followed by its extension into the calvarium. Of special importance here is the formation of a cholesteatoma within the middle ear. Cholesteatomas are common in people in this geographic location, usually associated with chronic otitis media. They are non-neoplastic, cystic lesions lined by keratinizing squamous epithelium or metaplastic mucus-secreting epithelium and filled with amorphous debris.[7] The pathogenesis behind their formation is still unclear, but a widely acknowledged theory is that the negative pressure and dysfunction of the Eustachian tube causes a deepening retraction pocket that, when obstructed, desquamated keratin cannot be cleared from the recess.[8] They are known to erode the ossicles, labyrinth, and adjacent bone by their production of cytokines such as RANKL and MMP's,[14] and it is likely this specific lesion permitted invasion of the calvarium in this case.

With the common occurrence of ear infections in infants and children, there is an extensive amount of published information regarding their pathogenesis and treatment in people, most of which revolves around the formation of biofilms. Biofilms are complex bacterial communities that adhere to the surface of implanted biomaterial or mucosa and play a major role in chronic ear infections.[6] In addition to enhancing adherence, biofilms increase bacterial virulence by protecting the microbes from immune effector mechanisms and increases their resistance to antimicrobial drugs.[9] In the ear, biofilms may contribute to cholesteatoma formation, as well as suppurative and non-suppurative otitis, and their formation can exacerbate the infection. This is why the first choice of treatment with internal ear infections in people is often surgery, and why all tissue with potential to harbor biofilms must be removed at that time or risk recurrence of infection.[6]

Conference participants were afforded the opportunity to review the intricate and minute anatomy of the outer, middle and inner ear, during which no less than thirty specific anatomical terms were described within the cochlea alone. Nomenclature aside, appropriate function of the ear requires vibration of the tympanic membrane by sound waves, which are then conducted into the cochlea via the ossicles of the middle ear (malleus, incus and stapes) by a push on the oval window. This movement incites a fluid wave within the cochlea, which is completely full of lymph fluid called endolymph. Where along the snail-shaped cochlea this wave intersects with the Organ of Corti and subsequently delivers information to the brain depends on its frequency. Of vital importance to this conduction system is the maintenance of a strong positive endocochlear potential within the endolymph, which requires precise control and recycling of potassium. In fact, potassium recycling defects in the cochlea is an important cause of deafness in people.[2]

**Contributing Institution:** Department of Pathobiological Sciences
School of Veterinary Medicine
Louisiana State University
http://www1.vetmed.lsu.edu//PBS/index.html
Louisiana Animal Disease Diagnostic Laboratory
http://www1.vetmed.lsu.edu/laddl/index.html

**References:**

1. Brook I. The role of anaerobic bacteria in chronic suppurative otitis media in children: Implications for medical therapy. *Anaerobe*. 2008;14(6):297-300.
2. Chen J, Zhao HB. The role of an inwardly rectifying K(+) channel (Kir4.1) in the inner ear and hearing loss. *Neuroscience*. 2014;265:137-146.
3. Eley BM, Cox SW. Proteolytic and hydrolytic enzymes from putative periodontal pathogens: characterization, molecular genetics, effects on host defenses and tissues and detection in gingival crevice fluid. *Periodontol*. 2000. 2003;31:105-24.
4. Ginn PE, Mansell JE, Rakich PM. Skin and appendages. In: Maxie MG, ed. *Jubb, Kennedy, and Palmer's Pathology of Domestic Animals*. 5th ed. Vol. 1. Philadelphia, PA: Elsevier; 2007:677-693.
5. Joint Pathology Center. http://www.askjpc.org/vspo/show_page.php?id=704.
6. Kaya E, Dag I, Incesulu A, Gurbuz MK, Acar M, Birdane L. Investigation of the presence of biofilms in chronic suppurative otitis media, nonsuppurative otitis media, and chronic otitis media with cholesteatoma by scanning electron microscopy. *Sci World J*. 2013:638715. doi: 10.1155/2013/638715. eCollection 2013.
7. Lingen MW. Head and neck. In: Kumar V, Abbas AK, Aster JC, eds. *Robbins and Cotran*

*Pathologic Basis of Disease*. 9th ed. Philadelphia, PA: Elsevier Saunders; 2015:740.
8. Maniu A, Harabagiu O, Perde Schrepler M, Catana A, Fanuta B, Mogoanta CA. Molecular biology of cholesteatoma. *Rom J Morphol Embryol*. 2014;55(1):7-13.
9. McAdam AJ, Milner DA, Sharpe AH. Infectious diseases. In: Kumar V, Abbas AK, Aster JC, eds. *Robbins and Cotran Pathologic Basis of Disease*. 9th ed. Philadelphia, PA: Elsevier Saunders; 2015:349.
10. Monasta L, Ronfani L, Marchetti F, et al. Burden of Disease Caused by Otitis Media: Systematic Review and Global Estimates. PLoS One. 2012;7(4):e36226.
11. Morris PS, Leach AJ. Acute and Chronic Otitis Media. Pediatr Clin North Am. 2009 Dec; 56(6):1383-99.
12. Soukos NS, Som S, Abernethy AD, et al. Phototargeting oral black-pigmented bacteria. *Antimicrob Agents Chemother*. 2005;49(4): 1391-6.
13. Verdaguer JM, Trinidad A, González-García JA, et al. Spontaneous otitis media in Wistar rats: an overlooked pathology in otological research. *Lab Anim* (NY). 2006;35(10):40-4.
14. Welkoborsky HJ. Current concepts of the pathogenesis of acquired middle ear cholesteatoma. *Laryngorhinootologie*. 2011;90(1):38-48.
15. Wilcock, BP. Eye and ear. In: Maxie MG, ed. *Jubb, Kennedy, and Palmer's Pathology of Domestic Animals*. 5th ed. Vol. 1. Philadelphia, PA: Elsevier; 2007:546-551.

**CASE II**: E 1061/14 (JPC 4048856).

**Signalment:** Adult female B6 mouse, *Mus musculus*.

**History:** The mouse was mated and suspected to be pregnant. About 14 days later the keepers suggested that the animal was not pregnant, but an abdominal swelling was reported. The animal showed a good general constitution, and food and water intake were unremarkable. The abdominal swelling was indolent. The animal was euthanized and a necropsy was performed. Formalin-fixed samples of the abdominal wall, ovaries, liver, colon and spleen were submitted for microscopic investigation.

**Gross Pathology:** The spleen was moderately enlarged and multiple, whitish nodules measuring up to 2 mm in diameter were observed. The liver showed a light brown coloration and was extensively and firmly attached to the small and large intestines as well as to abdominal fatty tissue. The ovaries and abdominal wall could not be identified grossly with certainty.

**Laboratory Results:** None.

**Histopathologic Description:** The slide shows a section of an abdominal mass of approximately 0.75 cm in diameter with adjacent skeletal muscle of the abdominal wall and abdominal fatty tissue. The mass is surrounded by a thick capsule consisting of fibroblasts and large amounts of collagenous fibers. In the center large areas of amorphous acellular eosinophilic material is present (necrosis). Additionally, there are segments of necrotic skin with keratin lamellae and necrotic hair follicles characterized by round to oval circles with central accumulation of dark brown coarse granular pigment. Furthermore, necrotic skeletal muscles are identifiable as eosinophilic straps with cross-striations. Islands of large pale basophilic cells arranged in a honey-comb-like pattern measuring up to 40 µm in diameter with pale eosinophilic predominantly centrally located shadows of nuclei (necrotic cartilage) are present. Adjacent to the necrotic cartilage, there are partly mineralized areas of necrotic bone tissue consisting of thin cortical structures and trabeculae without identifiable cellular elements. At the periphery of the mass, there is a marked accumulation of cellular debris mostly consisting of degenerate neutrophils with numerous viable neutrophils and as well as foamy macrophages. Within and around the fibrous capsule, a mild to moderate infiltration of plasma cells and lymphocytes is found. The serosa, abdominal striated muscle, and fatty tissue show a multifocal to coalescing moderate infiltration of lymphocytes and plasma cells. Adjacent to the mass parts of the exocrine pancreas are present (not in all sections), which is similarly infiltrated as described above.

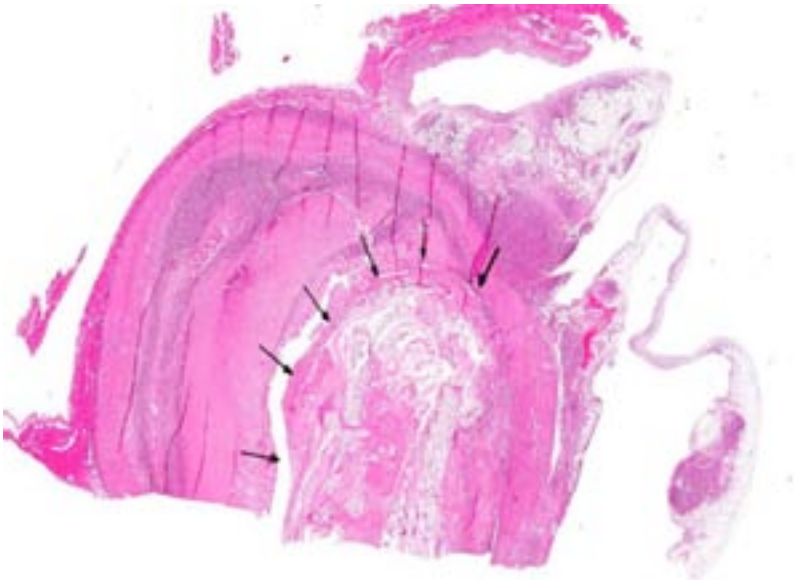

*2-1. Ectopic pregnancy, mouse: Within the abdominal cavity, there is a focally extensive abscess which contains plates of degenerating bone and cartilage (arrows). This degenerating fetus is contained within the abdominal cavity, representing an ectopic pregnancy. (HE 7X)*

**Contributor's Morphologic Diagnosis:** Abdominal cavity, Serositis, severe, pyogranulomatous, chronic with necrotic skin, musculature, cartilage and bone; findings consistent with abdominal pregnancy.

Myositis, pancreatitis, steatitis, multifocal to coalescing, moderate, lymphoplasmacytic, chronic.

**Contributor's Comment:** Abdominal pregnancy is a form of ectopic or extrauterine pregnancy that is characterized by an abdominal location of the embryo or fetus.[1,2,5] Especially in early stages of gestation, the zygote has the ability to adhere to several maternal tissues and to connect to

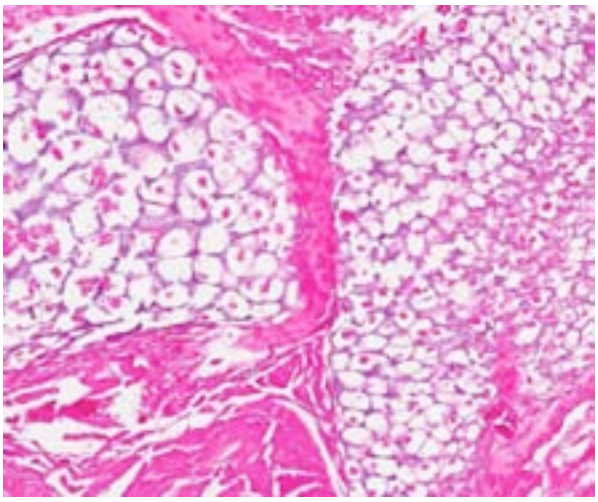

*2-2. Ectopic pregnancy, mouse: The degenerating fetus contains disorganized plates of bone undergoing intramembranous ossification. (HE 168X)*

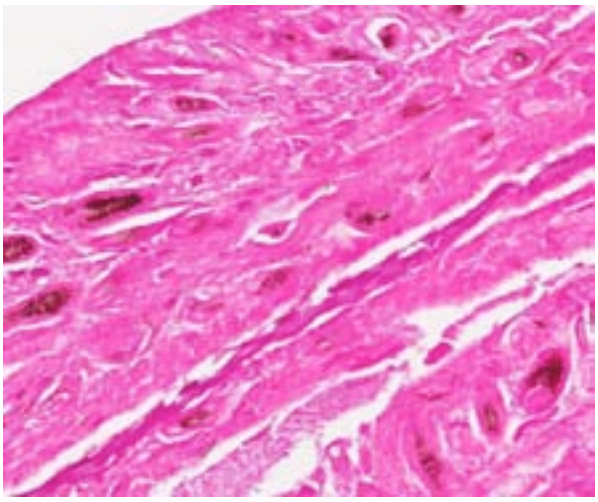

*2-3. Ectopic pregnancy, mouse: The degenerating fetus contains areas of necrotic skin with hair follicles (HE 168X)*

maternal blood vessels. Due to limitations of space and nutritional resources, embryonic or fetal death occurs in some cases concurrent with the observation of clinical signs of the mother.[2]

A distinction is made between primary and secondary ectopic pregnancy. In cases of primary ectopic pregnancy the zygote directly adheres to maternal tissue other than the uterus. Primary ectopic pregnancies in humans can be categorized into three subgroups.[1]

Ovarian pregnancy (*graviditas ovarica*): In these cases, the embryo develops in direct contact with the ovary. Only human cases have been reported so far.

Tube pregnancy (*graviditas tubaria*): It is the most frequently occurring primary ectopic pregnancy in humans that is often associated with severe intraabdominal hemorrhages. No cases have been reported in animals other than non-human primates.

Abdominal pregnancy (*graviditas abdominalis*): A true primary abdominal pregnancy has not been described in animals. One reason might be the fact that due to gastrointestinal movements in animals, the implantation of the zygote is inhibited. In contrast, due to the upright body position in humans, the zygote has a better chance to connect with extra-uterine maternal tissue caused by the relatively small pelvic cavity and the lesser influence of gastrointestinal movements in this area.

In secondary abdominal pregnancy the embryo or fetus starts to develop within the uterus. Subsequently, it is dislocated to the abdominal cavity and attached to extra-uterine maternal tissue with connection to maternal blood vessels. Secondary abdominal pregnancies are reported in all domestic animals with a declining frequency: cattle, rabbit, sheep, dog, pig, cat, goat and horse.[1,2,5] In mice, abdominal pregnancy has also been induced experimentally with living fetuses placed into the abdominal cavity.[4]

Secondary abdominal pregnancy is often caused by trauma or spontaneous uterine rupture. This process is called internal birth (*partus internus*). In most cases, when the abdominal pregnancy is recognized the cause of the uterine rupture cannot be identified anymore. Spontaneous uterine ruptures are often a consequence of uterine torsions or other pathological uterine conditions. Directly after dislocation of the embryo or fetus into the abdominal cavity the uterus contracts and uterine contractions stop immediately. The fate of the abdominal embryo or fetus depends on the ability to connect to maternal tissue and to ensure the connection to maternal blood vessels to guarantee nutritional supply. In cases with intact amniotic membranes the probability for an embryonic or fetal survival increases.[1,2,5]

In the maternal abdominal cavity, the embryo or fetus is initially recognized as a foreign body and within hours a circumscribed, serofibrinous inflammation starts which develops to an adhesive peritoneal reaction without involvement

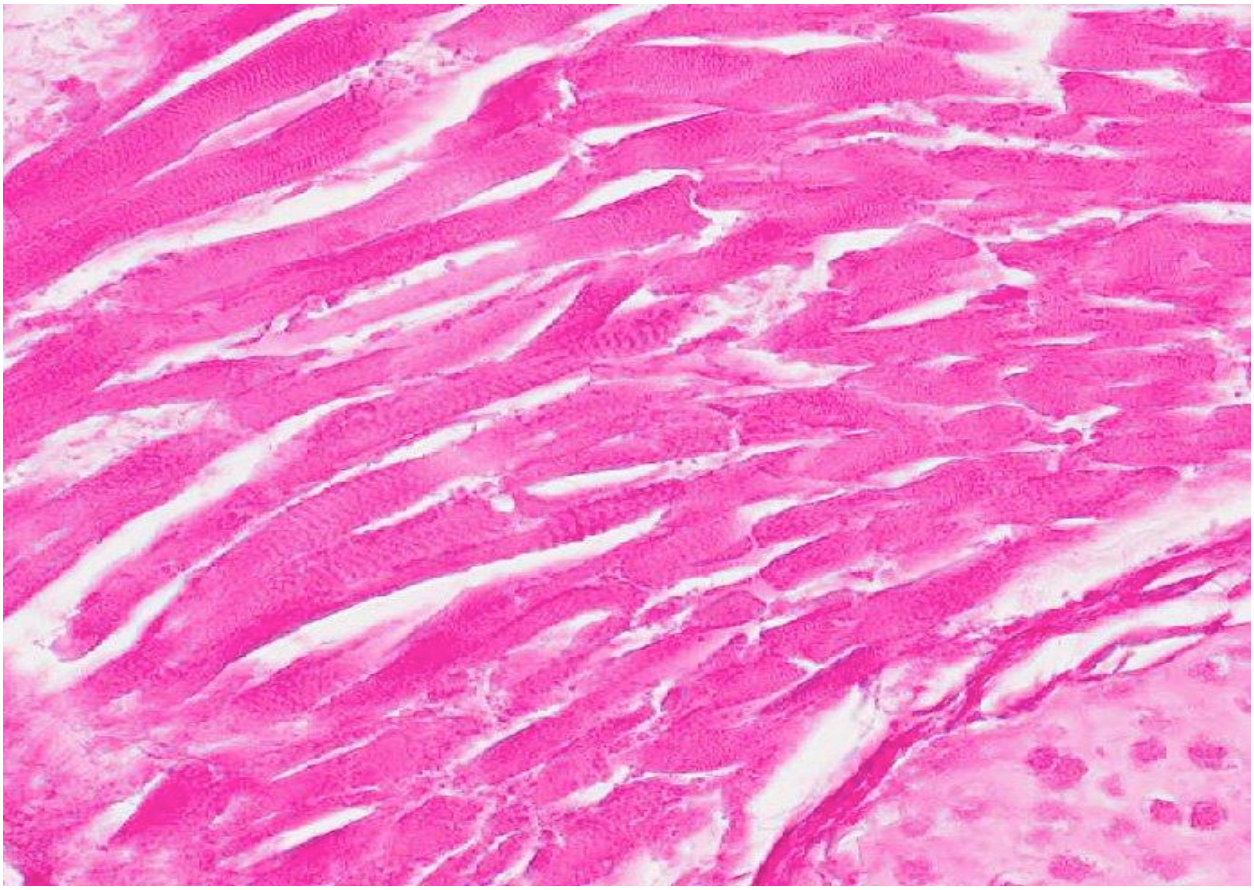

*2-4. Ectopic pregnancy, mouse: The degenerating fetus contains areas of necrotic skeletal muscle, characterized by the presence of cross-striations. (HE 320X)*

of infectious agents. Often a capsule is formed. In cases with neoplacentation, the placental fragments lose their species-specific properties and transform into irregularly formed islets of diffuse placental connections. Neoplacentations can occur in various abdominal organs. Neoplacentations within the mesentery or the great omentum normally do not cause clinical signs of the mother. Neoplacentations in other organs may be associated with severe clinical signs of the mother due to disturbances of normal organ function.

During the whole duration of abdominal pregnancy the embryo or fetus can die due to nutritional failure. If this happens the embryo or fetus will undergo mummification or maceration and may induce a reactive inflammatory reaction. This may lead to abscess formation and fistulation through the abdominal wall or inflammatory involvement of several abdominal organs.[2]

**JPC Diagnosis:** Uterus, abdominal cavity: Metritis and peritonitis, pyogranulomatous, focal, encapsulated, with myositis and a macerated fetus.

**Conference Comment:** This is an interesting and descriptively challenging case during which many participants debated whether the fetus was within the uterus or free in the abdominal cavity. Some sections contained a small piece of epithelium that to most looked like gestational uterine epithelial cells. Immunohistochemical staining of the section for smooth muscle actin demonstrated that smooth muscle was present surrounding much of the lesion. The combined findings left many to conclude the pregnancy began in the uterus that subsequently ruptured and adhered to the peritoneal wall. The contributor provides an excellent overview of ectopic pregnancies, of which only secondary abdominal pregnancy has been reported in animals, which supports the opinion of most participants.

Another important question pertaining to this case is regarding the age of the fetus. Many deliberated

as to its gestational age, and subsequently, how long prior to necropsy it had died. Ectopic pregnancies occur most commonly in the fallopian tube in people, and fetal development occurs as usual until, in some instances, its size outgrows the tissues ability to expand. This may cause a rupture 6-8 weeks into gestation of a fallopian tube pregnancy.[3] With an average gestation of just 20 days in mice, the history of mating 14 days prior to necropsy indicates this fetus may have been close to term. Whether the majority of this development occurred within the uterus prior to a rupture or largely took place while attached to the abdominal wall as observed in these slides remains a point of speculation.

**Contributing Institution:** Department of Pathology, University of Veterinary Medicine Hannover, Germany
http://www.tiho-hannover.de/kliniken-institute/institute/institut-fuer-pathologie/

**References:**

1. Corpa JM. Ectopic pregnancy in animals and humans. *Reproduction*. 2006;131:631-640.
2. De Kruif. Von den Früchten ausgehende Störungen der Gravidität. In: Richter J, Götze R eds. *Tiergeburtshilfe*. 4th ed. Berlin, Germany: Parey; 1993:146-147.
3. Ellenson LH, Pirog EC. The female genital tract. In: Kumar V, Abbas AK, Aster JC, eds. *Robbins and Cotran Pathologic Basis of Disease*. 9th ed. Philadelphia, PA: Elsevier Saunders; 2015:1036.
4. Hreshchyshyn MM, Hreshchyshyn RO. Experimentally induced abdominal pregnancy in mice. *Am J Obstet Gynecol.* 1964;89:829-832.
5. Weisbroth SH, Scher S. Spontaneous multiple abdominal pregnancies in a multiparous NCS mouse. *Lab Anim Care.* 1969;19:528-530.

**CASE III**: CP 8322 (JPC 4049001).

**Signalment:** 10-month-old female BALB/c, *Mus musculus.*

**History:** The mouse was group housed with other females in an individually ventilated cage (IVC) system. No experimental procedures had been performed on the mouse as she was part of a cohort being allowed to age prior to study commencement. The technicians noted a mass on the side of the face/neck, culled the animal and removed tissues for histological assessment.

**Gross Pathology:** A piece of haired skin with a 10 mm diameter cavitated, fluid filled mass was received in formalin. The mass had a multifocally thin wall (less than 1 mm fixed tissue thickness) but in other foci the wall of the cavitation was expanded by beige homogeneous tissue up to 5 mm in thickness. The fluid contained within the cavitated structure was clear. Thoracic and abdominal viscera were also submitted fixed in formalin and no other abnormalities were detected.

**Laboratory Results:** None.

**Histopathologic Description:** Within the subcutis of the haired skin, adjacent to the salivary tissue and lymph node, is an unencapsulated, but well-circumscribed, neoplastic mass, which is bluntly infiltrative in some tissue planes, and moderately densely cellular. The neoplastic cells are arranged in heterogeneous patterns including poorly defined clusters, occasionally in tubular structures, and also multifocally in sheets and broad bundles and streams, supported by a multifocally dense collagenous stroma. The cells are arranged around variably sized, but frequently large, cavitations and in some foci the cells palisade around the spaces. The neoplastic cells are pleomorphic polygonal to spindle-shaped, and are moderately sized, with indistinct cell margins and a moderate amount of eosinophilic cytoplasm. The nuclei are frequently oval and exhibit lightly stippled to clumped chromatin and a variable number of variably prominent nucleoli. The mitotic rate is high at 35 mitoses per 10 high power fields. There are foci of necrosis characterized by nuclear karyorrhexis and accumulations of amorphous eosinophilic material. Multifocal aggregates of small to moderate numbers of lymphocytes, with lesser numbers of plasma cells, are present multifocally. The cavitations within the mass multifocally contain strands of pale eosinophilic material and there are multifocal groupings of small numbers of macrophages, some of which contain grey to amphophilic intracytoplasmic material.

**Contributor's Morphologic Diagnosis:** Haired skin on side of face/ neck: Myoepithelial carcinoma.

**Contributor's Comment:** In the planes of tissue examined, the lesion is consistent with a myoepithelial carcinoma arising from the adjacent salivary tissue (not present on all sections).

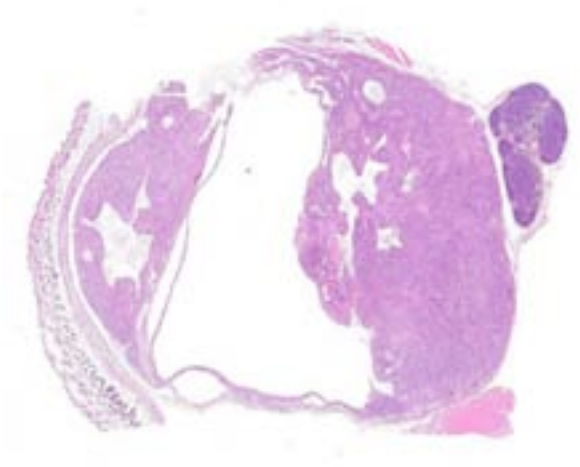

*3-1. Salivary gland, mouse: The salivary gland is effaced by a multicystic, expansile, moderately cellular neoplasm which elevates the overlying haired skin. (HE 7X)*

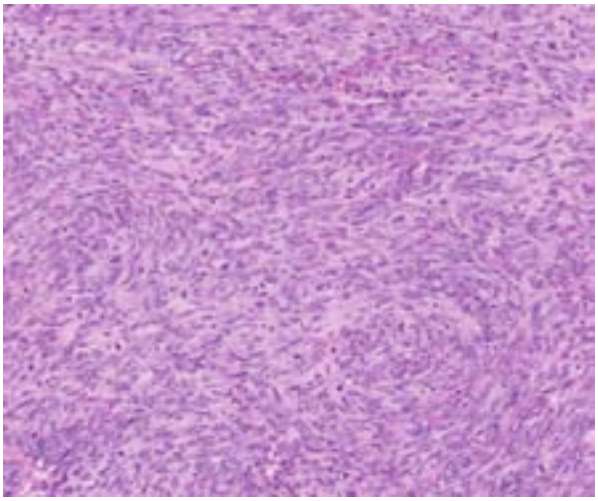

*3-2. Salivary gland, mouse: Neoplastic cells are arranged in short interlacing streams and bundles. (HE 75X)*

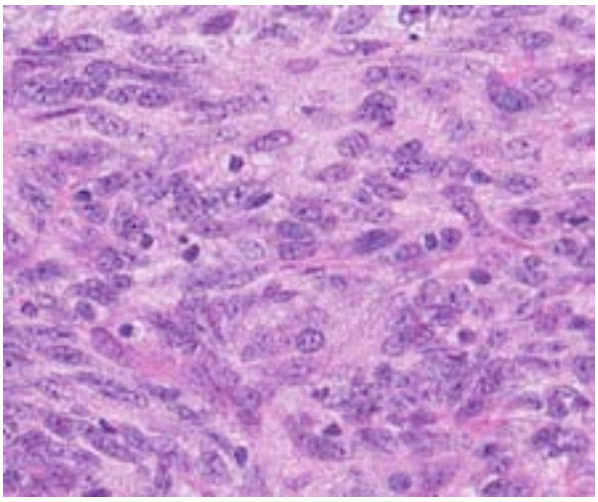

*3-3. Salivary gland, mouse: Neoplastic cells are spindled, with indistinct cell borders, abundant vacuolated cytoplasm, a vesicular chromatin pattern, and a brisk mitotic rate. (HE 356X)*

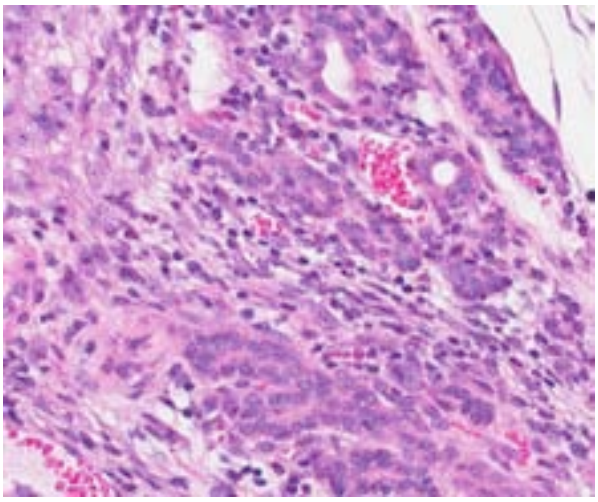

*3-4. Salivary gland, mouse: Atrophic salivary gland tissue is present at the edge of the neoplasm. (HE 320X)*

Alternative differential diagnoses based on the site and gross morphology included a Harderian gland cystadenoma, but the histological appearance of the specimen was most consistent with a tumor arising from the myoepithelial cells of the salivary gland. Myoepitheliomas generally exhibit a low mitotic rate,[6] but this example exhibited frequent mitoses and thus classification as a myoepithelial carcinoma was preferred. The cavitations exhibited by this mass are considered characteristic and are frequently the result of necrosis leading to the formation of "cyst-like" structures.[4] Had immunohistochemical staining been undertaken, myoepitheliomas stain positively for keratins 5 and 14, reflecting their myoepithelial origin.[6]

Although myoepithelial tumors are infrequent in most strains of mice, they are relatively more common in BALB/c mice, especially females, such as in the present case. They most frequently arise from the submaxillary and parotid salivary glands and present as swellings of the subcutaneous tissue of the ventral neck.[4] A retrospective study of 142 myoepitheliomas determined that these tumors also occur spontaneously in several other inbred strains of laboratory mice including A/HeJ, A/J, LLC.A/Ckc and NOD/Lt.[6] Recently, salivary carcinomas exhibiting myoepithelial and basal cell differentiation have been reported in the *Justy* mutant mouse strain (background: C3HeB/FeJ) which bears a recessive mutation in the *Gon4l* gene that regulates gene expression during development.[5]

Myoepithelial carcinomas are rare in humans and in the domestic species[3] although there are at least two reports of myoepithelial carcinoma (synonym: malignant myoepithelioma) in dogs.[1,2]

**JPC Diagnosis:** Parotid gland: Myoepithelioma.

**Conference Comment:** This is a rarely reported neoplasm in domestic species (other than the mouse), and without distinguishing features, its specific histogenesis is often left to immunohistochemistry. In this particular case, we ran pancytokeratin, vimentin and smooth muscle actin, with only pancytokeratin yielding positive staining. Myoepithelial cells are modified epithelial cells with contractile properties.[6] They exist in glandular tissue, such as salivary and mammary glands, and function by forcing secretions into and through a duct system with their contraction.[6] Myoepithelium stains positive for both epithelial and muscle markers; however, their staining seems to be more variable compared to the apparent high specificity of CK5 and CK14 as mentioned by the contributor.[1,5,6]

The question of malignancy was debated in this case, as some pointed out the well-circumscribed appearance and uniform cell population. We agree with the contributor, that the high mitotic rate and areas of necrosis are reason to worry, but elected to avoid a malignant modifier without definitive evidence such as vascular invasion.

**Contributing Institution:** Department of Veterinary Medicine, University of Cambridge Cambridge, UK
http://www.vet.cam.ac.uk/

**References:**

1. Faustino AM, Pereira PD. A salivary malignant myoepithelioma in a dog. *Vet J.* 2007:173:223-226.
2. Gorlin RJ, Barron CN, Chaudhry AP, et al. The oral and pharyngeal pathology of domestic animals: a study of 487 cases. *Am J Vet Res.* 1959:20:1032-1061.
3. Head KW, Else RW, Dubielzig RR. Tumors of the alimentary tract. In: Meuten D, ed. *Tumors in Domestic Animals*. 4th ed. Ames, Iowa: Iowa State Press; 2002:415.
4. Percy DH, Barthold SW. Mouse. In: Percy DH, Barthold SW, eds. *Pathology of Laboratory Rodents and Rabbits*. 3rd ed. Oxford, UK: Blackwell publishing; 2007:120-121.
5. Simons AL, Lu P, Gibson-Corley KN, et al. The *Justy* mutant mouse strain produces a spontaneous murine model of salivary gland cancer with myoepithelial and basal cell differentiation. *Lab Invest.* 2013:93:711-719.
6. Sundberg JP, Hanson CA, Roop DR, et al. Myoepitheliomas in inbred laboratory mice. *Vet Pathol.* 1991:28:313-323.

**CASE IV:** G 8397/12 (JPC 4033557).

**Signalment:** 18-year-old female putty-nosed monkey, *Cercopithecus nictitans.*

**History:** The monkey lived in a German zoo since 2007. After a fight among group members, the animal showed apathy, tachypnea and vomiting. Physical examination under general anesthesia revealed a perforating wound on the right lateral thorax, resulting in severe unilateral pyothorax, which was treated by drainage of the thoracic cavity and repeated wound cleaning, accompanied by administration of antibiotics and analgesics for a couple of days. The monkey showed good response to treatment and initially improved, before its clinical condition deteriorated after 10 days with additional development of neurological signs. Due to poor prognosis, the animal was euthanized and submitted for post mortem examination.

**Gross Pathology:** Focally extensive within the right ventrolateral chest wall, a chronic, well encapsulated, intramuscular to subpleural abscess was present, reaching from the sixth to ninth intercostal space into the mediastinum with adhesions to the caudal lung lobe and perforation of the costal pleura, accompanied by moderate unilateral fibrinous to hemorrhagic pleural effusion. The right lung showed diffuse necro-suppurative to fibrinous pleuropneumonia with marked compression atelectasis of mainly the caudal parts, whereas the left lung was poorly retracted, hyperemic, and edematous with multifocal miliary to mid-sized abscesses disseminated throughout all lobes. Cerebral as well as cerebellar grey and white matter revealed randomly distributed foci of acute hemorrhagic necrosis, accompanied by diffuse meningeal hyperemia and mild to moderate multifocal to coalescing suppurative meningitis.

**Laboratory Results:** *Aspergillus fumigatus* was isolated by fungal culture from the brain.

**Histopathologic Description:** Throughout grey and white matter as well as within meninges, there are multiple randomly distributed necrotic foci, composed of central debris, sometimes associated with bright eosinophilic material (Splendore Hoeppli phenomenon), and surrounded by numerous degenerate neutrophils and macrophages besides fewer lymphocytes and plasma cells. Frequently within necrotic centers, few to large numbers of faintly stained fungal hyphae of approximately 3-6 µm width, characterized by regular septation, thin, parallel walls, and dichotomous, progressive acute angle branching are present. Several small to mid-sized arterial blood vessels within the neuropil contain fibrin thrombi that are often admixed with the fungal hyphae described above, accompanied by moderate to marked fibrinoid change and necrosis of vessel walls. The surrounding tissue shows varying degrees of hemorrhage and lytic necrosis in combination with degenerate neutrophils, foamy macrophages (gitter cells), fewer lymphocytes, and plasma cells as well as moderate adjacent gliosis.

*4-1. Telencephalon, putty-nosed monkey: There is a focally extensive area of pallor (malacia) which comprises up to 66% of the section. (HE 7X)*

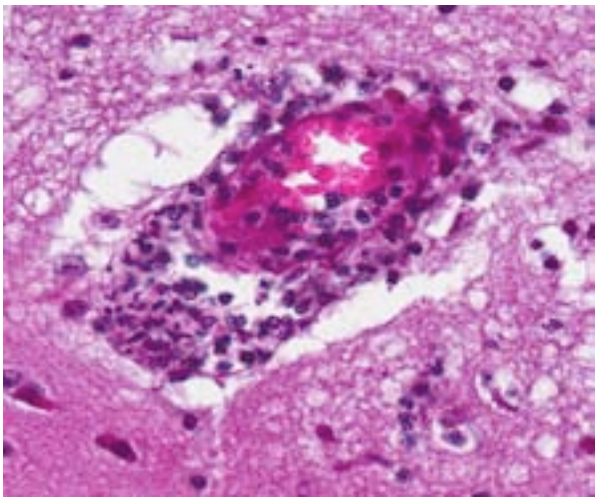

*4-2. Telencephalon, putty-nosed monkey: Throughout the area of necrosis, vessels walls are often expanded by numerous neutrophils (vasculitis) and surrounded by edema fluid. Surrounding neuropil is also edematous. (HE 360X)*

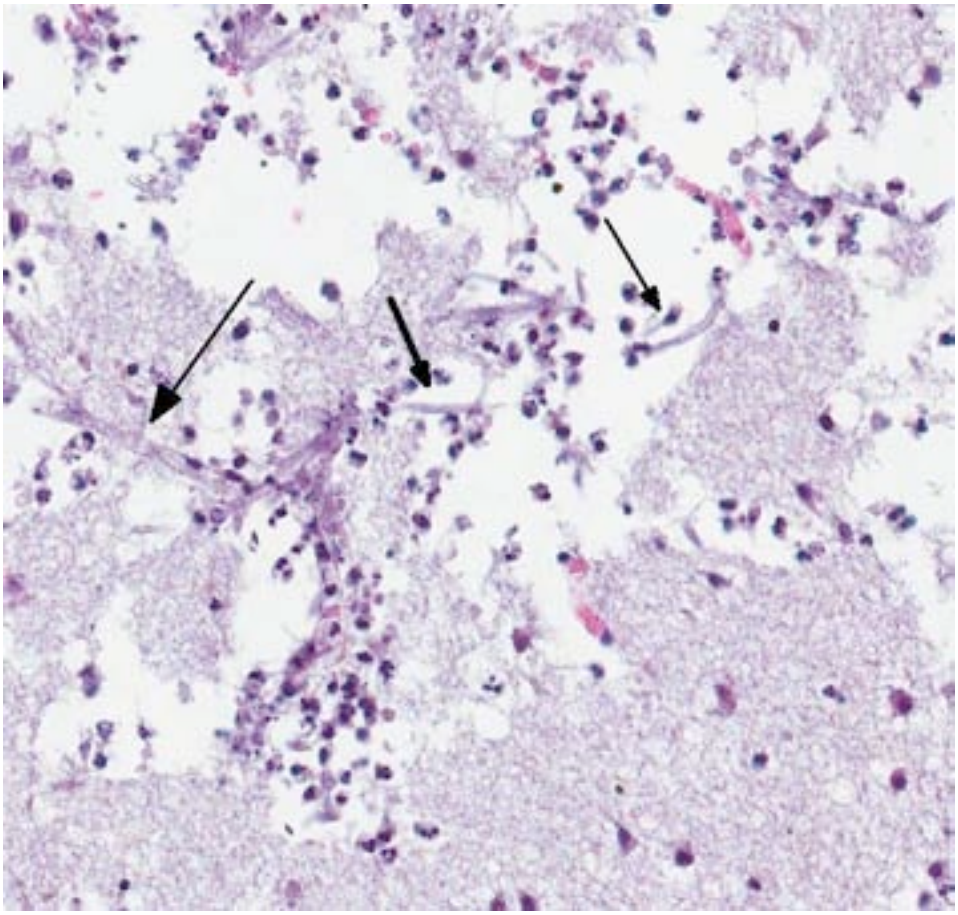

*4-3. Telencephalon, putty-nosed monkey: The necrotic tissue contains moderate numbers of septate fungal hyphae with parallel walls, dichotomous branching (consistent with Aspergillus sp.) both within vessels walls and within the neuropil, as shown here. (HE 400X)*

**Contributor's Morphologic Diagnosis:** Cerebral cortex: Meningoencephalitis, necrotizing, suppurative, acute, multifocal, marked, with multifocal thrombosis, necrosuppurative vasculitis, and numerous intralesional fungal hyphae consistent with *Aspergillus fumigatus*, putty-nosed monkey (*Cercopithecus nictitans*), nonhuman primate.

**Contributor's Comment:** More than 180 *Aspergillus* (*A.*) spp. have been described but only four species (*A. fumigatus*, *A. flavus*, *A. terreus*, *A. niger*) are commonly associated with invasive infection in primates,[5] with *Aspergillus fumigatus* being the most common cause (> 90 %) of human pulmonary fungal infections.[5,7] The uninucleate conidia, or spores, of *Aspergillus* sp. occur in soil, air, water and greatest numbers are found in hay and straw enriched with leaf and grass compost. They are easily dispersed by the wind and have a diameter small enough (2.5 to 3.5 µm) to reach down to the deep airways. They are considered to be the main vehicle for infective transmission, and when they get the chance to germinate inside the body, producing branched septate hyphae that invade tissues, different forms of aspergillosis can develop.[1]

However, the exact portal of entry for the fungal infection could not clearly be identified in the present case. It is possible that *Aspergillus* conidia entered through the perforating wound and germinated within the thoracic cavity, and from there they invaded the blood stream and spread to the lung and central nervous system. But it is also possible the infection route was via inhalation of *Apergillus* spores, resulting in penetration of distal alveolar spaces. Here, there are optimal environmental conditions for germination into angioinvasive filamentous hyphae that can produce local tissue damage, hemorrhage, infarction, and necrosis.[7]

In healthy, immunocompetent individuals, various elements of the pulmonary innate immune system are involved in recognition and elimination of inhaled *Aspergillus* conidia, thereby preventing colonization of the respiratory system. Ciliated and mucus secreting epithelial cells perform effective mucociliary clearance that is important for entrapment and elimination of inhaled conidia. Surfactant, mainly produced by type II pneumocytes and Clara cells, has been implicated in antimicrobial activity with surfactant protein A and D serving as collectins. Alveolar macrophages represent first line phagocytic defense by intracellular killing of swollen spores and prevention of germination. Recruited

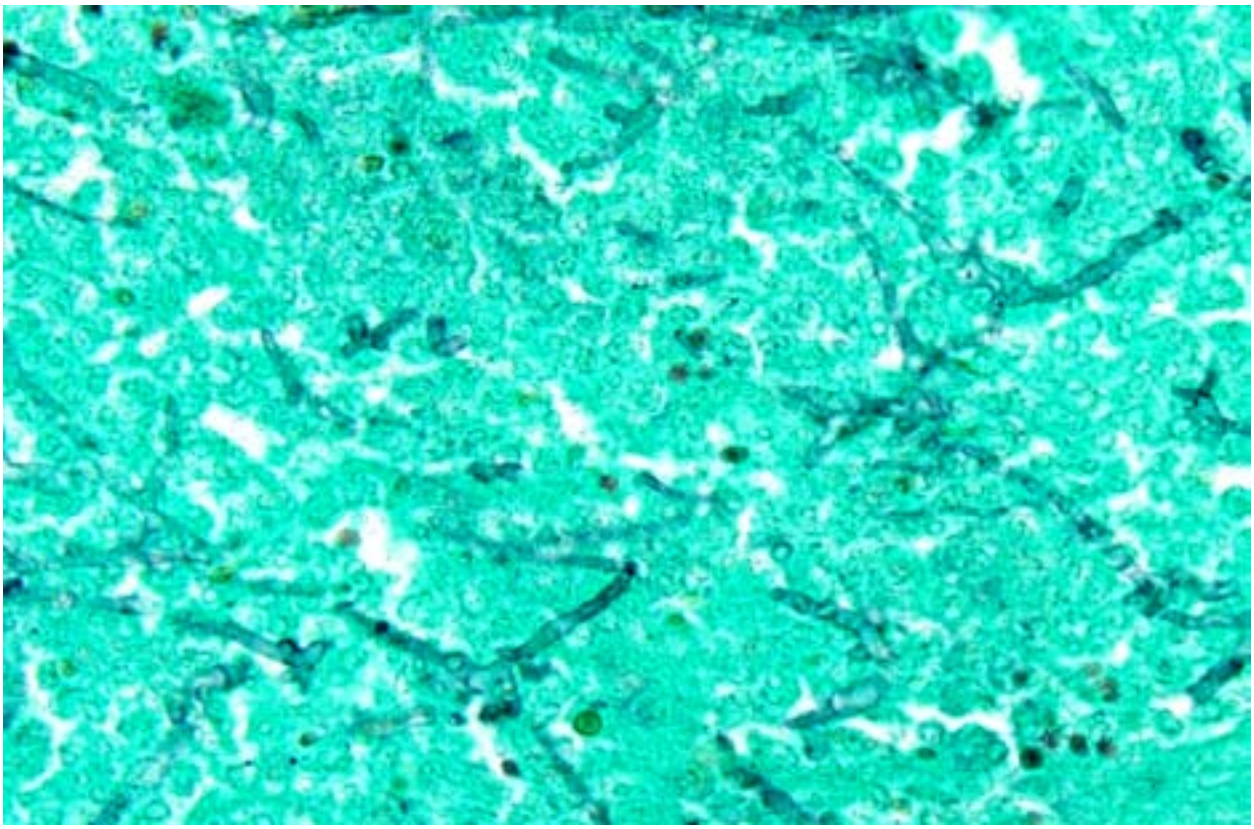

*4-4. Telencephalon, putty-nosed monkey: A silver stain better demonstrates the morphology and number of hyphae within the tissue. (Grocott Methenamine silver, 400X)*

neutrophils play an essential role by extracellular (degranulation) as well as intracellular (phagocytosis) elimination of aspergilli. Dectin-1, expressed by macrophages, neutrophils and dendritic cells, is an important receptor of innate antifungal defense being essential for spore recognition and phagocytosis, as well as production of oxygenated free radicals (fungicide al activity). Above that, certain Toll-like receptors (TLR) have been found to play a predominant role in the recognition of *A. fumigatus* (TLR2: recognition of spores, TLR4: recognition of spores and hyphae).[8]

On the other hand, several pathogenicity factors were found in different *Aspergillus* spp. to overcome certain host defense mechanisms such as endotoxins that inhibit epithelial ciliary activity, as well as a variety of proteases (including elastase, collagenase and trypsin) that damage epithelial cells and, thus, impair effective mucociliary clearance.[1,5] Furthermore, *A. fumigatus* produces a phospholipid capable of decreasing the binding of complement factor C3b to its surface, resulting in disturbed complement activation.[7] Also other fungal proteins of *A. fumigatus* are probably related to virulence by promoting mycelial growth in lung parenchyma or structural alterations of conidia that are resistant to host defense mechanisms.[1]

Moreover, it is likely that *Aspergillus* mycotoxins can work as virulence factors due to direct cytotoxic effects. In vitro studies revealed that aflatoxin (produced by *A. fumigatus*) suppresses the function of macrophages, and ochratoxin (produced by *A. ochraceus*) is cytotoxic to lymphocytes and suppresses lymphocytic, monocytic and granulocytic activity. As other possible immunosuppressive mycotoxins, gliotoxin, fumagillin, fumigacin, fumitremorgin A and Asp-hemolysin are discussed while different mycotoxins together may have synergistic effects. However, further in vivo studies are needed for confirmation of direct relation to *Aspergillus* pathogenesis.[6] Beyond that, melanin pigment, mannitol, catalases and superoxide dismutases are suggested as antioxidant defenses produced by *Aspergillus*.[4] Although it seems that certain antioxidant

molecules produced by *A. fumigatus* do not directly inhibit the oxidizing activity of phagocytes, inhibition of reactive oxygen species production by macrophages (e.g. with high blood cortisol levels or corticosteroid treatment) abolishes their ability to kill the spores while phagocytosis continues so that conidia can germinate and proliferate intracellularly.[8]

However, since pulmonary macrophages and neutrophils constitute a crucial part of first line innate host defense, neutropenia and long-term corticosteroid treatment or hyperglucocorticoidism, as observed in the present case, are generally regarded as major risk factors for the pathogenesis of invasive aspergillosis.[1,4]

**JPC Diagnosis:** Brain, cerebrum: Meningoencephalitis, necrosuppurative, multifocal, severe, with vasculitis, hemorrhage and numerous fungal hyphae.

**Conference Comment:** This is a great case exhibiting the vascular affinity of *Aspergillus* spp. within the brain of this monkey, with its severity alluding to suspicion of an underlying immune compromising condition such as chronic steroid administration. The contributor mentions this may have played a role, and describes the complex interactions of the fungi's virulence factors with the host's immune response; an interaction which often allows it to run amok in susceptible patients.

Aspergillosis is perhaps more readily recognized as the cause of granulomatous pneumonia and air sacculitis in avian species, mycotic rhinitis in dogs, abortion in cattle, secondary abomasal ulcers in ruminants following grain overload or mastitis, and hepatocyte megalocytosis and necrosis in dogs.[2,3] The latter is associated with production of aflatoxin of which there are several produced by *Aspergillus* spp. with $B_1$ being the most significant and best studied example.[10] Toxin production tends to be greatest in stored or unharvested mature grains. Among nonhuman primates, reports of infection are seemingly rare, limited to a single outbreak at the London Zoo in conjunction with tuberculosis. During this outbreak, Old World monkeys were affected by disseminated lesions in the lungs, liver, kidneys and spleen.[9]

**Contributing Institution:** Pathology Unit, German Primate Center, Göttingen, Germany www.dpz.eu

**References:**

1. Al-Alawi A, Ryan CF, Flint JD, et al. *Aspergillus*-related lung disease. *Can Respir J*. 2005;12(7):377-387.
2. Brown CC, Baker DC, Barker IK. Alimentary system. In: Maxie MG, ed. *Jubb, Kennedy, and Palmer's Pathology of Domestic Animals*. 5th ed. Vol. 2. Philadelphia, PA: Elsevier Saunders; 2007:229.
3. Caswell JL, Williams KJ. Respiratory system. In: Maxie MG, ed. *Jubb, Kennedy, and Palmer's Pathology of Domestic Animals*. 5th ed. Vol. 2. Philadelphia, PA: Elsevier Saunders; 2007:640.
4. Dagenais TRT, Keller NP. Pathogenesis of *Aspergillus fumigatus* in invasive aspergillosis. *Clin Microbiol Rev*. 2009;22:447-465.
5. Denning DW. Invasive aspergillosis. *Clin Infect Dis*. 1998;26(4):781-803.
6. Kamei K, Watanabe A. *Aspergillus* mycotoxins and their effect on the host. *Med Mycol*. 2005;Suppl43:S95-S99.
7. Latgé JP. *Aspergillus fumigatus* and aspergillosis. *Clin Microbiol Rev.*1999;12(2): 310-350.
8. Mansour MK, Tam JM, Vyas JM. The cell biology of the innate immune response to *Aspergillus fumigatus*. *Ann NY Acad Sci*. 2012;DOI: 10.1111:78-84.
9. Simmons J, Gibson S. Bacterial and mycotic diseases of nonhuman primates. In: Abee CR, Mansfield K, Tardiff S, Morris, T, eds. *Nonhuman Primates in Biomedical Research: Diseases*. 2nd ed. Vol. 2. San Diego, CA: Elsevier Inc. 2012:156-157.
10. Stalker MJ, Hayes MA. Liver and biliary system. In: Maxie MG, ed. *Jubb, Kennedy, and Palmer's Pathology of Domestic Animals*. 5th ed. Vol. 2. Philadelphia, PA: Elsevier Saunders; 2007:370-371.

**Joint Pathology Center**
**Veterinary Pathology Services**

# WEDNESDAY SLIDE CONFERENCE 2014-2015

## Conference 18

**11 February 2015**

**Guest Moderator:**
Timothy K. Cooper, DVM, PhD, DACVP
Penn State Milton S. Hershey Medical Center
College of Medicine

---

**CASE I:** A (JPC 4048645).

**Signalment:** 9-week-old mixed sex commercial meat rabbits, *Oryctolagus cuniculus.*

**History:** Some members of this group of 9-week-old rabbits were being raised on the barn floor because of insufficient numbers of cages. The rabbits raised on the floor were bedded on shavings. The bedding was changed weekly, and the floor was limed before applying new shavings. Only the rabbits being raised on the floor were dying. The rabbits were initially treated with amprolium for two weeks because of bloody diarrhea but the rabbits developed a bloated appearance, and so were retreated with amprolium for an additional two weeks. Two days following the last treatment, three rabbits were submitted for postmortem examination.

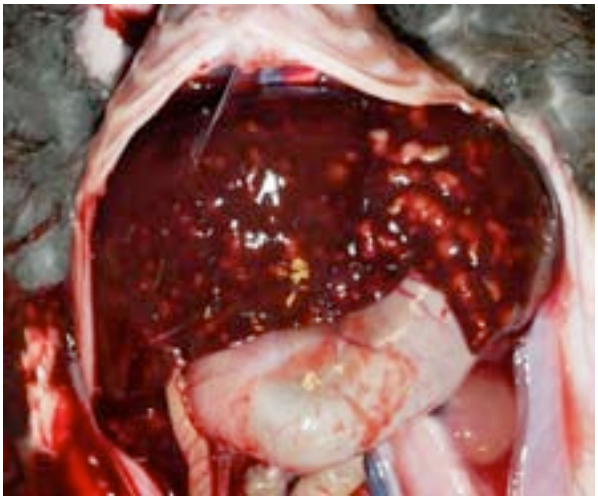

*1-1. Liver, rabbit: The liver was enlarged with numerous tortuous and cystic biliary duct scattered throughout. (Photo courtesy of: Animal Health Laboratory, University of Guelph, Guelph, Ontario, Canada. http://ahl.uoguelph.ca)*

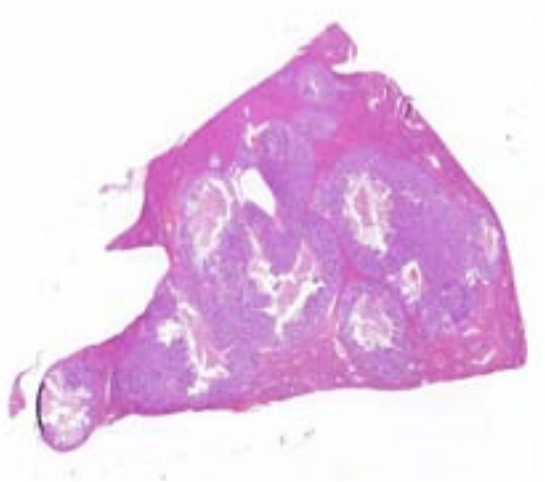

*1-2. Liver, rabbit: Biliary ducts are tortuous and markedly ectatic, replacing large amounts of hepatic parenchyma. (HE 6X)*

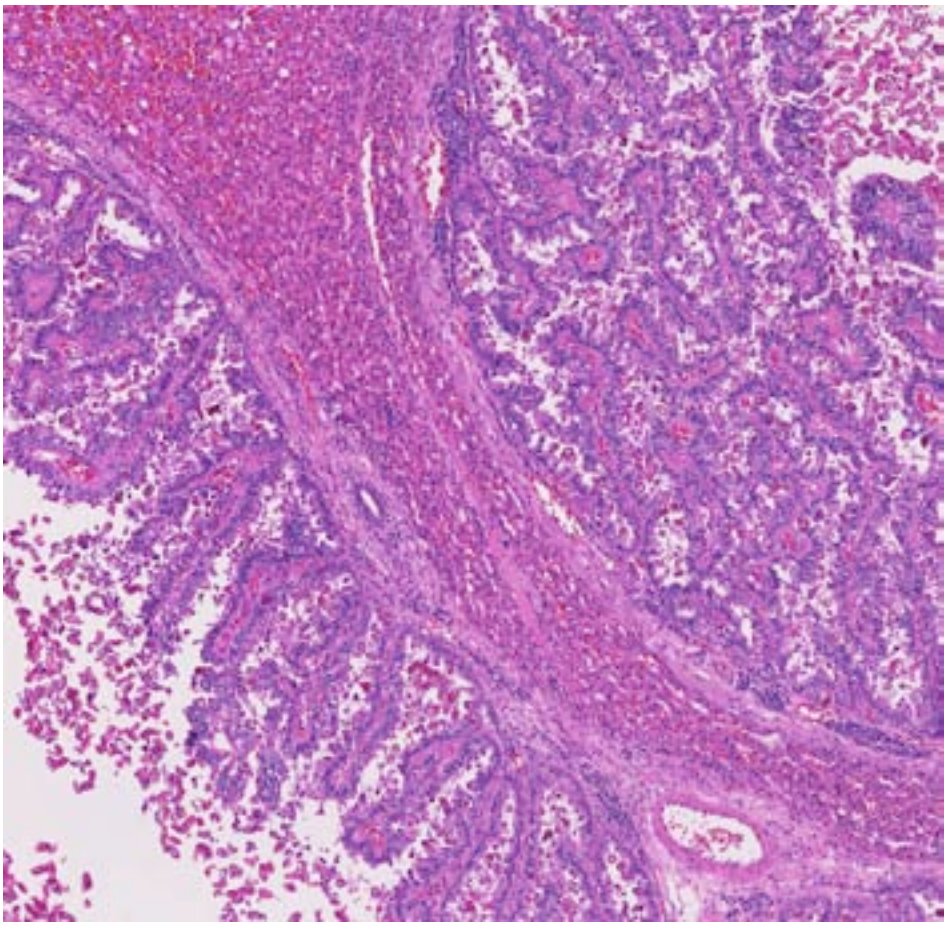

*1-3. Liver, rabbit: Dilated biliary ducts are lined by proliferating epithelium containing numerous life stages of Eimeria stiedae. (HE 38X)*

**Gross Pathology:** The rabbits were in very poor body condition with reduction in muscle mass and marked reduction in external and internal fat stores. Similar internal changes were noted for each. There was increased clear fluid in the abdominal cavity. Stomachs contained feed and the small intestine, cecum and sacculated colon had normal contents. The distal colon and rectum contained normal fecal pellets. The liver was dark red, enlarged with an irregular bosselated capsular surface and large numbers of variably sized, pale, cystic, round to elongate corded nodules filled with turbid pale green yellow fluid were scattered throughout the hepatic parenchyma. The gallbladder was thickened and contained similar cloudy fluid.

**Laboratory Results:** Parasitology: Oocysts with measurements consistent with *Eimeria stiedae* were identified in the biliary fluid collected from the cystic hepatic lesions. Fecal flotation revealed large numbers of a mixture of *Eimeria* spp. oocysts.

**Histopathologic Description:** Liver: There is generalized marked dilation of bile ducts causing compression of the surrounding hepatic parenchyma. Hyperplastic biliary epithelium forms papillary projections into duct lumens. Most epithelial cells are filled with asexual and sexual developmental stages of coccidial organisms and cystic duct lumina contain numerous oocysts. Few to moderate numbers of plasma cells and lymphocytes infiltrate within increased periductal fibrous tissue and within the connective tissue stroma of the proliferative biliary epithelium. Other portal tracts have mild cholangiolar proliferation, mildly increased periportal fibrosis and few to moderate numbers of mixed mononuclear cells within and around biliary epithelium. Occasional portal and hepatic veins contain low numbers of oocysts. Hepatocyte cords are markedly atrophied, and sinusoids are moderately congested and contain increased numbers of circulating neutrophils.

**Contributor's Morphologic Diagnosis:** 1. Marked proliferative and nonsuppurative cholangitis with large numbers of intralesional coccidial organisms. 2. Marked hepatic atrophy. 3. Ascites.

**Contributor's Comment:** While enteric coccidiosis continues to be one of the important potential causes of enteritis in commercial rabbitries in Ontario, hepatic coccidiosis is seldom identified in commercially raised rabbits submitted to our laboratory for diagnostic workup

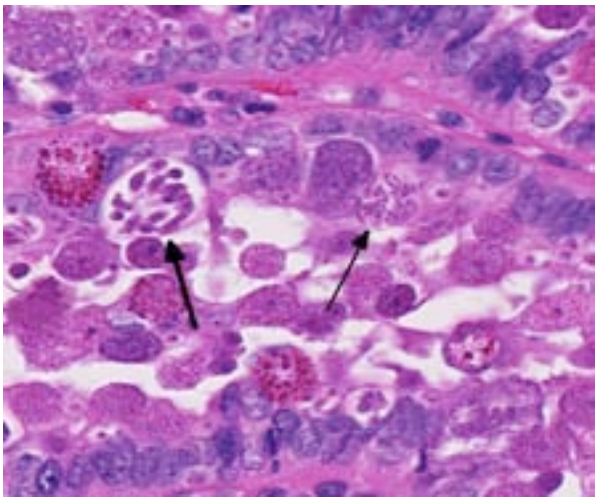

*1-4. Liver, rabbit: Developing schizonts containing numerous merozoites (arrows). (HE 400X)*

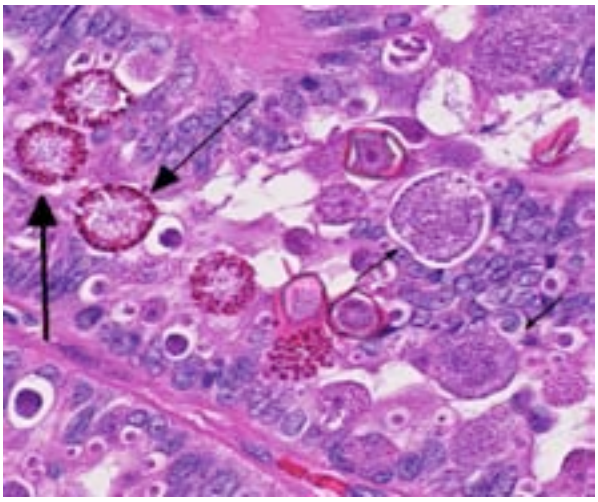

*1-5. Liver, rabbit: Gametes of Eimeria stiedae including macrogametes with brightly eosinophilic plastic bodies at the periphery (large arrows) and microgametes (small arrows). (HE 400X)*

of diarrhea. However, increasingly over the last few years, smaller collections of rabbits raised for meat or as pets are being housed on or provided access to the ground. Owners of these small rabbitries seek veterinary assistance for morbidity and mortality concerns and in turn, the diagnostic laboratory has received increased numbers of phone calls and pathology submissions from veterinary practitioners related to the diagnosis of hepatic coccidiosis in these rabbits.

Infection with *Eimeria stiedae* is usually subclinical and historically, hepatic coccidiosis has been associated with significant condemnations of livers from meat-type rabbits at processing but not with elevated mortality during grow-out.[7] However, if young, naïve rabbits are exposed to high enough levels of sporulated oocysts, clinical disease including anorexia, poor weight gain, weight loss, development of a distended abdomens, diarrhea and elevated mortality can occur.[2,7] In this particular situation, only the rabbits being reared on the floor were clinically affected and although the rabbits submitted for postmortem did not have diarrhea, histologically, they also had significant numbers of coccidial organisms within the intestinal mucosa and results of flotations conducted on feces from all rabbits indicated large numbers of mixed *Eimeria* spp. oocysts. Despite weekly cleaning and rebedding, the environment was heavily contaminated with coccidial oocysts and these rabbits were being continually challenged with both intestinal and hepatic coccidia.

Recommendations for the control of hepatic coccidiosis parallel the recommendations for control of intestinal coccidiosis, and sanitation is of great importance.[2,7] Coccidial oocysts are extremely resistant to environmental influences and no commonly available disinfectants will kill them. Removal of organic material from cages, feed pans and around waterers where oocysts can reside can help reduce the challenge.[7] Rabbits can develop long-lasting immunity to *Eimeria stiedae* as long as they are not exposed to an excessively high dose initially and are immunocompetent.[2]

With the advent of increased interest in raising small groups of rabbits and allowing them access to the ground, hepatic coccidiosis may re-emerge as a clinical disease.

**JPC Diagnosis:** Liver: Cholangitis, proliferative, multifocal to coalescing, chronic, severe, with intra-epithelial coccidia.

**Conference Comment:** There are over a thousand species of *Eimeria,* the vast majority of which are known to primarily infect the epithelial cells lining the gastrointestinal tract.[1] Hepatic coccidiosis is commonly reported in rabbits, known to occur in ferrets (see WSC 2009-2010, Conference 12, Case 2), and reported in some avian species which acquire extra-intestinal coccidiosis to include the liver and kidneys, albeit infrequently.[2,4] Each species has a host specific direct life cycle which originates with the unsporulated oocyst shed in the feces.

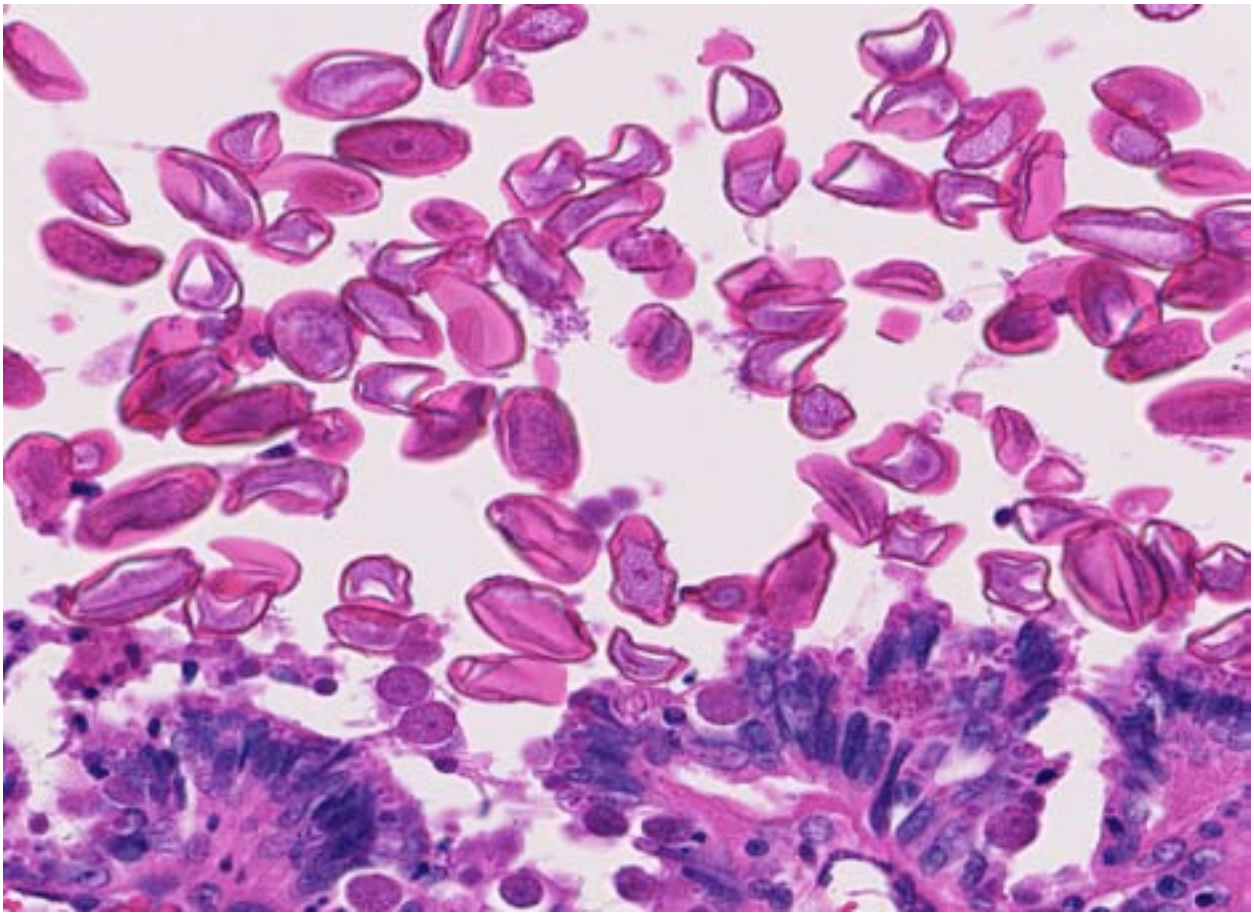

*1-6. Liver, rabbit: The lumen is filled with coccidial oocysts. (HE 400X)*

The oocyst initially contains a single cell called a sporont, and through a process known as sporulation or sporogony, the sporont develops into four sporocysts, each with two sporozoites. This appearance of the sporulated oocyst (4 sporocysts and 8 sporozoites) is a distinguishing feature of *Eimeria* spp. from other coccidian apicomplexans.[1] The sporulated oocyst is now infectious, and sporozoites will be released when ingested by the host.[1] The sporozoites invade epithelial cells and round up to become trophozoites which are the growing forms.[3] Trophozoites undergo asexual nuclear division, called both schizogony and merogony, to form a schizont/meront.[1,3,4] These two terms are used synonymously in most references of this stage, with the term schizogony referring to multiple nuclear divisions (as occurs in *Eimeria* spp. while merogony equates with nonspecific asexual division. Each schizont develops within it numerous merozoites, which following rupture of the host epithelial cell, are released to infect additional cells and subsequently develop into additional schizonts.[4] This process repeats over a variable number of generations depending on the individual species. For reasons still unknown, eventually some merozoites will infect epithelial cells and begin the sexual phase of the life cycle called gametogony.[3] The majority become females (macrogametocytes), while some become males (microgametocytes) which form numerous biflagellate microgametes within epithelial cells.[4] Each microgamete can fertilize a macrogamete to form a zygote known as the oocyst, which are then shed in the feces.[4] Among the phases of this elaborate life cycle, conference participants identified oocysts, schizonts containing merozoites, micro- and macrogametocytes, and micro- and macrogametes in abundance in this case.

In hepatic coccidiosis, this life cycle still begins within gastrointestinal epithelial cells, particularly in the duodenum. Following exposure, sporozoites have been documented in the regional lymph nodes within 12 hours, in bone marrow

within 24 hours, and in the liver within 48 hours.[6,7] Thus, spread by both hematogenous and lymphatic routes have been proposed. Additionally, the organism may infect mononuclear cells which aid in their dissemination.[7] Following gametogony in the biliary epithelium, the oocysts are shed in the bile and passed to the intestines.[7] Numerous oocysts are present in multiple blood vessels in many sections, a finding most participants attributed to an artifact of processing.

*Eimeria stiedae* have a characteristic appearance to the oocyst, with a thinning of the opercula that distinguishes it from all other coccidians in rabbits. There are eight other species of *Eimeria* known to infect rabbits and mixed infections are common, as demonstrated by the fecal results obtained in this case.

**Intestinal Coccidia of Rabbits**

*E. flavescens*
*E. magna*
*E. media*
*E. intestinalis*
*E. irresidua*
*E. perforans*
*E. piriformis*
*E. neoleporis*

**Contributing Institution:** Animal Health Laboratory, University of Guelph, Guelph, Ontario, Canada. http://ahl.uoguelph.ca

**References:**

1. Gardiner CH, Fayer R, Dubey JP. *An Atlas of Protozoan Parasites in Animal Tissues*. 2nd ed. Washington, D.C.: Armed Forces Institute of Pathology/ American Registry of Pathology; 1998.
2. Harkness, JE, PV Turner, S VandeWoude, Wheler CL. Coccidosis (Hepatic) in Rabbits. In: *Harkness and Wagner's Biology and Medicine of Rabbits and Rodents*. 5th ed. Ames, Iowa: Blackwell Publishing; 2010:272-275.
3. Kreier JP, Baker JR. *Parasitic Protozoa*. Winchester, MA: Allen & Unwin; 1987:134.
4. Levine ND. *Protozoan Parasites of Domestic Animals and of Man*. 2nd ed. Minneapolis, MN: Burgess Publishing Co; 1973:156-245.
5. Morgan KJ, Alley MR, Pomroy WE, Gartrell BD, Castro I, Howe L. Extra-intestinal coccidiosis in the kiwi (*Apteryx* spp.). *Avian Pathol.* 2013;42(2):137-146.
6. Owen D. Life cycle of *Eimeria stiedae*. *Nature*. 1970;227:304.
7. Percy DH, Barthold SW. Rabbit. In: *Pathology of Laboratory Rodents and Rabbits*. 3rd ed. Ames, Iowa, USA: Blackwell Publishing; 2007:253-307.

**CASE II**: B (JPC 4048646).

**Signalment:** 1.5-year-old female New Zealand white rabbit, *Oryctolagus cuniculus*.

**History:** In August of 2007, a pet rabbit was presented to an Ontario veterinary clinic with a 3-day history of lethargy, anorexia and facial swelling. The affected animal was one of a group of six housed in a large hutch on a grassy enclosure surrounded by a chain link fence. Chipmunks, other small mammals and occasionally birds were seen within the enclosure on a number of occasions and direct contact with other forms of wildlife could occur across the fence; two dogs also resided on the property.

During the examination, the rabbit was noted to be tachypneic. A 1-cm crust was noted on the nasal planum and skin over the right nares and upper lip was swollen. Excessive waxy debris was present in the left ear canal.

A presumptive diagnosis of *Pasteurella multocida*-induced pneumonia was made and oral antibiotic therapy (chloramphenicol palmitate) was prescribed and initiated. Mineral oil was infused in the left ear and when the luminal debris was removed, mild bleeding and ulceration of the epithelium was noted. Antibiotic ointment was instilled into the ear canal and the animal was discharged. Approximately 30 minutes after leaving the clinic, the owner reported that the animal began choking and bleeding from the nose. Shortly afterwards, the rabbit died and the body was submitted for postmortem examination.

**Gross Pathology:** The rabbit was in good body condition with abundant internal fat stores. Blood stained the inside of the left pinna and a blood clot was present at the base of the ear canal. A 1 cm round raised reddened area was noted on the nasal planum. Blood stained the perinasal and dewlap fur. The tracheal mucosa was mildly congested and there was generalized purple red mottling of the lungs with numerous, up to 3 mm, foci of hemorrhage on the pleural surface and in the parenchyma. Within the abdomen, the spleen was enlarged and congested. There was transmural reddening of the caudal 2 cm of the ileum and the lumen contained a blood clot.

**Laboratory Results:** Low numbers of *E. coli* were isolated from the lung. An alphaherpesvirus isolated from the lung and skin by cell culture was further identified by electron microscopy and

*2-1. Lung, rabbit (fixed specimen): There are multifocal mottled areas of hemorrhage scattered randomly through the parenchyma. (Photo courtesy of: Animal Health Laboratory, University of Guelph, Guelph, Ontario, Canada; http://ahl.uoguelph.ca)*

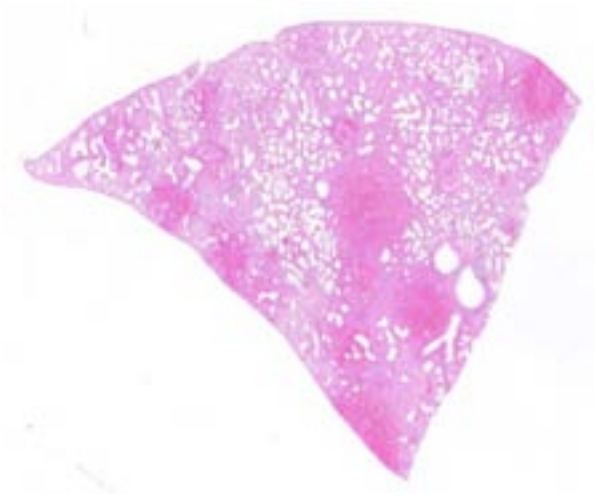

*2-2. Lung, rabbit: Areas of necrosis and hemorrhage correspond to that seen in the gross specimen. The intervening parenchyma is filled with edema fluid. (HE 7X)*

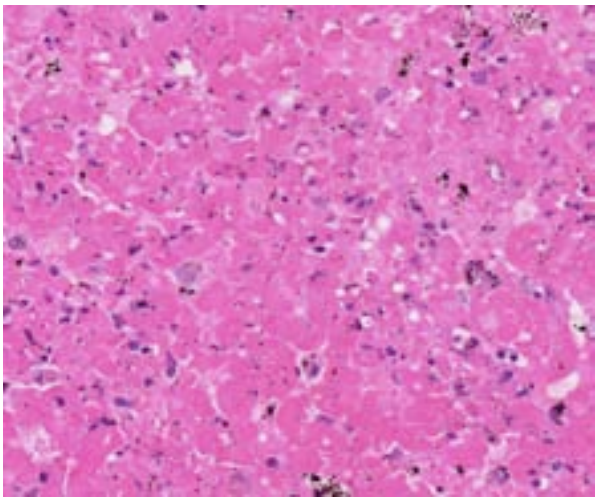

*2-3. Lung, rabbit: There are extensive areas of septal necrosis, with hemorrhage and fibrin deposition within coalescing alveoli. (HE 328X)*

ribonucleotide reductase gene sequencing as *leporid alphaherpesvirus*-4 (LHV-4).[1]

**Histopathologic Description:** There is marked generalized acute necrotizing and hemorrhagic bronchopneumonia with segmental bronchial epithelial proliferation and necrosis, large areas of alveolar necrosis and hemorrhage and flooding of alveoli by edema fluid, fibrin, heterophils and large macrophages. Numerous bronchiolar epithelial cells, bronchiolar epithelial syncytia, pneumocytes, endothelial cells and macrophages contain prominent glassy eosinophilic intranuclear viral inclusions. Several vessels have perivascular hemorrhage, edema, mural fibrinous necrosis, vasculitis and thrombosis. There is patchy alveolar overinflation and emphysema.

**Contributor's Morphologic Diagnosis:** Marked acute generalized necrotizing and hemorrhagic bronchopneumonia with syncytia containing numerous eosinophilic intranuclear viral inclusions.

**Contributor's Comment:** In the early 1990s, two herpes-virus like outbreaks with high mortality characterized by ulcerative dermatitis, pneumonia, splenic necrosis, and gastrointestinal hemorrhage were reported from commercial rabbitries in Alberta[4,6] and British Columbia.[4] In both cases, herpes-like viral particles were identified in formalin-fixed, paraffin-embedded tissue sections and herpesvirus was isolated from affected tissues, but neither isolate was further characterized. However, the disease was experimentally reproduced in meat-type rabbits using one of the isolates. In the summer of 2006, a commercial pet and agricultural rabbitry in Alaska also reported high morbidity and mortality associated with systemic herpesvirus infection.[3] Rabbits were housed outside in open-sided hutches, where mosquito and biting fly activity was high. Snowshoe hares were present in the surrounding area and feral domestic rabbits had been in close proximity to the hutches earlier in the spring. In the following spring and summer, several rabbits from this same rabbitry developed conjunctivitis and skin lesions; and one breeding rabbit that had recovered from clinical infection in the previous year experienced perinatal mortality. The herpesvirus was isolated and characterized as leporid herpesvirus-4.[2]

The case presented here is the first documented and characterized case of leporid herpesvirus-4 infection in a pet Canadian rabbit.[1] This viral disease should be included in the list of differential diagnoses for acute morbidity and mortality in domestic rabbits presenting with epistaxis or respiratory distress, which presently includes rabbit hemorrhagic disease virus (RHDV), peracute *Pasteurella multocida* septicemia or chronic *Pasteurella multocida* pleural/pulmonary abscessation with rupture.

**JPC Diagnosis:** Lung: Pneumonia, bronchointerstitial, necrohemorrhagic, multifocal to coalescing, acute, severe, with intranuclear viral inclusions and syncytia.

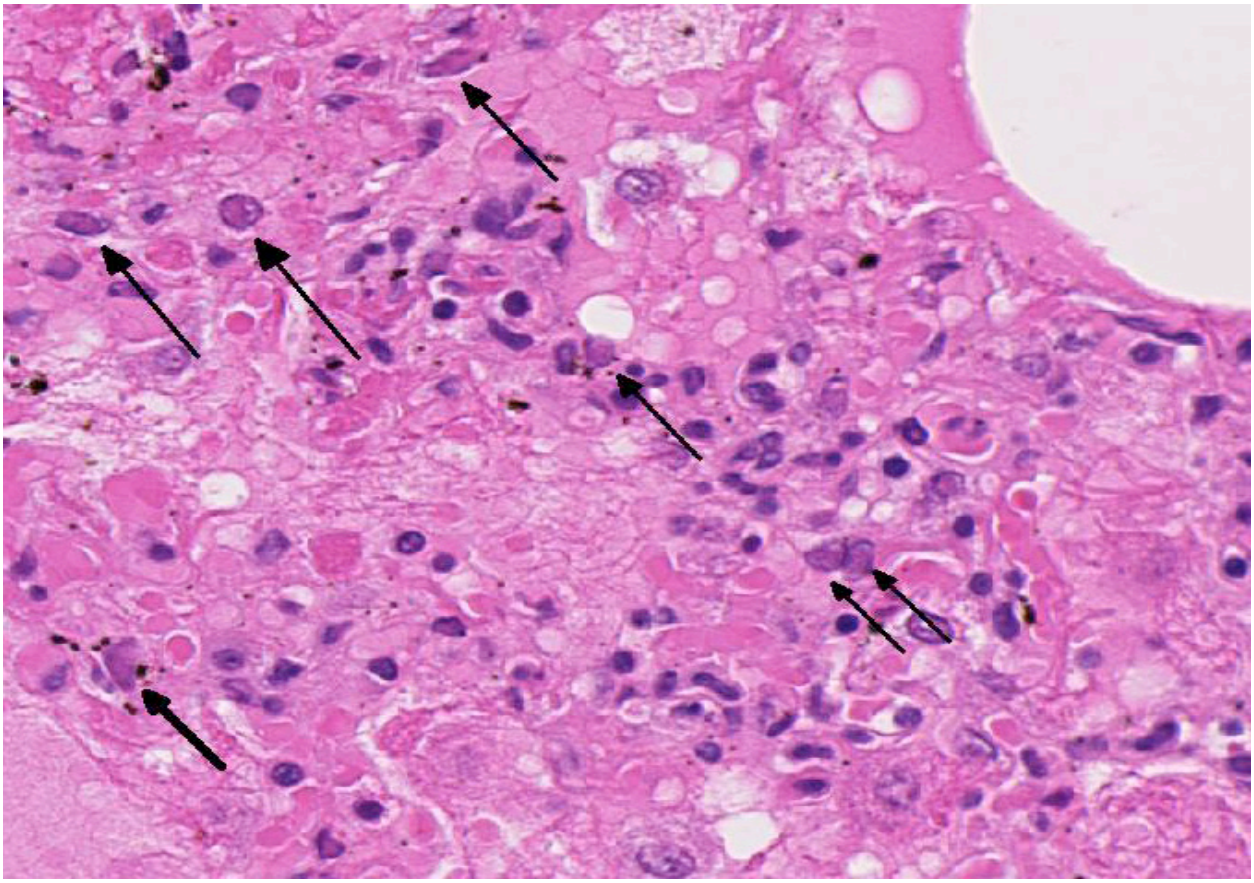

*2-4. Lung, rabbit: Within areas of necrosis, numerous cells of various lineage contain eosinophilic intranuclear viral inclusions. (HE 400X)*

**Conference Comment:** There are four known herpesviruses of rabbits, two of which are gammaherpesviruses that produce lymphoproliferative disease and neoplasia (*Leporid herpesvirus 1* and *Leporid herpesvirus 3*). *Leporid herpesvirus* 2 is also a gammaherpesvirus, but is capable of inducing encephalitis. Additionally, natural infections of *Human herpesvirus* 1 (herpes simplex) have been reported in rabbits causing a fatal encephalitis.[7] The virus demonstrated in this case, *Leporid herpesvirus* 4 (LHV4), is a novel herpesvirus with rare reports in the literature as the contributor highlighted.

LHV-4 is classified as an alphaherpesvirus on the basis of its rapid growth and cytopathic effect in cell culture.[5] This case illustrates the severity of bronchopneumonia which results from infection and leads to the reported 50% morbidity and 29% mortality rates.[6] Additionally, ulcerative rhinitis and splenic necrosis has been observed in experimental infections, and hemorrhagic dermatitis and myocarditis in natural infections.[5]

**Contributing Institution:** Animal Health Laboratory, University of Guelph, Guelph, Ontario, Canada; http://ahl.uoguelph.ca

**References:**

1. Brash ML, Nagy E, Pei Y, Carman S, Emery S, Smith AE, Turner PV. Acute hemorrhagic and necrotizing pneumonia, splenitis, and dermatitis in a pet rabbit caused by a novel herpesvirus (*leporid herpesvirus-4*). *Can Vet J*. 2010;51:1383-1386.
2. Jin L, Lohr CV, Vanarsdall AL, Baker RJ, Moerdyk-Schauwecker M, Levine C, et al. Characterization of a novel alphaherpesvirus associated with fatal infections of domestic rabbits. *Virol*. 2008;378:13-20.
3. Jin L, Valentine BA, Baker RJ, Lohr CV, Gerlach RF, Bildfell RJ, Moerdyk-Schauwecker M. An outbreak of fatal Herpesvirus infection in domestic rabbits in Alaska. *Vet Pathol*. 2008;45:369-374.
4. Onderka DK, Papp-Vid G, Perry AW. Fatal herpesvirus infection in commercial rabbits. *Can Vet J*. 1992;33:539-543.

5. Sunohara-Neilson JR, Brash M, Carman S, Nagy E, Turner PV. Experimental infection of New Zealand White rabbits (*Oryctolagus cuniculi)* with *Leporid herpesvirus* 4. *Comp Med*. 2013;63(5):422-431.
6. Swan C, Perry A, Papp-Vid G. Herpesvirus-like viral infection in a rabbit. *Can Vet J*. 1991;32:627-628.
7. Weissenbock H, Hainfellner JA, Berger J, Kasper I, Budka H. Naturally occurring herpes simplex encephalitis in a domestic rabbit (*Oryctolagus cuniculus*). *Vet Pathol.*1997;34(1): 44-47.

**CASE III**: 13-1079 (JPC 4031940).

**Signalment:** 2-year-old female rabbit, *Oryctolagus cuniculus*.

**History:** There is a ten-day history of increasing bloody discharge from the vulva. Abdominal palpation and abdominal radiographs revealed an enlarged uterus. An ovariohysterectomy was performed and the uterus was submitted.

**Gross Pathology:** Uterus was received in formalin. Uterine horns are enlarged and filled with brown to black watery fluid and blood clots.

**Laboratory Results:** The PCV before surgery was 14%.

**Histopathologic Description:** Uterus: A blood vessel in the endometrium is markedly dilated and filled with blood, laminated fibrin, and neutrophils mixed with karyorrhectic debris (thrombus). The endometrium overlying this area is thin with only 1 layer of low cuboidal cells and 2 to 3 layers of collagen separating it from the endometrium of the dilated vessel. The uterine lumen is markedly compressed by the aneurysmal vessels. In one section, the thrombus is adhered to the wall of the vessel (will vary with section). There are hemosiderin laden macrophages focally in the adjacent endometrium (in some sections).

**Contributor's Morphologic Diagnosis:** Uterus: Endometrial venous aneurysms.

**Contributor's Comment:** Hematuria in rabbits has been associated with uterine adenocarcinoma, uterine polyps, renal infarction, urolithiasis, cystitis, bladder polyps, pyelonephritis and uterine endometrial venous aneurysms.[2,3,7] The most common clinical signs with venous aneurysms are hematuria or urogenital bleeding.[1,2] Occasionally, the aneurysms are associated with mild anemia and proteinuria.[1] Varices and aneurysms of uterine subserosal and myometrial venous plexi, but not of endometrial vessels, have been reported in women. Similar endometrial aneurysms have been seen in rats and mice. In rabbits, at necropsy, clotted blood may be found within the uterine

*3-1. Uterus, rabbit: A large distended vein in the uterine wall contains a lamellated thrombus. (HE 7X)*

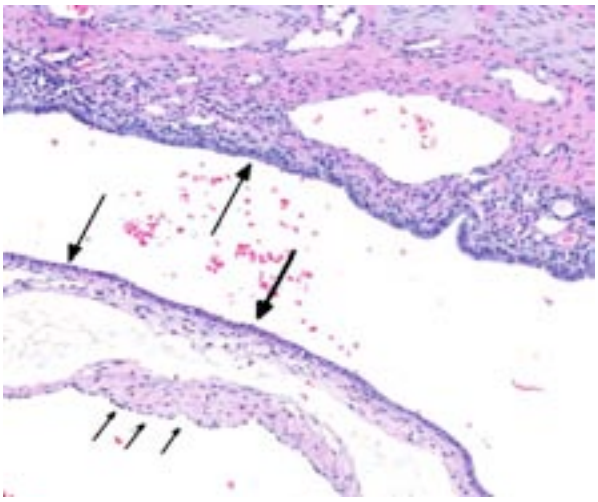

*3-2. Uterus, rabbit: The wall of the aneurysmal vein is endothelial- lined (small arrows). The vein is present within the uterine endometrium (large arrows). (HE 120X)*

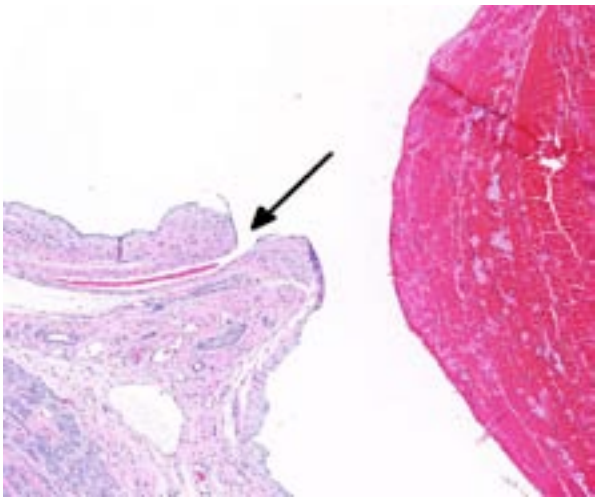

*3-3. Uterus, rabbit: The feeder vein of this aneurysm is visible in some sections. (HE 70X)*

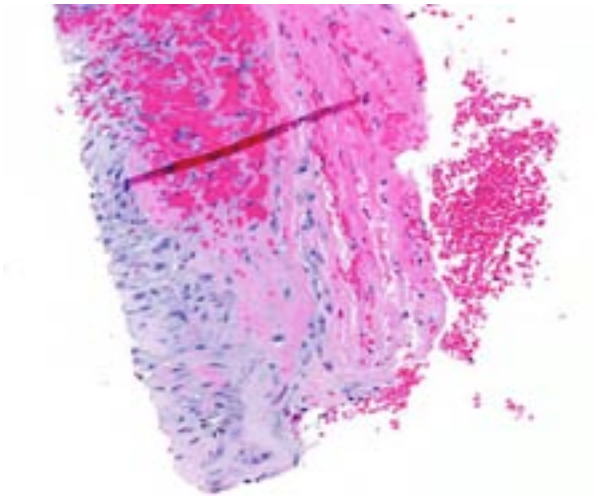

*3-4. Uterus, rabbit: At one edge of the thrombus, the proliferation of fibroblasts and immature collagen represents the nascent organization of this thrombus. (HE 120X)*

lumen.[6] Non-pregnant multiparous does are most affected.[7] The defect is likely congenital.[7]

**JPC Diagnosis:** Uterine horn: Endometrial venous aneurysm, with thrombosis.

**Conference Comment:** In rare sections in this case, the origin of the venous aneurysm is visible within the vessel wall. By definition, an aneurysm is a localized dilatation of a vessel due to widening of the lumen which causes an abnormal attenuated vascular wall. In normal branching vessels, the elastic fibers contract but are continuous when the area of branching is cut into histologic section. In this case, when present, a small vessel empties into this large aneurysm and the elastic fibers are lost at this point of transition, enabling participants to definitively identify it as the aneurysmal origin. Aneurysms should be contrasted with false aneurysms or dissections, which are a defect in the vascular wall leading to an extravascular hematoma.[6] Both aneurysms and dissections can rupture, often with catastrophic consequences.[6]

Aneurysms occur when the structure or function of the connective tissue within the vascular wall is compromised, often during the continuous remodeling process it undergoes to maintain structural integrity.[6] These defects can occur as a congenital condition or be acquired over time with progressive weakening of the wall. Increased expression of matrix metalloproteases (MMPs) and decreased expression of tissue inhibitors of metalloproteinases (TIMPs) often contributes to this degradation.[6] MMPs, which require metal ions such as zinc for their activity, are instrumental in the process of remodeling the extracellular matrix, to include vascular remodeling.[5] Additionally, MMPs play a prominent role in tumorigenesis due to their prominent role in cell turnover and migration, and regulating signal pathways of cell growth, inflammation and angiogenesis leading to a large body of research on these proteinases.[4] Specific to angiogenesis, MMP-2 and MMP-9 are cited as both pro and anti-angiogenic while MMP-1, MMP-7, and MMP-14 are specifically pro- while MMP-12 is anti-angiogenic.[4] MMPs are produced by a variety of cell types and regulated by growth factor and cytokine secretion. Their activity is

tightly controlled as they are rapidly depleted by TIMPs produced by most mesenchymal cells.[5] When this MMP/TIMP balance is altered, such as occurs with inflammation in atherosclerosis or vasculitis, the risk of aneurysm formation increases.[6]

**Contributing Institution:** Department of Biomedical and Diagnostic Sciences, College of Veterinary Medicine, University of Tennessee, Knoxville, TN

**References:**

1. Allison N. Anemic virgin female rabbits. *Lab Anim*. 2003;32(2):23-25.
2. Bray MV, Weir EC, Brownstein DG, Delano ML. Endometrial venous aneurysms in three New Zealand white rabbits. *Lab Anim Sci.* 1992;42(2): 360-362.
3. Garibaldi BA, Fox JG, Otto G, Murphy JC, Pecquet-Goad ME. Hematuria in rabbits. *Lab Anim Sci*. 1987;37(6):769.
4. Kessenbrock K, Plaks V, Werb Z. Matrix metalloproteinases: regulators of the tumor microenvironment. *Cell*. 2010;141:52-67.
5. Kumar V, Abbas AK, Aster JC. Inflammation and repair. In: Kumar V, Abbas AK, Aster JC, eds. *Robbins and Cotran Pathologic Basis of Disease*. 9th ed. Philadelphia, PA: Elsevier Saunders; 2015:105.
6. Mitchell RN. Blood vessels. In: Kumar V, Abbas AK, Aster JC, eds. *Robbins and Cotran Pathologic Basis of Disease*. 9th ed. Philadelphia, PA: Elsevier Saunders; 2015:501-502.
7. Percy DH, Barthold SW. Rabbit. In: *Pathology of Laboratory Rodents and Rabbits*. 3rd ed. Hoboken, NJ: Wiley-Blackwell; 2008:253-307.

**CASE IV:** N2013-1019 (JPC 4048674).

**Signalment:** Adult male chinchilla, *Chinchilla lanigera.*

**History:** The chinchilla was found dead with no reported premonitory signs. This animal was one of seven chinchillas submitted for necropsy during an approximately 3-week period that were either noted to exhibit respiratory distress and tachypnea or found dead without premonitory signs.

**Gross Pathology:** The caudal portion of the right cranial lung lobe was firm and mottled red to tan. Small amounts of soft to gelatinous, pale tan material were adhered to the pleural surface of the affected lung lobe. All lung lobes oozed a small volume of clear fluid on section.

**Laboratory Results:** Aerobic bacterial culture of the lung yielded the growth of many *Bordetella bronchiseptica*; *B. bronchiseptica* was also identified in three additional chinchillas with similar gross and histologic lesions. *Mycoplasma* culture and pneumovirus PCR were negative.

**Histopathologic Description:** In the most severely affected sections, 50-75% of airways and alveolar spaces are multifocally obscured and expanded by large numbers of heterophils that are often degenerate with poorly demarcated, round to streaming nuclei (oat cells), macrophages, small numbers of lymphocytes and plasma cells, aggregates of homogenous, eosinophilic material (fibrin), wispy to granular eosinophilic material (fibrin and proteinaceous fluid), and variable amounts of cellular and karyorrhectic debris (necrosis). Large numbers of small, <1 x 2 µm coccobacilli form dense intra- and extracellular colonies. Similar inflammation and necrosis also obscures and replaces alveolar septa. Bronchial and bronchiolar epithelial cells are often hypertrophic (reactive) with occasional areas of attenuation and infrequent piling of cells (hyperplasia). There are multifocal areas of acute alveolar hemorrhage and erythrophagocytosis. The adventitia surrounding pulmonary vessels and airways is often expanded by clear space with wispy, eosinophilic material and small numbers of heterophils, macrophages, lymphocytes and plasma cells. The alveolar spaces surrounding areas of intense inflammation contain copious amounts of wispy, eosinophilic material (edema) and moderate numbers of macrophages with foamy cytoplasm and fewer heterophils and lymphocytes. Moderate amounts of fibrin with small numbers of associated heterophils, macrophages and lymphocytes are adhered to the pleural surface multifocally; the underlying pleura is lined by plump, reactive mesothelial cells. In less severely affected sections, small to moderate numbers of heterophils infiltrate the bronchial and bronchiolar mucosa and are associated with small amounts of fibrin and edema. Alveolar septa are multifocally fragmented with the formation of large alveolar spaces (emphysema). Small numbers of lymphocytes, plasma cells and heterophils mildly expand perivascular spaces.

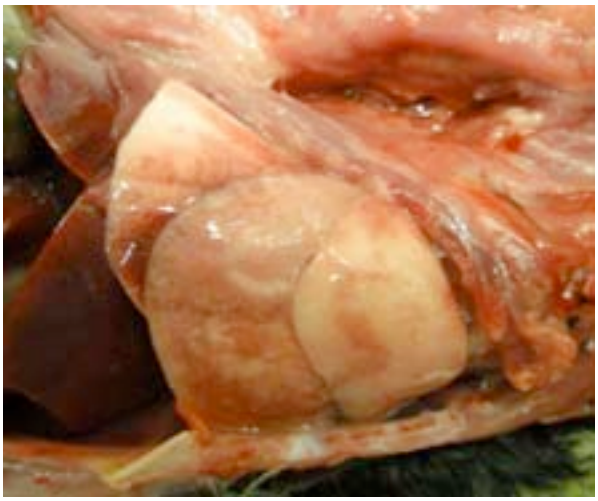

*4-1. Lung, chinchilla: The right lung lobes were firm and mottled red to tan. (Photo courtesy of: Wildlife Conservation Society, Zoological Health Program, Bronx, NY. www.wcs.org*

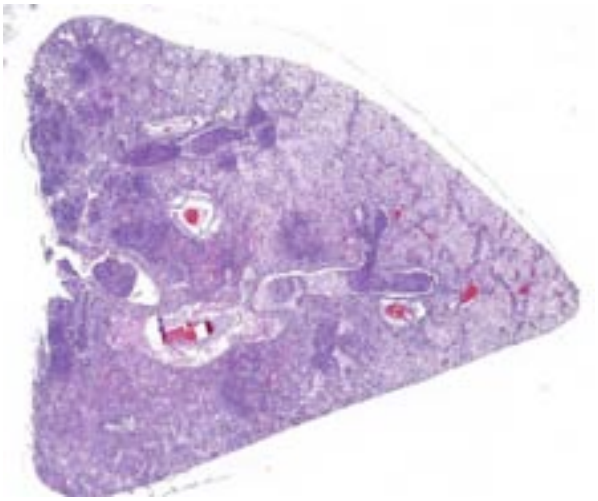

*4-2. Lung, chinchilla: The filling of airways with exuberant suppurative exudate clearly defines this pattern as a bronchopneumonia. (HE 9X)*

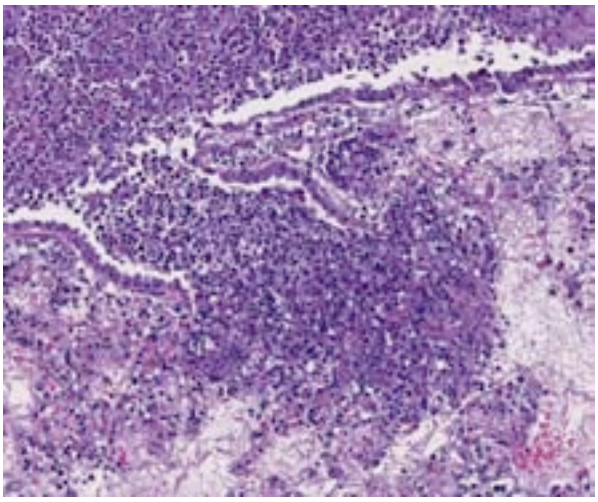

*4-3. Lung, chinchilla: Airways are filled with degenerate neutrophils which erupt through the ulcerated bronchiolar wall into surrounding alveolae. (HE 148X)*

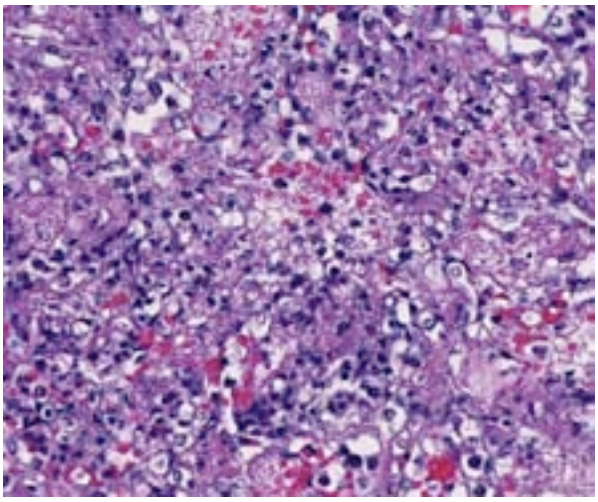

*4-4. Lung, chinchilla: Throughout the lung, in areas adjacent to airways, there are extensive areas of septal necrosis. (HE 228X)*

**Contributor's Morphologic Diagnosis:** Lung: Bronchopneumonia, necrosuppurative, fibrinous, acute, severe with oat cells, pulmonary edema, alveolar hemorrhage, fibrinous pleuritis and intralesional, intra- and extracellular coccobacilli colonies.

Nasal cavity (tissue not submitted): Rhinitis, mucopurulent, diffuse, moderate, subacute with intralesional, intra- and extracellular coccobacilli colonies and multifocal, mild mucosal erosion and ulceration.

**Contributor's Comment:** Gross, histologic and ancillary findings were consistent with a diagnosis of pulmonary and upper respiratory bordetellosis. *Bordetella bronchiseptica* was isolated from samples of lung for all chinchillas (*n=4)* that were submitted for aerobic bacterial culture, and all 7 chinchillas showed similar gross and histologic features. While *B. bronchiseptica* can commonly be a secondary, opportunistic pathogen, as lung samples were negative for consistent growth of other significant bacteria, *Bordetella* is believed to be the primary cause of disease in these chinchillas. Other significant associated findings in the affected chinchillas included rhinitis (*n*=3), tracheitis (*n*=2) and otitis media (*n*=1). Though not present in the submitted case, affected chinchillas with a more prolonged disease period demonstrated marked pneumocyte hyperplasia and hypertrophy; lung samples were negative for pneumovirus by quantitative PCR.

In small mammals, respiratory bordetellosis is most commonly reported in guinea pigs and rabbits; however, outbreaks in commercial chinchilla operations have been documented.[2] The contributor has also observed similar histologic changes, including the presence of prominent colonies of coccobacilli, in wild eastern gray squirrels (*Sciureus carolinensis*) with pulmonary bordetellosis. Other species in which *B. bronchiseptica* can be a significant pathogen include dogs (infectious tracheobronchitis), cats (tracheitis and bronchopneumonia) and pigs (atrophic rhinitis and neonatal pneumonia).

Like *Mannheimia* and *Actinobacillus spp.*, *Bordetella bronchiseptica* encodes a pore-forming, "repeat in toxin" (RTX) family virulence factor, adenylate cyclase toxin (ACT). ACT is an essential virulence factor that can: i) disable innate immunoprotective functions, including phagocytosis, chemotaxis, and superoxide production, ii) modulate immune responses through alterations in cytokine secretions, and iii) trigger apoptosis in macrophages.[5] Other important virulence factors of *B. bronchiseptica* include filamentous hemagglutinin (FHA), dermonecrotic toxin (DNT), tracheal cytotoxin, osteotoxin, fimbriae and a Type-III secretion system.[5]

**JPC Diagnosis:** Lung: Pleuropneumonia, necrotizing and fibrinosuppurative, acute, multifocal to coalescing, severe, with numerous bacilli.

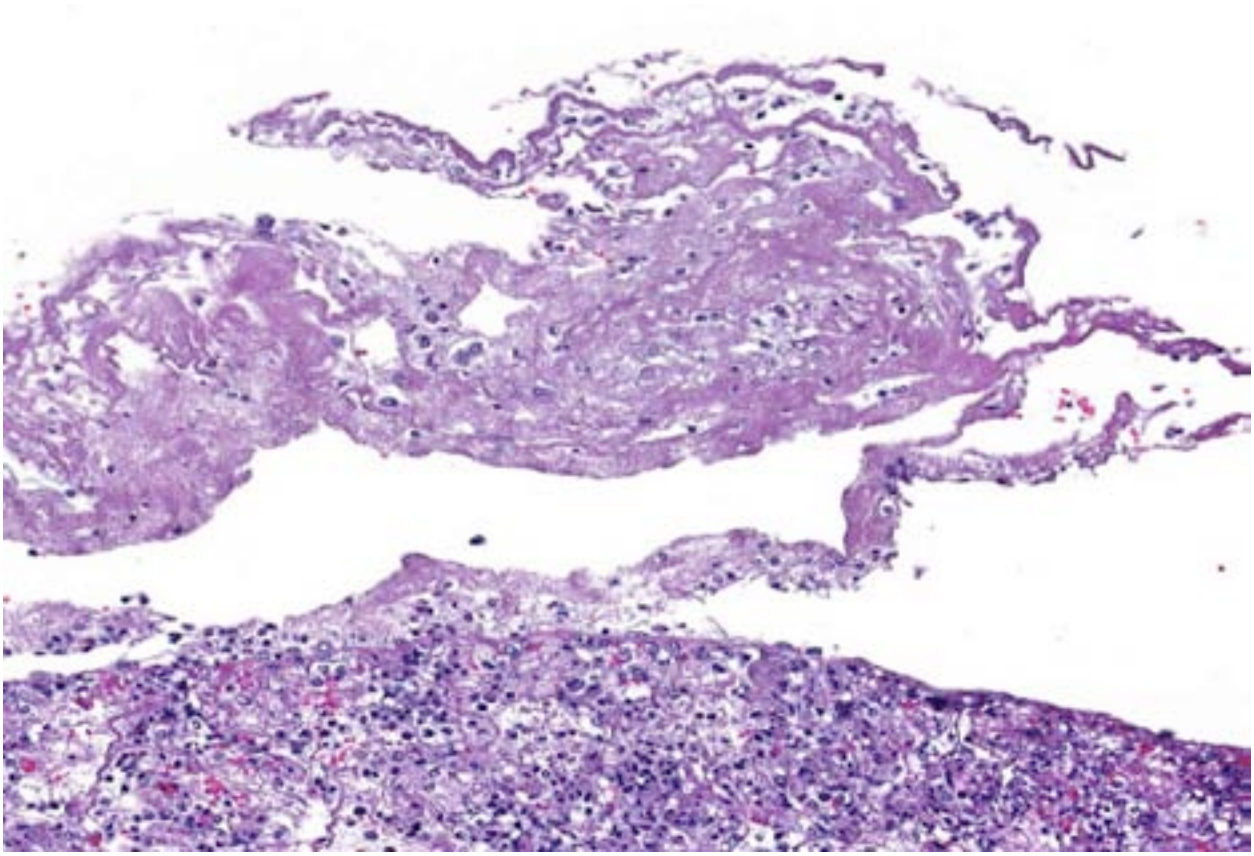

*4-5. Lung, chinchilla: The pleura is multifocally expanded by abundant fibrin, few degenerate neutrophils, and small amounts of cellular debris. (HE 320X)*

**Conference Comment:** This is a great descriptive case with an impressive abundance of fibrin within most alveolar airways and, in some sections, causing a thickening of the pleura. *Bordetella bronchiseptica* has an array of virulence factors as explained by the contributor, yet in many domestic animal species it is a known commensal organism of the upper respiratory tract. Its presence is not typically equitable with clinical disease unless an immune compromising event takes place in the host.[1] Of particular importance in laboratory species is its ability to take refuge within clinically normal rabbits, and subsequently spread to and wreak havoc in guinea pigs if housed in close proximity.[4] Pulmonary lesions are typically suppurative in most species, though fibrinous exudation within alveoli has been described in acute cases.[4] Fibrinous bronchopneumonias or pleuropneumonias are the result of severe pulmonary injury and, thus cause death earlier in the sequence of the inflammatory process than suppurative pneumonias.[3] Dramatic clinical signs and death can occur even in cases involving only 30% or less of the total pulmonary surface area.[3] Although lesions in this case had areas of suppurative inflammation, fibrin predominated and this finding correlates with the rapid onset and death provided in the case history.

**Contributing Institution:** Wildlife Conservation Society, Zoological Health Program, Bronx, NY. www.wcs.org

**References:**

1. Caswell JL, Williams KJ. Respiratory system. In: Maxie MG, ed. *Jubb, Kennedy, and Palmer's Pathology of Domestic Animals*. 5th ed. Philadelphia, PA: Elsevier Saunders; 2007:638-639.

2. Lazzari AM, de Vargas AC, Dutra V, et al. Infectious agents isolated from Chinchilla laniger. *Ciência Rural*. 2001;31:337-340.

3. Lopez A. Respiratory system, mediastinum, and pleurae. In: Zachary JF, McGavin MD, eds. *Pathologic Basis of Veterinary Disease*. 5th ed. St. Louis, MO: Elsevier Mosby; 2012:499-500.

4. Percy DH, Barthold SW. *Pathology of Laboratory Rodents and Rabbits*. 3rd ed.

Hoboken, NJ: Wiley-Blackwell; 2008:226-228, 267-268.
5. Register K, Harvill E. Bordetella. In: Gyles CL, Prescott JF, Songer G, Thoen CO, eds. *Pathogenesis of Bacterial Infections in Animals.* 4th ed. Ames, IA: Wiley-Blackwell; 2010:411-427.

**Joint Pathology Center**
**Veterinary Pathology Services**

# WEDNESDAY SLIDE CONFERENCE 2014-2015

## Conference 19

**1 April 2015**

---

**CASE I:** PA 4683 (JPC 3136052).

**Signalment:** Adult (age unspecified) female ferret, *Mustela putorius furo.*

**History:** This was one of several ferrets in this colony suffering from debilitation due to watery diarrhea. The animal died despite supportive care and a necropsy was performed by the overseeing clinical veterinarian.

**Gross Pathologic Findings:** No gross lesions were reported in the gastrointestinal tract. Lungs appeared collapsed and atelectatic, with multifocal pale, plaque like areas of discoloration noted throughout all lobes.

**Laboratory Results:** PCR evaluation of feces was positive for ferret enteric coronavirus (FECV).

*1-1. Lung, ferret: Numerous variably-sized white plaques are present within all lung lobes but are most concentrated in cranial lobes. (Photo courtesy of: Division of Laboratory Animal Resources, University of Pittsburgh. http://www.dlar.pitt.edu/)*

*1-2. Lung, ferret: Cross sections of lung tissue demonstrate the pleural location of the inflammatory nodules. (Photo courtesy of: Division of Laboratory Animal Resources, University of Pittsburgh. http://www.dlar.pitt.edu/)*

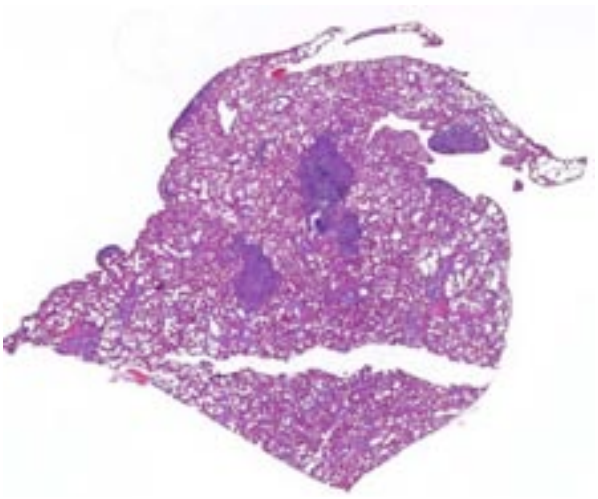

*1-3. Lung, ferret: Multiple 2-3mm inflammatory nodules are scattered throughout the lung parenchyma. (HE 6X)*

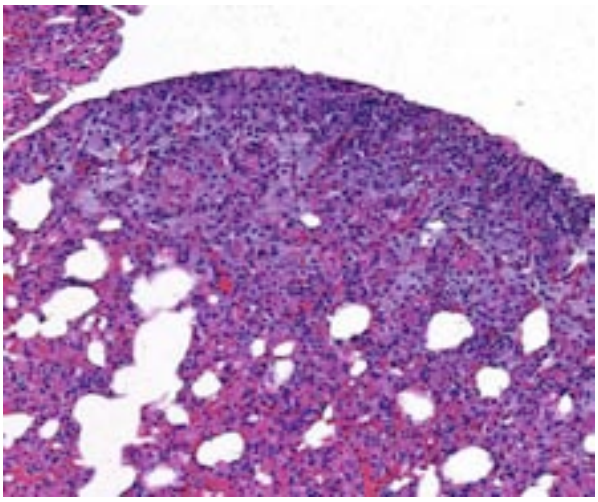

*1-4. Lung, ferret: Smaller subpleural inflammatory nodules are composed of foamy, lipid laden histiocytes admixed with fewer lymphocytes and plasma cells. (HE 128X)*

**Histopathologic Description:** Multiple slides were submitted from different blocks in this case and there is some variation in the appearance and distribution of lesions between cuts.

Multifocal, often coalescing areas of lipid pneumonia are present. These are often (correlative to the gross distribution of lesions seen) present in subpleural locations, although foci deep within pulmonary parenchyma are often noted. Some areas consist solely of homogeneous alveolar aggregates of foamy macrophages. Others are comprised of more dense mixed inflammatory infiltrates including histiocytes, lymphocytes, scattered neutrophils and occasional multinucleated giant cells. Cholesterol clefts and crystals are often seen in association with these latter areas. Infrequent focal areas of alveolar thickening and mild interstitial fibrosis are also noted in some lesions.

In general, most other adjacent lung tissue is atelectatic due to post-mortem collapse, but evidence of other concurrent chronic or active pulmonary disease processes (e.g. foreign body material, observable organisms, neoplasia, etc.) was not noted.

**Contributor's Morphologic Diagnosis:** Lipid pneumonia (lipogranulomas), subacute-chronic, multifocal and coalescing, mild to moderate (section dependent) – consistent morphologically with endogenous lipid pneumonia of ferrets.

**Contributor's Comment:** Endogenous lipid pneumonia is seen commonly as an incidental finding in ferrets[9,11] and was not thought to be related to the cause of death or of clinical significance in this animal. Although the specific cause of lipid pneumonia in general is often unknown, the entity has been reported widely over a large spectrum of species, both wild and domestic,[2,3,7,12,14] as well as in humans.[1,13] In general, such disease (i.e. lipid pneumonia) is often categorized as exogenous or endogenous (EnLP). The former is usually associated with aspiration from oral or nasal administration of mineral oil or petroleum-based compounds due to a failure to provoke either airway (glottic closure or cough) or mucociliary transport response mechanisms.[1] EnLP has a variety of both known and suspected causes as well as numerous other observed associations. Despite this, in many cases the exact underlying pathogenesis remains undetermined and is probably multifactorial.[3,7] In general, either bronchial obstruction or direct pneumocyte injury leads to overproduction of surfactant with high cholesterol content. Phagocytosis of this lipid leads to accumulations of foamy macrophages which may subsequently incite other inflammatory responses.[7] Other factors altering lipid mobilization and metabolism may also play a role. For example, the rapid mobilization of body fat by some mustelids has led to speculation that the lung could possibly act as a route for excretion of lipids.[5] A correlation with pulmonary nematode parasitic infestation has been made in several species.[2,7] EnLP has been previously reported in rats, where it was described

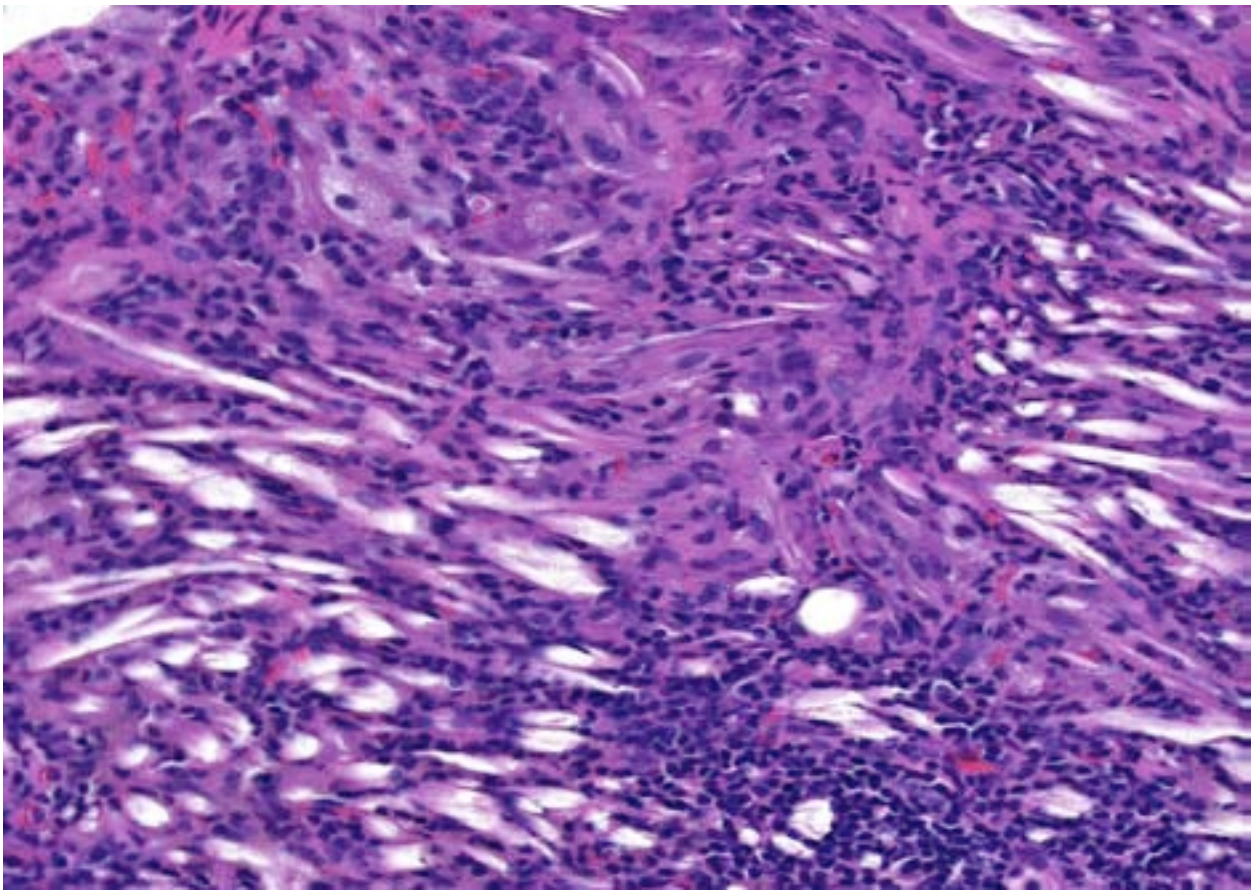

*1-5. Lung, ferret: Nodules of longer duration are larger, with increased numbers of lymphocytes and abundant cholesterol clefts. (HE 180X)*

with high spontaneous frequency under varying descriptive designations, including alveolar lipoproteinosis, multifocal histiocytosis, and alveolar proteinosis.[14] It is also well described in this species as a consequence of oral cadmium exposure (as well as other toxins), with subsequent type II pneumocyte hyperplasia and club (Clara) cell activation.[10]

In most cases when present, EnLP is an incidental finding secondary to some (often prior & undetermined) direct pneumocyte injury or bronchial obstructive process, and effort should be made to detect either resolved or active concurrent pulmonary disease. However, caution should be exercised in ascribing a major primary role in morbidity and mortality to these lesions alone.

The cause of death in this animal was thought to be debilitation and dehydration secondary to ferret enteric coronavirus infection (as suggested by a typical clinical presentation[15] and confirmed by PCR evaluation of feces). Microscopic assessment of the GI tract was of little additional benefit due to the degree of autolytic change present. Although the clinical presentation and other gross and histopathologic findings are distinctly different, the lesions of EnLP should not be mistaken for those associated with multisystemic coronavirus infection (resembling FIP) in ferrets.[4]

**JPC Diagnosis:** Lung: Pneumonia, granulomatous, subpleural, multifocal, moderate, with intrahistiocytic lipid vacuoles and cholesterol clefts.

**Conference Comment:** Endogenous lipid pneumonia (EnLP) is a common but obscure entity with an elusive pathogenesis that is diagnosed routinely in ferrets usually as an incidental finding. Its occurrence in cats and occasionally in dogs is less frequent and also of unknown significance; however, it is frequently reported in the vicinity of cancerous lesions in dogs, cats and people, possibly due to the accumulation of lipid breakdown products of

neoplastic cells.[8] This finding, in addition to other reports of EnLP's association with a variety of intrapulmonary and extrapulmonary conditions, indicates it may occur secondarily to underlying disease, equating its discovery as evidence supporting further pursuit of a primary illness.[6]

This case illustrates EnLP's classic histologic presentation as subpleural accumulations of histiocytes, lipid, and cholesterol. This distinctive subpleural location is curious given the proposed pathogenesis of pneumocyte damage and subsequent cholesterol release from disintegrating cell membranes.[7] Conference participants could not determine how such alveolar accumulations routinely end up forming subpleural nodules, and most agree with the contributor's suspicions of a multifactorial pathogenesis in the formation of EnLP.

**Contributing Institution:** Division of Laboratory Animal Resources, University of Pittsburgh
http://www.dlar.pitt.edu/

**References:**

1. Banjar H. Lipoid pneumonia: A review. Bahrain Medical Bulletin. 2003;25(1):36-39.
2. Brown CC. Endogenous lipid pneumonia in opossums from Louisiana. *Journal of Wildlife Diseases*. 1988;24(2):214-219.
3. Dungworth D. The respiratory system. In: Jubb K, Kennedy P, Palmer N, eds. *Pathology of Domestic Animals*. 3rd ed. Orlando, FL; Academic Press Inc: 1985;470-474.
4. Garner MM, et al. Clinicopathologic features of a systemic Coronavirus-associated disease resembling feline infectious peritonitis in the domestic (Mustela putorius). *Vet Pathol*. 2008;45:236-246.
5. Guarda F, Bollo E, Macchi E. Lipoid pneumonia in the Red fox (*Vulpes vulpes*). *JME*. 1997;4:13-16.
6. Himsworth CH, Malek S, Saville K, Allen AL. Endogenous lipid pneumonia and what lies beneath. *Can Vet J*. 2008;49(8):813-815.
7. Jones DJ, Norris CR, Samii VF, Griffey SM. Endogenous lipid pneumonia in cats: 24 cases (1985-1998). *JAVMA* 2000;216(9):1437-1440.
8. Lopez A. Respiratory system, mediastinum, and pleurae. In: Zachary JF, McGavin MD, eds. *Pathologic Basis of Veterinary Disease*. 5th ed. St. Louis, MO: Elsevier Mosby; 2012:530.
9. Marinez J, Reinacher M, Perpinan D, Ramis A. Identification of group 1 Coronavirus antigen in multisystemic granulomatous lesions in ferrets (mustela putorius furo). *J Comp Path*. 2008;138:54-58.
10. Molina AM, Raya AI, Carrasco L, Blanco A, Monterde JG, Rueda A, Moyano R. Endogenous lipid pneumonia in rats after subacute exposure to CdCl2. *Toxicology and Industrial Health*. 2008;24:677-681.
11. Personal communication, Dr. Bruce Williams
12. Raya AI, Fernandez-de Marco M, Nunez A, Afonso JC, Cortade LE, Carrasco L. Endogenous lipid pneumonia in a dog. *J Comp Path*. 2006;135:153-155.
13. Sharma A, Ohri S, Bambery P, Singh S. Idiopathic endogenous lipoid pneumonia. *Indian J Chest Dis Allied Sci*. 2006;48:143-145.
14. Weller W. Alveolar lipoproteinosis, rat. In: T.C. Jones, U. Mohr and RD Hunt, eds. *Monographs on Pathology of Laboratory Animals; Respiratory System*. Berlin: Springer-Verlag; 1985; 171-176.
15. Williams BH, Kiupel M, West KH, Raymond JT, Grant CK, Glickman LT. Coronavirus-associated epizootic catarrhal enteritis in ferrets. *JAVMA*. 2000;217(4):526-530.

**CASE II**: H10-131A; H10-126A (JPC 4049564).

**Signalment:** 12-week-old male Sprague-Dawley rat, *Rattus norvegicus* (09-1220); 12-week-old female Sprague-Dawley rat, *Rattus norvegicus* (09-1215).

**History:** These two rats were part of a larger study investigating the prevalence of lung lesions in Sprague-Dawley and athymic nude rats between 3 and 24 weeks of age, housed in either barrier or isolator facilities. The two rats submitted were both housed in a barrier facility from birth and were sacrificed at 12 weeks of age to look for gross and microscopic evidence of lung pathology.

**Gross Pathology:** No gross lesions were observed at routine post mortem examination; however, after 10% formalin infusion via the trachea and a minimum of 24 hours immersion fixation, multifocal (4-20), 0.5-1 mm white-grey foci were evident on all lung lobes (09-1215), or just the caudal lung lobes (09-1220).

**Laboratory Results:**

1. Aerobic and anaerobic culture of lung tissue did not culture any bacteria or fungi.

2. Surveillance of sentinel rats during this investigation was negative for pneumonia virus of mice, Theiler's encephalomyelitis virus (GD VII), Hantaan virus (Korean hemorrhagic fever), lymphocytic choriomeningitis virus, Sendai virus, reovirus-3, sialodacryoadenitis (rat coronavirus), rat parvoviruses (rat virus, rat parvovirus-1, Toolan H1 virus), *Corynebacterium kutscheri, Bordatella bronchiseptica, Pasteurella multocida, Streptococcus pneumonia, Streptococcus moniliformis, Staphylococcus aureus, Mycoplasma pulmonis, CAR bacillus, Clostridium piliforme, Salmonella enteriditis*, *Helicobacter* sp., nematodes, cestodes, intestinal protozoa (pathogenic species), *Encephalitozoon cuniculi* and arthropods.

3. PCR testing for *Pneumocystis carinii* was positive in lung tissue harvested from both rats at post mortem.

**Histopathologic Description:**

09-1215 - H10-0126A
09-1220 – H10-0131A

Lung: Multifocally, there are moderate amounts of perivascular, peri-bronchiolar, interstitial and

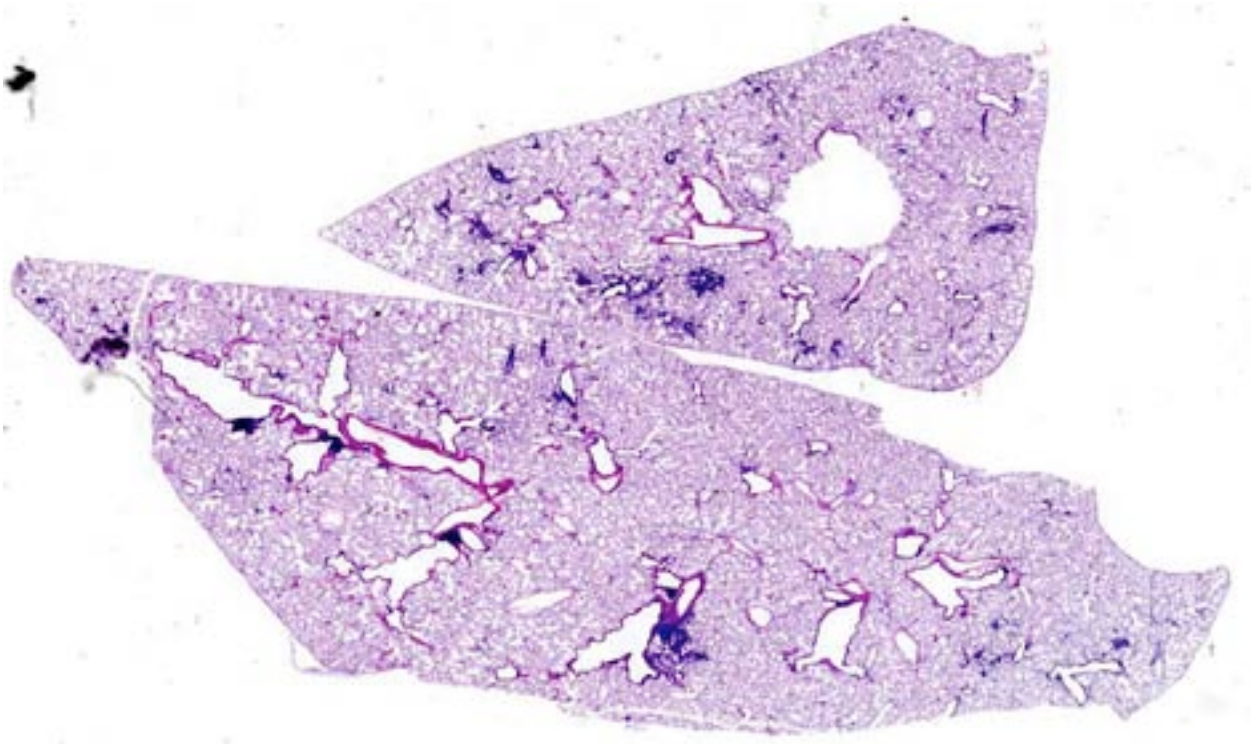

*2-1. Lung, rat: Multiple small foci of inflammation are scattered throughout the lung. (HE 6X)*

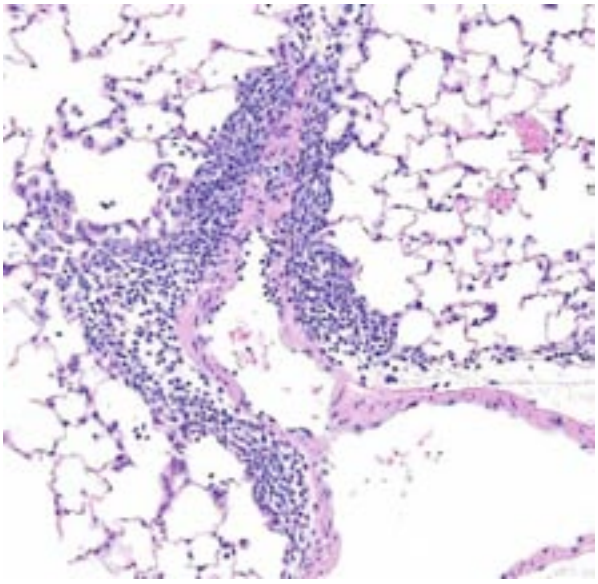

*2-2. Lung, rat: Multifocally, pulmonary arterioles are surrounded by moderate numbers of lymphocytes and histiocytes. (HE 96X)*

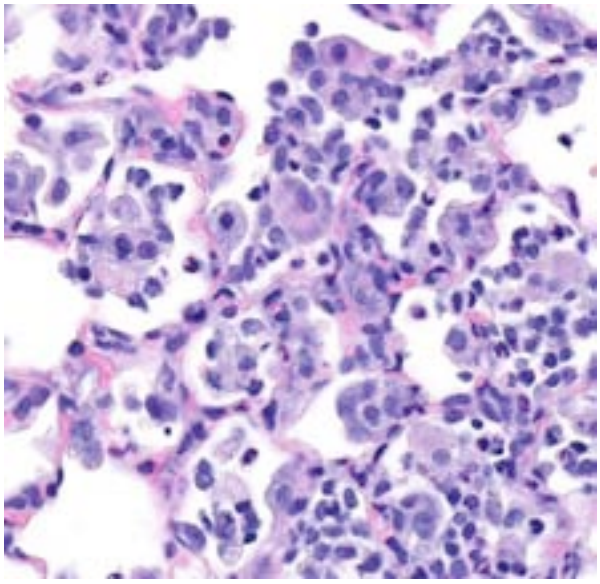

*2-3. Lung, rat: Multifocally, and randomly, alveoli contain low to moderate numbers of foamy macrophages and fewer neutrophils and are lined by type II pneumocytes. (HE 328X)*

alveolar hypercellularity. The majority of cells are pleomorphic lymphocytes and large foamy macrophages with fewer neutrophils and occasional plasma cells and eosinophils (mixed inflammatory cell interstitial pneumonia). In some slides the pleura is multifocally mildly expanded by a similar cellular infiltrate (pleuritis). Multifocally, the alveoli are filled with variable numbers of large foamy alveolar macrophages, occasional multinucleate giant cells, moderate amounts of cellular debris and are occasionally lined by plump cuboidal epithelium (mild type II pneumocyte hyperplasia). The perivascular lymphatics are occasionally moderately ectatic (perivascular oedema).

**Contributor's Morphologic Diagnosis:** Moderate, chronic, multifocal lymphoplasmacytic, neutrophilic and histiocytic interstitial pneumonia with occasional, mild type II pneumocyte hyperplasia.

**Contributor's Comment:** In the late 1990's distinctive and apparently novel pulmonary inflammatory lesions were identified and described in the lungs of laboratory rats from multiple institutions in the USA[2] and Europe.[7] These lesions included "pale or tan" macroscopic foci in the lungs and perivascular inflammatory cell cuffing throughout the lungs, accompanied by alveolar infiltrates of macrophages, neutrophils and lymphocytes, variably increased amounts of BALT and type II pneumocyte hyperplasia. Extensive serological testing, bacterial culture and protozoal identification testing failed to identify a causative agent. Electron microscopy failed to demonstrate the presence of viral-particles, although structures interpreted as bacterial bacilli were observed in the majority of rats with lung lesions.[2]

Further research undertaken in an attempt to isolate and transmit an infectious cause for the lung lesions led to the description of a novel enveloped virus and the disease was given the working name "rat respiratory virus" (RRV).[5,6] However, despite these early findings, other attempts at virus isolation from infected lungs were unsuccessful and the etiology of the pulmonary inflammatory lesions also known as "RRV" was undetermined and histopathology remained the only method of diagnosis (Albers, Simon et al. 2009).

In 2011 and 2012, two independent research groups, released publications containing convincing evidence that the fungal agent *Pneumocystis carinii* was the cause of the distinctive lung lesions known as RRV. Techniques used to demonstrate the correlation between the presence of *P. carinii* and the presence of the characteristic lung lesions included PCR, serology and experimental

infection studies.(Livingston, Besch-Williford et al. 2011, Henderson, Dole et al. 2012).

The gross and histopathological changes in the rat lungs submitted, combined with the negative microbial culture and serological testing results and positive PCR results for *Pneumocystis carinii*, led to the diagnosis of *Pneumocystis* pneumonia in these rats.

**JPC Diagnosis:** Lung: Pneumonia, interstitial, histiocytic, multifocal, mild, with multifocal lymphoplasmacytic perivascular inflammation.

**Conference Comment:** This case provides a detailed look at the rapid evolution of this mild but historically important pulmonary condition in rats. The contributor adequately outlined the historical aspects surrounding this lesion, and describes the current consensus identifying *Pneumocystis carinii* as the inciting agent. We performed Grocott's methenamine silver stain in an effort to identify an organism, but were only successful in observing one questionable fungal cyst.

*P. carinii* typically requires immune suppression for infection to cause clinical disease. In humans the organism is hypothesized to be continually present within the lungs from the first few years of life, often in the absence of overt pathology.[8] In certain rat colonies, *P. carinii* is apparently common and has been documented in the lungs of clinically healthy, immunocompetent rats; research suggests neonatal rats acquire it within hours after birth.[4] A survey of research institutions revealed 6% of rats had the characteristic perivascular lymphocyte accumulation associated with that described in the 1990's for RRV.[4] These lesions were reproduced experimentally in immunocompetent rats by inoculation of *P. carinii* and its transmissible potential was documented in independent studies.[3,4] Further, organism identification by PCR was highly correlated with lung pathology, and the organism was never identified in cases lacking the characteristic lung lesions, allowing characteristic microscopic changes to be an accurate predictor of *P. carinii* infection.[3] Despite the evidence, definitive causation can still not be assigned as the inoculum utilized in both studies was derived from infected rat lungs, thus the possibility of a second or primary agent remains, though that possibility is argued as highly improbable.[4] Regardless, both experimental and natural infections spontaneously resolve with time.[1,3]

**Contributing Institution:** Pathology Section; College of Veterinary Medicine; School of Veterinary and Life Sciences; Murdoch University http://www.murdoch.edu.au/School-of-Veterinary-and-Life-Sciences/Facilities-and-labs/College-of-Veterinary-Medicine/

**References:**

1. Albers TM, Simon MA, Clifford CB. Histopathology of naturally transmitted "rat respiratory virus": progression of lesions and proposed diagnostic criteria. *Vet Pathol*. 2009;46(5):992-999.
2. Elwell MR, Mahler JF, Rao GN. Have you seen this? Inflammatory lesions in the lungs of rats. *Toxicol Pathol.* 1997;25:529-531.
3. Henderson KS, Dole V, Parker NJ, Momtsios P, Banu L, Brouillette R, et al. Pneumocystis carinii causes a distinctive interstitial pneumonia in immunocompetent laboratory rats that had been attributed to "rat respiratory virus. *Vet Pathol*. 2012;49(3):440-52.
4. Livingston RS, Besch-Williford CL, Myles MH, Franklin CL, Crim MJ, Riley LK. Pneumocystis carinii infection causes lung lesions historically attributed to rat respiratory virus. *Comp Med*. 2011;61(1):45-59.
5. Riley L, Purdy G, Dodds J, et al. Idiopathic lung lesions in rats: search for a etiologic agent. *Contemp Top Lab Anim Sci.* 1997;36:46.
6. Riley L, Simmons J, Purdy G, et al. Research Update: idiopathic lung lesions in rats. *ACLAD News*. 1999;20:9-11.
7. Slaoui M, Dreef HC, van Esch. Inflammatory lesions in the lungs of Wistar rats. *Toxicol Pathol.* 1998;26:712-713, discussion 714.
8. Swain SD, Meissner N, Han S, Harmsen A. Pneumocystis infection in an immunocompetent host can promote collateral sensitization to respiratory antigens. *Infect Immun.* 2011;79(5): 1905-1914.

**CASE III**: MS14-887 (JPC 4052867).

**Signalment:** Adult female Adrenal Specific Prkar1a knockout (ADKO) mouse, *Mus musculus.*

**History:** Euthanized because of a large subcutaneous mass and abdominal distension.

**Gross Pathology:** A 15 mm diameter abscess is present in the subcutaneous layer of the dorsal left abdominal wall. This abscess extended into the abdomen and is contiguous with the left uterine horn. The subcutaneous portion measures approximately 15 mm in diameter. The abdominal aspect of the mass measures 31 x 12 x 12 mm. It is filled with thick yellow material, a swab of which is taken for bacterial culture. Abscesses are present within lumbar aortic lymph nodes. The mesenteric lymph node is markedly enlarged, swollen and diffusely pink. The liver and kidneys are pale and swollen. The spleen is approximately five times normal in size. It is adhered to the abdominal mass. The left lung is tan. The brain is not examined.

**Laboratory Results:** Bacteriology: Aerobic: *Pasteurella pneumotropica* present; Strict Anaerobe: *Peptostreptococcus anaerobius* present.

**Histopathologic Description:** The left uterine horn has severe necrosuppurative inflammation in the lumen and extending through the muscularis. Colonies of small bacterial rods are present.

The uterus also has a neoplastic cell population in the endometrium, myometrium and surrounding soft tissue. In some areas the neoplasm has sheets of oval to round cells with a moderate amount of amphophilic cytoplasm and eccentric nuclei. In the uterine wall the cells have a fusiform to spindle morphology. Nuclei are elongated to reniform with marginated chromatin. There are approximately 8 mitotic figures per ten 400X field. Similar neoplastic cells efface the pancreas and are present in the mesometrium, ovary, gall bladder, in abdominal lymph nodes and the spleen. Kidneys have cytoplasmic eosinophilic droplets in the proximal tubular epithelium.

*Immunohistochemistry results:* Performed on neoplastic aggregates present in the mesovarium and ovary: F4/80: Positive. Smooth muscle actin and desmin: Negative.

*Gram stain*: Uterus: The short bacterial rods are gram negative; occasional gram positive cocci are present.

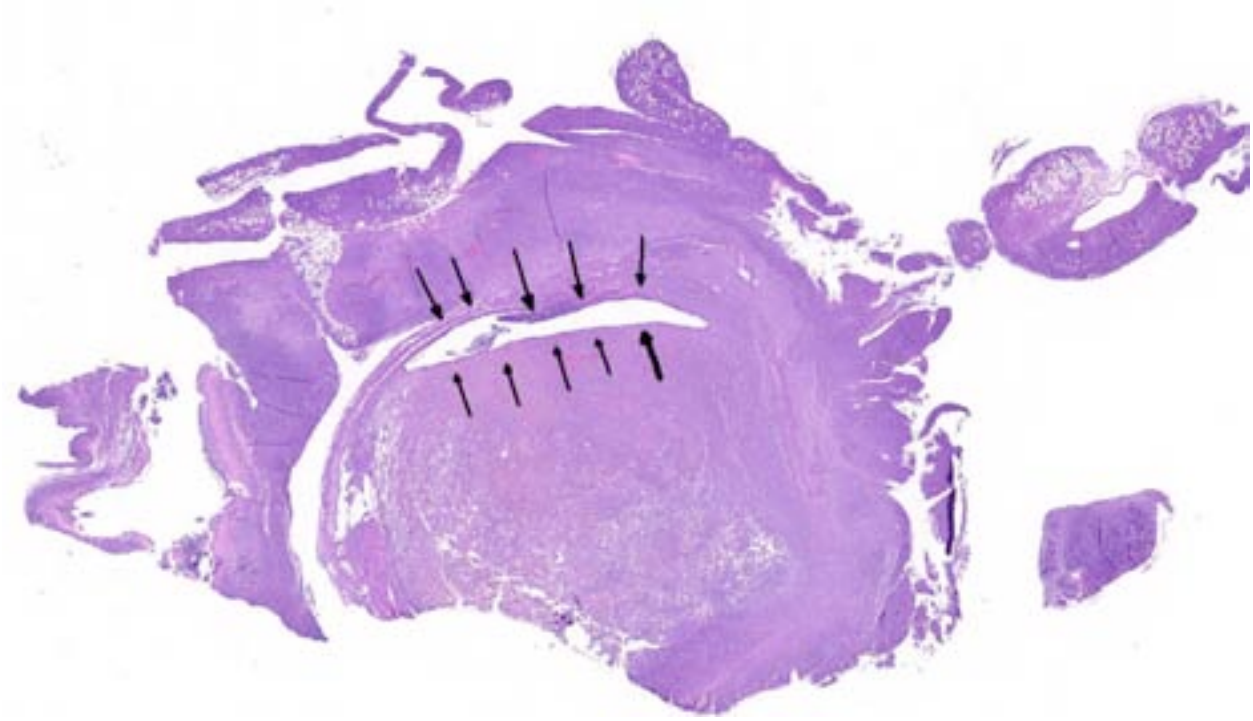

*3-1. Uterus, mouse: The wall of the uterus is markedly expanded by an infiltrative neoplasm which infiltrates the adjacent mesometrium, mesentery, and in this section, pancreas. Arrows delineate the compressed lumen. (HE 7X)*

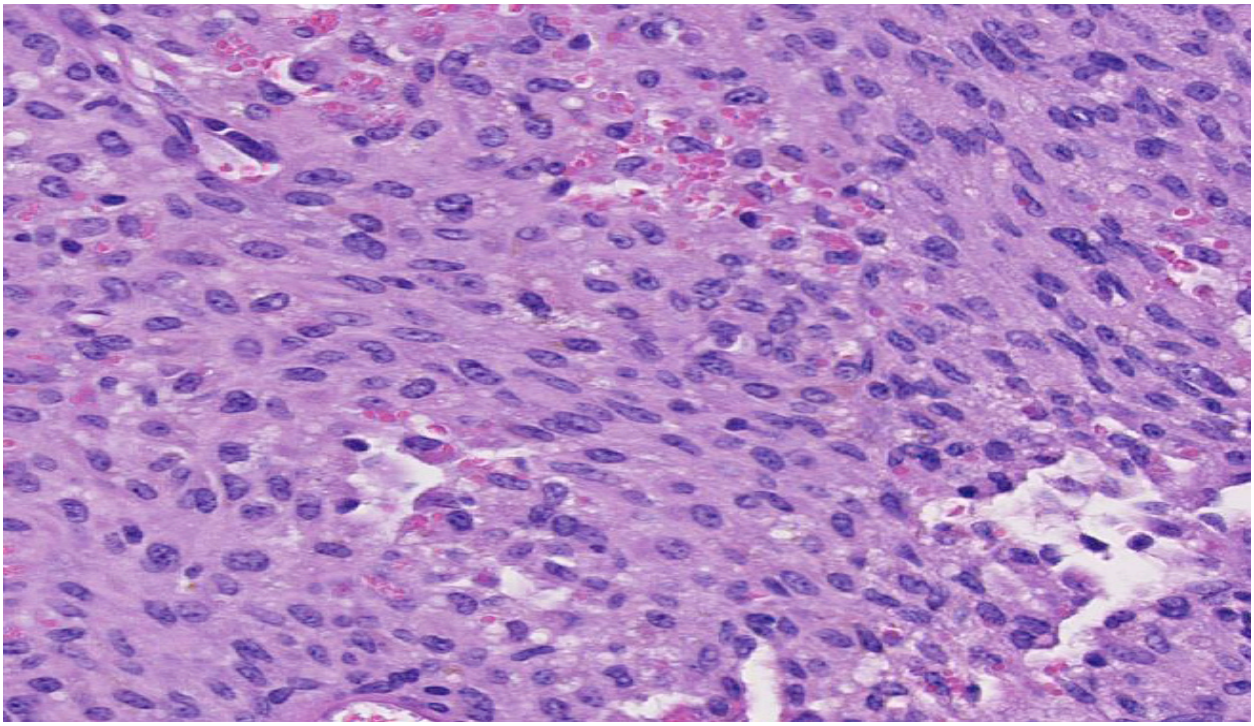

*3-2. Uterus, mouse: The neoplasm is composed of histiocytic round cells which often spindle. This morphology, coupled with an intrauterine location, is strongly suggestive of histiocytic sarcoma. (HE 120X)*

**Contributor's Morphologic Diagnosis:** Uterus: Histiocytic sarcoma; pyometra (Pasteurella).

**Contributor's Comment**: Histiocytic sarcoma is a neoplasm of monocyte origin. Incidence of histiocytic sarcoma in mice varies with strain, for example being rarely reported in 129/sSvJae and FVB/N mice to 15% in C57Bl in a study on comparing mortality between mouse strains.[1] Some histiocytic neoplasms have large cells with abundant cytoplasm and multinucleated cells; others have smaller oval to spindle cells.[4,8] Hyaline droplet accumulations in the kidney are commonly associated with histiocytic sarcoma. The droplets are caused by accumulations of lysozyme.[8] However, lymphomas and myelogenous leukemia in mice have been associated with hyaline droplets in the kidney.[3] In this case, spindle to round cell morphology, the presence of hyaline droplets in the kidney and strong positivity of neoplastic cells for F4/80 is consistent with a neoplasm of histiocytic in origin. A list of histiocyte markers is listed in the accompanying table.

Differential diagnoses for histiocytic sarcoma include stromal tumors like leiomyoma and Schwannoma, and other hematopoietic cell tumors such as histiocyte-associated lymphomas (HAL) and myelogenous leukemia. Significant populations of histiocytic cells can be present in lymphomas; the macrophages associated with HAL tend to be large and round with abundant cytoplasm. Histiocyte rich lymphomas can be distinguished by clonal rearrangements of Ig heavy chain (B-cell) or T-cell receptor loci in

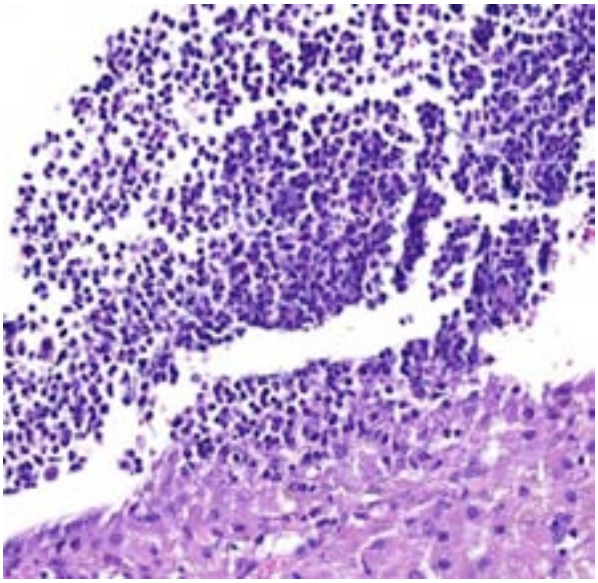

*3-3. Uterus, mouse: The lumen of the uterus contains numerous degenerate neutrophils and cellular debris, unassociated with the neoplasm, suggesting a concomitant uterine infection. (HE 340X)*

**Mouse Histiocyte markers**[9]

| Marker | Function | Cell location | Macrophage expression | Other tissues |
|---|---|---|---|---|
| **Arginase 1** | Arginine metabolism | Cytostolic | M2* macrophage | Other tissues |
| **CD68** | Lysosome/ phagosome A glycoprotein | Cytostolic | Tissue macrophages, thymus, lymph node, Kupffer cells, alveolar macrophages | Also other cells with lysozomes/ phagosomes |
| **CD163** | Scavenger receptor cysteine rich superfamily | Membrane | Monocytes and tissue macrophages except tingible body macrophages in germinal centers | |
| **F4/80** | Immune regulation[8] | Membrane | Tissue macrophage; not splenic white pulp | |
| **IAB1** | Actin/calcium binding protein | Cytoplasm and nucleus | All but alveolar macrophage and lymph node dendritic cells | |
| **$iNO_2$** | Nitric oxide expression | cytoplasmic | Activated macrophages via $CD_4TH1$ pathway | neutrophils |
| **Lysozyme** | Innate immune system | Cytoplasmic | Alveolar macrophage, Kupffer cells, Lymph node sinuses | Granulocytes, monocytes |
| **MAC 2** | Adhesion molecule | Cytoplasmic and membrane | All | Also various epithelial cells |
| **Mac3** | Glycoprotein | cytoplasm | Macrophages and dendritic cells | Epithelial, megakaryocytes, endothelial cells, granulocytes |
| **YM1** | Expression associated with inflammation | Cytoplasm | M2 macrophage, Alveolar macrophages | M2 |

*M2 macrophage: Macrophages involved in the $CD4TH_2$ pathway.

lymphocyte populations versus having IgH and TcR receptor genes in germline (non-rearranged) configuration. This is done by Southern blot analysis. If neoplastic cells lack IgH gene rearrangements, neoplasms of B-cell origin are excluded; however, rarely cells with histiocytic cell morphology have displayed IgH rearrangements. Some histiocyte-rich neoplasms have nodular proliferations of more pleomorphic macrophages increased numbers of mitotic figures and lymphocytes with clonal immune receptor and rearrangements; these may represent tumors with both neoplastic histiocytes and lymphocytes.[5] Immunohistochemistry for T-cell and B-cells were not performed in the submitted case.

*Pasteurella* is a common pathogen in laboratory mice that has been associated with uterine infections as well as male reproductive, ocular, ear, nasal, skin and mammary gland infections.[8] *Peptostreptococcus* has not been reported as a cause of spontaneous disease in mice but has been associated with genitourinary tract infections in people.[7]

**JPC Diagnosis: 1.** Uterus, mesometrium, pancreas, mesentery: Histiocytic sarcoma.
2. Uterus: Endometritis, necrotizing, diffuse, severe, with intra- and extracellular bacilli.

**Conference Comment:** Sections from three different blocks were provided for this case and equally distributed among conference participants and contributors; there is significant variation between different sections. Among them, histiocytic sarcoma is present within the pancreas, uterus and mesentery, inciting an array of extensive secondary pathologic changes in the affected organs, distorting tissue architecture and in some cases, rendering tissue identification impossible. The spleen is present in some sections although we did not observe the neoplasm within it. The neoplasm and secondary changes provide for a descriptively challenging case.

The contributor provides an excellent overview of histiocytic sarcoma in rodents and its immunohistochemical attributes. Immunohistochemistry has afforded greater clarity in teasing out cellular origin of various histiocytic diseases, effectively eliminating commonly used diagnoses such as malignant fibrous histiocytoma and splenic fibrohistiocytic nodules while identifying the majority of histiocytic proliferations in dogs and cats as Langerhans cell or interstitial dendritic cell origin.[6,11] Only hemophagocytic sarcoma is still recognized as originating from macrophages.[6] Histiocytic proliferative diseases may occur as neoplastic processes or dysregulated inflammatory processes in dogs, while only neoplastic processes are identified in cats.[6]

Histiocytic sarcoma is one of the few neoplasms known to cross the joint space and is often confused with synovial cell sarcoma when present at an articular surface. Synovial cell sarcomas are derived from type B synovial cells, which are specialized fibroblasts that readily attract large numbers of histiocytes. The two are differentiated by the dominant cell population and its CD18 expressivity.[6] Histiocytic sarcoma is one of three typically disseminated neoplasms in rodents, to also include hemangiosarcoma and lymphoma, that are believed to arise synchronously in multiple organs. It is interesting there is no mention of liver involvement in this case, where it occurs so commonly and was often cited as a primary location in older literature.[2]

Pyometra most commonly occurs following estrus in most species, while the uterus is under progesterone influence.[10] In mice, pyometra may also occur secondarily to mucometra, and *Klebsiella* spp. and *Pasteurella* spp. are the most commonly cultured organisms.[2,8]

**Contributing Institution:** National Institutes of Health, Division of Veterinary Resources
http://www.ors.od.nih.gov

**References:**

1. Brayton CF, Treuting PM, Ward JM. Pathobiology of aging mice and GEM: Background strains and experimental design. *Vet Path*. 2012;49(1):85-105.
2. Davis BJ, Dixon D, Herbert RA. Ovary, oviduct, uterus, cervix, and vagina. In: Maronpot RR, ed. *Pathology of the Mouse*. Vienna, IL: Cache River Press, Inc.; 1999:438.
3. Decker JH, Dochterman LW, Niquette AL, et al. Association of renal tubular hyaline droplets with lymphoma in CD-1 Mice. *Toxicol Pathol*. 2012;40(4):651-655.
4. Frith CH, Ward JM, Harlmen JH, et al. Hematopoietic system. In: *International Classification of Rodent Tumors: The Mouse*. Berlin, Germany: Springer-Verlag; 2001:430-431.
5. Hao X, Fredrickson TN, Chattopadhyay SK. The histopathologic and molecular basis for the diagnosis of histiocytic sarcoma and histiocyte–associated lymphoma of mice. *Vet Pathol*. 2010;47(3):434-445.
6. Moore PF. A review of histiocytic diseases of dogs and cats. *Vet Pathol*. 2014;51(1):167-184.
7. Murdoch DA. Gram-positive anaerobic cocci. *Clinical Microbiology Reviews*. 1998;11(1): 81-120.
8. Percy DH, Barthold SW. Mouse. In: *Pathology of Laboratory Rodents and Rabbits. 3rd ed*. Oxford, England: Blackwell Publishing Ltd; 2007:3-111.
9. Rehg JE, Bush D, Ward JM. The utility of immunohistochemistry for the identification of hematopoietic and lymphoid cells in normal tissues and interpretation of proliferative and inflammatory lesions of mice and rats. *Toxicol Pathol*. 2012;40(2):345-374.
10. Valli VE, Jacobs RM, Parodi AL, Vernau W, Moore PF. *Histological Classification of Hematopoietic Tumors of Domestic Animals*. 2nd series. Vol VIII. Washington, D.C.: Armed Forces Institute of Pathology/ American Registry of Pathology; 2002:48-49.
11. van den Berg TK, Kraal G. A function for the macrophage F4/80 molecule intolerance induction. *Trends in Immunology*. 2005;26(10): 506-509.

**CASE IV:** 09187 WFUHS (JPC 3165083).

**Signalment:** Adult male vervet monkey, *Chlorocebus aethiops.*

**History:** After arriving into the CDC quarantine, this animal was noted to have labored breathing and coughing and died on the morning of the next day. There were no experimental procedures performed on this animal.

**Gross Pathologic Findings:** A necropsy was performed as per the CDC quarantine animal necropsy protocol. While opening the diaphragm to enter the thoracic cavity, abundant yellowish-tan, opaque viscous liquid (pus) poured out. The lungs were mottled dark brown to tan to dull red, markedly consolidated, had a consistency similar to that of liver (hepatization of lung), and did not collapse with loss of thoracic cavity negative pressure. Multifocal, tan to white, well demarcated, variably sized pus-filled abscesses reaching up to 2.5 cm in diameter were found on cut sections. Only about 10 percent of apparently normal, remaining pulmonary parenchyma was present. The pleura was thickened and multifocally adhered to the dorsal and lateral thoracic walls. A variably thick layer of pus admixed with dull red to brown fibrillar material (fibrin) was present on the pleural surface and in the thoracic cavity. Mucus admixed with small plugs of pus were present in the distal bronchial lumina. The tracheobronchial lymph nodes were prominent.

**Gross Morphologic Diagnoses:** Pleuropneumonia, diffuse, chronic, severe, suppurative with abscessation and thoracic adhesions.

**Laboratory Results:** Bacterial culture from the lung - *Klebsiella pneumoniae* 3+

Filoviral ELISA – negative.

**Histopathologic Description:** The pulmonary architecture was extensively obscured by abundant suppurative inflammatory cellular infiltrate admixed with edema, necrotic debris and fibrin. Bronchioles and alveolar spaces were filled by numerous neutrophils, many degenerate, which often transmurally infiltrated and effaced alveolar and bronchiolar walls. The affected bronchioles were lined by attenuated epithelial cells lacking cilia and multifocally the epithelial lining was denuded. Most of the blood vessels were surrounded by thick fibrin strands and clear spaces (edema). The alveolar capillaries are congested and small hemorrhages are scattered throughout the pulmonary parenchyma. The pleura was expanded up to 150 microns in thickness by fibrin. Frequently within the airspaces, 1x2-4 micron bacterial rods occasionally arranged in chains were seen extracellularly or within macrophage cytoplasm.

*4-1. Lung, vervet monkey: The lungs were mottled dark brown to tan to dull red, markedly consolidated. The lungs contain several well demarcated, variably sized pus-filled abscesses ranging up to 2.5 cm in diameter. (Photo courtesy of: Animal Resources Program, Wake Forest University Health Sciences, Winston-Salem, NC http:// www1.wfubmc.edu/pathology/training/index.htm)*

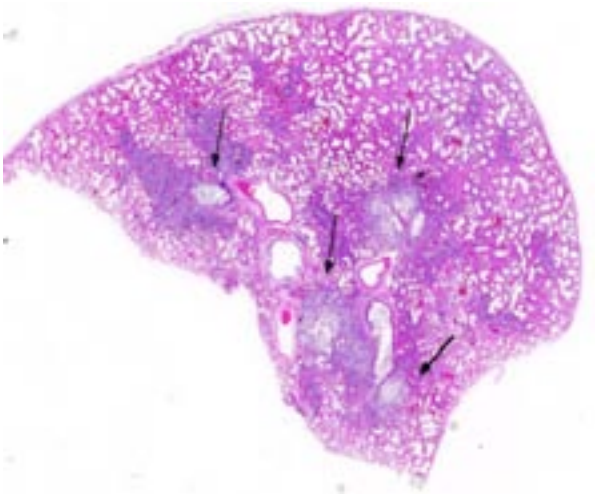

*4-2. Lung, vervet monkey: Numerous lucent areas are present within the diffusely inflamed parenchyma. (HE 6X)*

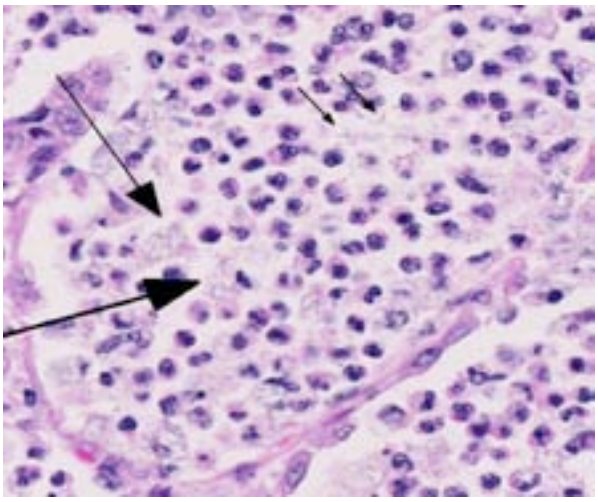

*4-3. Lung, vervet monkey: Lucent areas are composed of ruptured and confluent alveoli which are filled with numerous neutrophils and macrophages which often contain engulfed bacilli. (HE 400X)*

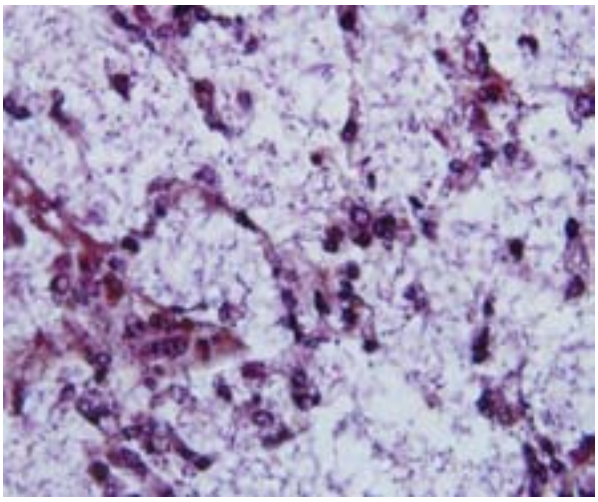

*4-4. Lung, vervet monkey: Gram stain of bacilli showing the distance between bacilli in areas of inflammation, corresponding to the presence of a capsule. (Brown-Hopps, 600X)*

Gram stain: Numerous gram negative 1x2-4 micron single or chains of bacilli were present at the areas of inflammation.

Acid fast stain: The bacterial rods were acid fast negative, but acid fast stain showed a prominent blue stained bacterial capsule.

**Contributor's Morphologic Diagnosis:** Pneumonia, bronchointerstitial, diffuse, severe, subacute, fibrinosuppurative with intralesional gram negative bacteria.

**Contributor's Comment:** *Klebsiella pneumoniae* is a gram-negative, aerobic, encapsulated, nonmotile rod-shaped bacteria of the family *Enterobacteriaceae*, which are ubiquitous in nature. It is one of the most important nosocomial bacterial infections in humans, which accounts for a significant proportion of urinary tract infections, pneumonia, septicemias, and soft tissue infections.[4] As opportunistic pathogens, *Klebsiella* spp. primarily attack immunocompromised individuals. It is also a frequent cause for pneumonia in nonhuman primates. Differentials for bacterial pneumonia in nonhuman primates include *Mycobacterium tuberculosis*, *Burkholderia* sp., *Klebsiella* sp., *Staphylococcus* sp., *Corynebacterium* sp., *Streptococcus* sp., *Nocardia* sp., *Actinomyces* sp, among others.

Based on the pathological findings, it is presumed that this animal was infected with *K. pneumoniae* and developed pneumonia prior to shipping to Wake Forest, although the transportation-associated stress likely aggravated the condition. Stress associated with shipping and transportation is known to increase the incidence of this infection. Multisystemic abscess formation in African green monkeys caused by invasive, hypermucoviscosity phenotype *Klebsiella pneumonia* has been reported.[6] Serotyping based on the capsular antigen type is the technique for further characterizing *Klebsiella* spp. *K. pneumoniae* characteristically produce vast amounts of capsular polysaccharide covering the bacterial surface.[5] K1 and K2 serotypes are most virulent and they were found to be significantly more resistant to phagocytosis than non-K1/K2 isolates.[1,5] The thick polysaccharide capsule (K antigen) of these bacteria creates a barrier that prevents opsonization and phagocytosis. In this case, capsular serotyping was not performed. This animal also had meningitis, epicarditis and renal arterial thrombosis which suggest bacterial septicemia. Also moderate myeloid hyperplasia in the bone marrow was observed as expected in bacterial infections.

**JPC Diagnosis:** Lung: Bronchopneumonia, fibrinosuppurative, chronic, multifocal, severe, with numerous intra- and extracellular bacilli.

**Conference Comment:** This is a classic case of the primate form of shipping fever, a disease affecting both New and Old World primates and can lead to sepsis and rapid death, which likely occurred in this case. The organisms are numerous in this example, and the thick capsule

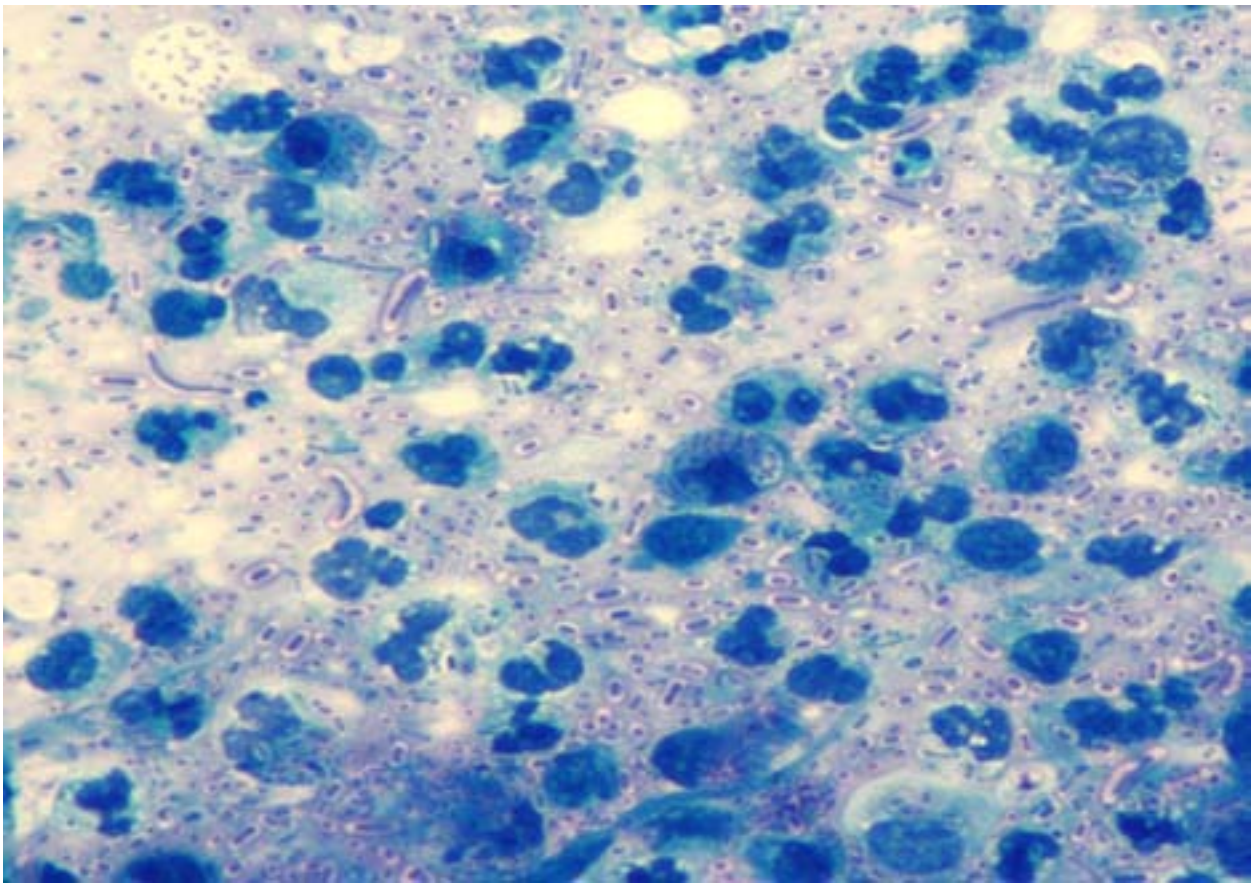

*4-4. Lung, vervet monkey: Gram stain of bacilli showing the distance between bacilli in areas of inflammation, corresponding to the presence of a capsule. (Brown-Hopps, 600X)*

so important to its pathogenesis is beautifully depicted in the image of the acid fast stain submitted by the contributor. This capsule also likely plays a role in the increased invasiveness and pathogenicity of the hypermucoviscosity phenotype (HMV), which carries greater resistance to oxidative-mediated killing and imparts a higher level of cytotoxicity upon the host.[2] HMV was first isolated from fatal human infections and was only recently described in nonhuman primates; it characteristically causes rampant abscesses affecting multiple organs.[6]

*K. pneumoniae* is associated with disease in other lab animal species as well, including enterotyphilitis and bronchopneumonia in rabbits, polyserositis and bronchopneumonia in guinea pigs, and lymph node and renal abscesses in mice and rats.[3] The closely related *K. oxytoca* causes suppurative endometritis and dermatitis readily in mice.[3] Among domestic species, *K. pneumoniae* causes urinary tract infections (dogs), mastitis (ruminants), cerebral abscesses (ruminants) and pneumonia (dogs).[7]

**Contributing Institution:** Animal Resources Program, Wake Forest University Health Sciences, Winston-Salem, NC
http://www1.wfubmc.edu/pathology/training/index.htm

**References:**

1. Chuang YP, Fang CT, Lai SY, Chang SC, Wang JT. Genetic determinants of capsular serotype K1 of Klebsiella pneumoniae causing primary pyogenic liver abscess. *J Infect Dis*. 2006;193:645-654.
2. Cox BL, Schiffer H, Dagget G Jr, et. al. Resistance of Klebsiella pneumonia to the innate immune system of African green monkeys. *Vet Microbiol*. 2015;176(1-2):134-142.
3. Percy DH, Barthold SW. *Pathology of Laboratory Rodents*. 3rd ed. Ames, IA: Blackwell Publishing; 2007:64, 152, 222, 275.
4. Podschun R, Ullmann U. Klebsiella spp. as nosocomial pathogens: epidemiology, taxonomy, typing methods, and pathogenicity factors. *Clin Microbiol Rev*. 1998;11:589-603.

5. Struve C, Bojer M, Nielsen EM, Hansen DS, Krogfelt KA. Investigation of the putative virulence gene magA in a worldwide collection of 495 Klebsiella isolates: magA is restricted to the gene cluster of Klebsiella pneumoniae capsule serotype K1. *J Med Microbiol*. 2005;54:1111-1113.
6. Twenhafel NA, Whitehouse CA, Stevens EL, Hottel HE, Foster CD, Gamble S, et al. Multisystemic abscesses in African green monkeys (Chlorocebus aethiops) with invasive Klebsiella pneumoniae--identification of the hypermucoviscosity phenotype. *Vet Pathol*. 2008;45:226-231.
7. Zachary JF, McGavin MD. *Pathologic Basis of Veterinary Disease*. 5th ed. St. Louis, MO: Elsevier Mosby; 2012:524, 637, 801, 1124.

**Joint Pathology Center**
**Veterinary Pathology Services**

# WEDNESDAY SLIDE CONFERENCE 2014-2015

## Conference 20

**18 April 2015**

**Guest Moderator:**
Amy C. Durham, DVM, ACVP
School of Veterinary Medicine Department of Pathobiology
University of Pennsylvania

---

**CASE I:** B1319791 (JPC 4048572).

**Signalment:** 9-year-old castrated male beagle dog, *Canis familiaris.*

**History:** The dog was referred to a veterinary surgeon for evaluation of a possible splenic mass. An abdominal ultrasound showed a 2 inch mass in the cranial aspect of the spleen, which was confirmed at surgery for a splenectomy. No other gross abnormalities were noted by the submitting veterinarian.

**Gross Pathology:** The surgeon reports a single splenic nodule and no other gross abnormalities.

**Laboratory Results:** Immunohistochemistry: The lymphocytes are strongly CD79a-positive and CD3-negative. PCR for antigen receptor rearrangement (performed by the Leukocyte Antigen Biology Laboratory at UC Davis): Molecular clonality analysis of IgH2, IgH3 and KDE (B cell) revealed polyclonal rearrangements.

**Histopathologic Description:** The splenic nodule consists of coalescing nodules of lymphocytes. The intervening tissue is congested with a mixture of plasma cells, myeloid and erythroid precursors, megakaryocytes and hemosiderophages. The coalescing lymphoid tissue consists mainly of marginal zone cells which are intermediate in size (nuclei approximately 1.5 times the diameter of a red blood cell). The cells have a scant to moderate

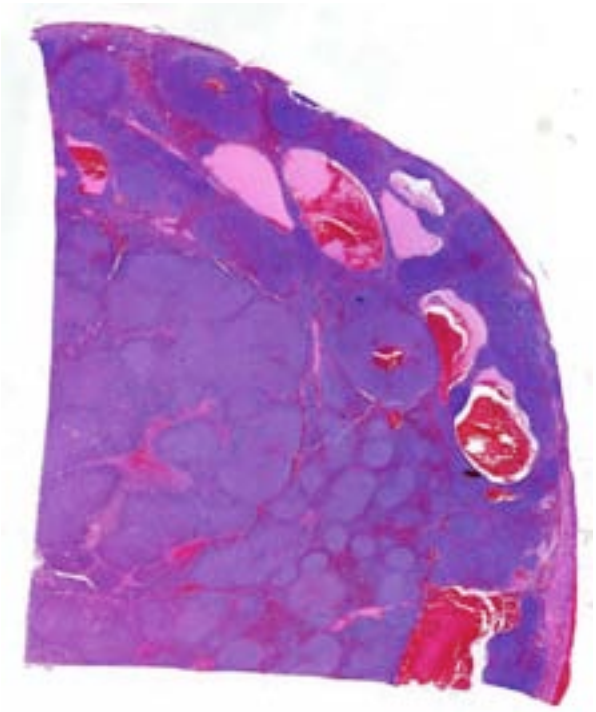

*1-1. Spleen, dog: Normal architecture is replaced by coalescing nodules of lymphocytes, separated by a mixed population of plasma cells and extramedullary hematopoiesis. (HE 4.5X)*

amount of eosinophilic cytoplasm and round to oval nuclei with a single prominent central nucleolus. Admixed throughout this proliferation are smaller numbers of larger cells with oval open nuclei (interpreted as dendritic cells), remaining germinal center cells, and scattered lymphocytes with small hyperchromatic nuclei (measuring 1 times the size of a red blood cell). Mitoses within the marginal zone cell population range from 0-2 in a single high power field.

**Contributor's Morphologic Diagnosis:** Splenic Marginal zone lymphoma (probable).

**Contributor's Comment:** Marginal zone lymphoma (MZL) is an indolent B-cell neoplasm derived from the cells of the marginal zone of lymphoid follicles. Three types of MZL with different clinical and molecular characteristics are recognized in humans: extranodal mucosa-associated lymphoid tissue (MALT) lymphoma, splenic MZL (SMZL) and nodal MZL (NMZL). In humans, SMZL is rare (1-3% of lymphomas) and usually involves the spleen, bone marrow, and blood. The disease can present as an incidental finding or with symptoms of splenomegaly. Anemia, lymphocytosis, or thrombocytopenia are reported in about 25% of cases.[7] Currently, there is no known genetic abnormality specific for SMZL, but deletions of chromosome 7q are found in 30-50% of cases.[5] Therapy for SMZL in humans remains controversial with options including splenectomy, various chemotherapeutic agents, or rituximab alone.[1,5,7] Most disease-related deaths in SMZL are associated with transformation to diffuse large B cell lymphoma.[5]

Indolent lymphomas in dogs include follicular, mantle cell, marginal zone, and T-zone lymphomas. Valli et al examined 66 dogs with indolent lymphoma which included 33 dogs with nodal MZL and 13 cases of splenic MZL; however, only 3 of these cases had outcome data available.[9] Two recent studies describe SMZL in 5 and 34 dogs, respectively, and provide better insight into clinical characteristics and outcome of this disease.[4,6] In the larger study by O'Brien et al, the overall median survival time (MST) after splenectomy was 383 days and dogs that had MZL as an incidental finding had a longer MST (1,153 days) compared to dogs with clinical signs associated with MZL (309 days). Other factors such as lymph node involvement, hemoabdomen, adjuvant chemotherapy, and concurrent malignancies did not influence survival.[4]

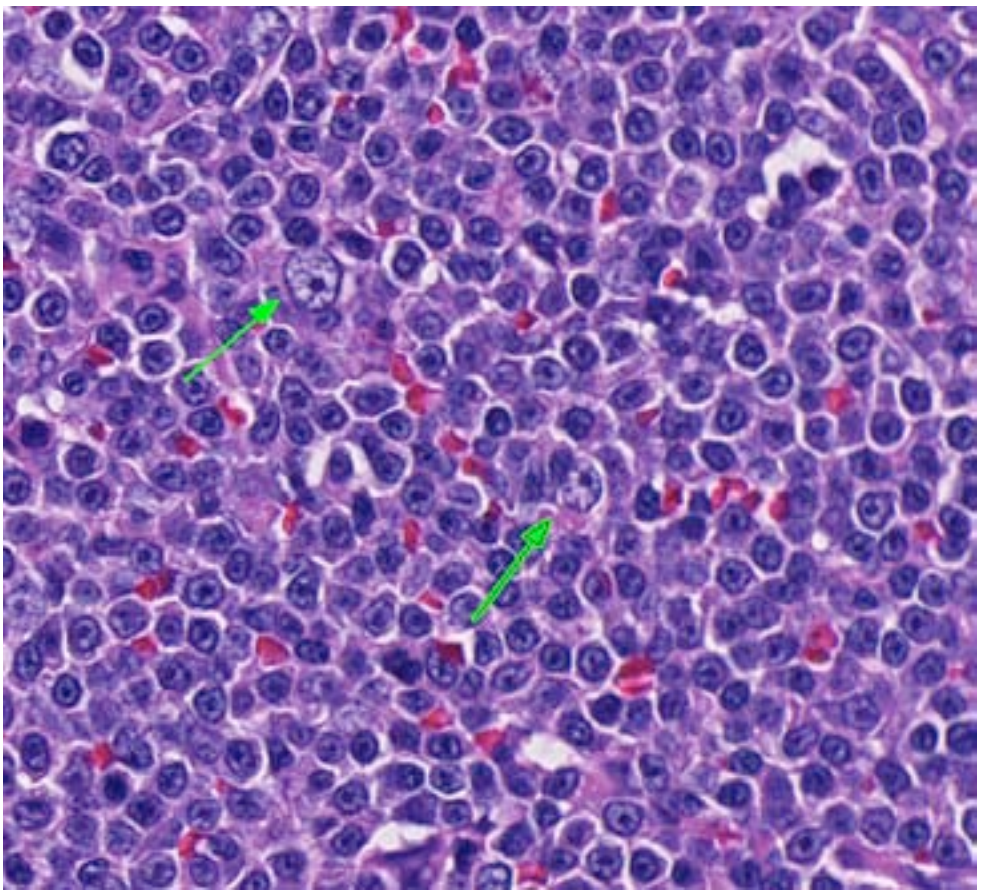

*1-2. Spleen, dog: The neoplasm consists mainly of marginal zone cells which are intermediate in size (nuclei approximately 1.5 times the diameter of a red blood cell), and have a high mitotic rate. Mitotic figures are rare. Scattered among these cells are fewer larger lymphocytes with a moderate amount of granular cytoplasm, and larger vesicular nuclei (centroblasts – green arrows). (HE 360X)*

Assessment of tissue architecture is needed for a diagnosis of MZL, and therefore, histopathology is required. MZL has a distinct nodular pattern in which the lighter-staining neoplastic marginal zone cells form a dense cuff around small foci of darkly stained mantle cells (fading follicles). The neoplastic marginal zone lymphocytes are intermediate in size, with nuclei measuring approximately 1.5 times the diameter of a red blood cell, and have a single prominent central nucleolus. Benign marginal zone hyperplasia (MZH) has a similar architectural appearance, although the expanded marginal zone is heterogeneous, containing a mixture of small and intermediate sized lymphocytes.[10] Differentiating between MZH and MZL is challenging because MZL arises on the background of MZH. Therefore, immunophenotyping and molecular clonality are ultimately required for a definitive diagnosis.

This case highlights the difficulty in differentiating between MZL and MZH and this distinction is especially difficult in the spleen of dogs. Lymphoid nodular hyperplasia and complex nodular hyperplasia ('fibrohistiocytic nodules') are common in the canine spleen; it is possible that many cases of nodular hyperplasia contain areas of MZL. In this case, the architectural feature of homogenous coalescing marginal zone cells was more suggestive of MZL than MZH. The fields in which there were up to 2 mitotic figures further supported this diagnosis, and is likely indicative of later stages of disease development, as mitoses increase with disease progression.[9,10]

As expected, the cells were CD79a positive and CD3 negative, indicating a B cell phenotype. Tissues were sent to the Leukocyte Antigen Biology Laboratory at UC Davis. Molecular clonality analysis of IgH2, IgH3, and KDE (B cell) revealed polyclonal rearrangements, which suggested a reactive process rather than a neoplasm. However, upon review of the histopathological and immunohistochemical findings, the reviewing pathologists at UC Davis were also highly suspicious of MZL and that the PARR testing might be a false negative result. The O'Brien paper also found a subset of cases (27%) that did not demonstrate a clonal population (pseudoclonal and polyclonal rearrangements)[3], which is consistent with the published sensitivity of this PCR-based test.[2,8] In that study, the polyclonal rearrangements were attributed to a mutation in V or J segments of Ig. Similarly, the most likely reasons for false negative results in this case are mutation of gene segments that are not covered by the primer sets or mutation of primer sites during somatic hypermutation. In support of this suspicion is the fact that the IgH3 locus did not show a robust polyclonal curve as would be expected in a hyperplastic lesion, but instead had non-reproducible peaks of variable height within a weak polyclonal background.

**JPC Diagnosis:** vSpleen: Lymphoma, intermediate size, low grade, consistent with marginal zone lymphoma.

**Conference Comment:** The contributor provides an exceptional overview to splenic marginal zone lymphoma and discusses its diagnostic challenges, specifically in distinguishing from hyperplastic nodules. Splenic nodular hyperplasia is a common finding in dogs and presents with variable histologic appearance depending on its cellular constituents. The simple or lymphoid form of hyperplasia is composed of discrete lymphocytes often forming follicles with germinal centers. The complex form of nodular hyperplasia additionally contains a proliferative stroma. Some variations of these lesions were previously diagnosed as fibrohistiocytic nodules, and recent advances in immunohistochemistry has led to their reclassification into a diverse group of diseases to include the above hyperplastic nodules, histiocytic sarcoma, and various subtypes of lymphoma.[3]

Using the grading criteria based on mitotic figures per single 400x field (indolent = 0-1, low = 2-5, intermediate = 5-10, high >10) and cell size determined by comparison to red blood cells (small = 1xRBC, intermediate = 1.5xRBC, large ≥ 2xRBC), we identified this neoplasm as intermediate size and low grade, with definitive classification of MZL requiring immunophenotyping and molecular clonality testing.[8]

**Contributing Institution:** University of Pennsylvania School of Veterinary Medicine
http://www.vet.upenn.edu/research/academic-departments/pathobiology

**References:**

1. Bennetta M, Schechterb GP. Treatment of splenic marginal zone lymphoma: splenectomy versus rituximab. *Semin Hematol*. 2010;47:143–147.

2. Burnett RC, Vernau W, Modiano JF, Olver CS, Moore PF, Avery AC. Diagnosis of canine lymphoid neoplasia using clonal rearrangements of antigen receptor genes. *Vet Pathol*. 2003;40:32-41.

3. Moore AS, Frimberger AE, Sullivan N, Moore PF. Histologic and immunohistochemical review of splenic fibrohistiocytic nodules in dogs. *J Vet Intern Med*. 2012;26:1164-1168.

4. O'Brien D, Moore PF, Vernau W, Peauroi JR, Rebhun RB, Rodriguez Jr. CO, Skorupski KA. Clinical characteristics and outcome in dogs with splenic marginal zone lymphoma. *J Vet Intern Med*. 2013;27:949–954.

5. Osciera D, Owenb R, Johnson S. Splenic marginal zone lymphoma. *Blood Reviews*. 2005;19:39–51.

6. Stefanello D, Valenti P, Zini E, Comazzi S, Gelain ME, Roccabianca P, et al. Splenic marginal zone lymphoma in 5 dogs (2001 –2008). *J Vet Intern Med*. 2011;25:90–93.

7. Traverse-Glehena A, Baseggiob L, Sallesc G, Felmanb P, Bergera F. Splenic marginal zone B-cell lymphoma: a distinct clinicopathological and molecular entity: recent advances in ontogeny and classification. *Current Opinion in Oncology*. 2011;23:441–448.

8. Valli VE, Kass PH, Myint MS, Scott F. Canine lymphomas: Association of classification type, disease stage, tumor subtype, mitotic rate, and treatment with survival. *Vet Pathol*. 2013;50(5):738-748.

9. Valli VE, Vernau W, de Lorimier LP, Graham PS, Moore PF. Canine indolent nodular lymphoma. *Vet Pathol*. 2006;43:241–256.

10. Valli VE, *Veterinary Comparative Hematopathology*. 1st ed. Ames, IA: Blackwell Pub; 2007.

**CASE II**: 09-12665 (JPC 3164837).

**Signalment:** 1.5-year-old spayed female Bassett hound, *Canis familiaris.*

**History:** The dog was presented to the veterinary teaching hospital with inappetence, severe hepatomegaly and icterus. Bloodwork showed circulating lymphoblasts that were fragile and therefore often misshapen. Within one day, the dog developed thrombocytopenia, melena and shock, and died. Unsuccessful therapy included 10,000 IU of L-asparaginase and 1mg/kg of dexamethasone the day prior to death.

**Gross Pathologic Findings:** The mucus membranes and internal organs were moderately icteric. The abdominal cavity contained 1L of watery red effusion. The liver and spleen were both markedly enlarged (2 and 3 times normal weight, respectively). The liver had a prominent reticular pattern. The stomach contained a large blood clot and several gastric ulcers were identified. Digested blood was present throughout the intestinal track. Cranial mesenteric lymph nodes were also enlarged.

**Laboratory Results:** The total WBC on this slide was 85, 600/microliter with lymphocytes composing 83,032/microliter of the total, neutrophils were at 2568/microliter. The HCT was decreased at 32% (38-56) and the platelets were decreased, 58,000/microliter (150,000-500,000).

| | |
|---|---|
| K+ | 6.1 (4-5.4) |
| Phosph | 12.4 (2.2-6.4) |
| Creatinine | 2.1 (0.7-1.6) |
| BUN | 109 (9-26) |

**Histopathologic Description:** Spleen: In several sections of the spleen, the white and red pulps were completely replaced by a highly cellular mass. The mass was composed of round lymphoid cells arranged in sheets and supported by a delicate fibrovascular stroma. The neoplastic cells had distinct margins with scant to moderate amounts of eosinophilic cytoplasm. Nuclei were round to pleomorphic, had a finely clumped chromatin pattern, and 1 to 2 nucleoli. The nuclear diameter of the neoplastic cells was equal to the diameter of two regional erythrocytes. Mitotic figures ranged from 5 to 12 in ten 400x random fields. The tumor was not immunophenotyped.

Lungs: Within the lumen of some of the small-size pulmonary arteries, there were clusters of neoplastic lymphoid cells and karyorrhectic debris. Fibrin thrombi were present in many pulmonary vessels.

Neoplastic infiltrates were also present in the bone marrow, liver, heart and multiple visceral lymph nodes (not shown).

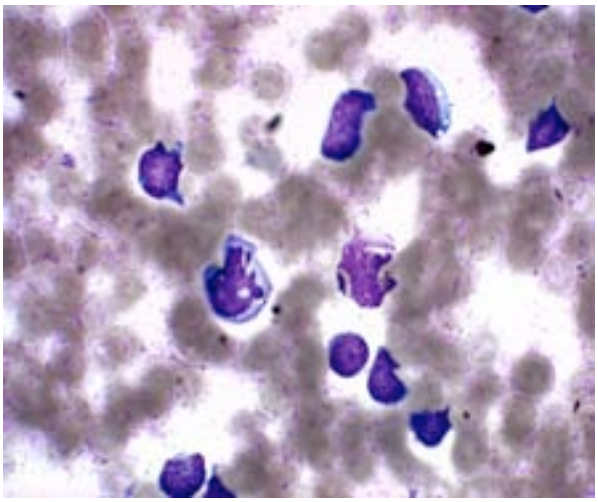

*2-1. Peripheral blood, dog: A blood smear showed circulating lymphoblasts that were fragile and therefore often misshapen. (Wright-Romanovsky, 1000X) (Photo courtesy of: Department of Veterinary Microbiology and Pathology, College of Veterinary Medicine, Washington State University, Pullman, WA 99164-7040, www.vetmed.wsu.edu)*

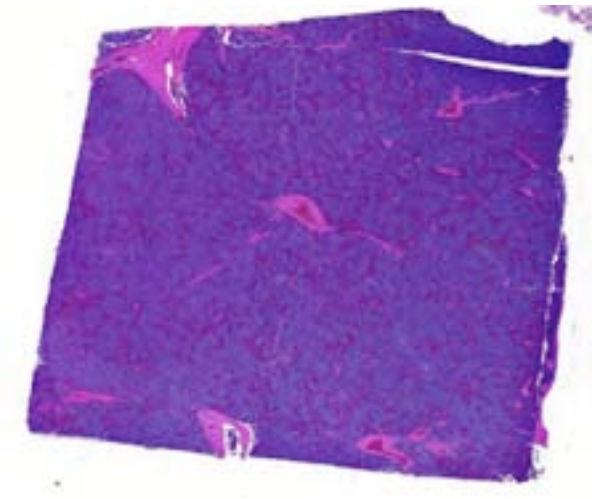

*2-2. Spleen, dog: Normal architecture is replaced by coalescing nodules of lymphocytes. (HE 4.5X)*

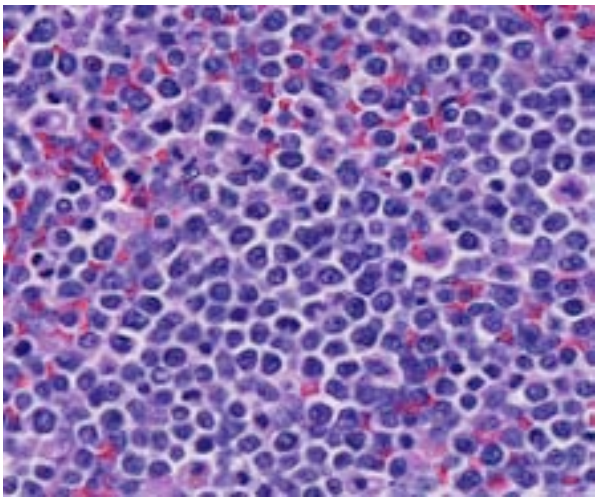

*2-3. Spleen, dog: Neoplastic lymphocytes are 1.5-2x the size of an erythrocyte, with large irregularly round, often indented nuclei. Mitotic figures range up to 10 per high power field. (HE 328X)*

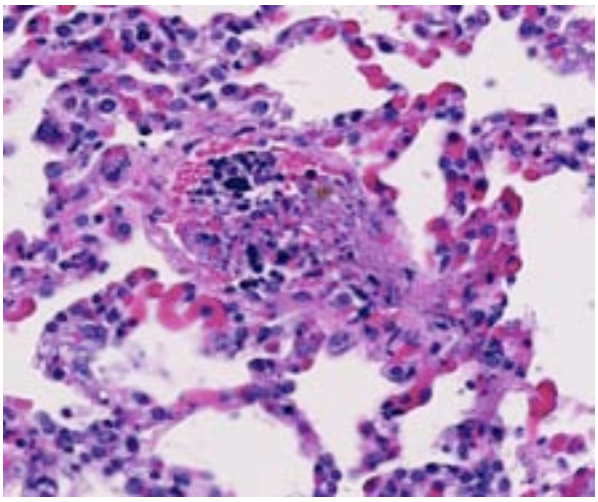

*2-4. Lung, dog: Neoplastic lymphocytes are present within moderate numbers with pulmonary capillaries. Within larger vessels, there are multifocal fibrin thrombi which contain neoplastic cells, cellular debris, and variably-sized globules of basophilic aggregated protein. (HE 284X)*

**Contributor's Morphologic Diagnosis:** 1) Multicentric lymphoblastic lymphosarcoma. 2) Intravascular chromatin emboli compatible with tumor lysis syndrome.

**Contributor's Comment:** Acute tumor lysis syndrome (ATLS) is a life-threatening metabolic derangement associated with rapid cell death in high volume tumors, most often leukemias and lymphomas. Although it can occur spontaneously in untreated individuals, the most common presentation is at some period after the institution of chemotherapy or radiation therapy.[2] Risk factors in human patients include tumors of high growth fraction, large tumor bulk and the form of therapy. It is most commonly induced by treatment with a variety of chemotherapeutic agents, including L-asparginase, but has also been seen after treatment with ionizing radiation, biological response modifiers, hormone therapy and glucocorticoid therapy.[2]

Clinical signs, which can include vomiting, lethargy, respiratory distress and cardiac arrest, are related to the massive release of intracellular purines, phosphorus, uric acid, potassium and lactate.[1] Common clinicopathologic abnormalities include hyperphosphatemia, hyperkalemia and acidosis. Individuals with renal insufficiency may be at greater risk for ATLS (due to reduced ability to clear metabolites from the blood) and ATLS patients are also at risk for developing renal failure if realkalinization of blood leads to calcium and phosphorus precipitation in the kidney.[2]

ATLS has been reported in dogs[5], a cat[1] and in mice with experimentally induced lymphoid malignancies.[6] The histologic lesion of ATLS, large chromatin emboli in blood vessels, especially in the lung, was recently described in a 129/SvEv mouse with experimentally induced acute myeloid leukemia that had been treated with valproic acid, a histone deacetylase inhibitor known to produce tumor lysis.[6]

In dogs, ATLS has been associated with dramatic reduction in tumor mass.[5] In this case, the dog had severe clinical signs and may have been manifesting ATLS, DIC or both at the time of presentation. However, both chemotherapeutic agents the dog received have been associated ATLS. Although no dramatic reduction in tumor size was noted clinically or pathologically, there was necrosis of tumor cells in the spleen, and the characteristic histologic lesions in the lung indicate that ATLS was most likely at least partly responsible for the dog's demise.

**JPC Diagnosis:** 1. Lung, Spleen: Lymphoma, intermediate to large cell, high grade. 2. Lung, septal capillaries: Neoplastic thrombi with necrosis.

**Conference Comment:** The tumor lysis syndrome occurs when neoplastic cells release more of their contents in the bloodstream than can

be handled by the body's normal homeostatic mechanisms, and is defined clinically as two or more of the following metabolic abnormalities appearing simultaneously: hyperuricemia, hyperkalemia, hyperphosphatemia and hypocalcemia. Hyperkalemia can cause fatal dysrhythmias. Hyperphosphatemia can precipitate as calcium phosphate crystals in multiple organs and also exacerbate hypocalcemia. Hypocalcemia itself leads to tetany, dysrhythmias and seizures. Uric acid accumulation can cause acute renal injury due to vasoconstriction, impaired autoregulation, decreased renal blood flow, oxidation, and inflammation. Additionally, the lysis of neoplastic cells induces the release of cytokines.[3] This combination of metabolic derangements often proves lethal due to multiple organ failure.

Lymphoblastic lymphoma (LBL) is a diffuse lymphoma characterized by a dispersed chromatin pattern which obscures nuclear detail, and thus has indistinct nucleoli. Of note, the term "lymphoblast" has been commonly misused in veterinary medicine. By definition, the lymphoblasts of LBL are *intermediate-sized cells* and not the large lymphocytes seen in cases of diffuse large B cell lymphoma or peripheral T cell lymphoma. LBL can look very similar to hepatosplenic lymphoma (HS-TCL) and both are comprised of T-cells. HS-TCL is centered on the liver and spleen; however, it occurs without significant lymph node involvement which was identified in this case.[4] Additionally, another distinct entity in the liver has been proposed called hepatocytotropic lymphoma (HC-TCL) for those subtypes that are not confined to the sinusoids but rather invade hepatic cords.[4] All three discussed subtypes, (LBL, HS-TCL, HC-TCL) are associated with a poor prognosis in dogs.[4,7]

**Contributing Institution:** Department of Veterinary Microbiology and Pathology
College of Veterinary Medicine
Washington State University
Pullman, WA
www.vetmed.wsu.edu

**References:**

1. Calia CM, Hohenhaus AE, et al. Acute tumor lysis syndrome in a cat with lymphoma. *J Vet Intern Med.* 1996;10:409-411.
2. Fleming DR, Doukas MA. Acute tumor lysis syndrome in hematologic malignancies. *Leuk and Lymphoma.* 1992;8:315-318.
3. Howard SC, Jones DP, Pui CH. The tumor lysis syndrome. *N Engl J Med.* 2011;364(19): 1844-1854.
4. Keller SM, Vernau W, Hodges J, et al. Hepatosplenic and hepatocytotropic T-cell lymphoma: two distinct types of T-cell lymphoma in dogs. *Vet Pathol.* 2013;50(2):281-290.
5. Myonakis ME, Koutinas AF, et al. Acute tumor lysis syndrome in a dog with B cell lymphoma. *Austr Vet J*. 2007;85:206-208.
6. Radaelli E, Marchesi F, et al. Diagnostic excercise: Sudden death in a mouse with experimentally induced acute myeloid leukemia. *Vet Pathol*. 2009;46:1301-1305.
7. Valli VE, Kass PH, Myint MS, Scott F. Canine lymphomas: Association of classification type, disease stage, tumor subtype, mitotic rate, and treatment with survival. *Vet Pathol*. 2013;50(5):738-748.

**CASE III**: B1316893 (JPC 4048571).

**Signalment:** 10-year-old castrated male golden retriever, *Canis familiaris.*

**History:** The dog was previously diagnosed with T-cell lymphoma based on PARR only. A CHOP (cyclophosphamide-doxorubicin-vincristine-prednisone)-based chemotherapy protocol commenced for 6 months with minimal response. One month after cessation of chemotherapy treatment, the lymph nodes enlarged further. A fine needle aspirate and biopsy was performed on the left mandibular lymph node at a referring practice and in-house cytology revealed a small to intermediate cell lymphoma with low mitotic index. The biopsy sample was submitted for histopathology and immunohistochemistry.

**Gross Pathology:** N/A

**Laboratory Results:** N/A

**Histopathologic Description:** Two sections of the lymph node are evaluated. The nodal architecture is almost completely obliterated by a somewhat nodular infiltrate. The fading follicles are compressed and pushed against the nodal trabeculae. The neoplastic cells are arranged in broad sheets and consist of intermediate sized round cells with nuclei approximately 1-1.5 times the diameter of a red blood cell. The cells have a small amount of lightly eosinophilic cytoplasm and the nuclei are round to oval with sharp shallow nuclear indentations. Mitoses are rare.

Immunohistochemical stains CD3, CD20 and CD79a were performed. The neoplastic cells have strong positive CD3 immunoreactivity. The peripheralized fading follicles have positive CD20 and CD79a immunoreactivity. This staining pattern confirms the diagnosis of a T-zone lymphoma.

**Contributor's Morphologic Diagnosis:** Left mandibular lymph node: T-zone lymphoma, intermediate cell.

**Contributor's Comment:** T-zone lymphoma (TZL), which is of T-cell lineage, is classified as

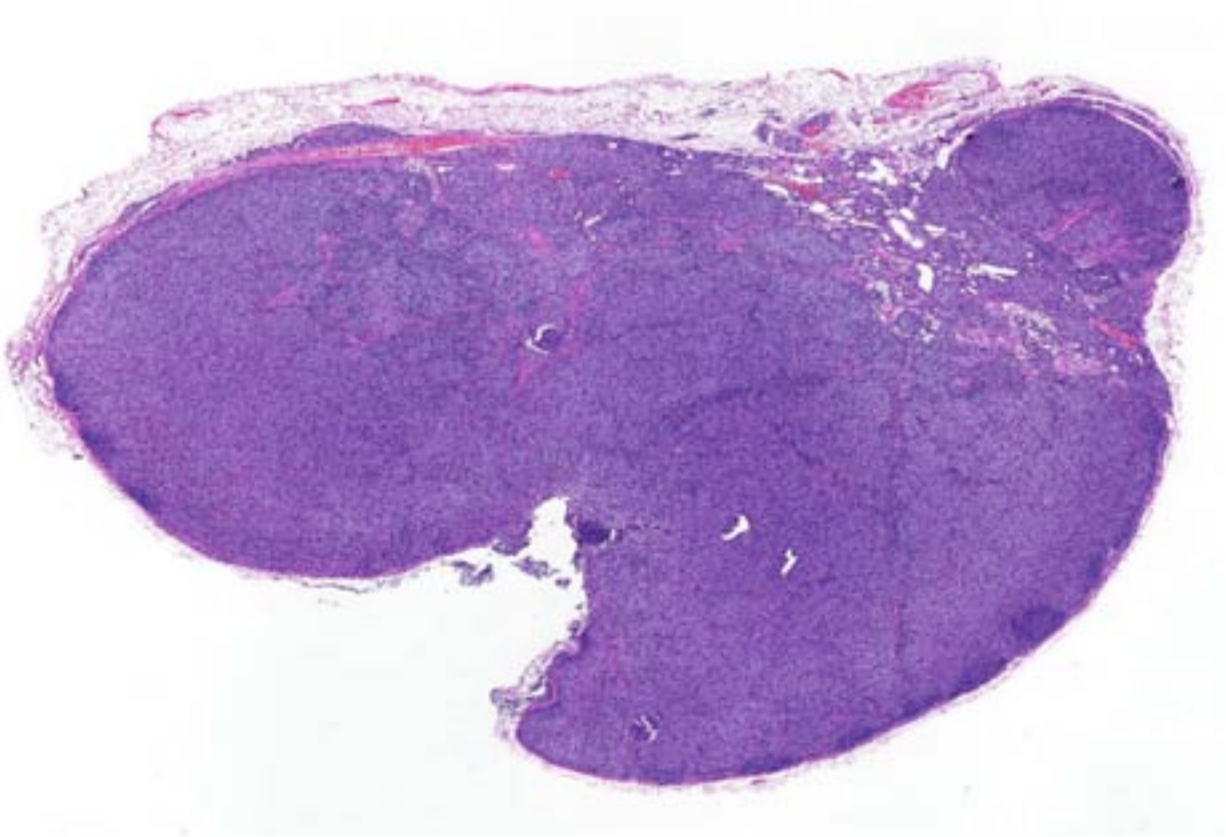

*3-1. Lymph node, dog: The lymph node architecture is largely replaced by a lymphoid neoplasm composed of expanding nodules of neoplastic cells. (HE 6X)*

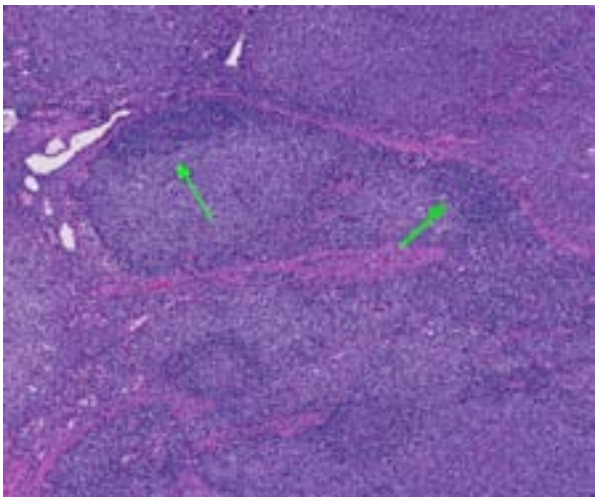

*3-2. Lymph node, dog: Expanding nodules neoplastic lymphocytes compress pre-existent follicular lymphocytes to the periphery (arrows) ("fading follicles"). (HE 75X)*

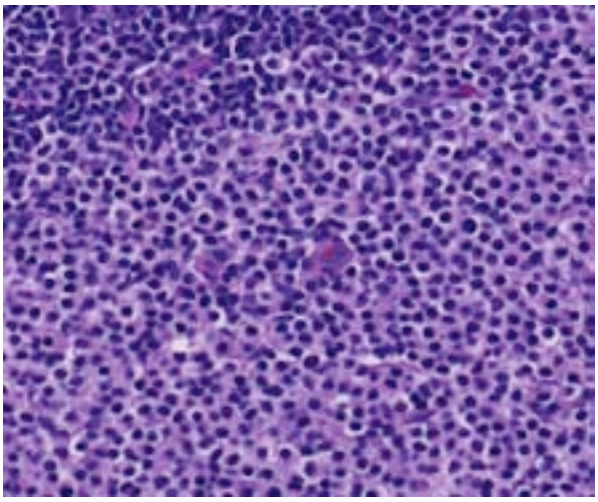

*3-3. Lymph node, dog: Neoplastic cells are small, with a moderate amount of cytoplasm and small round hyperchromatic nuclei. Mitotic figures are rare. (HE 380X)*

one of the subtypes of canine indolent lymphomas. Canine indolent lymphomas are a heterogeneous group of lymphoma subtypes that are similar to specific subtypes of non-Hodgkin's lymphomas in humans.[2] Other subtypes include, nodal and splenic marginal zone lymphoma, follicular lymphoma and mantle cell lymphoma, which are all of B-cell lineage, T-cell rich B-cell lymphoma, small lymphocytic lymphoma of B- and T-cell, and lymphoplasmacytic lymphoma.[2,7] These subtypes have a low mitotic index and slow clinical progression.[8] Dogs usually retain a normal appetite and physical activity, even in advanced stages of disease.[7]

T-zone lymphoma first appeared in the Kiel classification with a description of a nodal lymphoma that occurs rarely in humans.[7,8] In 2008, a description was added to the human WHO (World Health Organization) classification as a morphologic variant of peripheral T-cell lymphoma not otherwise specified (PTCL-NOS), and is characterized by a clonal expansion of T-zone lymphocytes that exhibit a unique architectural and cytomorphologic pattern.[2,5] Human TZL comprise only 1.5% of all cases of PTCL-NOS.[5] Although the true incidence of canine TZL is unknown, two recent publications indicate that they are relatively common, comprising between 15.5 and 62% of all canine indolent lymphomas, which themselves are reported to have an incidence rate of 29% of all canine lymphomas.[2,5,8] Almost all cases of TZL occur in peripheral lymph nodes with a predilection for the mandibular node, and usually have a history of a single enlarged lymph node for as long as a year.[7] A higher incidence rate is observed in the golden retriever and shih tzu breeds, and in the majority of cases, a lymphocytosis is frequently reported at the time of diagnosis.[2, 5]

The WHO system of classification of canine lymphomas defines TZL as a nodal T-cell lymphoma, in which neoplastic cells expand the paracortex and medullary cords without effacement of the nodal architecture.[7] The architecture of TZL has a signature pattern that results from the expanding population of neoplastic T-cells which peripheralizes fading atrophied germinal centers in the outer cortex and medulla. The capsule is usually focally thinned, the peripheral sinuses are compressed, and postcapillary venules are prominent. The intervening areas of paracortex are expanded by a uniform population of small or intermediate sized lymphocytes. There is no extension of the neoplasm into the peripheral sinuses or perinodal tissue. Areas of empty sinus ectasia are observed in the later stages. Two subtypes are categorized based on the nuclear size of the neoplastic T-cells compared to the diameter of a red blood cell (RBC). TZL of small cells have nuclei that are 1-1.25 x RBC, and TZL of intermediate-sized cells are 1.5 x RBC. Neoplastic cells have distinct cell borders with abundant cytoplasm. The nuclei have frequent sharp shallow indentations, are hyperchromatic with little internal detail, and inconspicuous nucleoli. The mitotic index is low, usually 0-1 on most 40x fields.

TZL must be differentiated from small lymphocytic lymphoma of T or B-cell type and benign small lymphocytes that are diagnosed via fine-needle aspirates.[7] B-cell proliferations symmetrically surround germinal centers. Small lymphocytic lymphomas are not associated with fading germinal centers or sinus ectasia, and the nuclei do not have consistent nuclear indentations.

Immunohistochemistry and flow cytometry are powerful tools when differentiating TZL from benign nodules of hyperplasia and other nodal lymphomas. TZL cells have a solid CD3 positive immunoreactivity and are negative for CD79a and CD20.[5,7] A recent study demonstrated CD45 immunophenotyping using flow cytometry on peripheral blood and lymph node aspirates.[5] CD45 is a tyrosine phosphatase that has a complex role in the regulation of signaling through the T-cell receptor, and in the regulation of cytokine receptor activation. Neoplastic T-cells do not express CD45. To date, there is no normal CD45 negative T-cell counterpart described in mice or people, and no evidence of CD45 negative T-cells in the blood or lymph nodes in normal or reactive canine lymph nodes. The loss of CD45 expression appears to be correlated with malignant transformation of T-cells; however, the mechanisms involved are not known.

**JPC Diagnosis:** Lymph node: T-zone lymphoma.

**Conference Comment:** The contributor presents an excellent case of T-zone lymphoma and adeptly outlines its histologic and cellular characteristics, which will aid in diagnosis of this common small to intermediate cell variant of nodal indolent lymphoma. This case illustrates the challenges of establishing a firm diagnosis to guide the treatment protocol. The initial diagnosis based on PARR led to the initiation of a treatment regimen that is largely ineffective with T-zone lymphomas due to their indolent nature because of their low mitotic rate. PARR is a PCR-based assay used for determining clonality. It can be useful in differentiating hyperplastic from neoplastic lesions and in monitoring response to treatment; however, it should be used in conjunction with other assessments including histopathology and immunohistochemistry in determining treatment strategy.[1]

Lymphoma can be readily diagnosed on fine needle aspirate; however, it is not yet possible to subclassify it by cytology alone. Aspirates of T-cell lymphomas do sometimes have a "hand mirror" morphology when smeared onto a slide which may allow the examiner to favor this classification.[3,6] These cells are mentioned in other sources as reactive lymphocytes with plasmacytoid features, thus their presence should be interpreted with caution.[4]

**Contributing Institution:** University of Pennsylvania School of Veterinary Medicine
Department of Pathobiology, 4005 MJR-VHUP
3900 Delancey Street
Philadelphia, PA
http://www.vet.upenn.edu/research/academic-departments/pathobiology

**References:**

1. Avery A. Molecular diagnostics of hematologic malignancies. *Top Companion Anim Med*. 2009;24(3):144-150.
2. Flood-Knapik KE, Durham AC, Gregor TP, Sánchez MD, Durney ME, Sorenmo KU. Clinical, histopathological and immunohistochemical characterization of canine indolent lymphoma. *Vet Comp Oncol*. 2013;11:272–286.
3. Han JY, Kim JS, Kim DH, et al. Cytologic features of ascetic fluid complicated by small cell variant T-cell prolymphocytic leukemia-a case report. *Korean J Cytopathol*. 2008;19(2):168-172.
4. Rizzi TE, Cowell RL, Tyler RD, Meinkoth JH. Effusions: abdominal, thoracic and pericardial. *Diagnostic Cytology and Hematology of the Dog and Cat*. 3rd ed. St. Louis, MO: Mosby Elsevier; 2008:240-241.
5. Seelig DM, Avery P, Webb T, et al. Canine t-zone lymphoma: Unique immunophenotypic features, outcome, and population characteristics. *J Vet Intern Med*. 2014;28:878–886.
6. Valli VE, Kass PH, San Myint M, Scott F. Canine lymphomas: Association of classification type, disease stage, tumor subtype, mitotic rate, and treatment with survival. *Vet Pathol*. 2013;50(5):738-748.
7. Valli VE, San Myint M, Barthel A, et al. Classification of canine malignant lymphomas according to the World Health Organization criteria. *Vet Pathol*. 2011;48:198–211.
8. Valli VE, Vernau W, Lorimier LP, Graham PS, Moore PF. Canine indolent nodular lymphoma. *Vet Pathol*. 2006;43:241–256.

**CASE IV:** 2008906084 (JPC 3103338).

**Signalment:** 11-year-old spayed female Japanese domestic, *Felis cattus*.

**History:**

2008.3.25 This cat showed diarrhea lasting for one month and gradual weight loss for one year from 4.82kg to 3.76kg. Diarrhea disappeared immediately after general treatment with an anti-diarrheal drug.

2008.5.12 Repeated vomiting appeared from recent two weeks with complete loss of appetite. A mass lesion was found in the abdominal cavity by X-ray examination and echography.

2008.5.13 Intestinal obstruction was confirmed in the small intestine by barium contrast study.

2008.5.14 The mass was surgically removed. The enlargement of the mesenteric lymph node was observed during a laparotomy.

**Gross Pathologic Findings:** The affected part of the small intestine was a mass lesion and consisted of severely thickened intestine wall with narrowing of the lumen.

**Laboratory Results:** Fine needle biopsy findings: Comparatively uniform lymphoblast-like cells were observed on the smear from needle biopsy of the mesenteric lymph node.

**Histopathologic Description:** Lymphoid cells proliferated throughout the entire intestinal wall from the mucosa to the serosa and resulted in severe thickening of intestinal wall. Numerous lymphoid follicles of varying size were formed in the muscular and serosal layer among the severely infiltrated tumor cells. Some follicles had clear germinal centers and incomplete mantle zones. The tumor cells other than follicle-forming cells had small to medium-sized nuclei that are round to irregularly indented and a have thick nuclear membrane. The nuclei had dense chromatin with multiple small distinct nucleoli (or with a small distinct nucleolus). The cytoplasm was pale and abundant. Mitotic figures were observed at rate of 7 cells per 10 high power fields. Small number of eosinophils infiltrated among the tumor cells and fibrous stroma was slightly increased in some areas with proliferated tumor cell.

Immunohistochemically, the majority of tumor cells were positive for CD3 and TIA-1, negative for CD79a and CD20. In the muscular layer where the lymph follicles formed, many cells forming the follicles were positive for CD79a and CD20 and negative for CD3 and TIA-1, whereas a few cells of germinal center were positive for CD3 and TIA-1.

Based on immunohistochemical findings, tumor cells have a T-cell phenotype in this lymphoma but lymph follicles formed in the tumor mass consisted of B-cells.

**Contributor's Morphologic Diagnosis:** Small intestine: Malignant lymphoma, T cell lymphoma.

**Contributor's Comment:** Hematopoietic tumors (lymphoma and mast cell tumors) are the most common type of neoplasia in the feline intestine.[7] In alimentary lymphoma, the tumors are usually of the B-cell origin, with few being T-cell origin.[4,7,11,15] B-cell lymphoma arises from the germinal center of the gut, MALT, and drainage lymph nodes.[6,7] In contrast, T-cell type of multicentric lymphoma proliferates from the paracortical area,[6,7] and T-cell lymphoma of the intestine usually involves the lamina propria with epitheliotropism to the mucosal epithelium.[2,8,15]

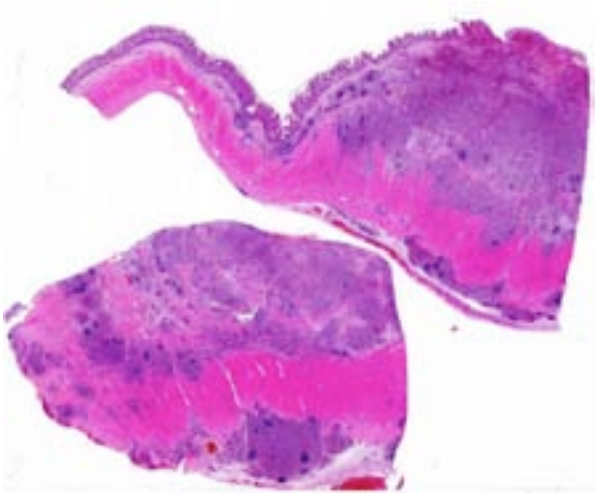

*4-1. Small intestine, cat: The intestinal wall is markedly expanded and transmurally effaced by sheets of neoplastic cells. (6X)*

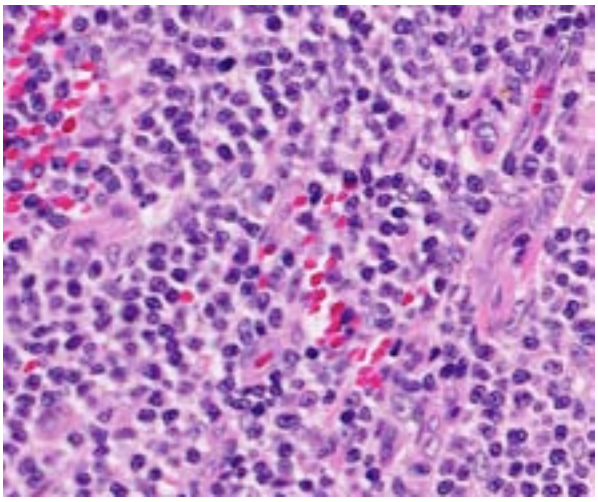

*4-2. Small intestine, cat: Neoplastic cells have small amounts of cytoplasm and irregularly round nuclei with small blue nucleoli. Mitotic figures are rare. (HE 350X)*

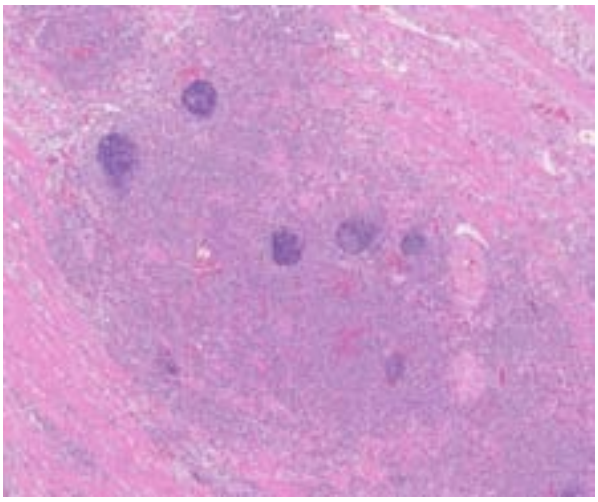

*4-3. Small intestine, cat: Non-neoplastic lymphoid follicles are scattered throughout all layers of the intestinal wall, including the muscular tunics. (HE 70X)*

The present case was characterized by formation of lymph follicles in the mass of tumoral proliferation. These lymph follicles were not original lymphoid tissue, because they were formed in muscular and serosal layers where there is no lymphatic tissue in the normal condition. In addition, this lymphoma had a T-cell phenotype and the follicles were composed of B-cell phenotype. Therefore, it was likely that lymphoid follicles were formed due to the reactive response to tumor cells or immunologic stimuli by the altered environment resulting in proliferation of tumor cells. The neoplastic cell proliferation forming lymph follicles was similar to lymphoma of mucosa-associated lymphoid tissue (MALT lymphoma) in morphologic growth pattern. MALT lymphoma and marginal zone lymphoma are B-cell lymphoma,[14] and the tumor cells encircle follicles outside the mantle cell layer in these types of lymphoma. Cytologically, T-cell lymphoma consists of smaller cells with low mitotic rate as in the present case. However, MALT lymphoma is usually composed of small lymphocytes with indented nuclei, or there may be a more mixed pattern with some larger lymphoid cells similar to the centrocytes and centroblasts of benign germinal centers.[14]

Intestinal T-cell lymphoma is characterized also by epitheliotropism of tumor cells.[2,8,15] Neoplastic lymphocytes usually are small round cells that resemble mature lymphocytes. However, epitheliotropism was not seen in the tumor cells of the present case. In a report of canine intestinal T-cell lymphoma, approximately 25% did not show epitheliotropic behavior.[14] In addition, in humans, MALT lymphoma usually forms lymphoepithelial lesions and tumor cells invade between mucosal epithelium. Lymphoepithelial lesions resemble epitheliotropism, but are characterized by centrocyte-like cell invasion and destruction of the epithelium. Therefore, epitheliotropism is not specific for T-cell lymphocytes and formation of lymph follicles is also not specific for B-cells.

**JPC Diagnosis:** Intestine, ileum: Lymphoma, intermediate size, low grade, transmural.

**Conference Comment:** The cellular morphology and epitheliotropic behavior presented in the small intestine of a cat is distinctive for T-cell lymphoma (TCL). Intestinal lymphomas can be further classified as mucosal or transmural based on depth of invasion. Epitheliotropism can occur in both types, and occurs most commonly in the villous epithelium. Mucosal T-cell lymphoma closely matches the WHO entity enteropathy-associated T-cell lymphoma (EATCL) type II. Transmural T-cell lymphomas more often can lead to intestinal obstruction and perforation and closely match the WHO entity EATCL type I.[9]

The most common presentation of lymphoma in cats has evolved as the success of FIV/FeLV testing and vaccination programs have been realized. In the 1970's, 70% of feline lymphoma cases in the U.S. were attributed to FeLV infection which dropped to less than 15% twenty years later.[1] Interestingly, as the prevalence of

these known oncogenic viruses have diminished, the incidence rate of lymphoma in cats appears to be increasing.[1,9] Retroviral-associated lymphomas commonly presented as mediastinal or multicentric forms in young cats.[3,12] The majority of lymphomas in cats now occur in the gastrointestinal tract.[9] Recent literature has also described a shift in prevalence from B-cell to T-cell lymphomas in intestinal lymphoma in cats.[9,12] Diffuse large B-cell lymphomas are considered most common in the stomach of cats.[9] Other subclassifications of significance in cats include large granular lymphocyte lymphoma which also occurs in the intestinal tract but often with more systemic involvement and is associated with a poor prognosis. T-cell rich large B-cell lymphoma is an indolent type with a mixed cell population to include bizarre giant or multinucleated cells and typically presents in a single lymph node.[3]

Conference participants were interested in the unique histologic presentation of lymphoma in this case, with the formation of multiple lymphoid follicles dispersed throughout all levels of the muscularis mucosa. Theories regarding their formation were exchanged, including immune stimulation by antigens or toxin absorption through the disrupted mucosal epithelium.

**Contributing Institution:** Department of Pathology, Setsunan University, 45-1 Nagaotohge-cho, Hirakata, Osaka 573-0101, JAPAN

**References:**

1. Beatty J. Viral causes of feline lymphoma: retroviruses and beyond. *Vet J*. 2014;201:174-180.
2. Carreras JK, Goldschmidt M, Lanb M, McLear RC, Drobatz KJ, Sorenmo KU. Feline Epitheliotropic intestinal malignant lymphoma: 10 cases(1997-2000). *J Vet Intern Med*. 2003;17:326-331.
3. Chino J, Fujino Y, Kobayashi T, et al. Cytomorphological and immunological classification of feline lymphomas: clinicopathological features of 76 cases. *J Vet Med Sci*. 2013;75(6):701-707.
4. Gabor LJ, Canfield PJ, Malik R. Immunophenotypic and histological characterization of 109 cases of feline lymhosarcoma. *Austrarian Veterinary Journal*. 1999;76:725-736.
5. Gabor LJ, Malik R, Canfield PJ. Clinical and anatomical features of lymphosarcoma in 118 cats. *Austrarian Veterinary Journal*. 1998;76:725-736.
6. Head KW, Cullen JM, Dubielzig RR, Else RW, Misdorp W, Patnaik AK, et al. Histological classification of alimentary tumors of domestic animals. In: *Histological Classification of Tumors of the American System of Domestic Animals*. 2nd Series. Vol. X, Washington, DC: Armed Forces Institute of Pathology/ American Registry of Pathology and the Worldwide Reference on Comparative Oncology; 2003:87-100.
7. Head KW, Else RW. Other tumors of the alimentary tract. In: Menten DJ, ed. *Tumors in Domestic Animals*. Fourth ed. Ames, Iowa: Iowa State Press; 2002:467-8, 471-3.
8. Krecic MR, Black SS. Epitheliotropic T-cell gastrointestinal tract lymphosarcoma with metastasis to lung and skeletal muscle in a cat. *J Am Vet Med Assoc*. 2000;216:524-529.
9. Moore PF, Rodriguez-Bertos A, Kass PH. Feline gastrointestinal lymphoma: mucosal architecture, immunophenotype, and molecular clonality. *Vet Pathol*. 2012;49(4):658-668.
10. Ozaki K, Yamagami T, Nomura K, Narama I. T-cell lymphoma with eosinophilic infiltration involving the intestinal tract in 11 dogs. *Vet Pathol*. 2006;43:339-344.
11. Patterson-Kene JC, Perrins Kugler B, Francis K. The possible prognostic significance of immunophenotype in feline alimentary lymphoma: a pilot study. *J Comp Path*. 2004;130:220-222.
12. Pohlman LM, Higginbotham ML, Welles EG, Johnson CM. Immunophenotypic and histologic classification of 50 cases of feline gastrointestinal lymphoma. *Vet Pathol*. 2009;46:259-268.
13. Vail DM. Hematopoietic tumors. In: Ettinger SJ, Feldman EC, eds. *Veterinary Internal Medicine*. 7th ed. Vol 2. St. Louis, MO: Saunders Elsevier; 2010:2149-2150.
14. Valli VE, Jacobs RM, Parodi AL, Vernau W, Moore PE. Histological classification of hematopoietic tumors of domestic animals. In: Histological Classification of Tumors of the American System of Domestic Animals. 2nd Series, Vol.Ⅷ. Washington, DC: Armed Forces Institute of Pathology/ American Registry of Pathology and the Worldwide Reference on Comparative Oncology; 2002:28-47.
15. Waly NE, Gruffydd-Jones TJ, Stoke CR, Day MJ. Immunohistochemical diagnosis of alimentary lymphomas and severe intestinal inflammation in cats. *J Comp Path*. 2005;133:253-260.

**Joint Pathology Center**
**Veterinary Pathology Services**

# WEDNESDAY SLIDE CONFERENCE 2014-2015

## Conference 21

**15 April 2015**

**Guest Moderator:**
Jey Koehler, DVM, PhD, ACVP
Histopathology Core Laboratory Department of Pathobiology
Auburn University College of Veterinary Medicine

---

**CASE I:** 13-45574 (JPC 4048670).

**Signalment:** 6-week-old neutered male mixed breed canine, *Canis familiaris*.

**History:** The puppy was presented to the referring DVM for wellness exam and vaccination. The puppy was vaccinated with Durammune-5, a combination vaccine against canine distemper, canine adenovirus 2, canine parainfluenza virus, and canine parvovirus at approximately 1 pm. The puppy died the next day and was presented to the diagnostic lab for necropsy examination.

**Gross Pathology:** The animal was in adequate nutritional condition evidenced by adequate visceral and subcutaneous adipose tissue stores. The oral mucous membranes and subcutaneous tissues were markedly pale. The thymus contained numerous, multifocal, pinpoint, dark red foci (petechial hemorrhages).

The peritoneal cavity contained 20 ml of dark red watery fluid. The intestines were segmentally filled with dark brown, slightly flocculent, viscous digesta. Mesenteric lymph nodes were dark red and moderately enlarged (up to 1.2 cm in diameter). Hepatic parenchyma and brain tissues were grossly unremarkable.

**Laboratory Results**: *Salmonella* PCR, parvovirus FA, distemper FA were all negative on intestine samples. Bacterial culture revealed heavy growth of *Escherichia coli* and moderate growth of *Proteus* sp. and beta *Escherichia coli* from the intestine. No bacteria were cultured from the spleen or urine. Fecal flotation revealed the presence of *Isospora* sp.

**Histopathologic Description:** Liver: Diffusely in the liver parenchyma are multiple coalescing foci of hepatocellular swelling and necrosis. These foci are typically centrilobular to midzonal and occasionally extend to periportal areas. Necrotic hepatocytes present with a hypereosinophilic, micro-vacuolated to wispy cytoplasm, and nuclear fragmentation (karyorrhexis), pyknosis or complete lack of nuclear staining. Sinusoids within necrotic foci are frequently expanded by erythrocytes (congestion and/or hemorrhages).

Throughout all zones of the hepatic lobule, numerous hepatocytes, few endothelial cells and rare Kupffer cells contain a large (up to 5 micron), solid amphophilic intranuclear viral inclusion body that marginates the chromatin and is often surrounded by a clear halo (Cowdry type-A).

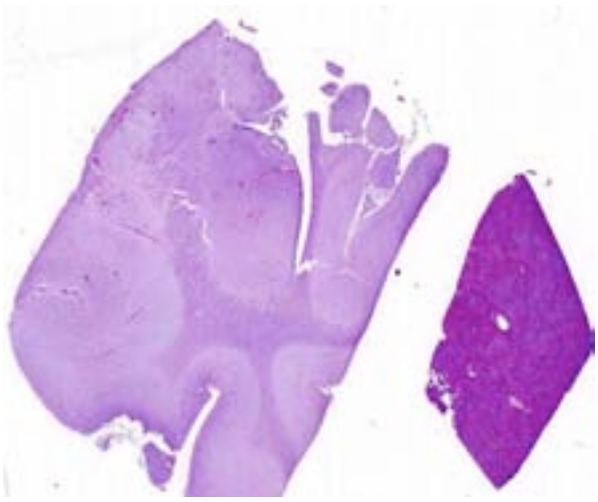

*1-1. Cerebrum and liver, dog: A subgross retiform pattern of hepatic necrosis is visible in the liver. (HE 6X)*

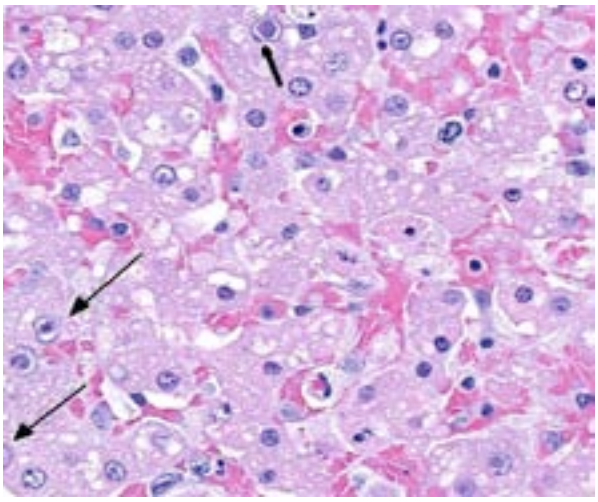

*1-2. Liver, dog: Hepatocytes at edges of necrotic areas contain large intranuclear adenoviral inclusions (arrows). Within necrotic areas (center), plate architecture is lost and hepatocyte nuclei are pyknotic or karyorrhectic. (HE 340X)*

Brain: Multifocally, extending from the caudal brainstem to the thalamus, hypothalamus and basal nuclei, endothelial cells in blood vessels are frequently necrotic and occasionally contain similar intranuclear viral inclusion bodies. Neighboring endothelial cells are enlarged (reactive). The tunica media is often hypereosinophilic and disorganized, and mixed with pyknotic nuclear debris (fibrinoid necrosis). In the surrounding blood vessels Virchow-Robin's spaces contain small numbers of lymphocytes, macrophages, necrotic cells and extravasated erythrocytes (hemorrhage). Similar but less extensive lesions are observed in meninges and cerebral cortex. The cerebellum was not affected.

Other significant histologic changes were identified in the following organs:

Thymus (hemorrhage and lymphocytolysis), spleen, Peyer's patches and lymph nodes (massive lymphoid and red pulp necrosis with very few inclusions), kidney (inclusions in glomeruli and vascular endothelial cells), heart (rare endothelial inclusions).

**Contributor's Morphologic Diagnosis:** Liver: Hepatitis, necrotizing, centrilobular to mild zonal, severe, acute with hepatocellular and endothelial intranuclear viral inclusion bodies.

Brain: Encephalitis, multifocal, moderate, acute, with vasculitis, hemorrhages and endothelial intranuclear viral inclusion bodies.

**Contributor's Comment:** Histopathology is consistent with canine adenovirus type I infection (CAV-1). There is no reported pathogenicity with subcutaneously administered modified live canine adenovirus and the incubation period of adenovirus is typically 4-9 days[7]; therefore, this dog was likely naturally infected with CAV-1 prior to vaccine administration. Vaccination against canine adenovirus has greatly decreased the incidence of infectious canine hepatitis (ICH) cases in domestic dogs, but subclinical infection is prevalent in undomesticated canines, and likely provides a reservoir for infection. The virus is very stable in the environment, and can be excreted in the urine from previously infected animals for up to 9 months.[7] Maternal antibodies are typically protective for puppies until the point at which they are no longer absorbed, typically around 5-7 weeks of age.[7] Maternal antibodies will also inactivate vaccine virus. Therefore, disease may develop in puppies exposed to the virus, whose dam was unvaccinated, who never nursed (were bottle-fed), or who were not vaccinated according to an appropriate schedule.

The pathogenesis of ICH begins with infection with CAV-1 after exposure to infectious saliva, feces, urine, or respiratory secretions. The virus initially localizes in tonsil and regional lymph nodes, finally spreading to the bloodstream approximately four days post infection. Primary targets of circulating CAV-1 include hepatocytes, Kupffer cells, glomerular endothelium, and uvea. Any vascular endothelium is susceptible, causing

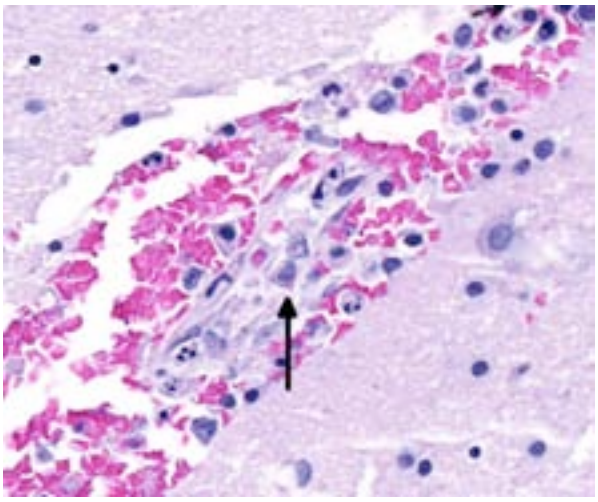

*1-3. Cerebrum, dog: Multifocally, capillary endothelium contains similar adenoviral inclusions. Adjacent endothelium is necrotic, and erythrocytes are extravasated around the damaged vessel. (HE 360X)*

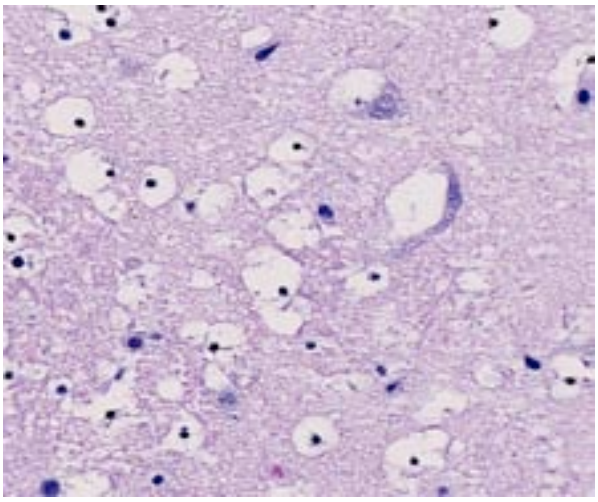

*1-4. Cerebrum, dog: In areas adjacent to damaged vasculature, large halos adjacent to neurons and oligodendrocytes suggest marked edema. (HE 256X)*

multifocal petechial hemorrhage, and severe widespread endothelial damage leads to disseminated intravascular coagulation (DIC).[7] Although adenovirus was first identified after noting viral inclusions in the brains of foxes with encephalitis, the CNS form is rare. Adenoviral tropism for the CNS has been suggested to be related to viral strain differences.[4]

The earliest clinical sign of ICH is a fever followed by tonsillar enlargement, depression, anorexia, tachycardia, tachypnea, vomiting, diarrhea, abdominal pain/distension (due to fluid accumulation and hepatic enlargement), and hemorrhage if liver damage is severe or endothelial damage is widespread. Neurologic signs (ataxia, hypersalivation, and seizures) may occur if there is CNS involvement. If the animal does not die from severe hepatic failure or DIC, approximately 7-14 days post infection, corneal edema (the classic "blue eye" lesion)[12] and azotemia, hematuria, and proteinuria (secondary to glomerulonephritis) are possible. As was seen in this case, sudden death with no previous clinical signs is possible when CNS infection occurs.[14]

Grossly, hepatic lesions typical of adenoviral infection (swollen mottled liver with gallbladder edema)[5,7] were not noted in this case. However, histologic lesions of multifocal hepatic necrosis, combined with striking intranuclear inclusions in hepatocytes and vascular endothelial cells in the liver and brain suggest etiology consistent with canine adenovirus type 1 (infectious canine hepatitis/CAV-1).

Histologically, typical lesions usually consist of centrilobular to midzonal hepatic necrosis with general sparing of periportal hepatocytes. Cowdry type A inclusions (marginated chromatin and clear halo around the inclusion) are seen in Kupffer cells, hepatocytes, and affected vascular endothelium. Lymphoid organs may be congested with necrosis of lymphoid follicles and intranuclear inclusions in vascular endothelium and histiocytes can be seen. Inclusions may also be found in glomerular or tubular renal epithelium, and central nervous system (CNS) vascular endothelium. Within the CNS, multifocal neuropil hemorrhages, perivascular accumulations of mononuclear cells, mixed with hemorrhage and occasionally fibrin, and intranuclear inclusions in vascular endothelial cells are evident, typically throughout the brainstem and caudate nuclei, often sparing the cerebral and cerebellar cortices.[14] Interestingly, in this case, lesions are noted extending into the cerebral cortex and meninges. Lesions in other organs are typically secondary to vascular endothelial damage and may consist of vascular necrosis, intravascular fibrin thrombi, hemorrhage, and edema.[7,13]

Adenoviral serotypes inducing disease in canines are from the family *Mastadenovirus* and include CAV-1, which causes the disease known as infectious canine hepatitis (ICH), and CAV-2, which is essential for the development of infectious tracheobronchitis (ITB).[7] Other

adenovirus families include *Aviadenovirus* (avian strains) and *Atadenovirus* (mammalian, avian, and some reptilian strains). Adenoviruses are typically host specific and produce multiple notable diseases (Table 1, chelonians, amphibians and fish not included). Typically, most adenoviral infections are subclinical, with serious illness only in young or immunocompromised individuals.[7]

**Table 1- Most important adenoviruses, affected species and major pathologic lesions**

| **Species Affected** | **Serotypes involved /Disease Name** | **Major Pathologic Findings** |
|---|---|---|
| ***Mastadenoviridae*** | | |
| Canine Ursidae | CAV-1 Infectious Canine Hepatitis | Intranuclear and intraepithelial inclusions in hepatocytes, Kupffer cells, endothelium and mononuclear cells with secondary necrosis |
| | CAV-2 Upper respiratory disease conjunctivitis | Important initiator of infectious tracheobronchitis (Kennel Cough) |
| Feline | | Rare, subclinical disease, only 1 confirmed fatal case |
| Bovine | BADV 3,4,10 | Sporadic enteric disease in 1-8 week old calves, tropism for vascular endothelium, lesions are secondary to thrombosis and ischemia |
| Porcine | PAdV-4- most common in Europe and North America | Typically non-clinical illness, may see pneumonia and enteritis, inclusions are in enterocytes- may be seen in non-clinically affected piglets |
| Equine | EAdV-1 (worldwide) | May cause pneumonia in SCID (Arabian) foals with intranuclear inclusions in alveolar epithelium, +/- pancreatic degeneration and necrosis with inclusions in pancreatic ducts |
| | EAdV-2 (Australia) | Diarrhea |
| Ovine Caprine | OAdV 1-3 GAdV-2 | Mild respiratory and GI disease in lambs and kids, inclusions within lamina propria in lambs, in endothelial cells in kids |
| Humans | Several strains | Respiratory disease and keratoconjunctivitis |
| Hamsters | Hamster strains | Enteric disease in less than 4 week old animals Intranuclear inclusions in intestinal epithelium Experimentally transmitted adenoviruses from other species can induce neoplasia |
| ***Aviadenovirus*** | | |
| Group I | Chickens Turkeys Geese Ducks Kestrel Pigeons | Inclusion Body Hepatitis | Vertically transmitted, hepatocellular hemorrhage and necrosis with intranuclear hepatocellular inclusions, may also see necrotizing pancreatitis with intranuclear inclusions |
| | Northern Virginia Quail | Quail Bronchitis | Necrotizing tracheitis, proliferative and necrotizing bronchitis and pneumonia with basophilic intranuclear inclusion in tracheal epithelium |
| | Chickens Quail | Inclusion Body Ventriculitis | |
| Group II | Turkey gallinaceous birds psittacine | Turkey Hemorrhagic Enteritis | Fibrino-necrotic membranes lining small intestine, intranuclear inclusions in lymphoblasts and macrophages in spleen, and small intestine lamina propria |
| | Pheasant | Marble Spleen Disease | Enlarged mottled spleen, congested and edematous lungs, splenic necrosis with large intranuclear inclusions |
| | Chicken | Group II splenomegaly virus | Usually causes no mortality. Lesions include splenic reticuloendothelial cell hyperplasia with intranuclear inclusions |
| ***Atadenovrius*** | | | |
| Group III | Chickens Ducks | Egg Drop Syndrome | Principle site of virus replication is pouch shell gland, if infection occurs before sexual maturity; virus is latent until maturity occurs. Loss of shell color, thin shelled eggs |
| Bovine | | BAdV-5, 6, 7, 8 | Enteric disease |
| Ovine Caprine | | OAD -D GAdV-1 | Enteric disease |
| Possums | | PAdV- 1 | Typically non clinical illness, interest in utilizing virus as a method to control populations as a vector for contraceptive antigens |
| Squamatids (lizards and snakes) | | Agamid AdV-1 (Bearded Dragons), SnAdV-1,2, (snakes), Eublepharid AdV-1 (geckos), Helodermatid AdV-1(gila monsters) | Hepatocellular necrosis with Intranuclear inclusions in hepatocytes. Inclusions also possible in enterocytes, renal epithelium, lung epithelium, myocardial endothelium, glial cells and brain endothelium |

**JPC Diagnosis:** Liver: Degeneration and necrosis, centrilobular to midzonal, multifocal to coalescing, severe, with numerous hepatocyte and endothelial intranuclear viral inclusions.

Cerebrum and thalamus: Vasculitis, necrotizing, diffuse, moderate, with hemorrhage, edema, and numerous endothelial intranuclear viral inclusions.

**Conference Comment:** This is a great diagnostic case that exhibits the pathognomonic combination

of intranuclear inclusions and brainstem hemorrhages in the dog. The contributor outlined adenoviruses of many species, of which only dogs, bears, oxen, goats, and lizards are mentioned as developing endotheliotropic manifestations of infection. Hemorrhages can occur in multiple organs in these species, and including the kidney, lung, brainstem, and long bones in dogs.[13] Intranuclear inclusions occur most prominently in endothelium and hepatocytes in dogs; however, they may also be observed in Kupffer cells and other differentiated cells.[13] Conference participants deliberated on whether some of the free individual cells with viral inclusions within the sinusoids and large vessels in this case are detached necrotic hepatocytes in the process of exiting the liver into the systemic circulation.

The brain lesions in this case appear to be most severe in the thalamus, where prominent cytotoxic edema of oligodendroglia is evident. Cytotoxic edema occurs due to altered cellular metabolism, often caused by ischemia, and presents as intracellular fluid accumulation. Cells of the CNS vary in their susceptibility to ischemic injury. Neurons are the most sensitive, with oligodendroglia, astrocytes, microglia, and endothelium following in decreasing order.[15] It is curious in this case that neurons are much less severely affected than oligodendroglia, which may allude to irregular or incomplete ischemic damage in this case. Other types of edema that occur within the CNS include vasogenic due to vascular injury, and hydrostatic from elevated pressure, which both results in extracellular fluid accumulation. Also hypo-osmotic edema from plasma microenvironment imbalances can cause both extracellular and intracellular fluid accumulation.[13]

**Contributing Institution:** University of Illinois College of Veterinary Medicine Department of Pathobiology and Veterinary Diagnostic Laboratory
http://vetmed.illinois.edu/path/

**References:**

1. Appel, M. et al. Pathogenicity of low-virulence strains of two canine adenovirus types. *American Journal of Veterinary Research*. 1973;4.4:543-550.
2. Brown CC, Baker DC, Baker IK. Alimentary system. In: Maxie MG, ed. *Jubb, Kennedy, and Palmer's Pathology of Domestic Animals*. 5th ed. Vol. 2. Philadelphia, PA: Saunders Elsevier; 2007:348-351.
3. Caswell, CL Williams KJ. Respiratory system. In: Maxie MG, ed. *Jubb, Kennedy, and Palmer's Pathology of Domestic Animals*. 5th ed. Vol. 2. Philadelphia, PA: Saunders Elsevier; 2007:630, 639.
4. Caudell D et al. Diagnosis of infectious canine hepatitisvirus (CAV-1) infection in puppies with encephalopathy. *J VET Diagn Invest*. 2005;17:58-61.
5. Decaro N et al. Canine adenoviruses and herpesviruses. *Vet Clin Small Anim*. 2008;38:799-814.
6. Fox JG et al. In: *Laboratory Animal Medicine*. 2nd ed. San Diego, CA: Academic Press; 2002:185.
7. Greene CG. Infectious canine hepatitis and canine acidophil cell hepatitis. In: *Infectious Disease of the Dog and Cat.* 3rd ed. St. Louis, MO: Saunders Elsevier; 2006:41-47.
8. Kennedy FA et al. Disseminated adenovirus infection in a cat. *J Vet Diagn Invest*. 1993;5:273–276.
9. Kennedy, FA Feline adenovirus infection. In: *Infectious Disease of the Dog and Cat*. 3rd ed. St. Louis, MO: Saunders Elsevier; 2006:143-144.
Marschang RE. Viruses infecting reptiles. *Viruses*. 10. 2011,3(11):2087-2126.
11. McFerran JB, et al. Avian adenoviruses. *Rev Sci Tech Off Int Epiz.* 2000;19(2):589-601.
12. Thompson D et al. Molecular confirmation of an adenovirus in brushtail possums (Trichosurus vulpecula). *Virus Res.* 2002;83(1-2):189-95.
13. Stalker MJ, Hayes MA. Liver and biliary system. In: Maxie MG, ed. *Jubb, Kennedy, and Palmer's Pathology of Domestic Animals*. 5th ed. Vol. 2. Philadelphia, PA: Saunders Elsevier; 2007:348-351.
14. Summers BA, Cummings JF, deLahunta. Inflammatory diseases of the central nervous system. In: *Veterinary Neuropathology*. Mosby-Year Book, Inc., St. Louis, MO: Mosbey-Year Book; 1995:117.
15. Zachary JF. Nervous system. In: Zachary JF, McGavin MD, eds. *Pathologic Basis of Veterinary Disease*. 5th ed. St. Louis, MO: Elsevier Mosby; 2012:781-791.

**CASE II**: 341368 (JPC 4049166).

**Signalment:** 6-year-old male Newfoundland Dog, *Canis familiaris.*

**History:** The animal presented to the small animal hospital at the University of Glasgow with acute tetraparesis following development of left thoracic limb lameness. MR imaging revealed the brainstem to be moderately atrophied with uneven margins. In addition MR imaging revealed that the cervical spinal cord was markedly atrophied with uneven and distorted margins, with an associated compensatory increase of surrounding CSF and faint intramedullary changes most apparent centrally within the cord.

**Gross Pathology:** On macroscopic examination, the brain was unremarkable but the brainstem and cervical spinal cord were moderately to markedly atrophic with increased CSF within the cervical region in concordance with MRI findings.

**Histopathologic Description:** Large numbers of ovoid to irregular, eosinophilic, intra-astrocytic hyaline structures consistent with Rosenthal fibers were distributed throughout the cerebellum, brainstem and spinal cord and to a lesser extent within supratentorial regions. Rosenthal fibers were most prominent within the subependymal and perivascular areas and within the subpial glia limitans, as would be expected for areas which ordinarily contain dense networks of astrocytic processes. Rosenthal fibers were found predominantly within the white matter but also to a lesser extent within the grey matter. Within affected areas, especially in the most severely affected areas of white matter there are also moderate numbers of abnormal astrocytes with large amounts of eosinophilic cytoplasm and marked karyomegaly. Occasional binucleate astrocytes were also noted in severely affected areas. Areas of white matter exhibiting the highest numbers of Rosenthal fibers, including the cerebellum, dorsal medulla oblongata, dorsal cervical spinal cord and piriform lobe, were also characterized by severe rarefaction of the surrounding white matter.

Rosenthal fibers, particularly at their periphery, show moderate GFAP immunostaining and moderate to strong ubiquitin immunostaining.

**Contributor's Morphologic Diagnosis:** Brain, cerebellum, brainstem and spinal cord: Encephalomyelopathy, multifocal, severe with subpial, perivascular and periependymal Rosenthal fiber accumulation, astrocytosis and astrocytic hypertrophy, consistent with Type II Alexander disease.

**Contributor's Comment:** The presence of Rosenthal fiber accumulation within the CNS is not a pathognomonic lesion of Alexander-like disease. Rosenthal fibers may be found in a variety of conditions including reactive astrocytosis and in some astrocytomas and the diagnosis of an Alexander-like disease must be based on recognition of the distribution of Rosenthal fibers within the CNS most prominently within the subpial glia limitans and in perivascular and periependymal locations. [13]

Alexander's disease in man is a primary astrocytic disorder with approximately 95% of patients harboring mutations in the GFAP gene. The age of onset is variable with cases reported from the prenatal period through until the sixth decade of life.[7] Alexander's disease is classically divided into infantile (0-2 years), juvenile (2-12 years) and adult (>12 years) onset forms; however, more recently a new classification limited to two categories (type I and type II) has been proposed focusing on lesion distribution and clinical presentation.[10] In the case of the two category classification, system age of onset remained a powerful predictor of disease type. It has been shown that phenotypic pattern and disease course alone more accurately classify cases of Alexander's disease and whereas all type I cases presented at an early age, type II cases occurred at all ages although generally with a later onset than type I cases. Type I disease is typically characterized by early onset commonly with seizures, spasticity, or developmental delays and diagnosis can be made based on the presence of at least four of the following five features on MR imaging: extensive cerebral white matter changes with a frontal predominance, a periventricular rim with high signal on T1-weighted images and low signal on T2-weighted images, abnormalities of the basal ganglia and thalami, brain stem abnormalities, and contrast enhancement of the ventricular lining, periventricular tissue or white matter of the frontal lobes, optic chiasm, fornix, basal ganglia, thalamus, dentate nucleus, or brain stem structures.[10,12] Type II disease is typically

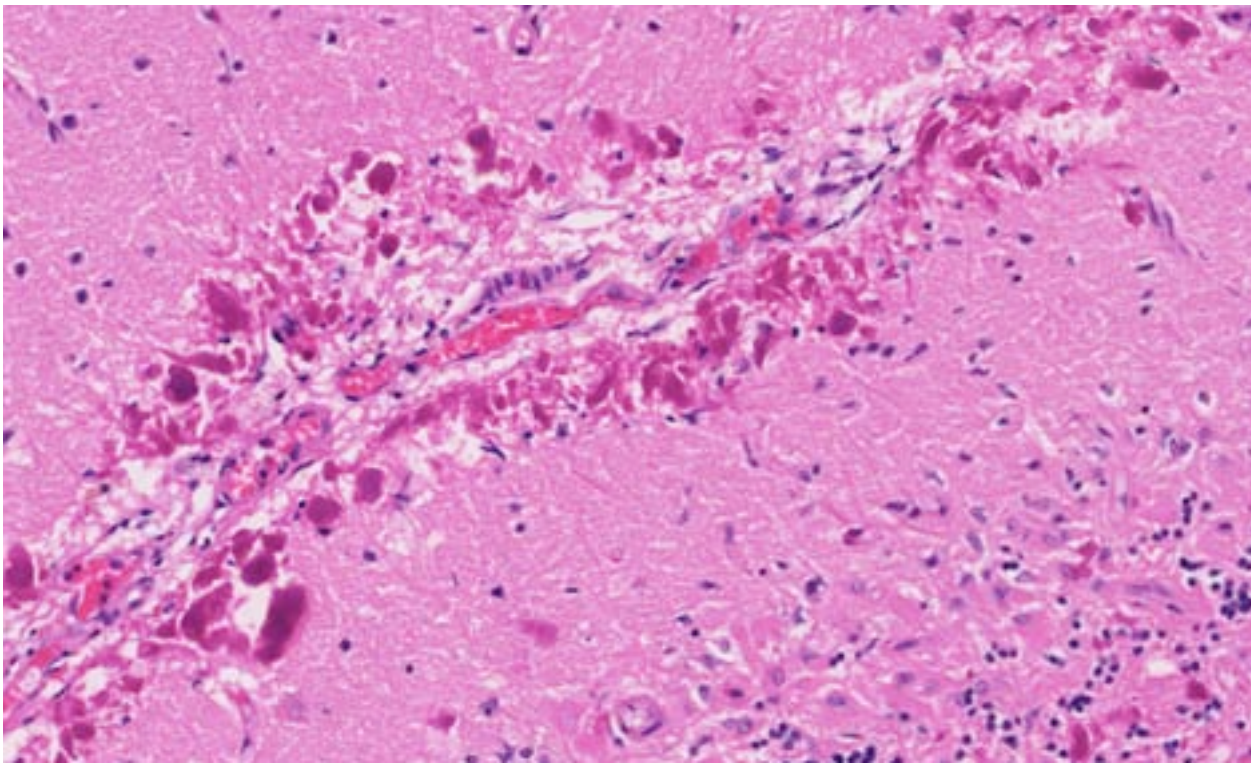

*2-1. Cerebellum, dog: Within the cerebellum, and to a lesser degree in the brainstem and cervical spinal cord, numerous brightly eosinophilic astrocyte processes consistent with Rosenthal fibers populate perivascular and subependymal areas. (HE 196X)*

later in onset and more often presents with signs of hindbrain dysfunction such as ataxia, palatal myoclonus and dysphagia. MR findings in type II disease show hindbrain predominance with atrophy of the medulla oblongata and cervical spinal cord.[4,5,8,9]

There have been seven previous reports of Alexander's disease in the dog, all of which predate the new human classification system.[1,2,3,6,11,14] Due to the distribution of lesions in this case with pronounced atrophy of the cervical spinal cord, Type II Alexander's disease was diagnosed.

**JPC Diagnosis:** Cerebellum: Hypertrophy, astrocytic processes, with accumulation of intermediate filament (Rosenthal fibers), diffuse, severe, with Purkinje and granular cell loss. Spinal cord, cervical: Hypertrophy, astrocytic processes, dorsal funiculi and subependymal, with accumulation of intermediate filament (Rosenthal fibers), moderate.

**Conference Comment:** This is a rarely reported disease in the veterinary literature, thus much of its understanding is derived from the documented cases in people where a functional mutation of the dominant GFAP gene has been identified.[1] The genetic equivalent in dogs has not been determined, although the similarities in presentation between animals and people strongly suggests a correlation. Rosenthal fibers consist of three major chemical components: GFAP, small heat shock proteins, and ubiquitin.[1] Their presence translates into increased expressivity with immunohistochemistry for GFAP, and coupled with their perivascular and periependymal location, are diagnostic for Alexander's disease (AD).[1] In AD, the mutant GFAP proteins are unable to form intermediate filaments and precipitate in aggregrates to cause derangements of astrocytic functions.[9] With the multiple functions of astrocytes, to include regulating the microenvironment of the CNS, repairing injured nervous tissue, and providing structural support;[15] it is reasonable to conclude their dysfunction can result in a variety of central nervous clinical manifestations. Among cases reported in dogs, depression, generalized tremors, progressive tetraparesis, spinal reflex deficits, and ataxia have all been observed.[1,11,14] The contributor described the different classifications of AD, and all previously reported cases in the dog could be considered the juvenile, or type II, form.[1]

**Contributing Institution:** Veterinary Diagnostic Services, School of Veterinary Medicine
College of Medical, Veterinary and Life Sciences, University of Glasgow
Bearsden Road
G61 1QH
Glasgow, United Kingdom
www.glasgow.ac.uk/vds

**References:**

1. Alemañ N, Marcaccini A, Espino L, et al. Rosenthal fiber encephalopathy in a dog resembling Alexander disease in humans. *Vet Pathol.* 2006;43:1025-1028.
2. Andrews EJ, Ward BC, Altman NH. Spontaneous animal models of human disease Elsevier; 1980.
3. Cox NR, Kwapien RP, Sorjonen DC, et al. Myeloencephalopathy resembling Alexander's disease in a Scottish terrier dog. *Acta Neuropathol.* 1986;71:163-166.
4. Farina L, Pareyson D, Minati L, et al. Can MR imaging diagnose adult-onset Alexander disease? *AJNR Am J Neuroradiol* 2008;29:1190-1196.
5. Graff-Radford J, Schwartz K, Gavrilova RH, et al. Neuroimaging and clinical features in type II (late-onset) Alexander disease. *Neurology.* 2014;82:49-56.
6. Ito T, Uchida K, Nakamura M, et al. Fibrinoid leukodystrophy (Alexander's disease-like disorder) in a young adult French bulldog. *J Vet Med Sci.* 2010;72:1387-1390.
7. Messing A, Brenner M, Feany MB, et al. Alexander disease. *J Neurosci.* 2012;32:5017-5023.
8. Namekawa M, Takiyama Y, Honda J, et al. Adult-onset Alexander disease with typical "tadpole" brainstem atrophy and unusual bilateral basal ganglia involvement: a case report and review of the literature. *BMC Neurology.* 2010;10: 21.
9. Pareyson D, Fancellu R, Mariotti C, et al. Adult-onset Alexander disease: a series of eleven unrelated cases with review of the literature. *Brain.* 2008;131:2321-2331.
10. Prust M, Wang J, Morizono H, et al. GFAP mutations, age at onset, and clinical subtypes in Alexander disease. *Neurology.* 2011;77:1287-1294.
11. Richardson JA, Tang K, Burns DK. Myeloencephalopathy with Rosenthal fiber formation in a miniature poodle. *Vet Pathol.* 1991;28:536-538.
12. van der Knaap MS, Naidu S, Breiter SN, et al. Alexander disease: diagnosis with MR imaging. *AJNR Am J Neuroradiol.* 2001;22:541-552.
13. Vandevelde M, Higgins R, Oevermann A. *Veterinary Neuropathology: Essentials of Theory and Practice*. John Wiley and Sons; 2012.
14. Weissenbock H, Obermaier G, Dahme E. Alexander's disease in a Bernese mountain dog. *Acta Neuropathol.* 1996;91:200-204.
15. Zachary JF. Nervous system. In: Zachary JF, McGavin MD, eds. *Pathologic Basis of Veterinary Disease*. 5th ed. St. Louis, MO: Elsevier Mosby; 2012:776-777.

**CASE III:** 14-69-6 (JPC 4048509).

**Signalment:** 14-year-old castrated male domestic short haired cat, *Felis catus.*

**History:** The cat presented with acute onset of seizures and nystagmus progressing to stupor, and was euthanized. It had a subtotal colectomy 3 years previously because of megacolon. One year previously the cat had been treated for constipation, pleural effusion of undetermined cause and pancytopenia, again of undetermined cause. At the time of euthanasia the cat was reportedly negative for FeLV, FIV and *Mycoplasma* infection.

**Gross Pathology:** The cat was in good nutritional condition. The brain was grossly normal externally and on transverse section. The heart was mildly rounded and had numerous delicate fibrinous and fibrous adhesions between the visceral and parietal pericardial surfaces. Bilaterally there was moderate pulmonary edema.

Incidental findings included a unilateral ectopic ureter, hematoma within the urinary bladder wall and abdominal wall musculature caused by cystocentesis, and bilateral polydactyly of the thoracic limbs.

**Laboratory Results:** None

**Histopathologic Description:** Thalamus and cerebral hemisphere; transverse section. [Depending on the level of the section, different slides contain some or all of the following structures: third ventricle, lateral ventricle, hippocampus, interthalamic adhesion, choroid plexus and ventral meningeal vessels.]

Scattered throughout the entire section, but most numerous in the ventral thalamus and adjacent leptomeningeal blood vessels, are several dozen variably-sized hypercellular foci up to 300 microns in diameter. Most are centered about small to medium-caliber arterioles and consist of mural and luminal proliferations of spindle cells. These form concentric whorls or haphazard tufts that frequently narrow or obliterate the lumen of affected vessels. Multifocally, luminal spindle cells form capillary clefts within which low numbers of red blood cells or fibrin thrombi are present. Spindle cells are bland, with a moderate amount of poorly demarcated smudged to very finely fibrillar eosinophilic cytoplasm. Nuclei are ovoid and pale with vesiculate to stippled chromatin and a single inconspicuous nucleolus. Mitotic figures are very rare. Multifocally, the perivascular (Virchow-Robin) space around both affected and unaffected parenchymal vessels is mildly expanded by clear space or lacy eosinophilic fluid (edema).

Immunohistochemistry was performed on this section. Approximately 50% of proliferating spindle cells showed strong immunoreactivity for factor VIII-related antigen and the remainder were

*3-1. Thoracic cavity, cat: The heart is mildly rounded and has numerous delicate fibrinous and fibrous adhesions between the visceral and parietal pericardial surfaces. Bilaterally, there is moderate pulmonary edema. (Photo courtesy of: Diagnostic Services Unit, Faculty of Veterinary Medicine, University of Calgary, Clinical Skills Building, 11877 85 St. NW,Calgary AB T3R 1J3 http://vet.ucalgary.ca/)*

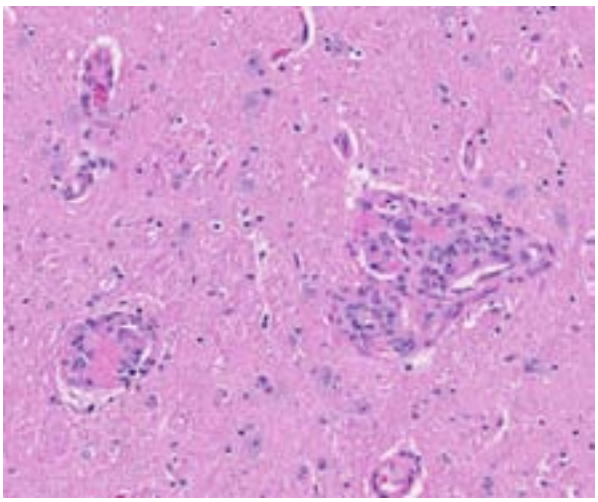

*3-2. Thalamus, cat: Thalamic arterioles are expanded by a luminal, occasionally concentric proliferation of spindle cells which narrow the lumen. Affected vessels multifocally contain fibrin thrombi. (HE 144X)*

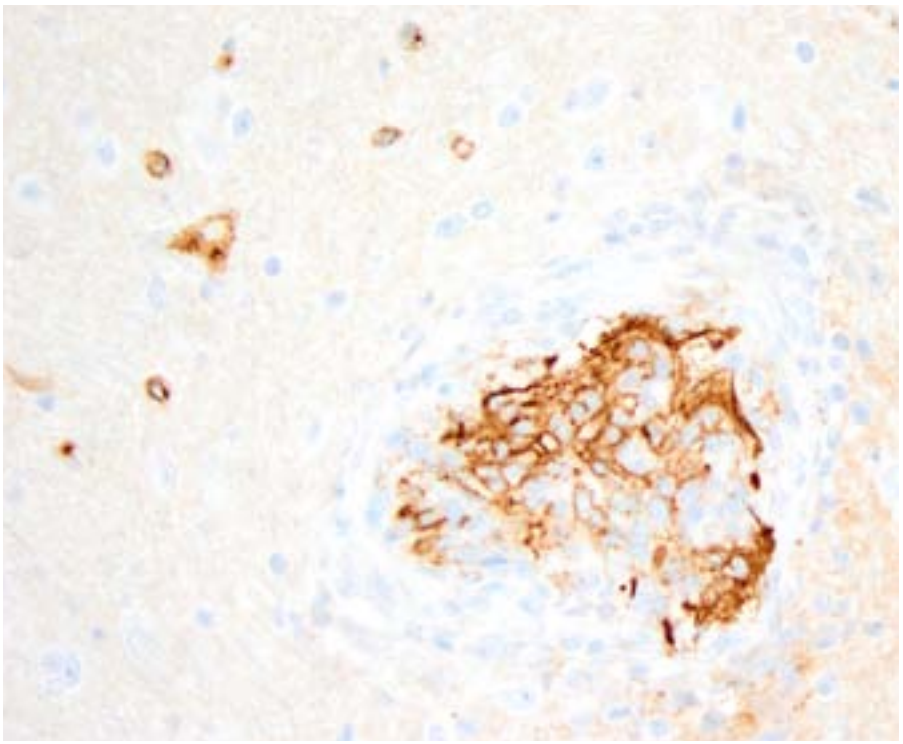

*3-3. Thalamus, cat: Within a thalamic arteriole, a proportion of proliferating intraluminal spindle cells exhibit diffuse moderately positive intracytoplasmic staining for Factor VIII-related antigen. (Photo courtesy of: Diagnostic Services Unit, Faculty of Veterinary Medicine, University of Calgary, Clinical Skills Building, 11877 85 St. NW, Calgary AB T3R 1J3 http://vet.ucalgary.ca/ (anti-VWF, 400X)*

strongly immunoreactive for smooth muscle actin. IHC for feline coronavirus was also performed. There was no immunoreactivity for feline coronavirus.

**Contributor's Morphologic Diagnosis:** Brain and leptomeninges: Marked multifocal intraluminal and mural vascular spindle cell proliferation (angioendotheliomatosis) with multifocal thrombosis and mild multifocal perivascular edema.

**Contributor's Comment:** Histologic and immunohistochemical changes are consistent with the condition of feline systemic reactive angioendotheliomatosis (FSRA). This is a rare condition of domestic cats characterized by intravascular proliferation of spindle cells in small blood vessels of many organs.[5] Although not named FSRA until recently,[5] diseases with similar sounding lesions have been described in sporadic case reports since the 1980s.[4,10,11] While FSRA appears to have no counterpart in other domestic species, a multisystemic disease with the same histologic lesions was reported in 2008 in a steer persistently infected by BVDV.[3] Diseases with similar vascular proliferations exist in humans but, unlike FSRA, these are restricted to the skin and are not fatal.[9]

In FSRA, the heart is the most consistently affected organ and myocardial dysfunction is the cause of illness reported in most cats.[5] The myocardial lesions of FSRA were described in an earlier case submitted to the Wednesday Slide Conference (Conference 03-2008; Case 2). In this current case, however, central nervous system disease caused the most important clinical signs, and the case was submitted as a reminder that FSRA is a multisystemic disease with a variety of clinical presentations. As such, FSRA should be considered in the differential diagnosis for cats with neurologic disease.

In this particular case, a specific cause for neurologic signs was not found in the brain sections examined. There was no evidence of obstructive hydrocephalus, severe edema or malacia in any section examined. However, myocardial dysfunction in FSRA is secondary to thrombosis and infarction[5] and it is possible that areas of infarction were present in the brain of this cat but not in sections examined histologically.

In addition to the myocardium and brain, other commonly affected organs in FSRA are the kidneys, spleen, lymph nodes, meninges, eyes and pancreas.[5] In the current cat, the most severely affected organs were the brain and heart, but milder vascular lesions were also present in the kidneys and the tunica muscularis of the gastrointestinal tract. Vascular lesions were not present in the urinary bladder and the mural hemorrhage noted at necropsy was attributed to cystocentesis.

The proliferating cells in FSRA are a mixture of endothelial cells and (presumed) pericytes, as

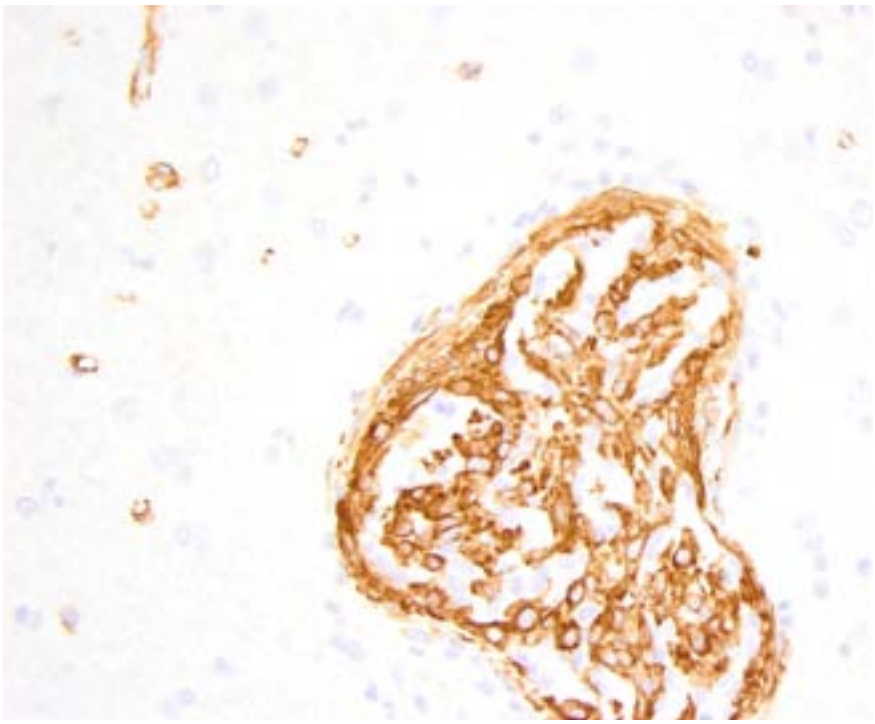

*3-4. Thoracic cavity, cat: Within a thalamic arteriole, a proportion of proliferating intraluminal spindle cells exhibit diffuse strongly positive intracytoplasmic staining for Factor VIII-related antigen. (Photo courtesy of: Diagnostic Services Unit, Faculty of Veterinary Medicine, University of Calgary, Clinical Skills Building, 11877 85 St. NW, Calgary AB T3R 1J3 http://vet.ucalgary.ca/ (anti-SMA, 400X)*

**JPC Diagnosis:** Diencephalon, arterioles: Pericyte and endothelial proliferation, occlusive, diffuse, severe, with necrotizing vasculitis, thrombosis, and mild gliosis.

**Conference Comment:** This case gives a unique look at a condition more readily recognized in the heart in cats. Conference participants deliberated whether proliferative, neoplastic, inflammatory or other processes could be ruled out based on current knowledge of the entity. Rather than arriving at a consensus, additional questions were raised such as whether the proliferative endothelial cells and pericytes are responsive to growth factors or exhibit decreased sensitivity to inhibitory stimuli. Too few cases of FSRA have been documented to determine a predilection for sex, breed, or age; and some examples offer evidence of possible infectious causes.[1,3,5]

identified by IHC for factor VIII-related antigen[5,10,11,13] and smooth muscle actin,[5,13] respectively. Because of the dual cell population and the lack of cellular atypia, lesions of FSRA are thought to represent an aberrant reactive process rather than neoplasia. (This is discussed in Fuji et al.'s 2005 review,[5] and by the previous submitter of a myocardial FSRA case to the 2008 Wednesday Slide Conference. Since their reviews of the literature, only one further case report on FSRA has been published.[13])

The cause of FSRA is unknown. In humans, certain vasoproliferative disorders are associated with infection by various *Bartonella* species,[6] and several mechanisms by which *Bartonella* spp. might induce endothelial proliferation have been shown.[7,8] Since 2010 a similar link has been investigated in certain vasoproliferative disorders of domestic animals, including FSRA in cats, hemangiopericytoma, hemangiosarcoma and bacillary angiomatosis in dogs and SRA in a steer.[1,2,12] The results of these studies are not conclusive but do suggest that further investigation into *Bartonella* infection and vasoproliferative disorders in domestic animals is justified.

While it consistently affects the heart, FSRA is usually observed in multiple organs of which the kidney, spleen, lymph node, gastrointestinal tract, brain, eye, and pancreas seem to be most common.[5] Regardless of affected organs, the disease is often fatal as the vasoproliferative lesions can induce thrombosis, hemorrhage, and necrosis of the myocardium causing acute myocardial failure.[5] Thrombotic thrombocytopenic purpura (TTP) has also been associated with FSRA, and consists of accumulations of large multidimers of vWF, possibly due to an acquired or genetic defect in vWF metalloprotease.[3] TTP may also be associated with certain drugs, viral infections, pregnancy, and systemic lupus erythematosus and may occur a single episode, relapsing intermittent episodes, or chronic unremitting forms.[3]

**Contributing Institution:** Diagnostic Services Unit
Faculty of Veterinary Medicine
University of Calgary
Calgary AB
http://vet.ucalgary.ca/

**References:**

1. Beerlage C, Varanat M, Linder K, Maggi RG, Cooley J, Kempf VAJ, et al. Bartonella vinsonii subsp berkhoffii and Bartonella henselae as potential causes of proliferative vascular diseases in animals. *Medical Microbiology and Immunology*. 2012;201:319-326.
2. Breitschwerdt EB, Linder KL, Day MJ, Maggi RG, Chomel BB, Kempf VAJ. Koch's postulates and the pathogenesis of comparative infectious disease causation associated with Bartonella species. *Journal of Comparative Pathology*. 2013;148:115-125.
3. Breshears MA, Johnson BJ. Systemic reactive angioendotheliomatosis-like syndrome in a steer presumed to be persistently infected with bovine viral diarrhea virus. *Veterinary Pathology*. 2008;45:645-649.
4. Dunn KA, Smith KC, Blunden AS. Fatal multisystemic intravascular lesions in a cat. *Veterinary Record.* 1997;140:128-129.
5. Fuji RN, Patton KM, Steinbach TJ, Schulman FY, Bradley GA, Brown TT, et al. Feline systemic reactive angioendotheliomatosis: Eight cases and literature review. *Veterinary Pathology*. **2005;**42:608-617.
6. Kaiser PO, Riess T, O'Rourke F, Linke D, Kempf VAJ. Bartonella spp.: Throwing light on uncommon human infections. *International Journal of Medical Microbiology*. 2011;301:7-15.
7. Kempf VAJ, Volkmann B, Schaller M, Sander CA, Alitalo K, Riess T, et al. Evidence of a leading role for VEGF in Bartonella henselae-induced endothelial cell proliferations. *Cellular Microbiology.* **2001;**3:623-632.
8. Riess T, Andersson SGE, Lupas A, Schaller M, Schafer A, Kyme P, et al. Bartonella adhesin A mediates a proangiogenic host cell response. *Journal of Experimental Medicine*. 2004;200:1267-1278.
7. Rongioletti F, Rebora A. Cutaneous reactive angiomatoses: Patterns and classification of reactive vascular proliferation. *Journal of the American Academy of Dermatology*. 2003;49:887-896.
10. Rothwell TLW, Xu FN, Wills EJ, Middleton DJ, Bow JL, Smith JS, et al. Unusual multisystemic vascular lesions in a cat. *Veterinary Pathology*. 1985;22:510-512.
11. Straumann Kunz US, Ossent P, Lottstolz G. Generalized intravascular proliferation in two cats: Endotheliosis or intravascular pseudoangiosarcoma? *Journal of Comparative Pathology*. 1993;109:99-102.
12. Yager JA, Best SJ, Maggi RG, Varanat M, Znajda N, Breitschwerdt EB. Bacillary angiomatosis in an immunosuppressed dog. *Veterinary Dermatology*. 2010;21:420-428.
13. Zielschot N, Kleinschmidt S, Wohlsein P. Feline systemic reactive angioendotheliomatosis in a cat. *Kleintierpraxis*. 2011;56:131-134.

**CASE IV**: P3900-14 (JPC 4048654).

**Signalment:** 7-week-old female crossbreed (unknown) porcine, *Sus scrofa domesticus.*

**History:** Dead pig, suspect meningitis.

**Gross Pathology:** The pig was in poor body condition with reduced muscle mass and minimal subcutaneous and internal fat stores (weight = 12.5 Kg). Both pinnae showed extensive areas of purple discoloration. The mandibular, cervical, mesenteric and lumbar lymph nodes were edematous and enlarged approximately two times normal size. The trachea contained abundant white froth. The lungs were expanded, rubbery, wet, heavy and non-collapsed (interpreted as interstitial pneumonia); the interlobular septa were expanded with clear gelatinous material (pulmonary edema). The pericardial sac contained approximately 25 ml of clear, yellow, watery fluid (hydropericardium). The epicardial fat was diffusely replaced by clear, translucent gelatinous material (serous atrophy). There was also serous atrophy of the perirenal fat. The kidneys exhibited multifocal to coalescing, 2-5 mm in diameter, white spots scattered throughout the cortex; confluence of these lesions produce expansion and distortion of one renal pole (interpreted as interstitial nephritis). The spleen showed a locally extensive, firm, dry, irregular area of tan discoloration involving the middle third of the organ and extending into the splenic parenchyma (interpreted as infarct). There was an extensive area of subarachnoid hemorrhage over the dorsal surface of the cerebellum. No other gross abnormalities were seen in the rest of the viscera.

**Laboratory Results:**

Bacteriology: There was no microbial growth from samples of kidney and spleen. A light growth of mixed flora was recovered from the meninges.

Virology: Ileum and tonsils tested positive for porcine circovirus type 2 by FAT and PCR.

Immunohistochemistry: Porcine circovirus type 2 antigen was present in the inflammatory infiltrate and affected blood vessels of cerebellum, choroid plexus and brain stem (Prairie Diagnostic Services, 52 Campus Dr, Saskatoon, SK. S7N 5B4)

**Histopathologic Description:** The cerebellum has multifocally extensive areas of hemorrhage, necrosis and edema involving the white and gray matter. The subarachnoid space and the stroma of the choroid plexus (4th ventricle) are markedly expanded with hemorrhage, variable deposits of fibrin, necrotic cell debris, and large collections of macrophages interspersed with many lymphocytes, fewer plasma cells, occasional neutrophils and rare eosinophils. The wall of many blood vessels is infiltrated with scant eosinophilic homogeneous to fibrillar material (fibrinoid degeneration), karyorrhectic debris, and occasional macrophages or neutrophils (vasculitis). Many of these blood vessels and parenchymal capillaries are occluded with fibrin

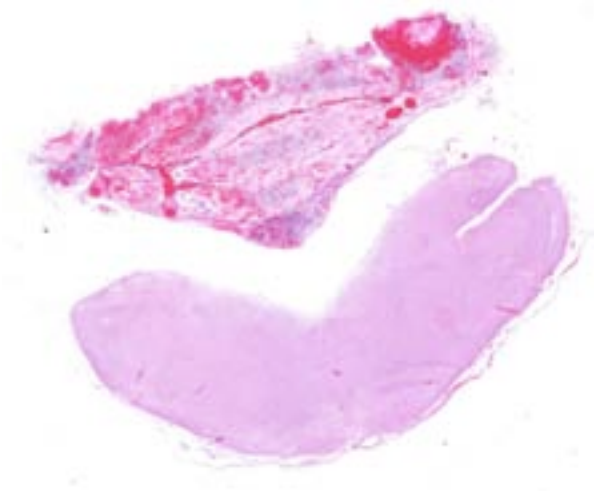

*4-1. Cerebrum, piglet: There is marked hemorrhage throughout the cerebellum. (HE 4X)*

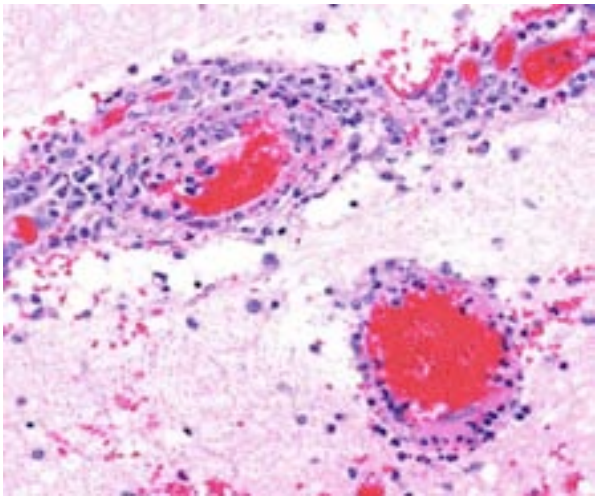

*4-2. Cerebellum, piglet: Multifocally, vascular walls are necrotic and surrounded by a prominent infiltrate of macrophages, lymphocytes, and fewer plasma cells and neutrophils. (HE 256X)*

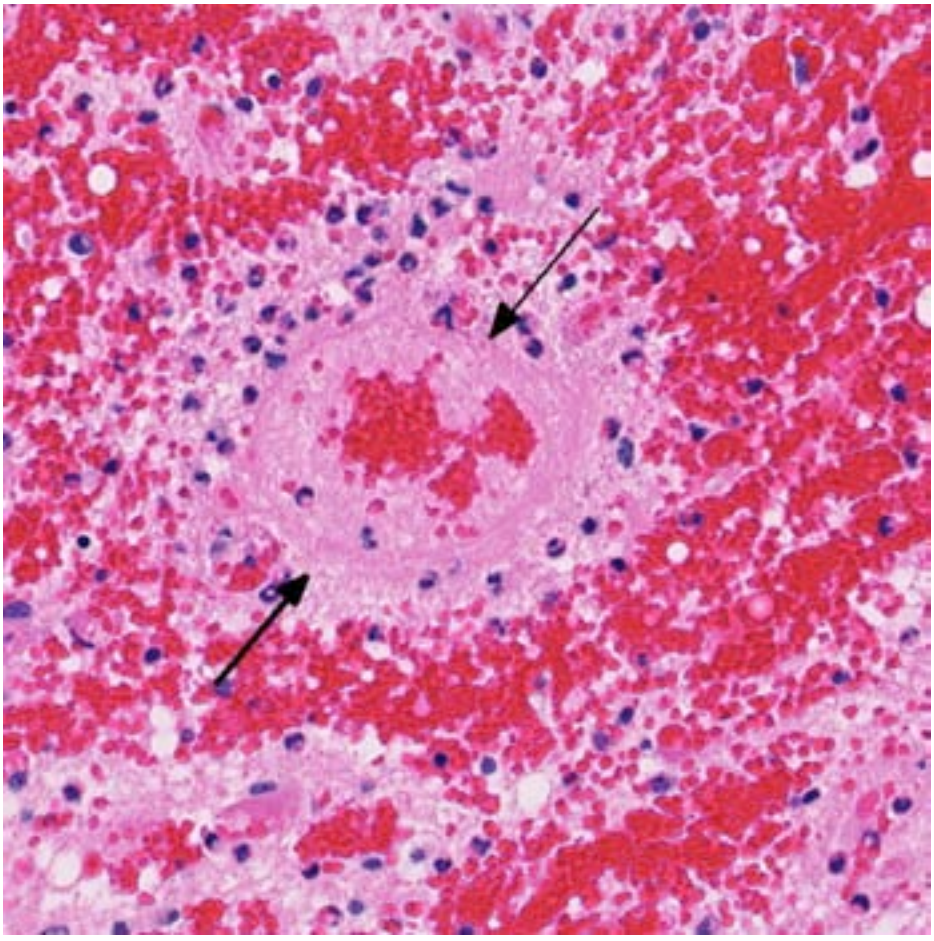

*4-3. Cerebellum, piglet: Hemorrhagic infarcts are centered on necrotic vessels. (HE 270X)*

thrombi. Within the neuropil are areas of spongiosis (edema) with scattered macrophages and neutrophils. Hypereosinophilic and shrunken neurons with karyolysis or nuclear pyknosis (neuronal necrosis) are seen primarily in the Purkinje and molecular cell layer among the areas of necrosis and hemorrhage. The ventricular space contains variably sized collections of erythrocytes admixed with fibrin, scant cell debris, histiocytes and lymphocytes. Vasculitis is also noted in the adjacent section of brain stem. Porcine circovirus type 2 antigen was present in the inflammatory infiltrate and affected blood vessels.

**Contributor's Morphologic Diagnosis:**
1. Cerebellum, choroid plexus, and brain stem: Vasculitis, fibrinonecrotizing and lymphohistiocytic, severe, diffuse, with severe, multifocal hemorrhage, necrosis, edema and thrombosis.
2. Lungs (not submitted): Interstitial pneumonia, lymphohistiocytic, diffuse, moderate, subacute.
3. Spleen (not submitted): Splenitis, granulomatous, diffuse, severe with locally extensive necrosis, fibrosis, and multifocal mineralization (chronic infarct).
4. Lymph nodes (not submitted): Lymphadenitis, histiocytic, multifocal, moderate, with diffuse lymphoid depletion, and scant intrahistiocytic cytoplasmic botryoid inclusions.
5. Ileum, Peyer's patches (not submitted): Lymphoid depletion, diffuse, severe.
6. Kidney (not submitted): Nephritis, interstitial, lymphohistiocytic, multifocal, moderate, with tubular degeneration, necrosis and regeneration, and interstitial fibrosis.
7. Tonsil (not submitted): Lymphoid depletion, diffuse, severe.

**Contributor's Comment:** Gross and microscopic findings are consistent with porcine circovirus type 2 (PCV2) infection (Post-weaning multisystemic wasting syndrome). Virology (FAT and PCR) and immunohistochemistry results confirmed the diagnosis. In addition, no significant bacterial isolates were recovered from this animal's samples.

Porcine circovirus (PCV) is a non-enveloped, single-stranded, circular DNA virus classified in the *Ciroviridae* family, genus *Circovirus*. There are two known PCV species, porcine circovirus type 1 (PCV1) and porcine circovirus type 2 (PCV2). PCV1 is non-cytopathic and non-pathogenic in swine. On the other hand, PCV2 is pathogenic in swine and associated with multiple disease entities. PCV2 is globally distributed and most herds are seropositive for anti-PCV2 antibodies.[8] Porcine circovirus type 2 infection

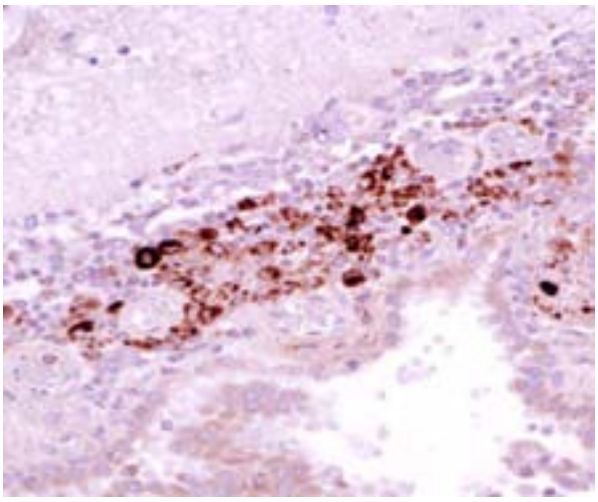

*4-4. Cerebellum, piglet: Cells within the perivascular infiltrates are strongly immunopositive for porcine circovirus-2 antigen. (Photo courtesy of: Atlantic Veterinary College, University of Prince Edward Island (http://home.upei.ca/).) (anti-PCV-2, 200X)*

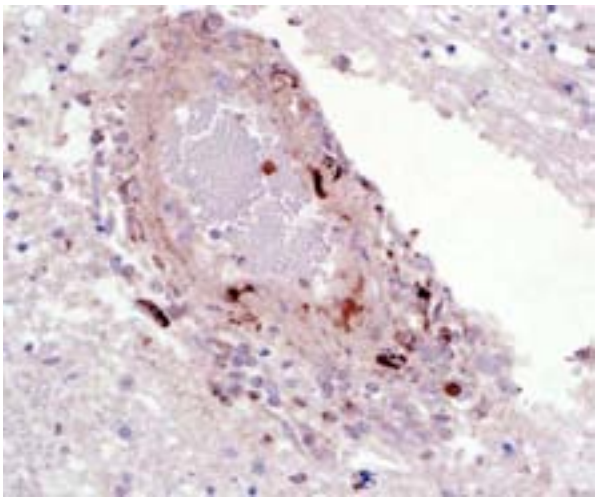

*4-5. Cerebellum, piglet: Scattered endothelial cells are strongly immunopositive for porcine circovirus-2 antigen. (Photo courtesy of: Atlantic Veterinary College, University of Prince Edward Island (http://home.upei.ca/).) (anti-PCV-2, 400X)*

occurs as maternally derived antibodies wane in post-weaned pigs (7-15 weeks of age) and results in either subclinical infection or clinical disease. Clinical disease associated with PCV2 infection can have multiple manifestations which include: post-weaning multisystemic wasting syndrome (PMWS), PCV2-associated respiratory disease, PCV2-associated enteritis, porcine dermatitis and nephropathy syndrome (PDNS), myocarditis/vasculitis, exudative dermatitis,[1,2] and cerebellar vasculitis.[3,11] Subclinical PCV2 infection may occur in apparently healthy pigs but this type of infection can reduce growth performance and increase susceptibility to other pathogens, or decrease the efficacy of vaccines.[9]

The PMWS is a systemic disease that clinically manifests between 7-15 weeks of age. It is characterized by wasting, dyspnea, lymphadenopathy, diarrhea, pallor and jaundice. Coughing, pyrexia, gastric ulceration, and meningitis have also been reported, but are sporadic.[5] Herd morbidity in PMWS herds is variable with 4-30% of the pigs affected. Mortality rates are often high (20-50%). The most consistent necropsy finding in PMWS pigs is generalized lymphadenopathy. PMWS pigs are frequently coinfected with other common bacterial and viral pathogens, and coinfection often complicates gross findings. Microscopically, lymphoid tissues from PMWS-affected pigs exhibit lymphoid depletion and replacement by histiocytic/granulomatous inflammation. Multinucleated (syncytial) giant cells, epithelioid macrophages and macrophage-associated intracytoplasmic botryoid-like basophilic inclusions are also commonly seen in lymphoid tissues (lymph node, tonsil, Peyer's patches, and spleen). Focal parenchymal coagulative and apoptotic necrosis in lymphoid tissues has also been described. Microscopic lesions in nonlymphoid tissues are characterized by lymphohistiocytic inflammation and include interstitial pneumonia, hepatitis, interstitial nephritis and enteritis/colitis. The diagnosis of PMWS is based on clinical signs of wasting which may or may not include respiratory distress and icterus, lymphoid depletion and granulomatous inflammation, and the presence of PCV2 antigen or nucleic acid associated with microscopic lesions.[12]

PCV2-associated respiratory disease and PCV2-associated enteritis can often overlap with PMWS or be a contributing factor in porcine respiratory disease complex (PRDC) and bacterial enteritis, respectively. Microscopically, there is lymphohistiocytic interstitial pneumonia sometimes associated with type II pneumocyte hypertrophy and hyperplasia, peribronchiolar fibrosis, and associated lymphoid hyperplasia. Within the intestine, the gut associated lymphoid tissue (GALT; Peyer's patches) exhibit similar changes as those described in PMWS. However, the diagnosis of PCV2-associated enteritis is appropriate when there is clinical diarrhea, lymphoid depletion and granulomatous inflammation are present in Peyer's patches but

not in other lymphoid tissues, and PCV2 DNA or antigen can be demonstrated within the lesions.[2]

Porcine dermatitis and nephropathy syndrome is a distinctive, sporadic, acute clinical entity of growing swine characterized by circular to coalescing, red to purple macules or raised papules and plaques that originate on the skin of the hind legs and perineal region. Lesions may become exudative, crusty, and eventually regress leaving dermal scars. Bilateral swollen kidneys with widely disseminated cortical petechial hemorrhages are also commonly observed. Increased mortality is seen in affected pigs older than three months of age. The typical microscopic lesion is necrotizing vasculitis and glomerulonephritis. Small to medium sized dermal and subcutaneous arterioles are cuffed by neutrophils, macrophages, lymphocytes, and plasma cells that are sometimes present within vascular walls. Arterioles are lined by plump endothelial cells, occasionally occluded by fibrin thrombi and walls can display multifocal hyalinization. Kidney sections exhibit distension of urinary spaces by fibrin intermixed with necrotic cellular debris and hemorrhage, periglomerular and interstitial lymphohistiocytic infiltrates, and distension of renal tubules with cellular and proteinaceous casts. Skin and glomerular lesions are characteristic of a type III hypersensitivity reaction with deposition of immune complexes. Multiple viral and bacterial pathogens have been implicated in PDNS, but PCV2 is considered a contributing factor.[2]

A striking finding in this particular case was the cerebellar vasculitis, particularly in absence of significant bacterial isolates. It is known that PCV2 produces nonsuppurative or granulomatous encephalitis with gliosis under experimental conditions and the PCV2 antigen has been identified in brain in these cases. However, in cases of naturally occurring encephalitis, PCV2 has been detected in brains of affected animals always in association with other pathogens that can cause encephalitis alone.[7] Cerebellar hemorrhage, edema and necrosis, resulting from necrotizing and lymphohistiocytic vasculitis (and thrombosis) is an uncommon feature that has also been previously described associated with PCV2 infection.[3,11] PVC2 antigen has been demonstrated in the inflammatory infiltrate and affected blood vessels as in this particular case. Similar to this case, the reported PCV2-associated cerebellar vasculitis exhibited some characteristics of PMWS and also changes consistent with PDNS[9] suggesting that a type III hypersensitivity reaction with deposition of immune complexes, as it has been considered in PDNS, might be involved in the pathogenesis of this lesion.

**JPC Diagnosis:** Cerebellum: Vasculitis, necrotizing, diffuse, severe, with thrombosis and multifocal to coalescing cerebellar necrosis.

**Conference Comment:** Despite the decreasing prevalence of PCV2 due to a successful vaccination campaign, it remains an important disease of swine throughout the world. This case serves as a reminder of maintaining PCV2 on the differential list for a multitude of different lesions in swine, as neural pathology associated with PCV2 infection occurs infrequently and is considered to be of minor importance.[8] PCV2 has the potential to cause disease in nine organ systems in various ways through its overlapping PCV-associated disease (PCVAD) manifestations outlined by the contributor. Perhaps most notably, PCV2 causes lymphoid depletion and histiocytic inflammation of lymphoid tissues.[8] This consistent lesion led some researchers to look for a porcine lentivirus during the initial presentation of PMWS just 20 years ago.[4]

The presence of vasculitis and fibrin in this case led many participants toward an etiology of *Streptococcus suis* or *Hemophilus parasuis*. Other differentials to consider for lymphohistiocytic encephalitis and cerebellar hemorrhage include *porcine parvovirus, porcine reproductive and respiratory syndrome virus,* and *hemagglutinating encephalomyelitis virus*.[8] Lymphohistiocytic and necrotizing vasculitis is well documented in PCV2-systemic disease, where it occurs most commonly in the mesenteric lymph nodes and kidney though many other organs may also be affected.[10] The virus appears to have a direct cytopathic effect on vascular endothelium, myocytes, and pericytes in these instances, although an indirect mechanism such as a hypersensitivity reaction may also be possible.[10]

**Contributing Institution:** Atlantic Veterinary College, University of Prince Edward Island (http://home.upei.ca/)

**References:**

1. Chae C. Postweaning multisystemic wasting syndrome: a review of aetiology, diagnosis and pathology. *Vet J.* 2004;168:41-49.
2. Chae C. A review of porcine circovirus 2-associated syndromes and diseases. *Vet J*. 2005;169:326-336.
3. Correa AM, et al. Brain lesions pigs affected with postweaing multisystemic wasting syndrome. *J Vet Diagn Invest*. 2007;19:109-12.
4. Ellis J. Porcine Circovirus: a historical perspective. *Vet Pathol.* 2014;51(2):315-327.
5. Harding JC. The clinical expression and emergence of porcine circovirus 2. *Vet Microbiol*. 2004;98:131-135.
6. Huang YY, Walther I, Martinson SA, Lopez A, Yason C, Godson DL, et al. Porcine circovirus 2 inclusion bodies in pulmonary and renal epithelial cells. *Vet Pathol.* 2008;45:640-644.
7. Maxie MG, Youssef S. Nervous System. In: Maxie MG, ed. *Jubb, Kenedy, and Palmer's Pathology of Domestic Animals.* 5th ed. Vol 1. Philadelphia, PA: Saunders Elsevier; 2007:430-431.
8. Opriessnig T, Langohr I. Current state of knowledge on porcine Circovirus type 2-associated lesions. *Vet Pathol.* 2013;50(1):23-38.
9. Opriessnig T, Meng XJ, Halbur PG. Porcine Circovirus Type 2 associated disease: Update on current terminology, clinical manifestations, pathogenesis, diagnosis, and intervention strategies. *J Vet Diagn Invest.* 2007;19:591- 615.
10. Resendes AR, Segales J. Characterization of vascular lesions in pigs affected by porcine Circovirus type 2-systemic disease. *Vet Pathol*. 2015;52(3):497-504.
11. Seeliger FA, Brügmann ML, Krüger L, Greiser-Wilkie I, Verspohl J, Segales J, et al. Porcine Circovirus Type 2-Associated Cerebellar Vasculitis in Postweaning Multisystemic Wasting Syndrome (PMWS)-Affected Pigs. *Vet Pathol*. 2007;44:621–634.
12. Sorden SD. Update on porcine circovirus and postweaning multisystemic wasting syndrome (PMWS). *Swine Hlth Prod*. 2000;8:133-136.

**Joint Pathology Center**
**Veterinary Pathology Services**

# WEDNESDAY SLIDE CONFERENCE 2014-2015

## Conference 22

**22 April 2015**

**Guest Moderator:**
Cynthia Mattan Bell, DVM, ACVP
University of Wisconsin School of Veterinary Medicine

---

**CASE I:** 459-12 (JPC 4017816).

**Signalment:** Tissue from a domestic duck, *Anas platyrhynchos domesticus*.

**History:** One duck was submitted for being lethargic with emaciation and ataxia.

**Gross Pathologic Findings:** No gross lesions were seen other than slight emaciation.

**Laboratory Results** (clinical pathology, microbiology, PCR, ELISA, etc.)**:** 1+ *Pasteurella multocida* and 1+ *E. coli* were isolated from the lung and liver swabs and no bacterial growth was obtained from the heart swab.

**Histopathologic Description:** The heart has multifocal small areas of necrosis and moderate multifocal mixed inflammation with heterophils, lymphocytes, and some histiocytes. Bacterial colonies and emboli are throughout the

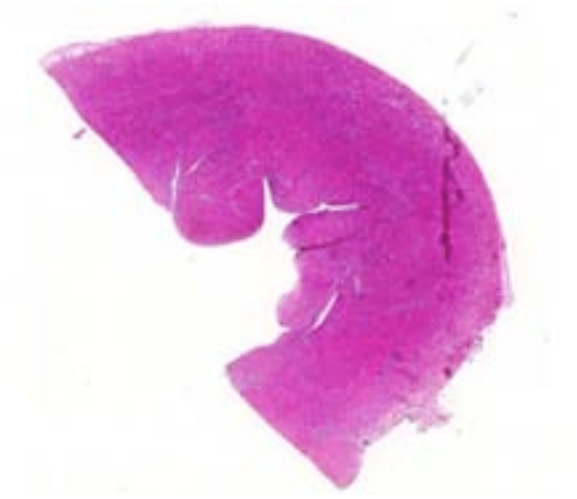

*1-1. Heart, duck: At subgross there is a cellular infiltration throughout the myocardium. (HE 3X)*

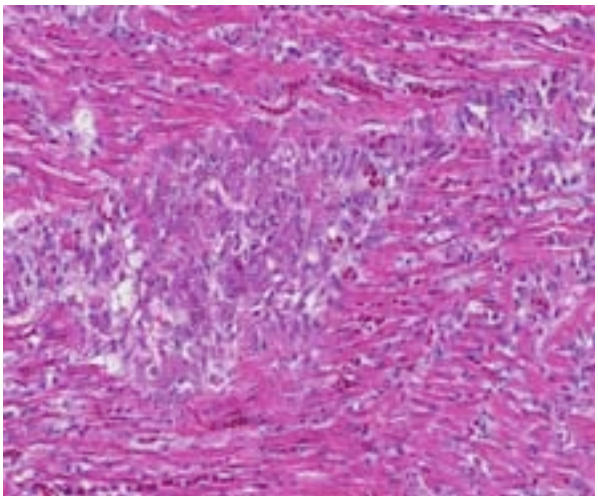

*1-2. Heart, duck: Large areas of necrotic cardiac muscle are infiltrated and replaced by numerous macrophages admixed with fewer multinucleated foreign-body type macrophages. (HE 224X)*

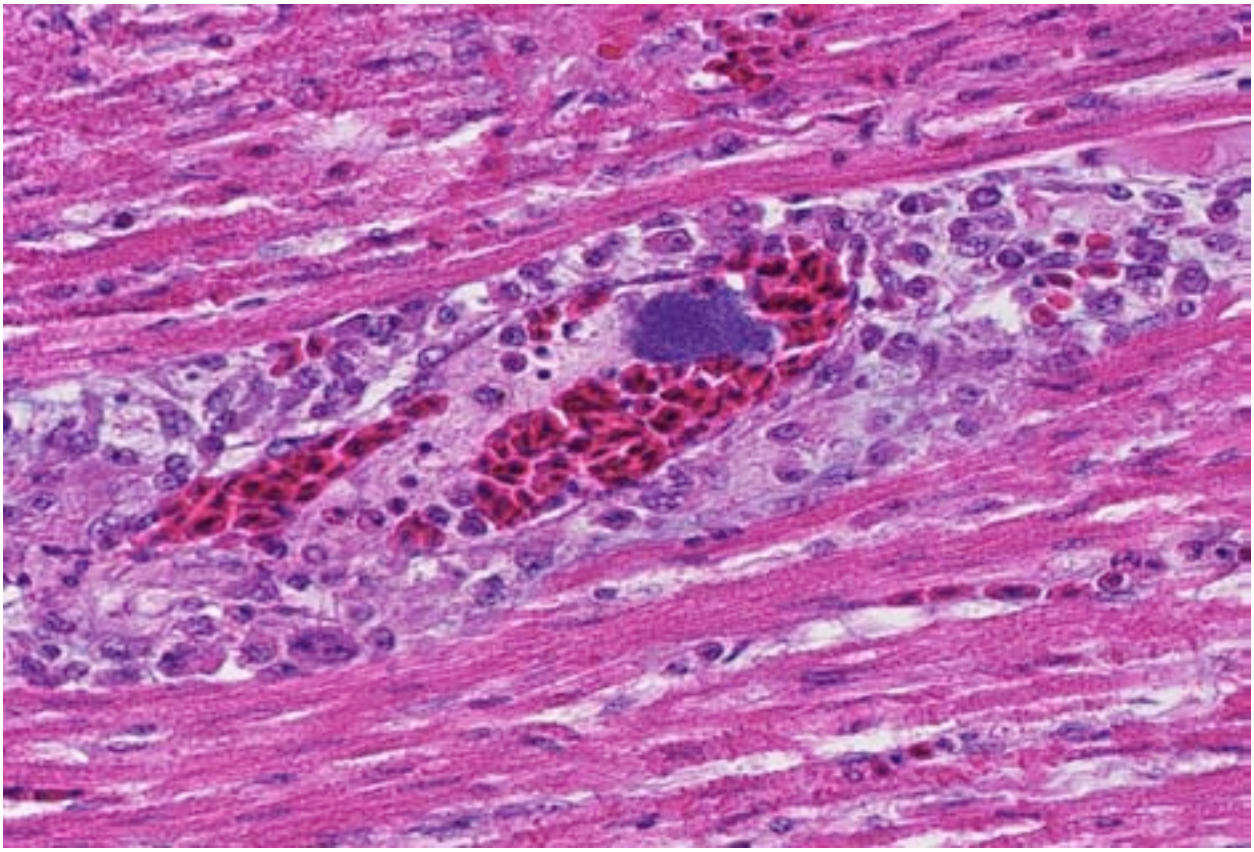

*1-3. Heart, duck: Bacterial emboli are present within numerous myocardial vessels, and there is often marked histiocytic perivascular inflammation. (HE 224X)*

myocardium. Mixed leukocytes with fibrin and a few multinucleated giant cells are on the epicardium. The lung section was congested and had a bacterial embolus but no inflammation and the liver was normal other than sinusoidal histiocytosis. No lesions were seen in the brain, intestine, and kidney sections (only heart from this case was submitted.)

**Contributor's Morphologic Diagnosis:** Multifocally necrotizing and subacute myocarditis.

**Contributor's Comment:** This is fowl cholera septicemia (*Pasteurella multocida*). *E. coli* was not thought to be significant and *P. multocida* is always considered to be significant from poultry. Chickens usually have a chronic disease with pasteurellosis, with infection in the combs and wattles. The bacteria can often also be isolated from internal organs. Turkeys and ducks are more likely to have an acute or peracute infection, often with many acute deaths.[3]

**JPC Diagnosis:** Heart: Myocarditis, necrotizing and histiocytic, multifocal to coalescing, severe, with vasculitis, thrombosis, fibrinous epicarditis, and intra- and extracellular bacterial colonies.

**Conference Comment:** *Pasteurella multocida*, the causative agent of fowl cholera, remains a major problem of poultry worldwide.[4] Disease manifestation can range from a mild localized infection to peracute systemic disease with high mortality.[2] The peracute forms are characterized by septicemic lesions, with petechial and ecchymotic hemorrhages in the fat and mucus membranes and necrosis of the liver and spleen.[2] The chronic form often involves the respiratory system as fibrinonecrotic pneumonia, but arthritis, peritionitis, and salpingitis also occurs.[2] Additionally, fibrinonecrotic dermatitis is observed in turkeys and broiler chickens (see 2011 WSC Conference 21, Case 1).

While all types of poultry are considered vulnerable to infection with *P. multocida*, there are species and age differences in susceptibility. Turkeys and waterfowl are considered the most

susceptible species while chickens are more resistant. All birds under 16 weeks of age also appear fairly resistant, though this effect is less pronounced in turkeys.[2]

Necrotizing myocarditis is not a typical finding with fowl cholera, allowing conference participants to review differentials for such a lesion in poultry. Specifically to ducks, *Riemerella anatipestifer* is a frequent cause of polyserositis including pericarditis in young ducklings of intensive production systems. *Salmonella pullorum* causes peritonitis and death in hatchling chicks or peritonitis, arthritis and pericarditis in adults. Coliform infections may lead to myocarditis, but usually with more abundant heterophilic inflammation and fibrin than present in this case. West Nile virus may perhaps be the best differential for necrotizing myocarditis of many avian species, with young chickens and geese being most likely to develop clinical disease and mortality.[1]

**Contributing Institution:** www.alpc.ar.gov

**References:**

1. Capua I. Arthropod-borne viruses. In: Pattison M, McMullin PF, Bradbury JM, Alexander DJ, eds. *Poultry Diseases*. 6th ed. Philadelphia, PA: Saunders Elseveier; 2008:421-422.
2. Christensen JP, Bojesen AM, Bisgaard M. Fowl Cholera. In: Pattison M, McMullin PF, Bradbury JM, Alexander DJ, eds. *Poultry Diseases*. 6th ed. Philadelphia, PA: Saunders Elsevier; 2008:149-154.
3. Glisson, JR, Hofacre, Cl, Christensen, FP. In: Saif YM, ed. *Fowl Cholera (Pasteurella and other related bacterial infections) in Diseases of Poultry.* 11th ed. Ames, IA; Iowa State Press: 2003:857-676.
4. Singh R, Remington B, Blackall P, Turni C. Epidemiology of fowl cholera in free range broilers. *Avian Dis*. 2014;58(1):124-128.

**CASE II**: D13-042840 (JPC 4048790).

**Signalment:** Adult female bald eagle, *Haliaeetus leukocephalus*.

**History:** This animal was admitted to The Raptor Center of the University of Minnesota on September 19, 2013. The animal was underweight and unable to fly. It had neurologic signs including nystagmus and muscle tremors. Blood lead levels were low. The animal was euthanatized one day after admission due to a grave prognosis for survival and rehabilitation.

**Gross Pathology:** The animal was moderately underweight. There was marked bilateral symmetrical pan-necrosis of the caudal third of the cerebral hemispheres with collapse of the parenchyma and increased quantity of cerebrospinal fluid ("hydrocephalus ex vacuo") when compared to a control brain of a bald eagle.

**Laboratory Result:** Cerebrospinal fluid and brain samples were positive for West Nile virus (WNV) and negative for Saint Louis encephalitis virus by PCR (performed at the Animal Health Diagnostic Center of Cornell University). West Nile virus antigen was detected in the cerebrum and retina by immunohistochemistry using a monoclonal antibody specific for the E protein of WNV (clone 7H2, Bioreliance).

**Histopathologic Description:** Both slides (C and D) are cross sections of the caudal aspects of cerebrum at around the level of the optic chiasm (with the more rostral aspect of the thalamus) and had similar histologic features. The lateral ventricles were dilated.

There was bilateral symmetric pan-necrosis of the gray matter of the dorsal aspect of the cerebral hemispheres ("pallium") along the lateral ventricles. The neuroparenchyma was collapsed and cavitated around what appeared to be a remaining scaffold of vasculature. The neuroparenchyma was largely infiltrated and replaced by numerous macrophages with gitter cell morphology in the pallium. In addition, there was a widespread massive lymphoplasmacytic perivascular infiltration. The endothelial cells were hypertrophied. Numerous cells contained basophilic granular material (interpreted to be calcified mitochondria) and occasional neurons were entirely calcified.

The gray matter adjacent and subjacent to the necrotic parenchyma was hypercellular. The hypercellularity was due to infiltration with lymphocytes and macrophages and due to infiltration by reactive astrocytes. These astrocytes were plump, had an increased amount of a faint eosinophilic cytoplasm and one and occasionally two enlarged vacuolar

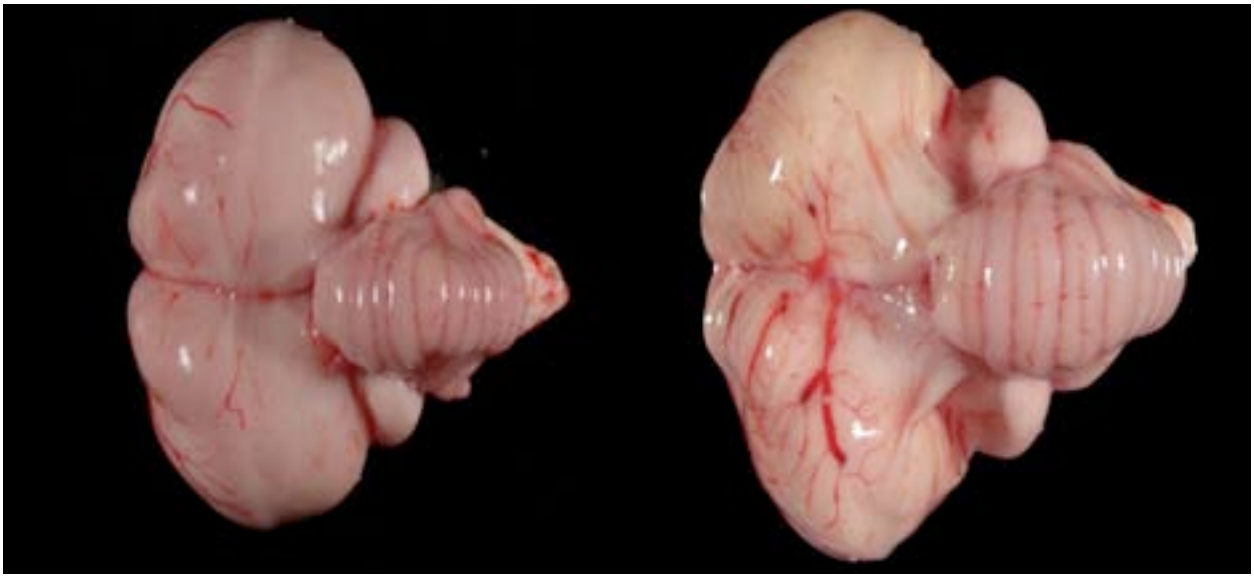

*2-1. Cerebrum, bald eagle: Brain of a female adult bald eagle (Haliaeetus leukocephalus; dorsal aspect), with control brain on left: There was marked bilateral symmetrical pan-necrosis of the caudal third of the cerebral hemispheres with collapse of the parenchyma. There was an increased quantity of cerebrospinal fluid ("hydrocephalus ex vacuo") that partly was collected for further testing and partly drained as the brain was removed from the brain cranial vault. (Photo courtesy of: Veterinary Population Medicine Department, 244 Veterinary Diagnostic Laboratory, 1333 Gortner Ave, St Paul, MN 55108, www.vdl@umn.edu)*

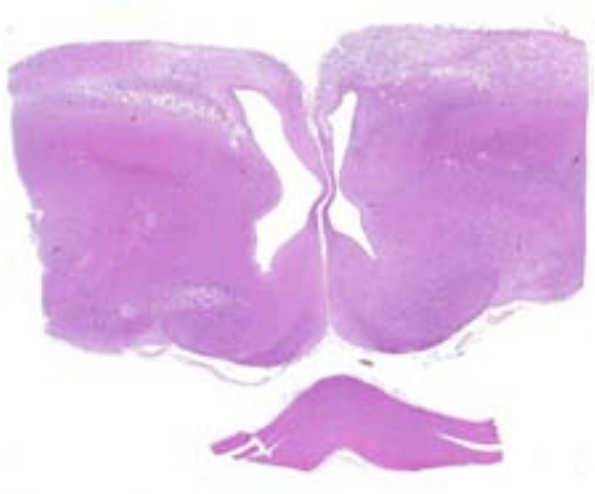

*2-2. Cerebrum, bald eagle: There is bilateral asymmetric necrosis and cavitation of the subpial grey matter in the dorsal aspect of the telencephalon, with bilateral distention of the third lateral ventricles. (HE 50X)*

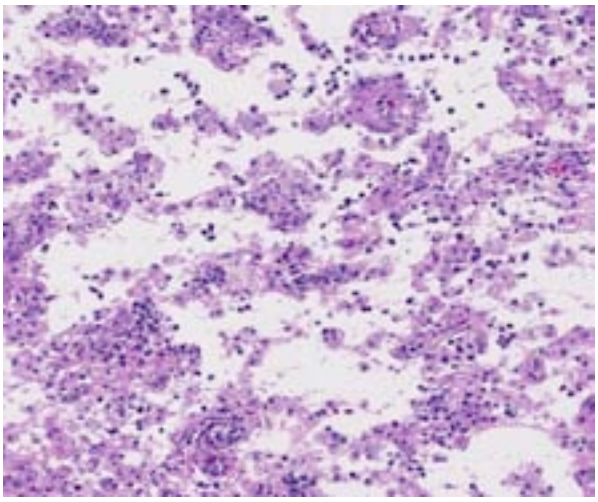

*2-3. Cerebrum, bald eagle: There are large asymmetrical areas of cavitary necrosis with remnant gliofibrillary strands separated by numerous Gitter cells. (HE 164X)*

("euchromatic") nuclei. Occasionally distinctly eosinophilic globules were present in the gray matter (interpreted to be spheroids).

White matter tracts such as the occipitomesencephalic tracts and optic tracts had a bilateral symmetric spongiform change characterized by the presence of numerous optically empty spaces ("interpreted as myelin sheath edema"). In addition, mild to moderate infiltrates of lymphocytes and plasma cells were present around capillaries of the white matter.

**Contributor's Morphologic Diagnosis:** Brain (cerebrum and thalamus), polioencephalitis, lymphoplasmacytic and histiocytic, chronic, marked with cerebral pan-necrosis and dilation of lateral ventricles ("hydrocephalus ex vacuo").

**Contributor's Comment:** The lesions were highly suggestive of an ischemic injury or massive viral encephalitis. A protozoal encephalitis (e.g. *Sarcocystis falcatula*) seemed to be unlikely based on the absence of protozoal organisms in the HE-stained sections although protozoal encephalitis cannot be ruled out entirely.[7] West Nile virus (WNV) is a member of the Japanese encephalitis and Saint Louis encephalitis antigenic complex (family: *Flaviviridae*). The virus is primarily transmitted by mosquitoes, but direct contact with infected animals and via oral uptake of virus infected tissues have also been reported. Raptors including bald eagles are frequently infected by WNV and succumb to West Nile disease.[1,4]

Gross lesions of WN disease in bald eagles may include macroscopically appreciable cerebral pan-necrosis as in the presented case in approximately half the cases and in individual cases may include myocarditis and endophthalmitis.[10] The presence of a triad of histopathological changes including encephalitis, endophthalmitis, and myocarditis are a hallmark of WN disease in bald eagles and other Accipitridae including Cooper's hawks (*Accipiter cooperi*), red tailed hawks (*Buteo jamaicensis*), and goshawks (*Accipiter gentilis*).[5,8-10] The pathogenesis of the cerebral pan-necrosis may include a vasogenic component due to damage of endothelial cells by the virus during an early phase of the infection or due to damage of the capillary integrity in the wake of the inflammatory response by extravasating inflammatory cells. Overt WNV-associated arterial necrosis has been described in kestrels and other falcons but does not appear to be a prominent feature of WN disease in hawks and eagles.[4,12] Alternatively or concurrently, the pathogenesis of the pan-necrosis may include direct cytolysis by the virus targeting neurons and possibly glial cells and/or cytolysis of neurons and glial cells as a result of bystander injury in the context of the antiviral immune response. High WNV antigen concentrations are present in the cerebrum (and cerebellum) of bald eagles with fairly acute WNV-associated encephalitis.[10] The cerebral necrosis was similar to a lesion described in one pigeon that was experimentally infected with highly pathogenic avian influenza virus.[2]

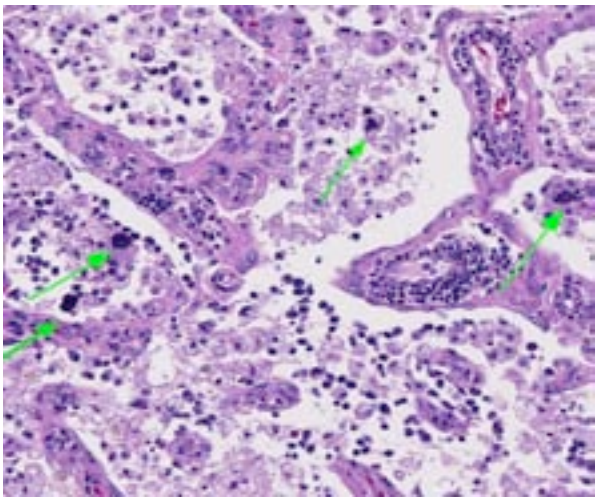

*2-4. Cerebrum, bald eagle: Multifocally throughout necrotic and inflamed neuropil, neurons and glial cells are replaced by crystalline mineral (arrows). (HE 164X)*

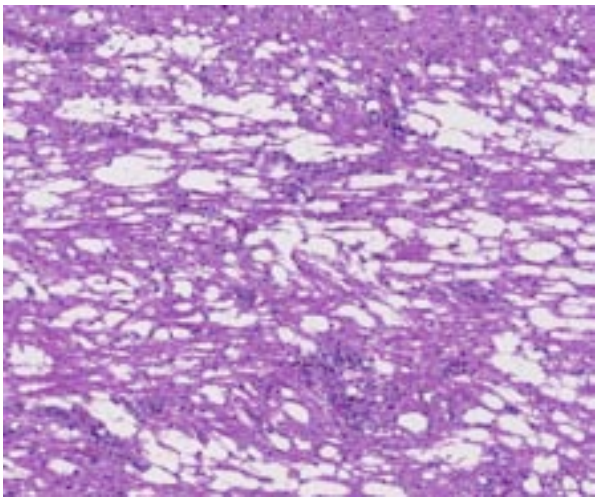

*2-5. Cerebrum, bald eagle: There is extensive spongiosis of white matter tracts. (HE 50X)*

Based on immunohistochemical analysis, brain (cerebrum and cerebellum), eyes (retina) and to a lesser extent heart and kidney harbor viral antigen similar to findings in other *Accipitridae*. PCR of brain tissue commonly yields a positive result in bald eagles with West Nile disease except for cases that had a significantly prolonged disease, e.g. because they were kept and cared for at a rehabilitation facility for months. In these animals, detection of WNV-specific antibodies in the CSF may be helpful to confirm WN encephalitis.[10]

**JPC Diagnosis:** Brain: Encephalitis, necrotizing, bilateral, severe, with lymphoplasmacytic perivascular cuffing, white matter spongiosis, mineralization and hydrocephalus *ex vacuo.*

**Conference Comment:** This is an exceptional example of West Nile virus (WNV), the arthropod-borne *Flavivirus* which utilizes many avian species as a natural reservoir. WNV is found throughout the world and is spread among the migratory bird population. Passeriformes are considered most susceptible to disease, to include the American crow, the blue jay, and the American robin. WNV is maintained in a silent mosquito-bird cycle in natural habitats until introduced into humanized areas where it cycles through humans and horses. This cycle accompanies a seasonal cycle, as the earliest infections arise in late spring and taper off in the fall. Human and horse cases are usually preceded by a few weeks of avian mortalities.[1]

WNV has a wide range of tissue tropism, thus there are no pathognomonic macroscopic lesions. Multiorgan hemorrhages are most characteristically found, and specifically to raptors, cerebral atrophy and malacia is often observed. Microscopically, lymphoplasmacytic and histiocytic inflammation, necrosis, and hemorrhage occur most commonly in the CNS, heart, kidney, spleen and liver. Paradoxically, the most susceptible species have the least amount of inflammation, and raptors that contract more chronic disease develop the triad of lesions described by the contributor.[1]

WNV contains two envelope glycoproteins, E1 and E2, which facilitate tropism for specific tissues.[11] Neuroinvasion requires crossing the blood-brain barrier and may be assisted by the release of proinflammatory cytokines.[11] The chemoreceptor CCR5 contributes to neuroinvasive resistance in humans, as those with CCR5 mutations have an increased rate of symptomatic infection, though this link has not been identified in animals.[3]

**Contributing Institution:** Veterinary Diagnostic Laboratory, University of Minnesota, www.vdl@umn.edu

**References:**

1. Gamino V, Höfle U. Pathology and tissue tropism of natural West Nile virus infection in birds: a review. *Vet Res.* 2013;44:39.
2. Klopfleisch R, Werner O, Mundt E, et al. Neurotropism of highly pathogenic avian

influenza virus A/Chicken/Indonesia/2003 (H5N1) in experimentally infected pigeons (Columbia livia f. domestica). *Vet Pathol*. 2006;43:463-470.
3. McAdam AJ, Milner DA, Sharpe AH. Infectious disease. In: Kumar V, Abbas AK, Aster JC, eds. *Pathologic Basis of Disease*. 9th ed. Philadelphia, PA: Elsevier Saunders; 2015:356-357.
4. Nemeth N, Gould D, Bowen R, Komar N. Natural and experimental West Nile virus infection in five raptor species. *J Wildl Dis.* 2006;42:1–13.
5. Pauli AM, Cruz-Martinez LA, Ponder J, et al. Ophthalmologic and oculopathologic findings in red tailed hawks and Cooper's hawks with naturally acquired West Nile virus infection. *J Am Vet Med Assoc*. 2007;231(8):1240-1248.
6. Pierson TC, Diamond MS. Flaviviruses. In: Knipe DM, Howley PM, Cohen JI, et al. eds. *Fields' Virology*. 6th ed. Philadelphia, PA: Lippincott, Williams & Wilkins, 2013:760-762.
7. Wünschmann A, Rejmanek D, Conrad PA, et al. Natural Sarcocystis falcatula infections in free ranging eagles in North America. *J Vet Diagn Invest.* 2010; 22:282-289.
8. Wünschmann A, Shivers J, Bender J, et al. Pathologic findings in red-tailed hawks (Buteo jamaicensis) and Cooper's hawks (Accipiter cooperi) naturally infected with West Nile virus. *Avian Dis.* 2004;48:570–580.
9. Wünschmann A, Shivers J, Bender J, et al. Pathologic and immunohistochemical findings in goshawks (Accipiter gentilis) and great horned owls (Bubo virginianus) naturally infected with West Nile virus. *Avian Dis.* 2005;49:252–259.
10. Wünschmann A, Timurkaan N, Armien AGA, et al. Clinical, pathological, and immunohistochemical findings in bald eagles (Haliaeetus leucocephalus) and golden eagles (Aquila chysaetos) naturally infected with West Nile virus. *J Vet Diagn Invest.* accepted for publication.
11. Zachary JF. Mechanisms of microbial infections. In: Zachary JF, McGavin MD, eds. *Pathologic Basis of Veterinary Disease*. 5th ed. St. Louis, MO: Elsevier Mosby; 2012:227-228.
12. Ziegler U, Angenvoort J, Fischer D, et al. Pathogenesis of West Nile virus lineage 1 and 2 in experimentally infected large falcons. *Vet Microbiol*. 2013;161:263-273.

**CASE III:** BB1705/10 (JPC 4002420).

**Signalment:** 14-year-old neutered male long-haired domestic cat, *Felis catus*.

**History:** The owner noticed a large, painless mass on the gingiva, which was surgically resected 6 days later at the local veterinary practice. The biopsy was sent to the R(D)SVS Veterinary Pathology Unit for histological examination.

**Gross Pathology:** Submitted for histological examination was a gingival lesion, lateral and adjacent to the left maxillary, third premolar tooth. This lesion was a 2cm x 1.4cm x 1.1cm, white nodule that was a little gritty and moderately firm. On cut section, it was homogeneous and white with a small number of irregular dark red areas.

**Histopathologic Description:** Gingival lesion (4 sections, slides A1 and A2): The submucosa is expanded and effaced by a densely cellular, poorly demarcated and locally invasive proliferation of epithelial cells arranged in anastomosing cords, ribbons and islands within a collagenous stroma. In this surrounding stroma there are moderate numbers of loosely spaced spindle cells. The cells at the periphery of the islands tend to palisade and range from cuboidal to low columnar. They have poorly defined cell borders, a small amount of basophilic cytoplasm, and a central, oval to indented nucleus with finely stippled chromatin and one nucleolus. The cells at the centre of the islands are stellate, with fibrillar cytoplasmic projections, indistinct cell borders and similar nuclear features to those described above. There is mild anisocytosis and anisokaryosis and mitotic figures average 2 per 10 high power fields (400X). Within the centre of many of the larger islands there are circular to globular aggregates of brightly eosinophilic, smudged to glassy, acellular and amorphous material which stains orange/red with apple green birefringence using a Congo red stain (amyloid). Some islands contain central squamous epithelial cells with associated refractile, lamellar, eosinophilic material, consistent with keratin. Cystic spaces within several islands are compatible with cystic degeneration and contain small numbers of neutrophils. A small number of small, irregular, deposits of eosinophilic material are superimposed with deeply basophilic material (mineralized bone, presumptive). The overlying mucosa is multifocally lost (ulcerated), with associated intense neutrophilic infiltration. Within the superficial submucosa there are clusters of lymphocytes and plasma cells, with neovascularisation and edema.

**Contributor's Morphologic Diagnosis:** Amyloid-producing odontogenic tumor with extensive mucosal ulceration - left maxillary gingival.

**Contributor's Comment:** Amyloid-producing odontogenic tumors fall into the category of tumors of odontogenic epithelial origin which do not produce odontogenic mesenchyme.[2] Pertinent

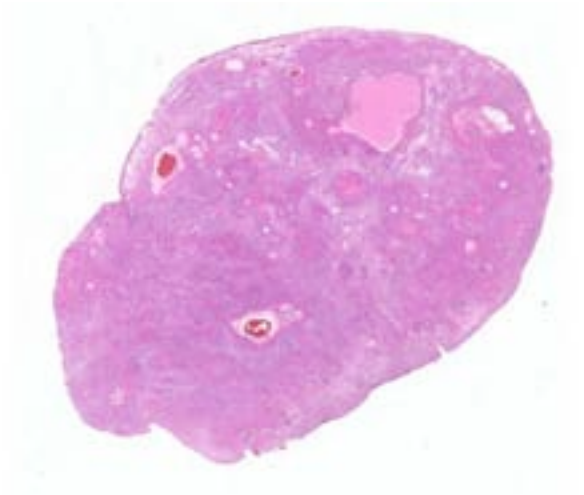

*3-1. Gingiva, cat: The gingiva contains a large, well demarcated neoplasm composed of islands and trabeculae of neoplastic cells. (HE 5X)*

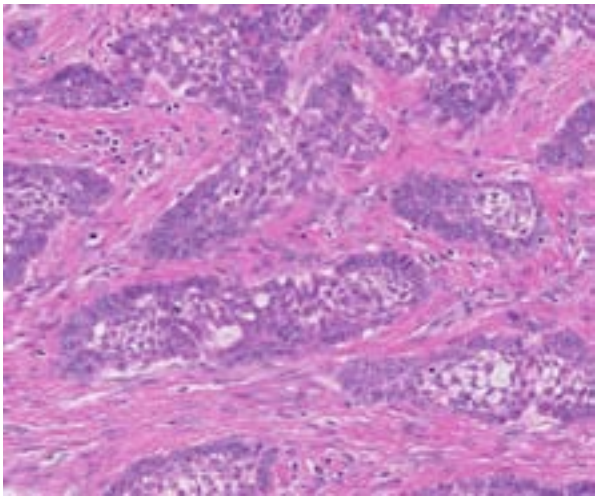

*3-2. Gingiva, cat: Islands and trabeculae of neoplastic cells are composed of numerous palisading columnar cells with prominent nuclei. (HE 150X)*

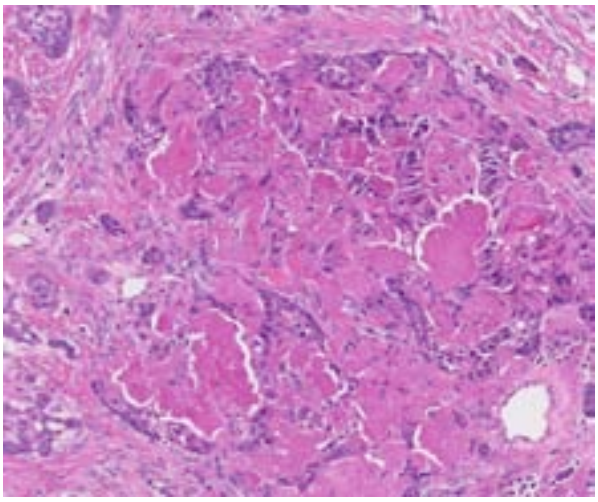

*3-3. Gingiva, cat: Occasionally, neoplastic cells surround a central focus of loosely arranged small spindle to stellate cells on a pale myxomatous matrix (stellate reticulum). (HE 260X)*

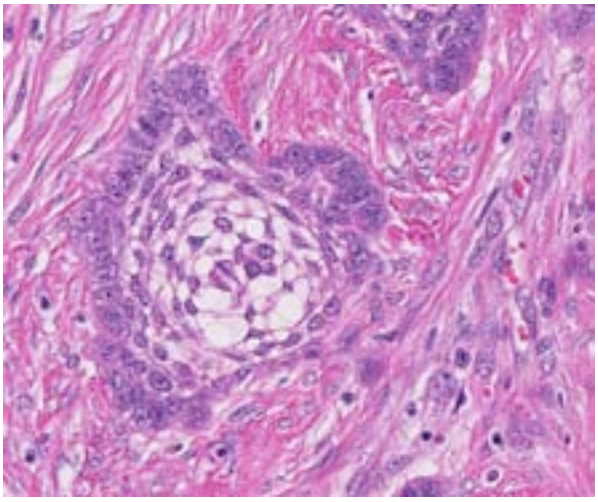

*3-4. Gingiva, cat: Occasionally, neoplastic cells surround a central focus of loosely arranged small spindle to stellate cells on a pale myxomatous matrix (stellate reticulum). (HE 260X)*

histological features include: Anastomosing cords and/or islands of odontogenic epithelium; peripheral palisading of those cells; apical crowding of the nucleus in the palisading cells; and loosely packed internal cells connected by long intercellular bridges, otherwise known as "stellate reticulum"; formation of extracellular deposits of eosinophilic glassy matrix in spherical nodular aggregates.[5]

In this case, the overlying mucosa is ulcerated, with associated neutrophilic infiltration. Additionally, there is accumulation of smudged, pale eosinophilic hyaline material, both within the islands and cords as well as between them. This material is consistent with amyloid, as it stains strongly with Congo red, and is pale green under polarized light.[10]

Amyloid-producing odontogenic tumors (APOT) have been described in dogs, cats and a Bengali tiger.[8-10] They have been reported as focally extensive, infiltrating, firm to friable lesions, frequently involving the entire maxilla.[2,8] These tumors are slowly progressive, locally invasive and can recur locally after excision.[11] There are no reports of metastasis of APOT in the literature.[4]

The histological feature that sets APOTs apart from ameloblastoma and acanthomatous ameloblastoma is the accumulation of amyloid between neoplastic epithelial cells. Other features are shared between these tumors.[5] Recently, the amyloid found in a single case of feline APOT was typed as odontogenic ameloblast-associated protein (formerly termed APin).[2]

Ultrastructurally in APOTs, cords and islands are delimited by a basement membrane, to which cuboidal to polygonal cells attach by hemidesmosomes. There are also numerous desmosomes between adjacent cells (consistent with epithelial cells). All these cells contain numerous tonofilaments, and pseudoinclusions containing 10nm thick filaments are occasionally noted. The ultrastructural presentation of the amyloid noted on light microscopy consists of intercellular accumulations of haphazardly arranged, non-branching, 10nm diameter filaments, which are frequently in direct contact with the epithelial cells.[3]

With regards to terminology APOTs have been designated calcifying epithelial odontogenic tumors in the past.[4] This designation has fallen out of favor, as this term is used to name an odontogenic tumor in humans that has a different histological presentation. Calcifying epithelial odontogenic tumors in humans frequently contain sheets of polyhedral cells, with extracellular mineralization of amyloid deposits and intracellular mineralization. Although these features are present in APOTs of dogs and cats, they are rare.[5]

**JPC Diagnosis:** Gingiva, left maxillary: Amyloid-producing odontogenic tumor.

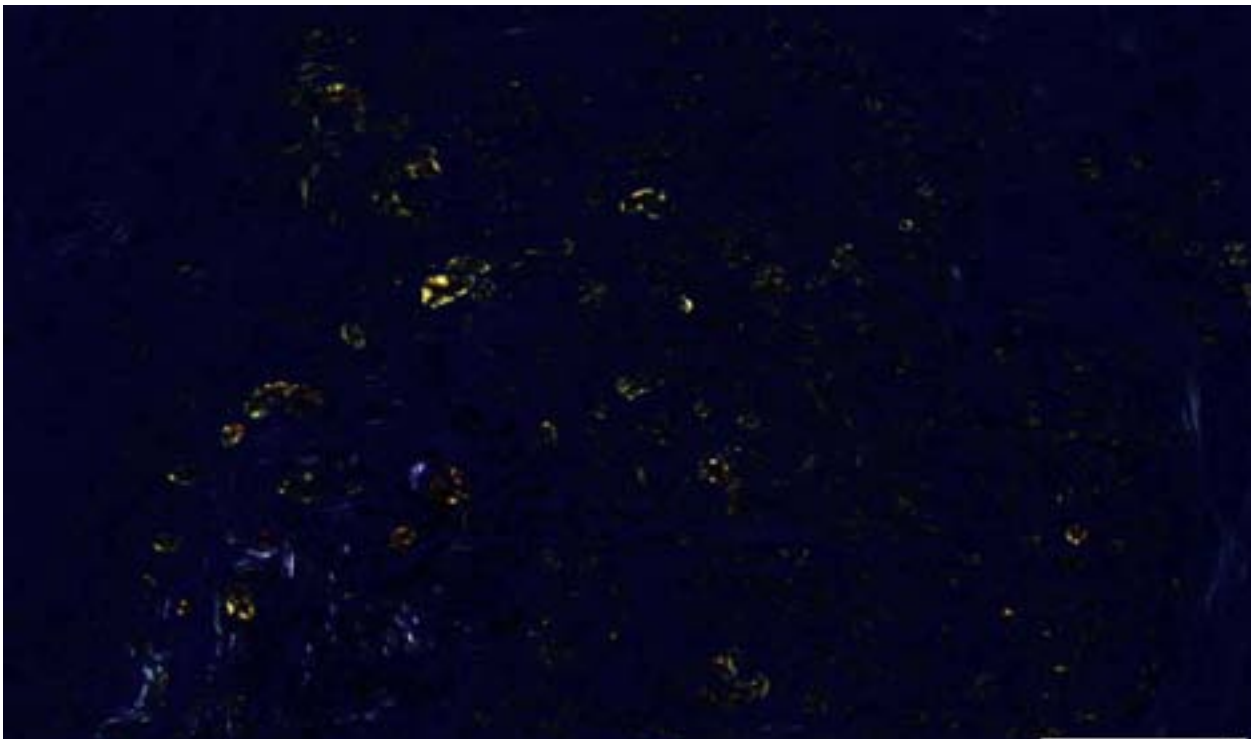

*3-5. Gingiva, cat: Congophilic islands of amyloid demonstrate apple-green birefringence under polarized light. (Photo courtesy of: Veterinary Pathology unit, Division of Veterinary Clinical Sciences, Roslin Institute and Royal (Dick) school of Veterinary Studies, The University of Edinburgh, Easter Bush Veterinary Centre, Roslin, Midlothian, EH25 9RG, UK http://www.ed.ac.uk/schools-departments/vet/services/pathology). (Congo Red, 200X)*

**Conference Comment:** Odontogenic tumors of dogs and cats are considered a diverse group of entities often with overlapping and controversial nomenclature. Amyloid-producing odontogenic tumors (APOT), calcifying epithelial odontogenic tumors (CEOT), and keratinizing ameloblastoma share all of the following features: benignity, odontogenic epithelium, and potential for both keratinization and amyloid deposition.[1] The amyloid in APOT has been demonstrated to be derived from ameloblasts, lending credence to its reclassification as amyloid-producing ameloblastoma.[7] The subjective distinguishing criteria and overlapping microscopic features indicate the possibility that all three of these oral tumors may be variants of a single entity.[1]

The majority of, if not all, odontogenic tumors can fit into one of three categories: epithelial, mixed or inductive, and mesenchymal. All of the various manifestations of ameloblastoma, including canine acanthomatous ameloblastoma, solid/multicystic ameloblastoma and the tumors previously discussed are epithelial derived. Mixed or inductive tumors consist of ameloblastic fibroma/fibro-odontoma and feline inductive odontogenic tumors. These are composed of proliferative odontogenic epithelium and odontogenic ectomesenchyme, often with inductive change, and may all occur along a single continuum. Finally, mesenchymal proliferations are perhaps most common, and consist of peripheral odontogenic fibroma (POF) and focal fibrous hyperplasia. The term POF has replaced the use of fibromatous epulis of periodontal ligament origin (FEPLO) among many veterinary surgical pathologists because epulis is a nonspecific term, and the lesion is derived from periosteal stroma rather than periodontal ligament. Both POF and FFH are recognized as separate entities, but also share overlapping clinical and pathologic features.[1]

**Contributing Institution:** Veterinary Pathology Unit, Division of Veterinary Clinical Sciences, Roslin Institute and Royal (Dick) School of Veterinary Studies, The University of Edinburgh, Easter Bush Veterinary Centre, Roslin, Midlothian, EH25 9RG, UK
http://www.ed.ac.uk/schools-departments/vet/services/pathology

**References:**

1. Bell CM, Soukup JW. Nomenclature and classification of odontogenic tumors – part II: clarification of specific nomenclature. *J Vet Dent*. 2014;31(4):234-243.
2. Bock P, Hach V, Baumgärtner W. Oral masses in two cats. *Vet Pathol* (ahead of print, 2011).
3. Breuer W, Geisel O, Linke RP, Hermanns W. Light microscopic, ultrastructural, and immunohistochemical examinations of 2 calcifying epithelial odontogenic tumors (CEOT) in a dog and a cat. *Vet Pathol*. 1994;31:415–420.
4. Gardner, DG, Dubielzig, RR. The so-called calcifying epithelial odontogenic tumour in dogs and cats (amyloid-producing odontogenic tumor). *J Comp Pathol*. 1994;111:221–230.
5. Head KW, Cullen JM, Dubielzig RR, Else RW, Misdorp W, Patnaik AK, et al. *Histological Classification of Tumors of the Alimentary System of Domestic Animals.* 2nd ed. Vol. X. Washington, DC; Armed Forces Institute of Pathology/ American Registry of Pathology. Washington DC, 2003:46-57.
6. Head KW, Else RW, Dubielzig RR. Tumors of the alimentary tract. In: Meuten DJ, ed. *Tumors in Domestic Animals*. 4th ed., pp. Ames, IA: Iowa State Press; 2002:402-410.
7. Hirayama K, Miyasho T, Ohmachi T, et al. Biochemical and immunohistochemical characterization of the amyloid in canine amyloid-producing odontogenic tumor. *Vet Pathol.* 2010;47:915-922.
8. Kang MS, Park MS, Kwon SW, Ma SA, Cho DY, Kim DY, et al. Amyloid-producing odontogenic tumour (calcifying epithelial odontogenic tumour) in the mandible of a Bengal tiger (*Panthera tigris tigris*). *J Comp Pathol*. 2006;134:236–240.
9. Langham RF, Bennett R, Koestner A. Amyloidosis associated with a calcifying ameloblastoma (calcifying epithelial odontoma) in a cat. *Vet Pathol*. 1984;21:549–550.
10. Myers RK, McGavin MD. Cellular and tissue responses to injury. In: McGavin MD, Zachary JF, eds. *Pathological Basis of Veterinary Disease*. 4th ed. Washington, DC; Mosby, Inc: 2003:45-46.
11. Poulet FM, Valentine BA, Summers BA. A survey of epithelial odontogenic tumors and cysts in dogs and cats. *Vet Pathol*. 1992;29:369–380.

**CASE IV**: 10728252 (JPC 3166465).

**Signalment:** 7-year-old castrated male Chinese Crested canine, *Canis familiaris*.

**History:** The dog originally presented in March 2009 with an oral gingival mass, mesial to the left mandibular canine tooth and first premolar. The mass was excised and recurred five months later. A partial rostral mandibulectomy was performed in February 2010.

**Gross Pathologic Findings:** The gingival mass was fluctuant to moderately firm and purple to red.

**Histopathologic Description:** Oral mucosa, mandible, left lower canine: The submucosa contains an unencapsulated, moderately demarcated, mildly infiltrative multinodular mass with a focal pedunculated region, composed of giant cells on a moderately vascular dense background of spindled stromal cells, interspersed by eosinophilic vascular connective tissue. Giant cells are polygonal to irregular with distinct cell borders, abundant pale basophilic granular to lightly vacuolated cytoplasm and up to 15-20 nuclei. Nuclei are round to oval to irregular with vesicular or finely stippled chromatin and generally one prominent nucleolus. Anisocytosis and anisokaryosis are 2-3 fold and mitoses are 11 in ten 400x high power fields. Scattered through the mass are moderate numbers of macrophages with intracytoplasmic dark tan to light brown granular material (hemosiderin) admixed with moderate multifocal hemorrhage. The overlying epithelium is moderately and diffusely hyperplastic and there is a focally extensive region of full thickness ulceration with replacement by moderate numbers of underlying viable and degenerate neutrophils and a small amount of necrotic cell debris. The superficial submucosa is multifocally edematous, characterized by pale staining and increased space between collagen fibers, and contains frequent thin walled vascular profiles admixed with plump fibroblasts (fibroplasia). Small populations of lymphocytes and plasma cells are noted within the submucosa at the periphery of the mass. The mass does not extend into the underlying bone or adjacent tooth and is completely excised with clean margins.

**Contributor's Morphologic Diagnosis:** Oral mucosa, mandible, left lower canine: Giant cell epulis with atypia.

**Contributor's Comment:** The oral mass in this dog was consistent with a giant cell epulis (GCE); however, the stromal spindle cells exhibited inconsistencies with the reported histologic features of this entity. In the stromal spindle cell population, mitoses were observed more frequently than expected for GCE, and anisokaryosis and anisocytosis were observed. Additional differential diagnoses include giant cell tumor of bone and soft parts, osteosarcoma (giant cell variant), or low grade spindle cell sarcoma with giant cells. This mass does not involve or infiltrate bone, contain osteoid, display severe cellular atypia or necrosis and is only present within the oral gingiva, making the first three possibilities less likely. In this case, the atypia observed may represent early neoplastic transformation of the spindle cell population, making differentiation between an atypical variant of GCE and low grade spindle cell sarcoma difficult. Recurrence of this mass may be explained by the incomplete excision of the previous (first) sample, or the presence of the atypical cell populations.

"Epulis" is a non-specific term referring to a benign local exophytic growth of the oral mucosa.[2] Epulides are common in the dog (up to 59% of benign canine oral neoplasms), and canine epulides can be divided into reactive lesions (giant cell epulis, fibrous epulis, pyogenic granuloma and reactive exocytosis) and peripheral odontogenic tumors (fibromatous epulis of the periodontal ligament, acanthomatous epulis (acanthomatous ameloblastoma) and calcifying epithelial odontogenic tumor (amyloid producing odontogenic tumor)).[5,11]

Giant cell epulis (GCE) was reported in a dog as early as 1917 but is a rare lesion, with little information available in the veterinary literature.[4-6,11,12] Classified under "Tumor-like Lesions" in the WHO Histologic Classification of Tumors of the Alimentary System of Domestic Animals, GCE is thought to represent a benign hyperplastic lesion rather than a true neoplastic process.[6,11,12] Despite the low number of documented cases, a variety of canine ages and breeds have been reported, with ages ranging from 1 to 11 years.[5,7,12] These masses arise from gingiva, most often adjacent to

the maxillary and mandibular premolars and are typically red to purple and lobulated.[11,12]

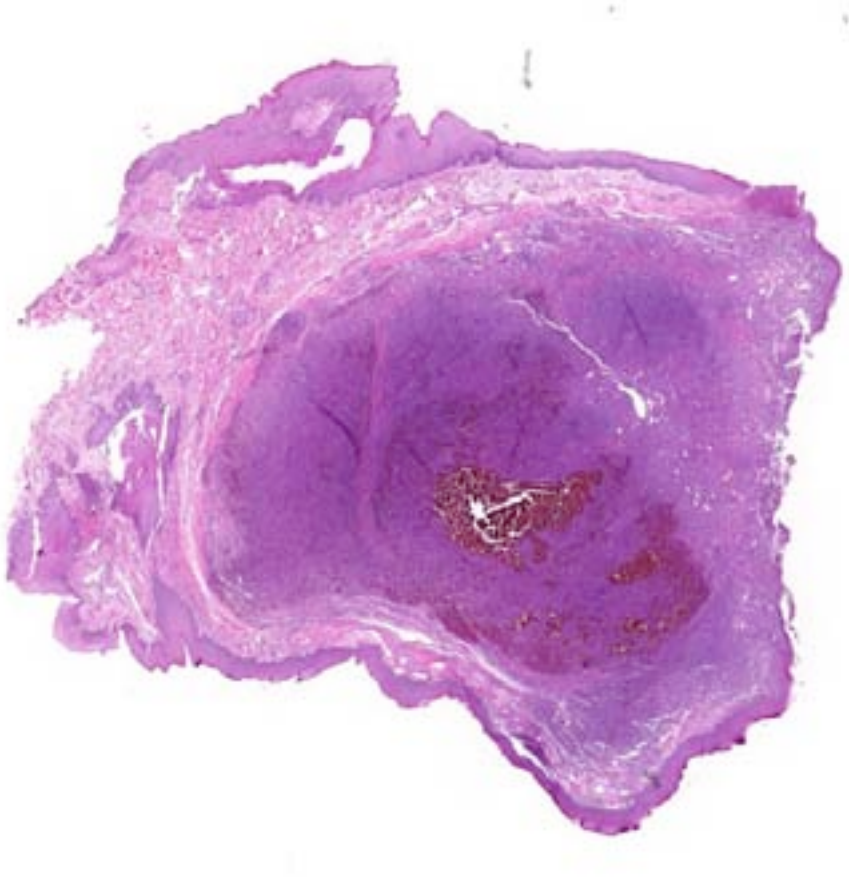

*4-1. Gingiva, dog: The gingiva contains an expansile, well-demarcated neoplasm. (HE 4X)*

Histologic features of canine and feline GCE are consistent with those reported for human patients.[4] GCE typically presents as a nonencapsulated, poorly demarcated vascular submucosal nodule covered by hyperplastic gingival epithelium that may be ulcerated.[1,2,5,11] Nodules consist of large numbers of randomly distributed multinucleated giant cells in a background of mononuclear stromal cells.[1,7-11] Multinucleated giant cells are irregularly shaped, often containing 10-20 visible nuclei with abundant eosinophilic cytoplasm, and may vary with respect to size (up to and exceeding 100 µm diameter), amount of cytoplasm, nuclear chromatin pattern and prominence of the nucleolus.[1,2,6-8,10,11] Within the giant cell population, cellular and nuclear pleomorphism are not seen and there are few to no mitoses.[2,4,11] The stroma is typically well vascularized and highly cellular, containing numerous round and spindle shaped mononuclear cells that exhibit rare mitoses.[1,2,5-8,10,11] The stroma shows varying degrees of mixed inflammation, as well as frequent hemorrhage, hemosiderosis and occasional osteoid or woven bone deposition.[1,2,5,7,8,10,12]

In the dog, GCE is reported to exhibit slow growth without invasion or metastasis.[4,6,11] Several references have reported no recurrence following removal (post-excision follow-up time ranged from 8-18 months).[5,11,12] In a retrospective study of 52 feline epulides by deBruijin et al (2007), GCE was the second most common type of epulis diagnosed, after fibromatous epulis.[2] In contrast to the behavior of canine GCE, the feline GCE in this study exhibited rapid growth and an aggressive clinical course, with seven out of thirteen recurring within two months of marginal excision.[2] The authors hypothesized that the high recurrence rate and poor prognosis of the GCE in the cat after marginal excision alone may be related to the rapid growth and poor demarcation of the lesion associated with the persistent inflammatory component.[2]

The origin of the multinucleated giant cells in GCE remains unknown. Ultrastructural and immune studies have shown the giant cells to be derived from macrophages, though they are not functional in terms of phagocytosis and bone resorption.[1,11] Due to the close association of GCE with bone, it has been suggested that giant cells are of osteoclast origin, though others have proposed that multinucleated giant cells form by fusion of infiltrating macrophages, as the stroma may contain chronic granulomatous inflammation.[2,4,12] Immunohistochemical studies

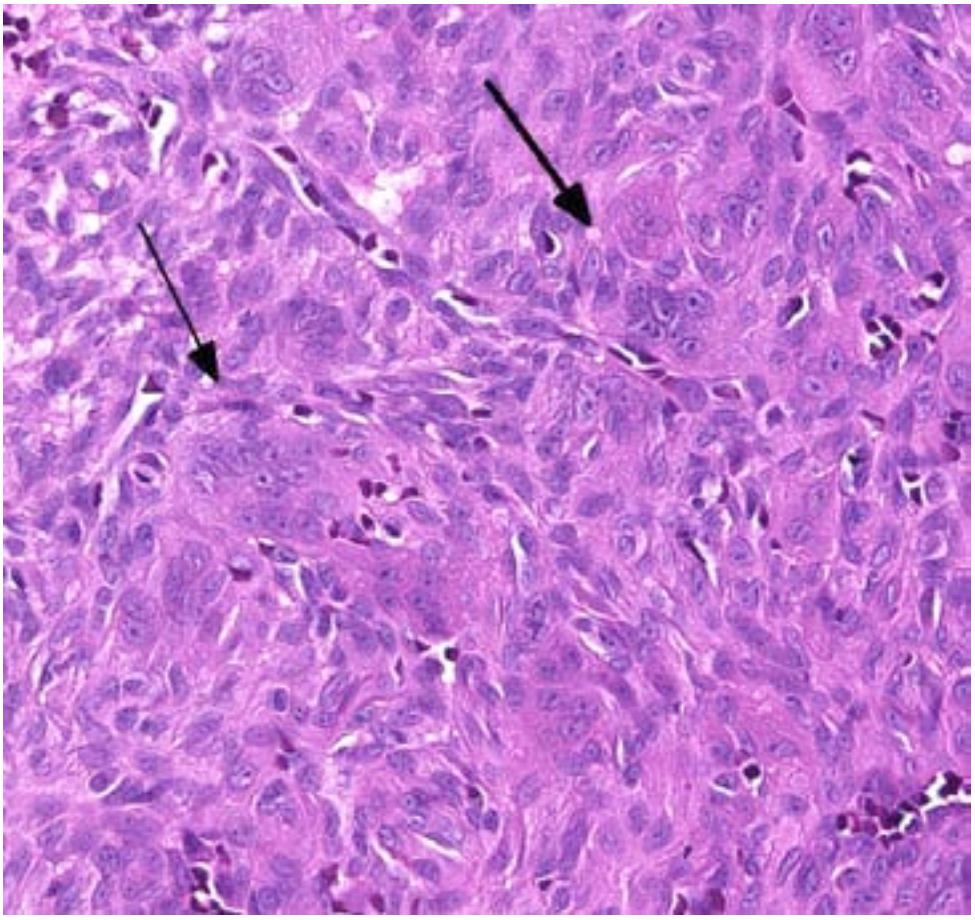

*4-2. Gingiva, dog: Neoplastic cells are spindled with prominent nucleoli. There are numerous polygonal multinucleated neoplastic cells scattered thoughout the neoplasm (arrows). (HE 248X)*

performed by deBruijn ND et al (2007) indicated that giant cells were strongly positive for vimentin and an osteoclast marker (tartrate-resistant acid phosphatase, TRAP) and negative for factor VIII.[2] Giant cell cytoplasm was also positive for the polyclonal antibody RANK, a cytokine leading to the differentiation of osteoclast progenitors into mature osteoblasts in the presence of its ligand (RANKL).[2] Therefore, the authors hypothesized that the giant cells are most likely formed from a monocyte/macrophage-like osteoclast precursor that differentiates into osteoclasts under the influence of mononuclear osteoblast-like stromal cells.

In humans, this lesion has been known by a variety of names, including peripheral giant cell tumor, peripheral giant cell granuloma, reparative giant cell granuloma, giant cell hyperplasia of the oral mucosa and osteoclastoma.[1,8,10] It accounts for approximately 1% of all oral pathologic lesions and occurs in all age groups, with the highest incidence in the fourth to sixth decade of life and the second highest incidence in the first to second decades.[1,8,9,11] It is generally accepted that this mass represents a benign hyperplastic lesion rather than a true neoplastic process, and it is known that chronic trauma or irritation can induce produce granulation tissue with chronic inflammation and fibroblast proliferation and manifest as reactive hyperplasia.[1,9-11] However, the inciting cause of GCE is not known and is controversial, with proposed causes including tooth extraction, poor dental restorations, dental malpositioning, ill fitting dentures, plaque, calculus or food impaction.[1,8-11]

The lesion originates from the connective tissue of the periosteum (mucoperiosteum or periodontal ligament) or from the periodontal membrane and is localized in the interdental papilla, edentulous alveolar margin or at the marginal gingival level.[1,8,10] The mass may involve the mandible or maxilla, though mandibular involvement is approximately 2.5 times more frequent than maxillary, and the premolar and anterior molar regions are most often affected.[1,8-11] Masses vary in size (though rarely exceed 2cm in diameter), are dark red to purple to blue, and can be polypoid, nodular or sessile.[1,8,10] The consistency of the mass depends on age of lesion because as time passes, an increased collagen component leads to increased firmness, and ulceration and bleeding can occur secondary to trauma.[1,8,10]

Behavior is variable, with growth ranging from silent to aggressive, affecting adjacent tissues by direct spread, though underlying bone is rarely affected.[1,9] The mass is not usually painful unless there is mucosal ulceration or erosion of the underlying bone, though swelling and dental mobility is common.[1,9,10] Occasional cases in children have been documented to be larger and more aggressive, with local bone destruction, displacement of the adjacent teeth and multiple recurrences.[1,9] Wide surgical excision with extensive clearing of the base of the lesion is usually curative, though when the periodontal membrane is affected, extraction of adjacent teeth may be necessary for full removal.[1,10,11] If resection is only superficial, recurrence is possible, though infrequent (5-11%).[1,8,10,11]

An interesting differential diagnosis in humans is brown tumor; a rare, non-neoplastic reactive growth associated with primary, secondary and/or tertiary hyperparathyroidism.[1,7-10] These masses are solitary or multiple, most often seen on the maxilla, ribs, clavicles and pelvic bones, and the name "brown tumor" is attributed to the gross brown discoloration of the affected tissue due to excessive hemorrhage and hemosiderosis.[6] The growth appears centrally in bone but can perforate the cortical layer, spreading towards the soft tissues, and cannot be distinguished from giant cell epulis based on histology.[1,10] However, this condition is often suspected when there are multiple lesions and recurrences despite adequate treatment.[1,9,10] Interestingly, a report by Headley et al (2008) described the occurrence of an oral lesion with features consistent with brown tumor in a 14-month-old English bulldog with renal secondary hyperparathyroidism due to chronic renal insufficiency.[7]

**JPC Diagnosis:** Oral mucosa, mandible: Peripheral giant cell granuloma.

**Conference Comment:** The contributor presents an uncommon proliferative non-neoplastic lesion observed in dogs, cats, and people; and then delivers a comprehensive review as currently understood in the literature. Conference participants observed the vascularization within some areas, and suggested the finding correlated with a reparative lesion.

A recent publication followed 26 diagnosed peripheral giant cell granulomas and concluded they are benign and rarely recur with even marginal surgical excision. Additionally, the number of giant cells and mitotic index of the lesions do not correlate with biologic behavior.[3]

**Contributing Institution:** The Animal Medical Center, Department of Pathology, 510 East 62nd St. New York, NY 10065**,** http://www.amcny.org/

**References:**

1. Chaparro-Avendano AV, Berini-Aytes L, Gay EC. Peripheral giant cell granuloma. A report of five cases and review of the literature. *Med Oral Patol Oral Cir Bucal.* 2005;10:48-57.
2. DeBruijn ND, et al. A clinicopathological study for 52 feline epulides. *Vet Pathol.* 2007;44:161-169.
3. Desoutter AV, Goldschmidt MH, Sanchez MD. Clinical and histological features of 26 canine peripheral giant cell granulomas (formerly giant cell epulis). *Vet Pathol.* 2012;49(6): 1018-1023.
4. Forman J, Reed CI. A fibro-blastoma of the alveolar border of the jaw containing giant cells (a giant cell epulis). *Ohio J Sci.* 1917;17(1):1-5.
5. Gardner DG. Epulides in the dog: a review. *J Oral Pathol Med.* 1996;25:32-37.
6. Head KW, et al. *Histological Classification of Tumors of the Alimentary System of Domestic Animals. 2nd Series*. World Health Organization International Histological Classification of Tumors of Domestic Animals, 2003.
7. Headley SA, et al. Oral lesions associated with renal secondary hyperparathyroidism in an English bulldog. *Semina: Ciencias Agrarias, Londrina*. 2008;29(2):407-412.
8. Rey JMG, et al. Peripheral giant-cell granuloma. Review of 13 cases. *Medicina Oral.* 2002;7:254-259.
9. Ruiz BD, et al. Reparative giant cell granuloma in a pediatric patient. *Med Oral Patol Oral Cir Bucal.* 2007;12:E331-335.
10. Shadman N, Ebrahimi SF, Jafari S, Eslami M. Peripheral giant cell granuloma: a review of 123 cases. *Dent Res J.* 2009;6(1):47-50.
11. Valentine BA, Eckhaus MA. Peripheral giant cell granuloma (giant cell epulis) in two dogs. *Vet Pathol.* 1986;23:340-341.
12. Yoshida K, et al. Clinicopathological study of canine oral epulides. *J Vet Med Sci.* 1999;61(8): 897-902.

**Joint Pathology Center**
**Veterinary Pathology Services**

# WEDNESDAY SLIDE CONFERENCE 2014-2015

## Conference 23

**29 April 2015**

**Guest Moderator:**
Charles Halsey, DVM, PhD, ACVP
Laboratory of Cancer Biology and Genetics Center for Cancer Research
National Cancer Institute, NIH

---

**CASE I:** NIAH2012-2 (JPC 4018762).

**Signalment:** 3-year-old female Holstein, *Bos Taurus.*

**History:** In a herd of 190 Holstein lactating cows, 9 cows died or were euthanized at 1 to 3 weeks after the onset of the clinical signs of fever, skin lesions, nasal discharge, decrease in milk production, and weight loss. Other characteristics of the skin lesions were multiple alopecia, dry scaling on the head, neck, vulva, and udder.

**Gross Pathology:** The lymph nodes, spleen, adrenal glands, kidneys, and liver were enlarged. The renal cortex was discolored and had multifocal to coalescing yellowish-gray nodules on both the capsular and cut surfaces.

**Laboratory Results:**

| | At clinical onset | At necrpsy (9 days after onset) |
|---|---|---|
| Temperature (°C) | 38.1 | 39.3 |
| Heart rate(/min) | 84 | 90 |
| Respiration rate (/min) | 56 | 30 |
| White blood cells (/ml) | 9,100 | 12,300 |

| | At clinical onset | At necrpsy (9 days after onset) |
|---|---|---|
| Packed cell volume (%) | 31 | 36 |
| Plasma protein level (g/dl) | 9.6 | 9.6 |

Flow cytometry analysis of the peripheral blood showed that the numbers of CD14+ monocytes (43.9%) and CD8 lymphocytes (19.1%) were significantly higher in the affected cows than in the normal lactating cows (CD14+ monocytes, 20.3 ± 1.6%; CD8 lymphocytes, 10.9 ± 1.3%). Further, the percentages of WC1 (3.5%) and IgM + lymphocytes (6.7%) were significantly lower in the affected cows than in the normal lactating cows (WC1+ cells, 12.7 ± 2.5%; IgM+ cells, 15.9 ± 2.6%).

No pathogens were isolated from the carcass.

**Histopathologic Description:** The interstitium throughout the renal cortex is replaced by multifocal to coalescing accumulations of inflammatory cells, mainly consisting of lymphocytes, macrophages, and multinucleated giant cells with moderate numbers of plasma cells. The arterioles are radially surrounded by the infiltrate. While some tubules are replaced with the infiltrate, other tubules throughout the cortex consist of diffuse mild vacuolation and contain

*1-1. Ox, kidney: There are multiple foci of hypercellularity scattered through the cortex. (HE 5X)*

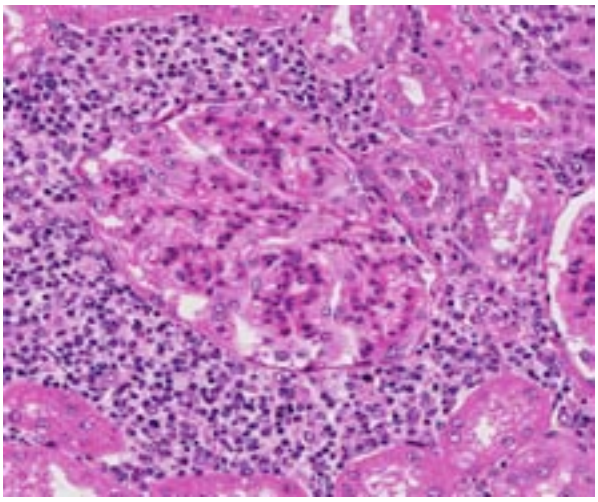

*1-2. Ox, kidney: The cellular infiltrate throughout the kidney is composed of numerous macrophages, lymphocytes, and fewer plasma cells. (HE 152X)*

eosinophilic stippled proteinaceous material. In addition, some areas show tubular and glomerular degeneration and necrosis, with protein casts and cellular debris in the tubular lumen.

Granulomatous inflammation with multinucleated giant cells was also detected in the adrenal glands, pancreas, thyroid, heart, mammary glands, liver, uterus, skin, and lymph nodes. The condition in the heart, mammary glands, and skin was accompanied with eosinophilic infiltration.

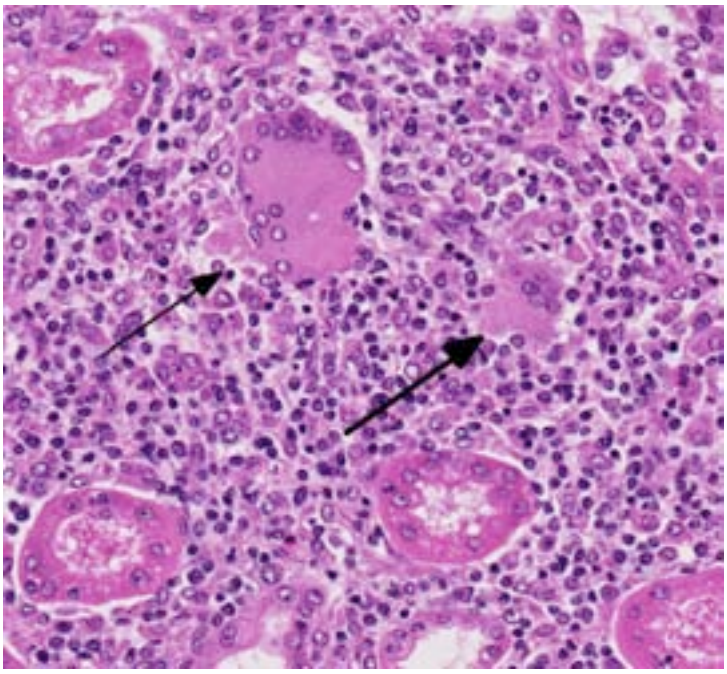

*1-3. Ox, kidney: Scattered throughout the infiltrate are low numbers of large multinucleated macrophages ranging up to 100 µm in diameter. (HE 185X)*

**Contributor's Morphologic Diagnosis:** Nephritis and diffuse, moderate to severe lymphogranulomatous inflammation.

**Contributor's Comment:** The outbreaks of the disease that were detected in various counties were characterized by systemic granulomatous inflammation; in cattle that is usually found to be induced by the ingestion of hairy vetch.

The granulomatous inflammation with the presence of multinucleated giant cells and the distribution of the lesions on the tissues show similar characteristics to those reported in hairy vetch toxicosis,[2,4,6] citrus pulp toxicosis,[3,7] and di-ureido isobutane (DUIB) toxicosis[1,5] in cattle. Various organs including the kidneys, heart, liver, spleen, adrenal glands, thyroid, lymph nodes, skin, and mammary gland are usually affected in these diseases.

Although the cause of the disease is an enigma, histopathological features suggest that a type 4 hypersensitivity reaction (key event) may play a role in the inflammatory reaction (pathogenesis).[6] We suggest that a plant constituent absorbed by the cows acts as an antigen that evokes a type 4 hypersensitivity reaction and granulomatous response. Alternatively, lectins may act as immunostimulants that directly stimulate T lymphocytes to initiate the

inflammatory cytokine response that characterizes the disease. However, in this case, the diet that was fed to cows in the farm did not contain vetch, citrus pulp, or DUIB.

**JPC Diagnosis:** Kidney: Nephritis, granulomatous, multifocal, moderate, with tubular degeneration and necrosis.

**Conference Comment:** Hairy vetch toxicosis is a diagnosis of exclusion, and the provided history of multiple lactating cows being affected is a typical presentation. Holstein and Angus cattle are most susceptible; and while the granulomatous inflammation is disseminated throughout a wide range of tissues in most cases, the lesion seems to be most frequently seen in the skin and the most severe lesions are seen in the kidney.[3,4] The heart is another common location in cattle, which distinguishes the disease from that in horses whom do not get myocardial involvement in addition to their lack of eosinophils in the granulomatous inflammation.[3]

The disease resembles a type 4 hypersensitivity reaction, although its pathogenesis is likely multifactorial as not all animals exposed develop lesions and lactating animals appear to be more susceptible.[4] The toxic principle was originally identified as prussic acid which is found in the seeds of *Vicia villosa* Roth (hairy vetch),[3] a forage commonly cultivated as winter cover or in row crop rotations due to its nitrogen-fixing ability. Other feed additives have been implicated (DUIB and citrus pulp), and this case serves as a reminder there are potentially other sources of a hapten or antigen capable of disease induction.

**Contributing Institution:** National Institute of Animal Health, Japan.
http://www.naro.affrc.go.jp/org/niah/

**References:**

1. Breukink HJ, Gruys E, Holzhauer C, Westenbroek AC. Pyrexia with dermatitis in dairy cows. *Vet Rec*. 1978;103:221-222.
2. Fighera RA, Barros CS. Systemic granulomatous disease in Brazilian cattle grazing pasture containing vetch (Vicia spp). *Vet Hum Toxicol*. 2004;46:62-66.
3. Hargis AM, Ginn PE. The integument. In: Zachary JF, McGavin MD, eds. *Pathologic Basis of Veterinary Disease*. 5th ed. St. Louis, MO: Elsevier Mosby; 2012:1018.
4. Iizuka A, Haritani M, Shiono M, Sato M, Fukuda O, Hagiwara A, et al. An outbreak of systemic granulomatous disease in cows with high milk yields. *J Vet Med Sci*. 2005;67:693-699.
5. Johnson B, Moore J, Woods LW, Galey FD. Systemic granulomatous disease in cattle in California associated with grazing hairy vetch (*Vicia villosa*). *J Vet Diagn Invest*. 1992;4:360-362.
6. Matsukawa K, Okada M, Kubo M. Pathomorphological findings of DUIB (1,1-Diureide isobutane) intoxication cases in dairy cattle. *J Coll Dairying*. 1983;10:197-204. (in Japanese with English summary)
7. Panciera RJ, Mosier DA, Ritchey JW. Hairy vetch (Vicia villosa Roth) poisoning in cattle: update and experimental induction of disease. *J Vet Diagn Invest*. 1992;4:318-325.
8. Saunders GK, Blodgett DJ, Hutchins TA, Prater RM, Robertson JL, Friday PA, et al. Suspected citrus pulp toxicosis in dairy cattle. *J Vet Diagn Invest* 2000;12:269-271.

**CASE II**: 50265 (JPC 4049053).

**Signalment:** 9-month-old male "sport horse", *Equus caballus*.

**History:** This horse presented with a 6-week history of lesions involving the dorsal cervical and nasal skin.

**Gross Pathology:** The liver was small and diffusely pale, with a firm consistency. The surface was irregular and pitted and contained numerous 0.5-1 cm raised white nodules that extended throughout the parenchyma.

**Laboratory Results**: Blood bile acids were 62 umol/L (reference range 0-20 um/L).

**Histopathologic Description:** In the liver, the most prominent lesion is marked biliary hyperplasia that has resulted in distortion of hepatic cords and hepatocyte individualization. The biliary hyperplasia is associated with fibrosis that extends between portal areas (bridging fibrosis). Also throughout the parenchyma, there are multiple variably sized nodules of hepatic regeneration that are often separated by a thin rim of fibrous connective tissue. Within portal areas, large numbers of hepatocytes that are characterized by an enlarged nucleus (up to 4 times normal size) with frequent intranuclear cytoplasmic invaginations and abundant, irregularly shaped, granular or vacuolated eosinophilic cytoplasm (megalocytes) are visible. Scattered throughout the liver, there are small numbers of hepatocellular mitotic figures. Additionally, Kupffer cells that often contain a greenish pigment that is interpreted as bile and few scattered lymphocytes are present.

**Contributor's Morphologic Diagnosis:** Chronic severe biliary hyperplasia, bridging fibrosis and nodular regeneration with prominent megalocytosis.

**Contributor's Comment:** The gross and histological lesions in this case are consistent with pyrrolizidine alkaloid toxicity. Pyrrolizidine alkaloids (PA's) are present in a wide variety of plants across the world. There are principally three families of plants that contain this toxin: Asteraceae (Compositae), Leguminosae (Fabaceae), and Boraginaceae.[7]

The most important genera are *Senecio, Cynoglossum, Amsinckia, Crotalaria, Echium, Trichodesma, and Heliotropium*. In New Zealand, PA toxicity in grazing animals is mostly associated with ragwort *(Senecio jacobaea)* poisoning. While ragwort is considered to be the most likely toxicant in this case, other possible causes of PA toxicity in New Zealand include: German ivy (Senecio mikanoides), groundsel (Senecio vulgaris), Paterson's curse (Echium plantagineum), viper's bugloss (E. vulgare), borage (Borago officinalis) and comfrey (Symphytum spp. & hybrids).[1]

Pyrrolizidinosis is usually a chronic disease but acute toxicity may occur due to the variations in

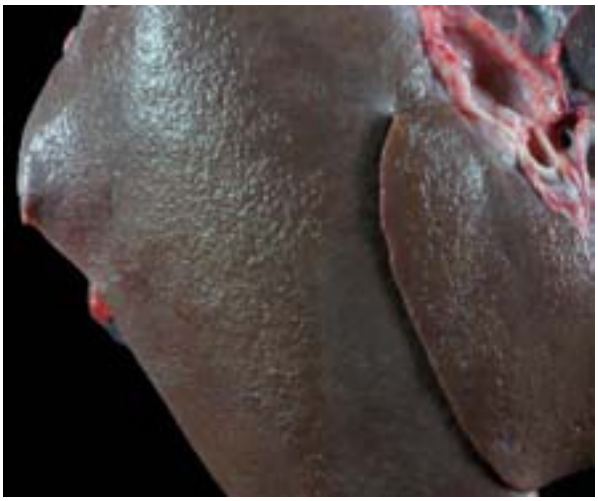

*2-1. Liver, horse: The liver is diffusely small, nodular, and pale. (Photo courtesy of: IVABS, Massey University, Palmerston North, New Zealand, http://www.massey.ac.nz)*

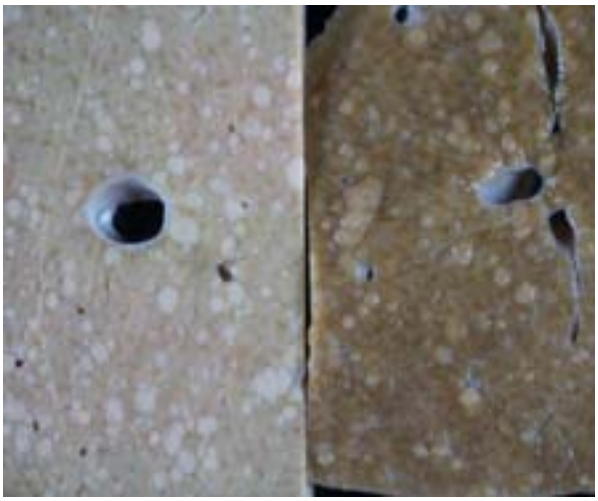

*2-2. Liver, horse: The surface was irregular and pitted and contained numerous 0.5-1 cm raised white nodules that extended throughout the parenchyma. (Photo courtesy of: IVABS, Massey University, Palmerston North, New Zealand, http://www.massey.ac.nz)*

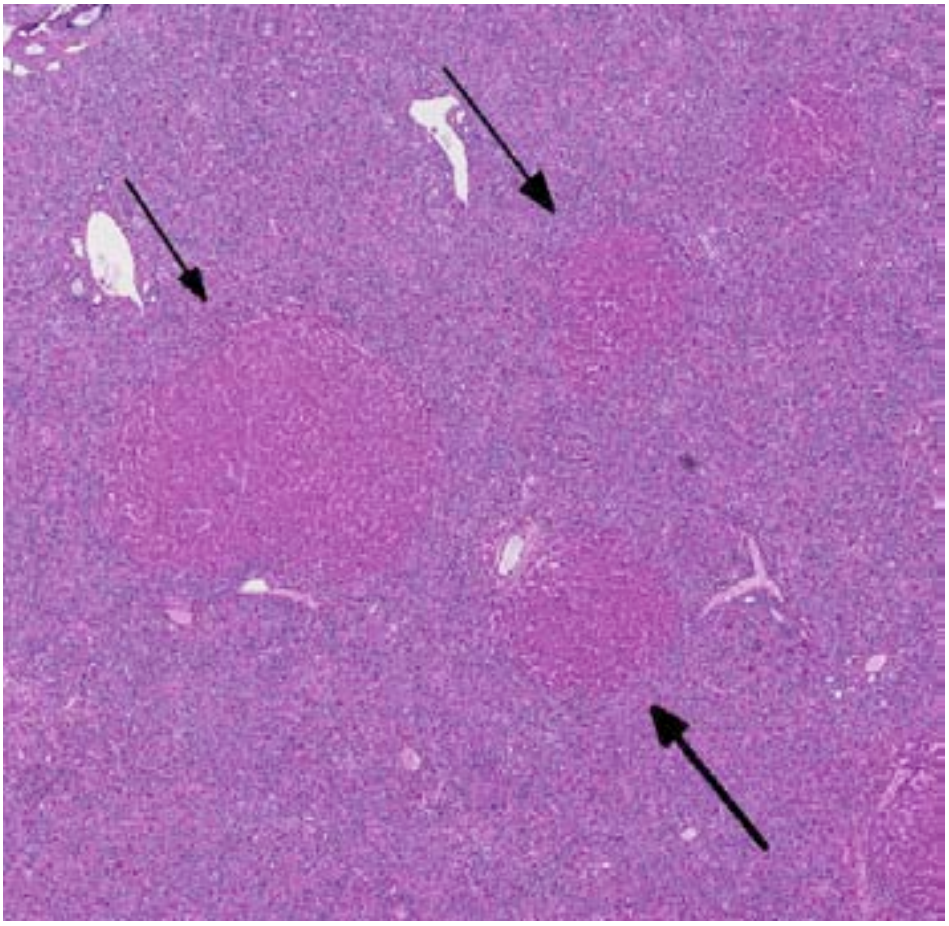

*2-3. Liver, horse: Much of the hepatic parenchyma is lost, with scattered islands of regenerative hepatocytes remaining (arrows). (HE 22X)*

PA's content that can occur between seasons and years.[1] PA's are hepatotoxic, carcinogenic, genotoxic, teratogenic and sometimes pneumotoxic.[7]

PA exists in the plant in two molecular forms: the hydrophilic nontoxic N-oxide (amine-oxide) and the lipophilic pro-toxic free or tertiary bases (retronecine, heliotridine and otonecine). Toxicity occurs when these free bases are converted into highly reactive and unstable alkylating pyrroles or pyrrolic derivatives by liver microsomal enzymes (cytochrome P-450 monooxygenases mainly CYP3A and CPY2B6). Subsequently the C-7 or C-9 position of the pyrrolic ring system becomes highly electrophilic and capable of binding to proteins and/or nucleic acids, leading to altered cell function and cell damage or death.[3] Individual animal variation in toxicity of PA's is mediated by the activity of the estereases that detoxify the alkylating pyrroles. Different PA's have different toxicity due to differences in total alkaloid content, structural features of the amino alcohol and the presence of other substitutions on the chemical ring that modify the rate and extent of the toxicity. Toxicity of PA's is due to necrosis, antimitotic action (crosslinks with DNA and inhibits mitosis with concomitant formation of megalocytes) and vascular damage mainly in the liver. Some alkylating pyrroles can escape the liver and reach the lung damaging capillaries and resulting in acute pulmonary edema and hydrothorax. Renal damage is also reported.[1]

Ragwort (tansy ragwort, Saint James' wort) is a biennial, perennial or annual weed with a diffuse root system. The alkaloids of ragwort include jacobine (major alkaloid), jaconine, jacoline, jacozine, senecionine and seneciphylline. All parts of the plants are toxic and animals normally eat the plant in small quantities either inadvertently or when forced due to lack of other food.[1] Pigs, horses, cattle, sheep, goats and chickens can be affected.[1,2] In humans, certain liver and other diseases have been attributed to the consumption of foods and herbal medicines prepared from pyrrolizidine alkaloid-containing plants.[6] Clinical signs in horses can be non-specific such as anorexia, weight loss, and diarrhea, photosensitization, icterus, or related to hepatic encephalopathy (depression, ataxia, circling, head pressing, blindness, collapse, coma and death).[2] There are three common histological patterns associated with pyrrolizidine poisoning: acute periacinar zonal necrosis, hepatic atrophy with formation of regenerative nodules, and atrophy and fibrosis without nodular regeneration. Megalocytes are usually most prominent in the

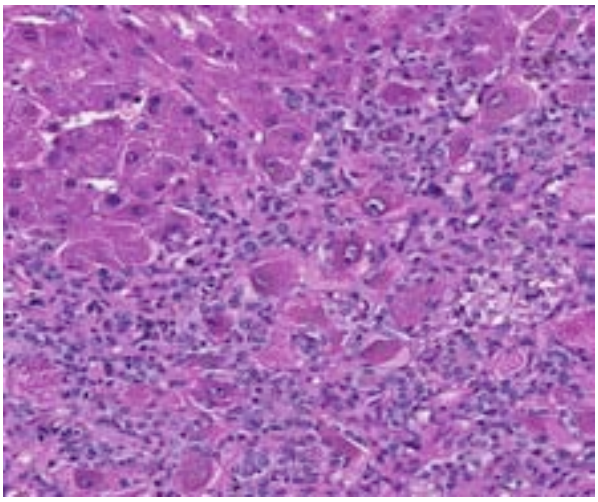

*2-4. Liver, horse: Remaining hepatocytes are separated by florid biliary hyperplasia. A regenerative hepatocellular nodule is at upper left. (HE 192X)*

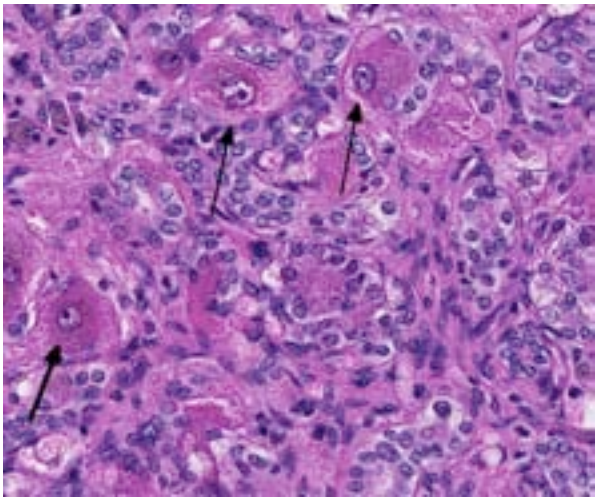

*2-5. Liver, horse: Numerous hepatocytes contain nuclei that are 3-5X normal size (arrows), referred to as "megalocytes". (HE 250X)*

second histological pattern. Megalocytosis is a progressive enlargement of liver cells to up to three times the normal diameter, with a proportionate increase in nuclear diameter. These are believed to be morphologically and functionally viable hypertrophic cells that are incapable of division due to the potent antimitotic action of the pyrrolizidine alkaloids. Some enlarged nuclei have cytoplasmic invaginations that can become entrapped as intranuclear inclusions.[6]

**JPC Diagnosis:** Liver: Florid biliary hyperplasia, portal and bridging, diffuse, severe, chronic, with nodular hyperplasia and hepatocellular megalocytosis, necrosis, and loss.

**Conference Comment:** Pyrrolizidine alkaloids (PA) are produced by over 6,000 plants as a deterrent from consumption by herbivores.[5] Most PA-producing plants are therefore unpalatable to grazing animals; however, when they invade pastures to the degree other forages are unavailable or their seeds contaminate prepared feeds, PA's become hepatotoxic by conversion to their metabolically activated form dehydropyrrolizidine.[4] Horses and pigs are more susceptible than ruminants in part because the toxin can be degraded in the rumen.[4]

The contributor discusses the three types of patterns of hepatic lesions associated with PA's. The acute form results from ingestion of a large quantity of toxin, as can occur in starving animals grazing drought stricken pasture. In the second form, likely present in the current case, repetitive prolonged exposure leads to the hepatic atrophy with megalocytosis. The third form, which lacks regenerative nodules, is due to prolonged exposure specifically to *Heliotropium* spp.[4]
The biliary hyperplasia is dramatic in this case, and often occurs in PA toxicosis. While this biliary reaction is commonly associated with bile duct obstructions or local portal inflammation and fibrosis, it is suspected to occur in toxicity cases such as PA, phomoposin, and aflatoxin due to sustained regenerative stimulus from an incapacitated atrophic liver.[4]

**Contributing Institution:** IVABS
Massey University
Palmerston North, New Zealand
http://www.massey.ac.nz

**References:**

1. Chambers, P. Poisonous plants of New Zealand. 2014 15/05/2014]; Available from: http://calve/pharm/toxSite/poisonplants/index.html.
2. Gava A, Barros CS. Senecio spp. poisoning of horses in southern Brazil. *Pesquisa Veterinária Brasileira.* 1997;17(1):36-40.
3. Molyneux R, et al. Pyrrolizidine alkaloid toxicity in livestock: a paradigm for human poisoning? *Food Additives & Contaminants: Part A*. 2011;28(3):293-307.
4. Stalker MJ, Hayes MA. Liver and biliary system. In: Maxie MG, ed. *Jubb, Kennedy, and Palmer's Pathology of Domestic Animals*. Vol 2. 5th ed. Philadelphia, PA: Elsevier Saunders;

2007:373-376.
5. Stegelmeier BL, Edgar JA, Colegate SM, et al. Pyrrolizidine alkaloid plants, metabolism and toxicity. *J Nat Toxins*. 1999;8(1):95-116.
6. Svoboda D, Reddy J, Bunyaratvej S. Hepatic Megalocytosis in Chronic Lasiocarpine Poisoning: Some Functional Studies. *The American Journal of Pathology*. 1971;65(2):399.
7. Wiedenfeld, H. Plants containing pyrrolizidine alkaloids: toxicity and problems. *Food Additives & Contaminants: Part A*. 2011;28(3):282-292.

**CASE III**: 090372-06 (JPC 4037988).

**Signalment:** Adult female New Zealand white rabbit, *Oryctolagus cuniculus.*

**History:** This rabbit was part of a study to determine the median lethal dose of aerosolized ricin. This rabbit was exposed to 4.41 ug/kg of aerosolized ricin and was found dead 24 hours after exposure. Research was conducted under an IACUC approved protocol in compliance with the Animal Welfare Act, PHS Policy, and other federal statutes and regulations relating to animals and experiments involving animals. The facility where this research was conducted is accredited by the Association for Assessment and Accreditation of Laboratory Animal Care, International and adheres to principles stated in the Guide for the Care and Use of Laboratory Animals, National Research Council, 2011.

**Gross Pathology:** The lungs were firm, bright red, edematous with rounded edges, mottled, and failed to collapse. The laryngeal and tracheal mucosa was dark red with multiple streaks of hemorrhage and blood tinged foam within the lumen. The connective tissue surrounding the organs within the mediastinum was gelatinous (edema). There was pleural effusion (20 ml of yellowish viscous fluid). There was blood staining of the hair on the face, and the nasal turbinates were slightly edematous and glistened on cut surface.

**Laboratory Results:** None.

**Histopathologic Description:** Lung: Diffusely, there are changes in all levels of the conducting, transitional, and exchange portions of the pulmonary parenchyma. The alveolar lumina are filled with large amounts of eosinophilic homogenous material (edema), eosinophilic finely fibrillar material (fibrin), sloughed necrotic cellular debris, hemorrhage, and heterophils. There is disruption and loss of the alveolar septa with replacement by cellular and karyorrhectic debris (necrosis) or the septa are segmentally expanded by congestion and edema. The connective tissue surrounding the bronchi, bronchioles, blood vessels and within the pleura is expanded by increased clear space (edema), fibrin, hemorrhage, and viable and degenerate heterophils. The epithelium lining bronchi and bronchioles are segmentally or completely lost and replaced by fibrin, edema, and necrotic cellular debris (necrosis) which occasionally fills the


*3-1. Lungs, rabbit: The lungs were firm, bright red, edematous with rounded edges, mottled, and failed to collapse. (Photo courtesy of: Pathology Division, USAMRIID, Building 1425, Fort Detrick, MD, 21702 http://www.usamriid.army.mil/)*

*3-2. Trachea, rabbit: The laryngeal and tracheal mucosa was dark red with multiple streaks of hemorrhage and blood tinged foam within the lumen. (Photo courtesy of: Pathology Division, USAMRIID, Building 1425, Fort Detrick, MD, 21702 http://www.usamriid.army.mil/)*

airway lumina. Lymphatics are moderately distended by fibrin and edema. Endothelial cells are often plump and protrude into the vascular lumen (reactive).

**Contributor's Morphologic Diagnosis:** Lung: Necrosis, interstitial and bronchiolar/bronchial epithelial, multifocal, moderate, with fibrin, peribronchovascular and pleural edema, hemorrhage, and acute inflammation.

**Contributor's Comment:** Ricin is a phytotoxin derived from the castor bean plant (*Ricinus communis*) that is found in all parts of the plant but is most highly concentrated in the seeds. It is listed as a Category B bioterrorism agent/toxin by the Centers for Disease Control and Prevention due to the potential use as a weapon of terrorism and as a biological warfare threat to military operations.[1]

Ricin is a glycoprotein composed of two glycoprotein chains (A and B) that are weakly linked by disulfide bonds. The B chain facilitates entry into the cell by binding to cell surface glycoproteins. The ricin A chain induces cellular necrosis by inhibition of protein synthesis through enzymatic alteration of the 28S ribosomal RNA loop contained within the 60S subunit.[1,3] The exotoxin, shiga toxin, produced by *Shigella dysenteriae* and *Escherichia coli* serotype O157:H7 have a similar mechanism of action.[7] Ricin also induces inflammation through the activation of mitogen activated protein kinases (MAPK), synthesis of proinflammatory RNA transcripts and production of increased levels of circulating cytokines and chemokines.[8]

All animals are potentially susceptible to toxicosis with ricin. The horse is the most sensitive domestic species. In contrast, sheep, cattle and pigs are more resistant while ducks and chickens are the most resistant. Cases of poisoning have resulted from the accident or deliberate introduction of beans or castor-cake with other feedstuffs. Mixture of feed in a plant previously used for castor seeds has even resulted in poisoning.[2]

The clinical signs and pathological changes in ricin intoxication are route specific.[3] The primary target of aerosolized ricin are the type I and II pneumocytes, and lesions following inhalation are primarily confined to the lungs and consist of intra-alveolar edema, acute alveolitis, and diffuse necrosis of the epithelium lining the lower respiratory tract.[1]

The gross lesions reported from experimental inhalation studies in rhesus macaques consist of focal hemorrhage in the intestines, brain, myocardium, and pleura.[7] Microscopic lesions consist of lymphocytic necrosis of lymphoid organs, hemorrhage, necrosis, hyaline droplets, and fibrin thrombi in the liver; hemorrhage and necrosis in the adrenal glands; tubular hyaline changes in the kidneys; degeneration and necrosis of the heart muscle; and congestion and hemorrhage of the gastrointestinal tract.[7]

Oral intoxication requires significantly more (up to 500X) material to reach toxic levels than by other routes of intoxication due to poor absorption in the digestive tract and possible enzymatic degradation in the digestive tract.[2,3] A review of 751 cases of castor bean ingestion in humans found a death rate of 1.9%.[3] The most common gross post-mortem findings reported in oral intoxication are multifocal ulceration and hemorrhages of the gastric and small intestinal mucosa. Findings in other organs systems are similar to parental introduction and include lymphoid necrosis in the mesenteric lymph nodes, gut-associated lymphoid tissue and spleen, as well as Kupffer cell and hepatocellular necrosis, diffuse nephritis and diffuse splenitis.[3]

In recent years, various extremist groups and individuals have used ricin in attacks or have been

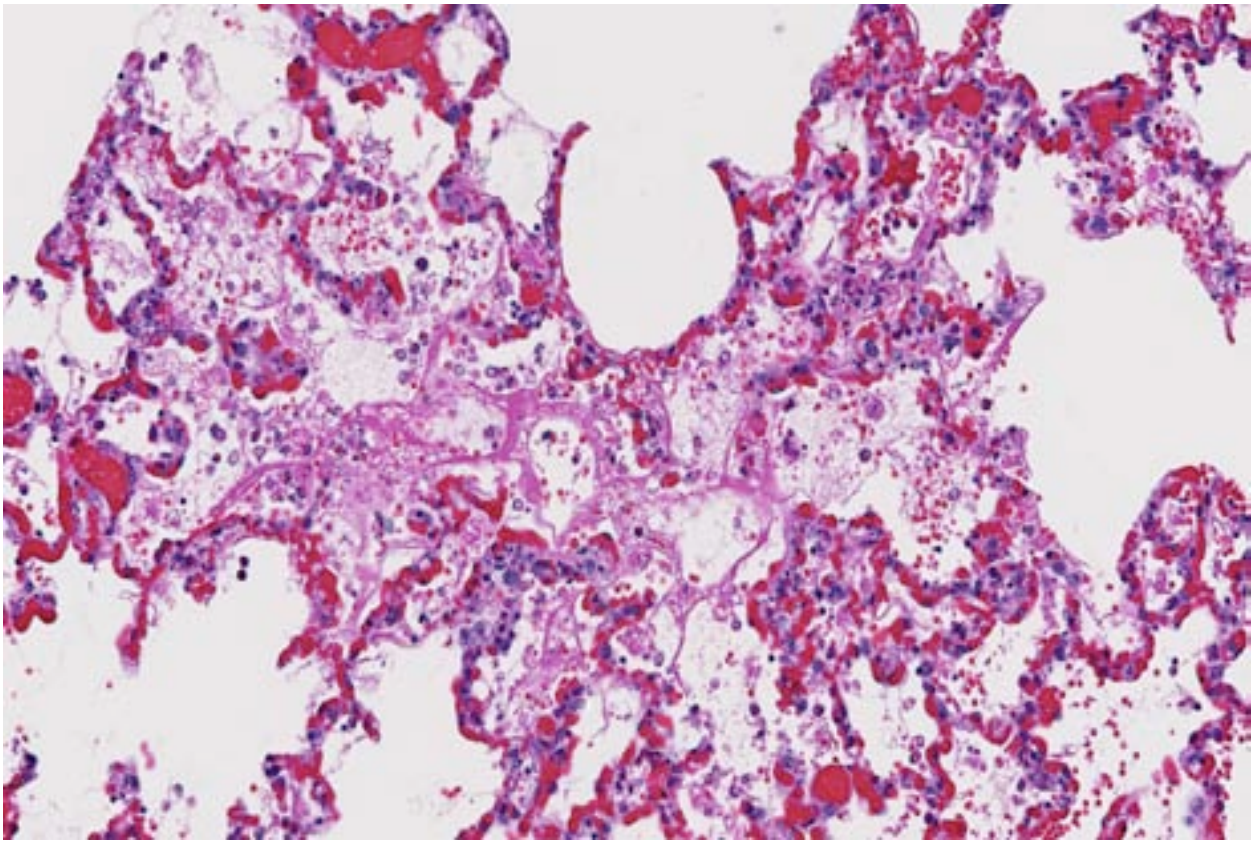

*3-3. Lung, rabbit: There is widespread septal necrosis. Alveoli contain variable amounts of hemorrhage, fibrin and edema, admixed with abundant cellular debris. In some areas, fibrin forms hyaline membranes. (HE 256X)*

arrested for the possession of ricin. This is attributed to the ready availability of castor beans, ease of toxin extraction, and popularization on the Internet. None of these attacks resulted in human intoxications; however, they demonstrate that ricin is well known.[3,6]

The ricin toxin is capable of inducing the formation of antibodies since it is a protein. Immunity in cattle and calves has been demonstrated by feeding increasing amounts of the bean.[2] Currently, there is no licensed vaccine available for use in humans; however, one is under development, and molecules that have been evaluated include a deglycosylated ricin A chain, formalin-inactivated toxoid, and recombinant ricin A chain.[3,4] A vaccine candidate produced by the latter technique shows the most promise and is in more advanced stages of development in clinical trials.[3]

The research described herein was sponsored by Defense Threat Reduction Agency / Joint Science and Technology Office for Chemical Biological Defense, CBM.VAXBT.03.10.RD.P.011.

Opinions, interpretations, conclusions, and recommendations are those of the author and are not necessarily endorsed by the U.S. Army.

**JPC Diagnosis:** Lung: Necrosis, interstitial, diffuse, with multifocal hyaline membrane formation.

**Conference Comment:** The contributor presents a rarely reported entity in the veterinary literature outside of experimental studies and delivers an excellent review of its pathogenesis and disease manifestations. Conference participants were struck by the widespread necrosis of Type I pneumocytes and largely unaffected septal capillaries in this case. The discussed differentials for toxic pneumonia in rabbits included paraquat toxicity and inhaled oxygen.

Aerogenous exposure is the most lethal form of ricin intoxication; however, a recent publication described two adult dogs that died 2-3 days following acute ingestion of fertilizer composed of residual castor bean plant material.[5] The dogs exhibited similar clinical signs as described in

human ingestion cases, with vomiting and abundant hemorrhagic diarrhea due to ulcerative gastroenteritis. The most prominent histopathologic lesions were multifocal renal tubular degeneration and necrosis. Reports of such intoxication in dogs are rare, and only 9% ended in death or euthanasia in a retrospective review of 98 cases over a 11 year time period.[5]

**Contributing Institution:** Pathology Division
USAMRIID
Building 1425
Fort Detrick, MD 21702
http://www.usamriid.army.mil

**References:**

1. Audi J, Belson M, Patel M, Schier J, Osterloh J. Ricin poisoning: a comprehensive review. *JAMA*. 2005;294(18):2342-2351.
2. Clarke EGC, Clarke ML. Poisonous plants. *Garner's Veterinary Toxicology*. Baltimore, MD: Williams and Wilkins Company; 1967:336-339.
3. Poli MA, Roy C, Huebner K, Franz DR, Jaax NK. Ricin. In: Dembek ZF, ed. *Medical Aspects of Biological Warfare*. Washington, DC: Borden Institute; 2007:323-335.
4. Reisler RB, Smith LA. The need for continued development of ricin countermeasures. *Adv Prev Med.* 2012;2012:149737.
5. Roels S, Coopman V, Vanhaelen P, Cordonnier J. Lethal ricine intoxication in two adult dogs: toxicologic and histopathologic findings. *J Vet Diagn Invest*. 2010;22(3):466-468.
5. Staff C. FBI searches for clues in ricin investigation http://www.cnn.com/2013/04/24/us/ricin-suspect-released/index.html?hpt=hp_inthenews. Accessed July 17, 2013.
6. Wilhelmsen CL, Pitt ML. Lesions of acute inhaled lethal ricin intoxication in rhesus monkeys. *Vet Pathol.* May 1996;33(3):296-302.
7. Wong J, Korcheva V, Jacoby DB, Magun B. Intrapulmonary delivery of ricin at high dosage triggers a systemic inflammatory response and glomerular damage. *Am J Pathol.* 2007;170(5): 1497-1510.

**CASE IV:** 14-2108 AFIP (JPC 4052872).

**Signalment:** Adult female Boer goat, *Capra hircus.*

**History:** Goats on a small holding with fair nutrition, Drenched with Q-drench 2 weeks ago. 25 goats, 2 sick, one found dead.

**Gross Pathology:** Generalised jaundice, liver swollen and finely mottled. Kidney swollen and moist with small (<1mm) white lesions scattered across surface. Lung, red with emphysema and foam in airways.

**Laboratory Results:** Gall bladder- profuse predominant growth of *Escherichia coli* (haemolytic).

**Histopathologic Description:** Liver: The periportal areas are moderately expanded by fibrosis that is sometimes bridging, along with biliary hyperplasia and infiltration of occasional lymphocytes. Disrupting and effacing bile duct epithelium, obliterating bile ducts and extending into surrounding fibrous tissue are abundant negatively stained outlines of acicular crystals, shrunken, individualized, hypereosinophilic and sloughed epithelial cells, cellular debris and occasional neutrophils. Within occasional remaining intact bile ducts are non-viable neutrophils and cellular debris. Crystals are occasionally present in adjacent hepatocytes and there is hyperplasia of Kupffer cells. Occasional hepatocytes are lost, shrunken and hypereosinophilic and replaced by neutrophils and cellular debris (necrosis). Remaining hepatocytes contain granular cytoplasm, often contain feathery vacuolation or occasionally contain variably sized, well defined cytoplasmic vacuoles (lipid), yellow-brown granular pigment (bilirubin) (cholestasis) and rare cytosegresomes.

**Contributor's Morphologic Diagnosis:** Liver; Cholangiohepatitis, necrotizing, moderate, chronic with biliary crystals and bridging portal fibrosis.

**Contributor's Comment:** This is a spectacular case of crystal-associated cholangiohepatopathy, and although crystals are not seen, their outlines are readily apparent. Crystal-associated cholangiohepatopathy is a progressive disease seen with ingestion of plants containing steroidal saponins that form crystals in bile ducts and less commonly hepatocytes, Kupffer cells and renal tubules.[1,4] Larger crystals are found with prolonged ingestion. This is a disease that primarily affects ruminants with sheep and goats being more commonly affected than cattle.[1]

The crystals are composed principally of calcium salts of the steroidal saponins that are metabolised in the rumen and liver to form episapogenin glucuronides. In the presence of calcium they can precipitate and form crystals.[5] Crystals can obstruct bile ducts and lead to icterus and secondary photosensitization.[2] It is still unclear whether the biliary crystals alone cause liver

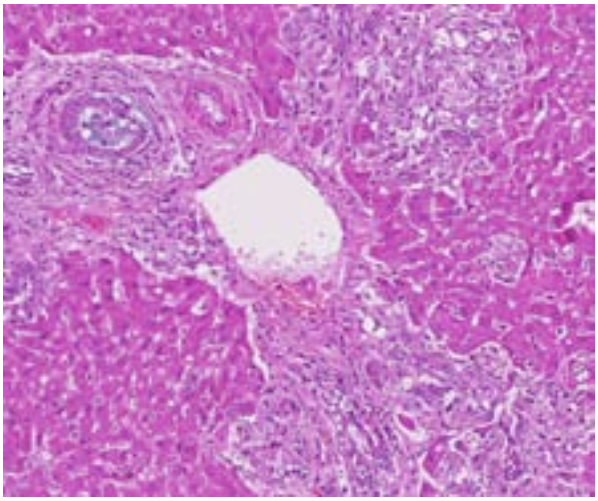

*4-1. Liver, goat: Portal areas are markedly expanded and often bridged by abundant fibrosis and moderate biliary hyperplasia. The fibrosis often breaches the limiting plate, effacing periportal hepatocytes. (HE 84X)*

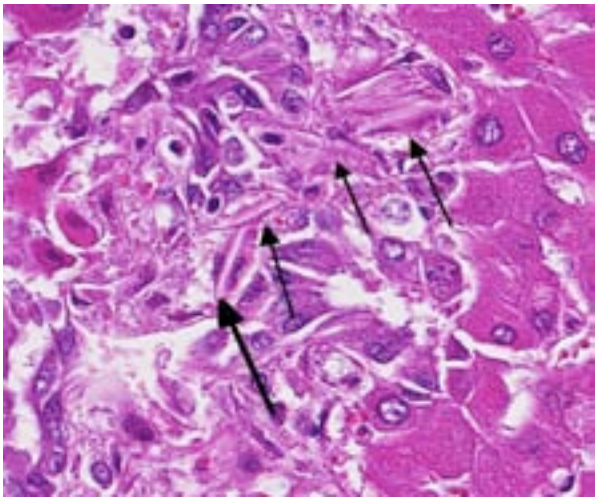

*4-2. Liver, goat: Within portal areas, often effacing proliferating biliary epithelium, are numerous outlines of acicular crystals. (HE 292X)*

damage or whether other toxins in the plants play a role.[1,5]

Levels of saponins vary greatly with age of plant, location and size and the plants are thus not always toxic. Outbreaks commonly occur in summer when young plants become wilted, especially if rain is followed by hot dry weather.[4]

Plants that are known to cause crystal-associated cholangiohepatopathy are included in **Table 1.**

Many plants contain steroidal saponins, but have not yet been documented as causing biliary crystals. *Solanales, Primulales, Ranunculales, Fabales, Sapindales, Poales* and *Liliales* are all orders of plants that contain steroidal saponins[1], so should not be ignored when investigating the etiology of crystal assosicated-cholangiohepatopathy.

In this case the significance of the *E.coli* is unclear. It may have been a post mortem contaminant, or a retrograde opportunist making use of the disrupted biliary epithelium.

**JPC Diagnosis:** Liver: Biliary hyperplasia, portal, diffuse, moderate, with intraductal crystal formation and periportal bridging fibrosis.

**Conference Comment:** Steroidal saponins are a type of glycoside, which, like alkaloids, are bitter and usually not readily consumed by domestic animals. Their metabolism to glucuronide conjugates result in the crystal formation evident in this case and subsequent hepatic disease secondary to biliary obstruction. Plants in early, rapid growth stages are most hazardous with the highest levels of saponins while mature plants can be grazed without incidence.[3]

Conference participants contrasted this entity with that of sporidesmin, the mycotoxin that causes biliary epithelial necrosis. Biliary hyperplasia with minimal inflammation is present in both entities and photosensitization is a common sequela, albeit through slightly different mechanisms. Saponins lead to biliary obstruction rather than necrosis, but both result in accumulation of phylloerythrin due to cholestasis inciting the characteristic skin manifestation of facial eczema when the affected animal is exposed to sunlight. [2]

**Table 1**

| Scientific name | Distribution | Common name |
|---|---|---|
| *Tribulus terrestris* | South Africa, Australia, North America | Puncture Vine |
| *Narthecium ossifragum* | Norway, UK | Bog asphodel |
| *Agave lecheguilla* | North America | Lecheguilla |
| *Nolina texana* | North America | Texan bear grass |
| *Brachiaria decumbens* | Brazil, Australia, Malaysia | Signal grass |
| *Panicum coloratum* | Australia, North America, Africa | Kleingrass |
| *Phytolacca octandra* | NZ, South America | Inkweed |

The contributor outlined the most well-known steroidal saponin-producing plants, of which *Tribulus terrestris* may be most readily recognized since it has caused enormous loss of sheep in South Africa, where it is known as "yellow bighead" due to icterus and marked facial edema.[5]

**Contributing Institution:** EMAI, State Diagnostic Veterinary Laboratory, Menangle, NSW Australia
http://www.dpi.nsw.gov.au/research/centres/emai

**References:**

1. Collett MG, Thompson KG, Christie RJ. Photosensitisation, crystal-associated cholangiohepatopathy, and acute tubular necrosis in calves following ingestion of Phytolacca octandra (inkweed). *New Zealand Vet J.* 2011;59:3.
2. Cullen J, Brown D. Hepatobiliary system and exocrine pancreas. In Zachary JF, McGavin MD, eds. *Pathologic Basis of Veterinary Disease.* 5th ed. St. Louis, MO; Elsevier Mosby:440.
3. Galey FD. Disorders caused by toxicants. In: Smith BP, ed. *Large Animal Internal Medicine*. 4th ed. St. Louis, MO: Mosby Elsevier; 2009:1697-1698.
4. McDonough SP, Woodbury AH, et al. Hepatogenous photosensitization of sheep in California associated with ingestion of *Tribulus terrestris* (puncture vine) *J Vet Diagn Invest.* 1994:6:392.
5. Stalker MJ, Hayes MA. Liver and biliary system. In: Maxie MG, ed. *Jubb, Kennedy and Palmer's Pathology of Domestic Animals*. 5th ed. Vol 2. Philadelphia, PA; Elsevier Saunders 2007:376-378.

**Joint Pathology Center**
**Veterinary Pathology Services**

# WEDNESDAY SLIDE CONFERENCE 2014-2015

## Conference 24

**06 May 2015**

---

**CASE I:** SP-12-7847 (JPC 4031937).

**Signalment:** 15-year-old castrated male domestic medium hair cat, *Felis catus*.

**History:** This cat had a 4-week history of hyphema and corneal opacity of the right eye (OD). Physical examination revealed dyscoria, epiphora, conjunctival hyperemia, 2+ buphthalmos, 2+ aqueous flare, hemorrhage within the anterior chamber, corneal midstromal neovascularization and edema, and increased intraocular pressure (54 mmHg) OD. The eye was enucleated and submitted for microscopic examination.

**Laboratory Results:** Three-view radiographs of the thorax revealed a soft tissue opacity in the left

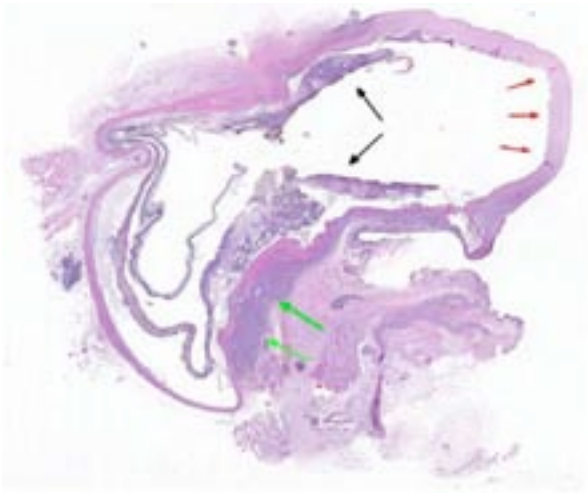

*1-1. Eye, cat: The specimen is collapsed from anterior to posterior. The cornea is at right (red arrows). An infiltrative neoplasm is present throughout the globe, markedly expanding the iris (black arrows), elevating the choroid and retina at the back of the globe, and extending through the sclera into the surrounding soft tissue (green arrows). (HE 3X)*

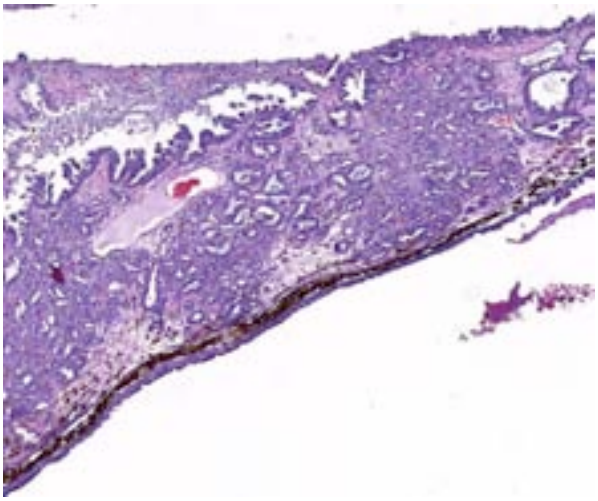

*1-2. Eye, cat: Closer view of the iris, which is expanded by an infiltrative epithelial neoplasm which forms variably sized tubules and acini, lined by papillary projections of neoplastic cells. Both the anterior and posterior aspects are lined by neoplastic cells. (HE 44X)*

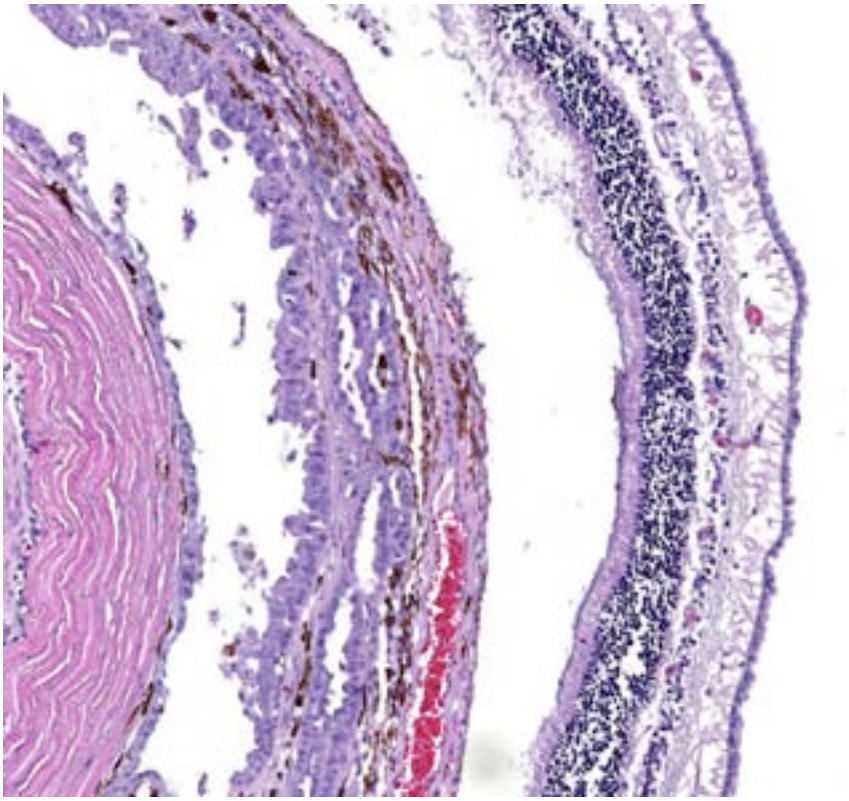

*1-3. Eye, cat: The retina (right) is detached and the anterior surface is lined by neoplastic cells. The underlying choroid (center) is lifted off the connective tissue by a lining of neoplastic cells forming papillary and micropapillary projections. (HE 96X)*

caudal lung lobe dorsally, the medial aspect of which appears to be associated with the left caudal lobar bronchus. Abdominal ultrasound did not reveal any abnormalities.

**Histopathologic Description:** The slides submitted to the conference contain the vertical section of a feline globe, which was collapsed as the result of a reported posterior rupture during enucleation. The globe is characterized by diffuse infiltration of the choroid and anterior uvea by a neoplastic population of epithelial cells causing extensive retinal detachment and complete occlusion of the filtration angles. The neoplastic cells are cuboidal to tall columnar and arranged in tubules, commonly containing either pale basophilic wispy material (mucin) or amorphous cell debris. Cells have indistinct cell borders and moderate to ample amount of eosinophilic cytoplasm, frequently with apical projections that stain basophilic with hematoxylin & eosin and magenta (i.e. positive) with the Periodic-Acid Schiff (PAS) reaction, consistent with mucus. The nuclei are round to oval and finely stippled with one or two prominent nucleoli. Anisocytosis and anisokaryosis are moderate. Twelve mitoses are counted in ten high power fields. Neoplastic cells focally infiltrate the deep corneal stroma anterior to the Descemet's membrane and extensively colonize the posterior aspect of the Descemet's membrane, as well as the iris, ciliary body and inner retina. Additionally, aggregates of neoplastic cells extend through the sclera into the episcleral stroma, with evidence of vascular invasion and, in the dependent portion, focal scleral thinning (staphyloma) and prominent regionally extensive periscleral desmoplastic spindle cell proliferation. Moderate numbers of lymphocytes and plasma cells are multifocally present within the uveal tract amongst the neoplastic population. The detached retina exhibits diffuse atrophy of the nerve fiber and ganglion cell layer, as well as multifocal edema. There is mild cupping of the optic nerve head with mild gliosis (not present in all sections). Mild midstromal neovascularization is present in the peripheral cornea. The lens (not present in the submitted sections) exhibits extensive subcortical cataractous change, characterized by eosinophilic spherical globules (Morgagnian globules) and migration of the epithelium along the posterior lens capsule. Within sections of eyelid (not submitted), moderate numbers of lymphocytes and plasma cells infiltrate the subepithelial stroma. Blood vessels are moderately congested, accompanied by mild acute edema.

**Contributor's Morphologic Diagnosis:** Eye: Metastatic carcinoma, with secondary glaucoma, retinal detachment and atrophy, multifocal uveitis, and cataractous change.

**Contributor's Comment:** The pattern of neoplastic cell infiltration in this case is typical of intraocular metastatic carcinoma.[1,2] With the exception of multicentric lymphoma, carcinomas are the neoplasms most frequently reported to

metastasize to the globe in cats.[1] The majority of intraocular metastases involve the posterior uvea likely because of the rich blood supply to this tissue.[1,2] Ophthalmoscopic findings in cats with angioinvasive pulmonary carcinoma typically include wedge-shaped areas of chorioretinal degeneration most prominent in the tapetal fundus radiating away from the optic disc. Vascular attenuation with areas of lumen occlusion, serous exudation, and retinal hemorrhage in the peripapillary retina are also common. The pathogenesis of the ophthalmoscopic lesions is thought to be neoplastic embolization of branches of the short posterior ciliary arteries, which supply retinal and choroidal circulation.[1] Histopathological examination of affected globes shows neoplastic cells within ocular blood vessel lumens and widespread retinal and tapetal necrosis. Growth of the metastatic lesions along the vascular endothelium leads to segmental loss of perfusion and subsequent necrosis of the overlying retina and choroid.[1,2]

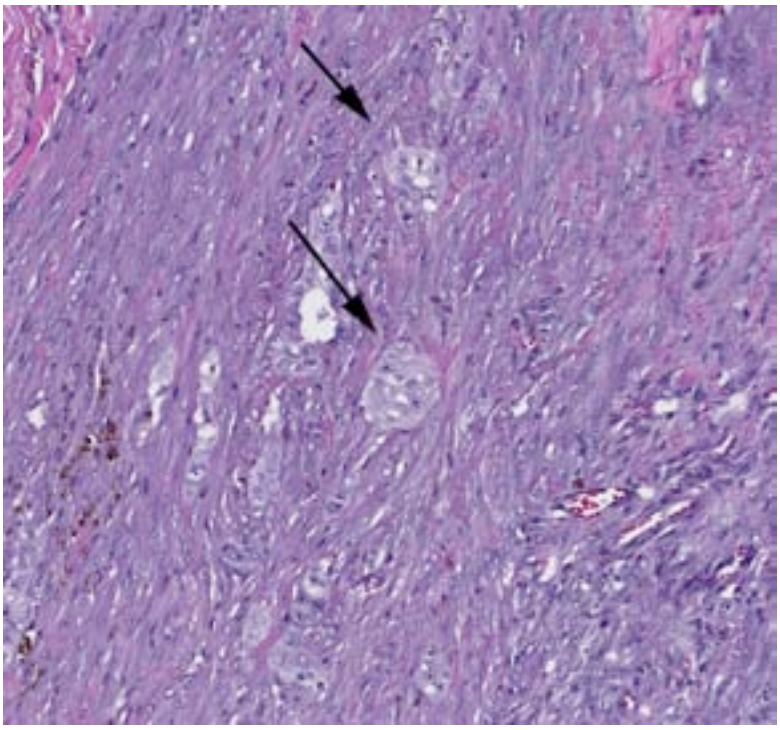

*1-4. Eye, cat: Within the extraocular soft tissues, nests of neoplastic cells are surrounded by a prominent desmoplastic response. (HE 92X)*

Carcinomas reported as metastasizing to the feline eye have been of pulmonary, sweat gland, mammary, uterine, and squamous cell origin.[1,2] In this case, the metastatic carcinoma in the eye was presumed to be of pulmonary origin based on the radiographic findings of a tissue opacity in the caudal lung, the most commonly affected lung field by primary lung tumors in cats.[4] CT scan and fine needle aspirate of this lung lesion with follow-up with the oncology team was recommended. The owners declined any further workup, however. The cat was euthanized three months later, at which point it was emaciated and unresponsive. No necropsy was performed.

Primary lung tumors are uncommon in cats, with older animals more commonly affected (mean age 12 years).[3,4] Lesions tend to be malignant and with a grave prognosis. When diagnosed early, with no evidence of metastatic disease, solitary lung tumors may be surgically resected. The degree of differentiation of the pulmonary neoplasm has been suggested to be a prognostic indicator, with cats with moderately differentiated primary lung tumors having reportedly a significantly longer survival time (median 698 days) than cats with poorly differentiated primary lung tumors (median 75 days).[5] However, early diagnosis is difficult since most cats initially present with nonspecific clinical signs or signs related to metastases.[3] Lameness, associated with metastasis to the bone and skin of the digits,[3] or visual deficits (associated with intraocular metastasis),[1] may be the only initial presenting sign. Intraocular metastasis may be underestimated since ophthalmoscopic and microscopic examinations are not performed on a routine basis in many cases. Other sites of metastasis of primary lung tumors in cats include skeletal muscle, and multiple thoracic and abdominal organs.[4] Thorough clinical examination and thoracic radiography can provide a high index of suspicion of the primary neoplasm.[4] Cytologic evaluation of cells obtained by fine-needle aspiration of the lung mass, as well as of cells collected from thoracic fluid or bronchoalveolar lavage can help determine the diagnosis.[3,4] Effective treatment has yet to be demonstrated for metastatic lung carcinomas in cats. As a result, most cats with metastatic lung

carcinoma die or are euthanized within 6 weeks of diagnosis.[5]

**JPC Diagnosis:** Eye: Metastatic carcinoma.

**Conference Comment:** This is an excellent descriptive slide with extensive ocular changes. Conference participants agreed the neoplasm is likely the result of metastasis from the pulmonary mass identified clinically. In the cat, lymphoma is by far the most prevalent metastatic tumor in the eye, although virtually any malignant neoplasm can localize within the uveal tract.[6]

Primary uveal neoplasms are common in dogs and cats and considerably more common than metastatic tumors, with the exception being metastatic uveal lymphoma in cats. Among primary ocular tumors, melanoma, lymphoma, posttraumatic sarcoma and iridociliary adenocarcinoma are most common in cats. Iridociliary adenocarcinoma is a reasonable differential in this case, but these typically benign neoplasms tend to infiltrate and expand the posterior chamber, often in solid sheets, in contrast to this case which filed along the uvea and choroid forming tubules.[6] Additionally, a PAS-positive basement membrane is highly conserved in these neoplasms and can aid in distinguishing from metastatic disease.[7] Extraocular metastasis from these primary tumors is rare or nonexistent; however, secondary complications are often significant, with glaucoma or intractable hyphema occurring most commonly.[6]

Of greater significance in cats are posttraumatic sarcomas, which are usually high-grade neoplasms of lens epithelial origin following lens rupture.[6] The majority of these are of the spindle cell variant and are often not recognized for years following a traumatic event. They are highly invasive within the globe though rarely metastasize. A round cell variant resembling lymphoma and osteo- or chondrosarcoma also occur following lens trauma, albeit at a much lower frequency.[2]

**Contributing Institution:** Diagnostic Center for Population and Animal Health, Michigan State University, 4125 Beaumont Road, Lansing, MI 48910
www.animalhealth.msu.edu

**References:**

1. Cassotis NJ, Dubielzig RR, Gilger BC, Davidson MG. Angioinvasive pulmonary carcinoma with posterior segment metastasis in four cats. *Vet Ophthalmol*. 1999;2(2):125–131.
2. Dubielzig RR, Ketring KL, McLellan GJ, Albert DM. Metastatic neoplasia. In: *Veterinary Ocular Pathology: A comparative review.* New York: Saunders Elsevier. 2010;97-103,309-315.
3. Goldfinch N, Argyle DJ. Feline lung-digit syndrome: unusual metastatic patterns of primary lung tumours in cats. *J Feline Med Surg*. 2012;14(3):202-8.
4. Hahn KA, McEntee MF. Primary lung tumors in cats: 86 cases (1979-1994). *J Am Vet Med Assoc.* 1997;211(10):1257-60.
5. Hahn KA, McEntee MF. Prognosis factors for survival in cats after removal of a primary lung tumor: 21 cases (1979-1994). *Vet Surg*. 1998;27(4):307-11.
6. Njaa BL, Wilcock BP. The ear and eye. In: Zachary JF, McGavin MD, eds. *Pathologic Basis of Veterinary Disease*. 5th ed. St. Louis, MO: Elsevier Saunders; 2012:1228-1230.
7. Wilcock B, Dubielzig RR, Render JA. Histological Classification of Ocular and Otic Tumors of Domestic Animals. Second Series. Vol IX. Washington, D.C.: Armed Forces Institute of Pathology/ American Registry of Pathology; 2002:26.

**CASE II**: 08-65258 (JPC 3152323).

**Signalment:** 7-year-old castrated male DLH cat, *Felis catus.*

**History:** The cat was seen at the AUCVM Small Animal Teaching Hospital critical care service with a 1-2 day history of pancytopenia, dehydration, and dull mentation according to the referring veterinarian. The owners had not seen the cat drinking or using the litter box for the past few days. The cat was indoor-only, with no other feline or canine housemates. He did have access to a screened porch and was on Frontline but no heartworm preventative. Upon arrival at the AUCVM, the cat was quiet and dull with marked icterus of the sclera and oral mucous membranes. The animal's temperature was 105.2°, pulse rate 120 bpm, and respirations were 88 bpm. The mucous membranes were dry and had a capillary refill time of -3 seconds. Heart and lung sounds were normal.

**Diagnostics:** Diagnostic tests included CBC, chemistry panel, and thoracic and abdominal radiographs. Radiographic findings included a prominent interstitial lung pattern, Pertinent CBC and chemistry findings are given here.

| **Parameter** | | |
|---|---|---|
| HCT(%) | 20.6 | 30-45 |
| MCV (fl) | 45.2 | 39-55 |
| MCHC (g/dL) | 33.1 | 30-36 |
| RDW | 18.3 | 11-17 |
| Platelets (/uL) | 28000 | 200,000-700,000 |
| Reticulocyte Count (/uL) | 3000 | 15,000-81,000 |
| WBC (/uL) | 2460 | 5,500-19,500 |
| Neutrophils (/uL) | 812 | 2,500-12,500 |
| Bands (/uL) | 1255 | 0-300 |
| Total Protein (g/dL) | 4.73 | 6.2-7.7 |
| Albumin (g/dL) | 2.0 | 2.8-4.2 |
| Globulin (g/dL) | 2.7 | 2.4-4.4 |
| Total Bilirubin (mg/dL) | 9.78 | 0. 1-0.2 |
| Blood Urea Nitrogen (mg/dL) | 50.1 | 5-30 |

**Treatment and Case Outcome:** Intravenous crystalloid fluids and broad-spectrum antibiotics were initiated on the night of 6/14/08, along with one unit of packed red blood cells. The next morning the cat was still dull and dysphoric and soon developed cardiac and respiratory arrest. Resuscitation efforts were unsuccessful. A necropsy was performed.

**Gross Pathologic Findings:** The cat was in good physical condition, but moderately overweight. All tissues were severely icteric. Multiple fleas were present. There was a significant amount of serosanguineous fluid in the trachea and large bronchi. The liver had a diffuse lobular pattern throughout the parenchyma. The edges of the liver lobes were rounded. There was a moderate amount of dark red to black fecal material in the large intestine. The spleen was markedly enlarged and bluish-black. The mesenteric lymph nodes were diffusely dark red.

**Histopathologic Description:** Blood vessels throughout the lung, liver, pancreas, adrenal glands, kidneys, and gastrointestinal tract are partially to almost completely occluded by few to numerous macrophages containing protozoal schizonts consistent with *Cytauxzoon felis*. Similar organisms are within macrophages filling subcapsular, cortical, and medullary sinuses of lymph nodes as well as within the splenic red pulp.

**Contributor's Diagnosis:** Parasitemia, diffuse, severe, whole body with intralesional schizonts

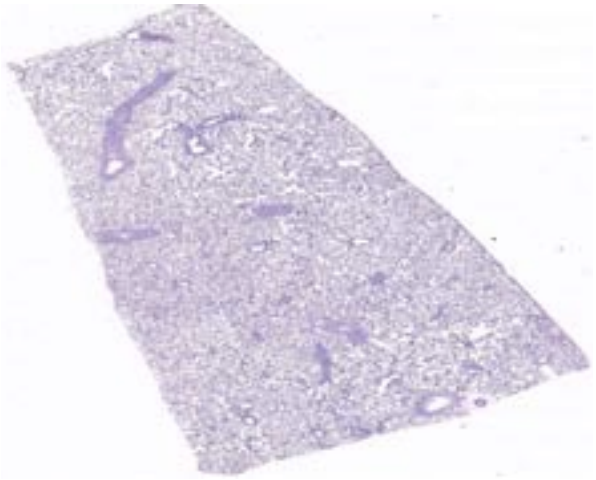

*2-1. Lung, cat: At subgross examination, while pulmonary vasculature is prominent, blood is not evident within larger vessels. Pulmonary fields appear crowded due to expansion of alveolar septa. (HE 3X)*

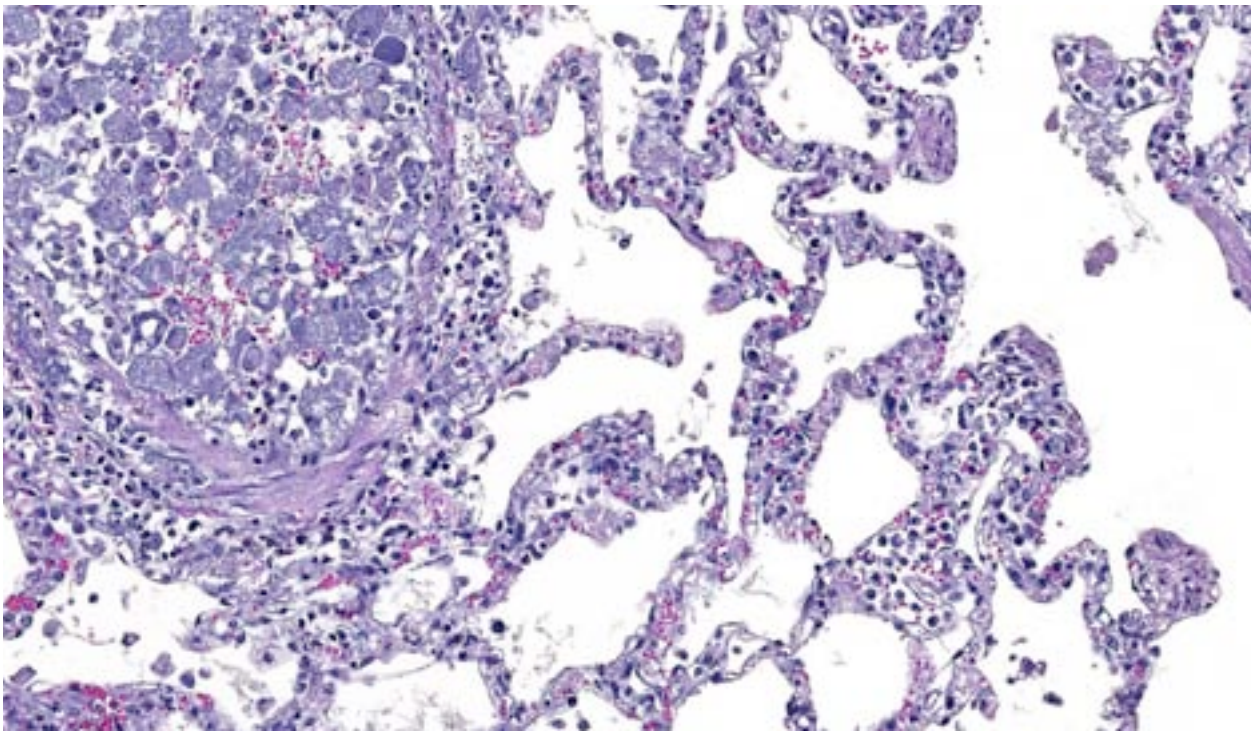

*2-2. Lung, cat: Alveolar septa are expanded up to 3x normal by numerous macrophages, dilated capillaries, edema, and fibrin. The adjacent pulmonary venule is expanded and almost occluded by the present of numerous macrophages enlarged by schizonts of Cytauxzoon felis. (HE 104X)*

containing protozoal organisms consistent with *Cytauxzoon felis*.

**Contributor's Comment:** *Cytauxzoon felis* is a protozoal parasite that infects wild and domestic cats. It is transmitted by a tick vector *(Dermocenter variabilis)*. Bobcats and possibly other wild felids are believed to serve as the reservoir host.[4] The organism exists in two tissue forms; a piroplasm erythrocyte stage and a schizont tissue phase found within macrophages primarily in the spleen, liver, and lung. Clinical findings include acute illness with fever, depression, anorexia, pallor, icterus, and usually death within a few days.[4] Some cats do survive natural infections.[2] Diagnostic findings often include pancytopenia with nonregenerative anemia. The urine in the early hemolytic phase is highly concentrated, acidic and contains large amounts of protein, bile and blood.[6]

Previously, antemortem diagnosis was made by identification of erythrocyte piroplasms, but PCR assays for this agent are now available. This more sensitive method of detection has lead to the identification of cats that either have subclinical infection or that have recovered from an infection and become chronic carriers.[2] Genetic variability of *Cytauxzoon felis* has been proposed as a possible explanation for why some animals recover from infection or fail to develop clinical signs.[1]

**JPC Diagnosis:** 1. Lymph node: Lymphadenitis, histiocytic, diffuse, mild, with lymphoid depletion, hemorrhage, thrombosis, and numerous intravascular intrahistiocytic schizonts.

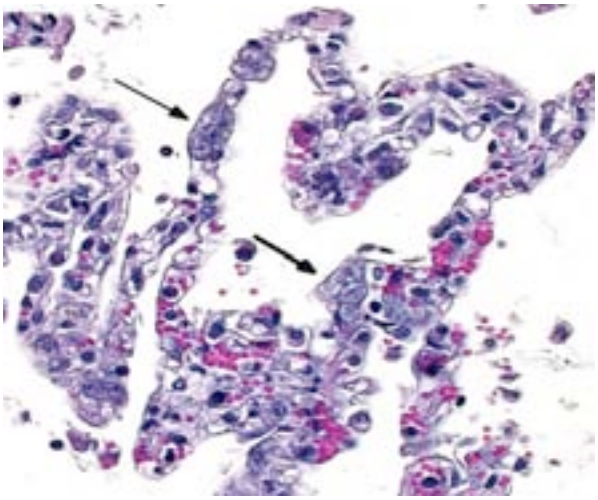

*2-3. Lung, cat: Occasional alveolar capillaries contain Cytauxzoon schizonts. (HE 292X)*

2. Lung: Pneumonia, interstitial, histiocytic, diffuse, mild, with numerous intravascular intrahistiocytic schizonts.

**Conference Comment:** Two different slides were distributed for this case, both exhibiting numerous intravascular apicomplexans typical of *Cytauxzoon felis*. *C. felis* spends its lifecycle in circulation following introduction through a tick vector. The schizonts within circulating macrophages demonstrated in this case are first cycle of schizogony, and in chronic disease, cytomeres are released and infect erythrocytes during the second cycle of schizogony to form the piroplasm ring (signet ring) often evident on cytology.[6]

The disease is uncommon, but often fatal in cats when it occurs.[4] The intrahistiocytic phase leads to systemic circulatory compromise due to partial or complete vascular obstruction.[4] The erythrocytic phase is characterized by persistent parasitemia with anemia which may exacerbate ischemic tissue damage. Ischemic damage can also cause cerebral necrosis, appearing similar in some respects to feline ischemic encephalopathy and thiamine deficiency.[3] Dyspnea is also a common clinical finding of infected cats, and interstitial pneumonia seems to be a consistent finding and may be the largest contributor to respiratory difficulty, possibly leading to acute respiratory distress syndrome in some cases.[5]

**Contributing Institution:** Department of Pathobiology, 166 Greene Hall, College of Veterinary Medicine, Auburn University, AL 36849-5519

**References:**

1. Brown HM, Berghaus RD, et al. Genetic variability of *Cytauxzoon felis* from 88 infected domestic cats in Arkansas and Georgia. *J Vet Diagn Invest*. 2009;21:59-63.
2. Brown HM, Latimer KS, et al. Detection of persistent *Cytauxzoon felis* infection by polymerase chain reaction in three asymptomatic domestic cats. *J Vet Digan Invest*. 2008;20:485-488.
3. Clarke LL, Rissi DR. Neuropathology of natural *Cytauxzoon felis* infection in domestic cats. *Vet Pathol*. 2015 Jan 8. pii: 0300985814564986. [Epub ahead of print]
4. Fry WM, McGavin MD. Bone marrow blood cells and lymphatic system In: McGavin MD, Zachary JF, eds. *Pathologic Basis of Veterinary Disease*. 4th ed., pp.783. Philadelphia, PA: Mosby; 2007:783.
5. Snider TA, Confer AW, Payton ME. Pulmonary histopathology of *Cytauxzoon felis* infections in the cat. *Vet Pathol*. 2010;47(4):698-702.
6. Valli VEO. Hematopoietic system In: Maxie MG, ed. *Jubb, Kennedy, and Palmer's Pathology of Domestic Animals*. Vol 3. 5th ed. Philadelphia, PA: Saunders; 2007:243.

**CASE III**: E 3476-12 (JPC 4048934).

**Signalment:** 11-year-old male Bobtail dog, *Canis familiaris*.

**History:** The dog was clinically presented with anorexia and weight loss. Ultrasonic examination revealed a thickening of the stomach wall. By laparotomy a mass of approximately 2.0 cm in diameter was excised from the pylorus.

**Gross Pathology:** One tissue sample measuring 2.2 x 1.4 x 1.2 cm was submitted for histologic examination.

**Histopathologic Description:** Stomach: Expanding the submucosa and elevating the overlying gastric mucosa there is a mostly well demarcated, but unencapsulated, densely cellular and partially infiltrative growing ovoid mass of up to 1.5 x 0.5 cm in dimension, which extends partially to the cut borders.

The cells are closely packed in sheets with a moderate amount of fibrovascular stroma. Single tumor cells are ovoid to polygonal, ranging in size from 20 to 30 µm in diameter. Cell borders are distinct. The moderate to abundant amount of eosinophilic cytoplasm is finely granular. Round to ovoid nuclei, ranging in size from 10 to 15 µm in diameter, are often located eccentrically within the cells. The chromatin is finely stippled, in some nuclei finely clumped with a distinct round centrally located eosinophilic nucleolus in each nucleus. Bi- and multinucleated tumor cells with up to three nuclei are frequent (> 5 / HPF). Anisocytosis and anisokaryosis are striking. The mitotic rate is low with up to 1 mitotic figure per high power field.

Preexisting vessels within the mass are thickened by increased numbers of spindle cells in the media (media hyperplasia) and deposition of extracellular, eosinophilic, fibrillar material (collagen).

Additionally, throughout the mass multifocal acute hemorrhages with extravasation of erythrocytes and fibrin, depositions of granular golden-brown pigment (hemosiderin) in macrophages and multiple areas of necrosis are present.

Submucosal tissue surrounding the neoplasm is expanded by edema, occasional hemorrhages, multiple hemosiderin-laden macrophages and moderate numbers of plasma cells.

**Contributor's Morphologic Diagnosis:** Stomach: Extramedullary plasmacytoma.

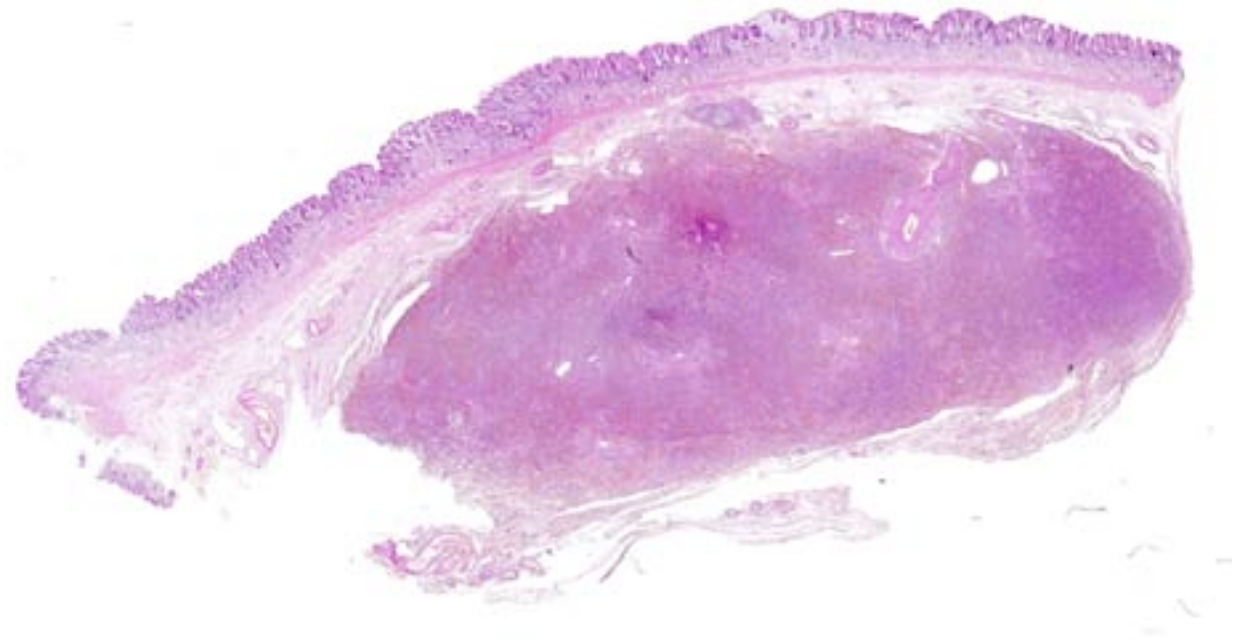

*3-1. Stomach, dog: Within the pyloric submucosa, there is an expansile, well-demarcated, densely cellular neoplasm. (HE 3X)*

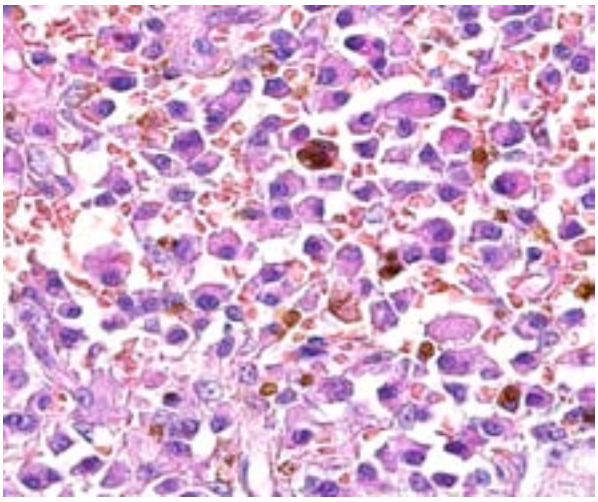

*3-2. Stomach, dog: The neoplasm is composed of uninucleated and multinucleate plasma cells. Numerous hemosiderin-laden macrophages are scattered throughout the neoplasm. (HE 300X)*

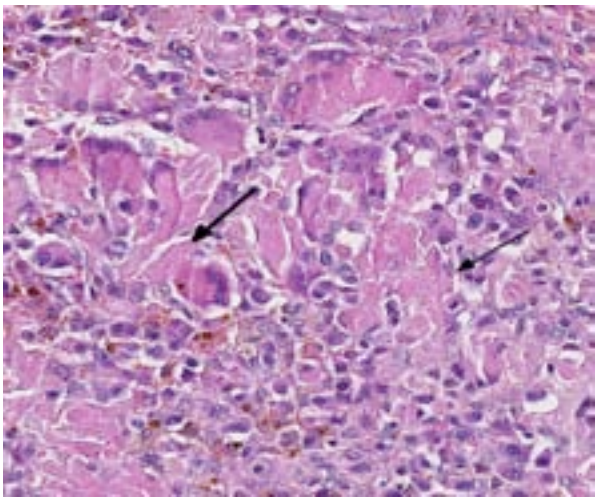

*3-3. Stomach, dog: Multifocally, neoplastic plasma cells are separated by homogenous to fibrillar eosinophilic material (presumed amyloid) which is occasionally engulfed by multinucleated foreign-body type macrophages. (HE 300X)*

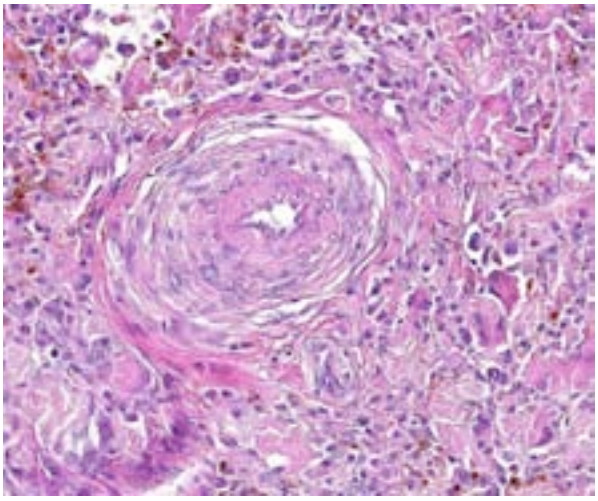

*3-4. Stomach, dog: Within the neoplasm there is marked hypertrophy of arteriolar walls. (HE 144X)*

**Contributor's Comment:** In veterinary medicine three forms of plasma cell tumors are distinguished. Multiple myeloma (MM) which arises in the bone marrow, cutaneous plasmacytomas and extramedullary plasmacytomas (EMP) which arise from sites other than the bone marrow. The synthesis of large amounts of monoclonal immunoglobulins, resulting most often in a monoclonal gammopathy, is a similarity of all plasma cell neoplasms.[4,5] The first report of a gastric plasmacytoma in a human patient was published in 1928 by Vasiliu and Popa and 1984 MacEwen and colleagues documented the first veterinary cases in two dogs.[6,15] Since then only few reports of intestinal extramedullary plasmacytomas in dogs, cats or horses exist.[3-7,13]

Clinically, gastric plasmacytomas appear nonspecific; occasionally epigastric pain, vomiting, anorexia weight loss and hemorrhages occur. Specific gross lesions are rare, as tumors cause more or less diffuse thickening of the stomach wall, like other round cell tumors. Histologically, gastric plasmacytomas are unencapsulated, but well demarcated, densely cellular masses, composed of variable mature, well- to poorly-differentiated round cells, which often contain typically eccentric located nuclei. Bi- and multinucleated cells with up to 5 nuclei per cell are a frequent finding.[5,8]

The deposition of AL-amyloid within tumor masses has been reported in few cases of EMP.[9,10,12] Congo red stain is useful to distinguish a gastric plasmacytoma from other round cell tumors, like malignant lymphoma or histiocytoma.[2,5] Congo red stain in this case failed to identify amyloid deposits.

The development of MM proceeding from EMP has not been determined in dogs, in contrast to humans.[8,13] In general, EMP located in the oral cavity tend to be benign, whereas EMP of the aboral digestive tract (esophagus, stomach, intestine, and rectum) tend to be more aggressive with potential to metastasize via the regional lymph nodes.[5]

**JPC Diagnosis:** Stomach: Extramedullary plasmacytoma.

**Conference Comment:** Extramedullary plasmacytomas are relatively common in older dogs, accounting for 2.4% of all canine tumors in a recent publication.[11] While they most often occur in the skin and mucus membranes, tumors of the abdominal viscera do occur, albeit with much less frequency.[11] Cutaneous and oral plasmacytomas are generally benign with no related clinical signs, and other references describe gastrointestinal plasmacytomas as more likely to be malignant.[1,14]

Conference participants agreed with the contributor's assessment that the preexisting vessels in the submucosa are moderately thickened, though it was suspected amyloid is also responsible for this expansion in addition to spindle cells. There is abundant hemosiderin within this neoplasm, often within apparent neoplastic plasma cells. Iron accumulation in neoplastic plasma cells is a feature identified in previously reported cases, with one author speculating it may be due to a mutation of heme-containing enzymes.[11]

Plasmacytomas, in addition to multiple myeloma, lymphoma and ehrlichiosis, have all been associated with a monoclonal gammopathy.[1] Bence-Jones proteinuria is another clinical feature associated with plasma cell tumors; which are light chains of immunoglobulins small enough to permit their passage through the glomerulus.[1] A noted cytologic feature of plasma cell tumors is a rim of red globular material around the neoplastic cells, termed "flame figures", which is another supportive diagnostic finding to these neoplasms.

**Contributing Institution:** Department of Veterinary Pathology, Freie Universität Berlin, Germany
http://www.vetmed.fu-berlin.de/en/einrichtungen/institute/we12/index.html

**References:**

1. Allison RW. Laboratory evaluation of plasma and serum proteins. In: Thrall MA, Weiser G, Allison RW, Campbell TW, eds. *Veterinary Hematology and Clinical Chemistry*. 2nd ed. Oxford, UK: Wiley-Blackwell; 2012:469-470.
2. Brunnert SR, Altman NH. Identification of immunoglobulin light chains in canine extramedullary plasmacytomas by thioflavine T and immunohistochemistry. *J Vet Diagn Invest*: official publication of the American Association of Veterinary Laboratory Diagnosticians, Inc. 1991;3:245-251.
3. Brunnert SR, Dee LA, Herron AJ, Altman NH. Gastric extramedullary plasmacytoma in a dog. *Journal of the American Veterinary Medical Association*. 1992;200:1501-1502.
4. Fry MM, McGavin MD. Bone marrow, blood cells and lymphatic system. In: McGavin MD, Zachary JF, eds. *Pathologic Basis of Veterinary Disease*.4th ed. St. Louis, MO: Penny Rudolph; 2007:802-803.
5. Jacobs RM, Messick JB, Valli VE. Tumors of the hemolymphatic system. In: Meuten DJ, ed. *Tumors in Domestic Animals*. 4th ed. Ames, Iowa: Blackwell Publishing Company; 2002:161-163.
6. MacEwen EG, Patnaik AK, Johnson GF, Hurvitz AI, Erlandson RA, Lieberman PH. Extramedullary plasmacytoma of the gastrointestinal tract in two dogs. *Journal of the American Veterinary Medical Association*. 1984;184:1396-1398.
7. Majzoub M, Breuer W, Platz SJ, Linke RP, Linke W, Hermanns W. Histopathologic and immunophenotypic characterization of extramedullary plasmacytomas in nine cats. *Veterinary Pathology*. 2003;40:249-253.
8. Nolan KD, Mone MC, Nelson EW. Plasma cell neoplasms. Review of disease progression and report of a new variant. *Surgical Oncology*. 2005;14:85-90.
9. Platz SJ, Breuer W, Geisel O, Linke RP, Hermanns W. Identification of lambda light chain amyloid in eight canine and two feline extramedullary plasmacytomas. Journal of Comparative Pathology. 1997;116: 45-54.
10. Ramos-Vara JA, Takahashi M, Ishihara T, Miller MA, Pace LW, Craft D, et al. Intestinal extramedullary plasmacytoma associated with amyloid deposition in three dogs: an ultrastructural and immunoelectron microscopic study. *Ultrastructural Pathology*. 1998;22:393-400.
11. Rannou B, Heilie P, Bedard C. Rectal plasmacytoma with intracellular hemosiderin in a dog. *Vet Pathol*. 2009;46(6):1181-1184.
12. Rowland PH, Linke RP. Immunohistochemical characterization of lambda light-chain-derived amyloid in one feline and five canine plasma cell tumors. *Veterinary Pathology*. 1994;31:390-393.

13. Smithson CW, Smith MM, Tappe J, Beaudin A, Bradley M. Multicentric oral plasmacytoma in 3 dogs. *Journal of Veterinary Dentistry*. 2012;29: 96-110.
14. Vail D. Solidtary and extramedullary plasmacytic tumors. In: Withrow SJ, Vail ME, eds. *Small Animal Clinical Oncology*. Philadelphia, PA: WB Saunders; 2007:779-783.
15. Vasiliu T, Popa R. Forme gastrointestinale des tumeurs dites plasmacytomes. *Comptes Rendus des Séances et Mémoires de la Société de Biologie.* 1928;98:738-740.

**CASE IV:** 149705 (JPC 4049500).

**Signalment:** 2.5-year-old female Bernese mountain dog, *Canis familiaris*.

**History:** A 2.5-year-old female Bernese mountain dog was referred to the Veterinary School of Nantes for a 3-month history of vomiting, weight loss, dysorexia and apathy. Physical examination revealed a marked amyotrophy and pale mucous membranes.

**Gross Pathology:** At necropsy, the dog had a poor condition score with pale and subicteric mucous membranes. Kidneys were diffusely pale, white-to-tan, with a marked generalized granular capsular surface. The cortex had numerous red-to-tan dots and had spongious aspect after formaldehyde fixation.

Other lesions included slight petechial hemorrhages of the stomach mucosa (confirmed by histology and associated with a laminar marked endothelial mineralization and necrosis on Alizarin red stain). Spleen was mildly firm, increased in size, and liver slightly and diffusely dark (HE and Perls stained slides: splenic and hepatic hemosiderosis and splenic macrophagous hyperplasia and extramedullary hematopoeïsis). 10 mL of serous pericardial effusion was found.

**Laboratory Results**: Clinical laboratory data oriented on chronic renal insufficiency with significant proteinuria suggesting a glomerular involvement. (BUN 38 md/dL; Creatinine 3.9 mg/dL; Albuminemia 2.0 g/dL; Proteinemia 3.9 g/dL; Proteinuria 0.48 g/dL; RPCU 8.6; Du=1.018). Blood count revealed a severe anemia, mildly regenerative, macrocytic with polychromasia, acanthocytes and schistocytes, compatible with an intravascular hemolytic process.

**Histopathologic Description:** Diffusely, glomerular tufts are enlarged with severe dilation of urinary chambers, increased tufts lobulation, thickening of the glomerular basement membrane, fibrotic changes including synechiae, capsular fibrosis and obsolescent glomeruli. Multifocally, hypertrophy and hyperplasia of parietal epithelial cells and periglomerular proliferation of myoepithelial arterioles were observed. Multifocally, within tubules, there is homogenous eosinophilic material (proteinuria), rare erythrocytes (hematuria), and rare intratubular karyorrhectic debris. A greyish material deposit was observed on tubular basement membrane and tubular epithelium (calcification). Interstitial lesions include aggregates of plasma cells, lymphocytes and fibrosis.

PAS staining: glomerular hypercellularity with both mesangial and endocapillary proliferation. Glomerular basement membranes are thickened.

Gomori Staining: multifocally, there are red dots in podocyte cytoplasm and basement membrane,

*4-1. Kidney, dog: Subgross examination of the section of kidney reveals cystic dilation of Bowman's capsules, and linear areas of fibrosis with a prominent cellular infiltrate. (HE 4X)*

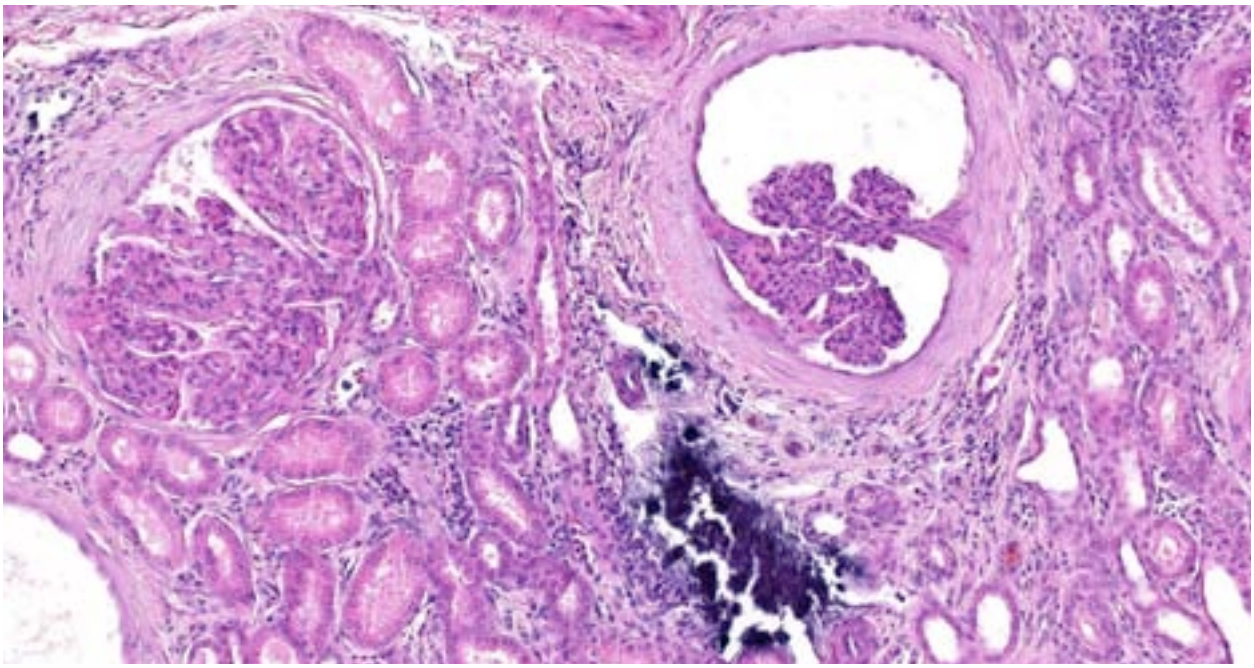

*4-2. Kidney, dog: The glomerular tuft at left is enlarged with marked segmentation, hypercellularity, synechiation, and periglomerular fibrosis. Tubules are separated by moderate amounts of collagen which contains moderate numbers of lymphocytes and plasma cells and large aggregates of crystalline mineral. (HE 120X)*

| ***Breed*** | ***Glomerulopathy*** |
|---|---|
| Beagle | Amyloidosis<br>Membranoproliferative glomerulonephritis |
| Bernese mountain dog | Membranoproliferative glomerulonephritis |
| Bull terrier | Hereditary nephritis |
| Bullmastiff | Focal and segmental glomerulosclerosis |
| English cocker spaniel | Hereditary nephritis |
| Dalmatian | Hereditary nephritis |
| Doberman pinscher | Glomerulosclerosis<br>Cystic glomerular atrophy |
| English foxhound<br>French mastiff | Amyloidosis<br>Juvenile glomerulopathy |
| Greyhound | Glomerular vasculopathy and necrosis |
| Newfoundland | Glomerulosclerosis |
| Pemprobe Welsh corgi | Cystic glomerular atrophy |
| Rottweiler | Atrophic glomerulopathy |
| Samoyed | Hereditary nephritis |
| Shar-Pei | Amyloidosis |
| Soft-coated wheaten terrier | Proliferative and sclerosing glomerulonephritis |

and there are fibrotic glomerular and interstitial changes.

**Contributor's Morphologic Diagnosis:**
Kidney: Glomerulonephritis, membranoproliferative, diffuse, marked, chronic, with proteinuria, glomerular microcysts and fibrotic changes.
Kidney: Interstitial nephritis, lymphoplasmocytic and fibrotic, mild, multifocal, chronic.

**Contributor's Comment:** Glomerular disease is major cause of chronic kidney disease in dogs. It results from alteration of the glomerular filtration barrier, which includes fenestrated endothelial cells, glomerular basement membrane, epithelial slit pores formed by podocytic processes.[3]

Defects in the glomerular selective filtration result in proteinuria and renal insufficiency, whose clinical spectra ranges from asymptomatic or proteinuric dogs, to non specific presentation (weight loss, apathy, anorexia), or evident signs of chronic renal insufficiency (polyuria, polydipsia, vomiting, halitosis).[6] Extrarenal complications of glomerular diseases include: nephrotic syndrome (hypoalbuminemia, proteinuria, hypercholesterolemia, edema, serous effusions); thromboembolism, secondary to loss of

antithrombin III; hypertensive illnesses; and microangiopathic anemia.[2,6]

Glomerular diseases can be acquired or congenital. Acquired glomerular injuries can result from:

1) Immune complex deposition (glomerulonephritis proliferative, membranous, membranoproliferative). Etiologies range from chronic infections (canine pyometra, *Borrelia burgdoferi*, etc.) to immune-mediated diseases (systemic erythematous lupus).[3]
2) In situ immune complex formation (anti-GBM glomerulonephritis). Antibodies bind on GBM antigens. It is rare in domestic animals, and suspected in several dogs. In humans, antibodies cross-reaction occurs by antigenic mimicry between streptococcus and GBM for instance.[3,6]
3) Damage by systemic factors affecting the glomeruli. It includes mesangial deposits like amyloidosis, focal segmental glomerulosclerosis, and minimal change disease.[6]

Congenital glomerulopathy gathers an increasing number of breeds, whose pathogeny and mode of inheritance often remains unknown and varies a lot between breeds. The table lists dog breeds with reported familial glomerulopathies.[3]

In Bernese mountain dogs, a familial glomerulopathy was reported by Minkus and collaborators in 1994. Lesions included membranoproliferative glomerulonephritis, with concomitant interstitial nephritis and high titer of IgG against *Borrelia burgdorferi*.[4] Since then, few reports were published, but one of them highlights an absence of correlation between proteinuria, the early sign of glomerular lesions, and the antibodies against *B.burgdoferi*.[1]

The present case deals with a 2.5-year-old Bernese mountain dog with chronic renal insufficiency and histologic lesions compatible with membranoproliferative glomerulonephritis and interstitial nephritis; however, immunofluorescence should have been performed to confirm it. A proliferation of myoepithelial periglomerular artierioles was also suspected and supports a probable hypertensive state that has not been clinically evaluated.

**JPC Diagnosis:** Kidney: Glomerulonephritis, membranoproliferative, diffuse, marked, chronic, with glomerulosclerosis, fibrosis, tubular mineralization, and mild lymphoplasmacytic nephritis.

**Conference Comment:** The contributor has provided an excellent and concise overview of glomerular disease as well as its specific manifestation in the Bernese mountain dog. Glomerulonephritis is most commonly caused by immune-mediated mechanisms and occurs in three distinct patterns. Proliferative glomerulonephritis is characterized by increased cellularity and is the most common variant observed in horses, usually due to equine infectious anemia or streptococcal antigen. In membranous glomerulonephritis, thickened basement membranes are the predominant change which most commonly occurs in cats. This case is representative of the membranoproliferative form of glomerular disease as most commonly observed in dogs.[5] Collectively, these conditions are generally acquired from accumulations of immune complexes due to low pathogenicity chronic infections with persistent antigenemia.[3] The contributor also highlights those recognized familial forms of glomerular disease in dogs which usually arise in younger animals as a result of various mutations affecting collagen formation or other unidentified mechanisms.[3,4]

**Contributing Institution:** Department of Pathology, Nantes-Atlantic National College of Veterinary Medicine, Food Science and Engineering - ONIRIS, 44 307 Nantes Cedex 03, France. www.oniris-nantes.fr

**References:**

1. Gerbe, B, Eichenberger S, Haug K, Wittenbrink MM, Reusch CE. Association of urine protein excretion and infection with*Borrelia burgdorferi*sensu lato in Bernese mountain dogs. *Vet J*. 2009 ;182(3),487-488.
2. Kumar V, Abbas AK, Fausto N, Aster JC. *Robbins and Cotran Pathologic Basis of Disease, Professional Edition: Expert Consult-Online*. Elsevier Health Sciences. 2009.
3. Maxie MG, Newman SJ. Urinary system. In: Maxie MG, ed. *Jubb, Kennedy and Palmer's Pathology of Domestic Animals*. 5th ed. Vol. 2.

Philadelphia, PA : Elsevier Saunders; 2007:459-461.
4. Minkus G, Breue, W, Wanke R, Reusch C, Leuterer G, Brem G, & Hermanns W. Familial nephropathy in Bernese mountain dogs. *Vet Pathol*. 1994;31(4),421-428.
5. Newman SJ. The urinary system. In: Zachary JF, McGavin MD, eds. *Pathologic Basis of Veterinary Disease.* 5th ed. St. Louis, MO : Elsevier Mosby; 2012:620-627.
6. Vaden SL. Glomerular disease. *TopCompanion Anim Med*. 2011;26(3),128-134.

**Joint Pathology Center**
**Veterinary Pathology Services**

# WEDNESDAY SLIDE CONFERENCE 2014-2015

## Conference 25

**13 May 2015**

---

**CASE I:** EV-UFMG 08/1116 (JPC 3136273).

**Signalment:** 4-month-old male Holstein calf, *Bos Taurus.*

**History:** This was an experimental calf. Soon after birth it was placed in an arthropod-free containment facility. The calf was inoculated with *Anaplasma marginale* when it was two months old. At the end of the experimental protocol, prior to release into the field, the calf was subjected to premunition with *Babesia bigemina* and *B. bovis*, after which it developed apathy and quickly progressed to death.

**Gross Pathologic Findings:** The calf was emaciated with moderate anemia and mild icterus. There was mild hydrothorax and

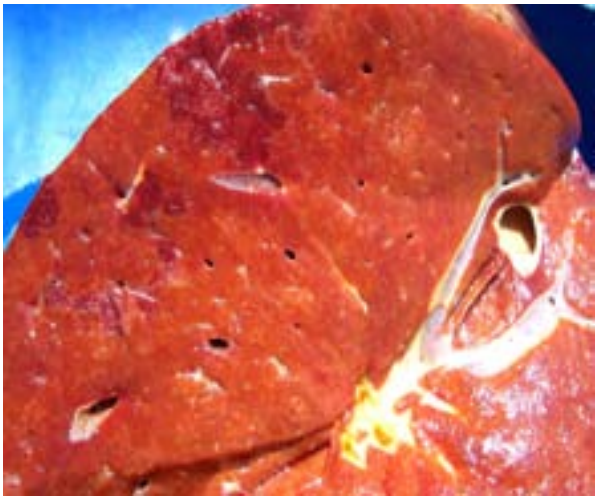

*1-1. Liver, calf: The liver is markedly enlarged and yellowish with focally extensive dark-red areas. Upon close inspection, there are numerous military white nodules within the parenchyma. (Photo courtesy of: Departamento de Clínica e Cirurgia Veterinárias, Escola de Veterinária, Universidade Federal de Minas Gerais, Belo Horizonte, MG, Brazil. http://www.vet.ufmg.br)*

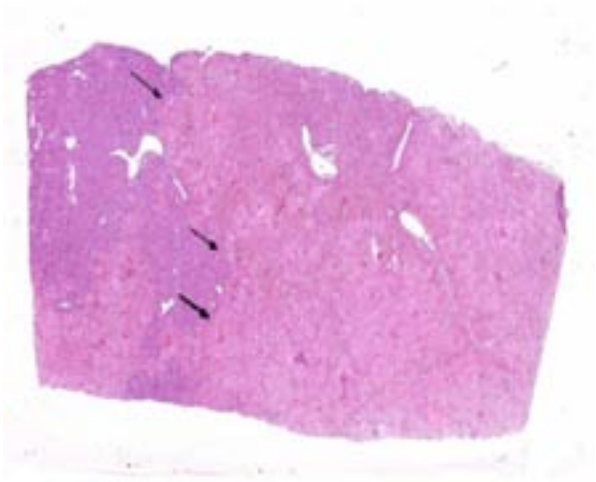

*1-2. Liver, calf: There are coalescing areas of coagulative necrosis within the submitted section of liver (arrows). (HE 5X)*

hydroperitoneum. In the lung there were multifocal mildly consolidated areas ranging from 0.3 to 0.5 cm in diameter distributed in all pulmonary lobes. The liver was markedly enlarged yellowish with focally extensive dark-red areas. There were multiple miliary white nodules in the parenchyma. There was also small amount of purulent exudate draining on the cut surface, and small thrombi were grossly observed. The spleen was moderately enlarged. Gross findings did not support babesiosis as a cause of death.

**Laboratory Results:** Microbiology: *Salmonella* sp. was isolated from the liver.

**Histopathologic Description:** In the liver there was multifocal random degeneration and necrosis associated with an intense neutrophilic infiltrate with some lymphocytes and macrophages. There were several intralesional bacterial colonies. A lymphoplasmacytic and histiocytic infiltrate predominates in portal areas. Several blood vessels had fibrinoid necrosis in the vascular wall associated with thrombosis, particularly in centrilobular veins. Some veins are completely obliterated by thrombosis.

In the spleen (section not submitted) there were numerous hemosiderin-laden macrophages and increased erythrophagocytosis, associated with moderate lymphoid depletion.

In the lungs (sections not submitted), there was an interstitial pneumonia characterized by marked thickening of the alveolar wall with interstitial infiltration of macrophages, lymphocytes and a few neutrophils. There was multifocal intra-alveolar accumulation of fibrin and a few neutrophils.

**Contributor's Morphologic Diagnosis:** Liver: Hepatitis, necrotizing, histiocytic and neutrophilic, multifocal, random, acute, associated with thrombosis and intralesional bacterial colonies.

**Contributor's Comment:** *Salmonella enterica* comprises more than 2,000 serotypes, including serotypes Dublin and Typhimurium that are often isolated from cattle. The most common clinical manifestation of *Salmonella* infection in cattle is an enteric disease characterized by diarrhea that is usually associated with acute fibrino-necrotizing enteritis.[9-11] However, systemic salmonellosis in cattle may occur in the absence of enteric disease,[5] as observed in the present case.

*Salmonella* is highly invasive, crossing the intestinal epithelial barrier inducing ruffling of the apical surface of the epithelial layer, which results in internalization of the organism within a cytosolic membrane bound vacuole. This process is dependent on the expression of several effector bacterial proteins that are translocated into the host cells through a type III secretion system encoded by the *Salmonella* pathogenicity island 1 (SPI-1).[9-12] Once the organism crosses the epithelial layer, it quickly localizes in the lamina propria, where it is found mostly within

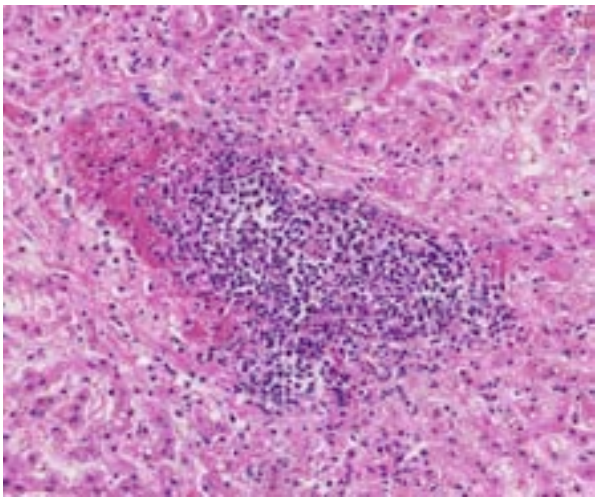

*1-3. Liver, calf: Numerous portal veins contain fibrinocellular thrombi and necrotic debris within the vascular wall (vasculitis). (HE 256X)*

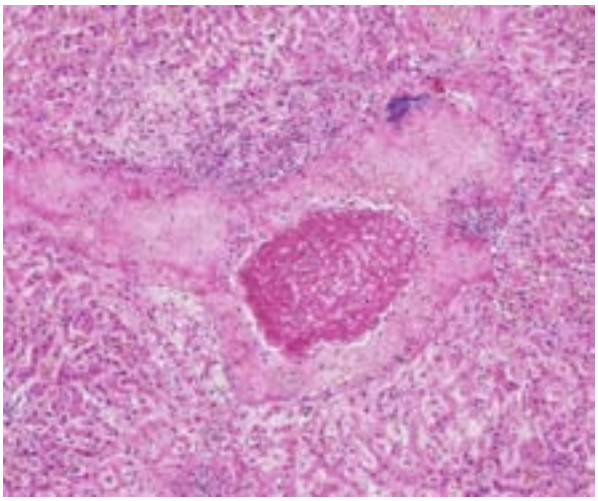

*1-5. Liver, calf: Areas of lytic necrosis are infiltrated by moderate numbers of neutrophils and histiocytes ("paratyphoid nodules"). There are aggregates of post-mortem bacilli throughout the section. (HE 256X)*

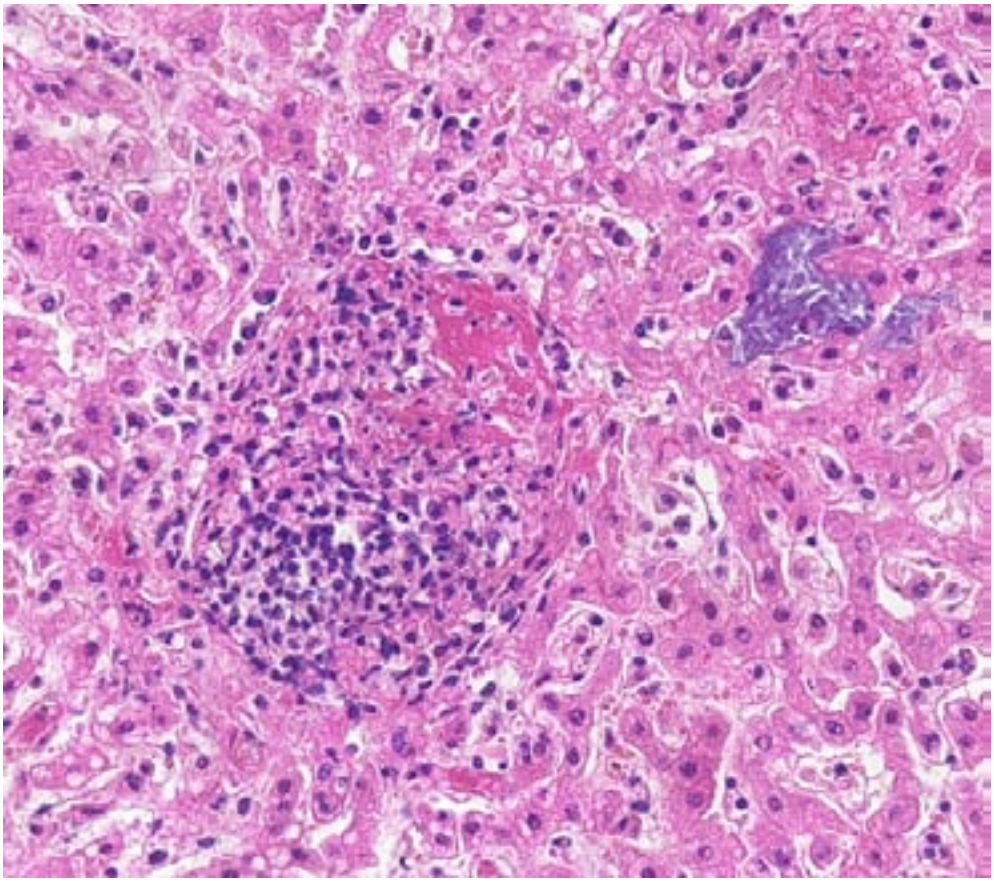

*1-5. Liver, calf: Areas of lytic necrosis are infiltrated by moderate numbers of neutrophils and histiocytes ("paratyphoid nodules"). There are aggregates of post-mortem bacilli throughout the section. (HE 256X)*

macrophages. *Salmonella* processes another type III secretion system encoded by SPI-2 that is activated as soon as the bacteria localizes in the phagosome. This SPI-2-encoded type III secretion system is essential for intracellular survival of the organism in macrophages and, therefore, systemic dissemination of the infection.[8]

In our empirical experience, *Salmonella* is usually not observed in HE-stained section, both in enteric and systemic sites of infection. Interestingly, in the present case there were abundant intralesional bacterial colonies, which likely represent postmortem overgrowth of the organism.

**JPC Diagnosis:** Liver: Hepatitis, necrotizing, multifocal, random, with vasculitis, thrombosis, and rare paratyphoid nodules.

**Conference Comment:** The accumulations of mixed mononuclear inflammatory cells multifocally scattered throughout the liver in this case are called "paratyphoid nodules" and are characteristic for the typhoidal form of salmonellosis.[3] Paratyphoid nodules or granulomas may also be found in the kidney, spleen, lymph nodes and bone marrow in cases of septicemic salmonellosis.[1] These contribute to the gross miliary pattern in affected organs, most often in the liver and spleen.[1] It is unclear whether these nodules are the result of a cell-mediated immune response or accumulate due to bacterial replication within macrophages.[1,7]

Typhoidal serotypes of *Salmonella* spp. are less common than the nontyphoidal forms in most species, including humans with the exception being in mice. Mice regularly develop septicemia with oral inoculation of *Salmonella* isolates, often without exhibiting gross and microscopic changes in the alimentary tract.[2,7]

The nontyphoidal or enteric form of salmonellosis, characterized by self-limiting enterocolitis or diarrhea in the absence of systemic disease, is a major cause of morbidity and mortality in calves and often over one billion human cases per year. While both are incriminated in cattle, *Salmonella enterica* serovar *Typhimurium* infects all species and is the most common isolate in people, while *S. enterica* serovar *Dublin* is more specific to cattle.[1,6] The similarity in enteric disease manifestation between cattle and humans and has led to their use as an experimental model for human infections.[6,11] Characteristic histopathology of nontyphoidal salmonellosis is the massive influx of neutrophils, which is also suggested as the

major triggering event of gastrointestinal necrosis and diarrhea.[6] Vasculitis and thrombosis is also prominent, and in severe cases can lead to rectal strictures in pigs who have poor collateral circulation.[4] Fibrinous cholecystitis is pathognomonic for acute enteric salmonellosis in calves.[4] Chronic enteric salmonellosis is characterized by discrete foci of necrosis and ulceration called "button ulcers" and seen most often in pigs but also cattle and horses.[4]

The colonies of coccobacilli and large numbers of rods found in some areas of the slide are both gram-positive, leading conference participants to conclude these are postmortem bacterial overgrowth not related to the *Salmonella* infection in this case.

**Contributing Institution:** Departamento de Clínica e Cirurgia Veterinárias, Escola de Veterinária, Universidade Federal de Minas Gerais, Belo Horizonte, MG, Brazil. http://www.vet.ufmg.br

**References**

1. Brown CC, Baker DC, Barker IK. Alimentary system. In: Maxie MG, ed. *Jubb, Kennedy, and Palmer's Pathology of Domestic Animals*. 5th ed. Vol 2. Philadelphia, PA: Elsevier Saunders; 2007:200-202.
2. Brown DE, Libby SJ, Moreland SM, et al. *Salmonella enterica* causes more severe inflammatory disease in C57/BL6 NrampI$^{G169}$ mice than SV129S6 mice. *Vet Pathol.* 2013;50(5): 867-876.
3. Cullen, JM, Brown DL. Hepatobiliary system and exocrine pancreas. In: Zachary JF, McGavin MD, eds. *Pathologic Basis of Veterinary Disease*. 5th ed. St. Louis, MO: Elsevier Mosby; 2012:433.
4. Gelberg HB. Alimentary system and the peritoneum, omentum, mesentery, and peritoneal cavity. In: Zachary JF, McGavin MD, eds. *Pathologic Basis of Veterinary Disease*. 5th ed. St. Louis, MO: Elsevier Mosby; 2012:376-377.
5. Morter RL, Armstrong CH, Amstutz HE, Thacker HL. Systemic salmonellosis in mature beef cows. *J Vet Diagn Invest*. 1989;1:22-24.
6. Nunes JS, Lawhon SD, Rossetti CA, et al. Morphologic and cytokine profile characterization of Salmonella enteric serovar typhimurium infection in calves with bovine leukocyte adhesion deficiency. *Vet Pathol.* 2010;47(2): 322-333.
7. Percy DH, Barthold SW. *Pathology of Laboratory Rodents and Rabbits* 3rd ed. Ames, IA: Blackwell Publishing; 2007:61-63.
8. Santos RL, Bäumler AJ. Cell tropism of *Salmonella enterica*. *Int J Med Microbiol*. 2004;294:225-233.
9. Santos RL, Tsolis RM, Bäumler AJ, Adams LG. Pathogenesis of *Salmonella*-induced enteritis: a review. *Braz J Med Biol Sci*. 2003;36:3-12.
10. Santos RL, Zhang S, Tsolis RM, Kingsley RA, Adams LG, Baumler AJ. Animal models of *Salmonella* infections: gastroenteritis vs. typhoid fever. *Microbes Infect*. 2001;3:1335-1344.
11. Santos RL, Zhang S, Tsolis RM, Bäumler AJ, Adams LG. Morphologic and molecular characterization of *Salmonella typhimurium* infection in neonatal calves. *Vet Pathol*. 2002;39:200-215.
12. Zhang S, Santos RL, Tsolis RM, Stender S, Hardt WD, Bäumler AJ, et al. The *Salmonella enterica* serotype Typhimurium effector proteins SipA, SopA, SopB, SopD and SopE2 act in concert to induce diarrhea in calves. *Infect Immun*. 2002;70:3843-3855.

**CASE II**: 08-4562 (JPC 3103756).

**Signalment:** 3-4 year-old ewes.

**History:** Chronic weight loss.

**Gross Pathology:** None.

**Laboratory Results:** None.

**Histopathologic Description:** The mucosa and submucosa is diffusely expanded and crypts are widely separated by extensive infiltration of epithelioid macrophages, a few multinucleated giant cells, plasma cells and lymphocytes. The macrophages are distended with cytoplasm containing fine, granular basophilic material which was demonstrated as acid fast bacilli (mycobacteria) by Ziehl Nielson stain. There is villous blunting and fusion. There are multifocal areas of necrosis in the mucosa. The submucosa contains dilated lymphatics. There is mild edema of serosa with small numbers of lymphocytes and plasma cell infiltration. In the associated mesentery there are multifocal areas of adipocyte necrosis and mineralization. The mesenteric blood vessels are infiltrated and surrounded by moderate numbers of lymphocytes and plasma cells. There is marked perivascular fibrosis.

**Contributor's Morphological Diagnoses:** Small intestine: Enteritis, granulomatous, diffuse, severe, chronic with villous atrophy, lymphangectasia and macrophages containing acid fast bacilli seen with Ziehl-Nielson stain. Mesentery: Fat necrosis and mineralization, multifocal with lymphoplasmacytic perivasculitis.

**Contributor's Comment:** Johne's disease (paratuberculosis) is a chronic intestinal disease of ruminants caused by *Mycobacterium avium* subspecies *paratuberculosis*. This disease is responsible for extensive economic losses worldwide related to fatality and loss of productivity. In small ruminants, Johne's disease is characterized by chronic wasting, decreased milk production and is rarely associated with diarrhea.[2] Gross thickening of bowel is not as remarkable as in cattle. Caseating granulomas (often mineralized), generally not seen in cattle, are commonly present in the intestine, lymphatics and lymph nodes of small ruminants.[2] Atrophy of fat due to malabsorption is a common finding in Johne's disease. However, in this case there is fat necrosis and mineralization. Widespread or focal necrosis of abdominal fat is frequently found in sheep and the pathogenesis is unknown.[2]

The route of disease transmission is fecal-oral route. After ingestion, the mycobacterium undergoes endocytosis by M cells of the dome epithelium over lymphoid follicles. It is proposed that integrin receptors on the apical surface of M cells bind fibronectin-opsonized bacteria, facilitating phagocytosis by these cells.[7] From M cells, the mycobacterium is transported in vacuoles to macrophages in subepithelial and intraepithelial areas of Peyer's patches and lamina propria.[1,2] After uptake by macrophages, the bacteria resist the degradative and killing

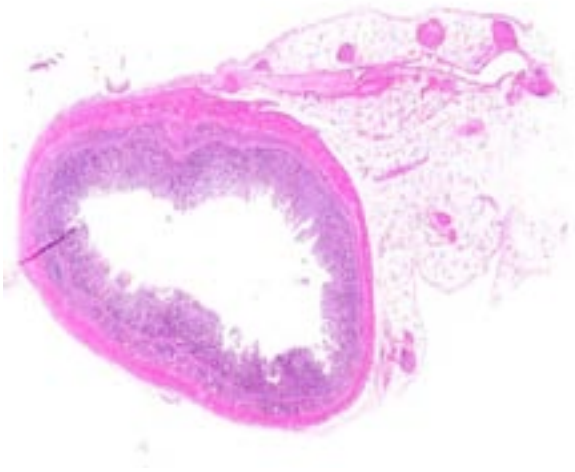

*2-1. Small intestine, sheep: There is marked blunting of intestinal villi, and vessels within the adjacent mesentery are prominent. (HE 5X)*

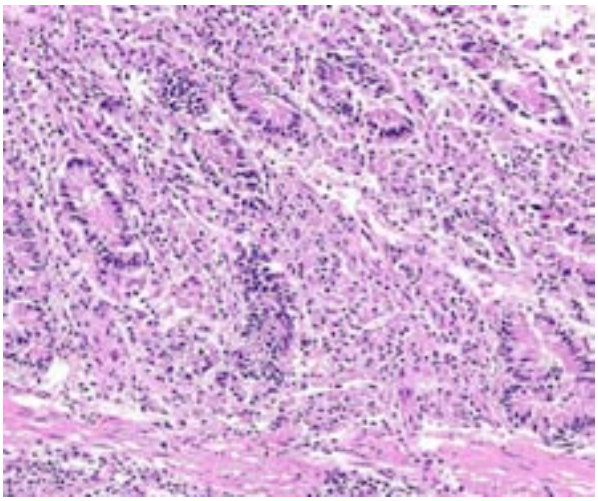

*2-2. Small intestine, sheep: There is marked crypt loss and remaining crypts are separated by large numbers of macrophages with abundant eosinophilic cytoplasm. (HE 125X)*

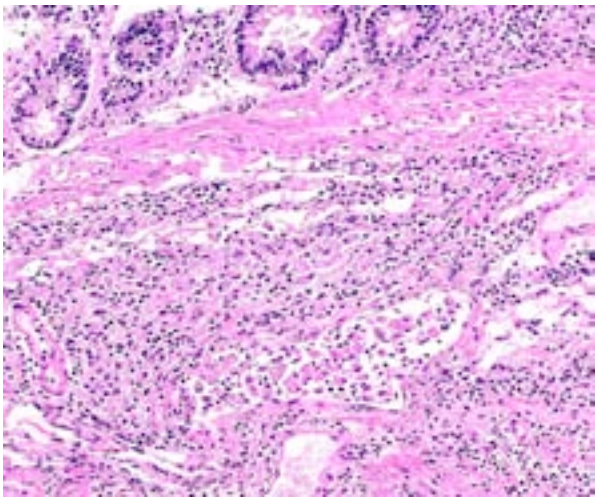

*2-3. Small intestine, sheep: The submucosa is also expanded by numerous macrophages and lymphocytes. Lymphatics are often distended and often contain macrophages as well. (HE 125X)*

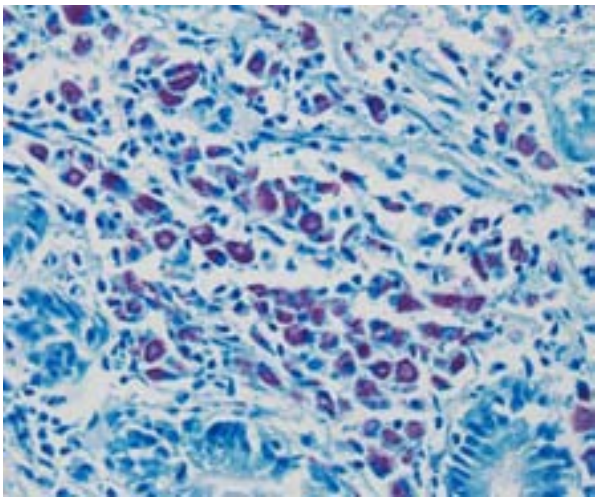

*2-4. Small intestine, sheep: Macrophages throughout the section contain numerous acid-fast bacilli. (Ziehl-Nielsen, 400X)*

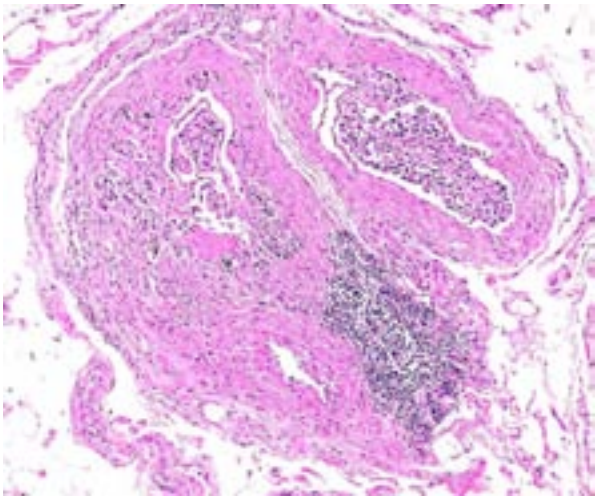

*2-5. Mesentery, sheep: There is chronic lymphangitis within the adjacent mesentery. (HE 90X)*

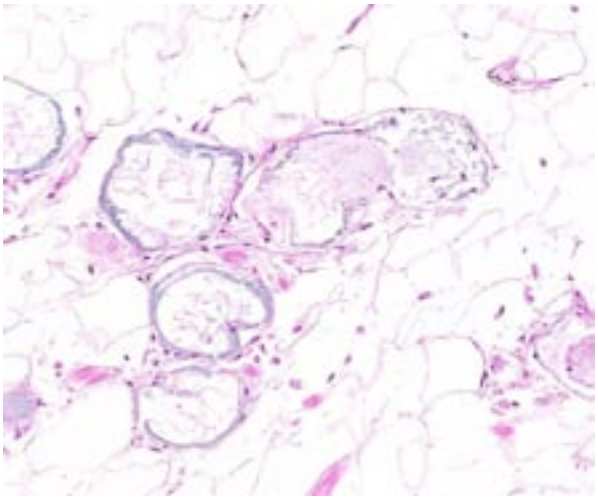

*2-6. Mesentery, sheep: There is multifocal necrosis and mineralization (saponification) of mesenteric adipocytes. (HE 148X)*

mechanisms of the macrophage via sulphatide production, which prevents phagosome-lysosome fusion, escape from the phagosome into the cytoplasm, glycolipid-mediated inhibition of nitric oxide production, and inhibition of the respiratory burst and oxidative killing mechanisms by superoxide dismutase and glycolipid production.[1]

Ovine Johne's disease has been noted as a problem in Australia and Europe. The disease in sheep can have three different forms with majority of the animals being asymptomatic. Among the clinically affected sheep, 30% are affected by paucibacillary (tuberculoid) form characterized by large number of T- lymphocytes, fewer eosinophils, macrophages and fewer bacteria in the gut. The rest of 70% have multibacillary (lepromatous) form with high levels of bacteria along with epithelioid macrophages and B lymphocytes infiltration,[5-8] as seen in this case. What determines the outcome of clinical disease is not entirely understood but various factors are implicated including the size of the infective dose, route of infection, mycobacterial strain virulence,[11] local and systemic immune status and age of the host, host resistance genes affecting antigen presentation and intracellular killing, and environmental factors.

In paratuberculosis, cell mediated immunity (CMI) plays a critical role in development of lesions and onset of clinical disease.[1,2] CMI develops relatively early in infection and, if effective, will lead to clearance of organisms and a resistant state.[1] The paucibacillary form is mediated by Th-1 response where bacterial growth within infected macrophage is controlled by IFN- and TNF-α production. The mulitibacillary form is mediated by Th-2 response with high production of IL-10 and little IFN- secretion and hence less control of intracellular bacterial growth.[5,8] It is interesting to note that the asymptomatic sheep are infected with mycobacterium but do not show any clinical or pathologic symptoms. The mechanism of disease resistance in asymptomatic animals is obscure. This differential activation of immune response to mycobacterium is speculated to be due to innate receptor engagement and signaling. Recently it is shown that different forms of sheep paratuberculosis have differential expression of pattern recognition receptors[5], including Toll-like receptors.[10]

**JPC Diagnosis:** 1. Intestine: Enteritis, granulomatous, diffuse, marked, with villar blunting, lymphangitis, and crypt loss.
2. Intestine: Fat necrosis with saponification.

**Conference Comment:** Johne's disease is problematic for livestock producers, as extended incubation times and average of 40% prevalence in infected herds coupled with intermittent bacterial shedding hinder eradication efforts. The problem is further exacerbated in small ruminant herds where diarrhea is not a typical clinical sign.[3] The disease only develops in older animals (over 19 months) and this complex epizootiology amounts to Johne's disease being one of the most important of the dairy industry.[3] Fecal culture is still the standard diagnostic test, but its poor reliability has led to investigation of many methods from qPCR of fecal samples to liver biopsies with mixed results, often requiring late stage disease development to establish meaningful sensitivity and specificity.[4,9]

The contributor discusses the pertinent differences of the cell-mediated immune response in relation to the two forms of disease, and we confirmed the lepromatous form in this case by repeating the acid-fast stains which revealed numerous intrahistiocytic bacteria. Clinical disease occurs due to the abundant granulomatous inflammation, and the lesions are often restricted to the ileum,[12] though the transmural granulomatous infiltration may also be observed in the colon and the organism has been cultured from a variety of organs.[1] Grossly the mesenteric lymph nodes are always enlarged and the classical intestinal change of diffuse mucosal thickening into transverse rugae is usually present in cattle.[1] In sheep and goats, the disease is characterized by chronic wasting and submandibular edema due to hypoproteinemia; the feces is usually normal in consistency and the gross enteric lesions are minimal, often missed at necropsy.[1]

**Contributing Institution:** Kansas State University

**References:**

1. Brown CC, Baker DC, Barker IK: Alimentary system. In: Maxie MG, ed. *Jubb, Kennedy and Palmer's Pathology of Domestic Animals*. 5th ed. Vol. 3. Philadelphia, PA: Elsevier Saunders; 2007:222-25, 285-286.
2. Clarke CJ. The pathology and pathogenesis of paratuberculosis in ruminants and other species. *J Comp Path*. 1997;116:217-261.
3. Gelberg HB. Alimentary system and the peritoneum, omentum, mesentery, and peritoneal cavity. In: Zachary JF, McGavin MD, eds. *Pathologic Basis of Veterinary Disease*. 5th ed. St. Louis, MO: Elsevier Mosby; 2012:385-387.
4. Laurin EL, Chaffer M, McClure SL, Keefe GP. The association of detection method, season, and lactation stage on identification of fecal shedding in mycobacterium avium ssp. Paratuberculosis infectious dairy cows. *J Diary Sci*. 2015;98(1):211-220.
5. Nalubamba K, Smeed J, Gossner A, Watkins C, Dalziel R, Hopkins J. Differential expression of pattern recognition receptors in the three pathological forms of sheep paratuberculosis. *Microbes Infect*. 2008;10(6):598-604.
6. Perez V, Garcia-Marin JF, Badiola JJ. Description and classification of different types of lesions associated with natural paratuberculosis infection in sheep. *J Comp Path*. 1996;114:107-122.
7. Sigurethardóttir OG, Valheim M, Press CM. Establishment of Mycobacterium avium subsp. paratuberculosis infection in the intestine of ruminants. *Adv Drug Deliv Rev*. 2004;19:56(6): 819-34.

8. Smeed JA, Watkins CA, Rhind SM, Hopkins J. Differential cytokine gene expression profiles in the three pathological forms of sheep paratuberculosis. *BMC Vet Res*. 2007;14:3:18.
9. Smith SL, Wilson PR, Collett MG, et al. Liver biopsy histopathology for diagnosis of Johne's disease in sheep. *Vet Pathol.* 2014;51(5):915-918.
10. Taylor DL, Zhong L, Begg DJ, de Silva K, Whittington RJ. Toll-like receptor genes are differentially expressed at the sites of infection during the progression of Johne's disease in outbred sheep. *Vet Immunol Immunopathol*. 2008;15;124(1-2):132-51.
11. Verna AE, Garcia-Pariente C, Muñoz M, Moreno O, García-Marin JF, Romano MI, et al. Variation in the immuno-pathological responses of lambs after experimental infection with different strains of Mycobacterium avium subsp. paratuberculosis. *Zoonoses Public Health*. 2007;54(6-7):243-52.

**CASE III**: 07-27354 (JPC 3105594).

**Signalment:** Young adult female caribou, *Rangifer tarandus.*

**History:** This specimen is one of a number of hunter-killed caribou that were submitted to the Canadian Cooperative Wildlife Health Centre due to concerns about the quality of the meat. In this case, only the head was submitted with the concern being the presence of "pus in the nose".

**Gross Pathologic Findings:** The head is from a young adult female caribou. Over the bridge of the nose about 2cm behind the nasal plenum there is a 3cm diameter area of thickened skin covered by a crusty surface exudate. The parotid lymph nodes are slightly enlarged. On section of the head, the anterior 4cm of both nasal cavities contain a large amount of muco-purulent yellow-brown tenacious exudate. The underlying mucosa is roughened and red. The nasal turbinates and pharyngeal mucosa appear normal.

**Laboratory Results:** N/A.

**Histopathologic Description:** Haired skin from nose. Segmentally, the epidermis is thickened and composed of or replaced by a variably thick layer of parakeratotic hyperkeratosis, fibrin, necrotic debris, bacterial colonies, pustules, fragmented hair shafts and vacuolated epithelial cells. Full thickness necrosis of the epithelium is present in many areas. Multifocally, throughout the dermis, hypodermis and underlying muscularis there are myriad 200 to 400 µm diameter intracellular protozoal cysts. A thick pale eosinophilic to pale blue capsule surrounds the bradyzoites contained within a parasitophorus vacuole. There is minimal inflammation or tissue reaction around most cysts. Occasionally cysts, particularly within the more superficial layers of the skin, appear to be dead and are infiltrated with macrophages, and multinucleate giant cells with smaller numbers of lymphocytes and plasma cells.

**Contributor's Morphologic Diagnosis:** Haired skin: Dermatitis, necrotizing, locally extensive, severe, chronic with myriad intralesional intracellular protozoal cysts consistent with *Besnoitia* sp.

**Contributor's Comment:** *Besnoitia* are apicomplexan parasites that parasitize numerous species including caribou, cattle, horses, reindeer, lizards, rodents and rabbits. Currently, there are 9 different named species of *Besnoitia*. Whether these are all truly distinct species is unclear as currently the life cycle of only a small number of

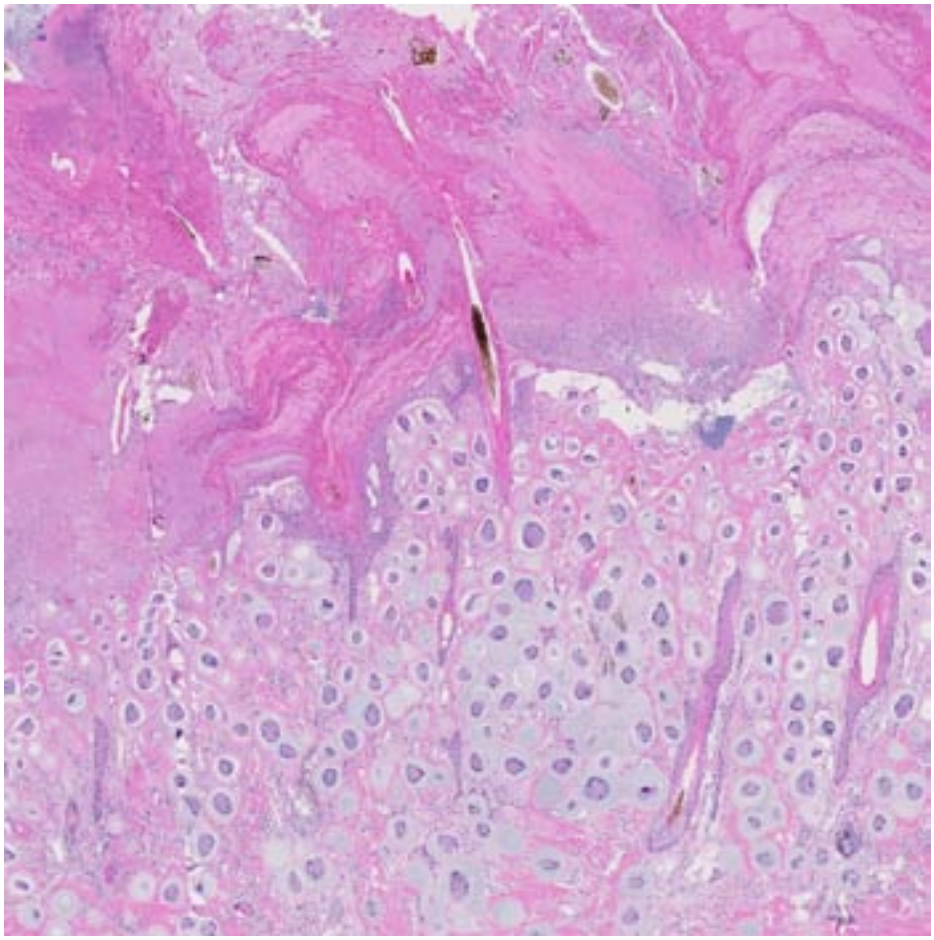

*3-1. Skin, caribou: The dermis is markedly expanded by numerous apicomplexan cysts which efface adnexa; the overlying epidermis is multifocally necrotic and diffusely and severely hyperkeratotic. (HE 22X)*

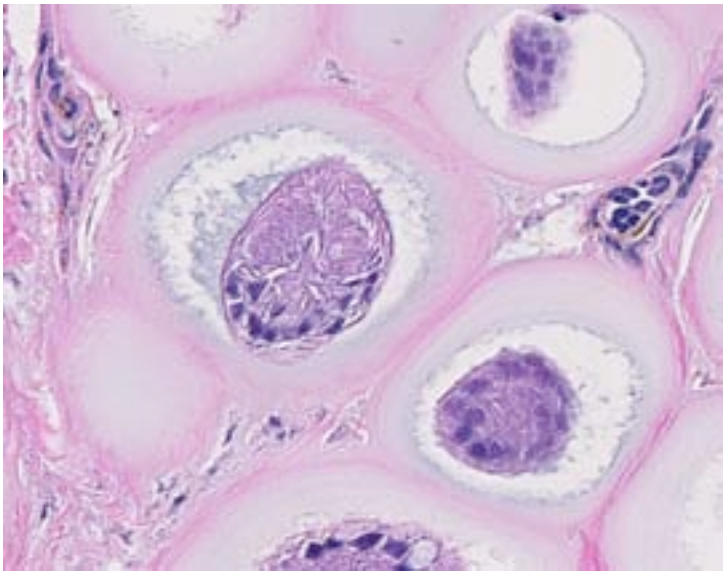

*3-2. Skin, caribou: Cysts have a 10-30 µm thick, hyaline and vacuolated blue-grey fibrous capsule that surrounds a 5-10 µm thick rim of host cell cytoplasm with multiple enlarged but flattened nuclei surrounding a parasitophorous vacuole containing numerous, densely packed crescentic 3-5 µm bradyzoites. (HE 316X)*

these species has been described and the taxonomy of the rest are based upon the species of the intermediate host.[2]

*B. tarandi* is the species of *Besnoitia* known to affect caribou and the closely related reindeer. The life cycle of this species is not currently known. The domestic cat is the definitive host for the 3 species with a known life cycle, but the definitive host for the *B. tarandi* is unknown although other *Felid* species such as cougars and lynx may be a possibility.[2]

An epizootic event of besnoitiosis occurred in a zoo in Manitoba starting in 1983.[4] The initial cases were diagnosed in 2 caribou (*Rangifer tarandus caribou*) that died of pneumonia. Over the course of 3 years besnoitiosis spread to mule deer (*Odocoileus hemionus hemionus*), reindeer (*Rangifer tarandus tarandus*) and a second isolated group of caribou. Twenty-eight caribou, 10 mule deer and 3 reindeer were euthanized or died as a result of this epizootic. The means of transmission in this case was thought to be biting flies.

In wild woodland caribou, besnoitiosis appears to be a relatively common (23% infection rate in one study) chronic and mild disease.[6] Lesions are most often confined to the skin of the extremities causing alopecia with mild skin thickening and crusting. In some cases however, the disease appears to be much more widespread and severe with ulceration of the skin, cysts in the sclera, conjunctiva, nasal mucosa, visceral serosa, tendons, tendon sheaths, hoofs and testes.[1,4] In this case, cysts were found within the nasal mucosa, sclera, conjunctiva, lymph nodes and meninges as well as the skin.

Although *B. tarandi* is not of zoonotic concern and meat from affected animals should be safe to eat, the relatively common prevalence, poorly understood natural history of the disease and the potential for transmission to other wildlife species makes besnoitiosis a disease of potential emerging concern for translocation of reindeer and caribou from arctic regions to more southern ones.

**JPC Diagnosis:** 1. Haired skin: Protozoal cysts, numerous.
2. Haired skin: Hyperplasia and hyperkeratosis, epidermal, diffuse, severe, with segmental epidermal necrosis and numerous mixed bacterial colonies.

**Conference Comment:** Most slides contain two sections of skin in this case which are variably affected with epidermal necrosis, parakeratotic hyperkeratosis and epidermal hyperplasia. While the protozoal cysts are diffuse throughout all areas, the most severe areas of hyperkeratosis also contain numerous aggregrates of mixed bacteria

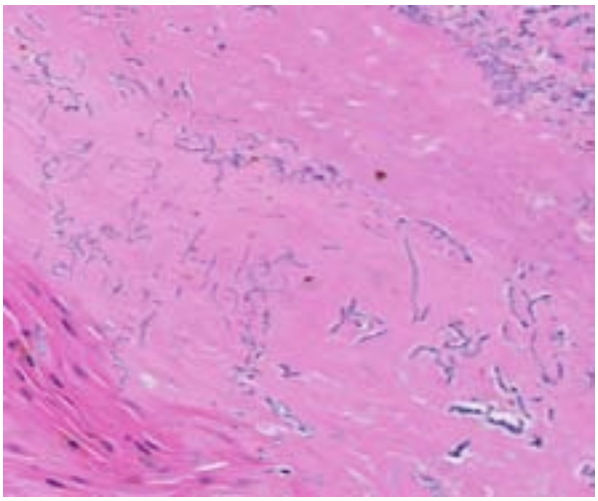

*3-3. Skin, caribou: In the overlying crust, there are abundant 1-2 µm, paired bacterial cocci (1 pt.) (zoospores) (1 pt.) haphazardly arranged in rows and forming long, branching, filaments (consistent with Dermatophilus congolensis). (HE 248X)*

including many with long filaments of parallel rows of coccoid bodies resembling railroad tracks. These are consistent with *Dermatophilus congolensis* and conference participants deliberated about the level of contribution the two infectious organisms played in lesion development. The parakeratosis and epidermal hyperplasia is quite characteristic of *D. congolensis* infections; however, histopathology from *Besnoitia* spp. infections is variable and nonspecific.[5]

*Besnoitia* spp. have a two-host life cycle with disease occurring in the definitive host.[3] The disease can be divided into acute, subacute, and chronic stages. The acute stage is characterized by tachyzoite proliferation within vascular endothelial cells. Bradyzoites proliferate during the subacute and chronic stages within mesenchymal cells resulting in the cyst formation such as observed in this case.[5]

Recently immunohistochemistry and other special stains were used to characterize the tissue cyst layers of *Besnoitia besnoiti* in cattle. Tissue cysts were found in multiple organs including the corium of the claw where they contributed to chronic laminitis. The cysts are composed of host cell wall with enlarged nuclei containing a parasitophorous vacuole with bradyzoites. Additionally, an inner and outer cyst wall were distinguished, and in chronic stages, extracystic zoites were observed.[5]

**Contributing Institution:** Department of Veterinary Pathology
Western College of Veterinary Medicine
52 Campus Dr
Saskatoon, Saskatchewan, Canada
www.usask.ca/wcvm/vetpath, www.ccwhc.ca

**References:**

1. Ayroud M, Leighton FA, Tessaro SV. The morphology and pathology of *Besnoitia* sp. In reindeer (*Rangifer tarandus tarandus*). *J Wildl Dis*. 1995;31(3):319-326.
2. Dubey JP, Sreekumar C, Rosenthal BM, Vianna MCB, Nylund M, Nikander S, et al. Redescription of *Besnoitia tarandi* (Protzoa:Apicomplexa) from the reindeer (*Rangifer tarandus*). *Int J Parasitol*. 2004;34:1273-1287.
3. Ginn PE, Mansell JL, Rakich PM. Skin and appendages. In: Maxie MG, ed. *Jubb, Kennedy, and Palmer's Pathology of Domestic Animals*. 5th ed. Vol 1. Philadelphia, PA: Elsevier Saunders; 2007:709-710.
4. Glover GJ, Swendrowski M, Cawthorn RJ. An epizootic of besnoitiosis in captive caribou (*Rangifer tarandus caribou*), reindeer (*Rangifer tarandus tarandus*), and mule deer (*Odocoileus hemionus hemionus*). *J Wildl Dis*. 1990;26:186-195.
5. Langenmayer MC, Gollnick NS, Majzoub-Altweck M, Scharr JC, Schares G, Hermanns W. Naturally acquired bovine besnoitiosis: histological and immunohistochemical findings in acute, subacute, and chronic disease. *Vet Pathol.* 2015;52(3):476-488.
6. Lewis RJ. Besnoitia infection in Woodland caribou. *Can Vet J.* 1989;30:436.

**CASE IV:** P678-12 (JPC 4032916).

**Signalment:** 2-year-old, female Scottish Highland heifer, *Bos Taurus.*

**History:** This heifer had a history of mild respiratory difficulty since birth. In the last month, multiple cutaneous nodules developed on the head, thorax and hind limbs, with pus draining from a few. This animal was the only one affected on the farm.

**Gross Pathology:** The animal was in poor body condition. There was diffuse facial swelling and deformity. On cut section, there were numerous encapsulated and fistulating abscesses, up to 5 cm in diameter, in the subcutaneous tissues and muscles of the maxillary and mandibular regions, and, minimally, the tongue; the pus was thick, yellowish, and no "sulfur granules" were detected. Similar abscesses were also present in: 1) the walls of the pharynx and proximal esophagus, 2) the cervical, prescapular, inguinal and tracheobronchial lymph nodes, 3) the subcutaneous tissues of the thorax and both hind limbs, and 4) the lungs. Multiple, often coalescing ulcers, 4 mm in diameter, were observed on the gingiva, tongue, soft palate and, to a lesser degree, esophagus.

**Laboratory Results:** The heifer tested negative for bovine viral diarrhea pestivirus by fluorescent antibody testing (FAT) on the oral and esophageal mucosa. Bacterial culture of abscesses in skin, lymph nodes and lung yielded a heavy growth of *Actinobacillus lignieresii*, in pure culture except in one lymph node in which *Trueperella pyogenes* was also identified.

**Histopathologic Description:** The submitted slide is a section of pharyngeal/cranial esophageal wall stained with hematoxylin-eosin-phloxin-saffron. The normal architecture is extensively obliterated by irregularly sized collections of degenerate neutrophils with variable numbers of surrounding and/or admixed macrophages (pyogranulomas), and dense fibrovascular (granulation) tissue infiltrated mainly by lymphocytes and plasma cells between pyogranulomas. Within these pyogranulomas, there are numerous structures composed of pale amphophilic, finely granular material (bacteria) surrounded by radiating, deeply eosinophilic, club-shaped material (Splendore-Hoeppli phenomenon). This material is multifocally and variably mineralized, with occasional associated multinucleated giant cells. A Gram stain showed the bacteria to be Gram-negative coccobacilli.

**Contributor's Morphologic Diagnosis:** Severe, multifocal chronic pyogranulomatous pharyngitis/esophagitis with Splendore-Hoppli material and intralesional Gram-negative coccobacilli.

**Contributor's Comment:** The final diagnosis was actinobacillosis. Actinobacillosis is mainly a disease of soft tissues of cattle and sheep, but it has also been reported in other species including

*4-1. Ox, head: There are numerous encapsulated and fistulating abscesses, up to 5 cm in diameter, in the subcutaneous tissues and muscles of the maxillary and mandibular regions. (Photo courtesy of: University of Montreal, Department of Pathology. http://www.medvet.umontreal.ca)*

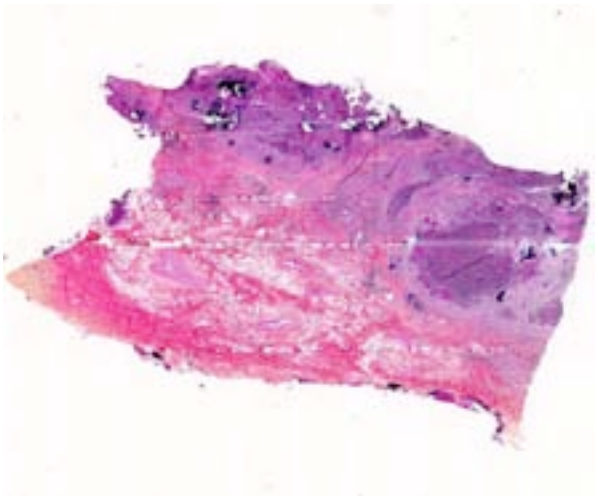

*4-2. Ox, fibrovascular tissues of head: The subcutaneous tissue is effaced by numerous coalescing pyogranulomas. (HE 5X)*

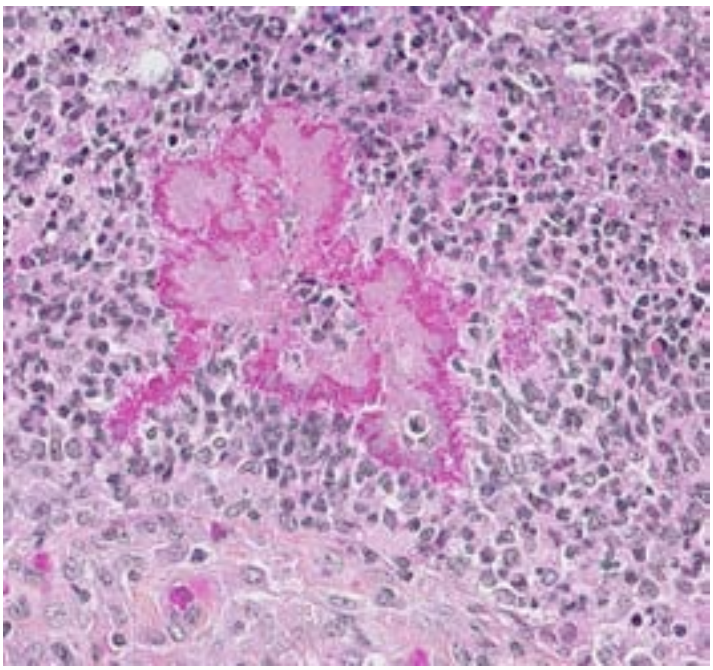

*4-3. Ox, fibrovascular tissues of head: The pyogranulomas are centered on colonies of bacilli encased in brightly eosinophilic Splendore-Hoeppli material. (HE 256X)*

pigs, goats, horses and dogs. *Actinobacillus lignieresii* is an opportunistic Gram-negative coccobacillary bacterium that is part of the normal flora of the oral cavity and rumen of cattle and sheep. Following trauma to the oral mucosa (e.g. plant material, teeth, etc.) or skin, *A. lignieresii* invades the underlying soft tissues and typically causes pyogranulomatous lesions, often with lymphagenous extension to regional lymph nodes (and thus lymphangitis and lymphadenitis).[1,2,3] Iatrogenic cases have been described, e.g. surgical wound contamination during cesarean sections.[1,3] *Actinobacillus lignieresii* is also a cause of bite wound infections in humans, especially horse bites.[3,4] Grossly, the lesions appear as variably-sized abscesses with abundant fibrous tissue, in which small granules, known as "sulfur granules", are usually seen. Microscopically, these lesions correspond to pyogranulomas, with abundant inflamed fibrous/fibrovascular tissue, centered on masses of coccobacilli surrounded by radiating club-shaped eosinophilic material (Splendore-Hoeppli phenomenon), and grossly seen as the granules.[2,3] Splendore-Hoeppli material can be seen in some bacterial, fungal and parasitic infections, but also in some non-infectious conditions; it is considered to be made up of immune complexes,[2] among others. Other bacteria that can cause similar microscopic lesions in cattle include *Staphylococcus aureus* and *Pseudomonas aeruginosa* (botryomycosis), and also *Actinomyces bovis*; the latter causes mainly a mandibular osteomyelitis, known as "lumpy jaw", but can sometimes involve soft tissues.[1,2,7]

In cattle, the most frequent presentation is a chronic glossitis known as "wooden tongue", due to the very firm consistency imparted by the abundant fibrous tissue.[1,2] The disease is usually sporadic, but small outbreaks have been reported.[1,2,3] Other reported locations include the skin of the head, neck and limbs, forestomachs, lungs, pharynx, esophagus and lungs.[1,2,3] Clinical signs depend on lesion size and distribution; subclinical lesions, especially in the tongue and lymph nodes of the head and neck, may be found as incidental findings at slaughter.[3] Intravenous sodium iodine is the treatment of choice, but successful surgical exeresis of localized lesions has been described.[1,7] In the present case, the tongue was minimally involved and no sulfur granules were observed; an underlying cause was not found. Dystrophic mineralization was prominent, especially in "older" lesions. The multiple ulcerations in the oral and proximal esophageal mucosae were considered to be the result of *A. lignieresii* infection, as they were associated with underlying pyogranulomatous lesions.

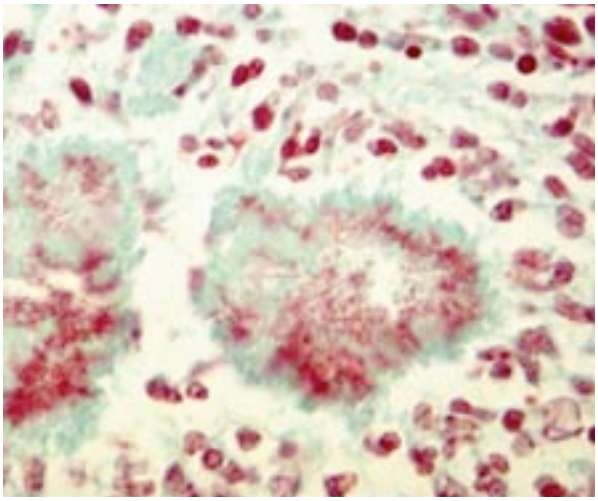

*4-4. Ox, fibrovascular tissues of head: A Gram stain demonstrates gram-negative bacilli within the Splenore-Hoeppli phenomenon. (Photo courtesy of: University of Montreal, Department of Pathology. http://www.medvet.umontreal.ca)*

**JPC Diagnosis:** Fibrovascular tissue: Cellulitis, pyogranulomatous, diffuse, severe, with Splendore-Hoeppli phenomenon, and numerous bacterial colonies.

**Conference Comment:** This is a classic case with challenging tissue identification as most sections lack discernible anatomic landmarks; however, the Splendore-Hoeppli phenomenon and club colonies leave few differentials for this lesion in the ox. Wooden tongue may be most aptly confused with lumpy jaw, the other classic large colony forming bacterial entity of the bovine oral cavity. Both *Actinobacillus lignieresii* and *Actinomyces bovis* form club colonies, but the colonies in actinomycosis are much larger with smaller and less discrete clubs.[6] The two can be readily distinguished by the invasion of bone in lumpy jaw or by gram stain as only *Actinomyces* is gram positive.[2]

As the contributor nicely explains, the bacteria is considered normal flora thus most cases of wooden tongue are sporadic with prevalence at slaughter of up to 3.6%. Interestingly, herd outbreaks have occurred with up to 73% morbidity and are likely associated with abrasive feedstuffs and crowded conditions.[4]

**Contributing Institution:** http://www.medvet.umontreal.ca

**References:**

1. Angelo P, Alessandro S, Noemi R, et al. An atypical case of respiratory actinobacillosis in a cow. *J Vet Sci*. 2009;10(3):265-7.
2. Brown CC, Baker DC, Barker IK. Alimentary system. In: Maxie MG, ed. *Jubb, Kennedy, and Palmer's Pathology of Domestic Animals*. Vol. 2. 5th ed. Philadelphia, PA: Elsevier Saunders; 2007:1-296.
3. Cahalan SD, Sheridan L, Akers CR, et al. Atypical cutaneous actinobacillosis in young beef cattle. *Vet Rec*. 2012;13;171(15):375.
4. Jones SL, Smith BP. Diseases of the alimentary tract. In: Smith BP, ed. *Large Animal Internal Medicine*. 4th ed. St. Louis, MO: Mosby Elsevier; 2009:782-784.
5. Peel MM, Hornidge KA, Luppino M, et al. *Actinobacillus* spp. and related bacteria in infected wounds of humans bitten by horses and sheep. *J Clin Microbiol*. 1991;29(11):2535-8.
6. Thompson K. Bones and joints. In: Maxie MG, ed. *Jubb, Kennedy, and Palmer's Pathology of Domestic Animals*. 5th ed. Vol. 2. Philadelphia, PA: Elsevier Saunders; 2007:98-99.
7. Thompson PN, Van der Lugt JJ, Olivier-Carstens A. Botryomycosis associated with *Pseudomonas aeruginosa* in the nasopharynx of a cow. *Vet Rec*. 2001:20;149(16):495-6.